UNIVERSITE D'AIX-MARSEILLE

ECOLE DOCTORALE SCIENCES DE LA VIE ET DE LA SANTE

INSTITUT DE BIOLOGIE DU DEVELOPPEMENT DE MARSEILLE

Thèse présentée pour obtenir le grade universitaire de docteur

Discipline : Biologie-Santé

AMBRA MASUZZO

Cellular and Molecular Dissection of Bacterial Peptidoglycan-mediated Drosophila melanogaster Behavioral Immunity

Dissection cellulaire et moléculaire de l'immunité comportementale de Drosophila melanogaster médiée par le peptidoglycane bactérien

To be defended on 27th November 2020 in front of the jury composed by:

Maria Luísa **VASCONCELOS**	Rapportrice
Serge **BIRMAN**	Rapporteur
Marc **DIONNE**	Examinateur
Julien **ROYET**	Directeur de thèse
Léopold C. **KURZ**	Co-Directeur de thèse

Per Anna.

Che tu possa sempre essere libera.

Acknowledgments

I want to thank all the people which have supported me during these four years, allowing me to live this adventure.

First of all, I want to thank Julien Royet, which gave me the opportunity to work in a wonderful scientific field. I am really grateful for the trust and the freedom Julien gave me during these years. He has been always available and supportive, in both professional and human points of view.

A big thank you goes to Leopold C. Kurz, which has guided me during these years. When I arrived in the lab, Leo taught me everything I know about flies. He always trusted me and encouraged me in the hardest moments.

I would like to thank all the member of Julien Royet's lab, I was lucky to work in such a great environment! A special thank you goes to Olivier. I will always remember our long talks about science, science fiction and life in general.

I want to thank Maria Luísa Vasconcelos, Marc Dionne and Serge Birman for reading my manuscript and accepting to be part of my Thesis Jury.

I want to thank the members of my Thesis Committee Yaël Grosjean, Serge Birman and Matthieu Cavey. Their advice helped me a lot to progress in my work.

Also, I want to thank our collaborators Yaël Grosjean, Gérard Manière, Frédéric Marion-Poll and Claudia Steiner. It has been stimulating to work and discuss with them.

I want to thank the animal and the imaging facility of the IBDM, for helping me with my experiments.

I want to thanks the LabEx which financially supported my thesis and the people working in administration, which always have been kind and helpful.

I am thankful to my friends here in Marseille and all over the world. Wherever they were they always supported me. I am grateful to have all of them in my life.

The biggest thank you goes to my family, which fill my life with love.

Abstract (French)

Dans la nature, les métazoaires cohabitent avec les micro-organismes avec lesquels ils ont développé des relations étroites. Ainsi, les épithéliums des animaux sont-ils recouverts de micro-organismes qui exercent chez l'hôte des fonctions à la fois protectrices et physiologiques. La présence de certaines espèces microbiennes peut être indicative, pour les animaux, de la qualité d'une source alimentaire ou d'un site de ponte favorable. C'est le cas pour la mouche *Drosophila melanogaster*, qui se nourrit et pond des œufs dans des fruits en décomposition. D'autre part, l'exposition à des microbes nocifs peut déclencher une infection et mettre en danger la vie de l'hôte. Pour éradiquer les agents pathogènes, les animaux ont développé différents mécanismes parmi lesquels l'activation d'une réponse immunitaire contre l'agent envahisseur. Les recherches menées ces dernières décennies ont permis de caractériser les cascades et les mécanismes moléculaires impliqués dans cette réponse immunitaire antimicrobienne. En plus de la réponse immunitaire canonique, les animaux adaptent leur comportement à la présence de micro-organismes nocifs pour : i) réduire leur exposition à l'agent pathogène et, donc, leur risque d'infection ii) éviter de propager l'infection à d'autres membres du groupe ii) protéger leur descendance vis-à-vis de l'exposition à l'agent pathogène. Cependant, on ne sait que peu de choses à ce jour sur les mécanismes qui sous-tendent les modifications comportementales induites par les microbes.

L'un des objectifs de notre laboratoire est d'identifier les acteurs cellulaires et moléculaires impliqués dans l'immunité comportementale. Il est bien documenté que le peptidoglycane dérivé des bactéries est le principal déclencheur de la réponse immunitaire humorale chez la drosophile et que sa reconnaissance par des récepteurs spécifiques déclenche la production de peptides antimicrobiens dépendante de la voie NF-κB. L'exposition des mouches au peptidoglycane bactérien déclenche non seulement une réponse antimicrobienne mais réduit également la ponte des femelles. Des travaux de l'équipe ont montré que le peptidoglycane active la signalisation NF-κB dans les neurones octopaminergiques, ce qui entraîne un blocage de la ponte chez la femelle. De plus, nous avons montré que cette réponse comportementale est régulée par une enzyme de dégradation du peptidoglycane appelée PGRP-LB (Kurz, C.L., Charroux, B. et al.,2017).

Au cours de la première partie de mon doctorat, j'ai identifié les neurones du système nerveux central de la mouche qui expriment la PGRP-LB. En outre, j'ai découvert qu'un sous-ensemble de ces neurones du cerveau est octopaminergique. En utilisant des stratégies génétiques, j'ai démontré que ce sous-ensemble de neurones régule la ponte des œufs lors de l'exposition au peptidoglycane. L'imagerie calcique m'a enfin permis de montrer que ces neurones octopaminergiques PGRP-LB+ détectent

directement le peptidoglycane bactérien et que cette détection entraîne l'inhibition de leur activité (Masuzzo, A. et al.,2019).

Dans la deuxième partie de mon doctorat, je me concentre sur la caractérisation des neurones non-octopaminergiques exprimant PGRP-LB. En particulier, je me suis focalisé sur une sous-population de neurones situés dans le proboscis des mouches qui projettent leurs axones dans la zone sous-œsophagienne du cerveau. J'ai montré que ces neurones correspondent à un sous-ensemble de neurones du goût pour la détection des composés amers. L'imagerie calcique montre que ces neurones réagissent au peptidoglycane bactérien et que cette réaction dépend de certains éléments de la cascade NF-κB. En outre, les neurones du goût pour la détection des composés sucrés réagissent également au peptidoglycane. Toutefois, dans ce cas, la réponse est totalement indépendante de la voie NF-κB. De plus, nous avons montré, à l'aide de tests comportementaux, que les mouches sont attirées par le peptidoglycane et que ce comportement résulte de l'intégration des signaux provenant des neurones du goût amer et du goût sucré (Masuzzo, A., Maniere, G., Steiner, C., et al. 2020. Manuscrit soumis).

En conclusion, les résultats que j'ai obtenus au cours de mon doctorat montrent qu'un composé bactérien unique, le peptidoglycane, induit à la fois la voie de signalisation NF-κB dans les cellules immunitaires « classiques » et dans les neurones immunocompétents, et déclenche ainsi une immunité canonique comportementale. Cependant, certains neurones, tels que les neurones du goût sucré, réagissent au peptidoglycane de manière indépendante de NF-κB, ce qui suggère que d'autres mécanismes sont nécessaires à la détection du peptidoglycane dans ces neurones. Ces résultats soulèvent des questions importantes tant pour le domaine de l'immunologie que pour celui des neurosciences, comme par exemple quelles sont les cibles moléculaires de l'activation du NF-κB dans les neurones et comment ces cibles sont capables de modifier l'activité des neurones.

Abstract (English)

In nature, metazoans co-habit with micro-organisms and have evolved tight relationships with them. Animal epithelial surfaces are covered by microbes, which have both protective and physiological functions. In the environment, the presence of certain microbial species can be indicative of a food source quality or associated with a convenient oviposition site. This is the case of *Drosophila melanogaster*, which feeds and lays eggs in rotten fruits. On the other hand, exposure to harmful microbes can lead to infection and put the host life at risk. Animals have evolved different mechanisms to eradicate pathogens. For instance, infection with pathogenic microbes triggers in the host the activation of a robust immune response against the invading agent. Last decades researches have successfully described and characterized the molecular cascades and mechanisms involved in this anti-microbial immune response. In addition to canonical immune response, animals adapt their behavior to the presence of harmful micro-organisms to: i) reduce their exposure to the pathogen and, thus, their risk of infection ii) avoid to spread the infection to other members of their group ii) protect the offspring from the exposure to the pathogen. However, up to date little is known about the mechanisms that underline microbe-induced behavioral modifications.

One of the goals of our laboratory is to identify the cellular and molecular actors involved in behavioral immunity. It is well known that bacteria-derived peptidoglycan is the main elicitor of the humoral immune response in *Drosophila melanogaster* and its recognition by specific receptors triggers the NF-κB-dependent production of anti-microbial peptides. In the lab was previously demonstrated that fly exposure to bacterial peptidoglycan not only triggers the antimicrobial response but also reduces female egg-laying. Indeed, peptidoglycan activates NF-κB signaling in octopaminergic neurons leading to female oviposition blockage. Moreover, we showed that this behavioral response is buffered by a dedicated peptidoglycan degrading enzyme known as PGRP-LB (Kurz, C.L., Charroux, B. et al.,2017).

During the first part of my Ph.D., I identified some neurons of the fly central nervous system which express PGRP-LB. In addition, I found that a subset of PGRP-LB neurons in the brain is also octopaminergic. By using intersectional strategies, I demonstrated that this specific subset of neurons regulates egg-laying upon peptidoglycan exposure. Furthermore, by using Ca^{2+} imaging, I showed that these octopaminergic/PGRP-LB expressing neurons directly sense the bacterial peptidoglycan and that this sensing leads to their neuronal activity inhibition (Masuzzo, A. et al.,2019).

In the second part of my Ph.D., I focus on the characterization of non-octopaminergic PGRP-LB expressing neurons. In particular, I focused on a subpopulation of these neurons which is located in the proboscis of flies and project their axons in the sub-esophageal zone of the brain. I showed that

these neurons correspond to a subset of taste neurons for the sensing of bitter compounds. In vivo Ca^{2+} experiments show that these neurons respond to bacterial peptidoglycan and that this response is dependent on some elements of the NF-κB cascade. In addition, also taste neurons for the detection of sweet compounds respond to peptidoglycan. However, in this case, the response is completely independent of the NF-κB pathway. Moreover, we showed by using the behavioral assays that flies are attracted to peptidoglycan and that this behavior results from the integration of the signals coming from both bitter and sweet taste neurons (Masuzzo, A., Maniere, G., Steiner, C., et al. 2020. Submitted manuscript).

The results I obtained during my Ph.D. show that the same bacterial elicitor (peptidoglycan) dually induces the NF-κB signaling pathway in immune-competent cells and neurons, and thus triggers both canonical and behavioral immunity. However, some neurons, i.e. taste sweet neurons, respond to peptidoglycan in an NF-κB independent way, suggesting that other mechanisms are required for the peptidoglycan detection in these neurons. These results raise important questions both for immune and neuroscience fields, such as which are the molecular targets of NF-κB activation in neurons and how these targets are able to modify neural activity.

Table of contents

List of Abbreviations iii
Introduction 1
1. *Drosophila melanogaster* immune system 1
1. Drosophila melanogaster as a model to study the innate immune response 1
1.2 Immune mechanisms in D. melanogaster 2
1.3 Methods to study immunity in D. melanogaster 2
1.4 Cellular immune response in D. melanogaster 4
1.5 The humoral immune response in D. melanogaster 5
1.6 Bacterial peptidoglycan: a key elicitor of the humoral immunity in D. melanogaster 6
1.6.1 Peptidoglycan structure 6
1.6.2 Release of soluble peptidoglycan fragments 8
1.7 Peptidoglycan recognition proteins in D. melanogaster 9
1.7.1 PGRPs as upstream receptors of the humoral immunity 10
1.7.2 PGRPs as regulators of the immune response 12
1.7.3 Peptidoglycan sensors in mammals 13
1.8 Major cascades involved in the humoral immune response in D. melanogaster 15
1.8.1 The Toll pathway 15
1.8.2 The DUOX system 17
1.8.3 The IMD pathway 19
1.8.3.1 Negative regulators of the IMD pathway 20
1.8.3.2 PGRP-LB as a key negative regulator of the IMD pathway 22
1.9 Antimicrobial peptides: key effectors of the humoral immune response 24
2. *D. melanogaster* as a model organism to study the behavior 26
2.1 Overview of the adult D. melanogaster Central Nervous System 26
2.2 Octopamine: a master molecule to modulate insect behaviors 28
2.2.1 Octopaminergic neurons in D. melanogaster 29
2.2.2 Octopamine-related behaviors in D. melanogaster 30
2.2.3 Octopamine and D. melanogaster egg-laying behavior 31
2.2.4 Neuronal circuits for egg-laying in D. melanogaster 34
2.3 Introduction to D. melanogaster Gustatory System 35
2.3.1 The gustatory organs of D. melanogaster 35
2.3.2 Taste modalities and receptors in D. melanogaster 38
2.3.3 Gustatory receptors 39

2.3.3.1 GRs expressed in GRNs for sugar detection ... 40
2.3.3.2 GRs expressed in GRNs for bitter detection ... 41
2.3.4 Ionotropic receptors related to taste ... 42
2.3.4 Taste-related pickpocket receptors ... 43
2.3.5 Transient receptor potential channels and taste ... 44
2.3.6 Overview of taste receptors and modalities in mammals ... 44
2.3.7 Sensory modulation of feeding behavior ... 46
2.3.8 Sweet bitter integration ... 49
3. Impact of bacterial infection in *D. melanogaster* nervous system and behaviors ... 51
3.1 Introduction to the concepts of sickness behavior and behavioral immune system ... 51
3.2 D. melanogaster as a model to study behavioral responses to microbes ... 52
3.3 Impact of bacterial exposure on D. melanogaster nervous system and behavior ... 53
3.3.1 Bacterial detection by D. melanogaster sensory nervous system ... 53
3.3.2 Bacteria-derived compounds can be sensed internally by D. melanogaster neurons ... 54
3.3.3 Neuronal signaling influences fly cellular immunity ... 56
3.3.4 Proteins of the canonical immune system are expressed in D. melanogaster neurons ... 56
3.5 Impact of bacterial exposure on mammal nervous system and behavior ... 58
Aims of the thesis ... 62
Results ... 63
Article 1 ... 63
Background relative to Article 2 ... 64
Article 2 ... 67
Supplementary figures Article 2 ... 68
Manuscript 3 ... 69
Conclusive remarks and future perspectives ... 70
Bibliography ... 76
Annex 1 ... 106

List of Abbreviations

AMMC: antennal mechanosensory and motor center

AMPs: antimicrobial peptides

AT2Rs: 2 angiotension II receptors

BBB: blood-brain barrier

cAMP: cyclic adenosine monophosphate

CGRP: calcitonin gene-related peptide

CNS: central nervous system

DAP: diaminopimelic acid

DCSO: dorsal cibarial sensory organ

DREDD: death related ced-3/Nedd2-like caspase

DSX: doublesex

DUOX: dual oxidase

E.c.c.: *Erwinia caratovora caratovora*

ECR: epithelial cell renewal

ENaC/DEG: epithelial sodium channel/degenerin

EVF: *Erwinia* virulence factor

FADD: FAS-associated domain

FPRs: formyl peptide receptors

FRU: fruitless

GABA: γ-aminobutyric acid

GNBP-1: Gram-negative bacteria-binding protein-1

GNPB-3: Gram-negative bacteria-binding protein-3

GPCRs: G-protein coupled receptors

GR: gustatory receptor

GRNs: gustatory receptor neurons

IAP2: inhibitor of apoptosis 2

IKK: IKβ kinase

ILC2: type 2 innate lymphoid cells

IMD: immune deficiency

IR: ionotropic receptor

IRC: immune responsive catalase

IRD5: immune response deficient 5

LPS: lipopolysaccharides

LSO: labral sensory organ

LTA: lipoteichoic acids

MBLs: mannose-binding lectins

MMP-2: matrix metalloproteinase-2

NE: norepinephrine

NF-κB: nuclear factor-κB

NLRs: NOD-like receptors

NOD: nucleotide-binding oligomerization domain

OA: octopamine

OBPs: odorant binding proteins

OANs: octopaminergic neurons

ORs: olfactory receptors

ORNs: olfactory receptors neurons

PAMPs: pathogen-associated molecular patterns

P.e.: *Pseudomonas entomophila*

PER: proboscis extension reflex

PGRPs: peptidoglycan recognition proteins

PHP: presynaptic homeostatic potentiation

PPK: pickpocket

PNS: peripheral nervous system

PRRs: pattern recognition receptors

RIPs: receptor-interacting proteins

ROS: reactive oxygen species

SEZ: subesophageal zone

sGPNs: sweet gustatory projection neurons

SP: sex peptide

SPR: sex peptide receptor

SPSNs: SPR positive sensory neurons

SPZ: Spätzle

TAK1: GF-β activated kinase 1

TβH: tyramine-β-hydroxylase

TCT: thracheal cytotoxin

TDC: tyrosine decarboxylase

TGF-β: transforming growth factor-β

TLRs: Toll-like receptors

TOR: target of rapamycin

TRCs: taste receptor cells

TRP: transient receptor potential channels

TRPA1: transient receptor potential cation channel subfamily A member 1

UDP: uridine diphosphate

VCSO: ventral cibarial sensory organ

VM: ventral midline

VNC: ventral nerve cord

WTA: wall teichoic acids

1. *Drosophila melanogaster* immune system

1. Drosophila melanogaster as a model to study the innate immune response

All animals have evolved strategies to protect themselves from pathogens. The immune system has the primary function to mount a response against invading agents, allowing the host to survive the infection. This response relies on the secretion of molecules and/or the action of specialized cells whose activity is directed against the pathogen. Two main immune branches have been described: innate and adaptative immunity. The innate immunity is based on the identification, by the host, of microbial conserved molecular patterns and allows a fast response against the pathogen. This response is conserved in metazoan, plants and fungi and, thus, considered one of the oldest evolved immune strategies. In contrast, only vertebrates evolved an adaptative immune response. The latter consists of an antigen-specific response that requires more time, generally within weeks, to be mounted. For a long time, researchers have focused on the study of adaptative immunity since it has been considered a more sophisticated and efficient defense mechanism. Conversely, innate immunity was thought to be a more rudimentary immune strategy. Nevertheless, when it was clear that innate immunity plays an active role in controlling adaptative immunity, the scientific community interest in this response increased (Janeway, 1989). Studies carried in various models, including the fruit fly *Drosophila melanogaster* (*D. melanogaster*), highlighted the importance of innate immunity in invertebrates and all animal kingdom. *D. melanogaster* is an excellent model to study the innate immune response. Indeed, its powerful genetic tools and the absence of an adaptative immunity were key to allow the identification of the molecular players of the innate immunity. Two major findings in *D. melanogaster* have been crucial to understanding the innate response: i) the characterization of the antimicrobial peptides (AMPs), the main effectors of the innate humoral response (Boman et al., 1972) ii) the identification of the Toll and the immune deficiency (IMD) pathways as the central molecular cascades controlling their production (Lemaitre et al., 1996, 1995). Notably, the identified molecular mechanisms underlying *D. melanogaster* innate immunity are highly conserved in vertebrates, supporting their ancient evolutionary origins.

1.2 Immune mechanisms in D. melanogaster

D. melanogaster relies on a great arsenal to fight invading microbes (**Figure 1**). First, the cuticle of flies constitutes a physical barrier that microbes hardly overcome. Nevertheless, cuticle damage and consequent septic injury can occur. For instance, some nematodes are able to break the fly cuticles, allowing the access of invading microbes in the hemolymph, the circulating fluid in insects (Vallet-Gely et al., 2008). Septic injury and, more generally, tissue damages lead to coagulation and melanization (Dziedziech et al., 2020; Tang, 2009). These two processes isolate the pathogen in the site of infection, preventing its spread. The diffusion of the infection in the hemolymph leads to the activation of the systemic immune response. The latter relies on the production of AMPs by mainly the fat body, homologs to the mammal liver, and specialized cells against the pathogen. In addition to septic injury, flies can be infected by ingesting contaminated food (oral infection). Indeed, flies feed on rotten fruits enriched in bacteria and fungi. In some cases, these food sources can be contaminated with pathogenic microbes. When flies are orally infected, the first line of defense is the intestine's local immune response, which includes the production of reactive oxygen species (ROS) and AMPs. In some cases, the local response is not enough to eradicate the pathogen. High microbial persistence in the gut can lead to the diffusion of bacterial components in the hemolymph and trigger the systemic immune response.

In this section, I will describe the main methods used to study immunity against bacteria in *D. melanogaster*. I will briefly introduce the different immune strategies against bacteria, focusing on the humoral immune response.

1.3 Methods to study immunity in D. melanogaster

In the laboratory, both septic injury and feeding are used to infect flies. Microbial infection effects can be studied in the short term (acute infection) or the long term (chronic infection). Usually, oral feeding is used to study both acute and chronic infections, while septic injury is mainly used to study acute infection. Also, septic injury is used to study the systemic effect of microbial infection, while oral infection is used to study both local and systemic effects. Distinct bacterial species are used to induce an immune response in flies. *Erwinia caratovora caratovora* (*E.c.c.*) is a naturally occurring opportunist pathogen widely used to study *D. melanogaster* immunity.Indeed, *E.c.c.* oral infection induces both the local and the systemic immune response without killing the animal (Basset et al., 2000). In nature, this bacterium is a phytopathogen that uses the fly as a vector of transmission.

Another bacterium used to infect flies is *Pseudomonas entomophila* (*P.e.*). This bacterium is highly pathogenic and perturbs host intestinal epithelial integrity after feeding. *P.e.* induces the local and, as a consequence of the rupture of the gut epithelia, the systemic immune response (Vodovar et al., 2005). *Serratia marcescens* (*S.m.*) is also highly pathogenic and septic injury with this bacterium kills the host within hours (Nehme et al., 2007). This bacteria is a good inducer of the local immune response, and systemic response to this bacterium is mainly based on phagocytic cells in the hemolymph (Bangham et al., 2006; Kocks et al., 2005). Thus, based on the bacterium and/or type of infection used in the laboratory, it is possible to study different aspects of the immune response.

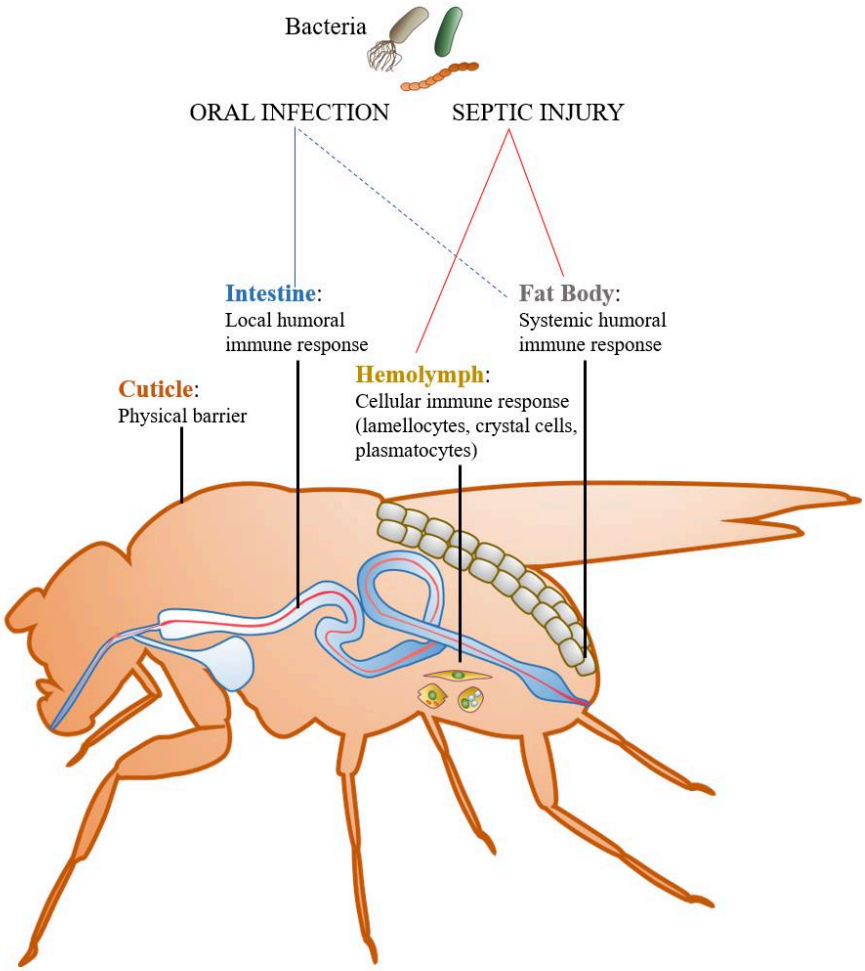

Figure 1. *D. melanogaster* strategies to overcome bacterial infection. The cuticle is a physical barrier that protects the fly from bacteria in the environment. Oral infection leads to the activation of the local immune response in the intestine. Bacterial persistence in the host gut can cause the passage of bacteria-derived molecules in the hemolymph and activation of the systemic humoral response in the fat body. Septic injury triggers the cellular immune response's activation and the systemic humoral response in the fat body.

1.4 Cellular immune response in D. melanogaster

The cellular immune response is mediated by specialized blood cells which function is to eradicate the pathogen or produce molecules against it directly. This response in *D. melanogaster* is mediated by three blood cell (hemocyte) types: plasmatocytes, lamellocytes and cristal cells (CCs) (**Figure 2**). Hematopoiesis, the process that leads to mature hemocyte production, occurs in two waves. The first takes place in the embryonic head mesoderm and causes the release of circulating mature hemocytes that are functional in larvae, in case of infection. The second occurs in the lymph gland, the major hematopoietic organ in larvae, and leads to the maturation of hematopoietic cells which will be circulating in the hemolymph of adult flies.

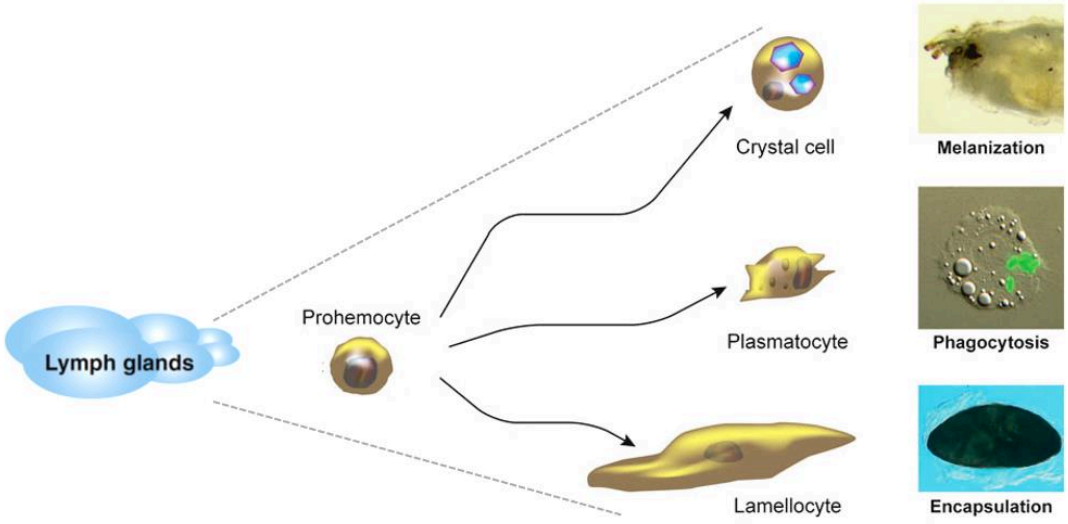

Figure 2. Cellular immunity in *D. melanogaster*. The lymph gland is the major hemopoietic organ in *D. melanogaster* larvae. Here the differentiation of mature hemocytes (crystal cells, plasmatocytes, lamellocytes) occurs. Mature hemocytes mediated different cellular immune responses: melanization (crystal cells), phagocytosis (plasmatocytes) and encapsulation (lamellocytes). Figure adapted from (Lemaitre and Hoffmann, 2007).

Plasmatocytes represent 90-95% of the mature hemocytes (Lemaitre and Hoffmann, 2007). These hemocytes phagocyte microbes or other types of molecules such as viral double-stranded RNA. Phagocytosis is started by the recognition of the pathogen by membrane receptors, such as Eater, Dscam and PeptidoGlycan Recognition Proteins (PGRPs). Importantly, plasmatocytes express AMPs after septic injury, contributing to the humoral immune response (Reichhart et al., 1992). Lamellocytes are involved in the encapsulation and their differentiation is inducible under determined

condition. Encapsulation consists in the formation of a multi-layered capsule around an invading agent. Generally, encapsulation is directed against microbes or bodies that can not be phagocyted. This process is used for instance to isolate eggs injected by parasitoid wasps in the larva hemocoel. Once encapsulated, the egg is destroyed by the release of toxic molecules such as ROS (Lemaitre and Hoffmann, 2007). CCs are a minor hemocyte population (around 5%) and are implicated in the melanization. The latter occurs when there is an injury and thus tissue damage. The phenoloxidase cascade-dependent biosynthesis of melanin is mediated by CCs and leads to the formation of a dark spot at the level of the damage. Melanin deposits prevent the dispersion of microbes from the wound site, preventing their entry in the host circulation (Tang, 2009).

1.5 The humoral immune response in D. melanogaster

The humoral immune response is based on microbicidal molecules' release, such as AMPs, in the extracellular space. These molecules can act locally or be released in the hemolymph, mounting a systemic immune response. Since the gut is one of the major entry points for pathogenic microbes, it is also the primary tissue where the local immune response takes place. Other tissues can also be involved in the AMPs production like salivary and labellar glands, Malpighian tubules, trachea, and reproductive tract (Ferrandon et al., 2007). In the gut, both ROS production and the IMD pathway-dependent AMP production are required to locally fight the infection (Kuraishi et al., 2013). These two mechanisms are molecularly independent. In addition to their role during the infection, both ROS production and the IMD pathway have physiological functions. Indeed, they are implicated in intestinal epithelial cell renewal (ECR) and in shaping the gut microbiome. Also, the Janus Kinase (JAK)/ signal transducers and activators of transcription (STAT) pathway is implicated in both humoral and cellular immune response (Agaisse and Perrimon, 2004). In the gut, this cascade contributes to the pathogen-induced ECR and, partially, to the AMP production (Buchon et al., 2009). The systemic humoral immune response is mediated mainly by the fat body cells. These cells can sense circulating bacterial components and secrete AMPs in response to bacterial infection. As mentioned before, also phagocytes contribute to AMP production.

In D. melanogaster, two are the major cascades implicated in the systemic humoral response: the IMD and the Toll pathway. Here below, I describe the main molecular actors, from the elicitors to the effectors, involved in the humoral immune response.

1.6 Bacterial peptidoglycan: a key elicitor of the humoral immunity in D. melanogaster

Activation of the innate immune system requires recognition by pattern recognition receptors (PRRs) of pathogen-associated molecular patterns (PAMPs). In general, PAMPs are highly conserved molecules that have a vital role for the microbe. For instance, components of the bacterial cell wall such as peptidoglycan (PGN), lipopolysaccharides (LPS) and, lipoteichoic acids (LTA) are classical PAMPs. Other examples are the fungal cell wall component β-1,3-glucan or virus-derived RNA or DNA molecules (Lemaitre and Hoffmann, 2007). Moreover, specific molecules secreted by microbes activate the immune response in the host. An example is uracil, which is produced by pathogenic but not, or in little doses, by symbiotic bacteria and triggers ROS production in the gut (see *Paragraph 1.8.2*).

PGN is the unique bacterial elicitor so far known for activating the IMD and Toll pathways in *D. melanogaster*. Furthermore, the Toll pathway can be activated by fungal β-1,3-glucan and fungal proteases (Gottar et al., 2006; Kim et al., 2000). Notably, LPS which is a renowned immune elicitor in vertebrates and invertebrates does not activate the humoral immune response in *D. melanogaster* (Kaneko et al., 2004; Leulier et al., 2003). Nevertheless, LPS detection in flies leads to aversive behaviors (Soldano et al., 2016; Yanagawa et al., 2019).

1.6.1 Peptidoglycan structure

The PGN is a component of almost all bacterial cell walls. Polymeric PGN maintains the cell wall structure and gives resistance to osmotic pressure (Irazoki et al., 2019). It also functions as a scaffold for anchoring other cell wall components such as teichoic acids (Neuhaus and Baddiley, 2003). Moreover, PGN is released as a signal for bacterial communication (Cloud-Hansen et al., 2006). The PGN monomer consists of a disaccharide and four amino acids. Among different bacterial species, slight differences in the composition of the monomeric PGN can be found. The PGN disaccharide is constituted by β-1,4-linked N-acetylglucosamine (GlcNAc) and N-acetylmuramic acid (MurNAc). The four amino acids, which differ among bacteria, are linked to the MurNAc (Schleifer and Kandler, 1972). Based on this aminoacidic component, two main types of PGN have been described: the diaminopimelic acid (DAP)-type PGN, and the lysine (Lys)-type PGN characteristic of Gram-negative and Gram-positive bacteria, respectively. The DAP-type PGN consists of L-alanine, D-glutamate, meso-DAP, and D-alanine. In the Lys-type PGN, the DAP residue is substituted by L-lysin. In the cell wall, the PGN forms polymers cross-linked directly or by short peptides. Generally,

the DAP-type PGN monomers are directly cross-linked, whereas the Lys-type PGN monomers are linked by variable short peptides (**Figure 3A** and **3B**).

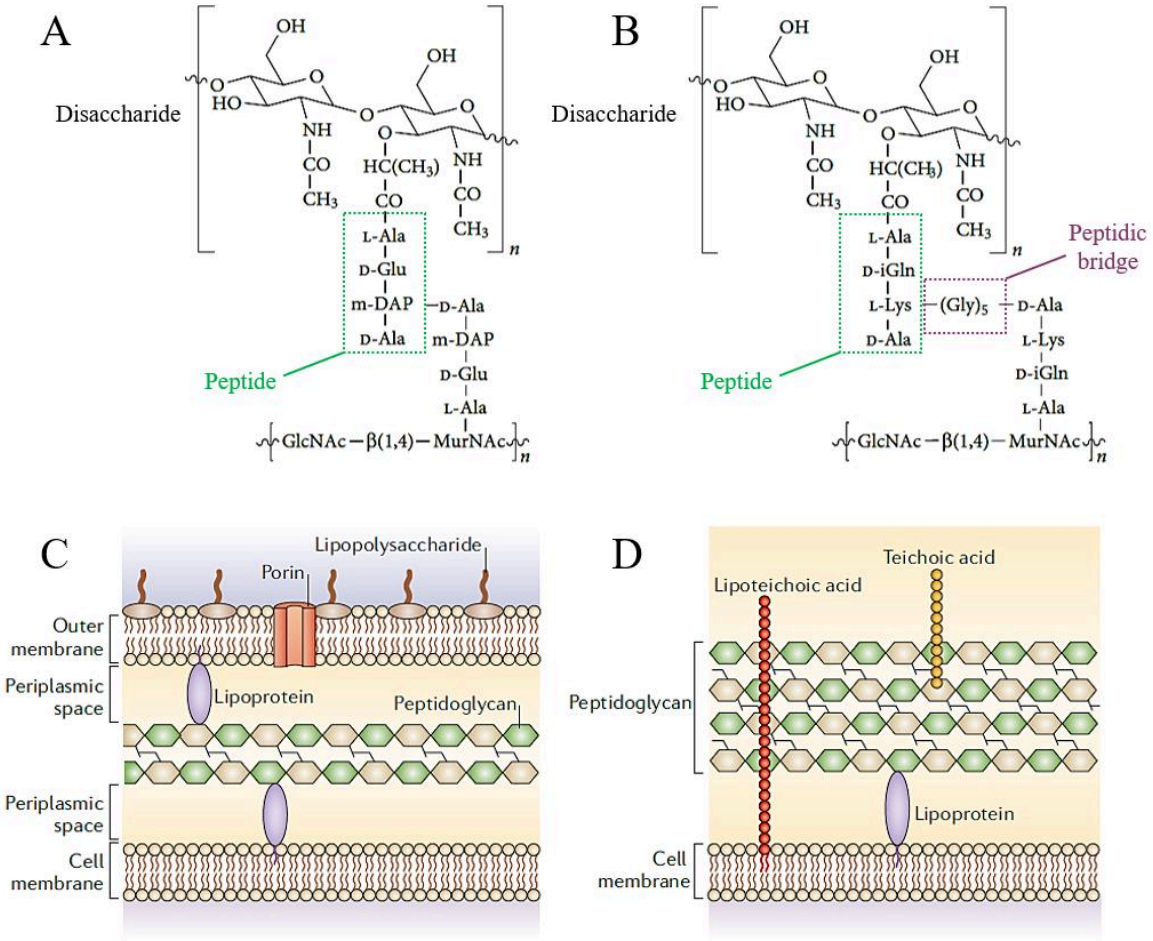

Figure 3. Peptidoglycan and bacterial cell wall. A Schematic of DAP-type peptidoglycan. PGN monomers are directly cross-linked. **B** Schematic of Lys-type peptidoglycan. Pepdic bridges link PGN monomers. **C** Gram-negative bacteria cell wall. Polymeric peptidoglycan forms a thin layer in the periplasmic space. Outer membrane and lipopolysaccharide cover the PGN. Other bacterial cell wall components are shown (i.e. porins and lipoproteins) **D** Gram-positive bacteria cell wall. Polymeric peptidoglycan forms a thick multilayer structure outside the outer membrane. Peptidoglycan functions as a scaffold for other structural molecules, such as lipoteichoic acid and teichoic acid. Figures from (Brown et al., 2015; Julien Royet and Dziarski, 2007).

As mentioned before, the DAP-type PGN is typical of Gram-negative bacteria and some Gram-positive species (i.e. *Bacillus sp.*). In these bacteria, the PGN polymers form a thin layer in the periplasmic space between the cell membrane and the outer membrane. The Gram-negative PGN is not directly exposed to the external environment but is covered by the outer membrane and the

lipopolysaccharides. Unlike the DAP-type PGN, the Lys-type PGN of Gram-positive bacteria forms a multilayer thick structure that is anchored to the cell membrane and is directly exposed to the external environment (**Figure 3C** and **3D**).

1.6.2 Release of soluble peptidoglycan fragments

The detection of circulating PGN plays a key role in the activation of the immune response. Bacterial growth and division lead to the release of PGN in the environment. The PGN turnover refers to the excision of PGN from the wall by specific enzymes during bacterial growth. It is estimated that in only one generation, around 50% of *Escherichia coli* (*E.coli*) PGN is disassembled from the wall as anhydromuropeptides (Doyle et al., 1988). Importantly, most of this released PGN (around 95 %) is reused via the PGN recycling pathway (Park and Uehara, 2008). This recycling process is energetically advantageous and reduces the amount of circulating PGN, which can activate the host immune system. The amount of PGN released by a bacterium is species-specific. For instance, the PGN turnover is higher in Gram-negative than in Gram-positive bacteria, with around 40–70% of PGN released as soluble fragments (Hasegawa et al., 2006). Soluble PGN fragments can be monomers, oligomers, or polymers and are differentially detected by the immune system. For instance, monomeric DAP-type PGN, also known as tracheal cytotoxin (TCT), is the minimal PGN module that induces the IMD pathway in *D. melanogaster* (Kaneko et al., 2006; Stenbak et al., 2004). Since TCT is released during cell growth and cell division, it might be perceived by the host as a signal of proliferating bacteria (Gendrin et al., 2009; Zaidman-Rémy et al., 2006).

PGN turnover requires the activity of different PGN cleaving enzymes. These proteins based on the cleavage site are divided into glycosidases (which cleave glycosidic bonds), amidases (which cleave between the amino acidic and the glycosidic components), and peptidases (which cleave amino acidic bounds) (Irazoki et al., 2019). Furthermore, some host enzymes can also cleave the PGN. The function of these enzymes is: i) to disrupt cell wall integrity (e.g. lysozyme) ii) to cleave the PGN in non-immunogenic fragments (e.g. PGRPs).

In the next session, I will present the PRRs used by *D. melanogaster* to detect the PGN.

1.7 Peptidoglycan recognition proteins in D. melanogaster

In *D. melanogaster*, the bacterial-derived PGN is detected by proteins of the PGRP family (Charroux et al., 2009; Julien Royet and Dziarski, 2007). PGRPs play an essential role in both humoral and cellular immunity and they act upstream the IMD and the Toll pathways. In flies, there are 13 genes encoding PGRPs and 19 peptides (Werner et al., 2000) (**Figure 4**). This protein family is widely spread in the animal kingdom, but not in basal metazoan (e.g. nematodes). Mammals have four PGRPs (i.e. PGLYRP-1–4; see *Paragraph 1.7.3*) (Liu et al., 2001). Unlike fly PGRPs, mammal PGRPs have a bactericidal function and they likely act to disrupt cell wall integrity. Instead, *D. melanogaster* PGRPs function as PGN sensors or amidases. Fly PGRPs are divided into short (S) and long (L) based on their transcripts' size. All PGRPs are characterized by at least one PGRP domain, homologous to the bacteriophage and bacterial type 2 amidases. Short PGRPs are peptides of around 200 amino acids and are characterized by an N-terminal signal peptide and a single C-terminal PGRP domain (Julien Royet and Dziarski, 2007).

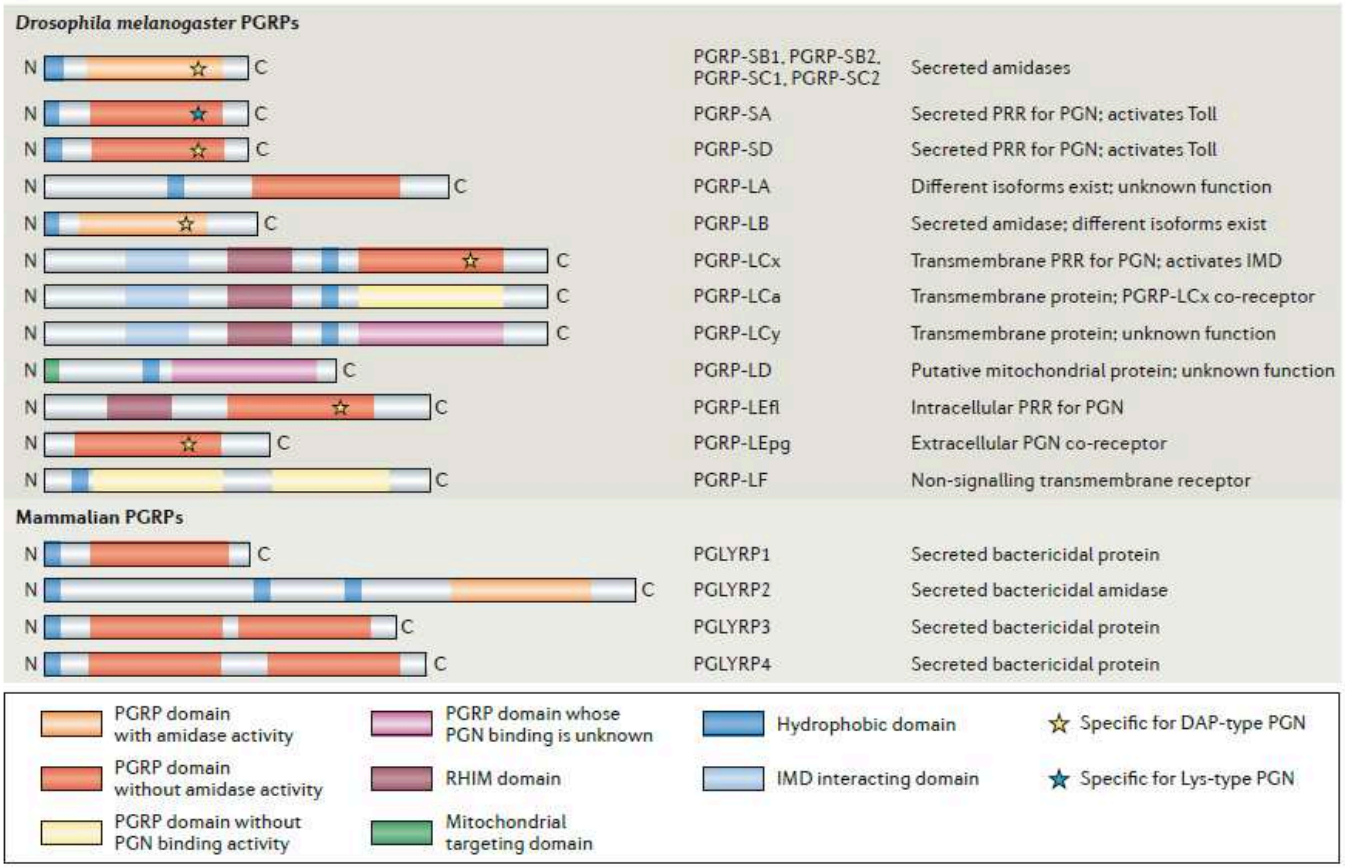

Figure 4. PGRPs in *D. melanogaster* and mammals. In the figure are shown the structure and the function of PGRPs. Figure adapted from (Royet et al., 2011).

PGRPs can be transmembrane (e.g. PGRP-LC), cytoplasmatic (e.g. PGRP-LE), or secreted (e.g. PGRP-LB). While some of these proteins are receptors for the PGN and trigger immune cascades' activation, others act as amidase and cleave the PGN in non-immunogenic fragments. Only one fly PGRP has been shown to have bactericidal activity in *in vitro* experiments. In particular, PGRP-SB1 has a bactericidal activity specifically against the bacterium *Bacillus megaterium* (Mellroth and Steiner, 2006).

Almost all PGRPs bind specifically the PGN and recognize both the disaccharide and the amino acid chain of this molecule. These proteins can recognize monomeric or/and polymeric PGN. Furthermore, PGRPs bind with different affinity DAP- and Lys-type PGN.

1.7.1 PGRPs as upstream receptors of the humoral immunity

Some *D. melanogaster* PGRPs functions as PRRs upstream of the Toll and the IMD pathways. PGRPs affinity for DAP- or Lys-type PGN leads to preferential activation of one pathway or the other one. Recognition of DAP-type PGN preferentially triggers the IMD pathway, whereas Lys-type PGN detection leads to Toll pathway activation. In 2001, Michel and collaborators demonstrated for the first time that *D. melanogaster* PGRPs function as PRRs and activators of the immune response. They showed that fly mutants for the secreted PGRP-SA are unable to activate the Toll pathway after Gram-positive bacteria infection and are hence more susceptible to this type of infection (Michel et al., 2001). Successive works have shown that PGRP-SA, PGRP-SD, and the Gram-negative bacteria-binding protein-1 (GNBP-1) cooperate in the recognition of the Lys-type PGN (Gobert et al., 2003; Park et al., 2007; Wang et al., 2008) and preferentially activate the Toll cascade in fat body cells. The recognition of fungal β-1,3-glucan, by the Gram-negative bacteria-binding protein-3 (GNBP-3) also activates this pathway (Gottar et al., 2006).

Two other PGRPs, i.e. PGRP-LC and PGRP-LE, have been shown to preferentially recognize DAP-type PGN and activate the IMD cascade (Bosco-Drayon et al., 2012; Choe, 2002; Kaneko et al., 2006; Leulier et al., 2003; Neyen et al., 2012; Takehana et al., 2004). PGRP-LC is the major DAP-type PGN receptor in the fat body and thus is mainly implicated in the systemic humoral response. Moreover, PGRP-LC cooperates with PGRP-LE to activate the local immune response in some zones of the intestine, such as the proventriculus and the ventriculus. On the other hand, PGRP-LE functions in the ventriculus, the intestinal Copper cells, and posterior midgut to detect PGN (**Figure 5**). Thus, PGRP-LE mainly mediates the activation of the local immune response (Royet and Charroux, 2013).

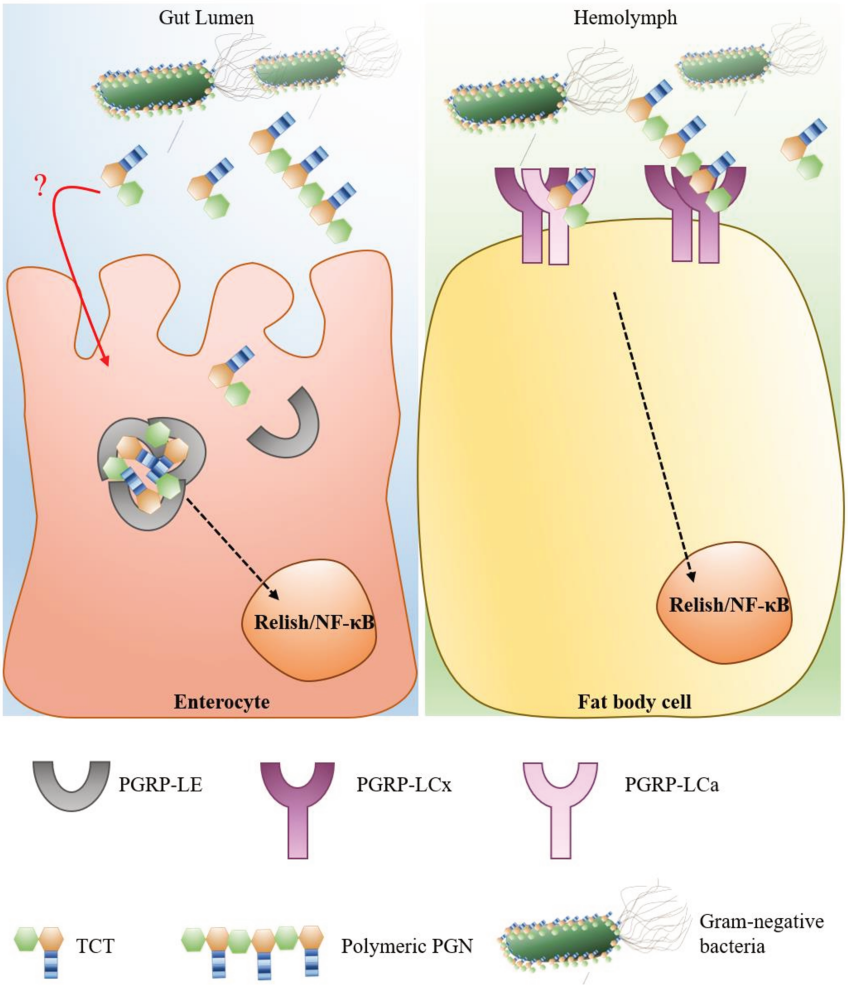

Figure 5. Detection of DAP-type PGN. Left In the gut, PGN detection is mainly mediated by the intracellular receptor PGRP-LE. Monomeric DAP-type PGN (TCT) enters the enterocyte via an unknown mechanism(s) and, in the cytoplasm, it is recognized by PGRP-LE. This recognition leads to oligomer formation. **Right** In the hemolymph, PGN is detected by PGRP-LC. While PGRP-LCx homodimers recognize polymeric PGN, PGRP-LCa-PGRP-LCx heterodimers recognize TCT. PGN detection triggers in all the case activation of the IMD/NF-κB pathway.

PGRP-LC is a transmembrane receptor and recognizes both polymeric and monomeric PGN. There are three PGRP-LC isoforms (PGRP-LCx, PGRP-LCa, and PGRP-LCy) which can form homodimers or heterodimers. PGRP-LCx homodimers recognize polymeric PGN, whereas heterodimers formed by PGRP-LCx and PGRP-LCa detect monomeric PGN (TCT) (Chang et al., 2006). PGRP-LE, similarly to mammals NOD-1 and NOD-2 receptors, is an intracellular receptor and detects TCT (Kaneko et al., 2006). Cytoplasmatic TCT leads to the formation of PGRP-LE oligomers and activation of the IMD pathway (Lim et al., 2006). How TCT is delivered inside the cell is still unclear. Works in mammals have shown that the transporters SLC5 are involved in the cytoplasmic delivery

of PGN (Charrière et al., 2010; Nakamura et al., 2014). However, other studies have shown that this family of transporters does not have the same role in flies (Capo et al., 2017; Paik et al., 2017). An RNAi screening by Paik and colleagues identified a transporter of the SLC46 family as a candidate PGN transporter in flies. Indeed, knockdown of this transporter leads to the decrease of IMD pathway activation in *in vitro* experiments, using S2 cells. Possibly this decreased response is due to reduced delivery of TCT in the cytoplasm of these cells. Importantly, knockdown of the mammal homolog transporter in human epithelial cells leads to a similar result. However, the cytoplasmic PGN delivery probably does not depend on a single class of transporters. Instead, different mechanisms, such as endocytosis or bacterial secretion system, might be involved.

Additionally, both PGRP-LC and PGRP-LE are implicated in the cellular immune response. For instance, PGRP-LE triggers the autophagy pathway following the detection of *Listeria monocytogenes* in the intracellular space (Yano et al., 2008). Moreover, PGRP-LE is also implicated in the activation of the prophenoloxidase cascade (Takehana et al., 2002). PGRP-LC and PGRP-SC1 are involved in the activation of the phagocytosis in the presence of *E.coli* and *Staphylococcus aureus*, respectively (Garver et al., 2006; Rämet et al., 2002). Notably, the fact that these PGRPs are involved in recognizing entire bacteria suggests that PGRPs can detect both soluble PGN fragments and bacterial cell wall PGN.

1.7.2 PGRPs as regulators of the immune response

Some PGPRs are modulators of the immune response. Indeed, these PGRPs have amidase activity and cleave the PGN in non-immunogenic fragments. In particular, they cleave the bond between the MurNAc and the L-alanine of PGN monomers (**Figure 6**) (Julien Royet and Dziarski, 2007). These amidase function as upstream negative regulators of the immune response. Indeed, by decreasing the amount of circulating PGN, these PGRPs prevent its binding to PGRP receptors. There are six catalytic PGRPs with regulatory function: PGRP-SC1A, PGRP-SC1B, PGRP-SC2, PGRP-LB, PGRP-SB1, and PGRP-SB2. Apart from some PGRP-LB isoforms (see *Paragraph 1.8.3.2*), the other regulatory PGRPs are secreted. Importantly, these PGRPs not only modulate the immune response upon infection but also contribute to the development of immune tolerance related to gut commensal bacteria. Among the regulatory PGRPs, PGRP-LB is a master negative regulator of both systemic and local immune response (see *Paragraph 1.8.3.2*) (Paredes et al., 2011; Zaidman-Rémy et al., 2006). PGRP-SC is mainly implicated in the modulation of the systemic immune response, while no clear function has been attributed to PGRP-SB. Indeed, even though this protein is upregulated upon infection, no increased immune response is observed in *PGRP-SB* mutants after oral or septic injury

(Paredes et al., 2011). Other PGRPs act as regulators by directly interacting with PGRP-LC. For instance, PGRP-LF by forming heterodimers with PGRP-LC prevents IMD pathway activation (Basbous et al., 2011). Also, a PGRP-LC isoform generated by alternative splicing has a regulatory function (i.e. rPGRP-LC). rPGRP-LC has a different cytosolic domain compared to the other PGRP-LC isoforms and is recruitment in the presence of polymeric PGN to prevent IMD pathway activation (Neyen et al., 2016). Notably, negative regulators are necessary to prevent exacerbated activation of the immune response. The lack of these regulators and the IMD pathway's overactivation have deleterious effects for the animal (see *Paragraph 1.8.3.1*). Furthermore, some PGRPs can positively regulate the activation of the immune response. A secreted isoform of PGRP-LE has been proposed to facilitate PGN recognition by PGRP-LC (Kaneko et al., 2006). Another PGRP, PGRP-SD, presents the PGN to PGRP-LC in the cell surface, enhancing IMD pathway activation (Iatsenko et al., 2016). Thus, PGRPs not only activate the humoral immune response but also finely modulate this response.

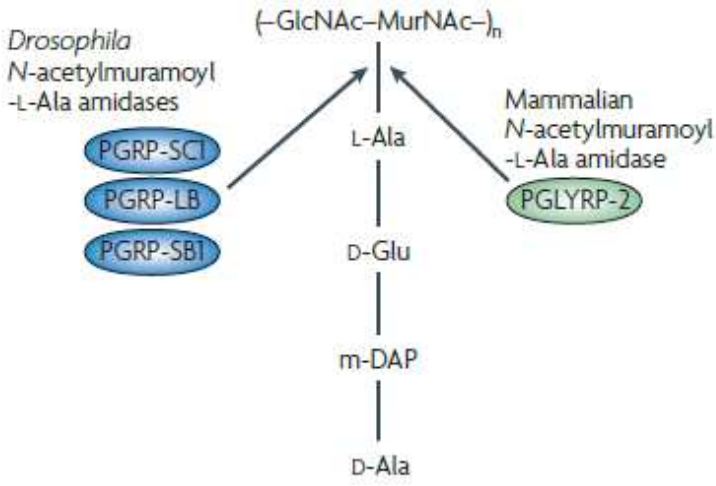

Figure 6. PGRP amidases in *D. melanogaster* and mammals. PGRP amidases cleave the bond between the MurNAc and the L-alanine of PGN monomers. The resulting fragments are non-immunogenic. In mammals, only PGLYRP-2 has been proposed to act as amidase. Figure adapted from (Julien Royet and Dziarski, 2007).

1.7.3 Peptidoglycan sensors in mammals

Mammals also have PGRPs to detect bacterial PGN. There are four secreted proteins in mammals (PGLYRP1-4). As mentioned before, the major difference with *D. melanogaster* PGRPs is that mammals PGLYRPs have a bactericidal function. PGLYRP-1 acts against both Gram-negative and

Gram-positive bacteria and it is expressed mainly in polymorphonuclear leukocytes (Tydell et al., 2006, 2002). PGLYRP-3 and PGLYRP-4 also have a bactericidal function, but they are mostly expressed in mucosal surfaces (Lu et al., 2006). These proteins probably act by recognizing the PGN in the cell wall and by perturbing its structural integrity. Moreover, it has been proposed that these proteins, by recognizing the PGN, facilitate phagocytosis (Dziarski et al., 2003). PGLYRP-2 is expressed in the liver and is thought to act as amidase (Wang et al., 2003). As *D. melanogaster* PGRP amidases, PGLYRP-2 might function as a negative regulator by sequestering circulating PGN.

In contrast to *D. melanogaster*, also other PGN sensors have been identified in mammals (**Figure 7**). Nucleotide-binding oligomerization domain (NOD) like receptors (NLRs) sense intracellular PGN. Many studies have focused on two of these receptors, i.e. NOD-1 and NOD-2. These receptors are expressed in different tissue types, with NOD-1 broadly expressed, while NOD-2 is mainly expressed in immune cells such as monocytes, macrophages and dendritic cells (Strober et al., 2006). NOD-1 recognizes the dipeptide D-Glu-mDAP typical of DAP-type PGN (Chamaillard et al., 2003; Girardin et al., 2003). NOD-2 recognizes the muramyl dipeptide (MDP), i.e. the MurNAc-D-Ala-D-Glu module, typical of both DAP- and Lys-type PGN (Inohara et al., 2003). PGN detection by NOD receptors leads to the activation of the nuclear factor-κB (NF-κB) pathway and inflammatory response (Caruso et al., 2014). Notably, mutations in NOD-2 gene sequence have been associated with pro-inflammatory diseases such as Crohn's disease and Blau syndrome (Hugot et al., 2001; Miceli-Richard et al., 2001; Ogura et al., 2001). As for PGRP-LE, PGN detection by NOD receptors implies its transport in the cytoplasm. SLC15 transporter family facilitates the transport of PGN in the cytoplasm and, consequentially, its NOD-2-mediated detection (Charrière et al., 2010; Nakamura et al., 2014). Also for mammals, different mechanisms have been proposed for cytosolic PGN delivery, including the bacteria secretion systems, endocytosis, and/or membrane transporters (Wolf and Underhill, 2018).

Among the mammals Toll-like receptors (TLRs), it has been proposed that TLR-2 recognizes distinct bacterial components, including the PGN (Dziarski and Gupta, 2005). Also, the receptor CD14 sense circulating PGN (Dziarski et al., 1998; Gupta et al., 1996). Both CD14 and TLR2 are membrane receptors expressed in different types of immune cells. Bacterial detection by these receptors leads to the secretion of pro-inflammatory cytokines. Hexokinase is a metabolic enzyme associated with the mitochondrial outer membrane. Wolf and collaborators showed that this enzyme is a sensor for PGN-derived GlcNAc and that this recognition triggers the release of hexokinase in the cytoplasm and inflammasome formation (Wolf et al., 2016).

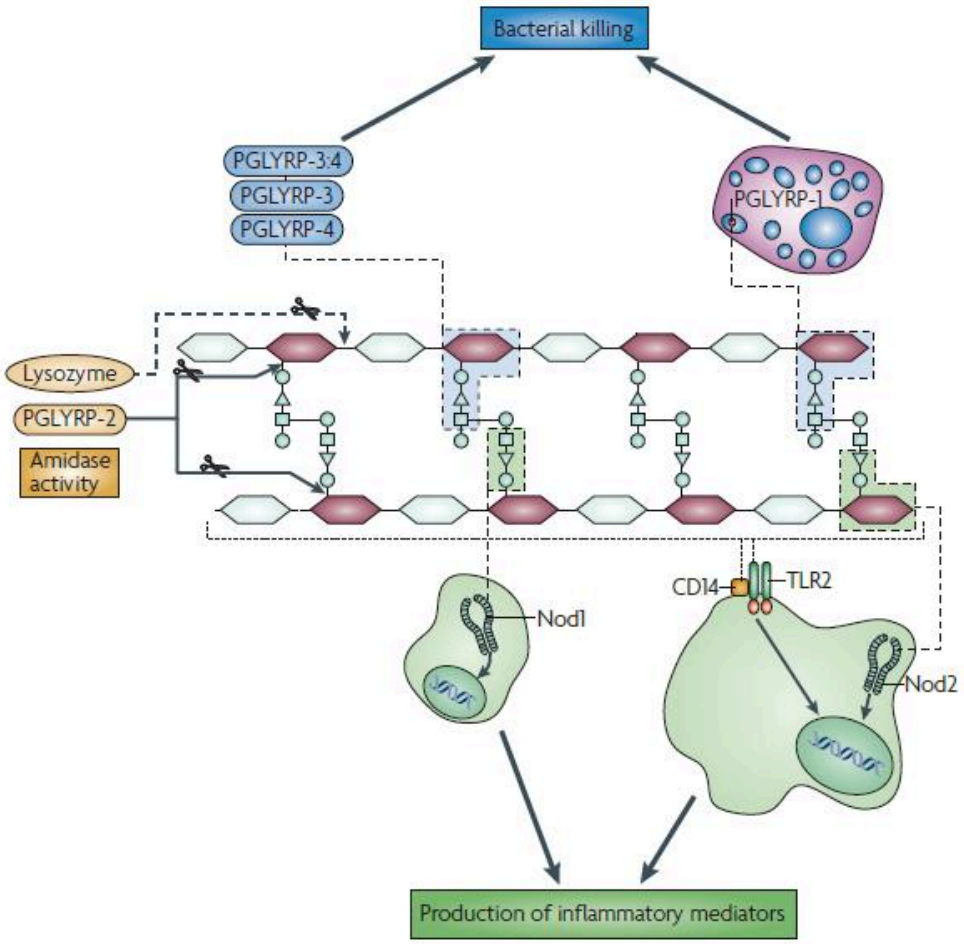

Figure 7. PGN recognition proteins in mammals. Secreted PGLYRP-1, PGLYRP-3, and PGLYRP-4 act as homo- or heterodimers and have microbicidal activity. Intracellular receptors NOD-1 and NOD-2 recognize PGN leading to the activation of the NF-κB pathway and inflammatory response. The membrane TLR-2 and CD14 also have been proposed to acts as PGN sensors. Lysozyme and PGLYRP-2 cleve the PGN in the indicated positions. Figure adapted from (Julien Royet and Dziarski, 2007).

1.8 Major cascades involved in the humoral immune response in D. melanogaster

1.8.1 The Toll pathway

At first, the Toll pathway was identified for its role in *D. melanogaster* embryo development (Anderson et al., 1985a, 1985b). One decade later, in a pioneering study of Lemaitre *et al.*, this cascade was found to be fundamental for the resistance to pathogenic fungi and the induction of the AMP drosomycin (Lemaitre et al., 1996). A few years later, it was shown that mammal TLRs have a similar function in the induction of the humoral response (Poltorak, 1998).

D. melanogaster Toll pathway resembles the mammal interleukin-1 and Toll-like receptors cascades. In contrast to mammal TLRs, *D. melanogaster* Toll receptors do not function as PRRs. Indeed, these

receptors do not directly recognize bacteria or bacterial components. Toll proteins are instead activated by NGF-like ligand of the Spätzle (Spz) family (**Figure 8**).

The Toll pathway is preferentially activated by fungal proteases, β-1,3-glucan and Lys-type PGN (Gram-positive bacteria). Activation of PRRs (PGRP-SA, PGRP-SD GNBP-1) by ad hoc ligands triggers the cleavage of Pro-Spz to its active form. Activated Spz binds Toll at the membrane, leading to its dimerization and the activation of the cascade (Jang et al., 2006; Weber et al., 2003). This activation requires the recruitment of a complex constituted by dMyd88, Tube, and Pelle (Sun et al., 2004, 2002; Tauszig-Delamasure et al., 2002; Towb et al., 1998). The activated complex leads to the phosphorylation and degradation of Cactus, an inhibitor of the transcriptor factor Dif (Belvin et al., 1995).

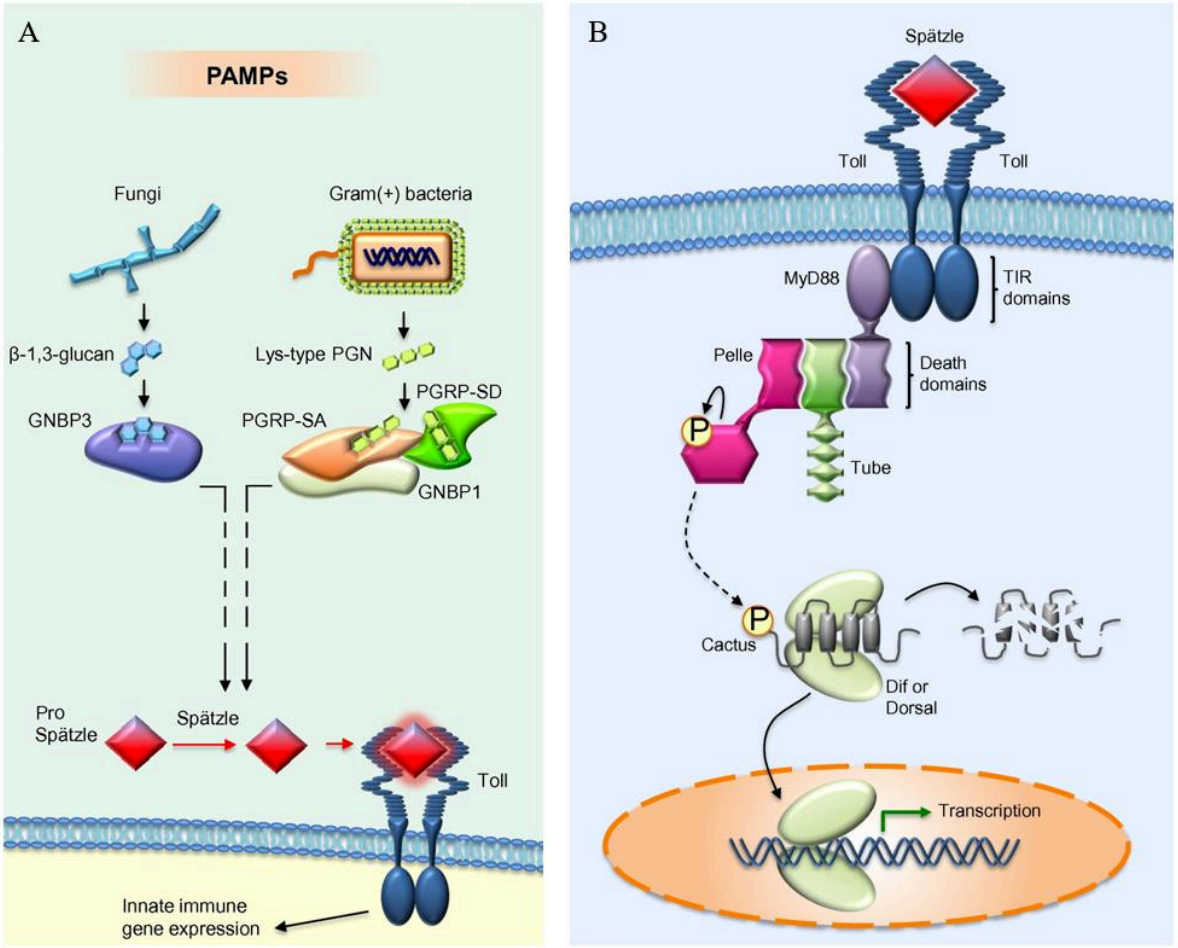

Figure 8. PAMP-mediated activation of the Toll pathway in *D. melanogaster*. A pathogen-associated molecular patterns (PAMPs) are detected in the hemolymph by pattern recognition receptors (i.e. GNBP-3; PGRP-SA, PGRP-SD and GNBP-1). This recognition triggers the cleavage of pro-spätzle. Activated spätzle binds Toll and activates the cascade. **B** Spätzle-Toll interaction triggers the activation of the MyD88/ Pelle/Tube complex and thus Cactus degradation. Dorsal and/or Dif translocate in the nucleus and activate immune gene expression. Figures adapted from (Lindsay and Wasserman, 2014).

Dif is one of the three NF-κB receptors present in *D. melanogaster*. The other two are Dorsal, downstream the same pathway, and Relish, downstream the IMD pathway. In larvae, both Dorsal and Dif control AMP expression, whereas only Dif regulates AMP production in adults (Manfruelli et al., 1999; Meng et al., 1999).

The Toll pathway is part of the systemic humoral immune response and it is induced only when its elicitors are present in the hemolymph. So far, this pathway does not seem to play any crucial role in the local immune response activation. Instead, two other cascades are essential for local immunity: the dual oxidase (DUOX)-associated ROS production and the IMD pathway.

1.8.2 The DUOX system

One of the most conserved weapons against bacterial infection is the production of ROS. In *D. melanogaster*, the release of these toxic molecules in the intestine lumen leads to bacteria killing. In the fly gut, ROS production is mediated by gut nicotinamide adenine dinucleotide phosphate (NADPH) DUOX. The DUOX complex comprises an extracellular peroxidase homology domain, an EF-hand domain, a transmembrane domain, a FAD-binding domain and a NADPH oxidase domain. The latter produces and releases H_2O_2 in the extracellular space. In the presence of Cl^-, H_2O_2 is converted into HOCl by the peroxidase homology domain. This process leads to the generation of toxic O_2^-. Moreover, the produced HOCl contributes to the response against the pathogen. Indeed, HOCl is sensed via the transient receptor potential cation channel, subfamily A, member 1 (TRPA1) in enteroendocrine cells, leading to an increase in defecation rate and thus, pathogens clearance (Du et al., 2016). The activity of DUOX is crucial for the host to limit bacterial proliferation and resist bacterial infection. Indeed, knockdown of DUOX in the gut epithelia leads to increased mortality in flies infected with *E.c.c.15*, due to a major bacterial persistence. In these animals, bacterial proliferation is associated with decreased ROS production (Ha et al., 2005a). DUOX activity is inducible upon infection and its molecular trigger is the bacterial uracil (Lee et al., 2013). The detection of this nucleobase leads to the activation of the Hedgehog signaling in the host epithelial cells, endosome formation and, consequentially, DUOX activation (Lee et al., 2015). Symbiotic bacteria do not produce uracil, whereas pathogenic bacteria such as *E.c.c.15* produce uracil and induce DUOX activity. A basal level of DUOX activity is caused by the release of a low amount of uracil by pathobiontic bacteria, such as *Lactobacillus brevis* or *Gluconobacter morbifer*. Perturbation of the microbiota can lead to increased uracil production by these bacteria, which become pathogenic (**Figure 9**). Conversely, *E.c.c.* unable to produce uracil, do not activate the DUOX system, and are therefore more pathogenic for the fly. Chronic DUOX activation is detrimental for the host since it

leads to loss of gut integrity. Since ROS also induce damages in the host cells, negative regulators are fundamental to prevent ROS accumulation. One of these is the immune responsive catalase (IRC) which eliminates H_2O_2 molecules (Ha et al., 2005b). Moreover, both DUOX activity and expression are finely regulated (Ha et al., 2009b, 2009a). Besides the principal role in the local immune response, DUOX system has been implicated in the maintenance of gut integrity, stem cell proliferation and activation of signal transduction (Lee and Kim, 2014).

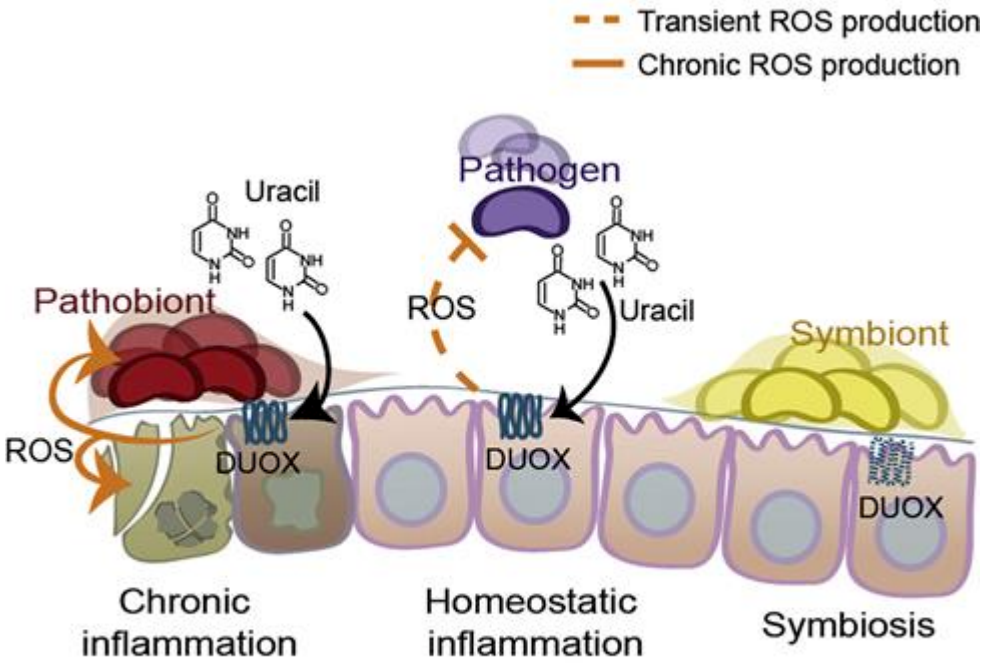

Figure 9. ROS production in *D. melanogaster* intestine. Bacterial-produced uracil triggers the activation of dual oxidase (DUOX) and the production of reactive oxygen species (ROS) in the gut. Transient ROS production is essential for intestinal epithelial maintenance, shaping the gut community and efficient pathogen clearance (homeostatic inflammation). In contrast, chronic ROS production is deleterious and leads to tissue damage. Figure from (Lee et al., 2013).

1.8.3 The IMD pathway

The IMD pathway plays a crucial role in the production of AMPs in response to Gram-negative bacteria. This cascade is involved in both local and systemic immune responses. Many components of this pathway are similar to members of the Tumor Necrosis Factor cascade pathway of mammals. The first identified member of this cascade was the death domain protein IMD. Indeed, a mutation in *imd* resulted in a defect in AMPs production upon microbial challenge (Lemaitre et al., 1995). The activation of this pathway depends on an intracellular receptor (PGRP-LE) and/or a transmembrane receptor (PGRP-LC) (see *Paragraph 1.7.1*) (**Figure 10**). The sensing of DAP-type PGN by one of these receptors leads to the interaction with the death domain protein IMD, a homolog of mammalian receptor-interacting proteins (RIPs) (Georgel et al., 2001). Activated IMD triggers two different processes required for the transcription factor NF-κB/Relish nuclear translocation: i) NF-κB/Relish phosphorylation ii) NF-κB/Relish cleavage (Ferrandon et al., 2007). Relish is similar to mammalian p100 and p105/NF-κB transcriptor factor precursors. Relish C-terminal contains a DNA binding domain, while the N-terminal contains ankyrin repeats, which have an inhibitory function. The first process requires the interaction between IMD and the FAS-associated domain (FADD) protein, which in turn recruits the death-related ced-3/Nedd2-like protein (DREDD), homologous of the caspase-8 (Leulier et al., 2002; Naitza et al., 2002). Consequently, DREDD is ubiquitinated and activated by the E3-ligase inhibitor of apoptosis 2 (Iap2). Activated DREDD cleaves IMD making it, in turn, available for ubiquitination. This event leads to the activation of the transforming growth factor-β (TGFβ)/activated kinase 1 (TAK1) complex, which activates the homologous of the mammalian IKK complex. In flies, this complex is composed of the immune-response deficient (IRD5)/IKKβ and Kenny/IKKγ subunits and its function is to phosphorylate Relish (Ertürk-Hasdemir et al., 2009). At this point, tagged Relish is cleaved by DREDD and translocates into the nucleus. In the nucleus, Relish activates the expression of its target genes, including genes encoding AMPs. Apart from its role in immunity, the IMD pathway contributes to shaping the gut bacterial community. A non-functional IMD pathway leads to the overgrowth of bacteria in the gut and dysbiosis (Buchon et al., 2009). Chronic activation of this cascade disrupts the equilibrium among commensal bacteria species, favoring the persistence of opportunist pathogen species (Ryu et al., 2008). Furthermore, since the IMD pathway is activated by PGN, a universal molecule that also characterizes commensal bacteria, its regulation is crucial. A copious number of negative regulators guarantee the efficient activation of the pathway only in the presence of pathogenic bacteria and tolerance for commensal bacteria.

1.8.3.1 Negative regulators of the IMD pathway

Since it functions in regulating gut homeostasis and immune response to pathogens, the IMD pathway must be finely regulated (**Figure 10**). Loss-of-function mutations in its negative regulators are associated with a detrimental overactivation of the pathway. Overactivation of the IMD pathway has been shown to have a dramatic effect on lifespan, survival to infection and gut integrity. For instance, loss-of-function mutations of the negative regulators PGRP-LB, PGRP-SC and/or Pirk, leads to decreased lifespan after *E.c.c.15* challenge. This phenotype is no longer present when core components of the pathway, such as DREDD, are simultaneously mutated. This demonstrates that the overactivation of the pathway is the cause of decreased host survival (Paredes et al., 2011). Importantly, non-infected mutant flies for PGRP-LB, PGRP-SC and/or Pirk also show decreased lifespan, suggesting that these proteins interact with commensal bacteria in normal conditions. In support of this hypothesis, the same flies raised in germ-free conditions show in comparison an increased lifespan. Furthermore, in the absence of infection, these mutants show a more sustained intestinal cell renewal compared to wild type animals. This is due to the fact that IMD pathway overactivation leads to tissue damage and consequently triggers cell renewal. Indeed, this phenotype is rescued when these flies are mutant also for DREDD.

IMD pathway overactivation also has other effects not related to chronic immune activation. Indeed, several elements of the IMD pathway belongs also to other cascades. For instance, IMD overactivation leads to developmental issues and activation of apoptotic pathways (Bischoff et al., 2006; Georgel et al., 1995; Maillet et al., 2008).

The numerous negative regulators act at different levels of the pathway. Some negative regulators act upstream at the level of the PGN detection. This is the case for the previously described PGRP amidases (see Paragraph 1.7.2). More downstream in the pathway, Pirk breaks PGRP-LC /IMD interaction and removes PGRP-LC from the membrane (Kleino et al., 2008). Both the abovementioned amidases and Pirk-related genes are Relish transcription targets and, thus inducible upon bacterial infection. Relish activity can also be negatively regulated. For instance, transglutaminase inhibits Relish translocation in the nucleus (Shibata et al., 2013). Another example is Caspar, which impairs the cleavage of Relish by DREDD and, thus, its nuclear translocation (Kim et al., 2006). Intriguingly, the transcriptor factor Caudal has been found to inhibits AMPs expression, but no other Relish targets expression (Lee and Ferrandon, 2011). Moreover, Caudal plays a crucial role in the maintenance of gut homeostasis. Caudal loss-of-function mutation leads to dysbiosis, host tissue damage and decreased lifespan (Ryu et al., 2008). Another inhibitor of Relish is Pickle, a protein of the IκB family. Pikle prevents in the nucleus the formation of Relish homodimers, required

for its transcriptional activity (Morris et al., 2016). Furthermore, post-translational modification of IMD pathway elements, such as ubiquitination modulates the pathway by modifying protein stability (Paquette et al., 2010; Zhou et al., 2005). Moreover, other molecular cascades, such as the JNK Ras/MAPK and JAK/STAT pathways, have been implicated in the IMD pathway modulation (Kim et al., 2007, 2005; Ragab et al., 2011).

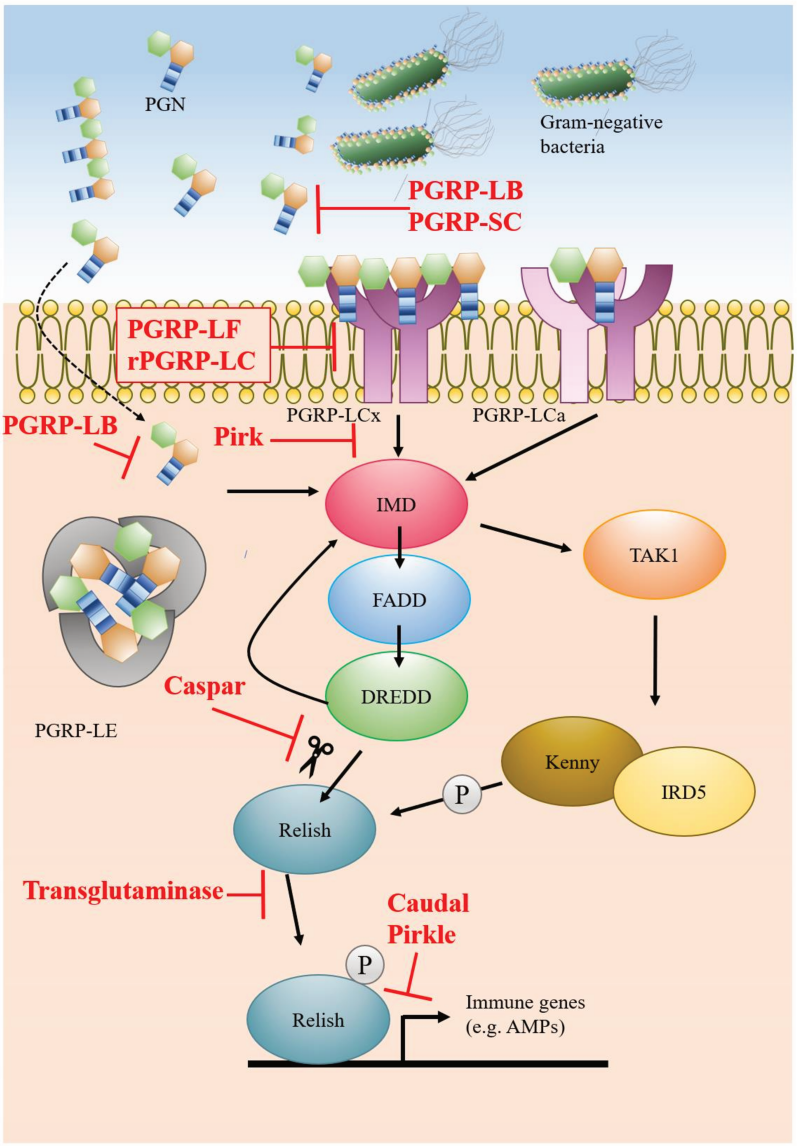

Figure 10. IMD pathway in *D. melanogaster*. The IMD pathway is activated by the detection of PGN by PGRP-LC and/or PGRP-LE. This recognition triggers the recruitment of IMD, FADD and DREDD. DREDD activates TAK1 which, in turn, activates the IRD5/Kenny complex. The latter phosphorylates Relish, which is then cleaved by DREDD. Cleaved Relish translocates in the nucleus and activates the expression of immune genes. In red are indicated some of the negative regulators of the pathway. Negative regulators act at different levels. PGRP-LB and PGRP-SC cleave the PGN in non-immunogenic fragments, preventing its recognition by PGRP-LC and/or PGRP-LE. PGRP-LF and rPGRP-LC inhibit the formation of functional PGRP-LC dimers. Pirk inhibits the recruitment of IMD. Caspar inhibits Relish cleavage, while transglutaminase inhibits Relish nuclear translocation. Caudal and Pirkle in the nucleus prevent the transcriptional activity of Relish.

1.8.3.2 PGRP-LB as a key negative regulator of the IMD pathway

Among the negative regulators of the IMD pathway, the amidase PGRP-LB has been shown to play an essential role in the modulation of both local and systemic immune responses (Paredes et al., 2011; Zaidman-Rémy et al., 2006). This amidase, by sequestrating circulating PGN, prevents IMD pathway activation. In *PGRP-LB* mutants, both septic injury and oral infection with *E.c.c.15* or DAP-type PGN lead to more higher and longer IMD pathway activation. This overactivation of the IMD pathway is rescued when PGRP-LB is overexpressed in the gut or the fat body of mutant flies. Also, when orally infected, *PGRP-LB* mutants show a higher fat body-mediated AMP production. This overactivation of the systemic response suggests that PGRP-LB acts locally in the gut to prevent PGN transfer in the hemolymph and consequent detection by the fat body cells. PGRP-LB expression is Relish-dependent and, thus, it is upregulated upon infection. Importantly, axenic flies express lower levels of PGRP-LB compared to flies raised in normal conditions, indicating that commensal bacteria induce its expression (Paredes et al., 2011; Zaidman-Rémy et al., 2006). This basal PGRP-LB expression has probably a homeostatic function and, by decreasing circulating PGN, allowed tolerance towards commensal bacteria. Overproliferation of pathogenic bacteria might lead to an increase in circulating PGN and saturation of PGRP-LB. Accumulation of circulating PGN leads then to recognition by its PGRP sensors and, in some cases (e.g. bacterial persistence), its translocation in the hemolymph. There are three PGRP-LB isoforms with two different functions (**Figure 11**). PGRP-LB^{PC} possesses a signal peptide that allows its secretion. In contrast, neither PGRP-LB^{PA} nor PGRP-LB^{PD} have such a sequence and are cytosolic (Charroux et al., 2018). While PGRP-LB^{PA} has only the amidase domain, PGRP-LB^{PD} has an additional N-terminal sequence of unknown function (Kurz et al., 2017). The secreted isoform PGRP-LB^{PC} is expressed in enterocytes and acts locally to prevent PGN translocation in the hemolymph and thus activation of the systemic response. When *PGRP-LB* mutants are orally infected, activation of the systemic immune response is rescued only when PGRP-LB^{PC} is overexpressed in enterocyte or fat body cells. On the contrary, no effect is observed when the two cytosolic isoforms are overexpressed. Overexpression of each isoform in enterocytes of *PGRP-LB* mutants rescues intestinal IMD pathway overactivation. Thus, all PGRP-LB isoforms are implicated in the modulation of the local immune response. Intriguingly, while the secreted isoform by sequestering the PGN prevents its binding to PGRP-LC, the two cytosolic isoforms prevent the response to PGN of the cytosolic receptor PGRP-LE. (Charroux et al., 2018).

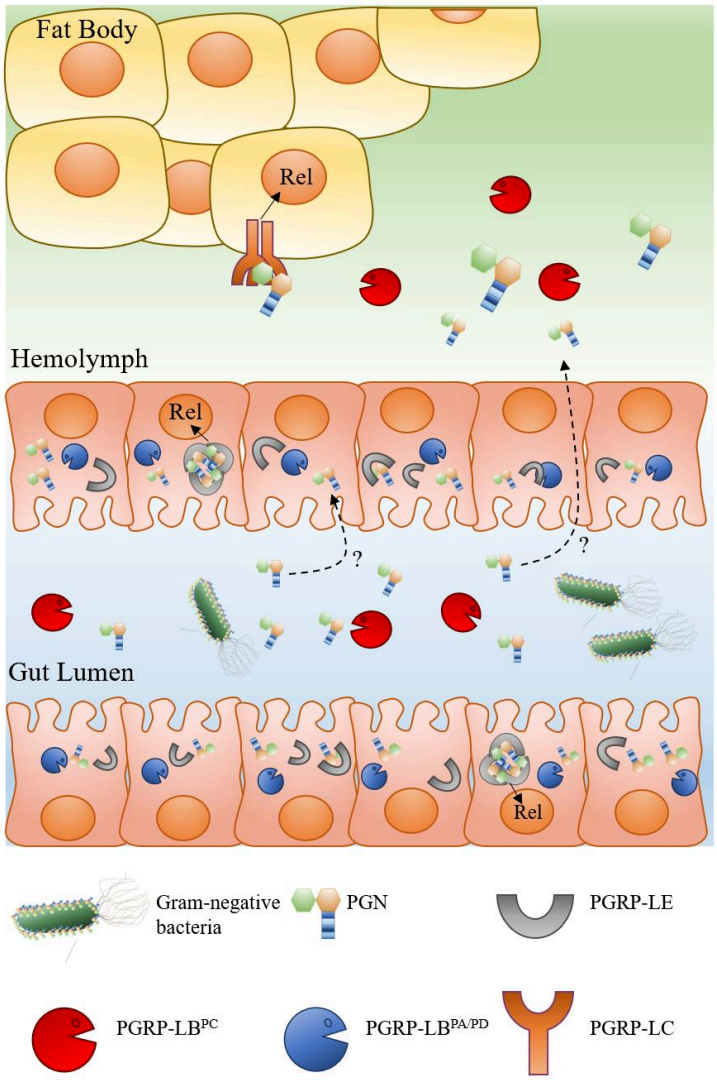

Figure 11. Regulation of the immune response by PGRP-LB isoforms. In the gut lumen, bacteria-derived PGN is detected and hydrolyzed by PGRP-LB^{PC}. When PGN is not hydrolyzed, it is recognized by PGRP receptors and triggers the activation of the IMD pathway. In the gut, this response is mediated mainly by the intracellular receptor PGRP-LE. Thus, uncleaved PGN enters (via un unknown mechanism) the enterocyte, where it can be detected by PGRP-LE or hydrolyzed by PGRP-LB^{PA} and PGRP-LB^{PD}. The fact that PGN can be cleaved by PGRP-LB isoforms in the gut lumen and the enterocyte cytoplasm guarantees tolerance for commensal bacteria and prevents constitutive activation of the IMD pathway. By hydrolyzing PGN, PGRP-LB^{PC} also prevents its transport (via an unknown mechanism) in the hemolymph and, thus, activation of the systemic immune response. This response is mediated by the receptor PGRP-LC, in fat body cells. PGRP-LB^{PC} in the hemolymph also prevents the activation of the systemic immune response.

1.9 Antimicrobial peptides: key effectors of the humoral immune response

AMPs are small, positively charged peptides and major effectors of *D. melanogaster* humoral immune response. These molecules kill bacteria and fungi by disrupting their cell wall integrity (Joo et al., 2016). The pioneering work of Boman and collaborators allowed to identify AMPs first in the silk moth *Hyalophora cecropia* and, later, in other insects, including the fruit fly (Boman et al., 1972; Steiner et al., 1981). Initially, AMPs were identified as short peptides inducible upon microbial infection and with microbicidal activity. Following studies in *D. melanogaster* led to the identification of the molecular cascades that regulate AMP expression, i.e. the IMD and the Toll pathways (Lemaitre et al., 1996, 1995). Since their characterization, AMPs have been used as a readout of the humoral immune response activation. Up to date, 21 AMPs have been described and classified into seven classes based on their *in vitro* antimicrobial activity. While some AMPs act preferentially against fungi (i.e drosomycins and metchnikowin), others act against bacteria (i.e. drosocin, attacins and dipetericins) or both fungi and bacteria (i.e. cecropins and defensin) (Hanson and Lemaitre, 2020). More recently, a new class of AMPs, called bomanins, has been identified (Clemmons et al., 2015). *In vivo* experiment using single or multiple *AMP* mutants revealed that while most of the "classical" AMPs are directed against Gram-negative bacteria and fungi, bomanins play an essential role in the response against Gram-positive bacteria and fungi (**Figure 12**) (Hanson et al., 2019). Moreover, the eradication of a specific microbe can require the synergic action of several AMPs or the action of individual AMPs. For instance, the eradication of *Enterobacter cloacae* and *Providencia rettgeri* mainly involves drosocin and diptericin, respectively (Hanson et al., 2019; Unckless et al., 2016). Furthermore, upon infection, the patterns of expression of AMPs can be variable. Apart from being expressed in the fat body, these molecules are differentially expressed in epithelial tissues (e.g. gut, trachea, reproduction tract), where they act in the local immune response (Ferrandon et al., 1998; Tzou et al., 2000). Thus, individual AMPs differential contribute to the immune response.

Besides their role in the immune response, AMPs have also been implicated in other processes such as aging, tumor elimination and neurodegeneration (Hanson and Lemaitre, 2020). More recently, AMPs have been shown to modulate behavioral responses (See *Paragraph 3.3.4*).

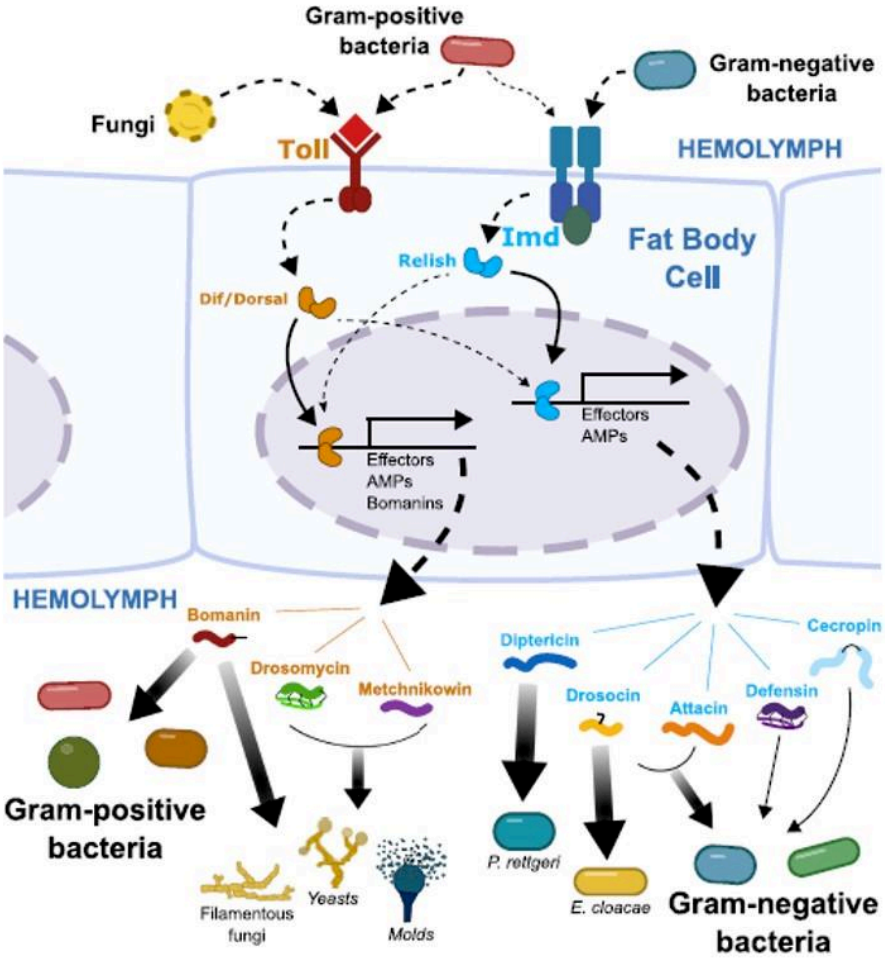

Figure 12. *D. melanogaster* AMP expression upon infection. Infection with fungi, Gram-positive or Gram-negative bacteria preferentially triggers the activation of the Toll or IMD pathway. The activation of these cascades leads to the production of specific classes of AMPs. While in some cases, the eradication of a specific pathogen is mediated by several AMPs, in other cases requires individual AMPs. For instance, drosocin plays a crucial role in the eradication of *Enterobacter cloacae*, whereas diptericin is needed for the eradication of *Providencia rettgeri*. Figure from (Hanson and Lemaitre, 2020).

2. *D. melanogaster* as a model organism to study the behavior

Like other insects, *D. melanogaster* displays a wide range of innate and learned behaviors. The availability of genetic tools, together with a relatively simple nervous system, make it an excellent model organism to study neuronal circuits and behaviors.

Historically, researches in the fly have massively contributed to the dissection of the genetic bases of behaviors (Kitamoto, 2002), such as learning and memory (Dubnau and Tully, 1998), sexual behavior (Yamamoto et al., 1997) or circadian rhythms (Hall, 2003). Traditional techniques used for functional studies such as electrophysiology and calcium imaging have been largely and successfully used in *D. melanogaster*. The use of binary expression systems (e.g. GAL4/Uas System) allows the target expression of ion channels or toxins which modulate the neuronal activity. For instance, the expression of the ion channel TRPA1 or Kir2.1 in specific neurons leads to their activation or inactivation, respectively (Venken et al., 2011). Furthermore, the anatomical and functional organization of the fly nervous system has been amply studied. Recently, efforts have been made to describe the fly brain connectome (Xu et al., 2020). Moreover, single-cell transcriptomics atlases of the *D. melanogaster* Central Nervous System (CNS) have been designed (Allen et al., 2020; Brunet Avalos et al., 2019; Davie et al., 2018). All these available tolls allow to map neural circuits associated with specific behaviors at the cellular level.

In this session, I will briefly describe the nervous system of adult flies. I will then focus on the octopaminergic and gustatory neurons as they are key components of my thesis.

2.1 Overview of the adult D. melanogaster Central Nervous System

The CNS of adult flies comprises the brain and the ventral nerve cord (VNC), which has functional similarities with the mammal spinal cord. Two main types of cells characterize the nervous system CNS: neurons and glial cells. It is estimated that 5-10% of *D. melanogaster* CNS cells are glial cells (Freeman, 2015). These cells support neurons and form the blood-brain barrier (BBB), which isolates the CNS from the hemolymph. Furthermore, glial cells, in particular astrocytes, have been shown to modulate neuronal circuits and, consequently, behavioral responses (Jackson et al., 2020; Ma et al., 2016). The fruit fly CNS counts approximately 150,000 neurons. Neuronal cellular bodies reside in the cortex, while neuronal axons and dendrites constitute the neuropils (Freeman, 2015). The brain is located in the head capsule and is formed by two optical lobes and the central brain, which hosts

higher brain centers (Ito et al., 2014). The brain and the VNC are connected through the cervical connective. The VNC is housed in the animal thorax and consists of three thoracic neuromeres and one abdominal neuromere (Court et al., 2020) (**Figure 13**).

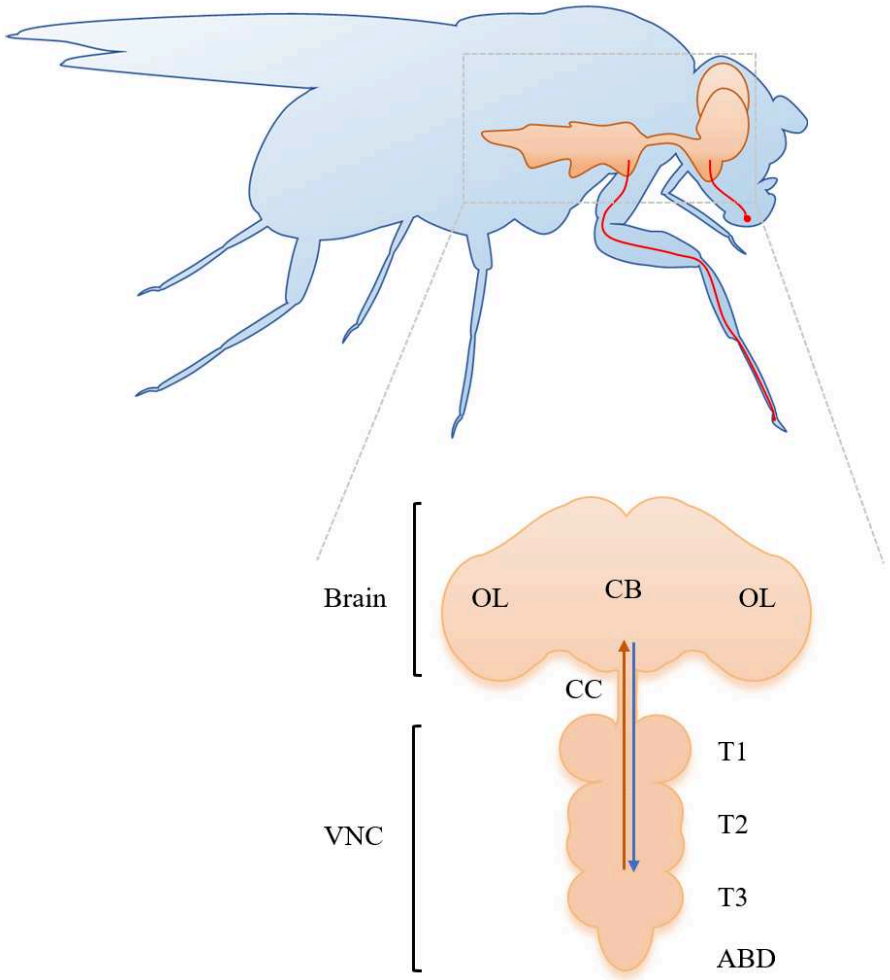

Figure 13. *D. melanogaster* central nervous system. Top The central nervous system (CNS) of *D. melanogaster* is composed of the brain (located in the head capsule) and the ventral nerve cord (VNC; in the thorax). The CNS receives sensory inputs from all the body (in red examples of sensory neurons that project in the CNS). **Bottom** The brain is composed of two optical lobes (OL) and the central brain (CB). The cervical connective connects the brain to VNC. The VNC consists of three thoracic neuromeres and one abdominal neuromere. Ascending neurons send inputs signal from the VNC to the brain (orange arrow), whereas descending neurons send output signals from the brain to the VNC (blue arrow).

The VNC collects sensory inputs from the periphery (e.g. from legs, reproductive tract, wings) and transfers them to the brain through ascending neurons. In the brain, several inputs are integrated and behavioral decisions are taken (Tsubouchi et al., 2017). Output signals from the brain are delivered in the VNC by descending neurons. In the VNC these signals trigger motor behaviors (Namiki et al.,

2018). In addition to these sensory-VNC-brain circuits, some behaviors are simple reflexes that are independent of the brain. For instance, local stimulation of the legs with dust triggers grooming behavior in headless flies (Corfas and Dudai, 1989). The brain also receives inputs directly from the sensory system. This is the case of sensory neurons located in the fly proboscis. These sensory neurons project directly in the subesophageal zone (SEZ) of the brain. The sensory inputs are then locally integrated or transferred from the SEZ to other brain zones to take feeding-related decisions. The related second-order neurons are starting to get characterized (see *Paragraph 2.3.7*) (Scott, 2018).

2.2 Octopamine: a master molecule to modulate insect behaviors

Octopamine (OA) is a biogenic amine found in plants, fungi and metazoan. In invertebrates, it acts as a neurotransmitter, neuromodulator and neurohormone. OA function in invertebrates is similar to the neurotransmitter norepinephrine (NE) in vertebrates. Both OA and NE levels increase during stressful situations and are implicated in the fight-or-flight response (Goldstein, 2010; Roeder, 1999). The latter refers to the physiological and behavioral changes which occurs during circumstances of stress or danger.

Octopamine was first identified in the salivary gland of *Octopus vulgaris* (Erspamer and Boretti, 1951). Two decades later, octopamine was shown to activate adenylate cyclase in cockroach VNC, suggesting a role for this molecule as a neurotransmitter in the CNS of insects (Nathanson and Greengard, 1973). Since then, the role of octopamine has been intensely studied in insects, where it has been implicated in a wide range of behaviors and physiological functions (Roeder, 2005, 1999). OA is produced both in the CNS and in non-neuronal tissues. It is synthesized from the amino acid tyrosine, which is converted into tyramine by the enzyme tyrosine decarboxylase (Tdc). In *D. melanogaster* there are two *tdc* genes: while *tdc2* is expressed in neurons, *tdc1* is expressed in non-neuronal cells of the abdomen (Cole et al., 2005). The amine tyramine is converted into octopamine by the enzyme tyramine-β-hydroxylase (Tβh) (**Figure 14**). Notably, both octopamine and tyramine function as neurotransmitters. They activate distinct receptors and, therefore, control different functions (Cole et al., 2005; El-Kholy et al., 2015).

Four G-protein coupled receptors (GPCRs, OAMB, Octβ1R, Octβ2R and Octβ3R) with specific expression patterns are activable by octopamine (El-Kholy et al., 2015). OAMB is expressed in the CNS and the female reproductive trait. *OAMB* mutant females are sterile and show ovulation defects (Lee et al., 2003). OA recognition by its receptors triggers an intracellular increase of second

messengers such as calcium or cyclic adenosine monophosphate (cAMP) (Balfanz et al., 2005; Koon et al., 2011). In other cases, OA recognition inhibits cAMP accumulation. In the larval neuromuscular junctions, octopaminergic and glutaminergic neurons express Octβ1R and Octβ2R receptors. While octopamine recognition by Octβ2R leads to an increase in cAMP and synaptic growth, octopamine recognition by Octβ1R has the opposite effect. The simultaneous expression of excitatory and inhibitory receptors guarantees normal synaptic plasticity, preventing synaptic termini overgrowth (Koon et al., 2011; Koon and Budnik, 2012).

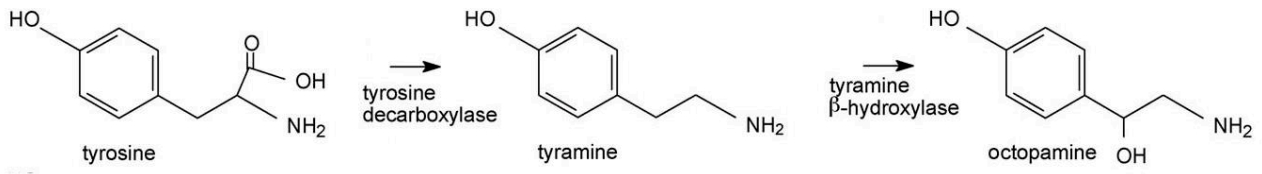

Figure 14. Octopamine synthesis in arthropods. The enzyme tyrosine decarboxylase converts tyrosine into tyramine. This amine is converted into octopamine by the enzyme tyramine-β-hydroxylase. Figure adapted from (Verlinden et al., 2010).

2.2.1 Octopaminergic neurons in D. melanogaster

In the CNS of *D. melanogaster* adults, there are around 138 octopaminergic neurons (OANs) (Rezával et al., 2014; Sinakevitch and Strausfeld, 2006). OANs innervate different parts of the fly body e.g. the reproductive trait, muscles, wings and antennae (Pauls et al., 2018). Since the OAN pattern of distribution in the CNS is highly conserved among different insect species, it has served for comparative neuroanatomy studies (Stevenson and Spörhase-Eichmann, 1995). Most OANs form clusters in the brain and VNC along the ventral midline (VM). Their patterns of projection in the periphery are stereotypical and conserved among arthropods (Braunig, 1997; Bräunig and Burrows, 2004; Busch and Tanimoto, 2010). Different OAN clusters innervate different zones in the brain, such as the lateral lobes, the SEZ, the fan-shape and the mushroom body. The major OAN cluster in the brain is the VM cluster, at the level of the SEZ (**Figure 15**) (Busch et al., 2009). Around 27 neurons belong to this cluster and they are organized in 3 subclusters located in different positions along the antero-posterior axis. The mandibular cluster (VMmd or VMI) is located more anteriorly, followed by the maxillary cluster (VMmx or VMII) and, more posteriorly, by the labial cluster (VMlb or VMIII). Moreover, these neurons are classified as ventral paired median (VPM) or ventral unpaired median (VUM) neurons, based on their projection patterns. VPM neurons project asymmetrically in

the SEZ or other brain zones, whereas VUM neurons present symmetrical projection patterns. Furthermore, VUM neurons can be ascending or descending, and thus innervate the VNC. Apart from the VM cluster, smaller clusters are present in other zones of the brain. The antennal lobe (AL) clusters are symmetrical and located ventrally the antennal lobes. Each AL cluster counts around eight neurons, which stereotypically project to the optical lobes. The ventrolateral (VL) protocerebrum clusters are located between the antennal lobe and the ventrolateral protocerebrum and each host two neurons (Busch et al., 2009; Busch and Tanimoto, 2010). In the VNC, OANs are also clustered with the vastest cluster at level of the abdominal neuromere.

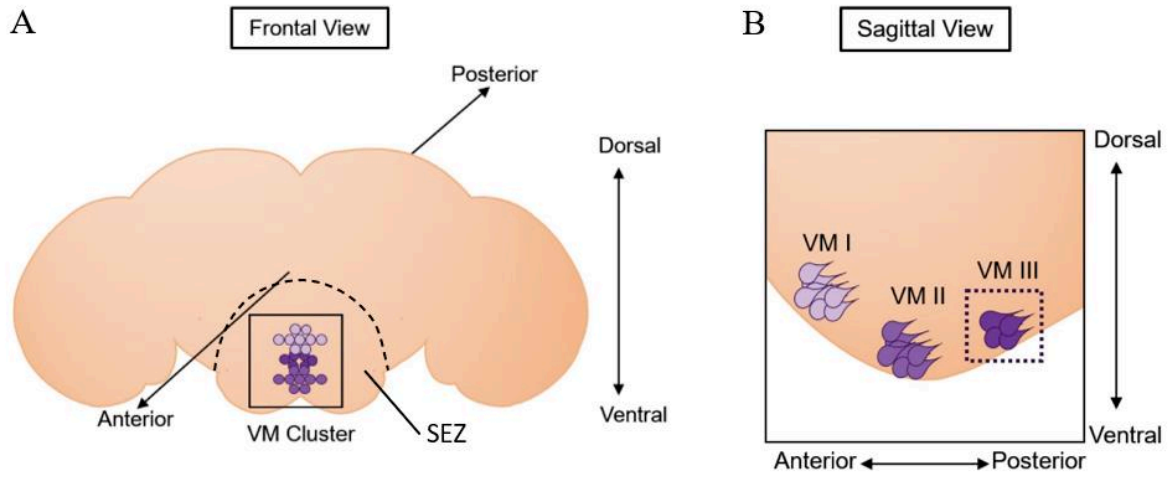

Figure 15. Octopaminergic VM cluster in *D. melanogaster*. Octopaminergic neurons are organized in clusters. The most significant cluster (around 27 neurons) in the brain is the ventral midline (VM) cluster at the level of the subesophageal zone (SEZ). Neurons in the VM cluster are organized in 3 subclusters, based on their position along the antero-posterior axis (VMI, VMII and VMIII).

2.2.2 Octopamine-related behaviors in D. melanogaster

Octopamine is implicated in a wide range of behaviors in insects. As mentioned before, OA is associated with excitatory signaling and modulates the fight-or-flight response. As NE, OA is implicated in the stress response (e.g. predator encounter) and leads to both metabolic and behavioral shifts necessary to adapt to environmental changes. OA modulates the energetic reserve's mobilization, muscle contraction and increases sensory perception (Bacon et al., 1995; Fields and Woodring, 1991; Malamud et al., 1988; Mentel et al., 2003; Mercer and Menzel, 1982). The impact of OA on insect behavior was studied at first by Hoyle's lab. Injection of OA in distinct parts of the

locust VNC leads to various behavioral responses, such as flight, running, or swimming (Sombati and Hoyle, 1984).

In *D. melanogaster*, OA is a master neurotransmitter broadly implicated in metabolic and behavioral responses, such as locomotion, courtship, post-mating behaviors, learning and memory, development, aggression, feeding and sleep (Andrews et al., 2014; Burke et al., 2012; Crocker and Sehgal, 2008; Hoyer et al., 2008; Iliadi et al., 2017; Li et al., 2016; Rezával et al., 2014; Schwaerzel et al., 2003; Selcho et al., 2012; Suver et al., 2012; Youn et al., 2018; Zhou et al., 2012, 2008). OA is also a modulator of the sensory system. For instance, OA signaling enhances visual interneurons activity during flight or walking (Suver et al., 2012). In *D. melanogaster* and other insects, OA modulates social behaviors, such as aggression, a behavior essential to guarantee access to nutritive sources and reproductive success. *D. melanogaster* males lacking octopamine (i.e. *tβh* mutants) do not show aggressive behavior towards other males (Hoyer et al., 2008). A small subset of around 5 OANs in the SEZ is sufficient to trigger aggression in socially grouped flies (Zhou et al., 2008). Aggression is also triggered by the recognition of pheromones by taste sensory neurons (Wang et al., 2011). A recent study identified a subset of taste sensory neurons in the fly proboscis required for aggression and forms synapses with OANs in the SEZ. Thus, OANs may function as second-order neurons in the CNS and collect inputs from the sensory system to modulate aggression (Andrews et al., 2014). OA has also been involved in feeding behavior modulation, which depends on the fly internal state and/or environmental inputs (Selcho and Pauls, 2019). For instance, the neuronal activity decrease of a subset of OANs (the OA-LVs) leads to the desensitization of bitter sensory neurons in starved flies. This process allows the fly to accept non-optimal nutritive sources when seeking food (LeDue et al., 2016). Another group of OANs in the SEZ, the OA-VPM4 neurons, modulates the response of sugar sensory neurons to sucrose. This modulation likely depends on the fly nutritive internal state (Youn et al., 2018). Furthermore, OA is also an essential regulator of sexual behavior and reproduction. In the next paragraphs, I will focus on the role of OA in egg-laying.

2.2.3 Octopamine and D. melanogaster egg-laying behavior

In *D. melanogaster*, as in many animals, mating and egg-laying are tightly interconnected. Mating induces deep physiological and behavioral changes in females. After mating, females decrease their receptivity and increase their rejection for males. At the same time, the production of mature eggs increases and oviposition occurs once the female finds an optimal site for offspring survival (Aranha and Vasconcelos, 2018). Octopamine is a major regulator of these post-mating behaviors, including egg-laying.

The D. melanogaster female reproductive tract is composed of two ovaries, the lateral and common oviducts, the spermatheca, the seminal receptacle, the accessory glands, the uterus and the vulva (**Figure 16**). The ovaries house ovarioles, in which oocyte maturation occurs. Each ovariole also includes a germarium, in which oocytes are assembled with nurse and follicular cells. The maturation of oocytes occurs in 14 stages. While the nurse cells die during the last stages, follicle cells form a layer around the mature oocyte. The latter is released from the ovary into the uterus through the lateral and common oviducts during ovulation. The follicle cell layer's rupture is critical to allow mature oocyte passage into the lateral oviduct. This process is called follicular trimming and the remaining follicle cells form a structure called corpus luteum. The follicular trimming requires the action of the matrix metalloproteinase-2 (MMP-2), an enzyme produced by the follicular cells and active only when ovulation happens (Deady et al., 2015). The released egg is fertilized once it reaches the uterus. The first phenotype observed in *tβh* mutant flies, lacking OA production, was female sterility. Even if these mutants produce mature eggs, they are not released from the ovaries (Monastirioti et al., 1996). This ovulation defect results in the accumulation of mature oocytes in the ovaries. Supplying these flies with exogenous OA is sufficient to trigger egg-laying. The induced expression of *tβh* in a population of neurons of the VNC also rescues the mutant phenotype (Monastirioti, 2003). However, *tβh* mutants not only do not produce OA but also accumulate the OA precursor tyramine (Monastirioti and Linn, 1996). Since tyramine is also implicated in behavioral modulation, the *tβh* mutant phenotypes could also be a consequence of tyramine accumulation. *tdc2* mutant females, which lack both octopamine and tyramine, are also sterile. However, in contrast to *tβh* mutants, these flies release the egg in the oviduct but do not lay it. This observation suggests that octopamine and tyramine contributes to ovulation at different levels (Cole et al., 2005). These two amines are also required to release the sperm from the seminal receptacle and the spermathecae (Avila et al., 2012). Instead, only OA is required for follicular trimming. By binding to the OAMB receptor expressed on follicular cells, OA triggers an intracellular Ca^{2+} increase which leads to the activation of the enzyme MMP-2 and follicular trimming (Deady and Sun, 2015). The ovulation defect of *tβh* mutants is due to impaired ovaries contraction. The ovaries are innervated by neurons located in the VNC abdominal ganglion. The release of octopamine, as well as glutamate, modulate oviduct contraction (Rodríguez-Valentín et al., 2006). *Ex vivo* experiments performed on the female genitalia tract showed that octopamine finely orchestrates muscle contraction leading to ovulation. It has been proposed that octopamine triggers the contraction of the ovary muscles and, in the meantime, relaxes oviduct muscles, allowing the egg passage (Middleton et al., 2006). How does OA modulate muscle contraction? Ovulation requires both OAMB and Octβ2R receptors expression in the oviduct epithelia (Lee et al., 2003; H.-G. Lee et al., 2009; Lim et al., 2014). It has been suggested that OA sensing in epithelial cells triggers

the production and release of nitric oxide, which by acting on muscles, leads to their relaxation (Lim et al., 2014). Ovulin, a protein of the male seminal liquid, modulates the action of OANs in muscle contraction, favoring ovulation (Rubinstein and Wolfner, 2013).

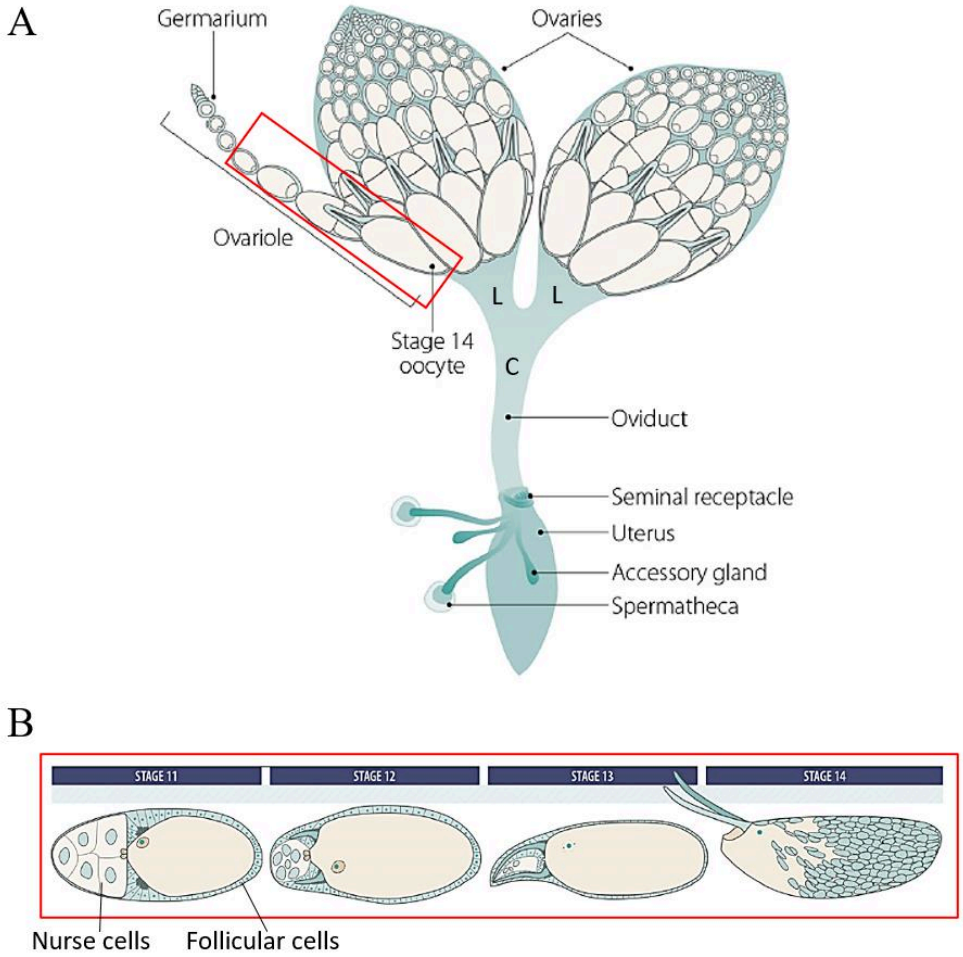

Figure 16. The reproductive trait of *D. melanogaster*. **A** The reproductive trait of *D. melanogaster* is composed of ovaries, lateral (L) and common (C) oviducts, seminal receptacle, accessory glands, spermatheca and uterus. Each ovary houses ovarioles, in which maturation of the oocytes occurs. Inthe germarium, oocytes are assembled with nurse and follicular cells. During maturation, the oocyte undergoes through different stages (from 1 to 14). **B** The latest stages of the oocyte maturation are shown (from stage 11 to 14). During the last stages, nurse cells die, while follicular cells are kept. The rupture of the follicular layer (follicular trimming) around the mature (stage 14) oocyte is necessary to release the egg into the lateral oviduct (Hughes et al., 2018).

2.2.4 Neuronal circuits for egg-laying in D. melanogaster

As previously mentioned, mating is one essential trigger event for egg-laying. In particular, post-mating behaviors are induced by a molecule contained in the male seminal fluid, i.e. the sex peptide (SP). This small peptide is initially sensed by the sex peptide receptor (SPR) expressed in SPR-positive sensory neurons (SPSNs) of the uterus and oviduct (Häsemeyer et al., 2009; Yang et al., 2009; Yapici et al., 2008). These sensory neurons express the sex-determination factors *doublesex* (*dsx*) and *fruitless* (*fru*) and the proprioceptive marker *pickpocket* (*ppk*) and project in the VNC abdominal ganglion (Häsemeyer et al., 2009; Rezával et al., 2012; Yang et al., 2009). It has been proposed that in the VNC, these neurons connect with a small subset of *dsx* expressing OANs (around 9 neurons) which are required to trigger post-mating behaviors (Rezával et al., 2014). However, another study argued that SPSNs that innervate the genitalia tract form synapses with another group of neurons in the abdominal ganglion called SP abdominal ganglion (SAG) neurons. Instead, the *dsx* expressing OANs would play other functions, such as the release of sperm from the sperm storage organs. SP detection by SPSNs after mating inhibits the SAG neurons and, by doing so, triggers post-mating behaviors (Feng et al., 2014). Other components of the neuronal circuit that links mating to egg-laying have been recently identified. SAG neurons project in the brain where they form synapses with cholinergic pC1 neurons. These neurons would act upstream of descending neurons called oviDNs. The latter are essential for egg-laying since their genetic impairment or activation leads to induction or inhibition of egg-laying, respectively. Thus, in the presence of SP, pC1 neurons would act on oviDNs by inhibiting them, leading to egg-laying (Wang et al., 2020).

2.3 Introduction to D. melanogaster Gustatory System

Testing the environment is a vital skill for animals to feed, reproduce and survive to predators or pathogens. *D. melanogaster* Peripheral Nervous System (PNS) is formed by sensory neurons located outside the CNS and innervating peripheric organs. These neurons collect input signals from the internal and external fly environment and transfer them to the CNS. In *D. melanogaster* there are 4 types of sensory structure: the chordotonal organs, the photoreceptors, the dendritic neurons and the external sensory organs (Jan and Jan, 1994). Neurons in the external sensory organs, such as taste bristles, expose their termini directly to the external environments and are mainly dedicated to the detection of surrounding chemicals. Chemosensory neurons express different types of receptors that detect odors, pheromones, tastants and noxious signals (Joseph and Carlson, 2015). All the inputs coming from the PNS are integrated into the CNS, where output behaviors are decided, also based on the animal's internal state. In the next paragraphs, I will focus on the detection of tastants by gustatory receptor neurons (GRNs). I will describe the main organs and receptors dedicated to tastant perception and how taste inputs modulate feeding behavior.

2.3.1 The gustatory organs of D. melanogaster

The gustatory system is dedicated to the tastant detection and inputs from this system are essential to take decisions, mainly related to feeding. Tastant detection is critical for the animal to feed in nutrient sources and avoid toxic molecules. Moreover, inputs coming from GRNs modulate other types of behaviors, such as mating, oviposition or grooming (Bray and Amrein, 2003; Guntur et al., 2017; Hu et al., 2015; Liu et al., 2017; Miyamoto and Amrein, 2008; Moon et al., 2009; Yanagawa et al., 2019; Yang et al., 2008). In *D. melanogaster*, taste organs are distributed all over the body, allowing the animal to navigate in its surrounding environment. Taste organs are found in the proboscis, legs, wing and female ovipositor. The proboscis, which is the fly mouth, hosts the highest number of taste structures. The proboscis tip is characterized by two symmetrical structures called labella, which directly enter in contact with chemicals. In *D. melanogaster*, there are three different types of taste organs (or sensilla): the taste bristles, the pores and the pegs (**Figure 17**) (Amrein and Thorne, 2005). Gustatory bristles are found in the labella (around 32 sensilla per each labellum), tarsi (around 30 sensilla per leg), wing margin (around 40 sensilla) and, female ovipositor (3 sensilla) (Falk et al., 1976; Nayak and Singh, 1983; Singh, 1997; Stocker, 1994). The number of taste bristles in the forelegs is sexually dimorphic, with around 37 taste bristles in females and around 50 in males (Nayak and Singh, 1983; Possidente and Murphey, 1989). Additional bristles in male forelegs express a

gustatory receptor (GR), Gr68a, dedicated to the detection of courtship-related pheromones (Bray and Amrein, 2003).

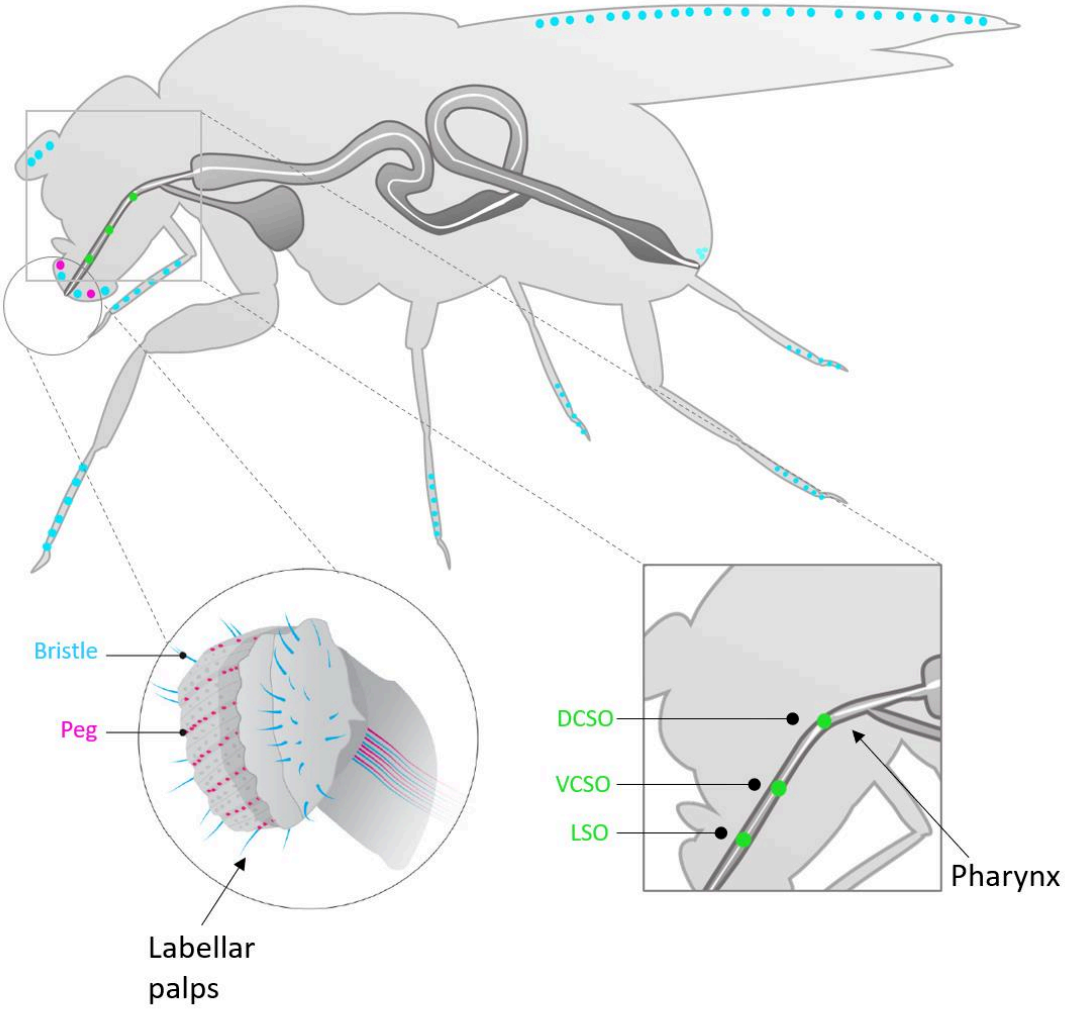

Figure 17. Taste organs in *D. melanogaster*. In *D. melanogaster*, there are three types of taste organs: bristles (light blu), pegs (fuchsia) and pores (green). Taste bristles are present in wings, labella, wings, leg tarsi and female ovipositor. Taste pegs are found in rows between the pseudotrachae of the labellar palps. Taste pores are internal taste organs lining the pharynx. The pores are called the labral sensory organ (LSO), the ventral cibarial sensory organ (VCSO) and the dorsal cibarial sensory organ (DCSO). Figure adapted from (Steck et al., 2018).

Taste bristles house 2-4 GRNs, one mechanosensory neuron and 3-4 accessory cells. These sensilla are classified as short (S), intermediated (I), or long (L). In the labella, while short and long sensilla house 4 GRNs, intermediate sensilla house 2 GRNs (**Figure 18**). In wings and legs, taste bristles are characterized by one mechanosensory neuron and four chemosensory neurons (Shanbhag et al., 2001). In a single sensillum, distinct types of GRNs detect different taste modalities (See *Paragraph*

2.3.2). Each bristle is delimited by a shaft that forms the hair and has an apical pore, which allows the access of chemicals in the bristle cavity. Here, GRN dendrites are bathed within a lymph rich of secretions produced by the accessory cells. These secretions facilitate the recognition of chemicals by taste receptors (Amrein and Thorne, 2005). GRN cell bodies are located at the sensillum base and send their axons to the CNS.

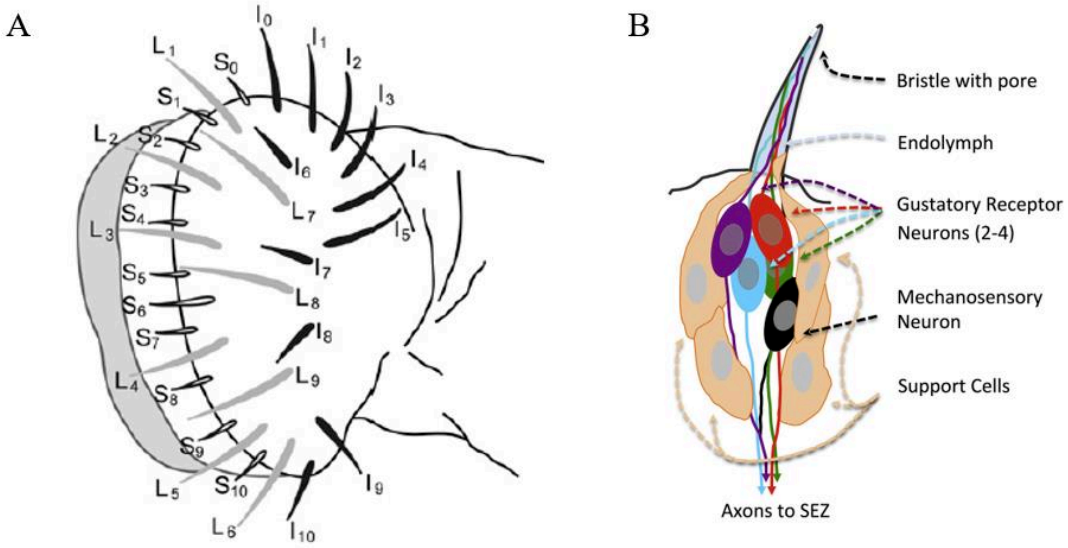

Figure 18. Taste Bristles in *D. melanogaster*. A Taste bristles are classified as short (S)-, intermediated (I)-, or long (L)-type sensilla. Numbers indicate specific sensilla. **B** Taste bristles house 2-4 GRNs, one mechanosensory neuron and 3-4 accessory cells. One pore at the tip allows the chemical access into the bristle cavity that is filled with endolymph. GRNs dendrites are in the bristle cavity, while axons are sent in the brain SEZ. Figure **A** from (Weiss et al., 2011). Figure **B** from (Amrein, 2016).

Taste pegs form rows between the pseudotrachae of the labella for a total of 30 pegs per each labellum (Falk et al., 1976). However, the number of these taste organs changes between the two sexes, with females having more taste pegs than males. Each peg houses one mechanosensory neuron and one GRN. The function of these structures is not clearly understood yet. In contrast to taste bristles, taste pegs are not directly exposed to chemicals. Indeed, peg GRNs enter in contact with tastants only when the fly extends its proboscis and opens the labellar palps (Shanbhag et al., 2001). Taste pores are the third type of taste organs and reside in the internal mouthpart, lining the pharynx. They are called the labral sensory organ (LSO), the ventral cibarial sensory organ (VCSO) and the dorsal cibarial sensory organ (DCSO) and are organized in sensilla with 1 to 8 chemosensory neurons and 1 or none

mechanosensory neuron (Stocker, 1994; Stocker and Schorderet, 1981). Since these organs are difficult to access, it has been hard to study their specific function. Moreover, as GRNs in these internal sensilla express similar GRs compared to taste bristles, it has been challenging to discriminate behavioral responses from one type of organ or the other (Chen and Dahanukar, 2017). However, because of their position, taste pores are thought to mediate food-quality control, once the food is ingested. Pharyngeal organs have been shown to sense sweet compounds and favorite sugars uptake by prolonging ingestion (LeDue et al., 2015). In addition, a recent report showed that stimulation of the pharynx with sugar trigger in starved flies foraging behavior (Murata et al., 2017).

2.3.2 Taste modalities and receptors in D. melanogaster

To sense chemicals, GRNs express receptors on the dendrites. In *D. melanogaster*, four types of receptors have been associated, mainly using electrophysiological recordings, with tastant detection: gustatory receptors (GRs), ionotropic receptors (IRs), pickpocket receptors (PPKs) and the transient receptor potential (TRP) channels (**Figure 19**) (Chen and Dahanukar, 2020; Scott, 2018). All these classes of receptors are expressed in GRNs and a single GRN can express several receptors. These receptors confer to the GRNs the capability to detect one or more taste modalities. Typically, GRNs detect sugars, bitter compounds, high salt concentration, law salt concentration and water. GRNs for the detection of water, sugars and bitter compounds are mutually exclusive. The detection of sugars by "sweet" GRNs is associated with appetitive behavior and attraction, whereas the detection of bitter compounds by "bitter" GRNs triggers aversive behaviors. What may appear as a binary system is much more subtle and includes fine tuning (see *Paragraph 2.3.8*). In contrast to the described taste modalities, which are mediated by well defined GRN classes, salt detection seems to be more complex. Low salt concentration simultaneously activates different GRNs, among which sweet GRNs. Analogously, hight salt concentration simultaneously activates different GRNs, among which bitter GRNs. While low salt detection triggers appetitive behavior, high salt detection leads to aversive behavior (Jaeger et al., 2018).

As mentioned before, labellar bristles can house 2 (I-type sensilla) or 4 (L- and S-type sensilla) GRNs. Electrophysiological responses to different tastants have allowed to better understand the organization of GRNs in these sensilla. All I-type sensilla house one bitter and one sweet GRN. L- and S-type sensilla house a low salt, a sugar and a water GRN. Almost all S-type sensilla and none L-type sensilla house also one bitter GRN (Liman et al., 2014; Weiss et al., 2011). Apart from the described taste modalities, GRNs also detect other types of chemicals. Indeed, GRNs respond to

acids, amino acids, fatty acids, polyamines, H_2O_2, carbonated water, ammonia and bacteria-derived molecules (Chen and Dahanukar, 2020).

I will describe below the main classes of taste receptors so far identified.

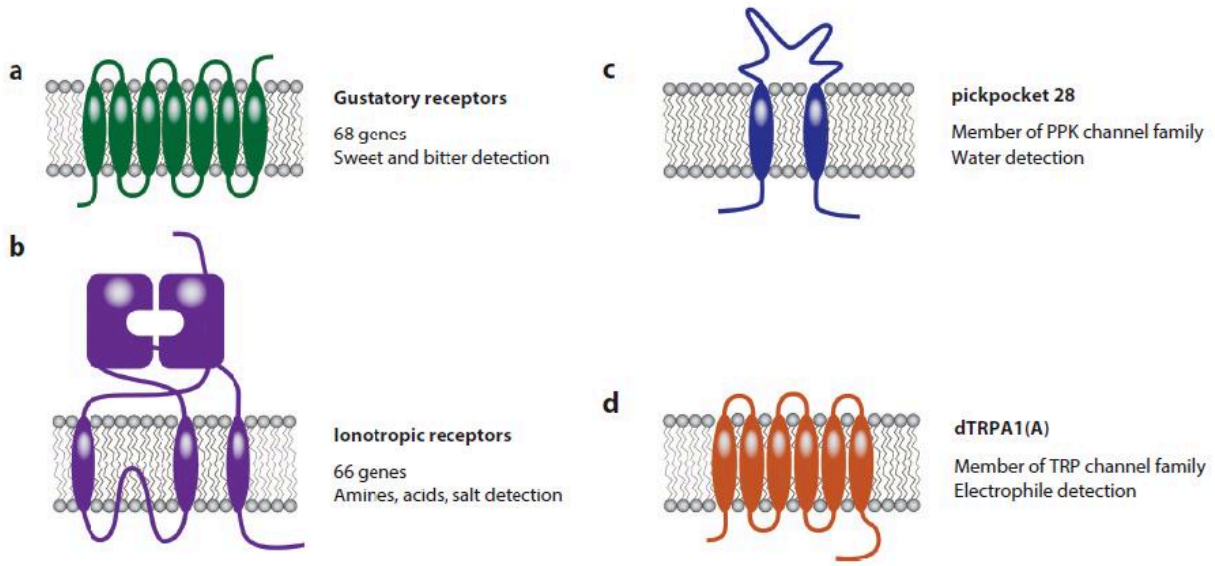

Figure 19. Taste receptors in *D. melanogaster*. In *D. melanogaster*, four types of receptors have been shown to detect tastasts: gustatory receptors (**a**), ionotropic receptors (**b**), pickpocket receptors and (**c**) receptors of the TRP channel family (**d**). Figure adapted from (Scott, 2018).

2.3.3 Gustatory receptors

GRs were the first taste receptors to be identified. A bioinformatic screen conducted by Carlson laboratory identified a family of 19 genes encoding membrane proteins expressed in the *D. melanogaster* labella and not expressed in *pox-neuro*^{70} mutants, in which taste is abrogated (Clyne et al., 2000). Following studies led to the identification of other members of this family for a total of 60 genes encoding 68 proteins (Dunipace et al., 2001; Robertson et al., 2003; Scott et al., 2001). GRs are seven transmembrane domain proteins with a conserved C-terminal domain. Until today, the mechanism of action of these receptors remains poorly understood. Since mammals taste receptors are GPCRs, it was initially thought that also GRs belonged to this superfamily (Chandrashekar et al., 2006). However, *D. melanogaster* GRs are not homologs to mammal taste receptors and they might function as ligand-gated ion channels (Sato et al., 2011). Moreover, *D. melanogaster* GRs are evolutionally related to odorant receptors (ORs), which have been also proposed to function as ligand-gated ion channels (Nakagawa et al., 2012; Sato et al., 2008; Wicher et al., 2008). Due to the difficulty

of studying GRs in heterologous systems, it is unclear if these receptors form homodimers and/or heterodimers. Furthermore, even if GRs were reported to be expressed in the taste organs, visualization of the endogenous receptors has not been achieved yet (Clyne et al., 2000; Dunipace et al., 2001; Scott et al., 2001). Nevertheless, several GAL4 lines have been generated to report the expression pattern of these receptors in neurons of the labellum, the pharynx and the legs (Chen and Dahanukar, 2017; Fujii et al., 2015; Jaeger et al., 2018; LeDue et al., 2015; Ling et al., 2014; Weiss et al., 2011). Behavioral and functional studies of single-gene mutants have shown that GRs expressed in GRNs detects mainly bitter and sweet compounds (see *Paragraph 2.3.3.1* and *2.3.3.2*). However, only for a few GRs, direct links tastant-receptor have been found. The fact that one GRN can express several GRs and that different GRs can detect a single tastant and *vice versa* makes these links hard to find. Moreover, GRs are expressed in neurons other than GRNs and can detect chemicals other than tastants. For instance, Gr43a and Gr64a are expressed in the CNS (Fujii et al., 2015; Miyamoto et al., 2012; Miyamoto and Amrein, 2014; Thorne and Amrein, 2008). Gr43a in the brain functions as an internal sensor for circulating fructose. Since hemolymph fructose concentration is high in fed flies and low in starved flies, Gr43a-dependent fructose detection probably informs the CNS on the animal feeding status (Miyamoto et al., 2012). GRs are also expressed in olfactory neurons (ORNs) of the antenna and/or the maxillary palps (Fujii et al., 2015; Jones et al., 2007; Suh et al., 2004; Yao and Carlson, 2010). Gr21a and Gr63a are expressed in the fly antenna and mediate CO_2 detection (Jones et al., 2007). Furthermore, GRs are expressed in gut enteroendocrine cells, multidendritic sensory cells on the abdominal wall and neurons innervating the reproductive traits (Park and Kwon, 2011a, 2011b; Shimono et al., 2009). Intriguingly, Gr28b has been involved in temperature sensation, suggesting that GRs might have other functions than detect chemicals (Ni et al., 2013).

2.3.3.1 GRs expressed in GRNs for sugar detection

Flies nourish on sources of food enriched with sugars and amino acids. The detection of these appetitive compounds is vital for animal survival and fitness. In *D. melanogaster* eight closely related GRs have been associated with the detection of sugars: Gr5a, Gr61a, Gr64a-f. The first GR associated with sugar detection was Gr5a. Dahanukar *et al.*, showed that the electrophysiological and behavioral response towards trehalose was diminished in *Gr5a* mutants and rescued when Gr5a expression was restored. Notably, *Gr5a* mutant flies responded to sucrose, suggesting specificity of this receptor for trehalose (Dahanukar et al., 2001). Gr5a is broadly expressed in taste organs and it is expressed in all sweet GRNs. Gr5a, Gr64a and Gr64f are required for the detection of most available sweet compounds. Gr5a and Gr64a functions are complementary: Gr5a detects primarily trehalose and

melezitose, whereas Gr64a responds mainly to maltose and sucrose (Dahanukar et al., 2007, 2001; Jiao et al., 2007; Ueno et al., 2001). Gr64f has been proposed to act as a co-receptor with Gr5a to detect trehalose and with Gr64a to detect sucrose, maltose and glucose (Jiao et al., 2008). Notably, Gr64a is not expressed in the labellum sensilla, whereas Gr5a and Gr64f are broadly expressed in the labella (Fujii et al., 2015). The expression of the remaining sweet GRs is limited to subsets of Gr5a expressing GRNs. In the legs, all sweet GRs are expressed in variable patterns (Fujii et al., 2015). More recently Gr43a has been also identified as sweet GR (see *Paragraph 2.3.3*). This receptor is expressed not only in taste organs but also in the brain, proventriculus and uterus. The particular pattern of expression of Gr43a suggests a role as a key nutrient internal sensor (Miyamoto et al., 2012; Miyamoto and Amrein, 2014). In the labellum, as well in the legs' tarsi, based on the sensilla type and the GRs pattern of expression, sweet GRNs have been divided into four groups (Fujii et al., 2015). Importantly, behavioral analysis of single-gene mutants showed that each GR is involved in the detection of a repertoire of sugars and at the contrary, each sugar is recognized by multiple receptors (Dahanukar et al., 2007; Fujii et al., 2015; Jiao et al., 2008, 2007; Slone et al., 2007). These data suggest that sweet GRs might function as multimeric complexes. However, the misexpression of single sweet GRs in the olfactory ab1C neuron confer sensitivity to one or more sweet tastants, strongly suggesting that each GRs directly recognizes its ligand/s. Nevertheless, this last result does not exclude the fact that sweet GRs can form multimeric complexes (Freeman et al., 2014).

2.3.3.2 GRs expressed in GRNs for bitter detection

The definition of bitter compounds is related to the type of behavior they trigger, i.e. aversive behavior. Many toxic compounds are perceived as bitter and, thus, their detection is fundamental for animal survival. Many plants also produce repellent compounds (e.g. L-canavanine, saponin) as a self-defense mechanism against insects. In *D. melanogaster*, the bitter receptor Gr66a is used as a hallmark of bitter neurons. In each labellum, Gr66a is expressed in around 25 neurons, which responds to bitter compounds and mediate aversive behavior (Lee et al., 2010; Y. Lee et al., 2009; Marella et al., 2006; Moon et al., 2006; Thorne et al., 2004). A work from Weiss and collaborators showed that the behavioral responses to different bitter tastants are variable, suggesting that distinct subsets of neurons are required to avoid different tastants. Consistently, the electrophysiological response of labellar sensilla to different bitter tastant is also variable. Based on the sensilla electrophysiological responses and expression patterns of different GRs, bitter GRNs were divided into 4 subtypes (Weiss et al., 2011). Among these subtypes, two respond to a wide spectrum of bitter compounds, whereas the other two respond to a narrower range. Bitter GRNs are expressed in I- and

S- (but S4 and S8), but not L-type sensilla. Moreover, they are by far more numerous than sweet GRs. Indeed, 33 GRs are expressed exclusively in bitter neurons, with Gr66a, Gr32a, Gr33a, Gr39a and Gr89a broadly expressed. Gr66a, Gr32a, Gr33a seem to play a key role in ligand recognition since the lack of one of these receptors impairs several bitter compounds' response. Thus, these receptors might act as co-receptors for tastant detection (Lee et al., 2010; Y. Lee et al., 2009; Moon et al., 2006). Each bitter GRN can express many (up to 29 in the labellum and 18 in the legs) or few (around 6) GRs (Ling et al., 2014; Weiss et al., 2011). Notably, a high number of expressed GRs positively correlates with the response to a wide range of tastants. In some cases, studies performed in single-gene mutants allowed to identify specific receptor-chemical correspondence. For instance, Gr93a detects caffeine, while Gr8a senses L-canavanine. However, ectopic expression of these receptors alone does not confer sensitivity to the respective tastants, suggesting that other GRs are required for their function (Lee et al., 2012; Y. Lee et al., 2009). Importantly, the heterologous co-expression of Gr8a Gr98b in Gr66a in sweet or salt taste neurons leads to a response to L-canavanine, suggesting that GRs function as heteromultimeric complexes. Furthermore, the recognition of L-canavanine by sweet GRNs leads to attractive behavior. Thus, neither GRs nor tastants, but the type of GRNs activated seems to dictate the output behavior (Shim et al., 2015). The possibility that GRs might function as multimeric complexes is reinforced by a study showing that misexpression of Gr32a, Gr66a and Gr59c is sufficient to detect lobeline, berberine and denatonium in sweet GRNs or S2 cells. Moreover, misexpression of Gr32a, Gr66a and Gr22e leads to the same result but confers the sensitivity to strychnine. So, different GR combinations seem to be required to detect specific tastant (Sung et al., 2017). Nevertheless, some GRs might act alone in tastant detection. This is the case for the detection of saponin, which only requires Gr28b (Sang et al., 2019). Remarkably, a recent report showed that overexpression, misexpression or knockout of single GRs has important global effects on the activity of GRNs. For instance, misexpression of GRs or endogenous GR deletion can lead to acquiring the response to new tastants (Delventhal and Carlson, 2016). Thus, the study of GRs might be complicated by the fact that these receptors interact in many different ways.

2.3.4 Ionotropic receptors related to taste

IRs are a family of 66 chemoreceptors related to ionotropic glutamate receptors (iGluRs) (Benton et al., 2009). They are three transmembrane receptors with an extracellular two-lobed ligand-binding domain and have been implicated in olfaction, taste, pheromones detection, thermosensation and hygrosensation (Chen and Dahanukar, 2020; Enjin et al., 2016; Knecht et al., 2016; Koh et al., 2014; Ni et al., 2016; Rytz et al., 2013). Most of the work on these receptors has focused on their role in

olfactory sensilla (Rytz et al., 2013). A group of 16 IRs is expressed in the antenna and function as odorant receptors to detect acids and amines (Ai et al., 2010; Min et al., 2013; Silbering et al., 2011; Yao et al., 2005). More recently, IRs' role in GRNs has been explored. The IR20a clade counts around 35 members and 16 GAL4 lines for different members of this clade are expressed in the fly labella (5 IRs), pharynx (8 IRs) legs (10 IRs) and wing (1 IR) (Koh et al., 2014). Four of the labellar IRs (Ir47a, Ir56b, Ir56d and Ir94e) are expressed in neurons that send projections in the CNS similar to those of sweet GRNs. One single labellar IR (Ir56a) is expressed in a subgroup of bitter GRNs. The fact that these labellar IRs are exclusively expressed in bitter or sweet taste neurons suggests that they have a role in the detection of aversive or appetitive tastants. Consistently, it has been shown that Ir56d expressing sweet GRNs mediate the attraction toward fatty acid, while Ir94e contributes to the attraction to low salt (Jaeger et al., 2018; Tauber et al., 2017). Moreover, other IRs not belonging to the Ir20a clade are expressed in GRNs. Among them, Ir76b is broadly expressed in taste and olfactory organs and it has been proposed to function as a co-receptor. In GRNs, Ir76b has been implicated in the detection of high and low salt, calcium, polyamines and amino acids (Croset et al., 2016; Ganguly et al., 2017; Hussain et al., 2016; Lee et al., 2017, 2018; Zhang et al., 2013a). Like Ir76b, Ir25a is also widely expressed in sensory neurons and has been proposed to act as a co-receptor in the detection of different chemicals (Chen and Dahanukar, 2020). Interestingly, another IR, Ir60a, which is expressed in a couple of sensory neurons in the pharynx inhibits sugar consumption. Indeed, while sucrose uptake increases when Ir60a neurons are genetically silenced, it decreases when they are activated. Behavioral and functional studies in *Ir60a* mutant animals confirmed that the sugar consumption modulation depends on this receptor. This negative feedback on sucrose uptake likely prevents overconsumption of this appetitive tastant. Notably, the role of Ir60a in regulating feeding seems to be limited to sucrose and high glucose concentrations (Joseph et al., 2017).

2.3.4 Taste-related pickpocket receptors

PPKs are two transmembrane domain proteins, belonging to the epithelial sodium channel/degenerin (ENaC/DEG) family. In *D. melanogaster*, there are 31 PPKs, implicated in locomotion, mechanical nociception and chemosensation (Ainsley et al., 2003; Chen and Dahanukar, 2020; Zhong et al., 2010). PPKs expressed in GRNs are necessary for pheromones (Ppk23, Ppk25 and Ppk29), calcium (Ppk23) and water detection (Ppk28) (Cameron et al., 2010; Chen et al., 2010; Lee et al., 2018; T. Liu et al., 2012; Liu et al., 2020, 2020; Lu et al., 2012; Park et al., 2006; Starostina et al., 2012; Thistle et al., 2012; Toda et al., 2012; Vijayan et al., 2014). Importantly, Pkk28 is necessary and sufficient

for water detection and, thus, it is considered a hallmark of water sensitive neurons (Cameron et al., 2010; Chen et al., 2010).

2.3.5 Transient receptor potential channels and taste

TRPs are an evolutionarily conserved superfamily of ion channels, implicated in a wide variety of sensory functions including thermosensation, olfaction, mechanosensation, hygrosensation, light sensation and taste (Fowler and Montell, 2013). Among them, the six transmembrane domain thermosensitive cation channel TRPA1 is expressed in GRNs. In a subset of bitter GRNs, TRPA1 mediates the molecular and behavioral responses to noxious signals (Kang et al., 2010; Kim et al., 2010). Furthermore, TRPA1 expression in bitter GRNs is required to detect and avoid bacterial LPS (Soldano et al., 2016). Painless, another member of the TRP family, is also expressed in GRNs and is required to sense isothiocyanate (ITC), a repellent molecule found in wasabi (Al-Anzi et al., 2006). Another receptor related to TRPs, the TRP-like (TRPL) cation channel, is expressed in GRNs and has been shown to sense the non-appetitive and non-toxic compound camphor. If short-term exposure to camphor leads to aversive behavior, long-term exposure provokes desensitization to this compound and thus acceptance. It has been proposed that camphor desensitization is mediated by the E3 ubiquitin ligase-dependent degradation of its receptor TRPL (Zhang et al., 2013b).

2.3.6 Overview of taste receptors and modalities in mammals

Although invertebrates and mammals' taste systems have independently evolved (Matsunami and Amrein, 2003; Yarmolinsky et al., 2009), some similarities can be found. As in *D. melanogaster*, mammals have a small number of taste modalities: sweet, bitter, umami, high and low salt and sour. In mammals, taste receptors are not expressed in sensory neurons, but in epithelial cells with a sensory function called taste receptor cells (TRCs) (**Figure 20**). Similarly to flies, different types of TRCs detect diverse taste modalities. In contrast to flies, were GRNs are present in different parts of the body, mammals TRCs are only expressed in the tongue and the palate, where they are organized in buds (Roper and Chaudhari, 2017). These structures are housed in papillae and count each 50 to 100 cells. The information from the papillae is collected by afferent nerves, which bring the input signals to the CNS. Mammalian taste receptors are mostly GPCRs and do not share similarity with *D. melanogaster* GRs (Clyne et al., 2000; Dunipace et al., 2001; Scott et al., 2001). Three heterodimeric GPCRs are dedicated to the detection of umami and sweet: T1R1, T1R2 and T1R3(Li et al., 2002; Nelson et al., 2002, 2001; Zhao et al., 2003). It has been proposed that different binding sites on each

of these receptors allow the detection of a wide range of compounds (Cui et al., 2006; Jiang et al., 2005, 2004; Winnig et al., 2007). T2Rs are GPCRs dedicated to the detection of bitter compounds. Depending on the species, T2R number ranges from 10 to 40 (around 30 in humans). Most of the pattern of expression of these receptor overlap, since a single TCR expresses many T2Rs. This is in contrast to what is observed in flies, where bitter GRs define specific patterns of expression (Weiss et al., 2011). The relatively small number of T2Rs implies that each of them is able to recognize several chemicals (Meyerhof, 2005). Receptors involved in the detection of sour and salt are still poorly understood (Roper and Chaudhari, 2017). Importantly, the ratio between sweet and bitter receptors is comparable to the ratio observed in flies, suggesting that the logic behind the perception of taste modalities could be similar. The hight number of bitter receptors, compared to the number of sweet receptors, could be explained with the fact that bitter compounds are structuraly more variable and complex than sugars.

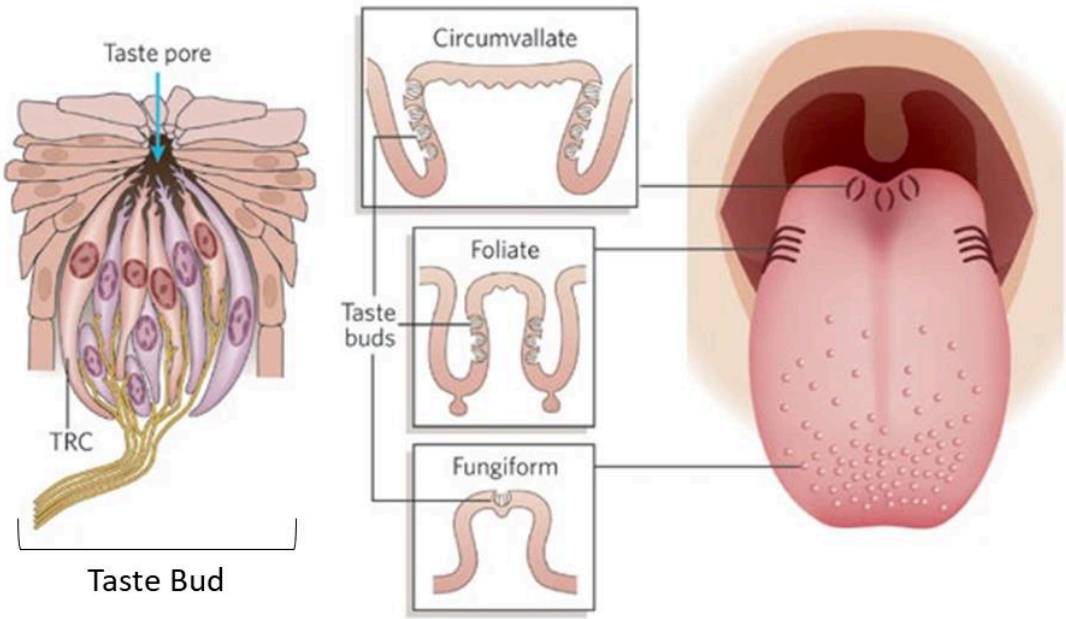

Figure 20. Taste in mammals. Taste buds are found in different types of papillae (circumvallate, foliate and fungiform) differentially distributed in the tongue. Each buds consist in 50-100 taste receptor cells (TRCs) which function is to detect tastants. A taste pore allows the access of tastants in the bud. Figure from (Chandrashekar et al., 2006).

2.3.7 Sensory modulation of feeding behavior

Feeding behavior is characterized by a sequence of behavioral modules orchestrated by the CNS (**Figure 21**). The initiation of foraging depends on the nutrient internal state and sensory cues (Pool and Scott, 2014). In addition to tastants, other properties of the food source, such as texture and odors, play an important role in determining attractive or aversive behaviors (Beshel and Zhong, 2013; Dweck et al., 2018; Sánchez-Alcañiz et al., 2017). Furthermore, the behavioral response to food is also linked to reward and memory (Krashes et al., 2009; C. Liu et al., 2012). Starved flies seek food and the detection of food by the sensory system leads to stop its search. The detection of gustatory cues at first requires neurons in the legs. In the case of appetitive compounds, the fly extends its proboscis, opens the labellar palps and starts ingestion. On the contrary, when bitter compounds are detected, the fly retracts its proboscis and moves forward. A food-quality check is performed by sensory neurons of the pharynx and determines the duration of the stay on the source of food (LeDue et al., 2015). Once the fly has consumed its meal, modulatory signals function to stop feeding and reactivate mobility.

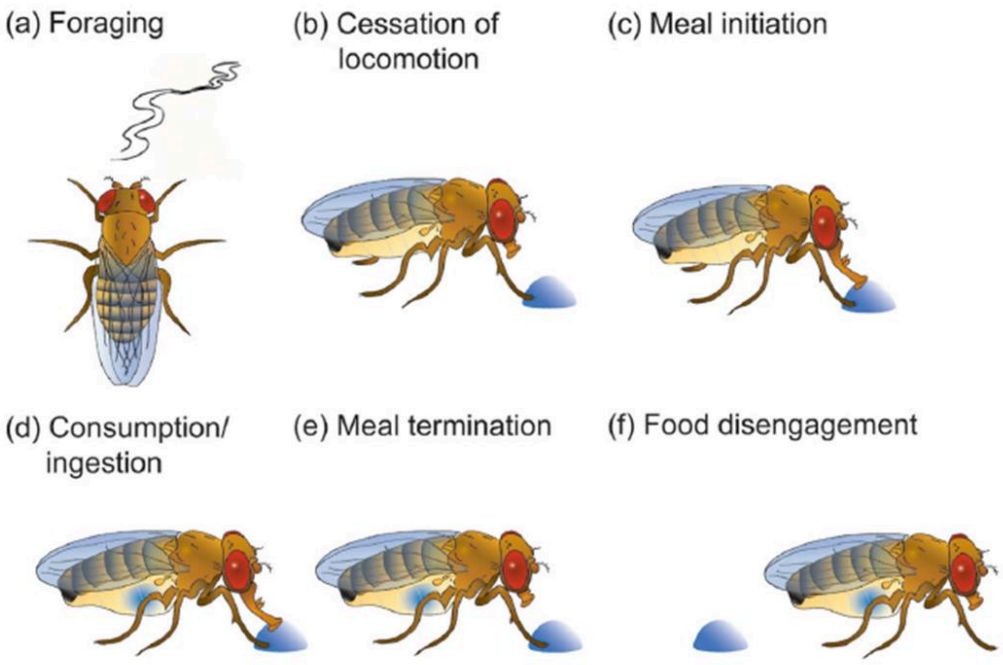

Figure 21. Feeding modules in *D. melanogaster*. Hungry flies seek food and move until they find a food source (**a**-**b**). The detection of the food involves the gustatory neurons in the legs. Ingestion is initiated and continues until modulatory signals induce meal termination (**c**-**e**). Fed flies start their locomotory activity again(**f**). Figure from (Pool and Scott, 2014).

The response by sweet or bitter GRNs to a food source is a strong determinant for attractive or aversive behaviors. GRNs of the legs projects in the VNC and through the cervical connective reach the SEZ in the brain. The SEZ represents the first relay for taste processing. Two functionally and anatomically diverse classes of sweet GRNs in the legs have been shown to control different behavioral modules based on their projection pattern. In particular, sweet GRNs projecting in the VNC determine the walk arrest when the fly encounters a sugar source, whereas sweet GRNs projecting in the SEZ, via the VNC modulate feeding initiation (Thoma et al., 2016). Proboscis GRNs project their axons via the labral nerve in the brain in the dorsal posterior SEZ. Pharyngeal GRNs project in the dorsal anterior SEZ, via the pharyngeal and accessory pharyngeal nerves (Stocker and Schorderet, 1981; Thorne et al., 2004; Wang et al., 2004). Both labellar and tarsal GRNs are required for proboscis extension reflex (PER) since mutant flies lacking these neurons no longer respond to stimuli (LeDue et al., 2015). In the SEZ, bitter and sweet GRNs have different patterns of projection, whereas water and sweet GRN projections are intermixed. Moreover, within a taste modality, GRNs from legs, labella or pharynx also have different projection patterns in the SEZ. Bitter labellar GRNs project to the medial SEZ where termini form a ring-shaped structure. In contrast, sweet labellar GRNs project in discrete ipsilateral SEZ regions and do not overlap with bitter GRNs projection (**Figure 22**) (Thorne et al., 2004; Wang et al., 2004). It is not clear if sweet and bitter inputs converge in the same downstream neurons or if there are two or more distinct neuronal circuits. Local circuits in the SEZ probably play a role in feeding behavior (Flood et al., 2013, Gordon and Scott, 2009, Melcher and Pankratz, 2005, Rajashekhar and Singh, 1994). However, taste inputs seem to convey also to higher brain centers, such as the mushroom body. The latter houses neurons which are activated upon sugar ingestion (Liu et al., 2012). Moreover, cues from the taste system need to be integrated with other types of inputs, including odors. Recent studies have started to identify second-order neurons belonging to taste circuits. A subset of 12 cholinergic interneurons in the SEZ, the IN1s, receives inputs from sweet pharyngeal GRNs. In hungry flies, sugar ingestion leads to an increase in IN1 neuronal activity. The activity of these neurons decreases over time, reflecting probably a state of satiety of the animal. Notably, activation of these neurons in fed flies leads to sustained food uptake, similarly to starved flies (Yapici et al., 2016). A behavioral screening identified sweet gustatory projection neurons (sGPNs) as second-order neuron candidates for sweet detection. sGPNs are located in the SEZ in close proximity to sweet GRN axons and they regulate proboscis extension and food uptake. Genetical modulation of these neurons induces or inhibits proboscis extension. Furthermore, labellum exposure to sucrose triggers a response in these neurons, which is higher in hungry flies. Based on the mapping of sGPNs presynaptic termini, two other regions, i.e. the antennal mechanosensory and motor center (AMMC) and motor center in the

deutocerebrum have been identified as higher-order brain centers for sweet taste (Kain and Dahanukar, 2015).

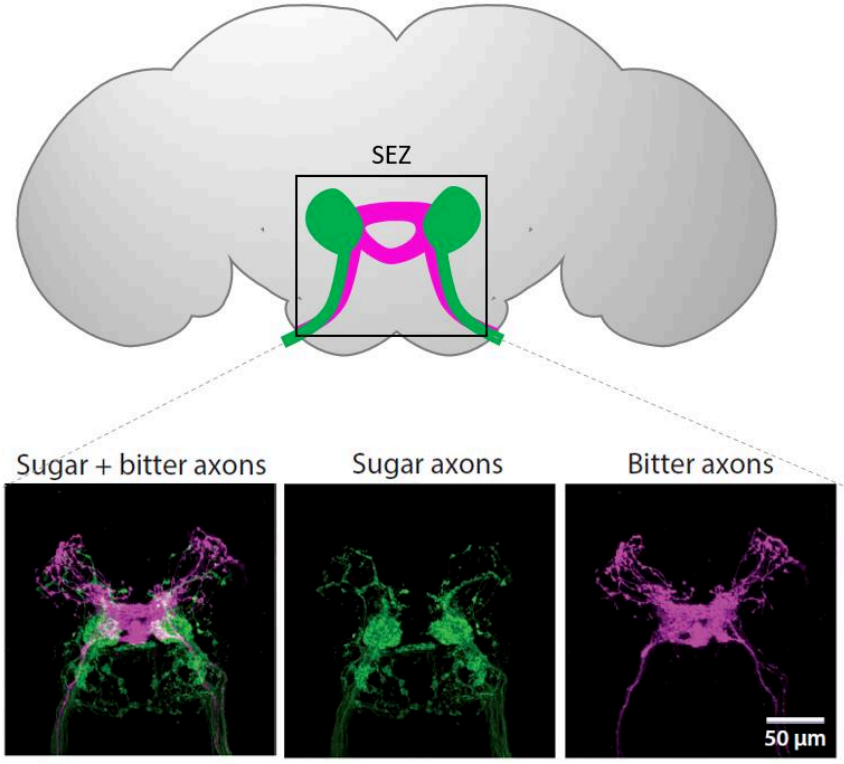

Figure 22. Different pattern of projection of labellar sweet and bitter GRNs. GRN axons project in the brain at the level of the subesophageal zone (SEZ). While bitter GRN axons (magenta) project to the medial SEZ, forming a ring-shaped structure, sweet GRN axons (green) project in discrete ipsilateral SEZ regions. At the bottom are microscopy pictures of GRN projections in the SEZ. Figure adapted from (Scott, 2018).

A couple of interneurons in the SEZ named FDGs responds to sucrose and are essential for sugar-induced feeding behavior. Interestingly, the activation of only one FDG leads to asymmetrical feeding behavior, suggesting that these neurons directly control motor neuron function. Also, FDGs respond to sucrose exposure only in starved flies, indicating that they might receive inputs about the fly internal state (Flood et al., 2013). In another study, *in vivo* calcium imaging in the brain was performed to assess which neurons are activated upon proboscis exposure to different stimuli. Stimulation with water, sucrose or bitter compounds led to the activation of different neuronal subsets in the brain. This result suggested that different taste modalities activate distinct neuronal circuits in the CNS. However, it is not possible to exclude that some of these circuits converge, since some cells

responded to more than one modality (D. T. Harris et al., 2015). In a recent work, the taste projection neurons (TPNs) have been proposed as second-order neuron candidates in the VNC. Neuronal arborizations of 3 classes of TPNs are found nearby axons of tarsal GRNs. These neurons respond selectiviely to different taste modalities (sugar and bitter), supporting the fact that different stimuli activate separated neuronal pathways. Although TPN activation induces PER, their inhibition does not abrogate PER, demonstrating that TPNs are dispensable for this behavior. In addition, two of the three identified TPNs are required for conditioned aversion behavior. Interestingly, inputs from these two TPN classes reach brain learning centers in the mushroom body (Kim et al., 2017).

2.3.8 Sweet bitter integration

While feeding behavior studies are carried out using single tastants, in nature, toxic and appetitive compounds are often detected in a mixture. Since these two classes of chemicals lead to opposite behaviors, GRNs responses to bitter and sweet compounds need to be finely regulated. The activity of sensory neurons, for instance, is modulated by the animal internal state. For example, bitter sensitivity decreases in starved flies, allowing them to feed in suboptimal food sources (LeDue et al., 2015). Moreover, it has been shown that the detection of bitter compounds can inhibit the activity of sweet GRNs (Charlu et al., 2013; Jeong et al., 2013). Indeed, the responsiveness of sweet GRNs is lower when exposed to a mixture of bitter and sweet compounds compared to when exposed to sugars only (Meunier et al., 2003). In rotten fruits, favorite sites for the fly to feed and lay eggs, carboxylic acids are present (Palma et al., 2011). It has been shown that bitter GRNs respond to carboxylic acids, mediating aversion to these compounds. When carboxylic acids are mixed with sucrose, they inhibit the sweet GRN response to sugar. Importantly, when bitter GRNs are silenced, the aversive behavior towards carboxylic acids is not entirely abolished, suggesting that two different mechanisms, one mediated by bitter and the other one by sweet GRNs, lead to avoidance of carboxylic acids (Charlu et al., 2013). In contrast, the response of tarsal bitter GRNs to bitter compounds is diminished when these tastants are present in a mixture with acids. Also, when acids are present in a mixture with bitter and sweet compounds, it causes a derepression of the response of tarsal sweet GRNs (Chen and Amrein, 2014). Another mechanism of sweet-bitter interaction relies on the presynaptic inhibition of sweet GRN responses (Chu et al., 2014). While sweet GRNs express $GABA_BR$ receptors, bitter GRNs do not. Brain GABAergic inhibitory neurons might inhibit sweet GRNs by releasing GABA in their proximity. When an antagonist of this receptor is used, the response of sweet GRNs to sucrose is higher, whereas the response of bitter GRNs to a bitter compound is not perturbed. In the presence of a sweet-bitter mixture, bitter compound detection by bitter GRNs might induce the release of GABA

in GABAergic interneurons and hence trigger inhibition of sweet GRNs (Chu et al., 2014). Notably, bitter compounds differ in the way they induce aversive behavior and inhibit sweet GRNs. For instance, L-canavanine induces aversive behavior by only activating bitter neurons, whereas strychnine induces aversive behavior by activating and inhibiting bitter and sweet GRNs, respectively (French et al., 2015). Furthermore, bitter GRNs activity can also be modulated by sweet GRNs. For instance, proboscis stimulation with a high sugar concentration decreases the response to bitter compounds of second-order neurons in the SEZ (D. T. Harris et al., 2015). Sweet-bitter modulation also takes place at the level of the GRN receptors. Odorant binding proteins (OBPs) are small secreted peptides that can facilitate ligand-odorant receptor recognition (Swarup et al., 2011). Many bitter compounds are structurally similar to odorants since they are small and hydrophobic. It has been proposed that OBPs modulate GRNs activity by interacting with tastants (Jeong et al., 2013; Swarup et al., 2014). OBP49a, which is expressed in labellar accessory cells, negatively regulates food uptake when bitter and sweet compounds are present in combination. Indeed, the response to sugar of sweet GRNs is diminished when sugar is in a mixture with bitter compounds. This reduction is abolished in *OPB49a* mutants, whereas this mutant response to single tastant is not perturbed. By directly acting on sweet GRN receptors, OBP49a might inhibit the activity of these neurons (Jeong et al., 2013). Thus, diverse mechanisms allow the integration of contradictory inputs, such as sweet/bitter inputs. The picture is more complicated if other sensory imputs (odors, texture, visual signals) are considered.

Note: part of this section is adapted from a manuscript accepted for publication (see **Annex 1**). The manuscript title is "*How bacteria impact host nervous system and behaviors: lessons from flies and worms*". The authors of this review are Ambra Masuzzo, Martina Montanari, Léopold Kurz, and Julien Royet. The manuscript publication is expected for December 2020 in *Trends in Neuroscience*.

3. Impact of bacterial infection in *D. melanogaster* nervous system and behaviors

3.1 Introduction to the concepts of sickness behavior and behavioral immune system

Over the last two decades, studies carried out in mammals and invertebrates demonstrated that when facing pathogenic microbes, animals can modify their behavior to avoid or reduce the exposure, defend themselves, their relatives, and/or offspring. Thus, along with the canonical immune responses, hosts have evolved behavioral responses against microbial infection (de Roode and Lefevre, 2012; Schaller, 2006).

The first observations linking microbial infection with host behavioral changes were done in mammals (Hart, 1988). Initially, the term "sickness behavior" was attributed to behaviors typically found in infected animals. Some examples are the loss of appetite, the increase in sleeping or depression observed in these animals. Importantly, these responses are also found in invertebrates such as insects, suggesting an essential role of this defense mechanism for the host survival and/or fitness (Adamo, 2006; Kazlauskas et al., 2016; Sullivan et al., 2016). However, the physiological relevance of sickness behavior is still partially understood. One possible role would be to save energy, necessary to mount the costly immune response. For instance, crickets infected with *Serratia marcescens* decrease their food uptake and, when given a choice, prefer to eat food with low-fat amount. This behavior might be a consequence of the high cost of lipid digestion. Thus crickets, by decreasing lipid uptake, would save energies to dedicate to the immune response (Adamo et al., 2010). Also, it has been proposed that sickness behavior reduces the risk of spreading the infection to the offspring (Shakhar and Shakhar, 2015). This possible role is supported by the observation that sick animals mate less and are socially isolated from healthy members of their group. Sickness behavior is also considered as a consequence of the activation of the immune system. The production of cytokines by immune cells and their action on the CNS can lead to behavioral changes in the host (Dantzer, 2001; Dantzer et al., 2008).

More recently, Mark Schaller coined a new term, “behavioral immunity,” to defined neuronally controlled mechanisms that allow animals to avoid and/or decrease its and others' exposure to a disease-causing agent (Schaller, 2006). In contrast to sickness behavior, which refers only to the behavioral response of sick animals, behavioral immunity also includes the behavioral response of healthy animals when they encounter a pathogen. Examples of behavioral immunity have been found in both vertebrates and invertebrates. Rodents isolate members of their group that are infected, while mandrill monkeys do not groom infected relatives (Arakawa et al., 2011; Boillat et al., 2015; Poirotte et al., 2017). Similarly, insects exposed to parasites groom themselves often, isolate themselves from the rest of the group, and are usually discarded for reproduction (Bos et al., 2012; de Roode and Lefevre, 2012; Heinze and Walter, 2010; Knell and Webberley, 2004; Leung et al., 2001). Since its conserved role and contribution to host survival to microbial exposure, behavioral immunity must be considered as an integral part of the host immune response.

3.2 D. melanogaster as a model to study behavioral responses to microbes

One crucial aspect of studying behavioral immunity is to understand how this response is modulated at a cellular and molecular level. How do neurons sense the presence of bacteria? How do the immune and nervous systems talk to each other and modulate their reciprocal activity? Which molecular and cellular pathways are required for behavioral changes when facing a pathogen? Even if in the last years, studies in mammals have strongly contributed to the field (see Paragraph 3.5), their complexity is an important limit on the study of behavioral immunity at a cellular and molecular level. On the other hand, even if insects display a wide variety of behavioral responses to pathogens, the lack of genetic tools for most of them is a limiting element to study behavioral responses. Therefore, genetically tractable models such as *D. melanogaster* and *C. elegans*, are excellent models to study behavioral immunity at the molecular and cellular level. In the last years, studies in *D. melanogaster* have not only unraveled the extreme pleiotropic modes of interactions that take place between microorganisms and the nervous system of animals but also begun to reveal the nature of the microbial elicitors, the type of neurons that detect them, and the behavioral consequences associated with their reciprocal interactions. In this section, I will present an overview of recent achievements in this animal model, with a specific emphasis on the interactions between bacteria and the host nervous system.

3.3 Impact of bacterial exposure on D. melanogaster nervous system and behavior

3.3.1 Bacterial detection by D. melanogaster sensory nervous system

D. melanogaster lives primarily on rotten fruits populated by microbes that synergistically ferment organic substrates to produce active compounds and metabolites (Christiaens et al., 2014; Fischer et al., 2017). Detecting these chemosensory molecules helps the flies to find nutrient-rich food, to select hospitable zones for egg-laying, and to avoid ecological niches contaminated with pathogens. In *D. melanogaster*, some constitutive elements of the bacterial cell wall and membrane can be directly sensed by sensory neurons. Detection of bacterial LPS by the esophageal bitter neurons via the TRPA1 receptor triggers feeding and oviposition avoidance (Soldano et al., 2016). When applied onto wing margins or legs, bacteria cell wall PGN induces grooming behavior (Yanagawa et al., 2019). Furthermore, also the fly olfactory system plays a key role in adapting behavior to the presence of bacteria. Geosmin, a volatile odorant produced by some fungi and bacteria acts as a strong fly repellent that can override innate attraction to vinegar and other food-related odorants (Stensmyr et al., 2012). Its activity is mediated by a single class of neurons expressing the odorant receptor Or56a and which target the DA2 glomerulus in the antennal lobe. Carnivore feces are enriched in bacteria that produce phenols. Phenol detection by Or46a expressing ORNs present in the fly palp triggers oviposition aversion (Mansourian et al., 2016). Activation of the geosmin and phenol circuitry is sufficient to induce a reduction in oviposition suggesting that they are powerful signals for the presence of potential infectious sites containing harmful microbes. Consistently, these signals have been shown to also be aversive in other insect species. Besides protecting flies from detrimental bacteria, the olfactory system can also mediate fly attraction to microbes. Indeed, the detection of bacterial short-chain fatty acid by Or30a neurons acts as an orexigenic signal for the larvae (Depetris-Chauvin et al., 2017). Optimal identification of a given bacteria species presumably requires the integration of multiple sensory modalities. Consistently, when given the choice between a sugar only and an *E.c.c.*-contaminated solution, flies are first attracted by the bacteria and after few hours repulsed by it. While the initial attractive phase depends on the olfactory Gr63a neurons, the second repulsive phase requires the bitter taste Gr66a neurons. Interestingly, by providing a food source for the flies, *E.c.c.* facilitates the potentiation of bitter neurons allowing the avoidance behavior to be established (Charroux et al., 2020). Altogether, these data demonstrate the roles played by the fly sensory neurons in detecting environmental bacteria and mounting behaviors to either avoid them if they are toxic or, on the contrary, to move towards them when they are beneficial (**Figure 23**).

3.3.2 Bacteria-derived compounds can be sensed internally by D. melanogaster neurons

While the pleiotropic roles played by gut-associated bacteria in fly development and physiology are amply documented, their influence on behavior only begins to be elucidated (Lesperance and Broderick, 2020). By acting via the olfactory system, gut-associated bacteria can influence fly preferences in food-seeking and choice of egg-laying sites (Qiao et al., 2019; Venu et al., 2014; Wong et al., 2017). However, internal bacteria can also alter neuronally controlled behaviors independently of the sensory system. When compared to their conventionally reared sibling, axenic flies show enhanced locomotion (Schretter et al., 2018). Gut recolonization by *Lactobacillus brevis* is sufficient to bring locomotion back to normal levels. Genetic and biochemical data demonstrated that bacteria-produced xylose isomerase is critical to sustaining normal fly locomotion. Although the exact mechanisms involved remain unclear, xylose isomerase mediates its effects by inactivating the CNS neurons that produce octopamine. The same neuromodulator is central to another bacteria-induced behavior modification in the fruit fly. When mated females are infected by bacteria, they reduce their oviposition to spare the energy required to fight infection or to prevent progeny development in a non-favorable environment (Kurz et al., 2017). Previous work has revealed that during an immune response, the detection of bacteria-derived PGN by PGRP receptors triggers an NF-κB-dependent production of AMPs in immune cells (J. Royet and Dziarski, 2007). Surprisingly, the same bacterial elicitor and the same signaling pathway regulate the reduction of female oviposition following bacterial infection (**Figure 23**) (Kurz et al., 2017). Therefore, a unique bacteria cell wall constituent and a common host signaling cascade are used in immune cells to mount an immune response and in CNS neurons to control fly behavior following infection. Interestingly, the biogenic amine octopamine was also shown to mediate the effects that the endosymbiotic *Wolbachia* bacteria can exert on *D. melanogaster* male aggressivity (Rohrscheib et al., 2015). Finally, pathogens can also modulate host behavior to their advantage. By changing the pheromone levels in the frass of the flies they infect, *Pseudomonas entomophila* attracts healthy flies leading to their contamination and favoring pathogen dispersal (Keesey et al., 2017). Fly mating behavior can also be influenced by bacteria that are associated with the host. Isogenic *D. melanogaster* populations prefer mating with partners with similar microbiota. Although it has been proposed that gut-associated bacteria influence mating preferences by changing host sex pheromone levels, the exact mechanism is still unclear (Sharon et al., 2010).

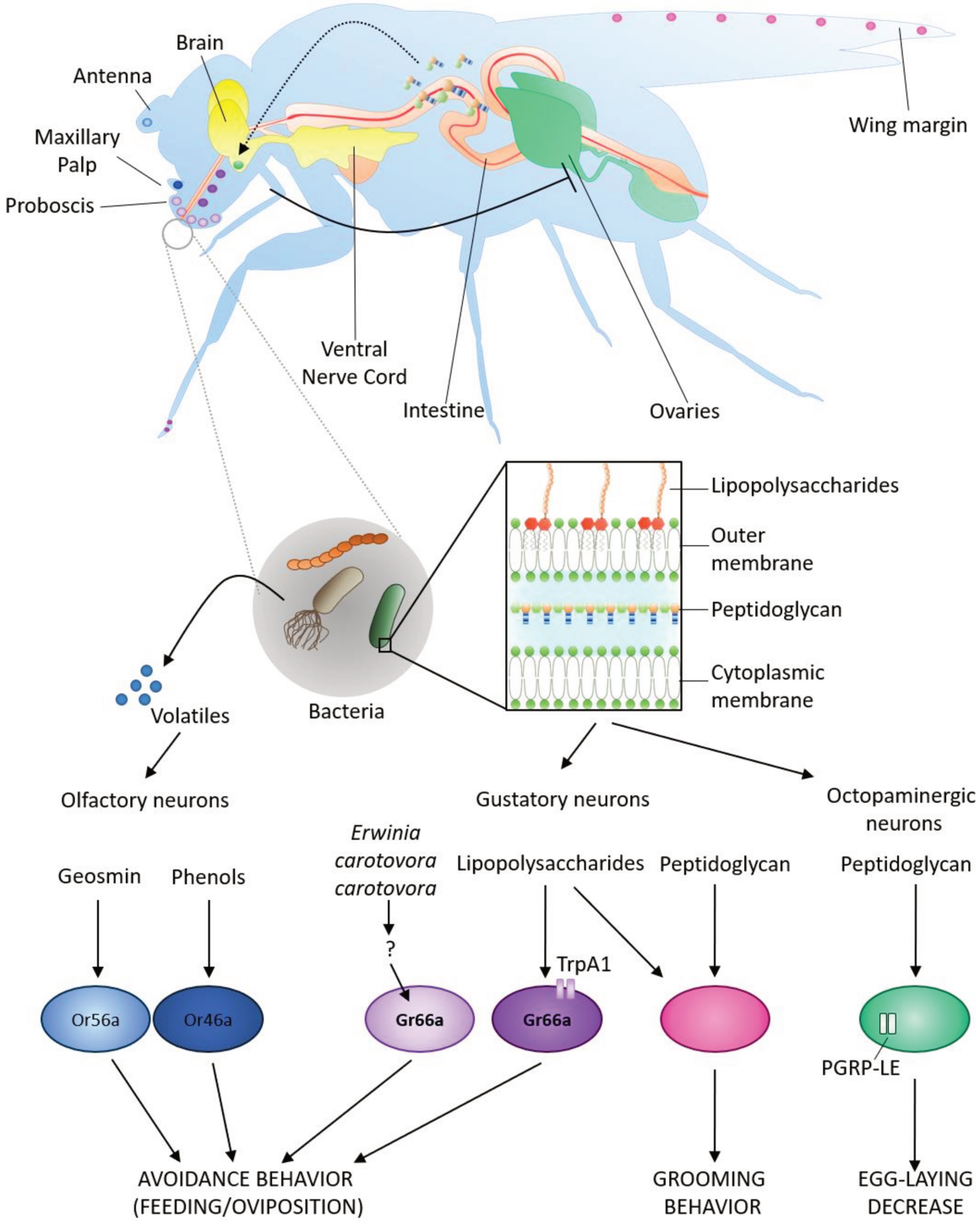

Figure 23. Interactions of bacteria with the *D. melanogaster* nervous system. Environmental bacteria produce metabolites and volatiles that can be directly sensed by the fly olfactory and gustatory neurons. The same is true for constituents of the bacteria cell wall, such as lipopolysaccharide (LPS) and peptidoglycan (PGN). Subsequent activation of sensory neurons induces host behavior changes such as bacteria avoidance or modulation in food intake, egg-laying rate or grooming.

3.3.3 Neuronal signaling influences fly cellular immunity

In *D. melanogaster*, professional phagocytes called plasmatocytes are mainly produced by the hematopoietic organ called the lymph gland and released into the blood. Their numbers and properties vary in response to developmental and environmental cues, some of which are of neuronal origin (Banerjee et al., 2019). Activin-β, a TGF-β family ligand that is expressed by sensory neurons of the peripheral nervous system, regulates the proliferation and adhesion of hemocytes. Agonist-mediated activation and transient silencing of these sensory neurons affect resident hemocyte numbers and localization (Makhijani et al., 2017). Environmentally-derived neuronal signals also control fly hematopoiesis. Activation of fly olfactory neurons leads to the secretion of GABA from neurosecretory cells into the circulation. Upon binding to its metabotropic receptors expressed on hematopoietic progenitors, GABA regulates the balance between maintenance and differentiation of these progenitors in the lymph gland (Shim et al., 2013). One candidate upstream sensor is the odorant receptor Or42 although the ligand(s) involved is still unknown. Neurons have also been implicated in connecting environmental gas level cues to myeloid differentiation. Both the inactivation of CO_2-sensing neurons and the stimulation of hypoxia-sensing neurons lead to an increase of Hypoxia-inducible factor-α in downstream neurons. In turn, these neurons release the JAK/STAT ligand Unpaired-3 which triggers Insulin-like peptide-6 production by the fat body cells. Once released into the circulation this hormone promotes crystal cell (one blood cell type) differentiation in the lymph gland (Cho et al., 2018). It would be of significant interest to decipher if and how bacterial infection directly modulates the activation of these olfactory and gas-sensitive neurons that function upstream of hematopoietic differentiation.

3.3.4 Proteins of the canonical immune system are expressed in D. melanogaster neurons

A role in the regulation of neuronal function and behavior by immune proteins has been reported in the fruit fly. In *D. melanogaster* neuromuscular junctions, perturbation of neurotransmitter receptors in the muscle cell enhances neurotransmitter release from the motor neuron, a phenomenon called presynaptic homeostatic potentiation (PHP). The immune pattern recognition receptor PGRP-LC and some downstream pathway components of the NF-κB/IMD pathway are required presynaptically to regulate PHP. However, the NF-κB/IMD signaling bifurcates downstream of the PGRP-LC receptor to achieve immediate modulation of the presynaptic release apparatus via the TGF-β activated kinase (TAK1), and prolonged maintenance of the homeostatic response via the transcription factor NF-κB/Relish (Harris et al., 2018; N. Harris et al., 2015). Since PHP has no obvious links with bacterial immunity, it is possible that PGRP-LC is activated at the synapse by an endogenous ligand. Besides

the regulation of neuronal function, the NF-κB/Relish protein has also been involved in sleep regulation. Together with other immune effectors, it turns out to be upregulated upon sleep deprivation (Williams et al., 2007). Consistently, flies mutant for NF-κB/Relish exhibit a reduced sleep period and, unlike their wild-type siblings, are unable to increase sleep upon bacterial infection (Kuo et al., 2010). Since both phenotypes are rescued by providing NF-κB/Relish in fat body cells, it is likely that NF-κB-regulated genes produced by fat body cells modulate sleep behavior. As mentioned above, the canonical NF-κB antibacterial pathway functions in neurons to regulate oviposition (Kurz et al., 2017). Although AMPs seem dispensable for this response (A.M., L.K. J.R. personal communication), they have been implicated in other neuronal activities. Nemuri, a peptide with antimicrobial properties expressed in few brain neurons is induced upon sleep deprivation. Flies in which Nemuri is overexpressed in neurons survive infection by *S. marcescens* or *S. pneumoniae* better than control flies. Nemuri could therefore act by prolonging sleep to promote fly survival after infection (Toda et al., 2019). Moreover, gain-of-function experiments suggest that when expressed in neurons (Drosocin) or glial cells (Metchnikowin) some AMPs could contribute to resilience to sleep deprivation (Dissel et al., 2015). Finally, genetic inactivation of Achilles, a neuronal gene showing a highly rhythmic expression pattern, results in dramatically high levels of immune response effectors, including AMPs (Li et al., 2017). As a result, flies are more resistant to immune challenge with bacteria. Other biological effects of immune genes on nervous function include memory formation. Diptericin B and the bacteria sensor GNBP-like3 are upregulated following behavioral training. Knock-down experiments revealed that while they both regulate long-term memory, Diptericin B functions in the head fat body and GNBP-like3 in neurons to prevent memory deficit (Barajas-Azpeleta et al., 2018). AMPs are produced as a result of immune stimulation, so it can be imagined that the formation of memories related to the event that determined their production may be beneficial for the fly. In contrast to previous examples, recent reports revealed that AMPs may also play a role in neurodegenerative diseases. Indeed, AMP accumulation has been shown to induce neuronal damage in flies. Hyperactivation of innate immunity in the brain as a result of genetic mutations or bacterial injection causes neurodegeneration linked to the neurotoxic effects of AMPs (Cao et al., 2013). With age, flies present an NF-κB-dependent constitutive AMP gene expression in glial cells which is accompanied by progressive neurodegeneration and locomotion decline (Kounatidis et al., 2017). Similarly, aging-associated expression of the AMP NLP-29 causes dendrite degeneration in *C. elegans*. By activating the orphan GPRC NPR-12, NLP-29 induces autophagy to mediate aging-associated dendrite degeneration, a mechanism also observed after infection by the fungus *Drechmeria coniospora* (E et al., 2018). This finding supports the existence of signaling pathways possibly linking microbial defense to degeneration. The growing number of immune proteins and

pathways involved in neuronal functions raises the broader question of how precisely should one delineate the range of phenomena to be considered strictly as immune response, and whether the definition of an immune cell should be expanded or reconsidered.

3.5 Impact of bacterial exposure on mammal nervous system and behavior

The crosstalk between the nervous and immune systems is a feature also found in vertebrates. In humans and other mammals, gut microbiota strongly influences brain physiology, behavior, neurodegenerative and neuropsychiatric disorders. The gut-brain axis has been implicated in pain, mood, depression, anxiety and other diseases (Foster and McVey Neufeld, 2013; Järbrink-Sehgal and Andreasson, 2020; Sauma and Casaccia, 2020). In mammals, sensory neurons express PRRs, such as Toll-like receptors (TLRs), that directly detect bacteria compounds (**Figure 24**) (Donnelly et al., 2020). Bacterial metabolites are sensed by sensory neurons, such as olfactory or nociceptive sensory neurons, modifying in this way host behavior (Yang and Chiu, 2017). N-formylated peptides are produced by mitochondria and bacteria and, in mammals, are recognized by GPCRs named formyl peptide receptors (FPRs). These molecules are strong elicitor of the cellular immune response (Le et al., 2002). Moreover, N-formylated peptides mediated bacterial recognition by sensory neurons. In mice, FPRs have been found expressed in olfactory neurons of the vomeronasal organ (VMO) (Liberles et al., 2009; Rivière et al., 2009). These neurons have been shown to respond *ex vivo* to *E.coli*-derived formyl peptide, suggesting that also mammals might use their olfactory system to detect potentially harmful bacteria (Rivière et al., 2009).

Some bacterial infections, such as skin or enteric infections by S. *aureus* and *Salmonella enterica* respectively, cause pain., It was initially thought that infection-related pain is a consequence of inflammation. More recently, Chiu *et al.* uncovered two mechanisms by which bacterial detection by nociceptive sensory neurons (known as nociceptors) mediates pain. First, nociceptors are activated by the detection of *S. aureus*-derived N-formylated peptide through the receptor FPR1. The inactivation of this receptor is sufficient to reduce pain. Also, *S. aureus* releases the toxin α-hemolysin, which by binding the nociceptor receptor ADAM10 forms pores at the membrane. The action of this toxin leads to cation influx and consequent neuronal firing (Chiu et al., 2013). Furthermore, nociceptors detect bacterial LPS via two independent receptors: TLR4 and TRPA1 (Diogenes et al., 2011; Ferraz et al., 2011; Meseguer et al., 2014). In the dental pulp, LPS recognition by TLR4 activates trigeminal nociceptor and triggers TRPV1 sensitization, increasing neuronal firing (Diogenes et al., 2011). Moreover, recognition of LPS via TRPA1 leads to nociceptor depolarization

and mediates local inflammation and mechanical hyperalgesia (Meseguer et al., 2014). Intriguingly, TRPA1 seems to be a conserved receptor for LPS among metazoans (Meseguer et al., 2014; Soldano et al., 2016). Also, some bacteria might hide from the host immune system by decreasing pain sensation. It is the case of *Mycobacterium ulcerans,* which causes painless skin lesions and ulcers. By releasing an antagonist (mycolactone) of nociceptor type 2 angiotension II receptors (AT2Rs), this bacterium provokes the nociceptor hyperpolarization and analgesia (Marion et al., 2014).

In mammals, neurons can also modulate the immune response to pathogens (Chu et al., 2020). Neurotransmitters and neuropeptides released by neurons are recognized by receptors expressed in immune cells (Godinho-Silva et al., 2019). Nociceptors release neurotransmitters and neuropeptides at the synaptic termini in the CNS to modulate behavior and at the level of the termini that innervate the periphery to modulate immune cells. Activation of nociceptors by noxious stimuli leads to signalization to the CNS. The signal can propagate back to the periphery along neighboring axons of the same neuron, leading to the release of neuronal molecules which are sensed by immune tissues (Chiu et al., 2012).

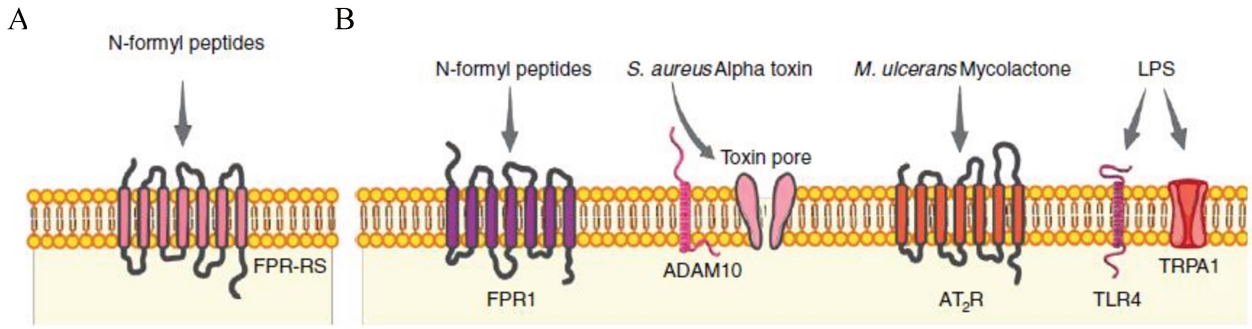

Figure 24. PRRs in sensory neurons in mammals. **A** Olfactory sensory neurons express FPRs for N-formyl detection. **B** Expression of PRRs in nociceptors. Figure adapted from (Yang and Chiu, 2017).

Recent researches have focused on neuro-immune modulation (**Figure 25**). For instance, cholinergic neurons in the gut and lung release a neuropeptide called NMU, which is recognized by the receptor NMUR1 in type 2 innate lymphoid (ILC2) cells and is required for helminth expulsion. Indeed NMU rapidly activates ILC2 cells and induce the production of cytokines that recruit eosinophils (Cardoso et al., 2017; Klose et al., 2017; Wallrapp et al., 2017). On the other hand, the release of neuropeptides can also negatively regulate the activity of immune cells (Moriyama et al., 2018; Nagashima et al., 2019). The neuropeptide CGRP acts on ILC2 cells to inhibit them and in turn, reduce helminth

clearance (Nagashima et al., 2019). Also, enteric neurons produce the cytokine IL-8, which by acting in Goblet cells, induce AMP production against *Salmonella typhimurium* infection (Jarret et al., 2020). Gut sympathetic neurons involved in stress response signal through norepinephrine (NE) to muscularis macrophages and ILC2 cells to modulate their response to bacterial and helminth infection. NE action on muscularis macrophages leads to a tissue-protective response to infection by preventing neuronal loss. NE action on ILC2 cells triggers cytokine production and helminth elimination (Gabanyi et al., 2016; Matheis et al., 2020). Bacteria can also use strategies to turn this neuro-immune interaction to their favor. *Streptococcus pyogenes* releases the toxin streptolysin S, which forms pores on the membrane of nociceptors, leading to pain. Activation of nociceptors by this bacterium also leads to the release of calcitonin gene-related peptide (CGRP), which acts on immune cells and inhibits neutrophil recruitment and thus bacteria clearance (Pinho-Ribeiro et al., 2018).

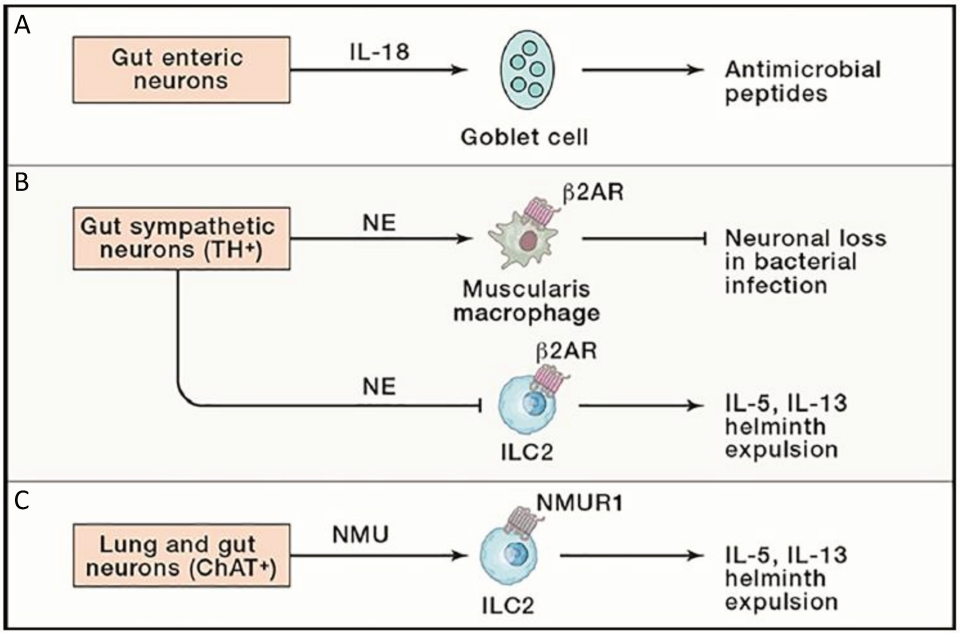

Figure 25. Neurons modulate the immune response. A IL-8 released by enteric neurons acts in Goblet cells to induce AMP production. **B** Norepinephrine (NE) released by gut sympathetic neurons acts on immune cells to prevent neuronal loss and produce cytokines. **C** Cholinergic ($ChAT^+$) neurons secrete NMU, which by acting on ILC2 cells, induces cytokine production. Figure adapted from (Chu et al., 2020).

Aims of the thesis

In nature, animals thrive in an environment with constant exposure to bacteria and other micro-organisms. The infection by harmful bacteria triggers in the host a robust immune response against the invading agent. In addition to canonical immune responses, animals, including insects, can adapt their behavior to avoid to be infected or to reduce the infection's effects. However, while anti-bacterial immune responses are well described, little is known about the molecular and cellular mechanisms that underline bacteria-induced behavioral modifications.

During my thesis, I studied the potential links between bacteria or bacterial-derived PGN, behavioral changes and immune signaling cascades in *D. melanogaster*. The fruit fly has been used for more than 30 years to decipher the molecular pathways orchestrating the innate immune responses. Studies in this model have highlighted the crucial role of the PGRP-mediated bacterial PGN recognition in the activation of the immune response. Moreover, *D. melanogaster* offers many advantages to study behavior. The available genetic tools allow to target specific cells and genes and perform functional studies. Its relatively simple and well-characterized CNS allows the precise mapping of neuronal circuits that underly behaviors. Moreover, like all insects, *D. melanogaster* displays a large repertoire of behaviors, which have been amply described.

The first project I worked on aimed at understanding how *E.c.c.* infection impacts the behavior of *D. melanogaster* larvae and at revealing the molecular players involved in this modulation (**Article 1**).

Previous work from the lab has shown that bacterial-derived PGN induces a decrease in egg-laying in *D. melanogaster* females. This response is mediated by the activation of the IMD/NF-κB pathway in octopaminergic neurons (Kurz et al., 2017). The second aim of my thesis was to identify the specific neuronal subset required for this behavioral response and to understand the mechanism by which bacterial PGN is sensed by these neurons (**Article 2**).

The third aim of my thesis was to identify other PGN sensing neurons, determine the mechanism(s) by which these neurons sense PGN and study their implication in behavior modulation (**Manuscript 3**).

The results I obtained during these years have been published (**Article 1** and **Article 2**) or have been submitted and are currently under review (**Manuscript 3**). In the following pages, I will present the results obtained during my thesis in the form of articles.

Article 1

Journal of Insect Physiology 99 (2017) 25–32

Contents lists available at ScienceDirect

Journal of Insect Physiology

journal homepage: www.elsevier.com/locate/jinsphys

Drosophila larvae food intake cessation following exposure to *Erwinia* contaminated media requires odor perception, *Trpa1* channel and *evf* virulence factor

Seydou Keita [1], Ambra Masuzzo [1], Julien Royet, C. Leopold Kurz *

Aix-Marseille Université (AMU), Centre National de la Recherche Scientifique (CNRS), UMR 7288, Institut de Biologie du Développement de Marseille (IBDM), 13288 Marseille cedex 9, France

ARTICLE INFO

Article history:
Received 20 October 2016
Received in revised form 31 January 2017
Accepted 16 February 2017
Available online 21 February 2017

Keywords:
Drosophila
Behavior
Olfaction
Food-intake
Bacteria

ABSTRACT

When exposed to microorganisms, animals use several protective strategies. On one hand, as elegantly exemplified in *Drosophila melanogaster*, the innate immune system recognizes microbial compounds and triggers an antimicrobial response. On the other hand, behaviors preventing an extensive contact with the microbes and thus reducing the risk of infection have been described. However, these reactions ranging from microbes aversion to intestinal transit increase or food intake decrease have been rarely defined at the molecular level. In this study, we set up an experimental system that allowed us to rapidly identify and quantify food intake decreases in *Drosophila* larvae exposed to media contaminated with bacteria. Specifically, we report a robust dose-dependent food intake decrease following exposure to the bacteria *Erwinia carotovora carotovora* strain *Ecc15*. We demonstrate that this response does not require *Imd* innate immune pathway, but rather the olfactory neuronal circuitry, the *Trpa1* receptor and the *evf* virulence factor. Finally, we show that *Ecc15* induce the same behavior in the invasive pest insect *Drosophila suzukii*.

© 2017 Elsevier Ltd. All rights reserved.

1. Introduction

In the wild, animals facing microbes have to rapidly appreciate the threat and react accordingly. In order to understand these complex interactions at the molecular level, the insect *Drosophila melanogaster* has been extensively and successfully used (Lemaitre and Hoffmann, 2007). Indeed, large amounts of transparent larvae can be infected following exposure to a food source contaminated with bacteria leading to a natural infection (Vallet-Gely et al., 2008). In this context, the Gram negative bacteria *Erwinia carotovora carotovora* (*Ecc15*) has been frequently used as it is a natural insect pathogen that induces host innate immunity, is genetically tractable and innocuous to mammals (Basset et al., 2000).

One facet of the *Drosophila* larvae response to microorganisms is innate immunity whose induction leads to production of molecules with antimicrobial properties. When exposed to Gram negative bacteria such as *Ecc15*, the peptidoglycan (PGN) released by the microbe when dividing or lysed triggers the Immune deficiency signaling cascades (IMD) and the subsequent production of antimicrobial peptides (AMP). PGRP-LC and PGRP-LE, that can bind PGN, are the upstream receptors of this cascade which signal through the caspase Dredd and *in fine* trigger NF-kB-like transcription factor Relish nuclear translocation (Lemaitre and Hoffmann, 2007; Charroux and Royet, 2012).

Moreover, reactive oxygen species (ROS) are produced by intestinal epithelial cells when exposed to bacteria. Precisely, uracil secreted by organisms including *Ecc15* is specifically recognized and induces a massive burst of ROS (Bae et al., 2010; Lee et al., 2013). In addition to these well-studied molecular responses, exposure to microbes also induces innate behaviors such as aversion (Stensmyr et al., 2012; Soldano et al., 2016), food intake decrease (Liehl et al., 2006) or intestinal transit increase (Du et al., 2016). This behavioral immunity represents a first line of defense that can prevent the animal from being in contact with a microbe or limit the duration of the contact, thus reducing the risk of being infected.

While observed and described in many animal species, these specific behaviors have been rarely deciphered at the molecular level from the host side as well as from the microbial side.

In this study, we present an experimental system to rapidly identify conditions influencing food intake in *Drosophila* larvae following bacterial contamination. On one hand, we demonstrate that

* Corresponding author.
E-mail address: leopold.kurz@univ-amu.fr (C.L. Kurz).
[1] These authors contributed equally to this work.

http://dx.doi.org/10.1016/j.jinsphys.2017.02.004
0022-1910/© 2017 Elsevier Ltd. All rights reserved.

exposure to *Ecc15* leads to a dose-dependent robust food intake decrease that neither requires the IMD signaling cascade nor uracil production by the bacteria. On the other hand, we identify the olfactory system, the *Drosophila Trpa1* channel and the *evf* virulence factor as being necessary for this food intake decrease, a phenomenon also conserved in the pest insect *Drosophila suzukii*.

2. Materials and methods

2.1. Bacterial strains and maintenance

For this study, the following bacterial strains were used: *Erwinia carotovora carotovora* 15 *2141* (*Ecc15*) (Basset et al., 2000), *Ecc15 PyrE::Tn5* (Lee et al., 2013), *Ecc15 evf* mutant (Basset et al., 2003) (obtained from F. Leulier), *Escherichia coli* (Dh5α Electromax, Invitrogen), *Pseudomonas aeruginosa* (PA14) (Rahme et al., 1995), *Serratia marcescens* (DB10) (Flyg et al., 1980). All the strains were grown in Luria-Bertani liquid media (LB) at 37 °C except *Ecc15* at 30 °C and shacked at 200 rpm. To concentrate bacteria and reach the requested OD, 250 mL overnight cultures were centrifuged 15 min at 2250 rcf, OD at 600 nm was measured and bacteria were diluted in PBS medium to the desired concentration.

2.2. Drosophila strains and maintenance

Adult flies and larvae were grown at 25 °C on standard yeast/-cornmeal medium supplemented with antibiotics in 12 h/12 h light/dark cycle controlled incubators. For 1 Liter of standard media, 8.2 g of agar (VWR, cat. #20768.361), 80 g of cornmeal flour (Westhove, Farigel maize H1) and 80 g of yeast extract (VWR, cat. #24979.413) were cooked for 10 min in boiling water. 5.2 g of Methylparaben sodium salt (MERCK, cat. #106756) and 4 mL of 99% propionic acid (CARLOERBA, cat. #409553) were added when the food had cooled down. For antibiotics, standard medium was supplemented with Ampicillin, Kanamycin, Tetracycline and Erythromycin at 50 μg/mL final concentrations. Media with antibiotics was used for stocks maintenance and larvae amplification in order to avoid any putative influence of the microbiota during the feeding assay experiments.

The following fly genotypes were used: OregonR (wild-type); CantonS (wild-type); *yw; w-*; *PGRP-LE*^{112} (Kaneko et al., 2004), *PGRP-LC*$^{\Delta E12}$ (Gottar et al., 2002) double mutant; *Dredd*^{D55} mutant (Leulier et al., 2000); *Relish*^{E20} mutant (Hedengren et al., 1999); *Orco*^{2} mutant (Larsson et al., 2004); *Trpa1*^{1}*; Df*(3R)ED5156 and *Drosophila suzukii* (kindly provided by B. Prudhomme).

2.3. Feeding-assay

For the feeding assay, L3 larvae were harvested from standard media using PBS, gently washed for 30 s in PBS then added using a brush to the container with the feeding-assay media composed of 20% yeast paste, 2% blue dye (blue food dye E133, 'Le meilleur du chef') and PBS 1X with (test) or without (control) bacteria or molecules. The assay is performed with 400 μL of feeding-assay media in an empty plastic fly tube as a container (VWR). Between 50 and 150 larvae are used per tube. Tubes are then sealed with parafilm and kept at 23 °C in the dark for the desired amount of time. Finally, larvae are harvested from assay tubes with PBS, washed 30 s with PBS then blue and white animals are counted. DTT (Invitrogen) was mixed to *Ecc15* to reach a final DTT concentration of 10 mM and a final *Ecc15* OD of 100. Uracil (Sigma) was freshly diluted in water and mixed to the dyed food to reach the desired concentrations; the assay was performed the same day.

2.4. Intestinal dye content measurements

The dye concentration in the food intake assay media was increased to 5% and larvae fed on the food intake assay media without dye were used as blank. The intestines were dissected in cold PBS1X. Five intestines per condition were transferred to 1.5 mL canonical tubes (VWR #16466-064) containing 0,75–1 mm glass beads (Retsch #22.222.0004) and 50 μL PBS1X then ground automatically using a grinder (Precellys® 24). Afterwards, the lysates were centrifuged at 15000 rpm and the OD at 630 nm was measured using a Nanodrop (Thermo Scientific™ NanoDrop™ 1000).

2.5. Preparation of heat killed bacteria

Pellet of centrifuged bacteria were diluted in PBS1X to reach the desired concentrations (*i.e.* OD50 and OD100). Afterwards, bacteria were heat killed by incubating the organisms at 90 °C for 10 min.

2.6. Preparation of supernatant

The supernatant from centrifuged bacterial culture was filtered (0,2 μm filters) and added to the dyed media. LB liquid media was added to the dyed food as control.

2.7. Colony-forming units (CFU) counting

The dyed media was prepared as previously described, without bacteria (control) or with *Ecc15* at an OD of 100. To not exclude the possibility of an effect of the larvae in the bacterial concentration, L3 staged larvae were added to the media. 50 μL of the media were collected at different time points (0 h, 1 h, 2 h, 4 h and 8 h). Bacterial counts were obtained by plating adequate dilutions of the media. 100 μL of the diluted media were plated in LB agar medium containing rifampicin. Plates were incubated at 30 °C for 24 h before the CFU counting. To exclude the possibility of contaminations due to the presence of the yeast in the media, we plated also the media without *Ecc15*.

2.8. Re-feeding assay

Larvae were left on media without bacteria or with *Ecc15* at an OD of 100 for 4 h. In both cases, the media did not contain dye. After 4 h, larvae have been washed with PBS1X and added in tubes containing media with fresh *Ecc* at an OD of 100 for 1 h. Afterwards, the counting of blue and white larvae was performed. As control, we counted larvae which were left in 2% dyed media without bacteria or with *Ecc15* at an OD of 100 for 5 h.

2.9. Pictures

Larvae were pictured after having been harvested and washed in PBS1X using a LEICA MZ FLIII binocular, Hamamatsu color camera and AxioVision 4.8 software.

2.10. Statistics

Ratios for fed and unfed animals were determined for each independent experiment. Then, the averages of the percentages of fed animals from several independent experiments were calculated and compared among treatments using the Prism software (GraphPad) and an unpaired Student *t*-test. P values below 0.05 were considered as statistically significant.

3. Results

3.1. Drosophila larvae reduce their food intake when exposed to Erwinia carotovora carotovora

In order to rapidly evaluate and quantify food intake defects in the transparent *Drosophila* larvae, we used two protocols. First, a rapid and stringent system allowing the screening of conditions impacting food intake was established. Late L3 larvae were fed yeast paste containing 2% blue dye for 1 h (see methods). In these conditions, more than 90% of the animals are blue and considered as fed (Fig. 1A and B). Molecules or bacteria such as *Erwinia carotovora carotovora* can be added to this control media at various concentrations. With a final optical density of 100 for *Ecc15* (*Ecc15*_100), we observed that larvae drastically diminished their food intake with 5% of the animals having dyed food in the intestine after 1 h (Fig. 1A and B). Based on this robust and highly reproducible phenotype, we developed a secondary test with 5% blue dye, a concentration necessary to confirm screening results via spectrophotometry (see methods). With a 5% blue dye set-up, spectrophotometry quantifications of large populations confirmed that larvae fed with *Ecc15* have an important food intake drop (Fig. 1C and D) with an OD related to the amount of food within the intestine divided by five when the media is contaminated with *Ecc15*_100. Thus, using a convenient screening method later confirmed by spectrophotometry, we demonstrated that *Drosophila* larvae strongly reduce their food-intake when exposed 1 h to the bacteria *Ecc15*. For the next steps of the study, we used the 2% blue dye and bacteria with a final OD of 50 or 100 for screening conditions and the 5% blue dye test to confirm interesting hits via spectrophotometry.

3.2. Drosophila larvae food-intake drop is Ecc15-specific, dose-dependent and requires the evf virulence factor

The feeding arrest consecutive to *Ecc15* exposure can either correspond to an effect of the bacteria on the animal independently of its ability to sense the bacteria or to a reaction of the host that has detected the bacteria. We first tested whether the effect was *Ecc15*-specific or related to virulence. We measured food intake in larvae exposed to Gram negative bacteria other than *Ecc15* such as *Escherichia coli* strain Dh5α, *Serratia marcescens* strain Db10 (Flyg et al., 1980) and *Pseudomonas aeruginosa* strain PA14 (Rahme et al., 1995; Apidianakis and Rahme, 2009; Igboin and Griffen, 2012)). Importantly, while *Serratia* and *Pseudomonas* are highly pathogenic, *E. coli* Dh5α is innocuous. Interestingly, our quantifications showed that although DH5α at an OD of 100 (*E. coli*_100) significantly reduced the food intake (70% of fed larvae compared to 92% for controls), this effect was minor compared to the 10% larvae with dyed food in the gut quantified with animals exposed to *Ecc15* at the same OD (Fig. 2A). Moreover, among the media contaminated with virulent bacteria, only *Pseudomonas* at an OD of 100 (*Pseudomonas*_100) triggered a significant decrease (68% of fed larvae), a reduction comparable to the drop measured with the avirulent *E. coli* and less marked than with *Ecc15*_50 or *Ecc15*_100 (Fig. 2A). Therefore, exposure of *Drosophila* larvae for 1 h to Gram negative bacteria significantly reduced their food-intake, but this host reaction is more important upon exposure to *Ecc15*.

In order to characterize the reaction of the host, we focused on the interaction between *Drosophila* and *Ecc15*. Considering that a molecule of microbial-origin sensed by the host or acting on it might act in a dose-dependent manner, we tested the feeding behavior of animals in media contaminated with *Ecc15* concentrations ranging from OD 1 (*Ecc15*_1) to OD 100 (*Ecc15*_100). We observed that while *Ecc15*_1 did not impair feeding (78% fed larvae versus 89% for control), *Ecc15*_10, *Ecc15*_50 and *Ecc15*_100 significantly impacted the population with 45%, 38% and 6% fed larvae, respectively (Fig. 2B and C). In order to control whether the food intake cessation following exposure to *Ecc15* was a behavior observed in genetic backgrounds other than Oregon and commonly used as wild-type, we assayed *yw*, *w*- and CantonS animals. Importantly, all these lines robustly reduced their food intake following exposure to *Ecc15*_50 and *Ecc15*_100 (Supplementary Fig. 1A).

Moreover, exposing larvae to heat-killed bacteria or filtered culture supernatant did not trigger the food intake cessation demonstrating that live *Ecc15* bacteria are necessary (Supplementary Fig. 1B–D). The blockage being of 90% with *Ecc15*_100 after 1 h, we wondered whether longer exposure times would exacerbate the phenotype. For this purpose, we exposed larvae to *Ecc15*_100 for 1 h, 2 h, 4 h and 8 h. Surprisingly, we noted that despite chronic exposure to *Ecc15*_100, the percentage of fed larvae increased significantly over time with 6%, 17%, 59% and 63% of fed animals after 1 h, 2 h, 4 h and 8 h, respectively (Fig. 2D). However, the difference in food uptake after 8 h exposure to *Ecc15*_100 was still significantly different from control animals exposed for 8 h to control media. Thus, *Ecc15*_100 is blocking the feeding behavior of almost all *Drosophila* larvae in a population, an effect that is transient and not fully reversed after 8 h. These observations indicated that either the amount of live bacteria declined over time during the assay or that larvae exposed to *Ecc15* for more than 1 h change their behavior. To address these questions, we quantified the amount of live *Ecc15* in our assay tubes containing larvae over a time period of 8 h. Strikingly, we observed that half the amount of initial bacteria remained alive after 4 h and 8 h (Supplementary Fig. 2A). In addition, we demonstrated that adding fresh *Ecc15* to larvae starting to eat again after having been exposed to *Ecc15* for 4 h could trigger a robust food intake cessation (Supplementary Fig. 2B). Consequently, the phenotype is certainly temporary during the long exposure due the bacterial decline in the media. While highly pathogenic bacteria such as *P. aeruginosa* or *S. marcescens* failed to trigger an important food intake cessation compared to *Erwinia*, we wondered whether the specificity of the *Ecc15*-induced behavior could be related to its virulence. A previous report identified the *evf* gene as an important virulence factor of *Ecc15* using forward genetic screens and *Drosophila* larvae as a host (Basset et al., 2003; Acosta Muniz et al., 2007). Thus, we compared the food intake cessation triggered by either *Ecc15* or *Ecc15 evf* mutant. Importantly, despite not being totally abolished as for animals fed with heat-killed bacteria (Supplementary Fig. 1B), the phenotype was less marked when larvae were exposed to *Ecc15 evf* mutant compared to *Ecc15* with 30% and 57% of fed larvae on *Ecc15*_100 and *Ecc15_evf*_100, respectively (Fig. 2E). The same trend was observed with the 5% blue dye and confirmed using spectrophotometry (Supplementary Fig. 3A and B). Taken together, these results suggested that *Drosophila* larvae are blocking their food intake when exposed to avirulent and virulent Gram-negative bacteria and that *Ecc15* is extremely potent to induce this process in an *evf* and dose-dependent manner.

3.3. Larval Ecc15-induced food intake drop is independent of the IMD pathway and does not require bacterial uracil

Ecc15 has been widely used as an inducer of the *Drosophila* innate immune response and more specifically of the IMD pathway (Lemaitre and Hoffmann, 2007; Charroux and Royet, 2012). We tested whether the IMD signaling cascade was required in the host for the food intake decrease upon exposure to bacteria. We compared the feeding activity of wild-type (WT) animals and IMD pathway mutants when fed with media contaminated with

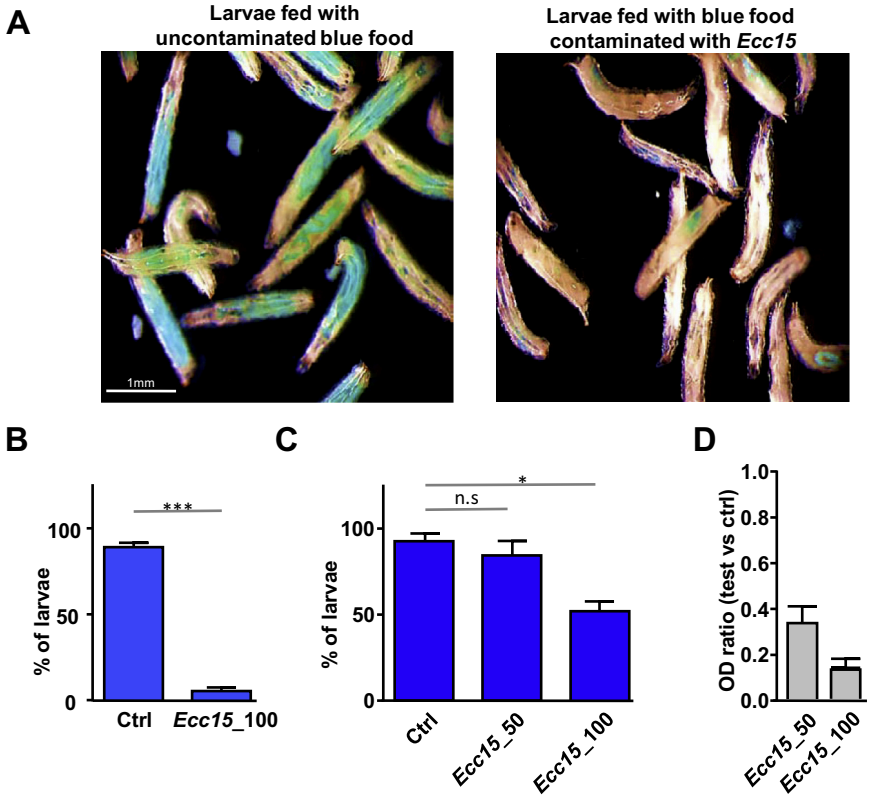

Fig. 1. Exposure to *Ecc15*-contaminated food reduces *Drosophila* larvae food-intake. (A) Pictures of L3 stage larvae fed 1 h with a media containing a blue dye (2%) to quantify the food-intake; media uncontaminated (left panel) or *Ecc15*-contaminated with a final OD of 100 (right panel). (B) Graphic representing the feeding percentage for larvae following 1 h exposure to uncontaminated food (Ctrl) or *Ecc15*_100 contaminated media. The whole animal population corresponds to 100% and the percentage of larvae with distinguishable dye within the intestine, considered as fed larvae, is represented (blue bar). The media contains a 2% blue dye. (C) Feeding percentage for WT animals fed 1 h without (Ctrl) or with *Ecc15* at a final OD of 50 (*Ecc15*_50) or 100 (*Ecc15*_100). The media contains a 5% blue dye. (D) Graphic representing the OD (630 nm) ratio between dissected intestine from larvae fed 1 h with a 5% blue dyed media contaminated (test) or not (Ctrl) with either Ecc_50 or Ecc_100. For B and C; shown is the average feeding percentage ± SEM from at least 3 independent trials with at least 250 larvae per genotype and condition used. For D; shown is average OD ratio ± SEM from at least 3 independent trials with at least 50 dissected intestines per genotype and condition used. * indicates $p < 0.05$; *** indicates $p < 0.001$; n.s. indicates $p > 0.05$, unpaired two-tailed Student-*t* test. (For interpretation of the references to colour in this figure legend, the reader is referred to the web version of this article.)

*Ecc15*_50 and *Ecc15*_100. We used mutants for: the peptidoglycan receptors PGRP-LC and PGRP-LE, the caspase Dredd and the NF-κB-like transcription factor Relish. All these mutants represent elements of the IMD pathway and have been previously shown as being unable to produce antimicrobial peptides following exposure to Gram-negative bacteria (Kaneko et al., 2004; Gottar et al., 2002; Leulier et al., 2000; Hedengren et al., 1999; Capo et al., 2016). When exposed to *Ecc15*_50 or *Ecc15*_100, these mutants were indistinguishable from the WT animals with severe and significant food intake impairments (Fig. 3A and B).

Therefore, the canonical IMD pathway is not required for *Drosophila* larvae to induce the food-intake blockage following exposure to *Ecc15*. Another innate immune pathway involves the perception of the uracil produced by bacteria, including *Ecc15*, and leads to the massive production of ROS. Consistently, exogenously provided uracil can trigger ROS production and an *Ecc15* mutant (*Ecc15 PyrE::Tn5*) that does not produce uracil no longer induces ROS production in fly gut (Lee et al., 2013). Finally, it has been observed that when exposed to *Ecc15*, larval intestinal transit is increased, an effect that requires the ROS produced following uracil perception and can be countered when the reducing agent Dithiothreitol (DTT) is added (Du et al., 2016; Lee et al., 2013). Consequently, we tested whether the perception of uracil was the trigger of the feeding arrest phenotype observed when larvae were exposed to *Ecc15*. As shown on Fig. 3C, uracil exogenously added to the media even at a concentration of 500 μM did not impair food intake relative to control. In addition, exposure to the *Ecc15 pyrE::Tn5* mutant at an OD of 100 significantly blocked food intake with 8% of fed larvae. Finally, DTT treatment of *Ecc15*_100 exposed larvae did not rescue the phenotype with 10% of the animals containing the dyed food in their intestine compared to 85% in control conditions. Taken together, we can conclude that neither the IMD pathway nor uracil perception in the host are required for the food intake blockage following exposure to *Ecc15*.

3.4. Food intake diminution following Ecc15 exposure requires the olfactory system and the Trpa1 channel

Drosophila possesses a complex olfactory system allowing animals to seek food and to avoid noxious components (Stensmyr et al., 2012). Numerous olfactory receptors (OR) have been identified (Vosshall, 2000) and they all need a co-receptor named *Orco* whose mutant is odor-irresponsive. Strikingly, while exposing WT animals to *Ecc15*_50 contaminated food led to 43% of fed larvae compared to 91% in control conditions, $Orco^2$ mutants did not reduce the food intake when exposed to bacteria (87% fed larvae on *Ecc15*_50 compared to 94% on control conditions) (Fig. 4A, B and Supplementary Fig. 4A–C). This observation was confirmed using 5% blue dye, spectrophotometry and *trans*-heterozygote animals having one $Orco^2$ allele and a deficiency covering the *Orco* gene (Supplementary Fig. 4B and C). Therefore, food-intake drop in *Drosophila* larvae following exposure to *Ecc15*-contaminated media was dependent on the olfactory system. This suggests that

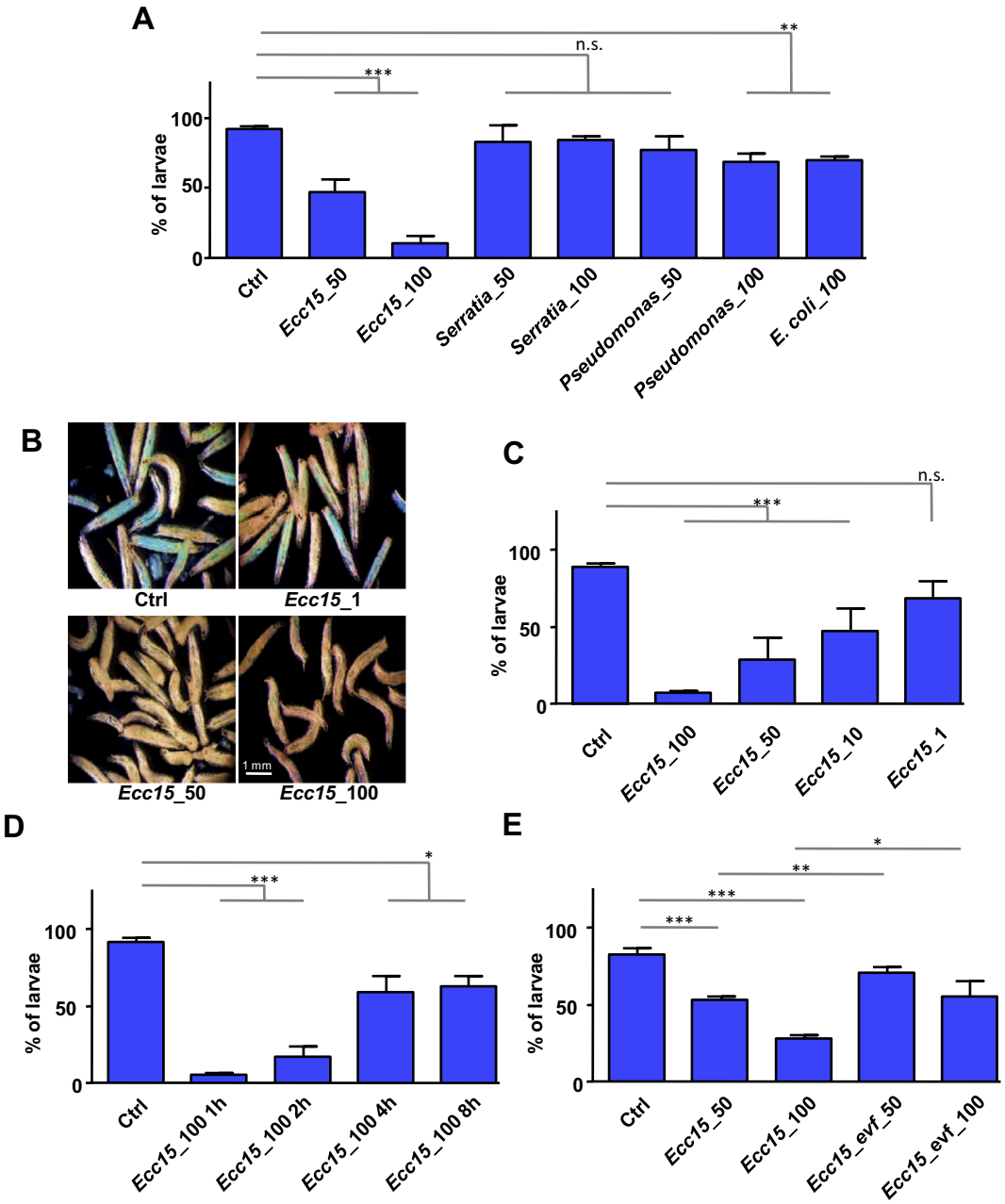

Fig. 2. Food-intake decrease following exposure to bacteria is *Ecc15*-specific, dose-dependent and temporary. (A) Feeding percentage for WT animals fed 1 h with a 2% blue dyed media without bacteria (Ctrl) or contaminated with *Ecc15* (*Ecc15*_50 and *Ecc15*_100), *S. marcescens* (*Serratia*_50 or *Serratia*_100), *P. aeruginosa* (*Pseudomonas*_50 or *Pseudomonas*_100) and *E. coli* (*E. coli*_50 or *E. coli*_100). (B) Pictures of L3 stage larvae fed 1 h with a 2% blue dyed media without (Ctrl) or with *Ecc15* at various final concentrations. (C) Feeding percentage for WT animals fed 1 h with a 2% blue dyed media without bacteria (Ctrl) or with *Ecc15* at various final concentrations. (D) Feeding percentage for WT animals fed 1 h, 2 h, 4 h or 8 h with a 2% blue dyed media without bacteria (Ctrl) or with *Ecc15*_100. As the percentage of fed animals after 1 h on Ctrl medium was not impacted by longer exposure, 1 h exposure is used as the reference. (E) Feeding percentage for WT animals fed 1 h with a 2% blue dyed media without bacteria (Ctrl), with *Ecc15* or *Ecc15* mutant for *evf* (*Ecc15_evf*) at OD50 and OD100 final concentrations. For A, C, D and E; shown is the average feeding percentage ± SEM from at least 2 independent trials with at least 100 larvae per genotype and condition used. *indicates $p < 0.05$; **indicates $p < 0.01$; ***indicates $p < 0.001$; n.s. indicates $p > 0.05$, unpaired two-tailed Student-*t* test. (For interpretation of the references to colour in this figure legend, the reader is referred to the web version of this article.)

a molecule produced by the bacteria and *Ecc15*-specific is rapidly perceived by the animal and triggers the feeding arrest behavior.

In addition to *Orco*, the transient receptor potential cation channel A1-encoding gene *Trpa1* has also been recently involved in behaviors triggered following exposure to bacteria (Du et al., 2016; Soldano et al., 2016). Thus, we tested the $Trpa1^{1}$ mutant of this receptor involved in nociception for feeding cessation following exposure to *Ecc15*. Importantly, exposure of $Trpa1^{1}$ mutant animals to *Ecc15*_50 contaminated media led to 78% of fed larvae compared to 31% for WT animals (Fig. 4B). This attenuated phenotype was confirmed using 5% blue dye and spectrophotometry (Supplementary Fig. 4D and E) demonstrating that the *Trpa1* receptor is required for the food intake blockage induced following exposure to *Ecc15*.

3.5. Food intake arrest following Ecc15 exposure can be triggered in *Drosophila suzukii*

In order to determine whether the ingestion arrest following exposure to *Ecc15* could be a response shared in other

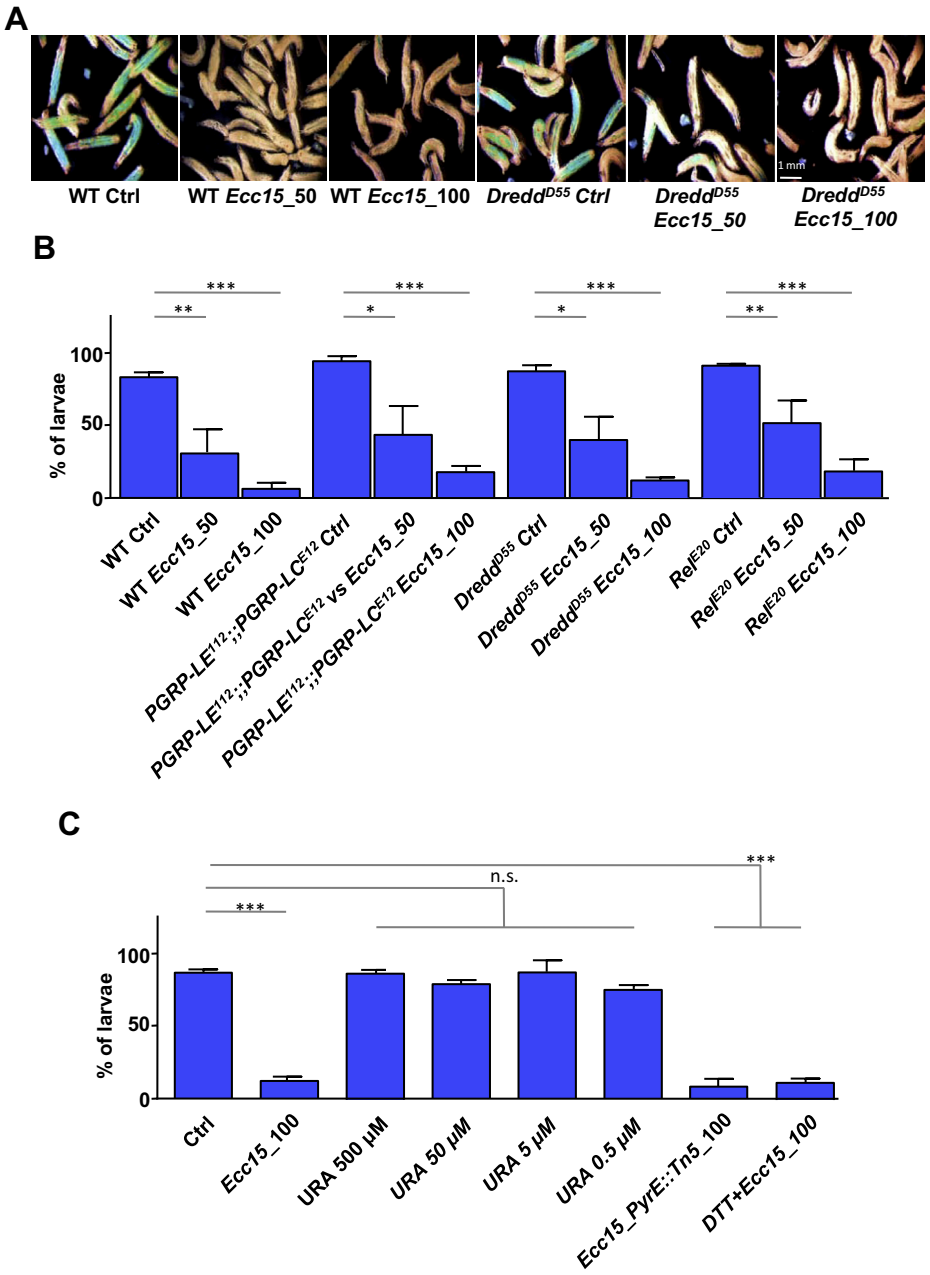

Fig. 3. Food-intake drop following exposure to *Ecc15* requires neither IMD pathway nor Uracil sensing. (A) Pictures of WT or *Dredd* mutant L3 stage larvae fed 1 h with a 2% blue dyed media without (Ctrl) or with *Ecc15* at final OD of 50 (*Ecc15*_50) or 100 (*Ecc15*_100). (B) Feeding percentage for WT, *PGRP-LE*; *PGRP-LC* double mutant, *Dredd* mutant and *Relish* mutant animals fed 1 h with a 2% blue dyed media without bacteria (Ctrl) or contaminated with *Ecc15* (*Ecc15*_50 and *Ecc15*_100). (C) Feeding percentage for WT larvae fed 1 h with a 2% blue dyed media without bacteria (Ctrl) or supplemented with: *Ecc15* at a final OD of 100 (*Ecc15*_100), uracil with several final concentrations, the *PyrE::Tn5* mutant of *Ecc15* deficient for uracil production at a final OD of 100 or a mixture of *Ecc15*_100 and Dithiothreitol (DTT at 10 mM final). For B and C; shown is the average feeding percentage ± SEM from at least 2 independent trials with at least 150 larvae per genotype and condition used. *indicates $p < 0.05$; **indicates $p < 0.01$; ***indicates $p < 0.001$; n.s. indicates $p > 0.05$, unpaired two-tailed Student-*t* test. (For interpretation of the references to colour in this figure legend, the reader is referred to the web version of this article.)

drosophilidae, we tested *Drosophila suzukii* in our experimental system. Contrary to *D. melanogaster*, this insect that originates from South Eastern Asia and is now found in Europe can successfully lay eggs on fresh fruits thereby becoming a major pest especially for vineyards (Adrion et al., 2014). Interestingly, comparably to *D. melanogaster*, *D. suzukii* larvae robustly diminished their food intake when the media was contaminated with *Ecc15* (Fig. 4E and F). This indicates that this behavioral response is not restricted to *D. melanogaster* and might be conserved among *Drosophila* species emphasizing the importance of this response for the insect fitness or survival.

4. Discussion

Behavioral responses of animals facing biotic stresses like parasites or microbes has been widely observed and need to be more extensively deciphered at the molecular level. As several sickness behaviors such as food-intake blockage are triggered upon exposure to bacteria from insects to mammals, understanding how these reactions are orchestrated is of great importance. In addition, the molecular dissection of the signaling pathways and neuronal circuitry required might be of potential interest for the control of agricultural pests or even blood-feeding insects.

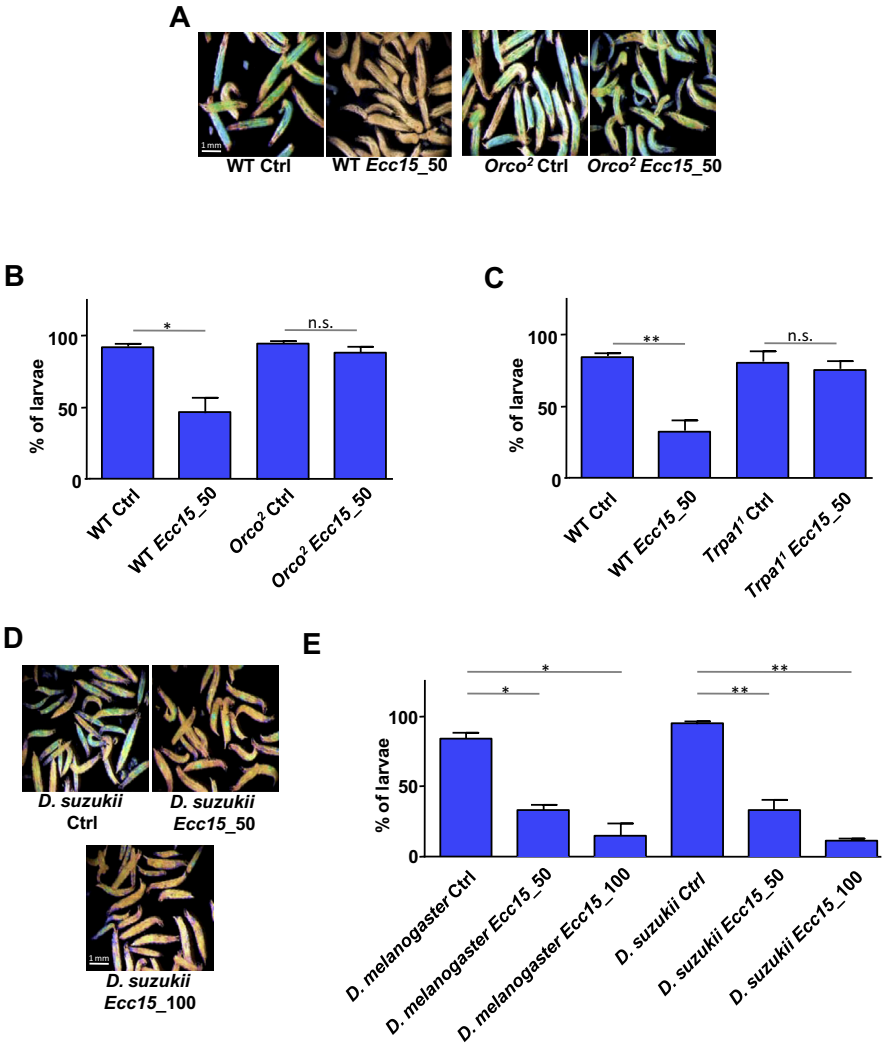

Fig. 4. Feeding depression following exposure to *Ecc15* requires the *Orco* and *Trpa1* genes and is not restricted to *D. melanogaster*. (A) Pictures of WT or *Orco*^{2} mutant L3 stage larvae fed 1 h with a 2% blue dyed media without (Ctrl) or with *Ecc15* at final OD of 50 (*Ecc15*_50). (B) Feeding percentage for WT or *Orco*^{2} mutant larvae fed 1 h with a 2% blue dyed media without bacteria (Ctrl) or contaminated with *Ecc15* at final OD of 50 (*Ecc15*_50). (C) Feeding percentage for WT or *Trpa1*^{1} mutant larvae fed 1 h with a 2% blue dyed media without bacteria (Ctrl) or contaminated with *Ecc15* at final OD of 50 (*Ecc15*_50). (D) Pictures of *D. suzukii* L3 stage larvae fed 1 h with a 2% blue dyed media without (Ctrl) or with *Ecc15* at final OD of 50 (*Ecc15*_50) or 100 (*Ecc15*_100). (E) Feeding percentage for *D. suzukii* larvae fed 1 h with a 2% blue dyed media without bacteria (Ctrl) or contaminated with *Ecc15* at final OD of 50 (*Ecc15*_50) or 100 (*Ecc15*_100). For B, C and E; shown is the average feeding percentage ± SEM from at least 3 independent trials with at least 150 larvae per condition used. *indicates $p < 0.05$; **indicates $p < 0.01$; n.s. indicates $p > 0.05$, unpaired two-tailed Student-*t* test. (For interpretation of the references to colour in this figure legend, the reader is referred to the web version of this article.)

For this study, an experimental system aiming at the rapid identification and quantification of conditions impairing food intake of *Drosophila* larvae exposed to media contaminated with bacteria was developed. We uncovered a robust and reproducible feeding-arrest when animals were in contact with *Ecc15*-contaminated food. While this behavioral response is independent of the canonical antibacterial innate immunity, it necessitates olfaction and the *Trpa1* receptor as well as the *evf* virulence factor.

The requirements for *Trpa1* and olfactory co-receptor *Orco* suggest that *Ecc15*-specific molecules are sensed by the larvae and trigger the food-intake drop. Interestingly, *Trpa1* has been recently involved in adult phenotypes triggered by LPS leading to gustatory and oviposition avoidances (Soldano et al., 2016). In contrast, we demonstrated with several bacterial strains that an almost complete food-intake blockage following exposure to contaminated media could only be trigger by *Erwinia* suggesting that LPS might not be the main trigger of the food-intake cessation phenotype, but rather *Ecc15*-specific molecules. *Orco* involvement suggests that odorant molecules are perceived and trigger the food intake blockage. Interestingly, a recent report demonstrated the involvement of an olfactory receptors and its related odorant molecule during an avoidance phenotype induced in *Drosophila* larvae by a wasp (Ebrahim et al., 2015). In addition, larval response to bitter compounds requires gustatory receptors and can lead to a food-intake cessation similar to the phenotype we observed following exposure to bacteria (Choi et al., 2016) suggesting that different cues may converge to a common behavior.

The *evf* virulence factor that we have shown in this study as being necessary for a full food-intake drop could be the trigger for the phenotype. Even though this virulence factor is known as being required for bacterial persistence within the intestine, our experimental set up involving a short exposure of 1 h suggests another role for *evf*. However, the feeding cessation following exposure to the *Ecc15 evf* mutant was still robust compared to the total absence of phenotype quantified following exposure to heat-killed bacteria. Consequently, the identity of the involved molecules is still an open question and the identification of the putative ligands is of importance for the complete deciphering of

the interaction between *Drosophila* larvae and the natural pathogen *Ecc15*. As an illustration, a recent report using adult flies unraveled how the perception by specific neurons of geosmin, a volatile molecule produced by soil microorganisms, induces a range of behaviors aiming at the protection of the animal and of its progeny (Stensmyr et al., 2012). The identification of the bacterial molecules responsible for the phenotype we described is a prerequisite for the elucidation of the neurons and receptors involved. Following the characterization of the active compounds, the neuronal circuitry and mainly the receptors could be targeted by chemical analogs to mimic *Ecc15*-dependent phenotypes and putatively impair fresh fruits colonization by *D. suzukii*.

Food intake cessation is a common response against infection and its efficiency has often been debated, but rarely studied. Indeed, despite detailed reports, the question remains as to whether feeding cessation is protective or not and the answer may be pathogen-specific (Ayres and Schneider, 2009; Wang et al., 2016). In our experimental system, in response to the natural pathogen *Ecc15*, larvae reduce their food intake, pupate and give rise to adults. Thus, either the induced sickness behavior we describe is sufficient to protect larval stages from *Ecc15* or the exposure conditions we used may not severely impact survival or development of the adult. In the future, it will be of interest using the system we describe to delineate whether food intake blockage is beneficial when larvae are fed with *Ecc15*-contaminated media or with a more virulent pathogen.

We believe that our observations and data establish a robust model that may help the understanding of a conserved sickness behavior with possible implications for pest control.

Funding sources

This work was supported by CNRS, Equipe FRM to Julien Royet "Equipe FRM DEQ20140329541".

Acknowledgements

We thank Won-Jae Lee and François Leulier for bacterial stocks. We thank member of the Julien Royet's team for advices, criticisms and comments on the study.

Appendix A. Supplementary data

Supplementary data associated with this article can be found, in the online version, at http://dx.doi.org/10.1016/j.jinsphys.2017.02.004.

References

Acosta Muniz, C., Jaillard, D., Lemaitre, B., Boccard, F., 2007. *Erwinia carotovora evf* antagonizes the elimination of bacteria in the gut of *Drosophila* larvae. Cell Microbiol. 9, 106–119.

Adrion, J.R., Kousathanas, A., Pascual, M., Burrack, H.J., Haddad, N.M., Bergland, A.O., Machado, H., Sackton, T.B., Schlenke, T.A., Watada, M., Wegmann, D., Singh, N.D., 2014. *Drosophila suzukii*: the genetic footprint of a recent, worldwide invasion. Mol. Biol. Evol. 31, 3148–3163.

Apidianakis, Y., Rahme, L.G., 2009. *Drosophila melanogaster* as a model host for studying *Pseudomonas aeruginosa* infection. Nat. Protoc. 4, 1285–1294.

Ayres, J.S., Schneider, D.S., 2009. The role of anorexia in resistance and tolerance to infections in *Drosophila*. PLoS Biol. 7, e1000150.

Bae, Y.S., Choi, M.K., Lee, W.J., 2010. Dual oxidase in mucosal immunity and host-microbe homeostasis. Trends Immunol. 31, 278–287.

Basset, A., Khush, R.S., Braun, A., Gardan, L., Boccard, F., Hoffmann, J.A., Lemaitre, B., 2000. The phytopathogenic bacteria *Erwinia carotovora* infects *Drosophila* and activates an immune response. Proc. Natl. Acad. Sci. U.S.A. 97, 3376–3381.

Basset, A., Tzou, P., Lemaitre, B., Boccard, F., 2003. A single gene that promotes interaction of a phytopathogenic bacterium with its insect vector, *Drosophila melanogaster*. EMBO Rep. 4, 205–209.

Capo, F., Charroux, B., Royet, J., 2016. Bacteria sensing mechanisms in *Drosophila* gut: local and systemic consequences. Dev. Comp. Immunol. 64, 11–21.

Charroux, B., Royet, J., 2012. Gut-microbiota interactions in non-mammals: what can we learn from *Drosophila*? Semin. Immunol. 24, 17–24.

Choi, J., van Giesen, L., Choi, M.S., Kang, K., Sprecher, S.G., Kwon, J.Y., 2016. A pair of pharyngeal gustatory receptor neurons regulates caffeine-dependent ingestion in *Drosophila* larvae. Front. Cell. Neurosci. 10, 181.

Du, E.J., Ahn, T.J., Kwon, I., Lee, J.H., Park, J.H., Park, S.H., Kang, T.M., Cho, H., Kim, T.J., Kim, H.W., Jun, Y., Lee, H.J., Lee, Y.S., Kwon, J.Y., Kang, K., 2016. *TrpA1* regulates defecation of food-borne pathogens under the control of the duox pathway. PLoS Genet. 12, e1005773.

Ebrahim, S.A., Dweck, H.K., Stokl, J., Hofferberth, J.E., Trona, F., Weniger, K., Rybak, J., Seki, Y., Stensmyr, M.C., Sachse, S., Hansson, B.S., Knaden, M., 2015. *Drosophila* avoids parasitoids by sensing their semiochemicals via a dedicated olfactory circuit. PLoS Biol. 13, e1002318.

Flyg, C., Kenne, K., Boman, H.G., 1980. Insect pathogenic properties of *Serratia marcescens*: phage-resistant mutants with a decreased resistance to Cecropia immunity and a decreased virulence to *Drosophila*. J. Gen. Microbiol. 120, 173–181.

Gottar, M., Gobert, V., Michel, T., Belvin, M., Duyk, G., Hoffmann, J.A., Ferrandon, D., Royet, J., 2002. The *Drosophila* immune response against Gram-negative bacteria is mediated by a peptidoglycan recognition protein. Nature 416, 640–644.

Hedengren, M., Asling, B., Dushay, M.S., Ando, I., Ekengren, S., Wihlborg, M., Hultmark, D., 1999. Relish, a central factor in the control of humoral but not cellular immunity in *Drosophila*. Mol. Cell 4, 827–837.

Igboin, C.O., Griffen, A.L., Leys, E.J., 2012. The *Drosophila melanogaster* host model. J. Oral Microbiol. 4.

Kaneko, T., Goldman, W.E., Mellroth, P., Steiner, H., Fukase, K., Kusumoto, S., Harley, W., Fox, A., Golenbock, D., Silverman, N., 2004. Monomeric and polymeric gram-negative peptidoglycan but not purified LPS stimulate the *Drosophila* IMD pathway. Immunity 20, 637–649.

Larsson, M.C., Domingos, A.I., Jones, W.D., Chiappe, M.E., Amrein, H., Vosshall, L.B., 2004. Or83b encodes a broadly expressed odorant receptor essential for *Drosophila* olfaction. Neuron 43, 703–714.

Lee, K.A., Kim, S.H., Kim, E.K., Ha, E.M., You, H., Kim, B., Kim, M.J., Kwon, Y., Ryu, J.H., Lee, W.J., 2013. Bacterial-derived uracil as a modulator of mucosal immunity and gut-microbe homeostasis in *Drosophila*. Cell 153, 797–811.

Lemaitre, B., Hoffmann, J., 2007. The host defense of *Drosophila melanogaster*. Annu Rev Immunol 25, 697–743.

Leulier, F., Rodriguez, A., Khush, R.S., Abrams, J.M., Lemaitre, B., 2000. The *Drosophila* caspase Dredd is required to resist gram-negative bacterial infection. EMBO Rep. 1, 353–358.

Liehl, P., Blight, M., Vodovar, N., Boccard, F., Lemaitre, B., 2006. Prevalence of local immune response against oral infection in a *Drosophila*/*Pseudomonas* infection model. PLoS Pathog. 2, e56.

Rahme, L.G., Stevens, E.J., Wolfort, S.F., Shao, J., Tompkins, R.G., Ausubel, F.M., 1995. Common virulence factors for bacterial pathogenicity in plants and animals. Science 268, 1899–1902.

Soldano, A., Alpizar, Y.A., Boonen, B., Franco, L., Lopez-Requena, A., Liu, G., Mora, N., Yaksi, E., Voets, T., Vennekens, R., Hassan, B.A., Talavera, K., 2016. Gustatory-mediated avoidance of bacterial lipopolysaccharides via TRPA1 activation in *Drosophila*. Elife 5.

Stensmyr, M.C., Dweck, H.K., Farhan, A., Ibba, I., Strutz, A., Mukunda, L., Linz, J., Grabe, V., Steck, K., Lavista-Llanos, S., Wicher, D., Sachse, S., Knaden, M., Becher, P.G., Seki, Y., Hansson, B.S., 2012. A conserved dedicated olfactory circuit for detecting harmful microbes in *Drosophila*. Cell 151, 1345–1357.

Vallet-Gely, I., Lemaitre, B., Boccard, F., 2008. Bacterial strategies to overcome insect defences. Nat. Rev. Microbiol. 6, 302–313.

Vosshall, L.B., 2000. Olfaction in *Drosophila*. Curr. Opin. Neurobiol. 10, 498–503.

Wang, A., Huen, S.C., Luan, H.H., Yu, S., Zhang, C., Gallezot, J.D., Booth, C.J., Medzhitov, R., 2016. Opposing effects of fasting metabolism on tissue tolerance in bacterial and viral inflammation. Cell 166 (1512–1525), e12.

Background relative to Article 2

During part of my thesis, I worked on a project related to the impact of bacterial PGN exposure on *D. melanogaster* egg-laying behavior. This project was a follow up on a previous publication of the laboratory (Kurz et al., 2017). Indeed, before I joined the team, Leopold C. Kurz and other colleagues decided to study the effect of bacterial infection on the fly behavior. Since bacterial chronic infection leads to drastic changes in the host physiology, they decide to study behavioral responses in the context of an acute infection. Thus, flies were transiently infected by feeding or injection and the effects of this infection were observed during the following hours. It was noticed that, after 6 hours, females injected with Gram-negative bacteria laid fewer eggs than uninfected siblings. This behavioral response to infection is transitory (no detectable drop after 24 hours) and reversible (**Figure 1A**). Few results indicated that the bacteria cell wall component PGN was the elicitor of then observed effects. First, the injection of highly purified PGN into the fly body cavity phenocopied the infection of bacteria. Second, the egg-laying drop was exacerbated in a mutant (PGRP-LB) in which a PGN cleaving enzyme is no longer functional (**Figure 1B**).

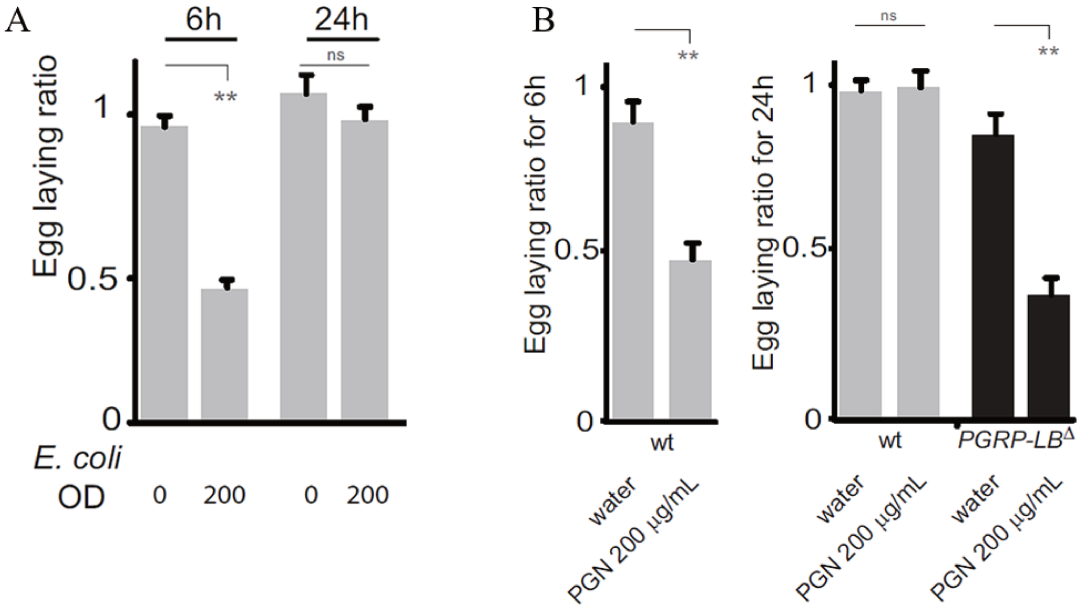

Figure 1. **A** Injection of *E.coli* leads to a reversible egg-laying drop. **B** Bacterial PGN injection is sufficient to trigger the egg-laying drop. This phenotype is exacerbated in PGRP-LB mutants. The egg-laying ratio is given by the number of eggs laid by a treated female over the average number of eggs laid by control females. Figures from (Kurz et al., 2017).

As PGRP-LB was an important negative regulator of this phenotype, it was assumed that cells expressing this protein would be the ones regulating the process. GAL4 lines for PGRP-LB were

generated to identify which cells control this phenotype. Since there are three PGRP-LB isoforms, 3 different lines were generated by cloning 3 Kb, 2.8 Kb and 3.8 Kb of genomic DNA upstream of the predicted transcription start site of each isoform upstream of the GAL4 coding sequences (**Figure 2A**). Among the PGRP-LB isoforms, only the cytosolic PGRP-LB^{PD} was required to buffer the effect of PGN injection on egg-laying. Indeed, only the overexpression of this isoform under the control of its putative driver (pLB1-GAL4) rescued the egg-laying defect in infected *PGRP-LB* mutant females (**Figure 2B**).

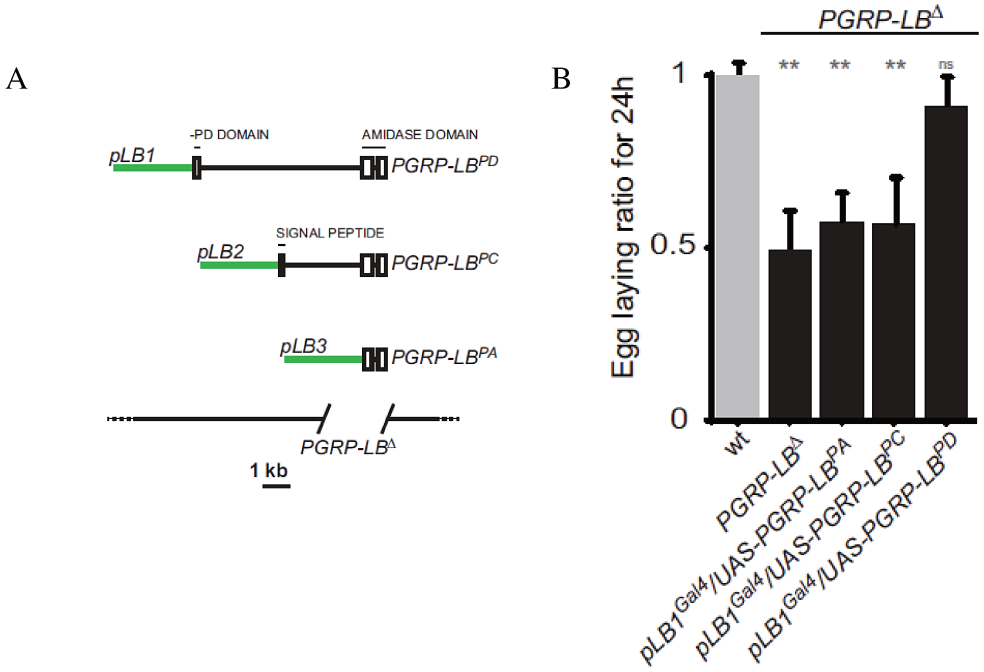

Figure 2. A Three isoforms produced by the PGRP-LB locus. In green are the fragments cloned to generate the PGRP-LB GAL4 lines. **B** Only the overexpression of one isoform (PGRP-LB ^{PD}) under the control of its putative GAL4 driver leads to rescue the egg-laying defect observed in *PGRP-LB* mutants. Figures from (Kurz et al., 2017).

Since octopaminergic neurons are major players in the egg-laying behavior, it was tested whether these neurons were implicated in the infection-related egg-laying defect. PGRP-LB^{PD} overexpression in octopaminergic neurons is sufficient to rescue the egg-laying defect of infected *PGRP-LB* mutant females showing that PGRP-LB is required in these neurons to modulate egg-laying (**Figure 3A**). Also, the knockdown of elements of the IMD pathway in PLB1+ cells or octopaminergic neurons abrogated the egg-laying drop observed in infected *PGRP-LB* mutant females (**Figure 3B** and **3C**). Thus, in this work, it was shown that upon PGN exposure, the canonical IMD pathway is required in pLB1+ cells and octopaminergic neurons to modulate egg-laying behavior.

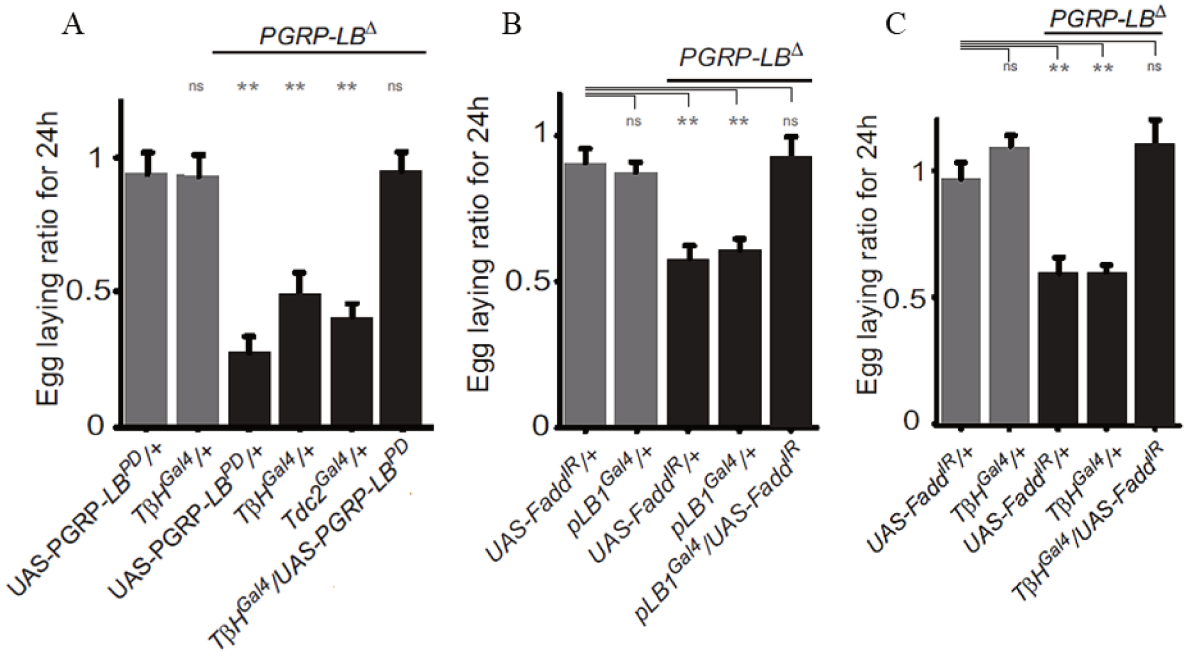

Figure 3. A Overexpression of PGRP-LB^{PD} in octopaminergic neurons (Tβh^{Gal4}) is sufficient to rescue the egg-laying defect of infected PGRP-LB mutant females. **B** and **C** Knockdown of an element of the IMD pathway (Fadd) in pLB1 cells (**B**) or octopaminergic neurons (**C**) leads to rescue of the egg-laying defect of infected PGRP-LB mutant females. Figures from (Kurz et al., 2017).

As a follow up of this work, I wanted to identify the specific neuron(s) dedicated to the egg-laying modulation upon PGN exposure. Furthermore, I studied how these neurons sense the PGN and how their activity modulates egg-laying.

Article 2

eLIFE elifesciences.org

RESEARCH ADVANCE

Peptidoglycan-dependent NF-κB activation in a small subset of brain octopaminergic neurons controls female oviposition

Ambra Masuzzo[1], Gérard Manière[2], Annelise Viallat-Lieutaud[1], Émilie Avazeri[1], Olivier Zugasti[1], Yaël Grosjean[2], C Léopold Kurz[1]*, Julien Royet[1]*

[1]Aix-Marseille Université, CNRS, IBDM, Marseille, France; [2]Centre des Sciences du Goût et de l'Alimentation, AgroSup Dijon, CNRS, INRA, Université Bourgogne Franche-Comté, Dijon, France

Abstract When facing microbes, animals engage in behaviors that lower the impact of the infection. We previously demonstrated that internal sensing of bacterial peptidoglycan reduces *Drosophila* female oviposition via NF-κB pathway activation in some neurons (Kurz et al., 2017). Although we showed that the neuromodulator octopamine is implicated, the identity of the involved neurons, as well as the physiological mechanism blocking egg-laying, remained unknown. In this study, we identified few ventral nerve cord and brain octopaminergic neurons expressing an NF-κB pathway component. We functionally demonstrated that NF-κB pathway activation in the brain, but not in the ventral nerve cord octopaminergic neurons, triggers an egg-laying drop in response to infection. Furthermore, we demonstrated via calcium imaging that the activity of these neurons can be directly modulated by peptidoglycan and that these cells do not control other octopamine-dependent behaviors such as female receptivity. This study shows that by sensing peptidoglycan and hence activating NF-κB cascade, a couple of brain neurons modulate a specific octopamine-dependent behavior to adapt female physiology status to their infectious state.
DOI: https://doi.org/10.7554/eLife.50559.001

***For correspondence:** leopold.kurz@univ-amu.fr (CLK); julien.royet@univ-amu.fr (JR)

Competing interests: The authors declare that no competing interests exist.

Funding: See page 51

Received: 25 July 2019
Accepted: 30 September 2019
Published: 29 October 2019

Reviewing editor: Bruno Lemaître, École Polytechnique Fédérale de Lausanne, Switzerland

© Copyright Masuzzo et al. This article is distributed under the terms of the Creative Commons Attribution License, which permits unrestricted use and redistribution provided that the original author and source are credited.

Introduction

Since eukaryotes live in an environment heavily contaminated by microorganisms, they have forged, over time, extremely complex relationships. Some of these interactions are affecting tissues and organs other than those whose function is to directly eliminate invading microorganisms. Along these lines, growing evidence indicates that bidirectional communication between the gut microbiota and the Central Nervous System (CNS) impacts host behaviors including anxiety, cognition, nociception and social interactions (***Cryan and O'Mahony, 2011***; ***Sharon et al., 2016***). Moreover, by modifying its behavior, an infected host can lower some of its physiological activities to concentrate its energy on pathogen elimination (***Adamo, 1999***; ***Adamo, 2014***). On the other hand, manipulating host behavior is a way for microbes to reduce the defenses of their hosts (***Elya et al., 2018***; ***Keesey et al., 2017***). The notion that hosts can react to microbes by changing their behaviors is called behavioral immunity and refers to a suite of mechanisms that allows organisms to detect the potential presence of disease-causing invaders and to engage in comportments that reduce the consequences of the infection at the level of the organism, the group and/or its offspring (***de Roode and Lefèvre, 2012***; ***Müller and Pawelec, 2014***). Although reported for a long time in invertebrates and mammals, only recent studies, mainly in *D. melanogaster* and *C. elegans*, have started to unravel the molecular aspects of these peculiar host-microbe interactions and especially to directly link

behavioral changes and immune activation (*Cao et al., 2017*; *Kacsoh et al., 2015a*; *Kacsoh et al., 2015b*; *Kacsoh et al., 2013*; *Lee and Mylonakis, 2017*; *Toda et al., 2019*; *Yanagawa et al., 2014*; *Zhai et al., 2018*). In a previous work, we have shown that some components of the NF-κB signaling cascade, which represents a major immune module in both invertebrates and vertebrates, are expressed outside classical immune organs and more precisely in some cells of the brain and the Ventral Nerve Cord (VNC) (*Kurz et al., 2017*). By performing functional studies, we demonstrated that the detection of a universal bacterial metabolite, called peptidoglycan (PGN), by neurons reduces female oviposition. Moreover, we demonstrated that octopamine (OA)-producing neurons which regulate many behaviors in flies, including oviposition, are also implicated in tuning egg-laying rate in response to bacteria (*Kurz et al., 2017*).

In the present study, we used genetic intersectional strategy to precisely map the neurons that, upon peptidoglycan sensing, trigger a reduction of female oviposition. Our results demonstrated that, out of around 20 neurons distributed in the brain and the VNC and expressing the immune modulator PGRP-LB (PeptidoGlycan-Recognition-Protein-LB), only a few are octopaminergic. We further demonstrated that peptidoglycan sensing and NF-κB activation in the VM III octopaminergic neuronal sub-cluster present in the brain is sufficient to modulate egg-laying, in infected females. Using calcium imaging, we showed that stimulation of brains by purified peptidoglycan blocks VM III octopaminergic neurons activity. Finally, our data are consistent with a model in which this peptidoglycan-dependent inhibition of brain neuronal activity impairs a specific ovulation event, called follicle trimming, hence functionally linking peptidoglycan detection to the reduction of egg production in infected females.

Results

The neuronal subpopulation of pLB1+ cells regulates egg-laying

pLB1-Gal4 is a reporter fly line that potentially recapitulates the *in vivo* expression pattern of one isoform of the immune regulator PGRP-LB (*Kurz et al., 2017*). By digesting bacteria-derived peptidoglycan inside the cells, this enzyme reduces the impact of peptidoglycan-dependent NF-κB signaling in cells that express it, thus acting as a negative regulator of the signaling cascade (*Charroux et al., 2018*). We have previously shown that cells expressing Gal4 in the pLB1 pattern (called pLB1+ cells) regulate egg-laying behavior in response to bacterial infection. The fact that the pLB1 expression pattern in the adult CNS delineates a network (*Figure 1A–B*) and that ectopic expression of proteins able to modify neuronal activity (such as Tetanus Toxin (TTx), Kir2.1 or Transient Receptor Potential cation channel, subfamily A, member 1 (TRPA1)) in these cells was sufficient to impact female egg-laying, suggested that at least some of the pLB1+ cells are neurons able to modulate oviposition (*Kurz et al., 2017*). However, since the pLB1-Gal4 line is also expressed in non-neuronal cells such as enterocytes or pericardiac cells (*Charroux et al., 2018*), we decided to confirm the neuronal identity of CNS-resident pLB1+ cells using imaging and functional assays. For that purpose, we used the flip-out method that allowed us to observe cells simultaneously positive for pLB1 and the pan-neuronal marker synaptobrevin (nSyb; nSyb>FLP/pLB1>stop>mGFP)(*del Valle Rodríguez et al., 2011*). This strategy confirmed the presence of a pLB1+ neuronal circuit in the brain and the VNC (*Figure 1C–D*) and outlined the position of the cell bodies. Considering data from the pLB1-Gal4 expression pattern as well as the intersectional strategy from multiple animals, we generated a map (*Figure 1E*) and a table (*Table 1*) with neuronal fibers and cell bodies of pLB1+ neurons. We detected pLB1+ neuronal projections in the SEZ of the brain (*Figure 1A*). In addition, the intersectional strategy using nSyb-LexA revealed, in the majority of the brains (12/20), a single pLB1+ neuron in the posterior part of the SEZ (*Figure 1C*) and few pLB1+ neurons in the same brain area in a minority of samples (5/20) (*Table 1*). In the VNC, the expression pattern was highly stereotyped with neuronal fibers present in all the segments, from the anterior thoracic segment (T1) to the Abdominal Ganglia (AbdG) (*Figure 1B and E*). From the analyses of all the samples (13/13), a network composed of 12 neurons and two isolated cell bodies localized in the posterior thoracic segment (T3) and the AbdG could be defined (*Table 1*, *Figure 1D–E*).

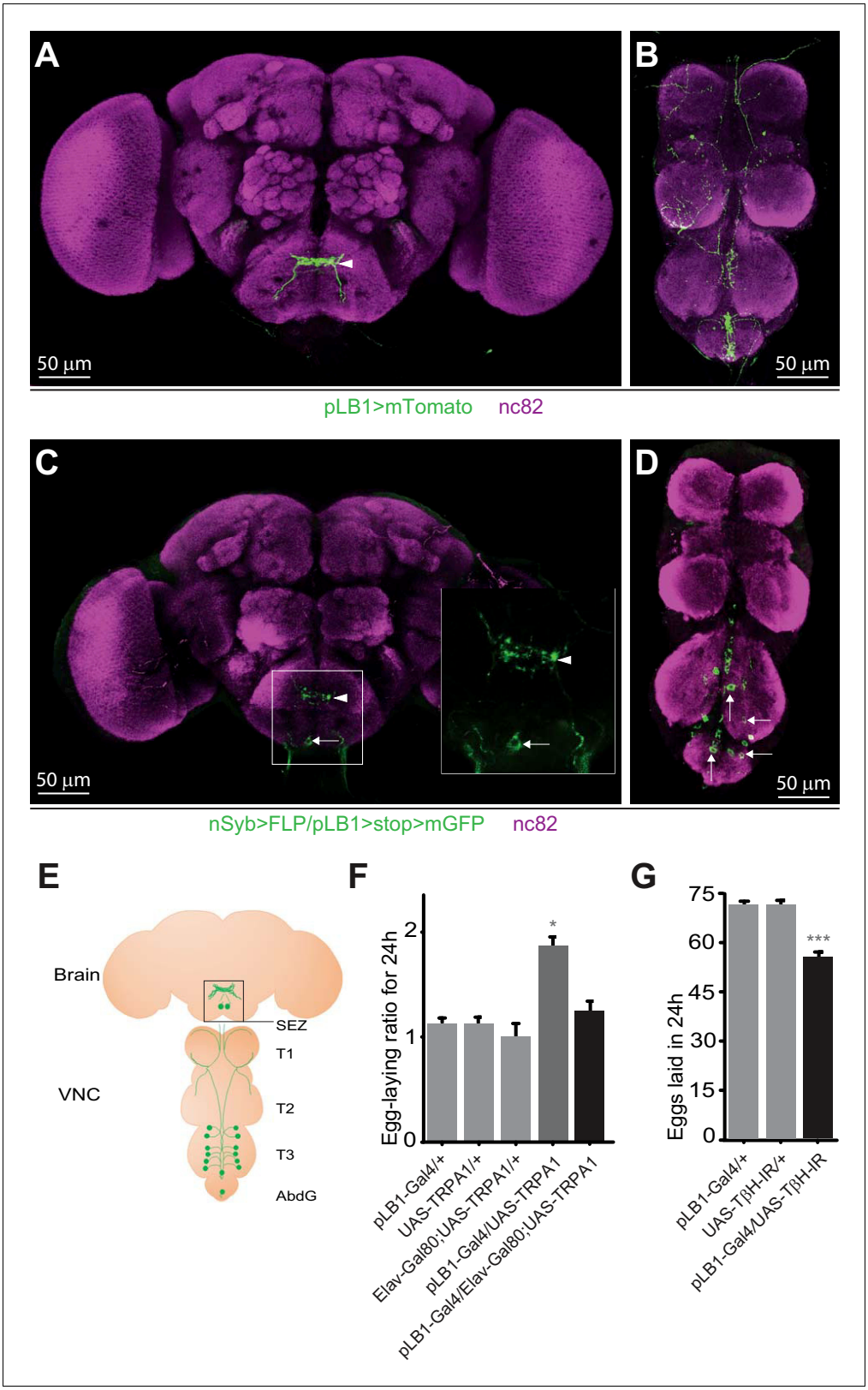

Figure 1. pLB1 is expressed in neurons modulating egg-laying via octopamine. (**A, B**); Immunodetection of cells expressing pLB1-Gal4/UAS-Tomato-mCD8 (pLB1>mTomato) in females. For the homogeneity of the different images, the red signal corresponding to Tomato-mCD8 was converted in green. In the brain (**A**), pLB1 is expressed in the Sub Esophageal Zone (SEZ) (arrowhead). In the ventral nerve cord (VNC) (**B**), the network links the brain to T1, T2, T3 and the Abdominal Ganglia (AbdG).(**C, D**); Pattern of cells co-expressing the neuronal markers nSyb and the pLB1 driver (nSyb>FLP/

Figure 1 continued on next page

Figure 1 continued

pLB1>stop>mGFP). The GFP can only be expressed if the stop sequence inserted upstream of the *gfp* gene is flipped-out in pLB1+/nSyb+ cells. In the brain (**C**), neuronal projections are found in the SEZ (arrowhead) as well as a cell body (arrow). The inserted box is a magnification of the SEZ. In the VNC (**D**), 8 to 14 cell bodies are revealed in T3 and AbdG.(**E**); Map representing projections and cell bodies of neurons expressing pLB1 in brain and VNC. (**F**); Preventing the expression of the transient receptor potential cation channel, subfamily A, member 1 (TRPA1) in pLB1+ neurons impairs the egg-laying increase in non-infected mated females. The egg-laying ratio for 24 hours (24 h) corresponds to the number of eggs laid by a female at the restrictive temperature (29˚C) over the average number of eggs laid by females of the same genotype at the permissive temperature (23˚C). (**G**); RNAi-mediated inactivation of the octopamine-producing enzyme TβH in pLB1+ cells reduces egg-laying. For (**A–D**), immuno-staining against the neuropil marker nc82 was used to stain the organ. For (**F**), shown is the average egg-laying ratio per 24 hours ± SEM (29˚C/23˚C) from at least two independent trials with at least 16 females per genotype and condition used. An egg-laying ratio of 1 indicates an absence of difference between the test and the control. For (**G**), shown is the average number of eggs laid per fly per 24 hours ± SEM from at least three independent trials with at least 58 females per genotype and condition used. * indicates $p<0.05$, *** indicates $p<0.0001$; non-parametric ANOVA, Dunn's multiple comparison test. Details including n values and genotypes can be found in the detailed lines, conditions and, statistics for the figure section.

DOI: https://doi.org/10.7554/eLife.50559.002

The following source data is available for figure 1:

Source data 1. Egg laying raw data for ***Figure 1F***.

DOI: https://doi.org/10.7554/eLife.50559.003

Source data 2. Egg laying raw data for ***Figure 1G***.

DOI: https://doi.org/10.7554/eLife.50559.004

Some pLB1+/octopaminergic neurons control egg-laying in response to infection

We have previously shown that the over-expression of TRPA1 (an ion channel increasing the excitability of neurons) in pLB1+ cells, enhances oviposition rate (***Kurz et al., 2017***). In order to demonstrate that the identified pLB1+ neurons functionally regulate egg-laying, we tested whether TRPA1 over-expression effect on egg-laying could be suppressed by the expression of the pan-neuronal Gal4 inhibitor, Elav-Gal80 (***Figure 1F***). Whereas TRPA1 expression in pLB1+ cells doubled the number of eggs produced by non-infected females compared to controls when shifted from 23˚C to 29˚C (from 40 eggs per day to 80 on average, 29˚C/23˚C ratio of 1.84), this effect was completely suppressed by co-expressing the Elav-Gal80 transgene. These data demonstrated that pLB1+ cells activation modulates egg-laying and that among the pLB1+ cells, a neuronal subgroup is responsible for this control. Our published results demonstrated that peptidoglycan-dependent NF-κB activation in octopaminergic neurons inhibits female egg-laying upon bacterial infection and that over-expressing the OA-producing enzyme Tyramine-β-hydroxylase (TβH) in pLB1+ cells counteracts this phenotype (***Kurz et al., 2017***). However, whether the peptidoglycan effect on egg-laying was mediated cell-autonomously via the modulation of OA signaling in pLB1+ cells remained an open question. The fact that some pLB1+ cells were neurons, led us to hypothesize that these neurons could be octopaminergic and thus able to modulate egg-laying via this neurotransmitter. To test this hypothesis, we analyzed the effects of reducing OA production in pLB1+ cells on egg-laying (***Figure 1G***). OA is synthesized from tyrosine by the sequential actions of Tyrosine decarboxylase (Tdc2) and TβH. Flies in which TβH RNAi was overexpressed in pLB1+ cells (UAS-TβH-IR), and hence OA production reduced, laid significantly fewer eggs than control flies. This result demonstrated that some pLB1+

Table 1. Number and position of GFP-positive cells in the CNS of nSyb>FLP/pLB1>stop>mGFP flies.

The cells positive for GFP are counted.

Organ	pLB1+ neurons	N events/total flies
Brain	0 1 in the SEZ 2-5 in the SEZ 6-10 in the SEZ	3/20 12/20 3/20 2/20
VNC	8-14 in T3 and AbdG	13/13

DOI: https://doi.org/10.7554/eLife.50559.071

neurons are indeed octopaminergic and that OA itself is implicated in the ability of these neurons to control egg-laying. Consistently, data from brain single-cell transcriptomics showed that some, but not all, brain Tdc2+ neurons also express mRNAs coding for NF-κB pathway components (***Davie et al., 2018***).

pLB1+/Tdc2+ neurons are present in the brain VM III sub-cluster and the VNC

To precisely map pLB1+ octopaminergic neurons, we stained brains and VNCs of nSyb>FLP/pLB1>stop>mGFP adult flies with an antibody against Tdc2 (***Figure 2A–B'***). This strategy identified very few pLB1+/Tdc2+ neurons in the brain SEZ (***Figure 2A–A"*** and ***Table 2A***). Complementary intersectional experiments between pLB1-Gal4 and Tdc2-LexA drivers, together with immunostaining against Tdc2, confirmed the existence in the majority of the stained brains (15/19) of either one or two pLB1+/Tdc2+ neurons in the posterior part of the SEZ (***Figure 2*** and ***Figure 2—figure supplement 1*** and ***Table 2B***). Using the same strategy as for the brain, we identified in 12 out of 32 flies tested, between one to three pLB1+/Tdc2+ neurons in the posterior region of the VNCs (***Figure 2B–B'*** and ***Table 2A*** and ***Figure 2—figure supplement 1***). In the absence of identified markers for the different octopaminergic clusters, it was difficult to unambiguously map these neurons. However, the position of the pLB1+ neurons along the dorso-ventral axis relative to Tdc2+ cells indicated that pLB1+/Tdc2+ neurons were part of the ventral midline (VM) cluster (***Figure 2—figure supplement 2***) (***Busch et al., 2009***). The latter can be further subdivided into three sub-clusters, based on their position along the antero-posterior axis (VM I, VM II, VM III respectively) (***Busch et al., 2009***; ***Schneider et al., 2012***). The single pLB1+/Tdc2+ neuron observed in most of the cases always belonged to the VM III sub-cluster (***Figure 2*** and ***Figure 2—figure supplement 3*** and ***Table 2A, B***). These data demonstrated that few brain octopaminergic neurons are pLB1+ and that this sub-population specifically belongs to the VM cluster with an emphasis for a single neuron in the VM III sub-cluster. Since Tdc2 is a marker for both tyraminergic and octopaminergic neurons, it is important to highlight that all Tdc2+ VM neurons have been shown to produce octopamine (***Schneider et al., 2012***). Although 8–14 pLB1+ neurons are reproducibly detected in the VNC, very few are octopaminergic (***Table 2A***). Interestingly, the pLB1+/Tdc2- cells of the T3 segment of the VNC seemed to be 12 interconnected neurons. In an attempt to characterize these non-octopaminergic pLB1+ neurons, we used specific Abs for neuropeptides expressed in a similar location in the VNC. These experiments demonstrated that pLB1+ VNC cells are neither Allatostatin A (***Chen et al., 2016***), Bursicon (***Peabody et al., 2008***), CCAP (Crustacean cardioactive peptide) (***Luan et al., 2006***), nor Leucokinin (***de Haro et al., 2010***) producing neurons (***Figure 2—figure supplements 4–7***).

pLB1+ neurons selectively control octopaminergic-dependent behaviors

It has been shown that a small subset of Tdc2 and Doublesex (Dsx) positive neurons (Tdc2+/Dsx+) present in the AbdG modulate OA-dependent behaviors, such as female receptivity, male rejection and egg deposition (***Rezával et al., 2014***). Since pLB1+ neurons also regulated egg deposition in mated females via OA (***Figure 1G***), as well as in virgins (***Kurz et al., 2017***), we tested whether these cells were involved in controlling other OA-dependent behaviors. As previously reported, we confirmed that virgin females in which Tdc2 neurons are inactivated (via the overexpression of Kir2.1, a potassium channel that hyperpolarizes neurons), presented an increased receptivity. Indeed, Tdc2-Gal4/UAS-Kir2.1 virgin presented a higher percentage of copulation and a lower latency than controls (***Rezával et al., 2014***) (***Figure 3A–B***). Furthermore, although not statistically significant, we observed a trend which suggested that the remating index of Tdc2-Gal4/UAS-Kir2.1 mated females was higher than in control flies (***Figure 3—figure supplement 1***), confirming previously published data (***Rezával et al., 2014***). Conversely, when we analyzed pLB1-Gal4/UAS-Kir.2.1 females, none of these OA-dependent behaviors were affected (***Figure 3A–B***, ***Figure 3—figure supplement 1***). These results suggested that pLB1+/Tdc2+ neurons are different from the ones regulating receptivity and post-mating behaviors in physiological conditions. Consistently, pLB1+/Tdc2+ neurons were also detected in males, whereas Tdc2+/Dsx+ ones are sexually dimorphic and absent in adult males (***Figure 3C–D'*** and ***Figure 3—figure supplements 2*** and ***3***) (***Rezával et al., 2014***). Besides intersectional strategy experiments using Dsx-FLP and Dsx-LexA drivers demonstrated that pLB1+ neurons

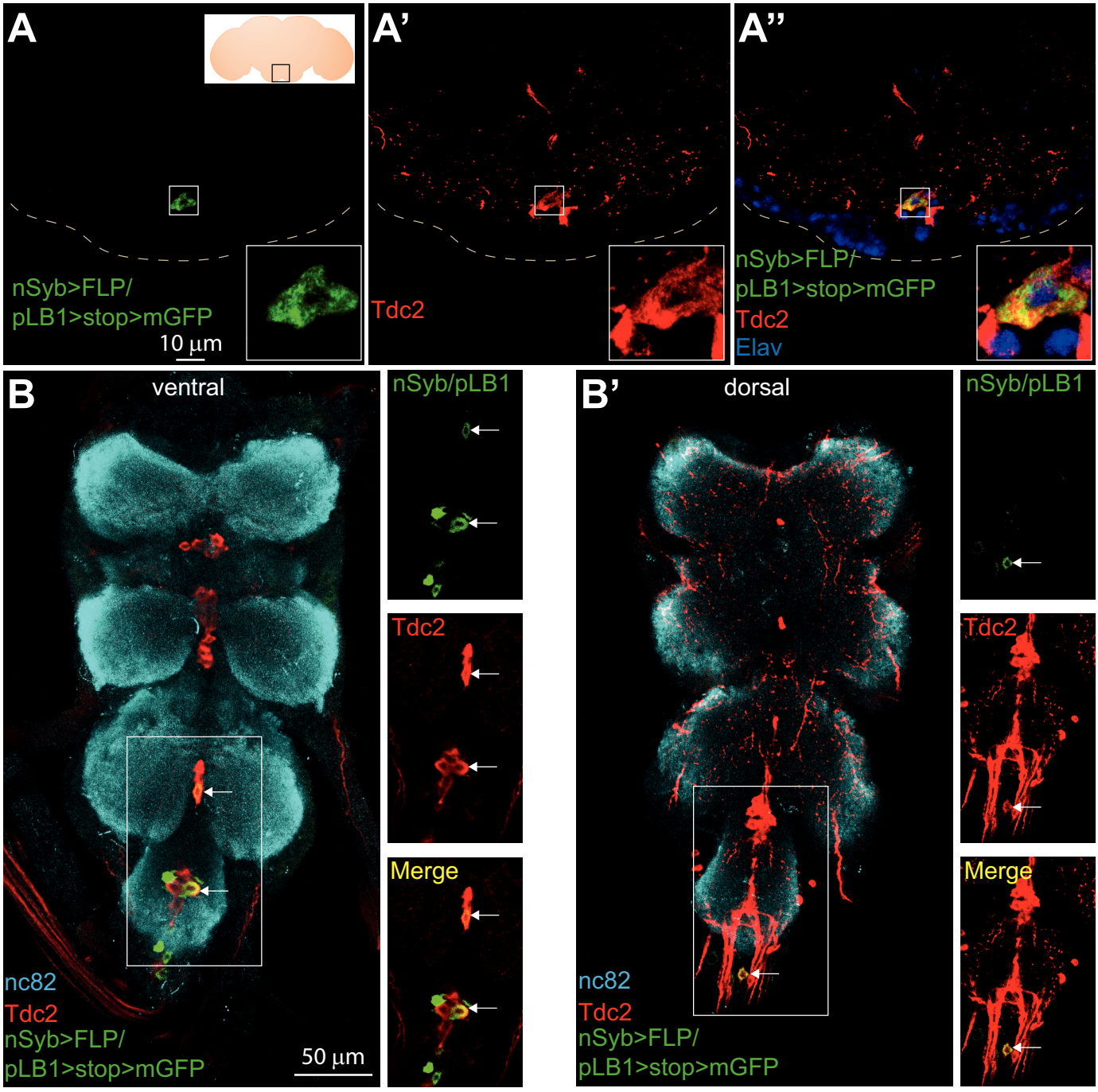

Figure 2. Some of the pLB1+ neurons are octopaminergic. (**A–B'**); Immuno-detection in the brain Sub Esophageal Zone (SEZ; **A–A''**) and ventral nerve cord (VNC; **B–B'**) of neurons expressing pLB1 (nSyb>FLP/pLB1>stop>mGFP) (**A,B and B'**) and producing the Tdc2 enzyme (**A', B and B'**). In (**A''**), the nuclear neuronal marker Elav was also immuno-detected. For (**A**), the inserted scheme represents the brain and the empty black square delineates the observed area. For (**A-A''**), the inserted box is a magnification of the outlined box and the dashed line represents the ventral limit of the brain. For (**B-B'**), staining against nc82 was used to delineate the shape of the VNC. For (**B–B'**), the merged channels of the outlined box are separated on the images on the right. Arrows point to pLB1+/Tdc2+ cells in the VNC. Details including genotypes can be found in the detailed lines, conditions and, statistics for the figure section.

DOI: https://doi.org/10.7554/eLife.50559.005

The following figure supplements are available for figure 2:

Figure supplement 1. Some octopaminergic neurons are pLB1+.

Figure 2 continued on next page

Figure 2 continued

DOI: https://doi.org/10.7554/eLife.50559.006

Figure supplement 2. Map of Tdc2 expressing neurons in the brain and VNC.

DOI: https://doi.org/10.7554/eLife.50559.007

Figure supplement 3. The pLB1+ octopaminergic neurons in the brain belong to the VM III sub-cluster.

DOI: https://doi.org/10.7554/eLife.50559.008

Figure supplement 4. pLB1-expressing neurons in the VNC do not produce Allatostatin A.

DOI: https://doi.org/10.7554/eLife.50559.009

Figure supplement 5. pLB1+ neurons in the VNC do not produce Bursicon.

DOI: https://doi.org/10.7554/eLife.50559.010

Figure supplement 6. pLB1+ neurons in the VNC do not produce CCAP.

DOI: https://doi.org/10.7554/eLife.50559.011

Figure supplement 7. pLB1+ neurons in the VNC do not produce Leucokinin.

DOI: https://doi.org/10.7554/eLife.50559.012

in the brain and the VNC were Dsx - (***Figure 3E–F'*** and ***Figure 3—figure supplement 4***). Altogether, these results demonstrated that the pLB1+/Tdc2+ neurons are different from the Tdc2+/Dsx + neurons that control female receptivity and post-mating behavior, including egg deposition, in uninfected flies.

NF-κB activation in pLB1+/Tdc2+ neurons reduces egg-laying rate of infected females

The above results led us to functionally test whether pLB1+/Tdc2+ neurons were i) able to control oviposition rate and ii) the ones that modulated egg-laying rate upon peptidoglycan sensing via the NF-κB pathway. For that purpose, we tested the consequences of functionally inactivating pLB1+/Tdc2+ neurons using an intersectional strategy that combined Gal4/UAS, LexA/Lex-Aop and a flippable Gal80 inhibitor (***del Valle Rodríguez et al., 2011***). As previously shown, the ectopic expression of the neuronal inhibitor TTx in pLB1+ cells strongly reduced female egg-laying (***Figure 4A***) (***Kurz et al., 2017***). While this effect was suppressed by the ubiquitous expression of the Gal80

Table 2. Number and position of pLB1+/Tdc2+ neurons.

(**A**); pLB1-Gal4, UAS>stop>GFPmCD8; LexAop-FLP/nSyb-LexA brains and ventral nerve cords (VNCs) stained with an anti-Tdc2 Ab. The cells positive for GFP and stained with the anti-Tdc2 Ab (pLB1+/Tdc2+) are counted (left). The cells positive for GFP and negative for the Tdc2 Ab (pLB1+/Tdc2-) are counted. (**B**); pLB1-Gal4, UAS>stop>GFPmCD8; LexAop-FLP/Tdc2-LexA brains and VNCs stained with an anti-Tdc2 Ab. The GFP+ cells (pLB1+/Tdc2+) also positive for Tdc2 Ab are counted (left). NR = non relevant. This intersectional strategy only reveals pLB1+/Tdc2+ cells.

(A) Organ	pLB1+/Tdc2+ neurons	pLB1+/Tdc2- neurons	N events/total flies
	(Strategy 1, see legend for details)		
Brain	0	0	1/18
	1 in the VMV III cluster	0	6/18
	1 in the VMV III cluster	2-4 in the SEZ	3/18
	2-5 in the VMV III cluster	0	8/18
VNC	0	8-14 in T3 and AbdG	11/14
	1 in the AbdG and 2 in T3	8-14 in T3 and AbdG	3/14
(B) Organ	**pLB1+/Tdc2+ neurons**	**pLB1+/Tdc2- neurons**	**N events/total flies**
	(Strategy 2, see legend for details)		
Brain	0	NR	4/19
	1 in the VMV III cluster	NR	13/19
	2 in the VMV III cluster	NR	2/19
VNC	0	NR	9/18
	1 in the AbdG	NR	7/18
	2 in the AbdG	NR	2/18

DOI: https://doi.org/10.7554/eLife.50559.072

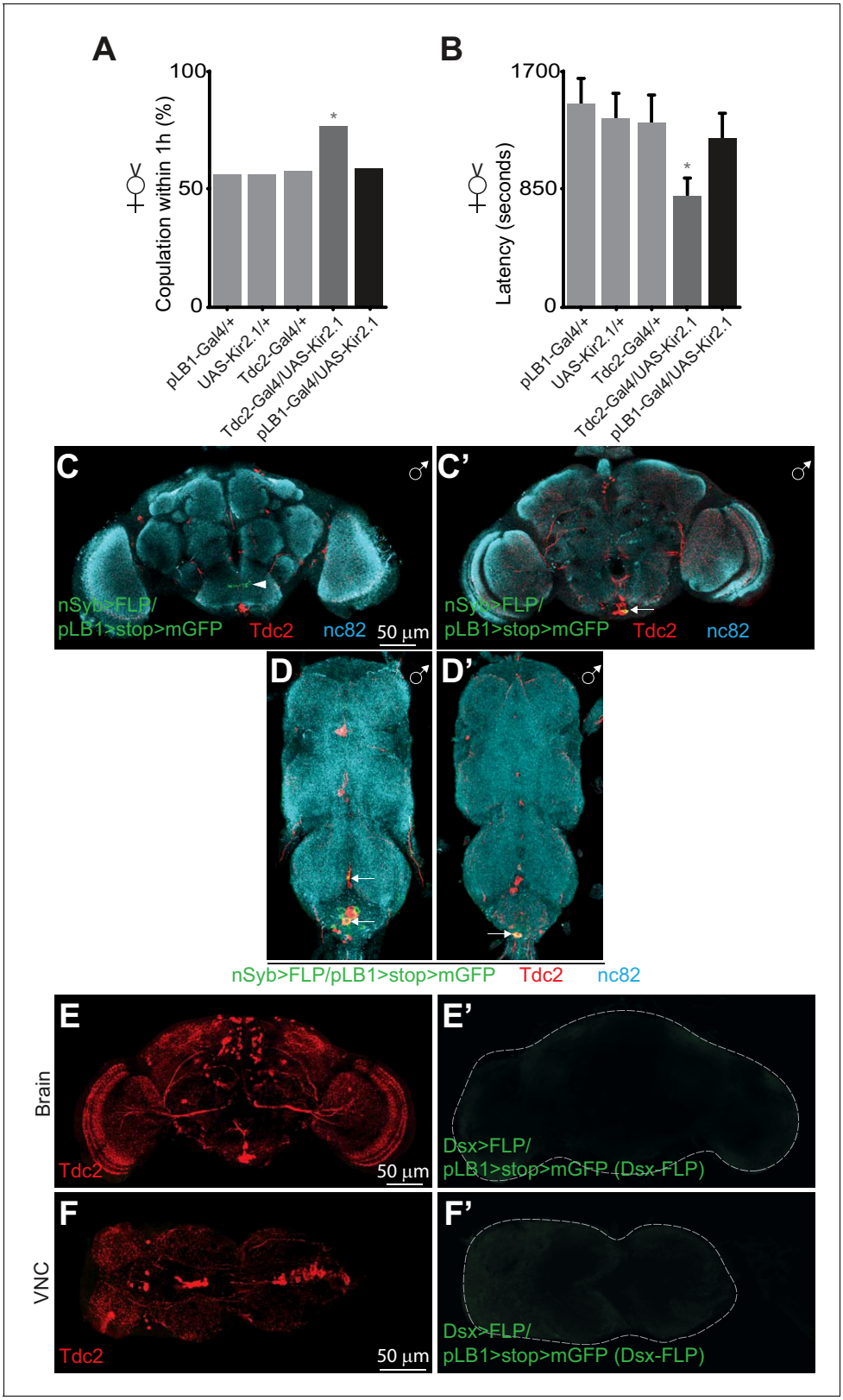

Figure 3. pLB1+ neurons are different from Tdc2+/Dsx+ neurons controlling receptivity. Impairing the activity of pLB1+ neurons via UAS-Kir2.1 neither reduces virgin copulation percentage (**A**) nor mating latency (**B**). (**C-D'**); In adult males, immuno-detection in the CNS of neurons expressing pLB1 and producing the Tdc2 enzyme. (**C** and **C'**) are the brain anterior and posterior views, respectively. (**D** and **D'**) are the ventral nerve cord (VNC) ventral and dorsal views, respectively. In adult females, immuno-detection in the brain (**E-E'**) and VNC (**F-F'**) of Dsx+/pLB1+ cells and producing the Tdc2 enzyme;

Figure 3 continued on next page

Figure 3 continued

no signal for Dsx+/pLB1+ cells is detectable. For (**A**), shown is the copulation percentage for virgins within 1 hour (1h) from six independent trials with a total of 70–80 females per genotype and condition used. All the tested flies were pooled for the calculation and error bars are not appropriate for this kind of representation. For (**B**), shown is the average latency time before mating for virgins from four independent trials with a total of 24 to 40 females per genotype and condition used. For (**C-D'**), staining against nc82 was used to delineate the shape of the brain and VNC. Arrows indicate the position of pLB1+ cell bodies. Arrowheads indicate projections. * indicates $p<0.05$; Fisher exact t-test (**A**) and non-parametric t-test, Mann-Whitney test (**B**). Details including n values and genotypes can be found in the detailed lines, conditions and, statistics for the figure section.

DOI: https://doi.org/10.7554/eLife.50559.013

The following figure supplements are available for figure 3:

Figure supplement 1. pLB1+ neurons may not control remating behavior.

DOI: https://doi.org/10.7554/eLife.50559.014

Figure supplement 2. pLB1+/Tdc2+ neurons are present in male brains.

DOI: https://doi.org/10.7554/eLife.50559.015

Figure supplement 3. pLB1+/Tdc2+ neurons are present in male VNC.

DOI: https://doi.org/10.7554/eLife.50559.016

Figure supplement 4. pLB1+ neurons are not Dsx+.

DOI: https://doi.org/10.7554/eLife.50559.017

inhibitor (Tub-Gal80), it was reestablished when Gal80 expression was specifically suppressed in Tdc2+ cells (***Figure 4A***). This result showed that TTx expression in pLB1+/Tdc2+ cells is sufficient to decrease egg-laying. Conversely, ectopic activation of the thermosensitive TRPA1 protein in pLB1+/Tdc2+ neurons was sufficient to trigger an increase of egg-laying compared to controls (***Figure 4B***). Next, using an RNAi transgene (UAS-Fadd-IR) targeting a cytosolic component of the NF-κB called Fadd (Fas-associated death domain protein), we assayed whether downregulation of NF-κB signaling specifically in pLB1+/Tdc2+ neurons was sufficient to abolish the egg-laying drop observed in females injected with peptidoglycan (***Figure 4C***) (***Leulier et al., 2002***; ***Naitza et al., 2002***). While control lines presented an egg-laying drop post peptidoglycan injection, this was no longer the case for females expressing the Fadd-IR transgene in pLB1+/Tdc2+ cells. This result showed that peptidoglycan-mediated activation of the NF-κB pathway in pLB1+/Tdc2+ neurons is the triggering event that reduces egg-laying upon bacterial peptidoglycan exposure.

Neurons that adapt female egg-laying behavior to infectious status are located in the brain

Next, to delineate which of the pLB1+ neurons located in the brain or the VNC were responsible for the egg-laying modulation in response to bacterial peptidoglycan, we used different strategies. First, we took advantage of the OTD-FLP transgene shown to be expressed in brain but not in VNC neurons (***Asahina et al., 2014***). We first tested whether this transgene was indeed expressed in brain pLB1+ cells. The presence of GFP+/Tdc2+ cells in brains of pLB1-Gal4/UAS>stop>GFP, OTD-FLP adult flies (OTD>FLP/pLB1>stop>mGFP), demonstrated that OTD is expressed in pLB1+/Tdc2+ neurons (***Figure 5—figure supplement 1***). Importantly, animals did not show any staining in the VNC, confirming the specificity of the OTD-FLP driver for the brain neurons (***Figure 5—figure supplement 1***). Once validated, this tool was used to test the effect of inactivating only brain pLB1+ neurons via the potassium channel Kir2.1. While control females laid an average of 60 eggs per day, ubiquitous inactivation of pLB1+ neurons via HS-FLP or targeted inactivation of brain pLB1+ neurons via the OTD-FLP, both resulted in a strong decrease of egg-laying rate with an average of 42 eggs per day (***Figure 5A***). These result was confirmed via a complementary approach using the Tsh-Gal80 abdominal driver inhibitor that blocks Gal4 activation in the thorax, including the VNC while sparing the brain Gal4 expressing cells. The efficiency of the Tsh-Gal80 transgene expression over pLB1-Gal4 was controlled and confirmed via microscopy (***Figure 5—figure supplement 1***). The egg-laying reduction seen upon Gal4-mediated Kir2.1 expression in pLB1+ cells was unaffected by Tsh-mediated expression of Gal80 (***Figure 5B***). Similar conclusions were drawn when UAS-Fadd-IR was used to modulate NF-κB pathway activity *in vivo*. Indeed, the suppression of egg-laying drop 6 hours post peptidoglycan injection mediated by the knockdown of the NF-κB cascade in Tdc2+ and pLB1 + cells was not observed when only thoracic neurons were targeted (***Figure 5C***) and persisted when Tsh-Gal80 was concomitantly expressed (***Figure 5D***). Taken together, these data supported a model

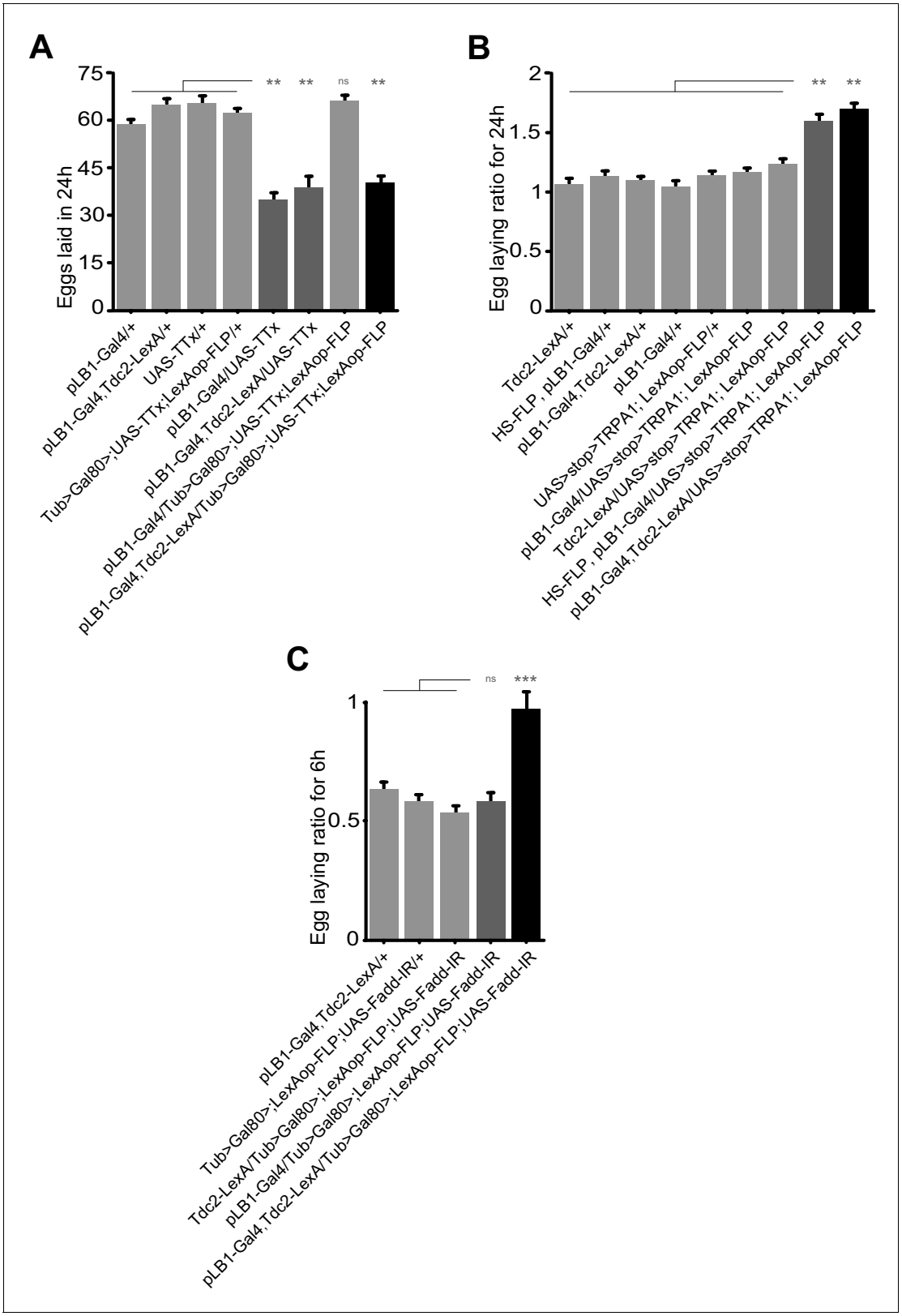

Figure 4. Egg-laying drop post peptidoglycan exposure is mediated by pLB1+/Tdc2+ neurons via the NF-κB pathway. (**A**); Impairing the activity of octopaminergic pLB1+ neurons reduces egg-laying. The ubiquitously expressed Tub-Gal80 that inhibits the activity of Gal4 can be flipped-out in cells expressing the LexA. Thus, only in cells co-expressing the Gal4 and the LexA the UAS-TTx will be expressed. (**B**); Increasing the activity of pLB1+ neurons augments egg-laying. The ubiquitously expressed Tub-Gal80 can be flipped-out only in cells expressing the heat shock (HS) flippase or the

Figure 4 continued on next page

Figure 4 continued

LexA. Thus, only in cells co-expressing the Gal4 and the LexA the UAS-TRPA1 will be expressed. (**C**); Octopaminergic pLB1+ neurons control the egg-laying drop post-peptidoglycan injection via Fadd. Only cells co-expressing the Gal4 and LexA express the Fadd RNAi (UAS-Fadd-IR) transgene. For (**A**), shown are the average numbers of eggs laid per fly per 24 hours ± SEM from at least two independent trials with at least 20 females per genotype and condition used. For (**B**), shown are the average egg-laying ratios per fly per 24 hours ± SEM from three independent trials with at least 35 females per genotype and condition used. For (**C**), shown are the average egg-laying ratios per fly per 6 hours ± SEM from at least two independent trials with at least 20 females per genotype and condition used. * indicates $p<0.05$; ** indicates $p<0.001$; *** indicates $p<0.0001$; n.s. indicates $p>0.05$, non-parametric ANOVA, Dunn's multiple comparison test. Details including n values and genotypes can be found in the detailed lines, conditions and, statistics for the figure section.

DOI: https://doi.org/10.7554/eLife.50559.018

The following source data is available for figure 4:

Source data 1. Egg laying raw data for ***Figure 4A***.

DOI: https://doi.org/10.7554/eLife.50559.019

Source data 2. Egg laying raw data for ***Figure 4B***.

DOI: https://doi.org/10.7554/eLife.50559.020

Source data 3. Egg laying raw data for ***Figure 4C***.

DOI: https://doi.org/10.7554/eLife.50559.021

in which the brain, and not the VNC pLB1+/Tdc2+ neurons, modulate egg-laying upon peptidoglycan-dependent NF-κB pathway triggering.

Some neurons that adapt female egg-laying behavior to infectious status are connected to VNC and express endogenous PGRP-LB protein

One important issue relates to the neuronal projections of the brain pLB1+/Tdc2+ cells. Unfortunately, the weak expression of the pLB1-Gal4 driver, prevented us to identify them. To overcome this problem, we generated a pLB1-LexA driver using the same DNA fragment as for the pLB1-Gal4 line. This tool allowed us to perform intersectional strategies to unlock, via the flippase/FRT system, the strong Tdc2-Gal4 driver in pLB1+ cells. In brains of pLB1-LexA/Tdc2-Gal4, UAS>stop>mCD8-GFP; LexAop-FLP (pLB1>FLP/Tdc2>stop>mGFP) flies, we detected five neuronal cell bodies (***Figure 6A***) and their neuronal projections (***Figure 6B–D***). In addition to the neurons already detected with the pLB1-Gal4 driver in the VM cluster, two AL2 octopaminergic neurons were detected (***Figure 6A***, left panel). The position of the identified pLB1+/Tdc2+ neuron within the VM I cluster, its symmetrical (unpaired) nature as well as the shape of its ascending projections make it likely to belong to the OA-VUMa4 class of neurons (***Busch et al., 2009***) (***Figure 6B***). The projection pattern of the two AL2 asymmetrical neurons in the ocular lobes identified them as OA-AL2i1 (***Figure 6C***) (***Busch et al., 2009***). The highly intricate and overlapping pattern of the pLB1+/Tdc2+ VM II neuron projections impaired its precise identification (data not shown). However, this neuron of the VM cluster has unpaired ascending projections, and thus belongs to the VUM class. With regard to pLB1+/Tdc2+ VM III neuron, it sends symmetrical projections descending towards the VNC which look very much like the ones of the described VUMd2 class of neurons, a class exclusively located in the VM III sub-cluster (***Figure 6D***) (***Busch et al., 2009***). Combined with our previous results demonstrating that the brain pLB1+/Tdc2+ neurons can modulate egg-lay following peptidoglycan exposure, we propose that peptidoglycan may interfere with the activity of the VUMd2 neuron that sends projections in the VNC (***Busch et al., 2009***).

Since all functional data relied on the pLB1-Gal4 construct and although previous rescue experiments suggested that this driver at least partially mimics PGRP-LB endogenous pattern (***Kurz et al., 2017***), we generated a PGRP-LB::GFP line in which all endogenous PGRP-LB isoforms were tagged with GFP at the endogenous locus. Brains of PGRP-LB::GFP flies showed intracellular localization of PGRP-LB protein (probably the cytosolic isoforms) in neurons of the octopaminergic VM and AL2 clusters (***Figure 7***). Of interest, few PGRP-LB::GFP+, but Tdc2- cells, were also detected (***Figure 7***, arrow). This result unambiguously demonstrated that the endogenous immune regulator PGRP-LB is produced by a subclass of octopaminergic neurons of the AL2, VM II, and VM III sub-clusters, among which are the pLB1 neurons.

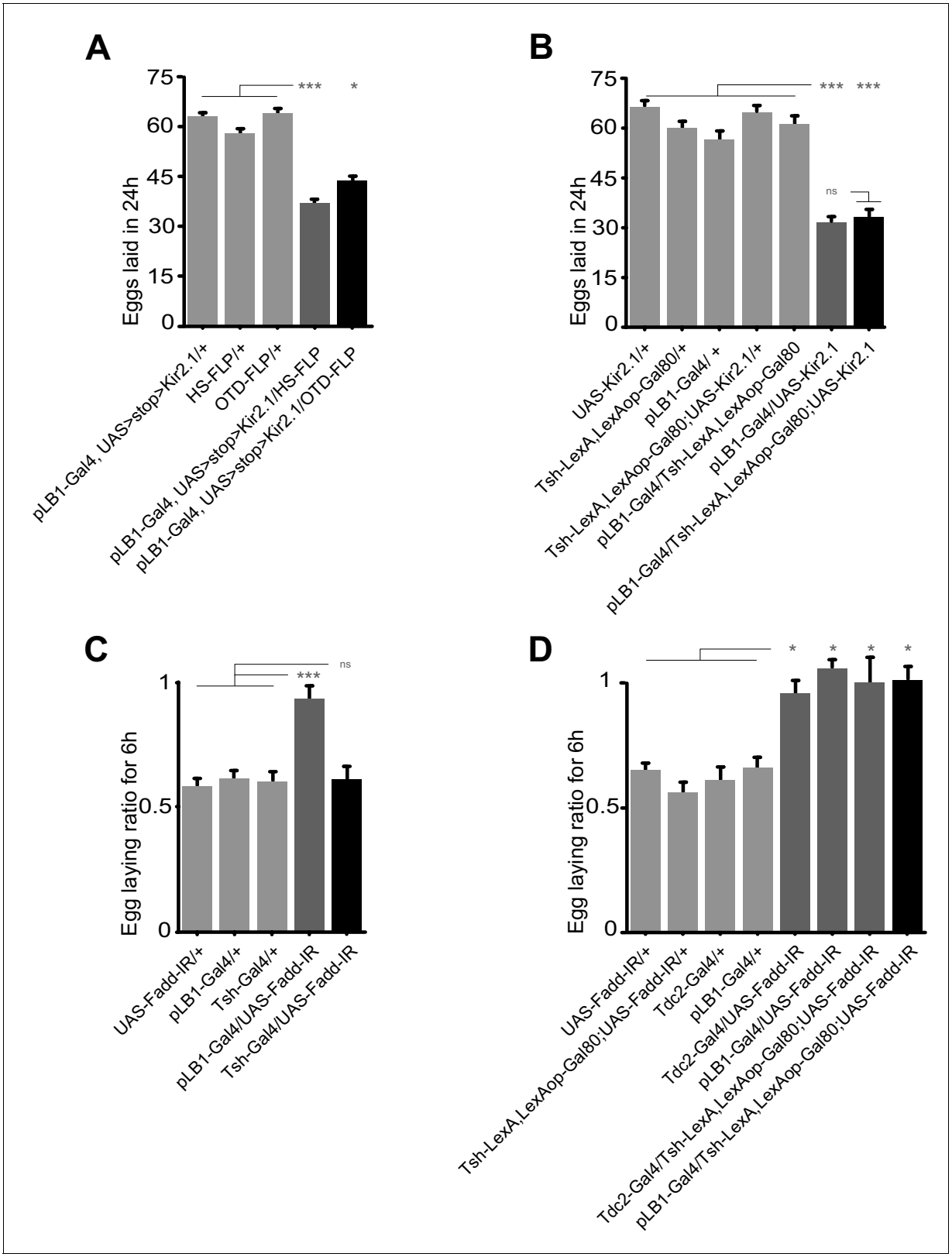

Figure 5. Egg-laying drop post peptidoglycan exposure is mediated by the brain, but not the VNC pLB1+ neurons. (**A**); Impairing the activity of pLB1+ cells of the brain reduces egg-laying. Only in cells co-expressing the FLP and the Gal4 will the UAS>stop>Kir2.1 be effective. Heat shock (HS) is ubiquitous while OTD is brain-restricted. (**B**); pLB1+ cells of the VNC are dispensable for the modulation of the egg-lay. The expression of LexAop-Gal80 antagonizes the activity of Gal4, thus preventing the effects of UAS-Kir2.1. Tsh-LexA drives the expression of Gal80 in the fly thorax, including the

Figure 5 continued on next page

Figure 5 continued

VNC. (**C**); RNAi-mediated Fadd (Fadd-IR) inactivation in the Tsh-Gal4+ cells does not prevent egg-lay drop post peptidoglycan injection. (**D**); RNAi-mediated Fadd inactivation in pLB1+ cells of the brain, but not of the VNC prevents egg-lay drop post peptidoglycan injection. The expression of LexAop-Gal80 antagonizes the activity of Gal4, thus preventing the effects of UAS-Fadd-IR, only in cells co-expressing the Gal4 and the LexA. For (**A and B**), shown are the average numbers of eggs laid per fly per 24 hours ± SEM from at least two independent trials with at least 20 females per genotype and condition used. For (**C and D**), shown are the average egg-laying ratios per fly per 6 hours ± SEM from at least two independent trials with at least 20 females per genotype and condition used. * indicates $p<0.05$; ** indicates $p<0.001$; *** indicates $p<0.0001$; n.s. indicates $p>0.05$, non-parametric ANOVA, Dunn's multiple comparison test. Details including n values and genotypes can be found in the detailed lines, conditions and, statistics for the figure section.

DOI: https://doi.org/10.7554/eLife.50559.022

The following source data and figure supplement are available for figure 5:

Source data 1. Egg laying raw data for ***Figure 5A***.

DOI: https://doi.org/10.7554/eLife.50559.024

Source data 2. Egg laying raw data for ***Figure 5B***.

DOI: https://doi.org/10.7554/eLife.50559.025

Source data 3. Egg laying raw data for ***Figure 5C***.

DOI: https://doi.org/10.7554/eLife.50559.026

Source data 4. Egg laying raw data for ***Figure 5D***.

DOI: https://doi.org/10.7554/eLife.50559.027

Figure supplement 1. OTD-FLP is expressed in pLB1+ neurons of the head, but not of the thorax whileTsh-LexA, LexAop-Gal80 efficiently silences pLB1-Gal4 in the thorax.

DOI: https://doi.org/10.7554/eLife.50559.023

Neurons that adapt female egg-laying behavior to infectious status are inhibited by peptidoglycan

To further test the effects of peptidoglycan on brain neurons, we performed calcium imaging using both *in vivo* and *ex vivo* methods. For that purpose, peptidoglycan solution was applied directly onto the brains of alive Tdc2-Gal4/UAS-GCaMP6s flies and GFP fluorescence intensity was monitored over time. We focused on octopaminergic neurons of the VM II/VM III sub-clusters (***Figure 8—figure supplement 1***) which, as shown above, contain the cells that express the pLB1 driver the most consistently and directly contact the VNC. In contrast to the control solution (Ringer's solution) (***Video 1***), brain stimulation by bacterial peptidoglycan induced a rapid and transient decrease of the GFP signal in VM II/III octopaminergic sub-clusters (***Figure 8A–C*** and ***Video 2***). To more precisely assay the response of pLB1+/Tdc2+ neurons upon peptidoglycan exposure, we performed *ex vivo* calcium imaging on dissected brains in which GCaMP6s was expressed in pLB1+/Tdc2+ cells only (pLB1>FLP/Tub>Gal80>,Tdc2>GCaMP6s, ***Figure 8D–F***). For the *ex vivo* experiments with dissected brains, we focused on the posterior part of the brain in which only the pLB1+/Tdc2+ neuron of the VM III cluster is detectable. Fluorescence intensity quantifications showed that direct stimulation of dissected brains by peptidoglycan triggered a reduction of calcium levels in this VM III pLB1 +/Tdc2+ neuron (***Video 4***) compared to control (***Video 3***). These results which indicated that peptidoglycan exposure inhibits pLB1+/Tdc2+ neuronal activity are coherent with functional data showing that blockage of pLB1+/Tdc2+ neurons by TTx or Kir2.1 overexpression reduces female egg-laying, a genetically triggered egg-lay drop that mimics the physiological response following peptidoglycan exposure. The differences observed between GCaMP kinetics in *ex vivo* (persistent drop post peptidoglycan stimulation) and *in vivo* (transient) experiments could reflect the fact that, for *in vivo* experiments, the imaged flies were alive with brains still connected to the rest of the nervous system including the VNC. In contrast, dissected brains disconnected from the periphery and the VNC were used for *ex vivo* experiments. Besides, whereas peptidoglycan was added to exposed brains still bathing in the surrounding hemolymph for the *in vivo* settings, it was added to brains bathing in Ringer's solution for *ex vivo* experiments.

pLB1+ neurons inhibition and peptidoglycan exposure temporary block mature oocytes release

We previously noticed that the egg-laying drop induced by bacterial or peptidoglycan injection was not associated with premature death of early-stage oocytes as described for wasp-exposed flies or

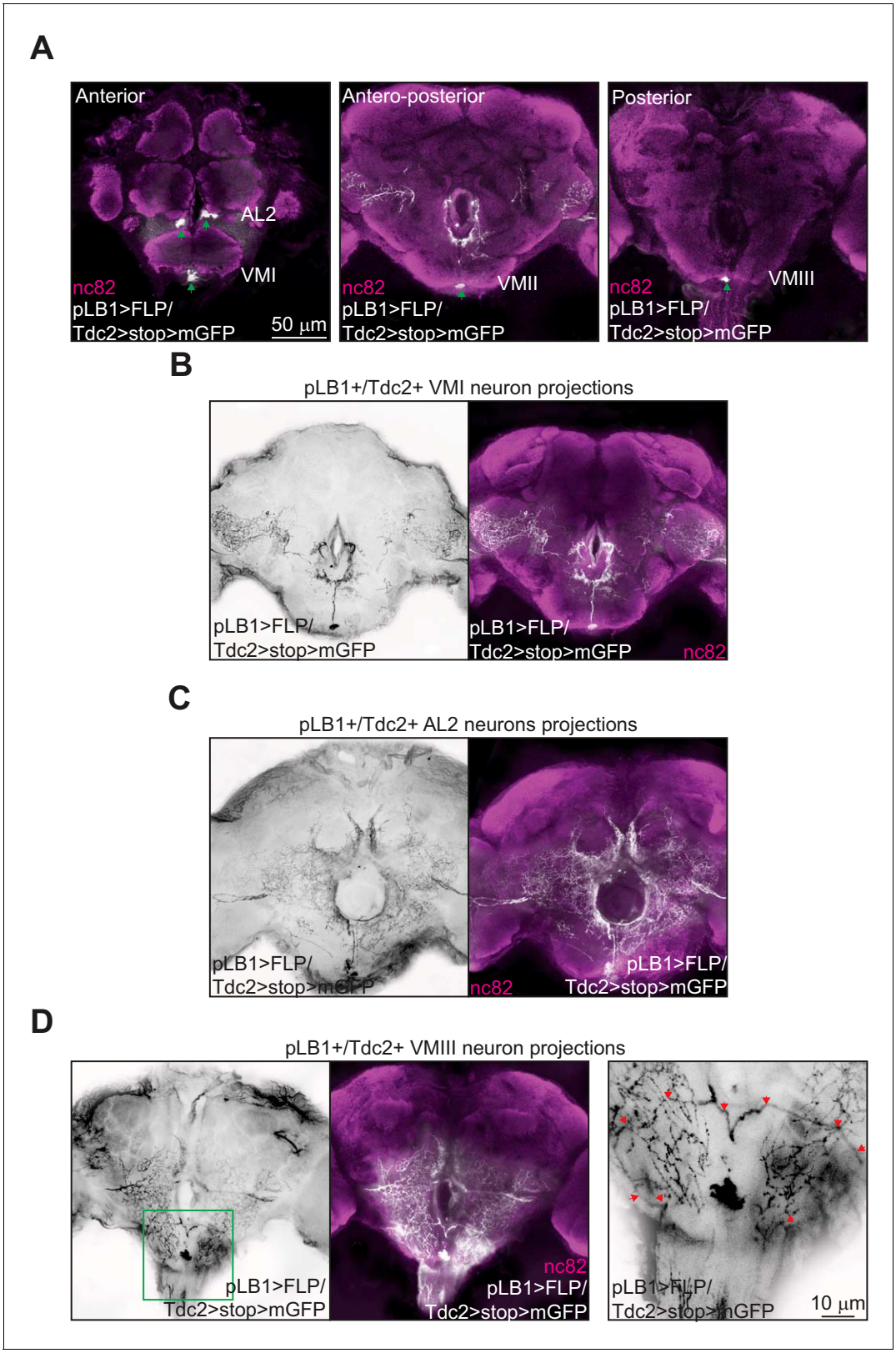

Figure 6. Brain pLB1+/Tdc2+ neurons project to the esophagus as well as to the VNC. (**A–D**); Immuno-detection in the brain of cells co-expressing the Tdc2-Gal4 and the pLB1-LexA drivers (pLB1>FLP/Tdc2>stop>mGFP). The GFP can only be expressed under the control of Tdc2 if the stop sequence inserted upstream of the *gfp* gene is flipped-out in pLB1+/Tdc2+ cells. (**A**); Five cellular bodies (green arrows) are detected in anterior, antero-posterior and posterior parts of the brain. (**B–D**); Specific stacks of the brain showing the projection patterns (in black) of the neurons present in VM I (**B**), AL2 (**C**)

Figure 6 continued on next page

Figure 6 continued

and VM III (**D**). In (**D**), the area delimited by the green box in the left panel is magnified on the right panel to show the descending projections (red arrows). Staining against nc82 was used to delineate the shape of the brain. Details including genotypes can be found in the detailed lines, conditions and, statistics for the figure section.

DOI: https://doi.org/10.7554/eLife.50559.028

insulin-related defects (***Pritchett and McCall, 2012***), but rather with a rapid accumulation of mature oocytes (stage 14) in the ovaries (***Kacsoh et al., 2015b***; ***Kurz et al., 2017***). By quantifying the effects of peptidoglycan exposure over time, we showed that this phenotype was reversible (***Figure 9A,B*** and ***Figure 9—figure supplement 1***). Whereas 6 hours after peptidoglycan injection, the amounts of stage 14 and 11–13 oocytes increased and decreased respectively, the effects were less pronounced after 24 hours and no longer detectable 48 hours post-injection. We then tested whether similar phenotypes could be obtained by a Kir2.1-mediated temporary inactivation of pLB1+ neurons using the Gal4/Gal80^{ts} system (***Figure 9C–E***). As for peptidoglycan injection, pLB1+ neurons transient inactivation led to stage 14 oocyte accumulation which was fully and progressively rescued by restoring normal pLB1+ neuronal function (***Figure 9C–E***, ***Figure 9—figure supplement 2***).

Peptidoglycan exposure modulates egg-laying by inhibiting follicular cell trimming

An important step occurring before oviposition is the transfer of the mature oocyte from the ovary to the lateral oviduct. This step which requires the rupture of the follicular cell layer and consequently allows the release of the oocyte in the oviduct is called follicle trimming. This process is OA-dependent and allows the mature oocyte to reach the lateral oviduct prior to its fertilization (***Lee et al., 2009***). Therefore, we tested whether the egg-laying drop observed upon inactivation of pLB1+ cells and peptidoglycan exposure were associated with a defect in follicle trimming. Ovaries of control lines (pLB1-Gal4/+ and +/UAS-Kir2.1) and animals with inactivated pLB1+ neurons (pLB1-Gal4/UAS-Kir2.1) were dissected when the females were five day-old, while water-injected and peptidoglycan-injected animals were dissected 6 hours after treatment. Following a DAPI staining, stage 14 oocytes were counted and the ratio of stage 14 oocytes covered by follicular cells quantified. We confirmed that compared to control lines, the inactivation of pLB1+ cells via Kir2.1 overexpression as well as the injection of peptidoglycan led to an accumulation of stage 14 oocytes (***Figure 10A–D, E and G***). Also, we observed a decrease of follicle trimming on mature oocytes after inactivation of pLB1+ cells via Kir2.1 overexpression or peptidoglycan injection compared to controls (***Figure 10F and H***). These results suggested that peptidoglycan exposure leads to a decrease of the OA-dependent rupture of follicular cells around mature oocytes and subsequently reduces the number of eggs laid by infected females.

Discussion

The present study demonstrated that some brain and VNC neurons are expressing endogenous peptidoglycan degrading enzyme PGRP-LB. Functional genetic intersection and calcium imaging data suggest a model in which, among them, very few brain pLB1+/Tdc2+ neurons belonging to the octopaminergic sub-cluster VM III sense peptidoglycan. The latter is likely to inhibit these (this) neurons leading to an NF-κB-dependent decrease of egg-laying in bacterially infected females (***Kurz et al., 2017***) (***Figure 11***). These results raise the question of the molecular and cellular mechanisms by which bacteria-derived peptidoglycan present in the hemolymph is able to reach this/these brain neuron/s. One model would be that circulating peptidoglycan can cross the blood-brain-barrier to reach brain neurons. In such a case, the selective expression of peptidoglycan sensor and NF-κB signaling components in some neurons, in this case, the pLB1+ neurons will confer them the ability to respond to peptidoglycan. In line with the idea that peptidoglycan can reach the brain, works in mice have shown that bacterial peptidoglycan derived from the gut microbiota can translocate into the brain where it is sensed by specific pattern-recognition receptors of the innate immune system (***Arentsen et al., 2017***; ***Arentsen et al., 2015***). However, precisely mapping the peptidoglycan localization in the brain and identifying the exact path followed by this gut-born bacteria metabolite to reach the brain will require peptidoglycan tracing methods which are not yet available.

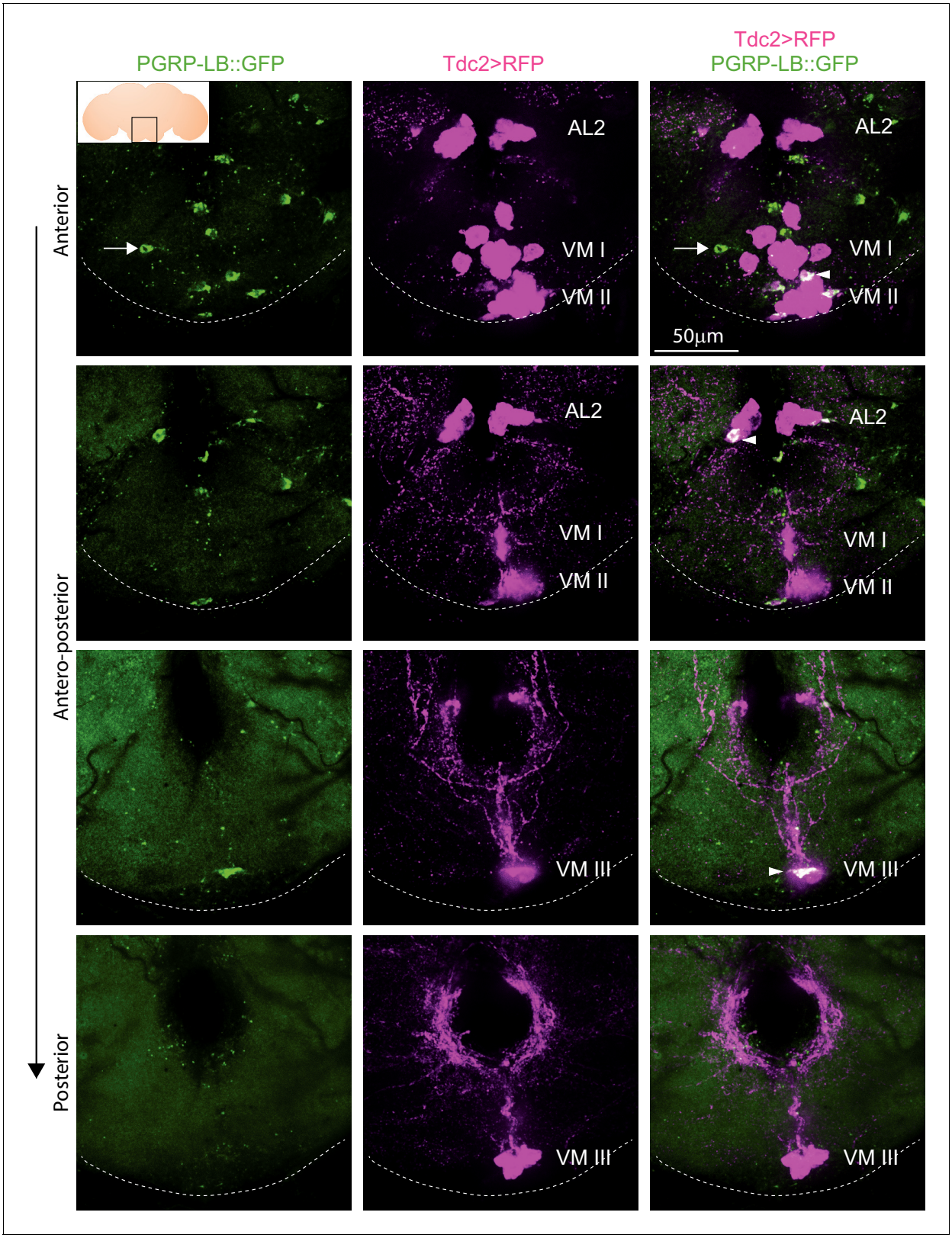

Figure 7. Endogenous PGRP-LB::GFP is expressed in Tdc2+ cells of the AL2 and VM clusters. Detection of PGRP-LB::GFP fusion protein as well as Tdc2 cells expressing RFP (Tdc2>RFP) without immunostaining . Only the area of the brain containing the octopaminergic AL2, VM I, VM II, and VM III clusters is shown with stacks corresponding to anterior, antero-medial, postero-medial and posterior views. The inserted scheme represents the brain, the empty black square delineates the area observed and the dashed line represents the ventral limit of the brain. Arrowheads point to Tdc2+/PGRP-

Figure 7 continued on next page

Figure 7 continued

LB::GFP+ cells and the arrow points to a Tdc2 negative cell containing PGRP-LB::GFP proteins. Details including genotypes can be found in the detailed lines, conditions and, statistics for the figure section.

DOI: https://doi.org/10.7554/eLife.50559.029

Alternatively, peptidoglycan could also be sensed by the pLB1+/Tdc2+ neurons at the level of the peripheric axonal or dendritic projections using a retrograde transport to bring peptidoglycan close to the cell body and hence allowing NF-κB activation. Further works and additional tools will be required to address these important questions.

It would be also important to understand how pLB1+/Tdc2+ VM III neurons regulate female egg-laying behavior in response to infection. Our results using the pLB1-LexA driver and a previously published anatomical map of brain octopaminergic neurons (**Busch et al., 2009**) indicate that some pLB1+/VM III neurons are sending descending neurites to the thoracic ganglia via cervical connectives. Analyzing the precise connectivity of these neurons will likely shed some light on these mechanisms.

A recent report showed that gut-resident *Lactobacillus brevis* can modify adult locomotion by acting on octopaminergic neurons via sugar metabolism (**Schretter et al., 2018**). This demonstrates that gut-associated bacteria have multiple ways to interact with the host behaviors. Alternatively, eukaryotes have developed different sensing mechanisms to adapt their behaviors to autochthonous or allochthonous bacteria. However, while the effects mediated by peptidoglycan on host egg-laying behavior are likely to be widespread since peptidoglycan is an universal bacterial cell-wall constituent, only bacteria producing xylose isomerase, such as *Lactobacillus brevis*, are expected to modify the walking activity of the colonized hosts. It should be mentioned that octopamine has also been shown to mediate neural regulation of immunity in *C. elegans* (**Sellegounder et al., 2018**).

Our data indicate that most pLB1+ neurons are not involved in controlling the egg-laying rate in response to infection and that a small fraction of them is octopaminergic. This suggests that most octopaminergic-dependent behaviors are unlikely to be affected by peptidoglycan exposure. Consistently, our data demonstrate that the receptivity of females to males, a behavior that is also under the control of octopamine, is not mediated by pLB1+ neurons. We, therefore, propose that by expressing sensors and effectors of the immune pathway in a small subset of neurons, flies render some of their behaviors controllable by bacteria-derived metabolite while maintaining others bacteria-unsensitive. Interestingly, pLB1+/Tdc2+ neurons that adapt female oviposition rate to their infectious status, are also present in males where they might regulate male-specific OA-dependent behaviors upon infection. One of the reported functions of octopaminergic circuitry is to modulate specific behaviors to environmental conditions (**Crocker and Sehgal, 2008**; **Rezával et al., 2014**; **Youn et al., 2018**). Such a modulatory function seems adapted to integrate immune signals allowing the fly to adapt to an environment enriched in microorganisms. Furthermore, the fact that some pLB1+ neurons are not octopaminergic, which is confirmed by using a PGRP-LB::GFP line in which all endogenous PGRP-LB protein isoforms are tagged, suggested that other neuronally controlled biological processes, yet to be identified, are likely to be influenced by PGN exposure. Identifying the exact nature of the non-octopaminergic pLB1+ neurons will be necessary to reveal the processes that they regulate. In addition, since pLB1+ neurons may represent only a subset of all the neurons that express immune pathway components, one could consider that other behaviors, yet to be identified, are controlled by bacteria.

The data from this study demonstrate that the response of few brain octopaminergic neurons to peptidoglycan is NF-κB pathway dependent, hence probably transcriptional. What are the NF-κB target genes mediating the effects of peptidoglycan in these neurons? Obvious candidates are the enzymes necessary for the production of octopamine itself which are Tdc2 and TβH. Consistently, providing ectopic TβH in pLB1+ neurons was shown to rescue egg-laying drop post infection (**Kurz et al., 2017**). Alternatively, antimicrobial peptides (AMPs) which are the main targets of NF-κB/Relish downstream of the innate immune pathways should also be considered. Although historically identified for their antimicrobial activity (**Ezekowitz and Hoffmann, 1996**), some recent reports indicate that AMPs play some important roles in the fly nervous system. Some AMPs, such as Metchnikowin, Drosocin, and Attacin, are implicated in sleep regulation (**Dissel et al., 2015**). Diptericin, a

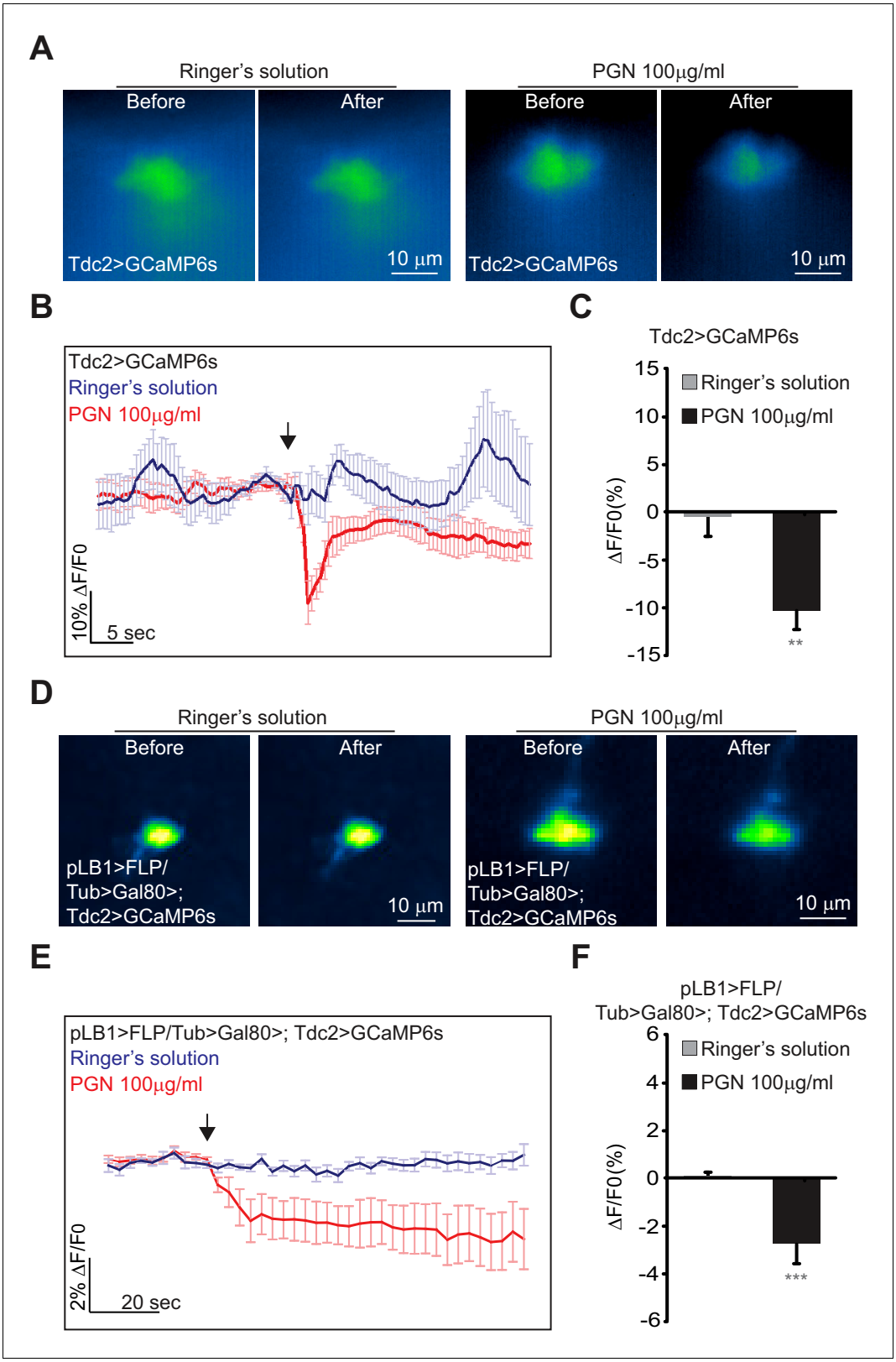

Figure 8. Real-time calcium imaging of Tdc2 VM II/III and pLB1+/Tdc2+ VM III neurons exposed to peptidoglycan. (**A–F**); Real-time calcium imaging using the calcium indicator GCaMP6s to reflect the *in vivo* neuronal activity of Tdc2 neurons (Tdc2>GCaMP6s) in VM II/VM III sub-clusters (**A–C**) or the *ex vivo* neuronal activity of Tdc2+/pLB1+ VM III neuron pLB1>FLP/Tub>Gal80>,Tdc2>GCaMP6s (**D–F**). (**A**); Representative images showing the GCaMP6s intensity before and after addition of either the control Ringer's solution (left panels) or the peptidoglycan (right panels). The images

Figure 8 continued on next page

Figure 8 continued

represent the average intensity of 4 frames before or after Ringer or peptidoglycan solution. (**B**); Averaged ± SEM time course of the GCaMP6s intensity variations (ΔF/F0 %) for Tdc2+ neurons of the VM II/VM III sub-clusters. The addition of Ringer's solution (n=8 flies) or peptidoglycan (n=13 flies) at a specific time is indicated by the arrow. (**C**); Averaged fluorescence intensity of negative peaks ± SEM for control (n=8) and peptidoglycan-treated flies (n=13). (**D**); Representative images showing the GCaMP6s intensity before and after the addition of either the control Ringer's solution (left panels) or the peptidoglycan (right panels). The images represent the average intensity of 4 frames before or after Ringer or peptidoglycan solution. (**E**); Averaged ± SEM time course of the GCaMP6s intensity variations (ΔF/F0 %) for Tdc2+/pLB1+ neuron of the VM III sub-cluster. The addition of Ringer's solution (n=10 flies) or peptidoglycan (n=12 flies) at a specific time is indicated by the arrow. (**F**); Averaged fluorescence intensity of negative peaks ± SEM for control (n=10) and peptidoglycan-treated flies (n=12) In (**C**), ** indicates p=0.001; in (**F**), *** indicates p=0.0001 non-parametric t-test, Mann-Whitney test. Details including n values and genotypes can be found in the detailed lines, conditions and, statistics for the figure section.

DOI: https://doi.org/10.7554/eLife.50559.030

The following figure supplement is available for figure 8:

Figure supplement 1. The *in vivo* and *ex vivo* real-time Calcium imaging approaches focused on neurons present in the VM II/III octopaminergic sub-cluster.

DOI: https://doi.org/10.7554/eLife.50559.031

well-characterized AMP, is important for a kind of non-associative learning, where ethanol preference is modified upon exposure to predatory wasps (***Bozler et al., 2017***). In addition, AMPs expressed in the fly adult head are involved in modulating long-term memory (***Barajas-Azpeleta et al., 2018***). Finally, the innate immune receptor PGRP-LC and downstream signaling are implicated in the regulation of the homeostatic plasticity of neuromuscular junction synapse by NF-κB/Relish-dependent and independent processes (***Harris et al., 2015***; ***Harris et al., 2018***). Further experiments will be necessary to test whether any of these cellular mechanisms are also at play in the regulation of neuronal-controlled behaviors by bacteria-derived metabolite in general and by PGN in particular.

Finally, it would be necessary to elucidate how neurons exposed to peptidoglycan modify intracytosolic calcium levels and identify a possible functional link with NF-κB signaling. Our previous and current results demonstrate that the egg-laying drop requires several elements of the IMD pathway, from the PGN-receptor PGRP-LE to the transcription factor NF-κB/Relish. It should be noted that a link between calcium levels and NF-κB activation in neurons has been reported in many mammalian studies (***Lilienbaum and Israël, 2003***; ***Lipton, 1997***; ***O'Neill and Kaltschmidt, 1997***). In addition, calcineurin, a Ca^{2+}-dependent phosphatase was shown to promote NF-κB dependent immune responses in the *Drosophila* larvae (***Dijkers and O'Farrell, 2007***). As for the causality between peptidoglycan stimulation and calcium decrease and despite the kinetic that does not suggest the involvement of a stereotypical signaling cascade, it should first be tested whether this step requires the elements of the IMD (Immune deficiency) pathway. If not, other receptors yet to be identified may mediate this fast response to peptidoglycan. Intriguingly, a recent study using the fly embryo linked a rapid modification of the calcium concentration in fly hemocytes undergoing phagocytosis of apoptotic corpses with the subsequent activity of the JNK pathway, the first event being a pre-requisite for the second (***Razzell et al., 2013***).

Materials and methods

Key resources table

Reagent type (species) or resource	Designation	Source or reference	Identifiers	Additional information
Genetic reagent (*D. melanogaster*)	pLB1-Gal4	(***Kurz et al., 2017***)		
Genetic reagent (*D. melanogaster*)	UAS-Kir2.1	Bloomington Drosophila Stock Center (***Hardie et al., 2001***)	BDSC Cat# 6595, RRID: BDSC_6595	

Continued on next page

Continued

Reagent type (species) or resource	Designation	Source or reference	Identifiers	Additional information
Genetic reagent (*D. melanogaster*)	UAS-TTx	Bloomington Drosophila Stock Center (**Sweeney et al., 1995**)	BDSC Cat# 28838, RRID: BDSC_28838	
Genetic reagent (*D. melanogaster*)	UAS-TRPA1	Bloomington Drosophila Stock Center	BDSC Cat# 26264, RRID: BDSC_26264	
Genetic reagent (*D. melanogaster*)	UAS-Fadd-IR	(**Khush et al., 2002**)		
Genetic reagent (*D. melanogaster*)	UAS> stop> GFPmCD8	Bloomington Drosophila Stock Center	BDSC Cat# 30125, RRID: BDSC_30125	
Genetic reagent (*D. melanogaster*)	nSyb-LexA	Bloomington Drosophila Stock Center	BDSC Cat# 51951, RRID: BDSC_51951	
Genetic reagent (*D. melanogaster*)	Tdc2-LexA	Bloomington Drosophila Stock Center	BDSC Cat# 52242, RRID: BDSC_52242	
Genetic reagent (*D. melanogaster*)	Tub>Gal80>	Bloomington Drosophila Stock Center	BDSC Cat# 38879, RRID: BDSC_38879	
Genetic reagent (*D. melanogaster*)	LexAop-FLP	Bloomington Drosophila Stock Center	BDSC Cat# 55819, RRID: BDSC_55819	
Genetic reagent (*D. melanogaster*)	8XLexAop2-FLP	Bloomington Drosophila Stock Center	BDSC Cat# 55820, RRID: BDSC_55820	
Genetic reagent (*D. melanogaster*)	UAS>stop > Kir2.1			
Genetic reagent (*D. melanogaster*)	UAS>stop> TRPA1	Bloomington Drosophila Stock Center	BDSC Cat# 66871, RRID: BDSC_66871	
Antibody	Rabbit polyclonal anti-Tdc2	Abcam	Cat# ab128225, RRID: AB_11142389	1:1000
Chemical compound	PGN from *E. coli*	Invivogen	14C14-MM	
Software, algorithm	Fiji	NIH	https://fiji.sc/	
Software, algorithm	GraphPad Prism 6	GraphPad	RRID: SCR_002798	

Drosophila melanogaster strains and maintenance

The following strains were used in this work: pLB1-Gal4 (**Kurz et al., 2017**); UAS-GFPnls (BDSC Cat# 4775, RRID:BDSC_4775); UAS-mCD8-Tomato (kindly provided by F. Schnorrer); UAS-TTx (**Sweeney et al., 1995**), (BDSC Cat# 28838, RRID:BDSC_28838); UAS-TRPA1 (BDSC Cat# 26264, RRID:BDSC_26264); UAS-Kir2.1 (BDSC Cat# 6595, RRID:BDSC_6595) (**Hardie et al., 2001**); UAS-

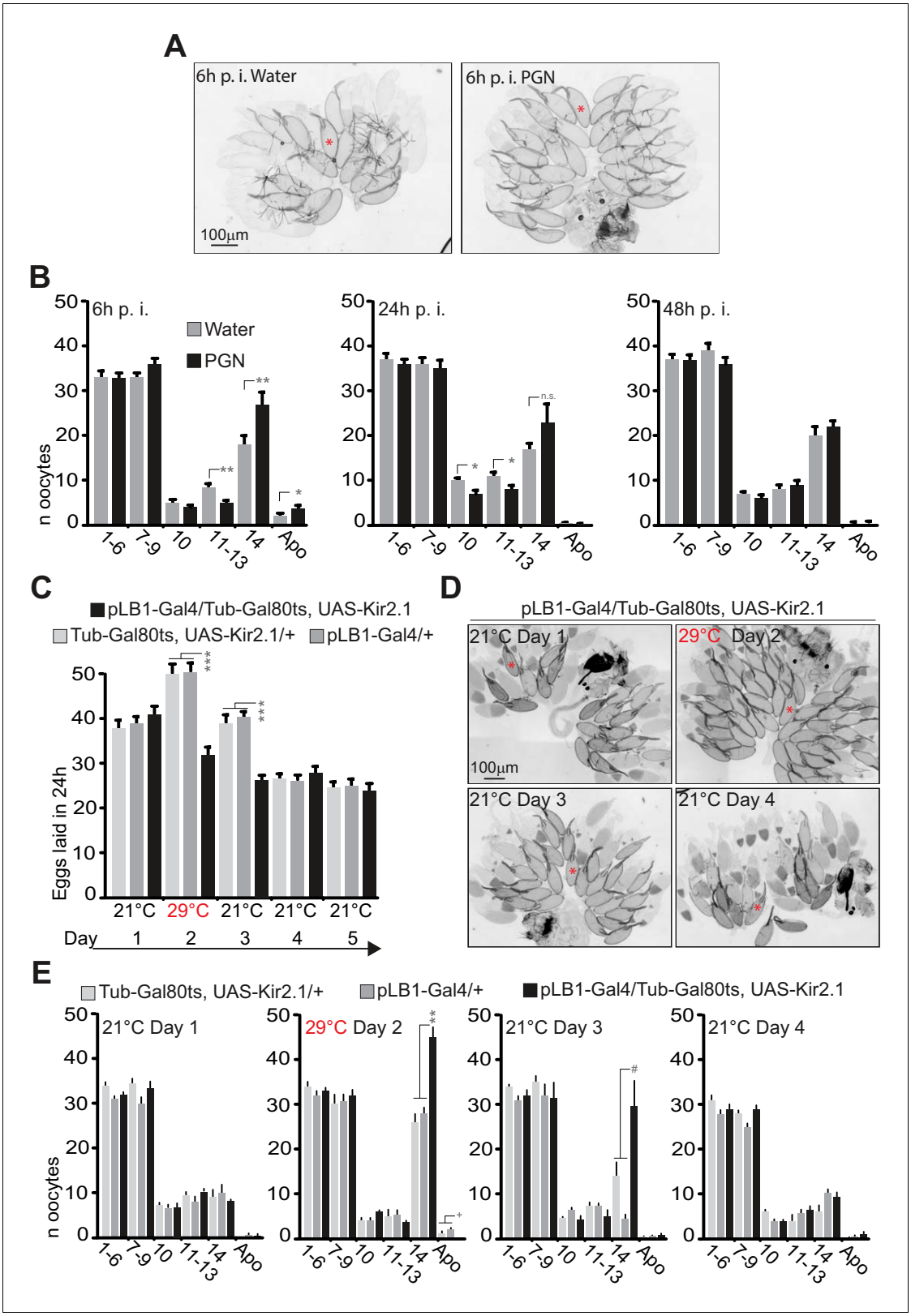

Figure 9. Peptidoglycan exposure as well as pLB1+ neurons conditional inactivation lead to a reversible mature oocyte accumulation. (**A–B**); Injection of peptidoglycan triggers a reversible accumulation of mature oocytes (stage14). (**A**); 6 hours (6h) post-treatment (p.i.), stage 14 oocytes accumulate in the ovaries of peptidoglycan-injected flies. Transmission light microscopy images of ovaries dissected from control flies (water injected) or peptidoglycan-injected animals 6h post-treatment. (**B**); peptidoglycan injection modifies the quantity and quality of oocytes by 6 h, leading to an accumulation of

Figure 9 continued on next page

Figure 9 continued

mature stage (stage14) eggs. The dynamic over three different time points (6h-24h-48h) post-treatment was assayed. (**C–E**); pLB1+ neurons reduced activity leads to stage 14 oocyte accumulation. (**C**); The conditional inactivation of pLB1+ neurons reduces egg-laying. At 21˚C, the ubiquitously produced Gal80^{ts} inactivates the Gal4 and thus the Kir 2.1 protein expression. At 29˚C, the Gal80^{ts} doesn't inactivate the Gal4, leading to the inhibited activity of pLB1+ neurons via Kir2.1. Switching back the animals to 21˚C inhibits the Gal4 activity via Gal80^{ts}. (**D**); Conditional inactivation of the pLB1+ neurons triggers a reversible stage 14 oocytes accumulation. Ovaries images of pLB1-Gal4/Tub-Gal80^{ts}, UAS-Kir2.1 flies were acquired with transmission light microscopy for 4 days at two different temperatures. (**E**); pLB1+ neurons conditional inactivation modifies the quantity and quality of oocytes,leading to an accumulation of stage 14 oocytes. The dynamic over four different time points and two different temperatures is shown. It is important to note that the switch from 21˚C to 29˚C might be stressful for all the lines since stage 14 oocytes accumulated in all of them. In (**A and D**), a prototypical stage 14 oocyte is indicated with a red asterisk. In (**B**), shown are the average numbers over time of different oocyte stages ± SEM from two cumulated independent trials with at least 18 females per genotype and condition used. In (**C**), shown are the average numbers of eggs laid per fly per 24h ± SEM over 5 days from two cumulated independent trials with at least 59 females per genotype and condition used. In (**E**), shown are the average numbers of different oocyte stages ± SEM over 4 days for one representative assay out of two independent trials with at least 10 females per genotype and condition used. For (**B**) and (**E**), on the *x* axis, 1–6 corresponds to early stages (from stage 1 to stage 6)oocytes ; 7–9 corresponds to the sum of stages 7, 8 and 9; 10 is for stage 10; 11–13 is for the sum of stages 11, 12 and 13; 14 is for stage 14 and Apo is for apoptotic events, all identified via DAPI staining. * indicates $p<0.05$; ** indicates $p<0.01$; *** indicates $p<0.0001$; $^{+}$ and $^{\#}$ indicate statistically significant differences between the test and the controls, but not all of them (see detailed statistics for ***Figure 9E***). In (**B**), non-parametric t-test, Mann-Whitney test; in (**C and E**), non-parametric ANOVA, Dunn's multiple comparison test between the genotypes or treatments. Details including n values and genotypes can be found in the detailed lines, conditions and, statistics for the figure section.

DOI: https://doi.org/10.7554/eLife.50559.036

The following source data and figure supplements are available for figure 9:

Source data 1. Egg laying raw date for ***Figure 9C***.

DOI: https://doi.org/10.7554/eLife.50559.039

Figure supplement 1. Peptidoglycan exposure leads to a reversible accumulation of stage 14 oocytes.

DOI: https://doi.org/10.7554/eLife.50559.037

Figure supplement 2. Conditional inactivation of pLB1+ neurons leads to a reversible accumulation of stage 14 oocytes.

DOI: https://doi.org/10.7554/eLife.50559.038

Fadd-IR (***Khush et al., 2002***) (Kindly provided by P. Meier); Tdc2-Gal4 (kindly provided by H. Scholz); nSyb-LexA (BDSC Cat# 51951, RRID:BDSC_51951); Elav-Gal80 (kindly provided by D. Herman); UAS>stop>GFPmCD8 (BDSC Cat# 30125, RRID:BDSC_30125); w- (BDSC Cat# 3605, RRID:BDSC_3605); UAS-TβH-IR (BDSC Cat# 27667, RRID:BDSC_27667); Tdc2-LexA (BDSC Cat# 52242, RRID:BDSC_52242); Tub>Gal80> (BDSC Cat# 38879, RRID:BDSC_38879); LexAop-FLP (BDSC Cat# 55819, RRID:BDSC_55819); 8XLexAop2-FLP (BDSC Cat# 55820, RRID:BDSC_55820); UAS>stop>-Kir2.1 (kindly provided by K Anderson's lab); HS-FLP (kindly provided by F. Schnorrer); OTD-FLP (kindly provided by K Anderson's Lab); Tsh-LexA, LexAop-Gal80 (kindly provided by S Birman's Lab); Tsh-Gal4 (kindly provided by M. Landgraf); 13XLexAop2-GFPmCD8 (BDSC Cat# 32203, RRID:BDSC_32203); LexAop-2xhrGFPnls (BDSC Cat# 29955, RRID:BDSC_29955); Dsx-LexA (BDSC Cat# 54785, RRID:BDSC_54785); Dsx-FLP (kindly provided by S. Goodwin). UAS>stop>TRPA1 (BDSC Cat# 66871, RRID:BDSC_66871); Tub-Gal80ts, UAS-Kir2.1 (kindly provided by B. Prud'homme's lab); UAS-GCaMP6s (BDSC Cat# 42746, RRID:BDSC_42746).

Flies were grown at 25˚C on a yeast/cornmeal medium in 12h/12h light/dark cycle-controlled incubators. For 1 L of food, 8.2 g of agar (VWR, cat. #20768.361), 80 g of cornmeal flour (Westhove, Farigel maize H1) and 80 g of yeast extract (VWR, cat. #24979.413) were cooked for 10 min in boiling water. 5.2 g of Methylparaben sodium salt (MERCK, cat. #106756) and 4 mL of 99% propionic acid (CARLOERBA, cat. #409553) were added when the food had cooled down.

Cloning pLB1-LexA pLB1 DNA fragment corresponding to pLB1-Gal4 (***Kurz et al., 2017***) was cloned by Gateway into pBP nlsLexA::p65Uw vector (RRID:Addgene_26230). This vector was injected into y^{1}w- P{nos-phiC31\int.NLS}X; P{CaryP}attP40 embryos (modified from BDSC Cat# 25709, RRID:BDSC_25709) and screened in F1 for white + transformants.

PGRP-LB::GFP

A PGRP-LB::GFP fusion protein transgenic line was obtained by inserting, via CRISPR mediated recombination, the eGFP cDNA at the C-term end of the PGRP-LB protein. The GFP cDNA was inserted in the 3' most coding exon, resulting in all PGRP-LB isoforms (RA; RC and RD) tagged with GFP. The P donor PGRP-LB-GFP was obtained by cloning the GFP cDNA flanked by 1 kb of PGRP-

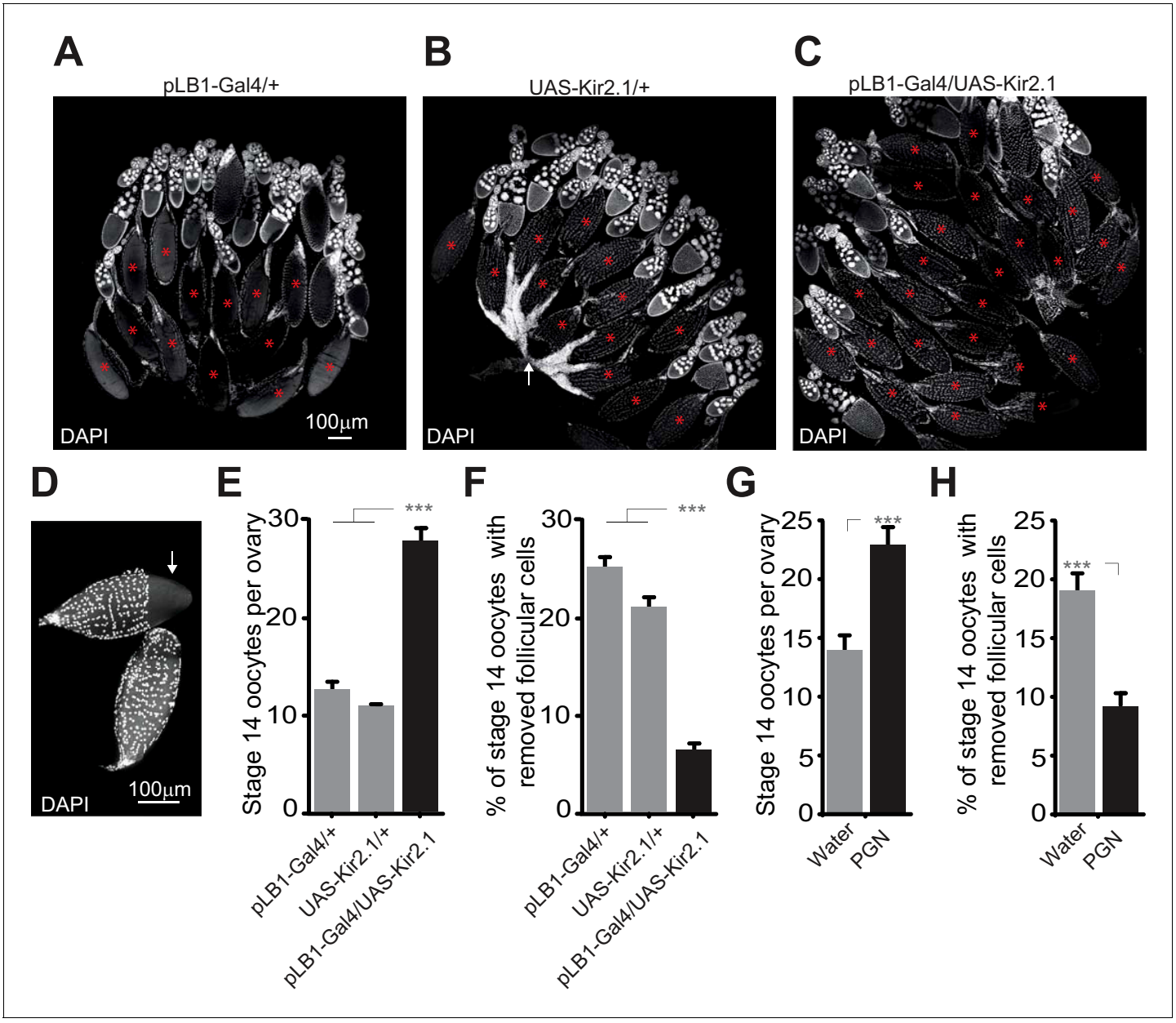

Figure 10. Impairing the activity of pLB1+ cells or injecting peptidoglycan leads to an accumulation of mature oocytes and a defect in follicular cells rupture. (**A–C**); Reducing the activity of pLB1+ cells leads to an accumulation of mature oocytes (stage14). DAPI staining of ovaries from control flies (**A and B**) or animals with reduced activity of the pLB1+ cells (**C**). Mature oocytes are indicated with a red asterisk and an oocyte with follicular cells ruptured is indicated with a white arrow. (**D**); Follicular cells surrounding the mature oocytes are removed before the entry in lateral oviducts. DAPI staining of stage 14 oocytes with follicular cells partly removed (white arrow) or fully covering the oocyte (bottom). (**E and G**); Stage 14 oocytes accumulate in the ovaries when pLB1+ cells activity is impaired (**E**) or when peptidoglycan is injected (**G**). (**F and H**); The ratio of mature oocytes with removed follicular cells is decreased when pLB1+ cells activity is impaired (**F**) or when peptidoglycan is injected (**H**). For (**E and G**), shown is the average number of stage 14 oocytes per ovary ± SEM in 5 day-old females (**E**) or 6 hours post-treatment (**G**) from three independent trials with at least 50 ovaries per genotype and condition used. For (**F and H**), shown are the ratios of stage 14 oocytes with removed follicular cells ± SEM in 5 day-old females (**F**) or 6 hours post-treatment (**H**) from three independent trials with at least 50 ovaries per genotype and condition used. For (**E and F**), *** indicates $p<0.0001$; non-parametric ANOVA, Dunn's multiple comparison test. For (**G and H**), *** indicates $p<0.0001$; non-parametric t-test, Mann-Whitney test. Details including n values and genotypes can be found in the detailed lines, conditions and, statistics for the figure section.

DOI: https://doi.org/10.7554/eLife.50559.040

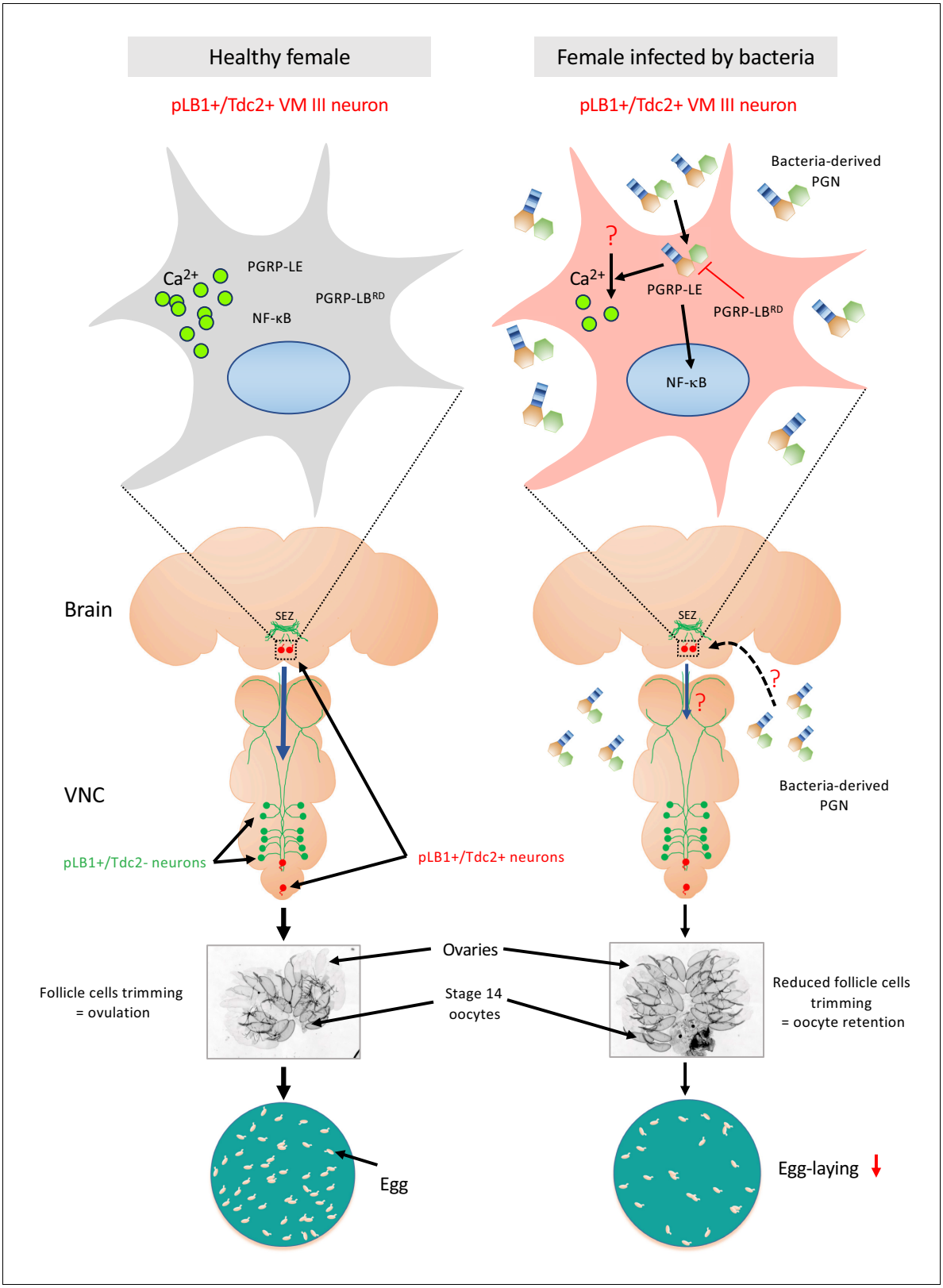

Figure 11. Diagram summarizing the effect of peptidoglycan sensing by pLB1+/Tdc2+ brain neurons on female oviposition. (**Left**) Around 20 neurons distributed in the brain and the ventral nerve cord (VNC) express immune genes such as PGRP-LB (called pLB1+ neurons, labeled in green and red). Among them, very few are also expressing the enzyme Tdc2 indicating that they are octopaminergic neurons (labeled in red), with the most robust pLB1 expression for those localized in the brain ventral midline, the VM cluster (delineated by the box with dashed line and schematically magnified in

Figure 11 continued on next page

Figure 11 continued

the top box). In homeostasic conditions, mated females produce mature oocytes surrounded by follicular cells. Rupture of these follicular cells (trimming) leads to egg ovulation. (**Right**) Upon bacterial infection either systemic or enteric, cell wall peptidoglycan (PGN) is released by proliferating bacteria and transported into the hemolymph. Intracytosolic peptidoglycan sensing via the PGRP-LE Rc, in the very few brain pLB1+/Tdc2+ neurons (but not in the VNC pLB1+/Tdc2+ neurons), leads to cell-autonomous NF-κB pathway activation. This causes a reduction of follicular cells trimming in mature (stage 14) oocytes, hence a reduction of egg-laying in infected females. Since some pLB1+/Tdc2+ neurons of the VM cluster (VM III sub-cluster specifically) are sending descending projections toward the VNC and that the direct addition of peptidoglycan reduces their intracytosolic calcium level, we believe that peptidoglycan directly reduces the activity of these cells. Then, these brain pLB1+/Tdc2+ cells could mediate their effect via secondary neurons present in the VNC. It remains to be understood how PGN from the hemolymph is reaching brain neurons, how PGN stimulation reduces calcium levels, how this is linked to NF-κB pathway signaling and whether secondary neurons modulate ovulation. Moreover, we believe that pLB1+/Tdc2- neurons control other behaviors that are probably modulated by infection.

DOI: https://doi.org/10.7554/eLife.50559.041

LB homology arms into the Bluescript vector using the following primers (fw 5' arm: CGGGC TGCAGGAATTCCAAACAGCTCGCACGCAAAATACAA, rv 5' arm: AACAGCTCCTCGCCCTTGC TCACGACCTTGGGCGCAGCTGGC; fw 3' arm: GCTGTACAAGCACCGGTCCACGTAGGCTGGA TTGGAGGGCCCTCA, rv 3' arm: GGGCCCCCCCTCGAGGCTGCCGCCGAAATCAATCCAATAGC). Guide RNA (GCTGCGCCCAAGGTCTAGGC), was cloned into pCFD3–dU6: 3 gRNA (RRID:Addgene_49410). y[1] M{w[+mC]=nos-Cas9.P}ZH-2A w[*] embryos were injected with both donor and guide vectors (pCFD3-gRNA ; P donor PGRP-LB::GFP). F1 larvae were screened for GFP expression and positive line were confirmed molecularly.

Oviposition assay

In order to ease the quantification of the laid eggs, a blue food dye (E133, Le meilleur du chef) was incorporated (1%) into the media used for the oviposition assays (Blue-tube). When the egg-laying index was used, it corresponds to the ratio between the number of eggs laid by a treated female and the average number of eggs per tube laid by the untreated animals during a specific time. An oviposition ratio of 1 indicates that the treatment did not impact the oviposition of the tested female during the time course of the experiment. *PGN injections*: one-day-old animals were harvested from tubes kept at 25˚C. Males and females were mixed in one tube with no more than 40 individuals per tube and the proportion male: female was 1:1. Tubes were kept at 25˚C and flies shifted to fresh tubes every 2 days. On day 5, females were used for injections. PGN or endotoxin-free water was used and injected using a nanojector (Nanojet II, Drummond Scientific Company, PA, USA). PGN is from *E. coli* (Invivogen, ref 14C14-MM, CA, USA) and was resuspended in endotoxin-free water at 200 µg/mL. 60 nL of PGN solution was injected in the thorax. All the flies including control animals

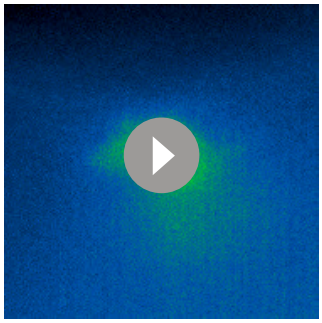

Video 1. Effect of Ringer's solution stimulation on Tdc2>GCaMP6s VM II/III neurons *in vivo*. GFP recording of an *in vivo* Tdc2>GCaMP6s fly brain in the VM II/III octopaminergic sub-clusters region. Brains of flies from which the head capsule has been removed were exposed to Ringer's solution. GFP signal was recorded every 500 ms.

DOI: https://doi.org/10.7554/eLife.50559.032

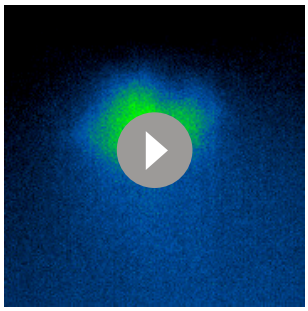

Video 2. Effect of peptidoglycan solution stimulation on Tdc2>GCaMP6sVM II/III neurons *in vivo*. GFP recording of an *in vivo* Tdc2>GCaMP6s fly brain in the VM II/III octopaminergic sub-clusters region. Brains of flies from which the head capsule has been removed were exposed to peptidoglycan solution. GFP signal was recorded every 500 ms.

DOI: https://doi.org/10.7554/eLife.50559.033

Video 3. Effect of Ringer's solution stimulation on pLB1>FLP/Tub>Gal80>,Tdc2>GCaMP6s VM III neurons *ex vivo*. GFP recording of an *ex vivo* pLB1>FLP/Tub>Gal80>,Tdc2>GCaMP6s fly brain in the VM III octopaminergic sub-cluster region. Dissected brains were mounted in Ringer's solution and stimulated with the same control solution. GFP signal was recorded every 2 s.
DOI: https://doi.org/10.7554/eLife.50559.034

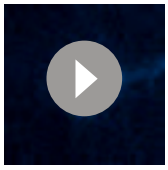

Video 4. Effect of peptidoglycan solution stimulation on pLB1>FLP/Tub>Gal80>,Tdc2>GCaMP6s VM III neurons *ex vivo*. GFP recording of an *ex vivo* pLB1>FLP/Tub>Gal80>,Tdc2>GCaMP6s fly brain in the VM III octopaminergic cluster region. Dissected brains were mounted in Ringer's solution and stimulated with peptidoglycan solution. GFP signal was recorded every 2 s.
DOI: https://doi.org/10.7554/eLife.50559.035

were anesthetized on CO_2 pad. *Egg-lay assay*: Treated animals were then transferred on fresh Blue-tube with dry yeast (Fermipan) added on top of each tube right before the egg-lay period. When PGN injection was tested, animals were allowed to lay eggs for 6h, two females per tube. Otherwise, flies were one per tube and laid eggs during 24h. In order to maximize the efficiency of the transgenes, animals were stored at 29˚C one day before the treatment and kept at this temperature during the egg-lay assay (except for experiments involving thermosensitive transgenes). Injections were always performed between ZT0 and ZT6. Eggs were counted for each tube 6h or 24h later. The eggs were not blindly counted. Raw egg counts are available as Data source.

Mating assay

Virgin females were collected after eclosion and kept in groups of 10–15 individuals at 25˚C, whereas naïve males where singularly isolated after eclosion and kept at 25˚C. Mating experiments were performed in a behavioral room at 24˚C. To assay fly receptivity, a 6 days-old virgin female was introduced in a laboratory made chamber (17 mm diameter x 8 mm height) with a naïve w- male. During 10 min, flies recovered from the flipping and adapted to the new chamber. Then, flies were recorded with a camera (Logitech HD pro webcam c920) for 1h and receptivity was quantified as the percentage of flies that mated within this time. Latency was defined as the time at which mating was starting. Successfully mated females were isolated in vials where they laid eggs for 48h at 25˚C. Mated females were again introduced in a chamber with a naïve w- male to assay re-mating. The latter was defined as the percentage of mated pairs within 1h.

Ovaries content and trimming quantification

Flies were reared and harvested as for the oviposition assays. After a 20s EtOH bath, animals were dissected at RT in 1X phosphate-buffered saline (PBS), then ovaries were fixed for 10 min in 4% paraformaldehyde on ice and rinsed three times in 1X PBS. The ovaries were then incubated with DAPI in the dark for 10 min. Finally, ovaries were gently opened on a glass slide in a 1X PBS drop. Oocytes stages, apoptotic events and trimming were visually quantified per ovary using DAPI and an AxioImager APO Z1 apotome microscope (Zeiss, Germany).

Imaging and Immuno-cytochemistry

Adult brains and VNCs were dissected in PBS and fixed for 15 min in 4% paraformaldehyde at RT. After fixation, the tissues were rinsed three times for 10 min in PBS-T (PBS + 0.3% Triton X-100) and blocked in 2,5% bovine serum albumin (BSA; Sigma-Aldrich) in PBS-T for 30 min. Next, samples were incubated with the first antibody diluted in 0,5% BSA in PBS-T overnight at 4˚C. The tissues were then washed three times and incubated with the secondary antibody diluted in 0,5% BSA in PBS-T for 2h at RT. Samples were rinsed three times and mounted on slides using Vectashield (Vector Laboratories, Ca, USA) fluorescent mounting medium, with or without DAPI. Images were captured with either a Leica SP8 confocal microscope (in this case, tissues were scanned with 20X oil immersion objective) or an AxioImager APO Z1 apotome microscope (10X or 20x air objectives were used). For the detection of endogenous PGRP-LB::GFP, brains of PGRP-LB::GFP Tdc2-Gal4/UAS-

Tomato-mCD8 flies were dissected in PBS, fixed on ice for 3 min, washed three times and then mounted without immuno-staining. Images were captured with a Spinning Disk Ropper 2 Cam.

Calcium imaging

For *in vivo* calcium imaging studies, fed mated females were aged from 5 to 7 days. The preparation consisted of a fly suspended by the neck on a plexiglass block (2 × 2×2.5 cm). Flies were anesthetized on ice for 1h. The flies, with the proboscis facing the center of the block, were immobilized using an insect pine (0.1 mm diameter) placed on the neck. The ends of the pin were fixed on the block with beeswax (Deiberit 502, Siladent, 209212). Then the head was glued on the block with a drop of rosin (Gum rosin, Sigma-Aldrich, 60895); dissolved in ethanol at 70%) to avoid any movements. Therefore, the anterior part of the head is oriented towards the objective of the microscope. Flies were placed in a humidified box to allow the rosin to harden for 1h. A plastic coverslip with a hole corresponding to the head width was placed on top of the head and fixed on the block with beeswax. The plastic coverslip was sealed on the cuticle with two-component silicon (Kwik-Sil, World Precision Instruments). 100 µL of Ringer's saline (130 mM NaCl, 5 mM KCl, 2 mM $MgCl_2$, 2 mM $CaCl_2$, 36 mM saccharose, 5 mM HEPES, pH 7.3) were placed on the head. The antenna area, the tracheas, and the fat body were removed. The gut was cut without damaging the brain to allow visual access to the ventral part of the SEZ. The exposed brain was rinsed twice with 100 µL of Ringer's saline. GCaMP6s fluorescence was viewed with a Leica DM600B microscope under a 25x water objective. GCaMP6s was excited using a Lumencor diode light source at 482 nm ±25. Emitted light was collected through a 505–530 nm band-pass filter. Images were collected every 500ms using an Orca Flash 4.0 camera and processed using Leica MM AF 2.2.9. Each experiment consisted of 70 to 100 images (before application) followed by 160 images of recording after the addition of 100 µL Ringer's saline (control) or 100 µL of PGN solution (200 µg PGN/mL diluted in Ringer's saline for a final PGN concentration on the preparation of 100 µg/mL).

For the *ex vivo* calcium imaging, 5–7 day-old females were immobilized on ice and brains were dissected in Ringer's saline and were located in a silicone (SYLGARD 184 Silicone Elastomer Kit, DOW) coated cover slip. To avoid any movements during the recording, brains were fixed to the silicone support by using two insect pins at the level of the optical lobes. A 50 µL drop of Ringer's solution was used to cover the brain. GCaMP6s fluorescence was recorded with a Confocal spinning disk Yokogawa coupled with a Nikon Ti Eclipse inverted microscope and 2 CMOS capture cameras (Evolve 512) under a 20x air objective. For *GCaMPs excitation*, a laser wavelength at 491 nm (30% laser power; time of exposure 200 ms) was used. Images were taken every 2s and each experiment consisted in around 40 measurements (before application) followed by 100 recording images after the addition of 50 µL Ringer's saline (control) or 50 µL of PGN solution (for a final PGN concentration on the preparation of 100 µg/mL). Data were analyzed using FIJI (https://fiji.sc/) as previously described (***Silbering et al., 2012***).

Statistical analyses and graphics

The Prism software (GraphPad Prism, RRID:SCR_002798) was used for statistical analyses. Our sets of data were tested for normality using the D'Agostino-Pearson omnibus test, and some of our data did not pass the normality test. Consequently, we used non-parametric tests for all the data sets, that is the unpaired ANOVA, Kruskal-Wallis test and specifically the Dunn's multiple comparisons test as well as the unpaired Mann-Whitney two-tailed test. In addition, for mating and remating datasets, we used the Fisher exact t-test. Moreover, we do not show one experiment representative of the different biological replicates, but all the data generated during the independent experiments in one graph.

Antibodies table

Antibody	Source	Dilution
Chicken anti-GFP	Aves Labs Cat# GFP-1020, RRID:AB_10000240	1:1000

Continued on next page

Continued

Antibody	Source	Dilution
Rabbit anti-RFP	Rockland Cat# 600-401-379, RRID:AB_2209751	1:1000
Rat anti-RFP [5F8]	ChromoTek Cat# 5f8-100, RRID:AB_2336064	1:1000
Mouse anti-NC82	DSHB Cat# nc82, RRID:AB_2314866	1:40
Rat anti-Elav-7E8A10	DSHB Cat# Rat-Elav-7E8A10 anti-elav, RRID:AB_528218	1:50
Rabbit anti-Tdc2	Abcam Cat# ab128225, RRID:AB_11142389	1:1000
Rabbit anti-A-Allatostatin	Jena Bioscience (ABD-062)	1:2000
Rabbit anti-CCAP	Jena Bioscience (ABD-033)	1:6000
Rat anti-leukokinin	P. Herrero's lab gift	1:1000
Rabbit anti-leukokinin	Dick R Nässel's lab gift	1:2000
Alexa Fluor 488 Donkey anti-Chicken IgY (IgG) (H+L)	Jackson Immuno Research Labs Cat# 703-545-155, RRID:AB_2340375	1:500
Alexa Fluor568 donkey anti-mouse IgG (H+L)	Thermo Fisher Scientific Cat# A10037, RRID:AB_2534013	1:500
Alexa Fluor647 donkey anti-mouse IgG (H+L)	Jackson Immuno Research Labs Cat# 715-605-151, RRID:AB_2340863	1:500
Alexa Fluor 488 donkey anti-rabbit IgG (H+L)	Thermo Fisher Scientific Cat# A-21206, RRID:AB_2535792	1:500
Alexa Fluor 568 donkey anti-rabbit IgG (H+L)	Thermo Fisher Scientific Cat# A10042, RRID:AB_2534017	1:500
Cy 3 donkey anti-rat IgG (H+L)	Jackson Immuno Research Labs Cat# 712-165-153, RRID:AB_2340667	1:500
Alexa Fluor647 donkey anti-rat IgG (H+L)	Jackson Immuno Research Labs Cat# 712-605-153, RRID:AB_2340694	1:500
Rabbit anti-Bursicon	B. White's lab gift	1 :2500

Detailed lines, conditions and, statistics for the figures

Lines and conditions used for *Figure 1*

For 1A and 1B:

Genotypes of tested animals

- pLB1-Gal4; UAS-Tomato-mCD8

Reagents and tools

- antibody against nc82; antibody against Tomato; Leica SP8 confocal microscope

For 1C, 1D:
Genotypes of tested animals

- pLB1-Gal4, UAS > stop > GFPmCD8; LexAop-FLP/nSyb-LexA

Reagents and tools

- antibody against nc82; antibody against GFP; Leica SP8 confocal microscope

For 1F:
Genotypes of tested animals (at 23˚C: n flies/mean eggs exp1/mean eggs exp2 //at 29˚C: n flies/mean eggs exp1/mean eggs exp2)

- pLB1-Gal4/+ (20/43.7/49.4 //20/52.5/51.6)
- UAS-TRPA1/+ (16/29.17/50.5 //19/39.4/46.6)
- Elav-Gal80; UAS-TRPA1/+ (20/50.3/48.4 //20/52.7/45.7)
- pLB1-Gal4/UAS-TRPA1 (17/43.4/45 //19/78/85)
- Elav-Gal80; UAS-TRPA1/pLB1-Gal4 (19/41.7/41.7 //19/46.6/58.4)

Detailed statistics for ***Figure 1F***

Dunn's multiple comparisons test	Significant	Summary	Adjusted P Value
pLB1-Gal4/+ vs. +/UAS-TRPA1; Elav-Gal80	No	ns	>0,9999
pLB1-Gal4/+ vs. +/UAS-TRPA1	No	ns	>0,9999
pLB1-Gal4/+ vs. pLB1-Gal4/UAS-TRPA1	Yes	****	<0,0001
pLB1-Gal4/+ vs. pLB1-Gal4/UAS-TRPA1; Elav-Gal80	No	ns	>0,9999
+/UAS-TRPA1; Elav-G80 vs. 0 > UAS-TRPA1	No	ns	>0,9999
+/UAS-TRPA1; Elav-G80 vs. pLB1 > UAS-TRPA1	Yes	****	<0,0001
+/UAS-TRPA1; Elav-G80 vs. LB1 > UAS-TRPA1; Elav-Gal80	No	ns	0,0793
+/UAS-TRPA1 vs. pLB1 > UAS-TRPA1	Yes	****	<0,0001
+/UAS-TRPA1 vs. p LB1-Gal4/UAS-TRPA1; Elav-Gal80	No	ns	>0,9999
pLB1-Gal4/UAS-TRPA1 vs. pLB1-Gal4/UAS-TRPA1; Elav-Gal80	Yes	*	0,0189

For 1G:
Genotypes of tested animals (at 29˚C: n flies/mean eggs exp1/mean eggs exp2/mean eggs exp3)

- pLB1-Gal4/+ (59/71/73/72)
- UAS-TβH-IR/+ (58/74/70/72)
- pLB1-Gal4/UAS- TβH-IR (59/50/54/60.5)

Detailed statistics for ***Figure 1G***

Dunn's multiple comparisons test	Significant	Summary	Adjusted P Value
pLB1-Gal4/UAS-TβH IR vs+/UAS-TβH-IR	Yes	****	<0,0001
pLB1-Gal4/UAS-TβH-IR vs. pLB1-Gal4/+	Yes	****	<0,0001
+/UAS-TβH-IR vs. pLB1-Gal4/+	No	ns	>0,9999

Lines and conditions used for *Figure 2*

For 2A-A'':

Genotypes of tested animals

- pLB1-Gal4, UAS > stop > GFPmCD8; LexAop-FLP/nSyb-LexA

Reagents and tools

- antibody against Tdc2; antibody against GFP; antibody against Elav; Leica SP8 confocal microscope

For 2B-B':

Genotypes of tested animals

- pLB1-Gal4, UAS > stop > GFPmCD8; LexAop-FLP/nSyb-LexA

Reagents and tools

- antibody against Tdc2; antibody against GFP; antibody against nc82; Leica SP8 confocal microscope

Lines and conditions used for *Figure 2—figure supplement 1*

For 2A-A''':

Genotypes of tested animals

- pLB1-Gal4, UAS > stop > GFPmCD8; LexAopFLP/Tdc2-LexA

Reagents and tools

- antibody against Tdc2; antibody against GFP; antibody against nc82; Leica SP8 confocal microscope

For 2B-B''':

Genotypes of tested animals

- pLB1-Gal4, UAS > stop > GFPmCD8; LexAopFLP/Tdc2-LexA

Reagents and tools

- antibody against Tdc2; antibody against GFP; antibody against nc82; Leica SP8 confocal microscope

Lines and conditions used for *Figure 2—figure supplement 2*

Genotypes of tested animals

- Tdc2-LexA, LexAop-GFPnls/LexAop-GFPmCD8

Reagents and tools

- antibody against GFP; antibody against nc82; Leica SP8 confocal microscope

Lines and conditions used for *Figure 2—figure supplement 3*

Genotypes of tested animals

- pLB1-Gal4, UAS > stop > GFPmCD8; LexAop-FLP/nSyb-LexA

Reagents and tools

- antibody against Tdc2; antibody against GFP; Leica SP8 confocal microscope

Lines and conditions used for *Figure 2—figure supplement 4*

Genotypes of tested animals

- pLB1-Gal4, UAS > stop > GFPmCD8; LexAopFLP/nSyb-LexA

Reagents and tools

- antibody against Allatostatin A; antibody against GFP; antibody against nc82; Leica SP8 confocal microscope

Lines and conditions used for *Figure 2—figure supplement 5*

Genotypes of tested animals

- pLB1-Gal4, UAS > stop > GFPmCD8; LexAopFLP/nSyb-LexA

Reagents and tools

- antibody against Bursicon (from B. White); antibody against GFP; antibody against nc82; Leica SP8 confocal microscope

Lines and conditions used for *Figure 2—figure supplement 6*

Genotypes of tested animals

- pLB1-Gal4, UAS > stop > GFPmCD8; LexAopFLP/nSyb-LexA

Reagents and tools

- antibody against CCAP (From B. White); antibody against GFP; antibody against nc82; Leica SP8 confocal microscope

Lines and conditions used for *Figure 2—figure supplement 7*

Genotypes of tested animals

- pLB1-Gal4, UAS > stop > GFPmCD8; LexAopFLP/nSyb-LexA

Reagents and tools

- antibody against Leucokinin (from D. Nassel and P. Herrero); antibody against GFP; antibody against nc82; Leica SP8 confocal microscope

Lines and conditions used for *Figure 3*

For 3A:

Genotypes of tested animals (n flies/mean % exp1/mean % exp2/mean % exp3/mean% exp4/mean% exp5/mean % exp6)

- pLB1-Gal4/+ (70/50%/50%/60%/60%/50%/55%)
- UAS-Kir2.1/+ (70/60%/40%/80%/80%/50%/40%)
- Tdc2-Gal4/+ (80/60%/60%/60%/40%/60%/50%)
- Tdc2-Gal4/UAS-Kir2.1 (80/100%/70%/100%/70%/50%/67%)
- pLB1-Gal4/UAS-Kir2.1 (80/70%/50%/80%/60%/30%/47%)

Detailed statistics for *Figure 3A*

Fisher's exact test	Significant	Summary	Adjusted P Value
pLB1-Gal4/+ vs. UAS-Kir2.1/+	No	ns	1
pLB1-Gal4/+ vs. Tdc2-Gal4/+	No	ns	0,87
pLB1-Gal4/+ vs. Tdc2-Gal4/UAS-Kir2.1	Yes	**	0009

Continued on next page

Continued

Fisher's exact test	Significant	Summary	Adjusted P Value
pLB1-Gal4/+ vs. pLB1-Gal4/UAS-Kir2.1	No	ns	0.74
Tdc2-Gal4/+ vs. UAS-Kir2.1/+	No	ns	0,87
Tdc2-Gal4/+ vs. Tdc2-Gal4/UAS-Kir2.1	Yes	*	0018
Tdc2-Gal4/+ vs. pLB1-Gal4/UAS-Kir2.1	No	ns	1
UAS-Kir2.1/+ vs. Tdc2-Gal4/UAS-Kir2.1	Yes	**	0009
UAS-Kir2.1/+ vs. pLB1-Gal4/UAS-Kir2.1	No	ns	0,74
Tdc2-Gal4/UAS-Kir2.1 vs. pLB1-Gal4/UAS-Kir2.1	Yes	*	0028

For 3B:

Genotypes of tested animals (n flies/mean time in seconds exp1/mean time in seconds exp2/mean time in seconds exp3/mean time in seconds exp4)

- pLB1-Gal4/+ (27/1528/1382/1395/1480)
- UAS-Kir2.1/+ (24/1643/1160/1087/1740)
- Tdc2-Gal4/+ (31/1896/640/1729/1171)
- Tdc2-Gal4/UAS-Kir2.1 (40/770/674/815/868)
- pLB1-Gal4/UAS-Kir2.1 (34/1214/931/1109/1443)

Detailed statistics for ***Figure 3B***

Mann-Whitney test	Significant	Summary	Adjusted P Value
pLB1-Gal4/+ vs. UAS-Kir2.1/+	No	ns	0,7341
pLB1-Gal4/+ vs. Tdc2-Gal4/+	No	ns	0,5641
pLB1-Gal4/+ vs. Tdc2-Gal4/UAS-Kir2.1	Yes	**	0,0081
pLB1-Gal4/+ vs. pLB1-Gal4/UAS-Kir2.1	No	ns	0,3415
Tdc2-Gal4/+ vs. UAS-Kir2.1/+	No	ns	0,8652
Tdc2-Gal4/+ vs. Tdc2-Gal4/UAS-Kir2.1	Yes	*	0,0272
Tdc2-Gal4/+ vs. pLB1-Gal4/UAS-Kir2.1	No	ns	0,7180
UAS-Kir2.1/+ vs. Tdc2-Gal4/UAS-Kir2.1	Yes	*	0,0234
UAS-Kir2.1/+ vs. pLB1-Gal4/UAS-Kir2.1	No	ns	0,6584
Tdc2-Gal4/UAS-Kir2.1 vs. pLB1-Gal4/UAS-Kir2.1	Yes	*	0,0471

For 3C-D':

Genotypes of tested animals

- Males pLB1-Gal4, UAS > stop > GFPmCD8; LexAop-FLP/nSyb-LexA

Reagents and tools

- antibody against Tdc2; antibody against GFP; antibody against nc82; Leica SP8 confocal microscope

For 3E-F':
Genotypes of tested animals

- pLB1-Gal4, UAS > stop > GFPmCD8/Dsx-FLP

Reagents and tools

- antibody against Tdc2; antibody against GFP; Leica SP8 confocal microscope

Lines and conditions used for *Figure 3—figure supplement 1*

Genotypes of tested animals; (n flies/mean % exp1/mean % exp2/mean % exp3/mean% exp4) pLB1-Gal4/+ (44/0%/0%/0%/0%)

- UAS-Kir2.1/+ (42/0%/0%/14%/0%)
- Tdc2-Gal4/+ (55/0%/0%/0%/0%)
- Tdc2-Gal4/UAS-Kir2.1 (53/20%/20%/4%/0%)
- pLB1-Gal4/UAS-Kir2.1 (42/0%/0%/4%/0%)

Detailed statistics for *Figure 3—figure supplement 1*

Fisher's exact test	Significant	Summary	Adjusted P Value
pLB1-Gal4/+ vs. Tdc2-Gal4/UAS-Kir2.1	No	ns	0,2
Tdc2-Gal4/+ vs. Tdc2-Gal4/UAS-Kir2.1	No	ns	0,1
UAS-Kir2.1/+ vs. Tdc2-Gal4/UAS-Kir2.1	No	ns	0,6
Tdc2-Gal4/UAS-Kir2.1 vs. pLB1-Gal4/UAS-Kir2.1	No	ns	0,6

Lines and conditions used for *Figure 3—figure supplement 2*

Genotypes of tested animals

- pLB1-Gal4, UAS > stop > GFPmCD8; LexAop-FLP/nSyb-LexA

Reagents and tools

- antibody against Tdc2; antibody against GFP; antibody against nc82; Leica SP8 confocal microscope

Lines and conditions used for *Figure 3—figure supplement 3*

Genotypes of tested animals

- pLB1-Gal4, UAS > stop > GFPmCD8; LexAop-FLP/nSyb-LexA

Reagents and tools

- antibody against Tdc2; antibody against GFP; antibody against nc82; Leica SP8 confocal microscope

Lines and conditions used for *Figure 3—figure supplement 4*

For 4A-A''':
Genotypes of tested animals

- pLB1-Gal4, UAS > stop > GFPmCD8; LexAop-FLP/Dsx-LexA

Reagents and tools

- antibody against Tdc2; antibody against GFP; Leica SP8 confocal microscope

For 4B-B''':
Genotypes of tested animals

- pLB1-Gal4, UAS > stop > GFPmCD8; LexAop-FLP/Dsx-FLP

Reagents and tools

- antibody against Tdc2; antibody against GFP; Leica SP8 confocal microscope

Lines and conditions used for *Figure 4*

For 4A:

Genotypes of tested animals; (at 29°C: n flies/mean eggs exp1/mean eggs exp2/mean eggs exp3)

- pLB1-Gal4/+ (34/51/65/-)
- pLB1-Gal4, Tdc2-LexA/+ (51/70/63/63)
- UAS-TTx/+ (38/61/72/-)
- Tub >Gal80>; UAS-TTx; LexAop-FLP/+ (49/61/64/63)
- pLB1-Gal4/UAS-TTx (39/27/44)
- pLB1-Gal4, TDC2-LexA/UAS-TTx (20/39/-/-)
- pLB1-Gal4/Tub >Gal80>; UAS-TTx; LexAop-FLP (50/65/71/62)
- pLB1-Gal4, Tdc2-LexA/Tub >Gal80>; UAS-TTx; LexAop-FLP (54/40/41/42)

Detailed statistics for *Figure 4A*

Dunn's multiple comparisons test	Significant	Summary	Adjusted P Value
+/Tub > Gal80>; UAS-TTx; LexAop-FLP vs. +/UAS-TTx	No	ns	>0,9999
+/Tub > Gal80>; UAS-TTx; LexAop-FLP vs. pLB1-Gal4,pTdc2-LexA/+	No	ns	>0,9999
+/Tub > Gal80>; UAS-TTx; LexAop-FLP vs. pLB1-Gal4/Tub > Gal80>; UAS-TTx; LexAop-FLP	No	ns	>0,9999
+/Tub > Gal80>; UAS-TTx; LexAop-FLP vs. LB1_G4,Tdc2_ LexA/Tub > Gal80>; UAS-TTx; LexAop-FLP	Yes	****	<0,0001
+/Tub > Gal80>; UAS-TTx; LexAop-FLP vs. pLB1-Gal4/UAS-TTx	Yes	****	<0,0001
+/Tub > Gal80>; UAS-TTx; LexAop-FLP vs. pLB1-Gal4,Tdc2-LexA/UAS-TTx	Yes	****	<0,0001
+/Tub > Gal80>; UAS-TTx; LexAop-FLP vs. pLB1-Gal4/+	No	ns	>0,9999
+/UAS-TTx vs. pLB1-Gal4,Tdc2-LexA/+	No	ns	>0,9999

Continued on next page

Continued

Dunn's multiple comparisons test	Significant	Summary	Adjusted P Value
+/UAS-TTx vs. pLB1-Gal4/Tub > Gal80>; UAS-TTx;LexAop-FLP	No	ns	>0,9999
+/UAS-TTx vs. pLB1-Gal4,Tdc2-LexA/Tub > Gal80>; UAS-TTx;LexAop-FLP	Yes	****	<0,0001
+/UAS-TTx vs. pLB1Gal4/UAS-TTx	Yes	****	<0,0001
+/UAS-TTx vs. pLB1Gal4,Tdc2-LexA/UAS-TTX	Yes	****	<0,0001
+/UAS-TTx vs. pLB1-Gal4/+	No	ns	0,5856
pLB1-Gal4,Tdc2-LexA/+ vs. pLB1-Gal4/Tub > Gal80>; UAS-TTx; LexAop-FLP	No	ns	>0,9999
pLB1-Gal4,Tdc2-LexA/+ vs. pLB1-Gal4,Tdc2-LexA/Tub > Gal80>; UAS-TTx;LexAop-FLP	Yes	****	<0,0001
pLB1-Gal4,Tdc2-LexA/+ vs. pLB1-Gal4/UAS-TTx	Yes	****	<0,0001
pLB1-Gal4,Tdc2-LexA/+ vs. pLB1-Gal4,Tdc2-LexA/UAS-TTx	Yes	****	<0,0001
pLB1-Gal4,Tdc2-LexA/+ vs. pLB1-Gal4/+	No	ns	>0,9999
pLB1-Gal4/Tub > Gal80>; UAS-TTx; LexAop-FLP vs. pLB1-Gal4,Tdc2-LexA/Tub > Gal80>; UAS-TTx;LexAop-FLP	Yes	****	<0,0001
pLB1-Gal4/Tub > Gal80>;UAS-TTx; LexAop-FLP vs. pLB1-Gal4/UAS-TTx	Yes	****	<0,0001
pLB1-Gal4/Tub > Gal80>; UAS-TTx; LexAop-FLP vs. pLB1-Gal4,Tdc2-LexA/UAS-TTx	Yes	****	<0,0001
pLB1-Gal4/Tub > Gal80>;UAS-TTx; LexAop-FLP vs. pLB1-Gal4/+	No	ns	0,3232
pLB1-Gal4,Tdc2-LexA/Tub > Gal80>; UAS-TTx;LexAop-FLP vs. pLB1-Gal4/UAS-TTx	No	ns	>0,9999
pLB1-Gal4,Tdc2-LexA/Tub > Gal80>; UAS-TTx;LexAop-FLP vs. LB1-Gal4; Tdc2-LexA/UAS-TTx	No	ns	>0,9999
pLB1-Gal4,Tdc2-LexA/Tub > Gal80>; UAS-TTx;LexAop-FLP vs. pLB1-Gal4/+	Yes	***	0,0003
pLB1-Gal4/UAS-TTx vs. pLB1-Gal4,Tdc2-LexA/UAS-TTx	No	ns	>0,9999
pLB1-Gal4/UAS-TTx vs. pLB1-Gal4/+	Yes	****	<0,0001
pLB1-Gal4,Tdc2-LexA/UAS-TTx vs. pLB1-Gal4/+	Yes	**	0,0054

For 4B:

Genotypes of tested animals (at 23˚C: n flies/mean eggs exp1/mean eggs exp2/mean eggs exp3 //at 29˚C: n flies/mean eggs exp1/mean eggs exp2/mean eggs exp3)

- Tdc2-LexA/+ (35/42/45/36//37/42/39/41)
- HS-FLP; pLB1-Gal4/+ (40/38.5/39/36//39/39.5/42/43)
- pLB1-Gal4, Tdc2-LexA/+ (40/38/40/32//39/44/38/36)
- pLB1-Gal4/+ (40/44/42/31//39/45/46/32)
- UAS > stop > TRPA1; LexAop-FLP/+ (40/45/45/34//40/48/47/43)
- pLB1-Gal4/UAS > stop > TRPA1; LexAop-FLP (40/39/37/35//40/44/44/42)
- Tdc2-LexA/UAS > stop > TRPA1; LexAop-FLP (40/34/32/35//37/35/37/34)
- HS-FLP; pLB1-Gal4/UAS > stop > TRPA1; LexAop-FLP (39/37/36/31//40/59/60/49)
- pLB1-Gal4, Tdc2-LexA/UAS > stop > TRPA1; LexAop-FLP (40/37/32/28//40/54/57/51)

Detailed statistics for *Figure 4B*

Dunn's multiple comparisons test	Significant?	Summary	Adjusted P Value
Tdc2Lex > 0 vs. LB1Gal4/HS-FLP > 0	No	ns	>0,9999
Tdc2Lex > 0 vs. LB1Gal4/Tdc2Lex > 0	No	ns	>0,9999
Tdc2Lex > 0 vs. LB1Gal4 > 0	No	ns	>0,9999
Tdc2Lex > 0 vs. 0 > stop > TRPA1/LexAopFLP	No	ns	>0,9999
Tdc2Lex > 0 vs. LB1G4/Tdc2Lex > stop > TRPA1/LexAopFLP	Yes	****	<0,0001
Tdc2Lex > 0 vs. LB1G4/HS-FLP > stop > TRAP1/LexAopFLP	Yes	****	<0,0001
Tdc2Lex > 0 vs. LB1G4 > stop > TRPA1/LexaopFLP	No	ns	>0,9999
Tdc2Lex > 0 vs. Tdc2Lex > stop > TRPA1/Lexaop-FLP	No	ns	0,7602
LB1Gal4/HS-FLP > 0 vs. LB1Gal4/Tdc2Lex > 0	No	ns	>0,9999
LB1Gal4/HS-FLP > 0 vs. LB1Gal4 > 0	No	ns	>0,9999
LB1Gal4/HS-FLP > 0 vs. 0 > stop > TRPA1/LexAopFLP	No	ns	>0,9999
LB1Gal4/HS-FLP > 0 vs. LB1G4/Tdc2Lex > stop > TRPA1/LexAopFLP	Yes	****	<0,0001
LB1Gal4/HS-FLP > 0 vs. LB1G4/HS-FLP > stop > TRAP1/LexAopFLP	Yes	****	<0,0001
LB1Gal4/HS-FLP > 0 vs. LB1G4 > stop > TRPA1/LexaopFLP	No	ns	>0,9999
LB1Gal4/HS-FLP > 0 vs. Tdc2Lex > stop > TRPA1/Lexaop-FLP	No	ns	>0,9999
LB1Gal4/Tdc2Lex > 0 vs. LB1Gal4 > 0	No	ns	>0,9999
LB1Gal4/Tdc2Lex > 0 vs. 0 > stop > TRPA1/LexAopFLP	No	ns	>0,9999
LB1Gal4/Tdc2Lex > 0 vs. LB1G4/Tdc2Lex > stop > TRPA1/LexAopFLP	Yes	****	<0,0001
LB1Gal4/Tdc2Lex > 0 vs. LB1G4/HS-FLP > stop > TRAP1/LexAopFLP	Yes	****	<0,0001
LB1Gal4/Tdc2Lex > 0 vs. LB1G4 > stop > TRPA1/LexaopFLP	No	ns	>0,9999
LB1Gal4/Tdc2Lex > 0 vs. Tdc2Lex > stop > TRPA1/Lexaop-FLP	No	ns	0,6815
LB1Gal4 > 0 vs. 0 > stop > TRPA1/LexAopFLP	No	ns	>0,9999
LB1Gal4 > 0 vs. LB1G4/Tdc2Lex > stop > TRPA1/LexAopFLP	Yes	****	<0,0001
LB1Gal4 > 0 vs. LB1G4/HS-FLP > stop > TRAP1/LexAopFLP	Yes	****	<0,0001
LB1Gal4 > 0 vs. LB1G4 > stop > TRPA1/LexaopFLP	No	ns	>0,9999
LB1Gal4 > 0 vs. Tdc2Lex > stop > TRPA1/Lexaop-FLP	No	ns	0,6919

Continued on next page

Continued

Dunn's multiple comparisons test	Significant?	Summary	Adjusted P Value
0 > stop > TRPA1/LexAopFLP vs. LB1G4/Tdc2Lex > stop > TRPA1/LexAopFLP	Yes	****	<0,0001
0 > stop > TRPA1/LexAopFLP vs. LB1G4/HS-FLP > stop > TRAP1/LexAopFLP	Yes	****	<0,0001
0 > stop > TRPA1/LexAopFLP vs. LB1G4 > stop > TRPA1/LexaopFLP	No	ns	>0,9999
0 > stop > TRPA1/LexAopFLP vs. Tdc2Lex > stop > TRPA1/Lexaop-FLP	No	ns	>0,9999
LB1G4/Tdc2Lex > stop > TRPA1/LexAopFLP vs. LB1G4/HS-FLP > stop > TRAP1/LexAopFLP	No	ns	>0,9999
LB1G4/Tdc2Lex > stop > TRPA1/LexAopFLP vs. LB1G4 > stop > TRPA1/LexaopFLP	Yes	****	<0,0001
LB1G4/Tdc2Lex > stop > TRPA1/LexAopFLP vs. Tdc2Lex > stop > TRPA1/Lexaop-FLP	Yes	****	<0,0001
LB1G4/HS-FLP > stop > TRAP1/LexAopFLP vs. LB1G4 > stop > TRPA1/LexaopFLP	Yes	****	<0,0001
LB1G4/HS-FLP > stop > TRAP1/ LexAopFLP vs. Tdc2Lex > stop > TRPA1/Lexaop-FLP	Yes	**	0,0012
LB1G4 > stop > TRPA1/LexaopFLP vs. Tdc2Lex > stop > TRPA1/Lexaop-FLP	No	ns	>0,9999

For 4C:

Genotypes of tested animals (at 29˚C: n flies for water injection: PGN injection /mean eggs laid post water injection: PGN injection exp1/ mean eggs laid post water injection: PGN injection exp2)

- pLB1-Gal4, Tdc2-LexA/+ (51:51/32:19/19:10)
- Tub >Gal80>; LexAop-FLP; UAS-Fadd-IR/+ (52:52/26:16/28:17)
- Tdc2-LexA/Tub >Gal80>; LexAop-FLP; UAS-Fadd-IR (58:58/24:14/25:14)
- pLB1-Gal4/Tub >Gal80>; LexAop-FLP; UAS-Fadd-IR (58:58/26:16/33:17)
- pLB1-Gal4, Tdc2-LexA/Tub >Gal80>; LexAop-FLP; UAS-Fadd-IR (47:47/37:30/23:22)

Reagents and tools

- PGN/Water/Nanojector

Detailed statistics for *Figure 4C*

Dunn's multiple comparisons test	Significant	Summary	Adjusted P Value
pLB1-Gal4,Tdc2-LexA/Tub > Gal80>; LexAop-FLP;UAS-Fadd IR vs. pLB1-Gal4,Tdc2-LexA/+	Yes	***	0,0001
pLB1-Gal4,Tdc2-LexA/Tub > Gal80>; LexAop-FLP;UAS-Fadd IRvs. pLB1-Gal4/Tub > Gal80>; LexAop-FLP;UAS-Fadd IR	Yes	****	<0,0001
pLB1-Gal4,Tdc2-LexA/Tub > Gal80>; LexAop-FLP;UAS-Fadd IR vs. Tdc2-LexA/Tub > Gal80>; LexAop-FLP;UAS-Fadd IR	Yes	****	<0,0001
pLB1-Gal4,Tdc2-LexA/Tub > Gal80>; LexAop-FLP;UAS-Fadd IR vs. +/Tub > Gal80>; LexAop-FLP;UAS-Fadd IR	Yes	****	<0,0001
pLB1-Gal4,Tdc2-LexA/+ vs. pLB1-Gal4/Tub > Gal80>; LexAop-FLP;UAS-Fadd IR	No	ns	0,5730

Continued on next page

Continued

Dunn's multiple comparisons test	Significant	Summary	Adjusted P Value
pLB1-Gal4,Tdc2-LexA/+ vs. Tdc2-LexA/Tub > Gal80>; LexAop-FLP;UAS-Fadd IR	No	ns	>0,9999
pLB1-Gal4,Tdc2-LexA/+ vs. +/Tub > Gal80>; LexAop-FLP;UAS-Fadd IR	No	ns	>0,9999
pLB1-Gal4/Tub > Gal80>; LexAop-FLP;UAS-Fadd IR vs. Tdc2-LexA/Tub > Gal80>; L exAop-FLP;UAS-Fadd IR	No	ns	>0,9999
pLB1-Gal4/Tub > Gal80>; LexAop-FLP;UAS-Fadd IR vs. +/Tub > Gal80>; LexAop-FLP;UAS-Fadd IR	No	ns	>0,9999
Tdc2-LexA/Tub > Gal80>; LexAop-FLP;UAS-Fadd IR vs. +/Tub > Gal80>; LexAop-FLP;UAS-Fadd IR	No	ns	>0,9999

Lines and conditions used for *Figure 5*

For 5A:

Genotypes of tested animals (at 29˚C: n flies/mean eggs exp1/mean eggs exp2)

- pLB1-Gal4, UAS > stop > Kir2.1/+ (40/63/63)
- HS-FLP/+ (34/58/58)
- OTD-FLP/+ (39/63/66)
- pLB1-Gal4, UAS > stop > Kir2.1/HS-FLP (40/35/39)
- pLB1-Gal4, UAS > stop > Kir2.1/OTD-FLP (40/46/49)

Detailed statistics for *Figure 5A*

Dunn's multiple comparisons test	Significant	Summary	Adjusted P Value
HS-FLP/+ vs. pLB1-Gal4, UAS > stop > Kir2.1/+	No	ns	0,3044
HS-FLP/+ vs. OTD-FLP/+	No	ns	0,1434
HS-FLP/+ vs. pLB1-Gal4, UAS > stop > Kir2.1/OTD-FLP	Yes	**	0,0060
HS-FLP/+ vs. pLB1-Gal4, UAS > stop > Kir2.1/HS-FLP	Yes	****	<0,0001
pLB1-Gal4, UAS > stop > Kir2.1/+ vs. OTD-FLP/+	No	ns	>0,9999
pLB1-Gal4,UAS > stop > Kir2.1/+ vs. pLB1-Gal4,UAS > stop > Kir2.1/OTD-FLP	Yes	****	<0,0001
pLB1-Gal4,UAS > stop > Kir2.1/+ vs. pLB1-Gal4,UAS > stop > Kir2.1/HS-FLP	Yes	****	<0,0001
OTD-FLP/+ vs. pLB1-Gal4, UAS > stop > Kir2.1/OTD-FLP	Yes	****	<0,0001
OTD-FLP/+ vs. pLB1Gal4, UAS > stop > Kir2.1/HS-FLP	Yes	****	<0,0001
pLB1-Gal4,UAS > stop > Kir2.1/OTD-FLP vs. pLB1-Gal4, UAS > stop > Kir2.1/HS-FLP	Yes	*	0,0255

For 5B:

Genotypes of tested animals (at 29˚C: n flies/mean eggs exp1/mean eggs exp2/ mean eggs exp3)

- UAS-Kir2.1/+ (50/51/70/70)
- Tsh-LexA, LexAop-Gal80/+ (48/50/70/68)

- pLB1-Gal4/+ (49/51/59/56)
- Tsh-LexA, LexAop-Gal80; UAS-Kir2.1/+ (50/46/70/68)
- pLB1-Gal4/Tsh-LexA, LexAop-Gal80 (50/39/67/67)
- pLB1-Gal4/UAS-Kir2.1 (69/28/28/41)
- pLB1-Gal4/Tsh-LexA, LexAop-Gal80; UAS-Kir2.1 (56/21/37/40)

Detailed statistics for *Figure 5B*

Dunn's multiple comparisons test	Significant	Summary	Adjusted P Value
pLB1-Gal4/UAS-Kir2.1 vs. pLB1-Gal4/UAS-Kir2.1; Tsh-LexA, LexAop-Gal80	No	ns	>0,9999
pLB1-Gal4/UASKir2.1 vs. pLB1-Gal4/Tsh-LexA, LexAop-Gal80	Yes	****	<0,0001
pLB1-Gal4/UAS-Kir2.1 vs. +/Tsh-LexA, LexAop-Gal80; UAS-Kir2.1	Yes	****	<0,0001
pLB1-Gal4/UAS-Kir2.1 vs. +/UAS-Kir2.1	Yes	****	<0,0001
pLB1-Gal4/UAS-Kir2.1 vs. +/Tsh-LexA, Lexaop-Gal80	Yes	****	<0,0001
pLB1-Gal4/UAS-Kir2.1 vs. pLB1-Gal4/+	Yes	****	<0,0001
pLB1-Gal4/UASKir2.1; Tsh-LexA, LexAop-Gal80 vs. pLB1-Gal4/Tsh-LexA, LexAop-Gal80	Yes	****	<0,0001
pLB1-Gal4/UAS-Kir2.1; Tsh-LexA, LexAop-Gal80 vs. +/Tsh-LexA, LexAop-Gal80; UAS-Kir2.1	Yes	****	<0,0001
pLB1-Gal4/UAS-Kir2.1; Tsh-LexA, LexAop-Gal80vs. +/UAS-Kir2.1	Yes	****	<0,0001
pLB1-Gal4/UAS-Kir2.1; Tsh-LexA, LexAop-Gal80 vs. +/Tsh-LexA, LexAop-Gal80	Yes	****	<0,0001
pLB1-Gal4/UAS-Kir2.1; Tsh-LexA, LexAop-Gal80 vs. pLB1-Gal4/+	Yes	****	<0,0001
pLB1-Gal4/Tsh-LexA, LexAop-Gal80 vs. +/Tsh-LexA, LexAop-Gal80;UAS-Kir2.1	No	ns	>0,9999
pLB1-Gal4/Tsh-LexA, LexAop-Gal80 vs. +/UAS-Kir2.1	No	ns	>0,9999
pLB1-Gal4/Tsh-LexA, LexAop-Gal80 vs. +/Tsh-LexA, LexAop-Gal80	No	ns	>0,9999
pLB1-Gal4/Tsh-LexA, LexAop-Gal80 vs. pLB1-Gal4/+	No	ns	>0,9999
+/Tsh-LexA, LexAop-Gal80;UAS-Kir2.1 vs. +/UAS-Kir2.1	No	ns	>0,9999

Continued on next page

Continued

Dunn's multiple comparisons test	Significant	Summary	Adjusted P Value
+/Tsh-LexA, Lexaop-Gal80;UAS-Kir2.1vs. +/Tsh-LexA, LexAop-Gal80	No	ns	>0,9999
+/Tsh-LexA, LexAop-Gal80;UAS-Kir2.1 vs. pLB1-Gal4/+	No	ns	>0,9999
+/UAS-Kir2.1 vs. +/Tsh-LexA, LexAop-Gal80	No	ns	>0,9999
+/UAS-Kir2.1 vs. pLB1-Gal4/+	No	ns	0,1350
+/Tsh-LexA, LexAop-Gal80 vs. pLB1-Gal4/+	No	ns	0,3431

For 5C:

Genotypes of tested animals (at 29˚C: n flies for water injection: PGN injection/mean eggs laid post water injection: PGN injection exp1/mean eggs laid post water injection: PGN injection exp2)

- UAS-Fadd-IR/+ (40:40/40:26/27:13)
- pLB1-Gal4/+ (40:40/43:28/30:17)
- Tsh-Gal4/+ (40:40/45:28/25:14)
- pLB1-Gal4/UAS-Fadd-IR (40:36/43:40/28:26)
- Tsh-Gal4/UAS-Fadd-IR (28:29/33:22/23:11)

Reagents and tools

- PGN/Water/Nanojector

Detailed statistics for *Figure 5C*

Dunn's multiple comparisons test	Significant	Summary	Adjusted P Value
pLB1-Gal4/+ vs. Tsh-Gal4/UAS-FaddIR	No	ns	>0,9999
pLB1-Gal4/+ vs. Tsh-Gal4/+	No	ns	>0,9999
pLB1-Gal4/+ vs. pLB1-Gal4/UAS-FaddIR	Yes	****	<0,0001
pLB1-Gal4/+ vs. +/UAS-FaddIR	No	ns	>0,9999
Tsh-Gal4/UAS-FaddIRvs. Tsh-Gal4/+	No	ns	>0,9999
Tsh-Gal-4/UAS-FaddIR vs. pLB1-Gal4/UAS-FaddIR	Yes	****	<0,0001
Tsh-Gal4/UAS-FaddIR vs. +/UAS-FaddIR	No	ns	>0,9999
Tsh-Gal4/+vs. pLB1-Gal4/UAS-FaddIR	Yes	****	<0,0001
Tsh-Gal4/+ vs. +/UAS-FaddIR	No	ns	>0,9999
pLB1-Gal4/UAS-FaddIR vs. +/UAS-FaddIR	Yes	****	<0,0001

For 5D:

Genotypes of tested animals (at 29˚C: n flies/mean ratio eggs water vs PGN exp1+exp2)

- UAS-Fadd-IR/+ (40/0.65)
- Tsh-LexA, LexAop-Gal80; UAS-Fadd-IR/+ (36/0.56)
- Tdc2-Gal4/+ (40/0.61) pLB1-Gal4/+ (38/0.66)
- Tdc2-Gal4/UAS-Fadd-IR (40/0.96)
- pLB1-Gal4/UAS-Fadd-IR (38/1.05)
- Tdc2-Gal4/Tsh-LexA, LexAop-Gal80; UAS-Fadd-IR (14/1.00)
- pLB1-Gal4/Tsh-LexA, LexAop-Gal80; UAS-Fadd-IR (32/0.92)

Reagents and tools

- PGN/Water/Nanojector

Detailed statistics for *Figure 5D*

Dunn's multiple comparisons test	Significant?	Summary	Adjusted P Value
Tdc2-Gal4/UAS-Fadd IR; Tsh-Lexa, LexAop-Gal80 vs. +/UAS-Fadd IR;Tsh-LexA, LexAop-Gal80	Yes	*	0,0236
Tdc2-Gal4/UAS-Fadd IR; Tsh-LexA, LexAop-Gal80 vs. Tdc2-Gal4/+	No	ns	0,0759
Tdc2-Gal4/UAS-Fadd IR; Tsh-LexA, LexAop-Gal80 vs. Tdc2-Gal4/UAS-Fadd IR	No	ns	>0,9999
Tdc2-Gal4/UAS-Fadd IR; Tsh-LexA, LexAop-Gal80 vs. +/UAS-Fadd IR	No	ns	0,1743
Tdc2-Gal4/UAS-Fadd IR; Tsh-LexA, LexAop-Gal80 vs. pLB1-Gal4/+	No	ns	0,2508
Tdc2-Gal4/UAS-Fadd IR; Tsh-LexA, LexAop-Gal80 vs. pLB1-Gal4/UAS-Fadd IR	No	ns	>0,9999
Tdc2-Gal4/UAS-Fadd IR; Tsh-LexA, LexAop-Gal80 vs. pLB1-Gal4/UAS-Fadd IR; Tsh-LexA, LexAop-Gal80	No	ns	>0,9999
+/UAS-Fadd IR;Tsh-LexA, LexAopGal80 vs. Tdc2-Gal4/+	No	ns	>0,9999
+/UAS-Fadd IR;Tsh-LexA, LexAop-Gal80 vs. Tdc2-Gal4/UAS-Fadd IR	Yes	***	0,0001
+/UAS-Fadd IR;Tsh-LexA, LexAop-Gal80 vs. +/UAS-Fadd IR	No	ns	>0,9999
+/UAS-Fadd IR;Tsh-LexA, LexAop-Gal80 vs. pLB1-Gal4/+	No	ns	>0,9999
+/UAS-Fadd IR;Tsh-LexA, LexAop-Gal80 vs. pLB1-Gal4/UAS-Fadd IR	Yes	****	<0,0001
+/UAS-Fadd IR;Tsh-LexA, LexAop-Gal80 vs. pLB1-Gal4/UAS-Fadd IR; Tsh-LexA, LexAop-Gal80	Yes	**	0,0036
Tdc2-Gal4/+ vs. Tdc2-Gal4/UAS-Fadd IR	Yes	***	0,0008
Tdc2-Gal4/+ vs. +/UAS-Fadd IR	No	ns	>0,9999
Tdc2-Gal4/+ vs. pLB1-Gal4/+	No	ns	>0,9999
Tdc2-Gal4/+ vs. pLB1-Gal4/UAS-Fadd IR	Yes	****	<0,0001

Continued on next page

Continued

Dunn's multiple comparisons test	Significant?	Summary	Adjusted P Value
Tdc2-Gal4/+ vs. pLB1-Gal4/UAS-Fadd IR;Tsh-LexA, LexAop-Gal80	Yes	*	0,0180
Tdc2-Gal4/UAS-Fadd IR vs. +/UAS-Fadd IR	Yes	**	0,0036
Tdc2-Gal4/UAS-Fadd IR vs. pLB1-Gal4/+	Yes	**	0,0078
Tdc2-Gal4/UAS-Fadd IR vs. pLB1-Gal4/UAS-Fadd IR	No	ns	>0,9999
Tdc2-Gal4/UAS-Fadd IR vs. pLB1-Gal4/UAS-Fadd IR;Tsh-LexA, LexAop-Gal80	No	ns	>0,9999
+/UAS-Fadd IR vs. pLB1-Gal4/+	No	ns	>0,9999
+/UAS-Fadd IR vs. pLB1-Gal4/UAS-Fadd IR	Yes	****	<0,0001
+/UAS-Fadd IR vs. pLB1Gal4/UAS-Fadd IR; Tsh-LexA, LexAop-Gal80	No	ns	0,0601
pLB1-Gal4/+ vs. pLB1-Gal4/UAS-Fadd IR	Yes	****	<0,0001
pLB1-Gal4/+ vs. pLB1-Gal4/UAS-Fadd IR;Tsh-LexA, LexAop-Gal80	No	ns	0,1049
pLB1-Gal4/UAS-Fadd IR vs. pLB1-Gal4/UAS-Fadd IR; Tsh-LexA, LexAop-Gal80	No	ns	>0,9999

Lines and conditions used for ***Figure 5—figure supplement 1***

For 1A-C''':

Genotypes of tested animals

- pLB1-Gal4, UAS > stop > GFPmCD8/OTD-FLP

Reagents and tools

- antibody against Tdc2; antibody against GFP; Leica SP8 confocal microscope

For 1D-D':

Genotypes of tested animals

- pLB1-Gal4; UAS-Tomato-mCD8/Tsh-LexA, LexAop-Gal80

Reagents and tools

- antibody against nc82; antibody against GFP; Leica SP8 confocal microscope

Lines and conditions used for ***Figure 6***

Genotypes of tested animals

- pLB1-LexA/Tdc2-Gal4, UAS > stop > GFPmCD8; Lexaop-FLP

Reagents and tools

- antibody against GFP; antibody against nc82; Leica SP8 confocal microscope

Lines and conditions used for ***Figure 7***

Genotypes of tested animals

- pgrp-lb::gfp/Tdc-2-Gal4, UAS-Tomato-mCD8GFP

Reagents and tools

- No antibody staining; Leica SP8 confocal microscope

Lines and conditions used for *Figure 8*

For A-C: *in vivo*

Genotypes and number (n) of tested animals

- Tdc2-Gal4, UAS-GCaMP6s
- Ringer's: n = 8 PGN: n = 13

Reagents and tools

- Leica SP8 confocal microscope, PGN, Ringer's solution

For D-F: *ex vivo*

Genotypes and number (n) of tested animals

- pLB1-LexA; LexAop-FLP/Tub > Gal80>; Tdc2-Gal4, UAS-GCaMP6s
- Ringer's; n = 10 PGN; n = 12

Reagents and tools

- Spinning Disk Ropper 2 Cam, PGN, Ringer's solution

Detailed statistics for *Figure 8C*

Mann-Whitney test

Table Analyzed	Data 1
Column B	PGN 100 µg/mL
vs	vs
Column C	PGN 100 µg/mL VM1
Mann Whitney test	
P value	0,0010
Exact or approximate P value?	Gaussian Approximation
P value summary	***
Are medians signif. different? (p<0.05)	Yes
One- or two-tailed P value?	Two-tailed
Sum of ranks in column B,C	97, 134
Mann-Whitney U	6000

Detailed statistics for *Figure 8F*

Table Analyzed	Data 1
Column A	Ringer's Solution
vs	vs
Column B	PGN 100microg/mL
Mann Whitney test	
P value	0,0001
Exact or approximate P value?	Gaussian Approximation

Continued on next page

Continued

Table Analyzed	Data 1
P value summary	***
Are medians signif. different? (p<0.05)	Yes
One- or two-tailed P value?	Two-tailed
Sum of ranks in column A,B	173, 80
Mann-Whitney U	2000

Lines and conditions used for *Figure 9*

For 9A:

Genotypes of tested animals

- w-

Reagents and tools

- Axio-Imager APO Z1 apotome microscope

For 9B:

Genotypes of tested animals (at 25˚C: n flies for water injection: PGN injection)

(mix of two independent experiments; mean stage 1–6 post water injection: PGN injection/mean stage 7–9 post water injection: PGN injection/mean stage 10 post water injection: PGN injection/mean stage 11–13 post water injection: PGN injection/mean stage 14 post water injection: PGN injection/mean Apoptotic oocytes post water injection: PGN injection)

- w- (17:20)
- 6h p. i. (33:32.7/33.2:35.7/5:3.85/8.5:5/18.1:27/2.1:3.7)
- 24h p. i. (36.7:36.5/36.1:35.2/9.5:7.3/11.2:8.1/17.3:23/0.5:0.3)
- 48h p. i. (36.7:39/39:36/7:6/7.8:9/20.5:21.8/0.35:0.45)

Reagents and tools

- PGN/Water/Nanojector

Detailed statistics for *Figure 9B*

Table Analyzed	oocytes count 6 hr water/PGN combo set 2 + set 1
Column G	st14 PGN200
vs.	vs,
Column A	st14 water
Mann-Whitney test	
P value	0,0085
Exact or approximate P value?	Exact
P value summary	**
Significantly different (p<0.05)?	Yes
One- or two-tailed P value?	Two-tailed
Sum of ranks in column A,G	238, 465
Mann-Whitney U	85
Difference between medians	
Median of column A	15, n = 17
Median of column G	24, n = 20
Difference: Actual	9

Continued on next page

Continued

Table Analyzed	oocytes count 6 hr water/PGN combo set 2 + set 1
Difference: Hodges-Lehmann	7

Table Analyzed	oocytes count 6 hr water/PGN combo set 2 + set 1
Column H	st11-13 PGN200
vs.	vs,
Column B	st 11–13 water
Mann Whitney test	
P value	0,0004
Exact or approximate P value?	Exact
P value summary	***
Significantly different (p<0.05)?	Yes
One- or two-tailed P value?	Two-tailed
Sum of ranks in column B,H	434,5, 268,5
Mann-Whitney U	58,5
Difference between medians	
Median of column B	9, n = 17
Median of column H	5, n = 20
Difference: Actual	-4
Difference: Hodges-Lehmann	-3

Table Analyzed	oocytes count 6 hr water/PGN combo set 2 + set 1
Column L	Apoptotic oocytes
vs.	vs,
Column F	Apoptotic oocytes
Mann Whitney test	
P value	0,0350
Exact or approximate P value?	Exact
P value summary	*
Significantly different (p<0.05)?	Yes
One- or two-tailed P value?	Two-tailed
Sum of ranks in column F,L	255,5, 447,5
Mann-Whitney U	102,5
Difference between medians	
Median of column F	0, n = 17
Median of column L	3,5, n = 20
Difference: Actual	3,5

Continued on next page

Continued

Table Analyzed	oocytes count 6 hr water/PGN combo set 2 + set 1
Difference: Hodges-Lehmann	1

Table Analyzed	oocytes count 24 hr water/PGN combo set 2 + set1
Column H	st11-13 PGN200
vs.	vs,
Column B	st 11–13 water
Mann Whitney test	
P value	0,0155
Exact or approximate P value?	Exact
P value summary	*
Significantly different (p<0.05)?	Yes
One- or two-tailed P value?	Two-tailed
Sum of ranks in column B,H	432,5, 308,5
Mann-Whitney U	98,5
Difference between medians	
Median of column B	12, n = 18
Median of column H	8,5, n = 20
Difference: Actual	−3,5
Difference: Hodges-Lehmann	-3

Table Analyzed	oocytes count 24 hr water/PGN combo set 2 + set1
Column I	st10 PGN200
vs.	vs,
Column C	st 10 water
Mann Whitney test	
P value	0,0266
Exact or approximate P value?	Exact
P value summary	*
Significantly different (p<0.05)?	Yes
One- or two-tailed P value?	Two-tailed
Sum of ranks in column C,I	426, 315
Mann-Whitney U	105
Difference between medians	
Median of column C	9,5, n = 18
Median of column I	6, n = 20
Difference: Actual	−3,5
Difference: Hodges-Lehmann	-2

For 9C:

Genotypes of tested animals (n flies/mean eggs day 1 (21˚C) exp1-2/mean eggs day 2 (29˚C) exp 1–2/mean eggs day 3 (21˚C) exp1−2/mean eggs day 4 (21˚C) exp 1–2/mean eggs day 5 (21˚C) exp 1–2)

- pLB1-Gal4/+ (60/46.9–30.5/57.8–43.1/46.6–34.5/28.4–24.1/31.4–18.5)
- Tub-Gal80ts, UAS-Kir2.1/+ (60/48–27.5/60-40.6/45–32.8/29-24.3/31–18)
- pLB1-Gal4/Tub-Gal80ts, UAS-Kir2.1 (60/50-32/40.1–24.8/29.3–23.4/29.3–26.7/29.3–19.5)

Detailed statistics for *Figure 9C*

Dunn's multiple comparisons test	Significant?	Summary	Adjusted P Value
T80ts > Kir 29d2 vs. LB1 > 0 29d2	No	ns	>0,9999
T80ts > Kir 29d2 vs. Lb1/T80ts > Kir 29d2	Yes	****	<0,0001
LB1 > 0 29d2 vs. Lb1/T80ts > Kir 29d2	Yes	****	<0,0001
T80ts > Kir 23d3 vs. LB1 > 0 23d3	No	ns	0,6535
T80ts > Kir 23d3 vs. Lb1/T80ts > Kir 23d3	Yes	****	<0,0001
LB1 > 0 23d3 vs. Lb1/T80ts > Kir 23d3	Yes	****	<0,0001

For 9D:

Genotypes of tested animals

- pLB1-Gal4/Tub-Gal80ts, UAS-Kir2.1

Reagents and tools

- Axio-Imager APO Z1 apotome microscope

For 9E:

Genotypes of tested animals (n flies Day 1-2-3-4 (mix of two independent experiments)); mean stage 1–6 Day 1-2-3−4/mean stage 7–9 Day 1-2-3−4/mean stage 10 Day 1-2-3−4/mean stage 11–13 Day 1-2-3−4/mean stage 14 Day 1-2-3−4/mean Apoptotic oocytes Day 1-2-3-4)

- pLB1-Gal4/+ (10-11-9-10; 30.9–31.8-31.4–28.6/30.1–30.7-32-25.3/6.6–3.9-6.4–4.2-/8–4.9-7.4–5.7/9.8–27.9-4.4–10.3/0.7–1.8-0.7–0.4)
- Tub-Gal80ts, UAS-Kir2.1/+ (10-10-9-10; 33.9–34.1-34-31.3/34.5–30.2-35-28.2/7.3–4.1-4.6–6.1/9.6–5.4-7.4–3.8/9.2–26.1-13.8-6/0-1.1–0.5-0.2)
- pLB1-Gal4/Tub-Gal80ts, UAS-Kir2.1 (10-9-11-10; 32-32-31.9–29.1/33.4–31.9-31.5–28.7/6.8–6.1-4.3–3.9/10.3–3.8-5-6.4/8.2–45.2-29.6–9.4/0.4-0-0.9–1)

Detailed statistics for *Figure 9E*

Day 2 (29˚C)

Dunn's multiple comparisons test	Significant?	Summary	Adjusted P Value
st14 Lb1 > 0 vs. st14 0/T80ts > Kir	No	ns	>0,9999
st14 Lb1 > 0 vs. st14 LB1/T80ts > Kir	Yes	**	0,0013

Continued on next page

Continued

Dunn's multiple comparisons test	Significant?	Summary	Adjusted P Value
st14 0/T80ts > Kir vs. st14 LB1/T80ts > Kir	Yes	***	0,0007

Dunn's multiple comparisons test	Significant?	Summary	Adjusted P Value
Apoptotic oocytes LB1 > 0 vs. Apoptotic oocytes 0/T80ts > Kir	No	ns	0,3395
Apoptotic oocytes LB1 > 0 vs. Apoptotic oocytes LB1/T80ts > Kir	Yes	**	0,0021
Apoptotic oocytes 0/T80ts > Kir vs. Apoptotic oocytes LB1/T80ts > Kir	No	ns	0,2155

Day 3 (21˚C)

Dunn's multiple comparisons test	Significant?	Summary	Adjusted P Value
st14 Lb1 > 0 vs. st14 0/T80ts > Kir	No	ns	0,0586
st14 Lb1 > 0 vs. st14 LB1/T80ts > Kir	Yes	***	0,0001
st14 0/T80ts > Kir vs. st14 LB1/T80ts > Kir	No	ns	0,2082

Lines and conditions used for ***Figure 9—figure supplement 1***

Genotypes of tested animals

- w-

Reagents and tools

- PGN/Water/Nanojector; Axio-Imager APO Z1 apotome microscope, DAPI

Lines and conditions used for ***Figure 9—figure supplement 2***

Genotypes of tested animals

- pLB1-Gal4/+
- Tub-Gal80ts, UAS-Kir2.1/+
- pLB1-Gal4/Tub-Gal80ts, UAS-Kir2.1

Reagents and tools

- Axio-Imager APO Z1 apotome microscope, DAPI

Lines and conditions used for ***Figure 10***

For 10A-C:

Genotypes of tested animals

- pLB1-Gal4/+
- UAS-Kir2.1/+
- pLB1-Gal4/UAS-Kir2.1

Reagents and tools

- DAPI
- Axio-Imager APO Z1 apotome microscope

For 10D:
Genotypes of tested animals

- w-

Reagents and tools

- DAPI
- Axio-Imager APO Z1 apotome microscope

For 10E and 10F:
Genotypes of tested animals (at 29˚C: n flies/mean stage 14 exp1/mean stage 14 exp2/mean stage 14 exp3//trimming % exp1/trimming % exp2/trimming % exp3)

- pLB1-Gal4/+ (64/11/12/15//30/24/19)
- UAS-Kir2.1/+ (64/14/12/8//22/24/18)
- pLB1-Gal4/UAS-Kir2.1 (61/25/26/35//8/7/3)

Detailed statistics for *Figure 10E*

Dunn's multiple comparisons test	Significant	Summary	Adjusted P Value
pLB1-Gal4/+ vs. +/UAS-Kir2.1	No	ns	>0,9999
pLB1-Gal4/+ vs. pLB1-Gal4/UAS-Kir2.1	Yes	****	<0,0001
+/UAS-Kir2.1 vs. pLB1-Gal4/UAS-Kir2.1	Yes	****	<0,0001

Detailed statistics for *Figure 10F*

Dunn's multiple comparisons test	Significant	Summary	Adjusted P Value
pLB1-Gal4/+vs. +/UAS-Kir2.1	No	ns	0,2023
pLB1-Gal4/+ vs. pLB1-Gal4/UAS-Kir2.1	Yes	****	<0,0001
+/UAS-Kir2.1 vs. pLB1-Gal4/UAS-Kir2.1	Yes	****	<0,0001

For 10G and 10H:
Genotypes of tested animals

- w-

(at 29˚C: n flies for water injection: PGN injection/mean stage 14 post water injection: PGN injection exp1/mean stage14 post water injection: PGN injection exp2/mean stage14 post water injection: PGN injection exp3//trimming% water: PGN exp1/trimming % water: PGN exp2/trimming % water: PGN exp3)

- (55:57/12:20/14:27/15:23//18:8/19:7/19:11)

Reagents and tools

- PGN/Water/Nanojector

Detailed statistics for *Figure 10G*

Mann-Whitney test	
P value	<0,0001
Exact or approximate P value?	Exact
P value summary	****
Significantly different (p<0.05)?	Yes
One- or two-tailed P value?	Two-tailed
Sum of ranks in column A,B	2312, 4016
Mann-Whitney U	772
Difference between medians	
Median of column A	12, n = 55
Median of column B	21, n = 57
Difference: Actual	9
Difference: Hodges-Lehmann	8

Detailed statistics for *Figure 10H*

Mann-Whitney test	
P value	<0,0001
Exact or approximate P value?	Exact
P value summary	****
Significantly different (p<0.05)?	Yes
One- or two-tailed P value?	Two-tailed
Sum of ranks in column A,B	3979, 2350
Mann-Whitney U	696,5
Difference between medians	
Median of column A	0,2, n = 55
Median of column B	0,07407, n = 57
Difference: Actual	−0,1259
Difference: Hodges-Lehmann	−0,1003

Acknowledgements

We thank R Tavignot for help in screening for PGRP-LB::GFP transformants and JC Patel for advices with calcium imaging. This work was supported by CNRS and Agence Nationale de la recherche, ANR-11-LABX-0054 (Investissements d'Avenir–Labex INFORM), ANR BACNEURODRO (ANR-17-CE16-0023-01), Institut Universitaire de France to JR. This work was performed using France-BioImaging infrastructure supported by (ANR-10 INBS-04–01). Research in YG's laboratory is supported by the CNRS, the 'Université de Bourgogne Franche-Comté", the Conseil Régional Bourgogne Franche-Comte (PARI grant), the FEDER (European Funding for Regional Economical Development), and the European Council (ERC starting grant, GliSFCo-311403).

Additional information

Funding

Funder	Grant reference number	Author
Agence Nationale de la Recherche	11-LABX-0054	Julien Royet

The funders had no role in study design, data collection and interpretation, or the decision to submit the work for publication.

Author contributions

Ambra Masuzzo, Conceptualization, Formal analysis, Investigation, Writing—original draft, Writing—review and editing; Gérard Manière, Conceptualization, Validation, Investigation, Methodology; Annelise Viallat-Lieutaud, Conceptualization, Data curation, Investigation; Émilie Avazeri, Olivier Zugasti, Investigation; Yaël Grosjean, Conceptualization, Supervision, Project administration; C Léopold Kurz, Conceptualization, Data curation, Formal analysis, Supervision, Validation, Investigation, Methodology, Writing—original draft, Writing—review and editing; Julien Royet, Conceptualization, Supervision, Funding acquisition, Validation, Writing—original draft, Project administration, Writing—review and editing

Author ORCIDs

Ambra Masuzzo https://orcid.org/0000-0002-2933-8924
C Léopold Kurz https://orcid.org/0000-0001-7081-3208
Julien Royet https://orcid.org/0000-0002-5671-4833

Decision letter and Author response

Decision letter https://doi.org/10.7554/eLife.50559.047
Author response https://doi.org/10.7554/eLife.50559.048

Additional files

Supplementary files

- Transparent reporting form DOI: https://doi.org/10.7554/eLife.50559.073

Data availability

All data generated or analysed during this study are included in the manuscript and supporting files.

References

Adamo SA. 1999. Evidence for adaptive changes in egg laying in crickets exposed to Bacteria and parasites. *Animal Behaviour* **57**:117–124. DOI: https://doi.org/10.1006/anbe.1998.0999, PMID: 10053078

Adamo SA. 2014. Parasitic aphrodisiacs: manipulation of the hosts' behavioral defenses by sexually transmitted parasites. *Integrative and Comparative Biology* **54**:159–165. DOI: https://doi.org/10.1093/icb/icu036, PMID: 24813461

Arentsen T, Raith H, Qian Y, Forssberg H, Diaz Heijtz R. 2015. Host Microbiota modulates development of social preference in mice. *Microbial Ecology in Health & Disease* **26**:29719. DOI: https://doi.org/10.3402/mehd.v26.29719, PMID: 26679775

Arentsen T, Qian Y, Gkotzis S, Femenia T, Wang T, Udekwu K, Forssberg H, Diaz Heijtz R. 2017. The bacterial peptidoglycan-sensing molecule Pglyrp2 modulates brain development and behavior. *Molecular Psychiatry* **22**:257–266. DOI: https://doi.org/10.1038/mp.2016.182, PMID: 27843150

Asahina K, Watanabe K, Duistermars BJ, Hoopfer E, González CR, Eyjólfsdóttir EA, Perona P, Anderson DJ. 2014. Tachykinin-expressing neurons control male-specific aggressive arousal in Drosophila. *Cell* **156**:221–235. DOI: https://doi.org/10.1016/j.cell.2013.11.045, PMID: 24439378

Barajas-Azpeleta R, Wu J, Gill J, Welte R, Seidel C, McKinney S, Dissel S, Si K. 2018. Antimicrobial peptides modulate long-term memory. *PLOS Genetics* **14**:e1007440. DOI: https://doi.org/10.1371/journal.pgen.1007440, PMID: 30312294

Bozler J, Kacsoh BZ, Chen H, Theurkauf WE, Weng Z, Bosco G. 2017. A systems level approach to temporal expression dynamics in Drosophila reveals clusters of long term memory genes. *PLOS Genetics* **13**:e1007054. DOI: https://doi.org/10.1371/journal.pgen.1007054, PMID: 29084214

Busch S, Selcho M, Ito K, Tanimoto H. 2009. A map of octopaminergic neurons in the Drosophila brain. *The Journal of Comparative Neurology* **513**:643–667. DOI: https://doi.org/10.1002/cne.21966, PMID: 19235225

Cao X, Kajino-Sakamoto R, Doss A, Aballay A. 2017. Distinct roles of sensory neurons in mediating pathogen avoidance and Neuropeptide-Dependent immune regulation. *Cell Reports* **21**:1442–1451. DOI: https://doi.org/10.1016/j.celrep.2017.10.050, PMID: 29117551

Charroux B, Capo F, Kurz CL, Peslier S, Chaduli D, Viallat-Lieutaud A, Royet J. 2018. Cytosolic and secreted Peptidoglycan-Degrading enzymes in Drosophila respectively control local and systemic immune responses to Microbiota. *Cell Host & Microbe* **23**:215–228. DOI: https://doi.org/10.1016/j.chom.2017.12.007, PMID: 29398649

Chen J, Reiher W, Hermann-Luibl C, Sellami A, Cognigni P, Kondo S, Helfrich-Förster C, Veenstra JA, Wegener C. 2016. Allatostatin A signalling in Drosophila regulates feeding and sleep and is modulated by PDF. *PLOS Genetics* **12**:e1006346. DOI: https://doi.org/10.1371/journal.pgen.1006346, PMID: 27689358

Crocker A, Sehgal A. 2008. Octopamine regulates sleep in Drosophila through protein kinase A-dependent mechanisms. *Journal of Neuroscience* **28**:9377–9385. DOI: https://doi.org/10.1523/JNEUROSCI.3072-08a.2008, PMID: 18799671

Cryan JF, O'Mahony SM. 2011. The microbiome-gut-brain Axis: from bowel to behavior. *Neurogastroenterology & Motility* **23**:187–192. DOI: https://doi.org/10.1111/j.1365-2982.2010.01664.x, PMID: 21303428

Davie K, Janssens J, Koldere D, De Waegeneer M, Pech U, Kreft Ł, Aibar S, Makhzami S, Christiaens V, Bravo González-Blas C, Poovathingal S, Hulselmans G, Spanier KI, Moerman T, Vanspauwen B, Geurs S, Voet T, Lammertyn J, Thienpont B, Liu S, et al. 2018. A Single-Cell transcriptome atlas of the aging Drosophila brain. *Cell* **174**:982–998. DOI: https://doi.org/10.1016/j.cell.2018.05.057, PMID: 29909982

de Haro M, Al-Ramahi I, Benito-Sipos J, López-Arias B, Dorado B, Veenstra JA, Herrero P. 2010. Detailed analysis of leucokinin-expressing neurons and their candidate functions in the Drosophila nervous system. *Cell and Tissue Research* **339**:321–336. DOI: https://doi.org/10.1007/s00441-009-0890-y, PMID: 19941006

de Roode JC, Lefèvre T. 2012. Behavioral immunity in insects. *Insects* **3**:789–820. DOI: https://doi.org/10.3390/insects3030789, PMID: 26466629

del Valle Rodríguez A, Didiano D, Desplan C. 2011. Power tools for gene expression and clonal analysis in Drosophila. *Nature Methods* **9**:47–55. DOI: https://doi.org/10.1038/nmeth.1800, PMID: 22205518

Dijkers PF, O'Farrell PH. 2007. Drosophila calcineurin promotes induction of innate immune responses. *Current Biology* **17**:2087–2093. DOI: https://doi.org/10.1016/j.cub.2007.11.001, PMID: 18060786

Dissel S, Seugnet L, Thimgan MS, Silverman N, Angadi V, Thacher PV, Burnham MM, Shaw PJ. 2015. Differential activation of immune factors in neurons and Glia contribute to individual differences in resilience/vulnerability to sleep disruption. *Brain, Behavior, and Immunity* **47**:75–85. DOI: https://doi.org/10.1016/j.bbi.2014.09.019, PMID: 25451614

Elya C, Lok TC, Spencer QE, McCausland H, Martinez CC, Eisen M. 2018. Robust manipulation of the behavior of *Drosophila Melanogaster* by a fungal pathogen in the laboratory. *eLife* **7**:e34414. DOI: https://doi.org/10.7554/eLife.34414, PMID: 30047862

Ezekowitz RAB, Hoffmann JA. 1996. Innate immunity. *Current Opinion in Immunology* **8**:1–2. DOI: https://doi.org/10.1016/S0952-7915(96)80096-3, PMID: 8793969

Hardie RC, Raghu P, Moore S, Juusola M, Baines RA, Sweeney ST. 2001. Calcium influx via TRP channels is required to maintain PIP2 levels in Drosophila photoreceptors. *Neuron* **30**:149–159. DOI: https://doi.org/10.1016/S0896-6273(01)00269-0, PMID: 11343651

Harris N, Braiser DJ, Dickman DK, Fetter RD, Tong A, Davis GW. 2015. The innate immune receptor PGRP-LC controls presynaptic homeostatic plasticity. *Neuron* **88**:1157–1164. DOI: https://doi.org/10.1016/j.neuron.2015.10.049, PMID: 26687223

Harris N, Fetter RD, Brasier DJ, Tong A, Davis GW. 2018. Molecular interface of neuronal innate immunity, synaptic vesicle stabilization, and presynaptic homeostatic plasticity. *Neuron* **100**:1163–1179. DOI: https://doi.org/10.1016/j.neuron.2018.09.048, PMID: 30344041

Kacsoh BZ, Lynch ZR, Mortimer NT, Schlenke TA. 2013. Fruit flies medicate offspring after seeing parasites. *Science* **339**:947–950. DOI: https://doi.org/10.1126/science.1229625, PMID: 23430653

Kacsoh BZ, Bozler J, Hodge S, Ramaswami M, Bosco G. 2015a. A novel paradigm for nonassociative long-term memory in Drosophila: predator-induced changes in oviposition behavior. *Genetics* **199**:1143–1157. DOI: https://doi.org/10.1534/genetics.114.172221, PMID: 25633088

Kacsoh BZ, Bozler J, Ramaswami M, Bosco G. 2015b. Social communication of predator-induced changes in Drosophila behavior and germ line physiology. *eLife* **4**:e07423. DOI: https://doi.org/10.7554/eLife.07423

Keesey IW, Koerte S, Khallaf MA, Retzke T, Guillou A, Grosse-Wilde E, Buchon N, Knaden M, Hansson BS. 2017. Pathogenic Bacteria enhance dispersal through alteration of Drosophila social communication. *Nature Communications* **8**:265. DOI: https://doi.org/10.1038/s41467-017-00334-9, PMID: 28814724

Khush RS, Leulier F, Lemaitre B. 2002. Immunology. pathogen surveillance–the flies have it. *Science* **296**:273–275. DOI: https://doi.org/10.1126/science.1071208, PMID: 11951023

Kurz CL, Charroux B, Chaduli D, Viallat-Lieutaud A, Royet J. 2017. Peptidoglycan sensing by octopaminergic neurons modulates *Drosophila* oviposition. *eLife* **6**:e21937. DOI: https://doi.org/10.7554/eLife.21937, PMID: 28264763

Lee HG, Rohila S, Han KA. 2009. The octopamine receptor OAMB mediates ovulation via Ca2+/calmodulin-dependent protein kinase II in the Drosophila oviduct epithelium. *PLOS ONE* **4**:e4716. DOI: https://doi.org/10.1371/journal.pone.0004716, PMID: 19262750

Lee K, Mylonakis E. 2017. An Intestine-Derived neuropeptide controls avoidance behavior in Caenorhabditis elegans. *Cell Reports* **20**:2501–2512. DOI: https://doi.org/10.1016/j.celrep.2017.08.053, PMID: 28877481

Leulier F, Vidal S, Saigo K, Ueda R, Lemaitre B. 2002. Inducible expression of double-stranded RNA reveals a role for dFADD in the regulation of the antibacterial response in Drosophila adults. *Current Biology* **12**:996–1000. DOI: https://doi.org/10.1016/S0960-9822(02)00873-4, PMID: 12123572

Lilienbaum A, Israël A. 2003. From calcium to NF-kappa B signaling pathways in neurons. *Molecular and Cellular Biology* **23**:2680–2698. DOI: https://doi.org/10.1128/MCB.23.8.2680-2698.2003, PMID: 12665571

Lipton SA. 1997. Janus faces of NF-kappa B: neurodestruction versus neuroprotection. *Nature Medicine* **3**:20–22. DOI: https://doi.org/10.1038/nm0197-20, PMID: 8986730

Luan H, Lemon WC, Peabody NC, Pohl JB, Zelensky PK, Wang D, Nitabach MN, Holmes TC, White BH. 2006. Functional dissection of a neuronal network required for cuticle tanning and wing expansion in Drosophila. *Journal of Neuroscience* **26**:573–584. DOI: https://doi.org/10.1523/JNEUROSCI.3916-05.2006, PMID: 16407556

Müller L, Pawelec G. 2014. Aging and immunity - impact of behavioral intervention. *Brain, Behavior, and Immunity* **39**:8–22. DOI: https://doi.org/10.1016/j.bbi.2013.11.015, PMID: 24315935

Naitza S, Rossé C, Kappler C, Georgel P, Belvin M, Gubb D, Camonis J, Hoffmann JA, Reichhart JM. 2002. The Drosophila immune defense against gram-negative infection requires the death protein dFADD. *Immunity* **17**:575–581. DOI: https://doi.org/10.1016/S1074-7613(02)00454-5, PMID: 12433364

O'Neill LA, Kaltschmidt C. 1997. NF-kappa B: a crucial transcription factor for glial and neuronal cell function. *Trends in Neurosciences* **20**:252–258. DOI: https://doi.org/10.1016/S0166-2236(96)01035-1, PMID: 9185306

Peabody NC, Diao F, Luan H, Wang H, Dewey EM, Honegger HW, White BH. 2008. Bursicon functions within the Drosophila CNS to modulate wing expansion behavior, hormone secretion, and cell death. *Journal of Neuroscience* **28**:14379–14391. DOI: https://doi.org/10.1523/JNEUROSCI.2842-08.2008, PMID: 19118171

Pritchett TL, McCall K. 2012. Role of the insulin/Tor signaling network in starvation-induced programmed cell death in Drosophila oogenesis. *Cell Death & Differentiation* **19**:1069–1079. DOI: https://doi.org/10.1038/cdd.2011.200, PMID: 22240900

Razzell W, Evans IR, Martin P, Wood W. 2013. Calcium flashes orchestrate the wound inflammatory response through DUOX activation and hydrogen peroxide release. *Current Biology* **23**:424–429. DOI: https://doi.org/10.1016/j.cub.2013.01.058, PMID: 23394834

Rezával C, Nojima T, Neville MC, Lin AC, Goodwin SF. 2014. Sexually dimorphic octopaminergic neurons modulate female postmating behaviors in Drosophila. *Current Biology* **24**:725–730. DOI: https://doi.org/10.1016/j.cub.2013.12.051, PMID: 24631243

Schneider A, Ruppert M, Hendrich O, Giang T, Ogueta M, Hampel S, Vollbach M, Büschges A, Scholz H. 2012. Neuronal basis of innate olfactory attraction to ethanol in Drosophila. *PLOS ONE* **7**:e52007. DOI: https://doi.org/10.1371/journal.pone.0052007, PMID: 23284851

Schretter CE, Vielmetter J, Bartos I, Marka Z, Marka S, Argade S, Mazmanian SK. 2018. A gut microbial factor modulates locomotor behaviour in Drosophila. *Nature* **563**:402–406. DOI: https://doi.org/10.1038/s41586-018-0634-9, PMID: 30356215

Sellegounder D, Yuan CH, Wibisono P, Liu Y, Sun J. 2018. Octopaminergic signaling mediates neural regulation of innate immunity in *Caenorhabditis elegans*. *mBio* **9**:e01645-18. DOI: https://doi.org/10.1128/mBio.01645-18, PMID: 30301853

Sharon G, Sampson TR, Geschwind DH, Mazmanian SK. 2016. The central nervous system and the gut microbiome. *Cell* **167**:915–932. DOI: https://doi.org/10.1016/j.cell.2016.10.027, PMID: 27814521

Silbering AF, Bell R, Galizia CG, Benton R. 2012. Calcium imaging of Odor-evoked responses in the Drosophila antennal lobe. *Journal of Visualized Experiments* **14**:2976. DOI: https://doi.org/10.3791/2976

Sweeney ST, Broadie K, Keane J, Niemann H, O'Kane CJ. 1995. Targeted expression of tetanus toxin light chain in Drosophila specifically eliminates synaptic transmission and causes behavioral defects. *Neuron* **14**:341–351. DOI: https://doi.org/10.1016/0896-6273(95)90290-2, PMID: 7857643

Toda H, Williams JA, Gulledge M, Sehgal A. 2019. A sleep-inducing gene, *nemuri*, links sleep and immune function in *Drosophila*. *Science* **363**:509–515. DOI: https://doi.org/10.1126/science.aat1650, PMID: 30705188

Yanagawa A, Guigue AM, Marion-Poll F. 2014. Hygienic grooming is induced by contact chemicals in Drosophila Melanogaster. *Frontiers in Behavioral Neuroscience* **8**:254. DOI: https://doi.org/10.3389/fnbeh.2014.00254, PMID: 25100963

Youn H, Kirkhart C, Chia J, Scott K. 2018. A subset of octopaminergic neurons that promotes feeding initiation in Drosophila Melanogaster. *PLOS ONE* **13**:e0198362. DOI: https://doi.org/10.1371/journal.pone.0198362, PMID: 29949586

Zhai Z, Huang X, Yin Y. 2018. Beyond immunity: the imd pathway as a coordinator of host defense, organismal physiology and behavior. *Developmental & Comparative Immunology* **83**:51–59. DOI: https://doi.org/10.1016/j.dci.2017.11.008, PMID: 29146454

Supplementary figures Article 2

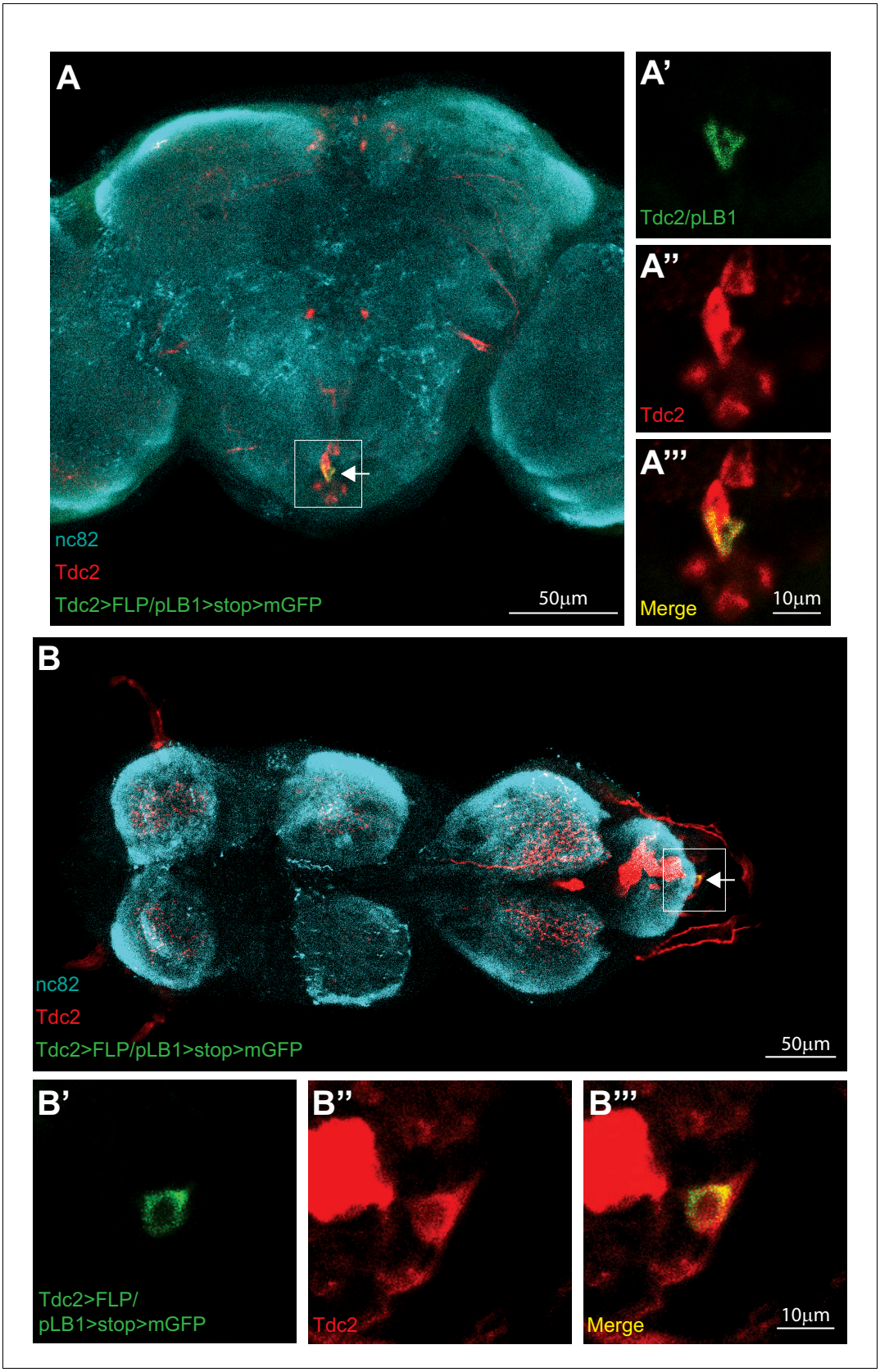

Figure 2—figure supplement 1. Some octopaminergic neurons are pLB1+. Immuno-detection in the brain (**A-A'''**) and ventral nerve cord (VNC; **B-B'''**) of cells co-expressing Tdc2 and pLB1 (Tdc2>FLP/pLB1>stop>mGFP). The GFP can only be expressed if the stop sequence inserted upstream of the

Figure 2—figure supplement 1 continued on next page

Figure 2—figure supplement 1 continued

gfp gene is flipped-out in pLB1+/Tdc2+ cells. For (**A and B**), the area outlined in the box is magnified in (**A'-A'''**) and (**B'-B'''**), respectively. Staining against nc82 was used to delineate the shape of the brain (**A**) and VNC (**B**). The arrow indicates neurons co-expressing pLB1 and Tdc2. Details including genotypes can be found in the detailed lines, conditions and, statistics for the figure section.

DOI: https://doi.org/10.7554/eLife.50559.006

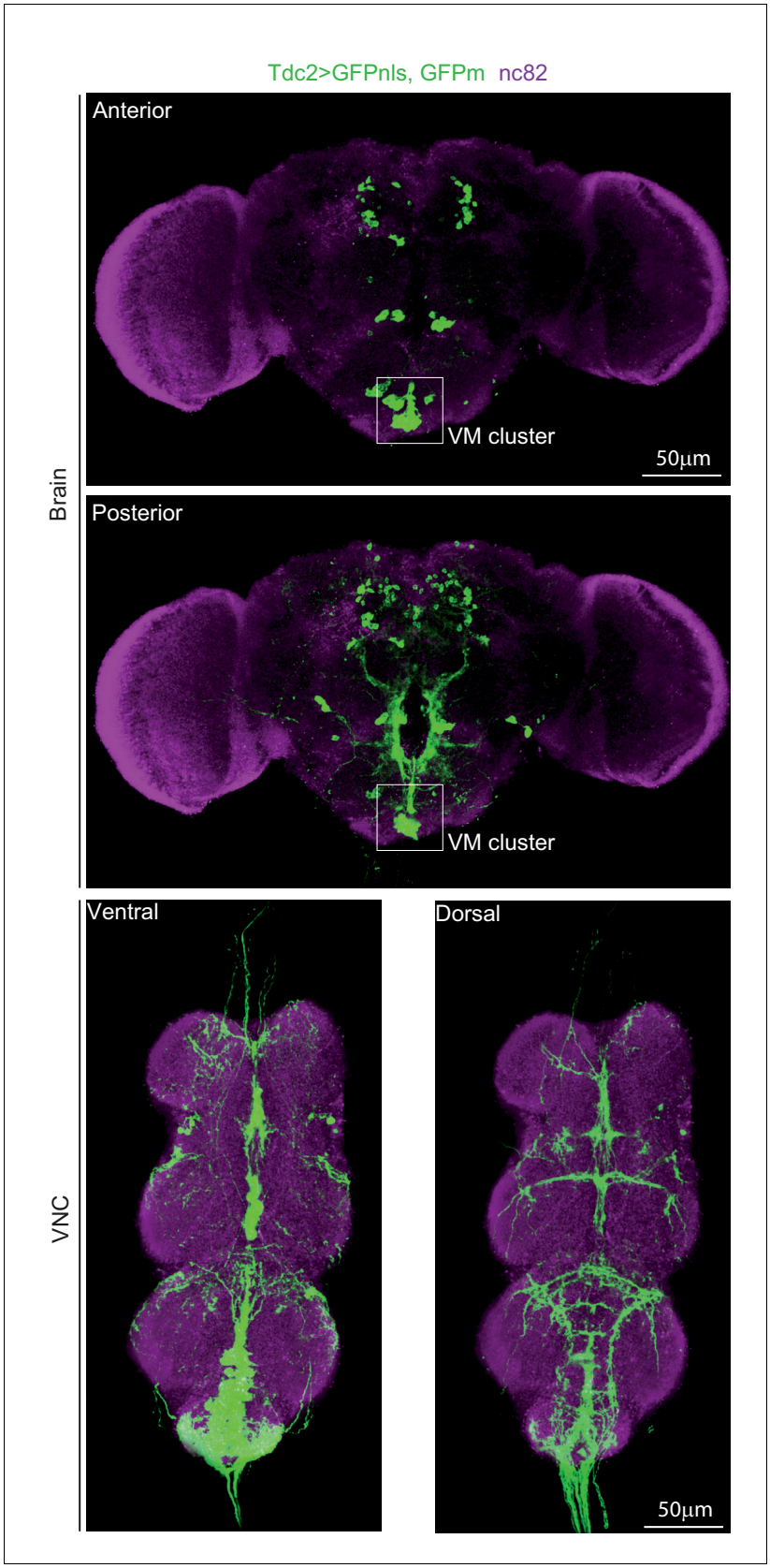

Figure 2—figure supplement 2. Map of Tdc2 expressing neurons in the brain and VNC. Immunodetection in the brain and ventral nerve cord (VNC) of cells expressing Tdc2. The area in the brain outlined in the box corresponds

Figure 2—figure supplement 2 continued on next page

Figure 2—figure supplement 2 continued

to the VM cluster. In the projection of the anterior view of the brain, VM I and VM II sub-clusters are visible. In the projection of the posterior view of the brain, the VM III sub-cluster is visible. Details including genotypes can be found in the detailed lines, conditions and, statistics for the figure section.

DOI: https://doi.org/10.7554/eLife.50559.007

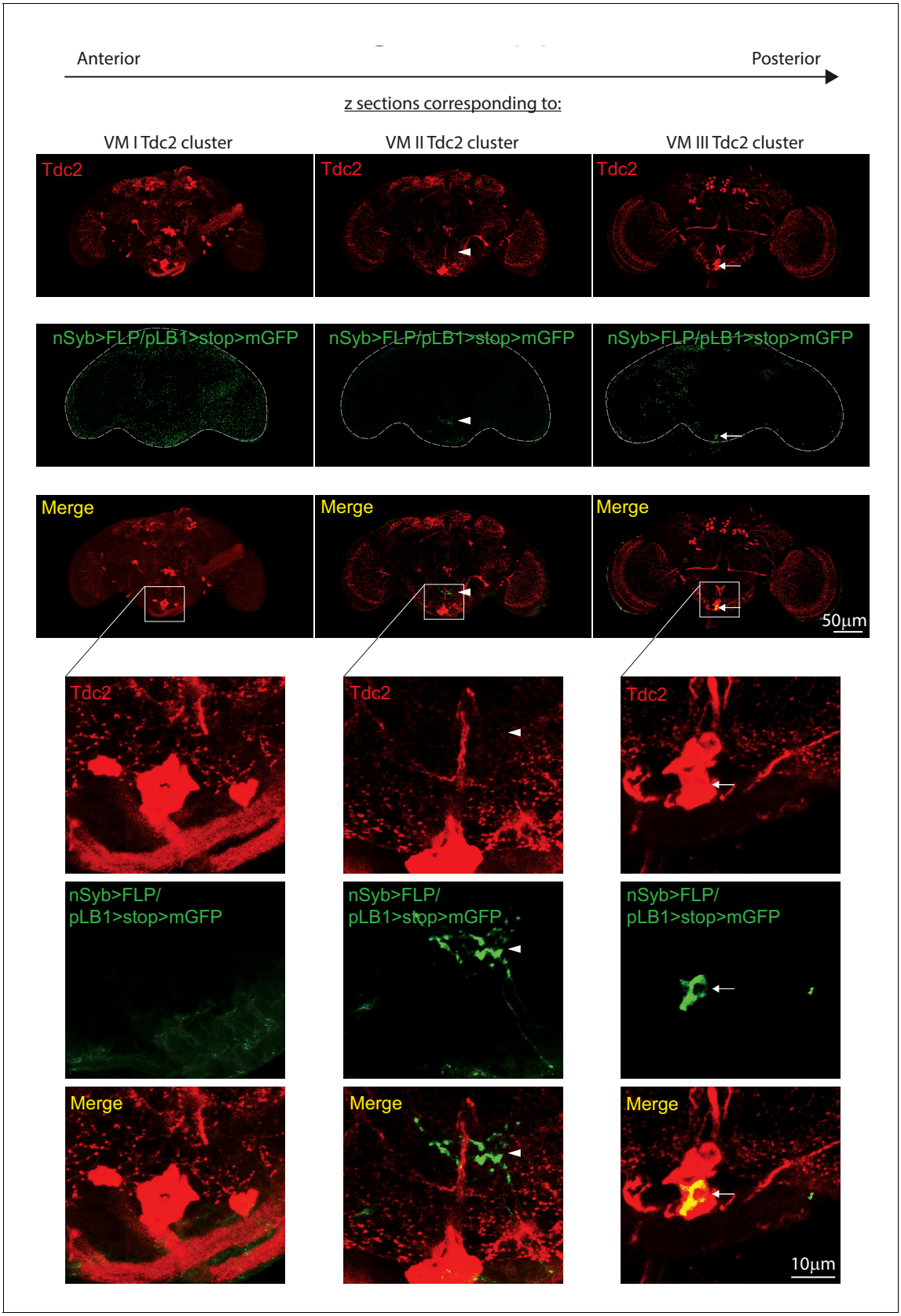

Figure 2—figure supplement 3. The pLB1+ octopaminergic neurons in the brain belong to the VM III sub-cluster. Immuno-detection in the brain of neurons expressing pLB1 (nSyb>FLP/pLB1>stop>mGFP) and producing the enzyme Tdc2. Brain stacks from anterior to posterior with focal plane

Figure 2—figure supplement 3 continued on next page

Figure 2—figure supplement 3 continued

corresponding to VM I, VM II and VM III octopaminergic sub-clusters are shown. The sub-clusters delimited by the outlined box are magnified and the individual channels shown. Arrows indicate cell bodies and arrowheads projections of pLB1+ neurons. Details including genotypes can be found in the detailed lines, conditions and, statistics for the figure section.

DOI: https://doi.org/10.7554/eLife.50559.008

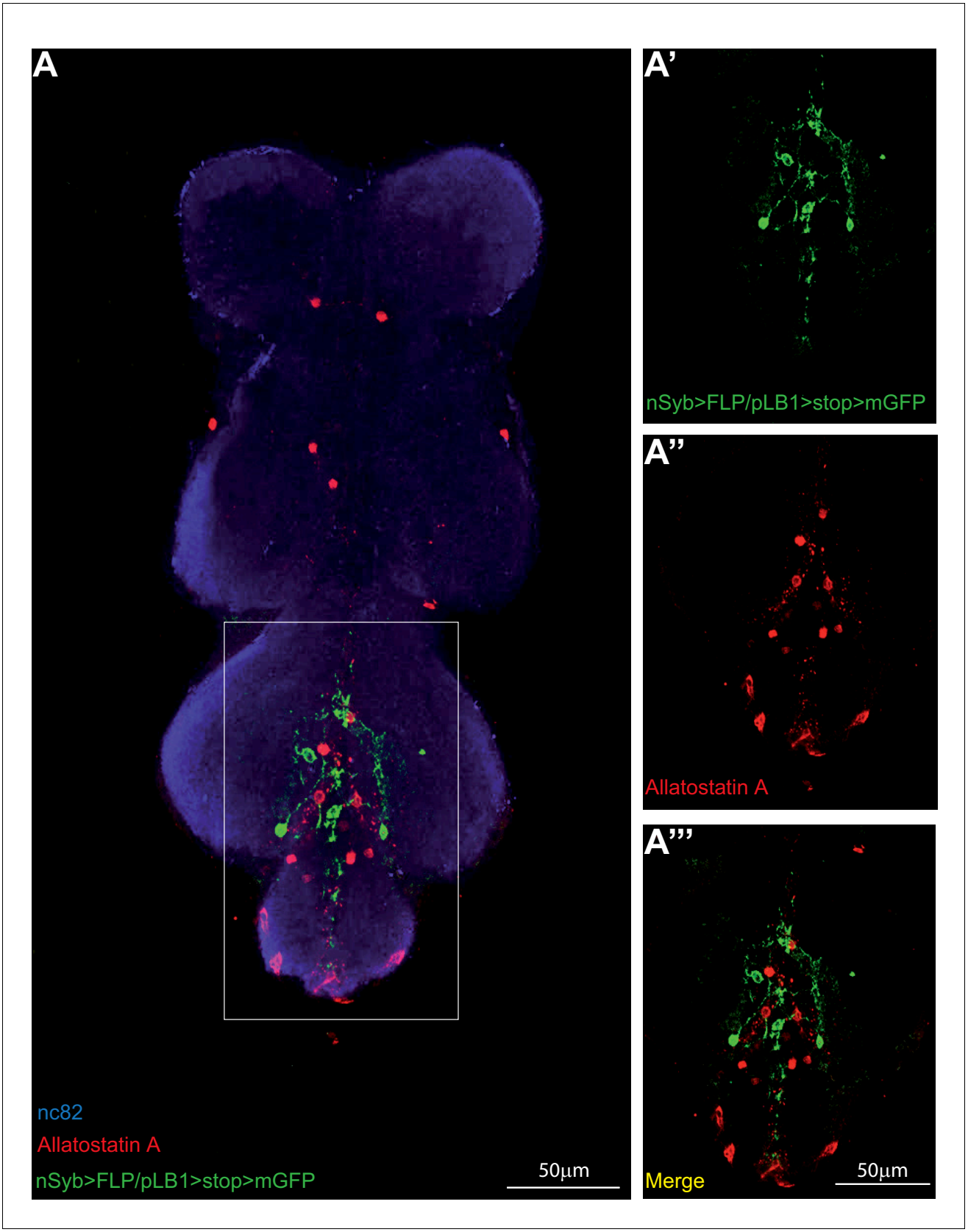

Figure 2—figure supplement 4. pLB1-expressing neurons in the VNC do not produce Allatostatin A. (**A-A'''**); Immuno-detection in the ventral nerve cord (VNC) of neurons expressing pLB1 (nSyb>FLP/pLB1>stop>mGFP) and producing the Allatostatin A neuropeptide. Shown is a maximum intensity

Figure 2—figure supplement 4 continued on next page

Figure 2—figure supplement 4 continued

projection. The area outlined in the box is magnified in (**A'-A'''**). Staining against nc82 was used to delineate the shape of the VNC (**A**). Details including genotypes can be found in the detailed lines, conditions and, statistics for the figure section.

DOI: https://doi.org/10.7554/eLife.50559.009

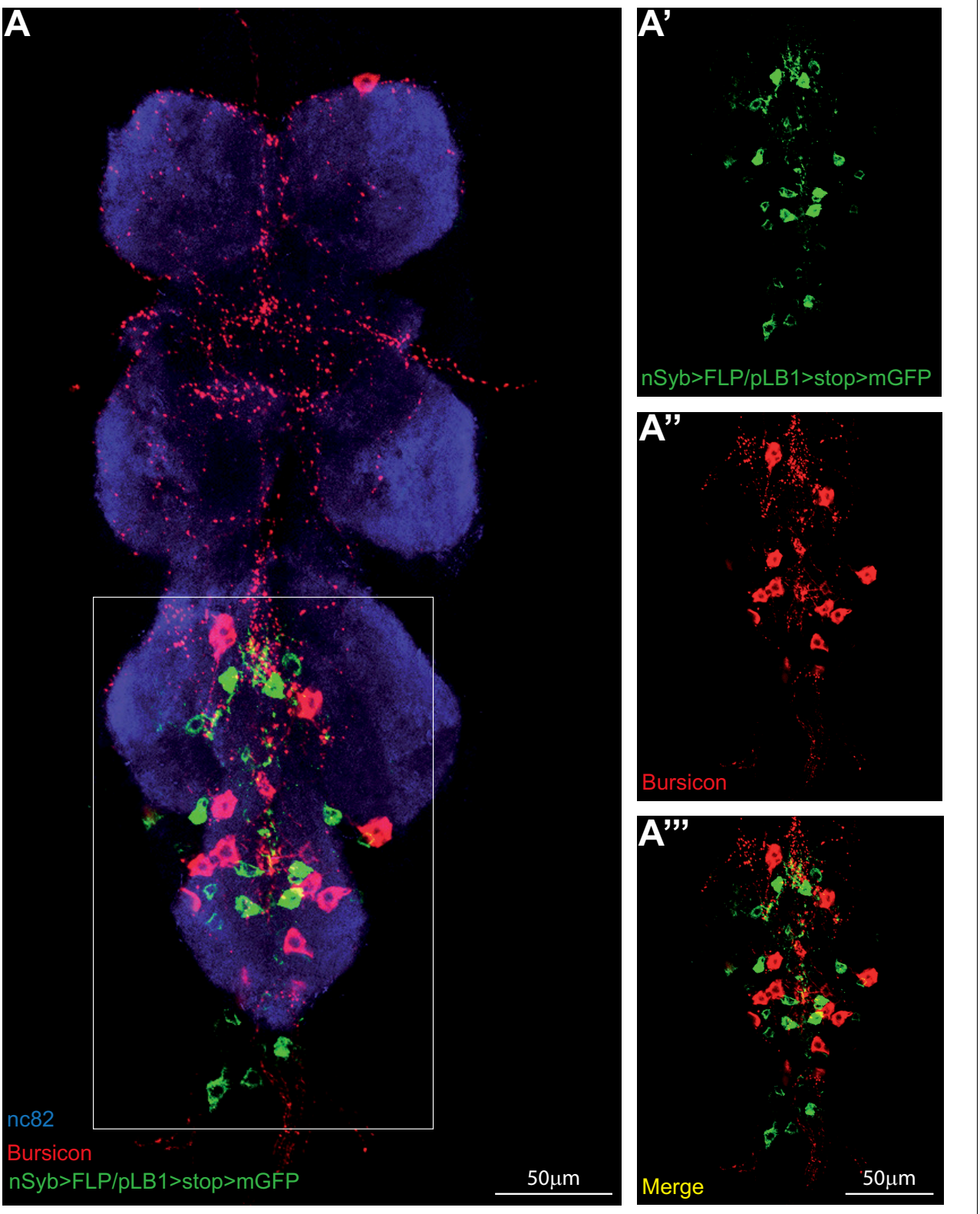

Figure 2—figure supplement 5. pLB1+ neurons in the VNC do not produce Bursicon. (**A-A'''**); Immuno-detection in the ventral nerve cord (VNC) of neurons expressing pLB1 (nSyb>FLP/pLB1>stop>mGFP), and producing the Bursicon neuropeptide. Shown is a maximum intensity projection. The area

Figure 2—figure supplement 5 continued on next page

Figure 2—figure supplement 5 continued

outlined in the box is magnified in (**A'-A'''**). Staining against nc82 was used to delineate the shape of the VNC (**A**). Details including genotypes can be found in the detailed lines, conditions and, statistics for the figure section.

DOI: https://doi.org/10.7554/eLife.50559.010

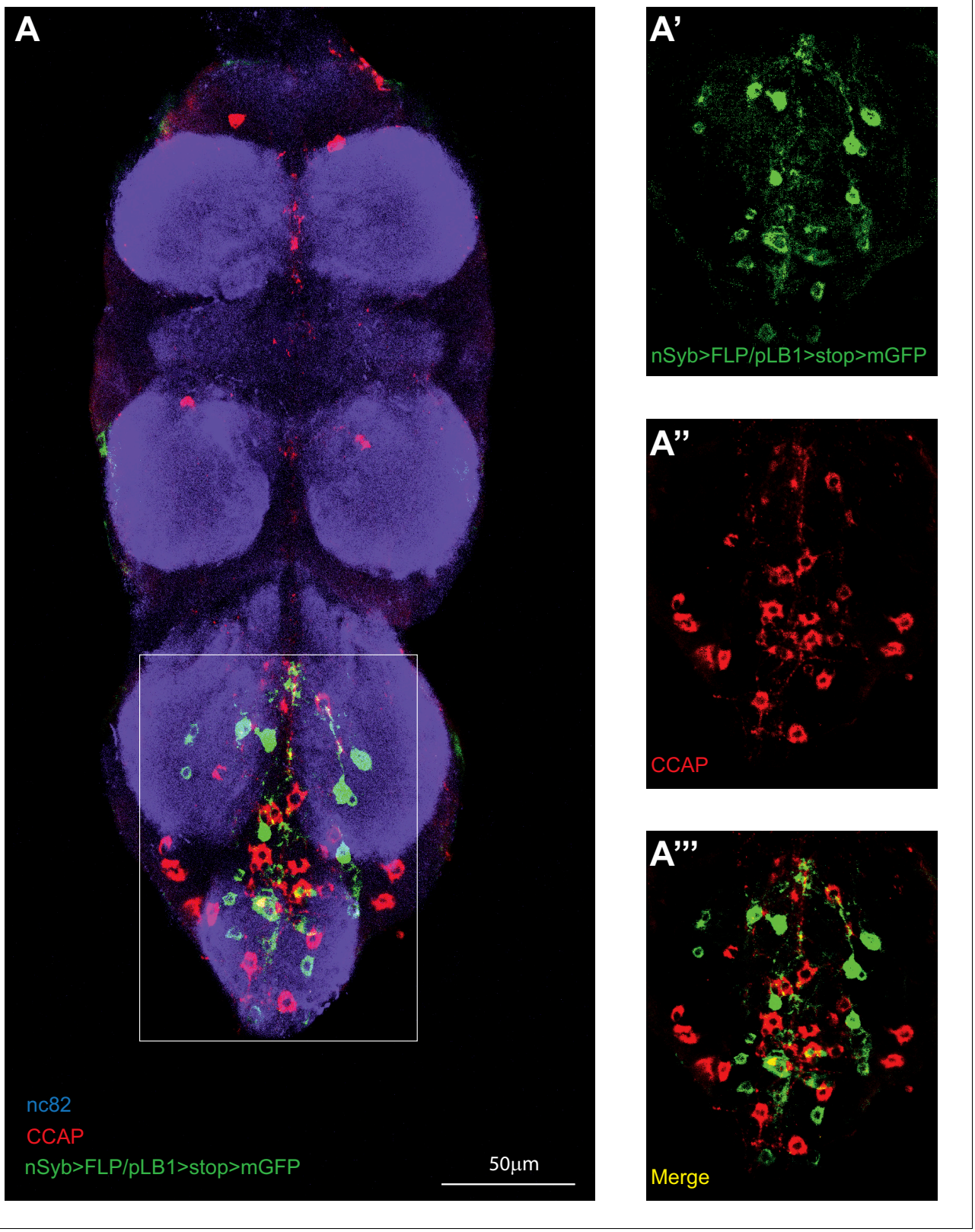

Figure 2—figure supplement 6. pLB1+ neurons in the VNC do not produce CCAP. (**A-'''**); Immuno-detection in the ventral nerve cord (VNC) of neurons expressing pLB1 (nSyb>FLP/pLB1>stop>mGFP)and producing the Crustacean cardioactive peptide (CCAP). Shown is a maximum intensity

Figure 2—figure supplement 6 continued on next page

Figure 2—figure supplement 6 continued

projection. The area outlined in the box is magnified in (**A'-A'''**). Staining against nc82 was used to delineate the shape of the VNC (**A**). Details including genotypes can be found in the detailed lines, conditions and, statistics for the figure section.

DOI: https://doi.org/10.7554/eLife.50559.011

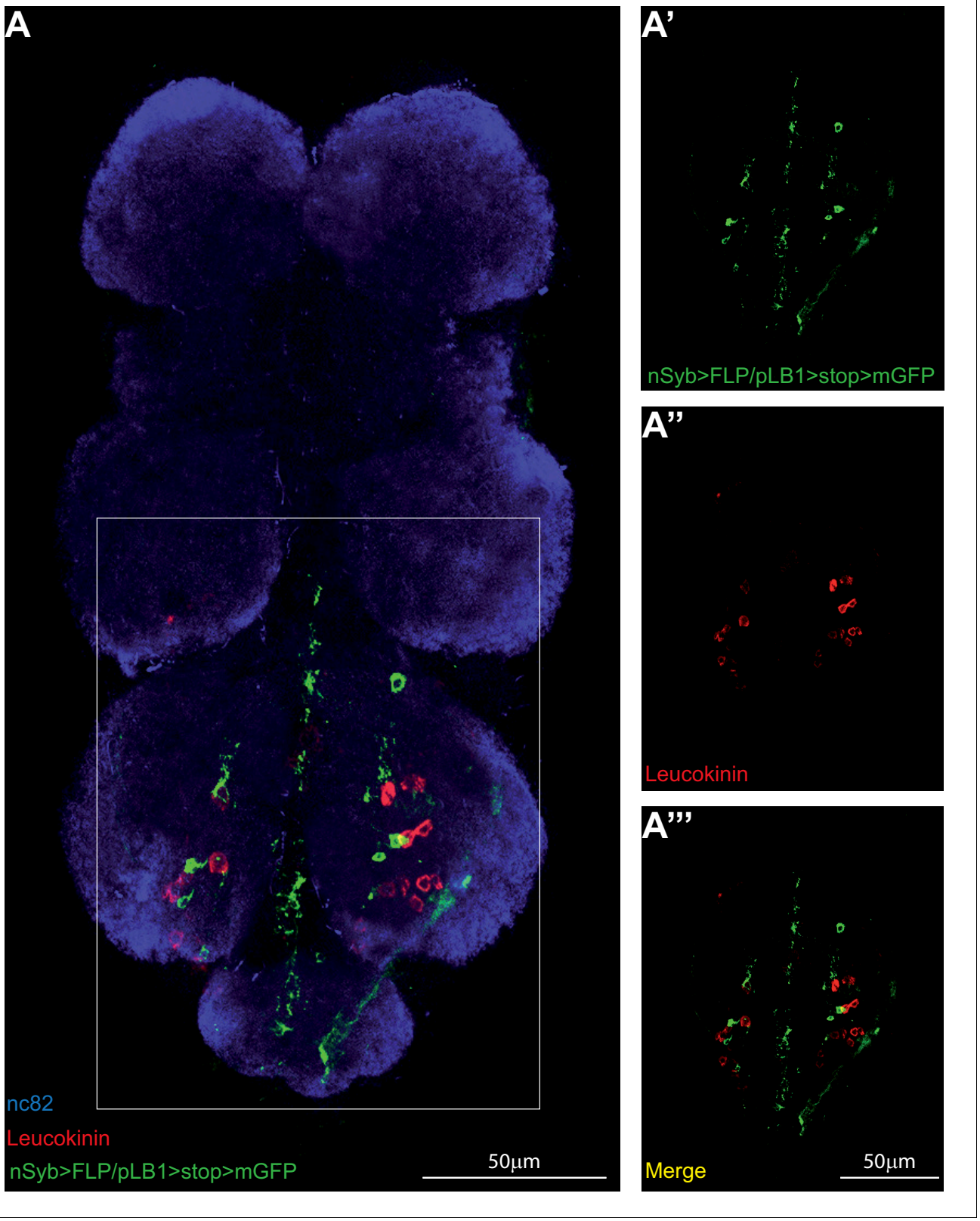

Figure 2—figure supplement 7. pLB1+ neurons in the VNC do not produce Leucokinin. (**A-A'''**); Immuno-detection in the ventral nerve cord (VNC) of neurons expressing pLB1 (nSyb>FLP/pLB1>stop>mGFP) and producing the Leucokinin neuropeptide. Shown is a maximum intensity projection. The

Figure 2—figure supplement 7 continued on next page

Figure 2—figure supplement 7 continued

area outlined in the box is magnified in (**A'-A'''**). Staining against nc82 was used to delineate the shape of the VNC (**A**). Details including genotypes can be found in the detailed lines, conditions and, statistics for the figure section.

DOI: https://doi.org/10.7554/eLife.50559.012

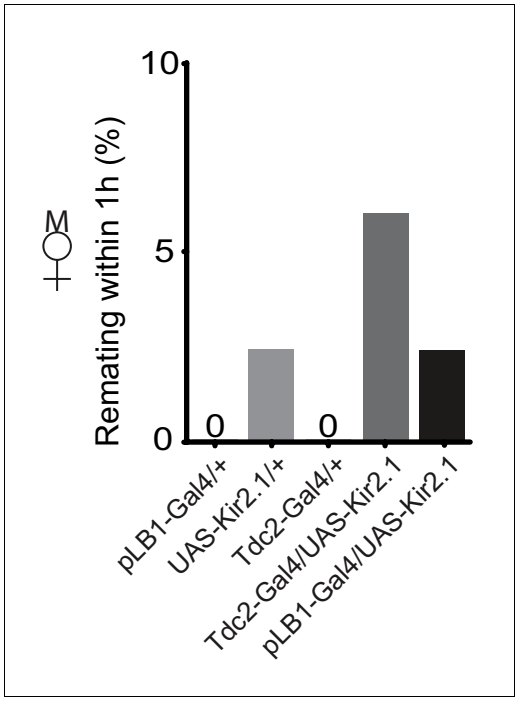

Figure 3—figure supplement 1. pLB1+ neurons may not control remating behavior. Impairing the activity of pLB1 neurons via UAS-Kir2.1 does not increase the remating percentage. Shown is the average remating percentage for mated females per 1 hour (1h) from four independent trials with a total of 42 to 55 females per genotype and condition used. For statistics, Fisher exact t-test was used and despite the trends, there were no statistically significant differences. Details including n values and genotypes can be found in the detailed lines, conditions and, statistics for the figure section.

DOI: https://doi.org/10.7554/eLife.50559.014

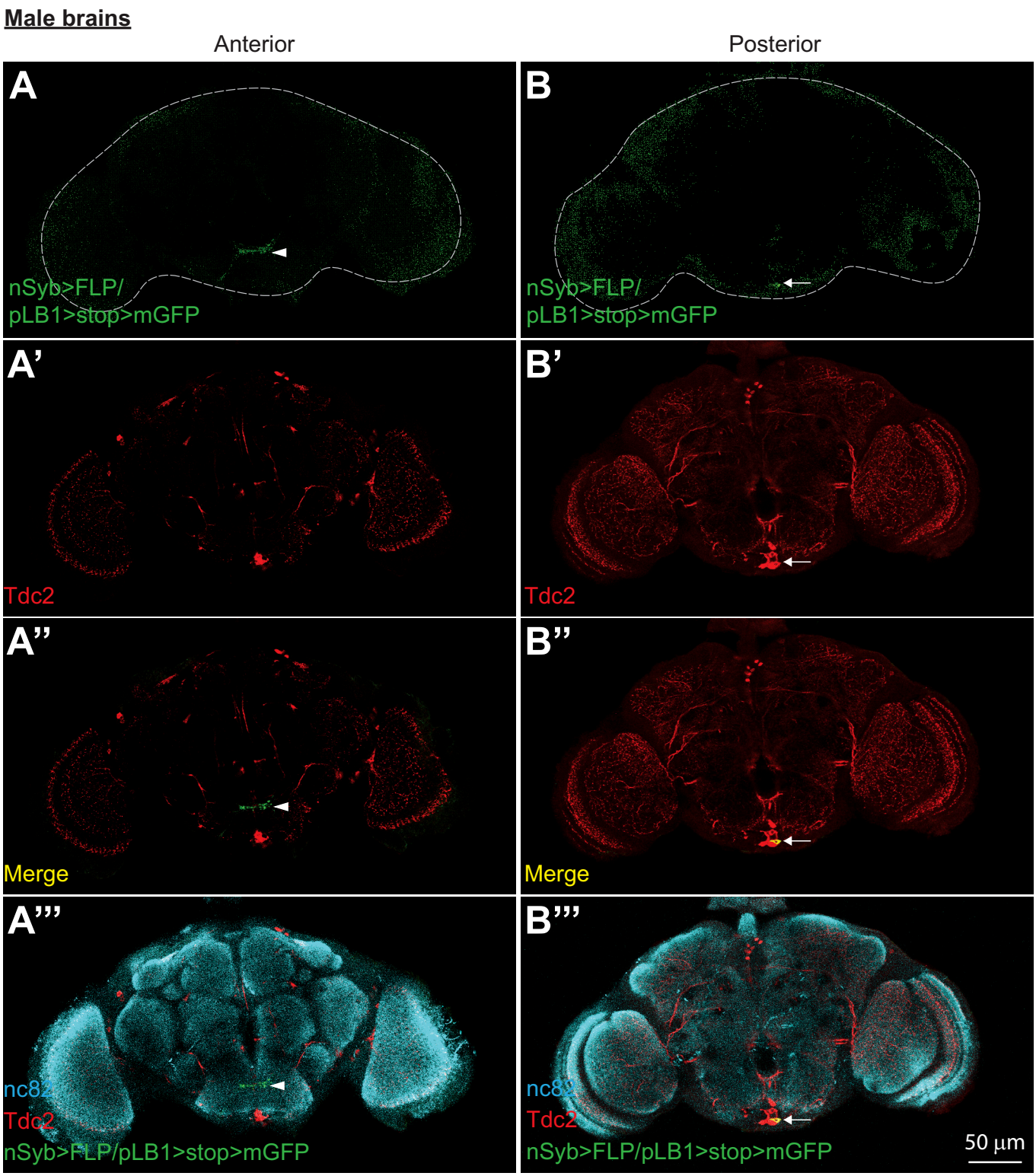

Figure 3—figure supplement 2. pLB1+/Tdc2+ neurons are present in male brains. In adult males, immuno-detection in the anterior (**A-A'''**) and posterior (**B-B'''**) part of the brain of neurons expressing pLB1 and producing the enzyme Tdc2. For (**A''' and B'''**), staining against nc82 was used to

Figure 3—figure supplement 2 continued on next page

Figure 3—figure supplement 2 continued

delineate the shape of the brain. Arrows indicate position of pLB1+ cell bodies. Arrowheads indicate projections. Details including genotypes can be found in the detailed lines, conditions and, statistics for the figure section.

DOI: https://doi.org/10.7554/eLife.50559.015

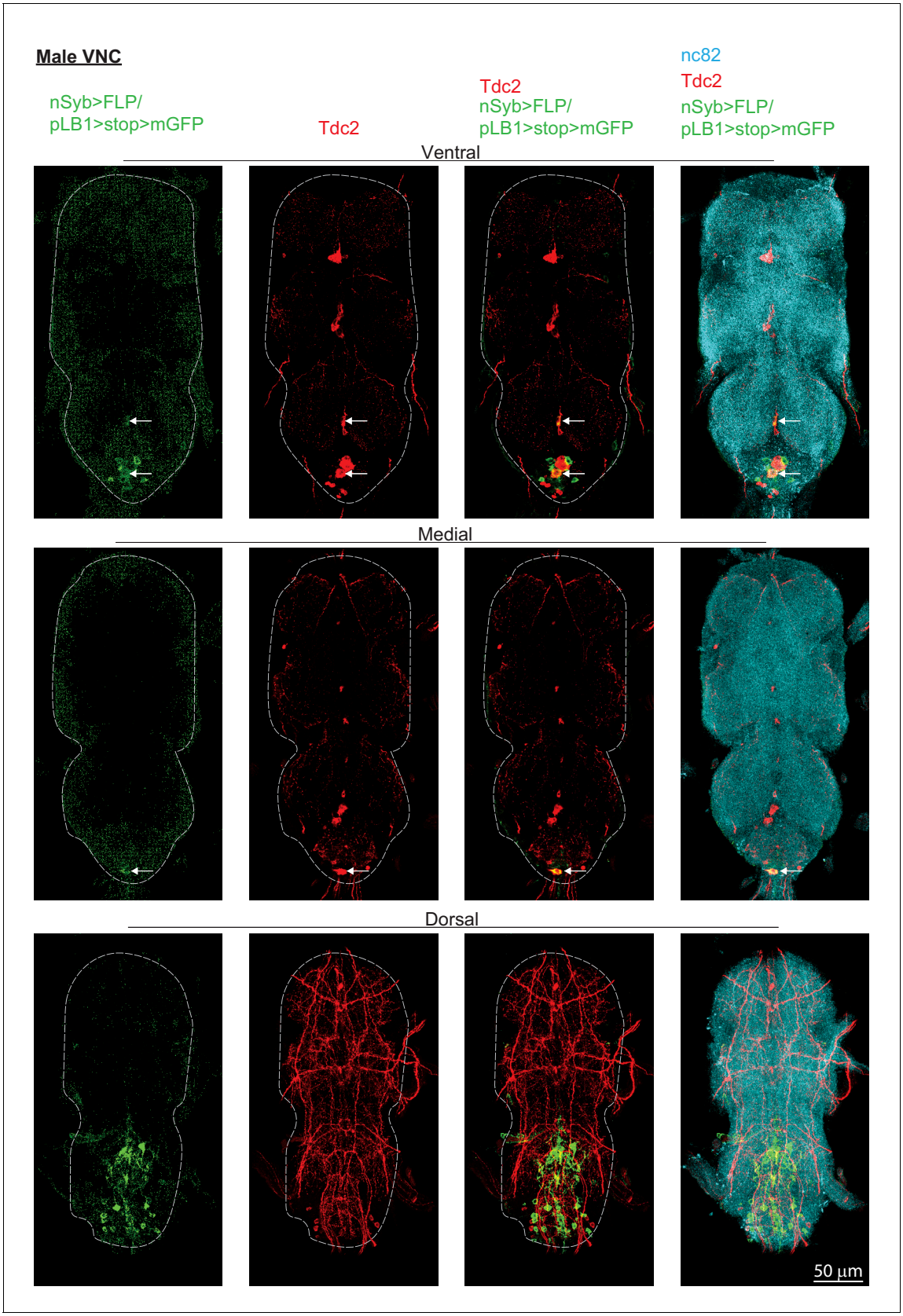

Figure 3—figure supplement 3. pLB1+/Tdc2+ neurons are present in male VNC. In adult males, immuno-detection in the ventral, medial and dorsal part of the ventral nerve cord (VNC) of neurons expressing pLB1 and producing the enzyme Tdc2. Staining against nc82 was used to delineate the

Figure 3—figure supplement 3 continued on next page

Figure 3—figure supplement 3 continued

shape of the VNC. Arrows indicate the positions of pLB1+ cell bodies. Details including genotypes can be found in the detailed lines, conditions and, statistics for the figure section.

DOI: https://doi.org/10.7554/eLife.50559.016

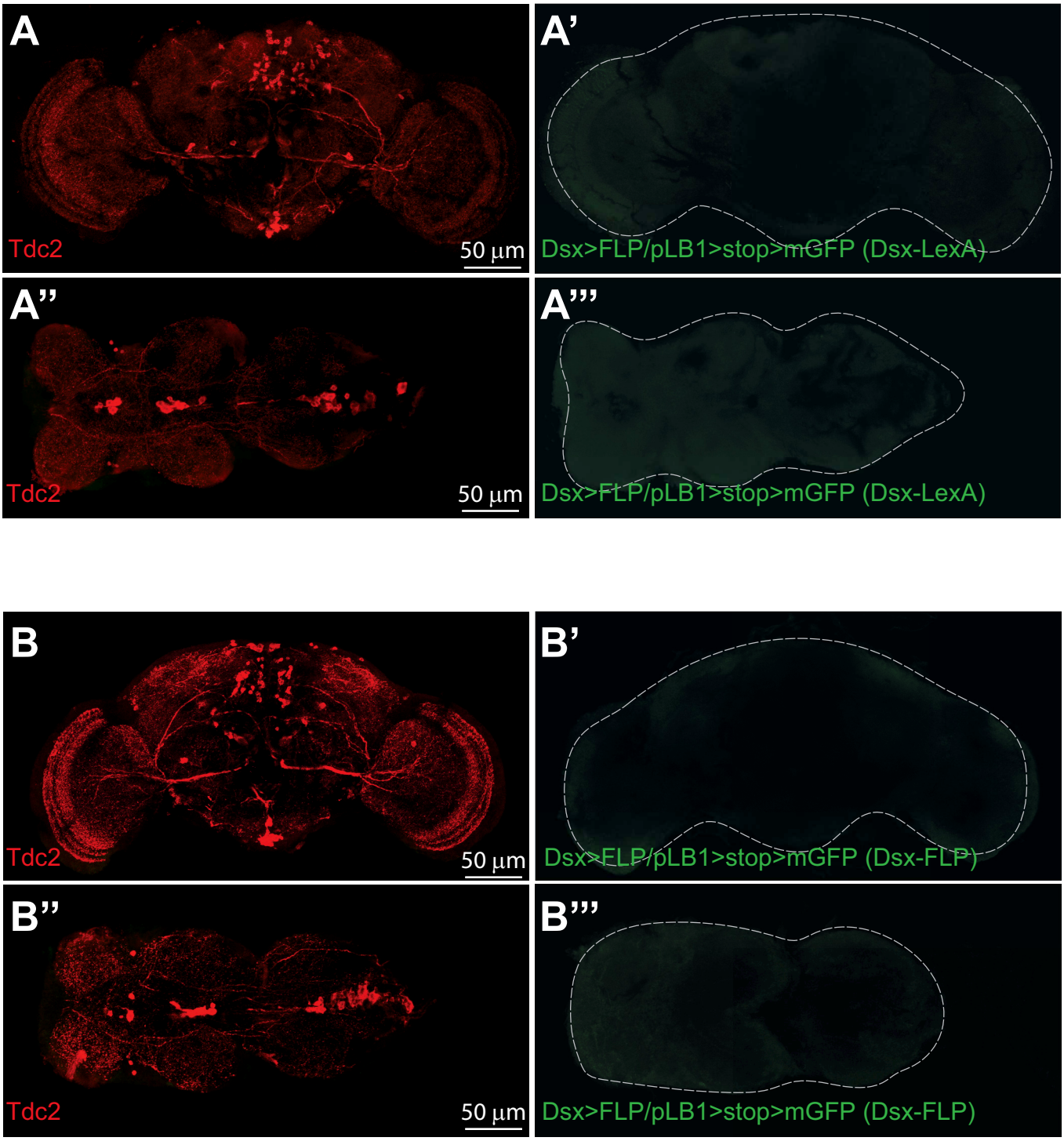

Figure 3—figure supplement 4. pLB1+ neurons are not Dsx+. In adult females, immuno-detection in the brain (**A-A', B-B'**) and ventral nerve cord (**A''-A''', B''-B'''**) of Dsx+ cells expressing pLB1 and producing the enzyme Tdc2 via intersectional strategy and the use of either Dsx-LexA (**A' and A'''**) or Dsx-FLP (**B' and B'''**); no signal for Dsx+/pLB1+ cells is detectable. Details including genotypes can be found in the detailed lines, conditions and, statistics for the figure section.

DOI: https://doi.org/10.7554/eLife.50559.017

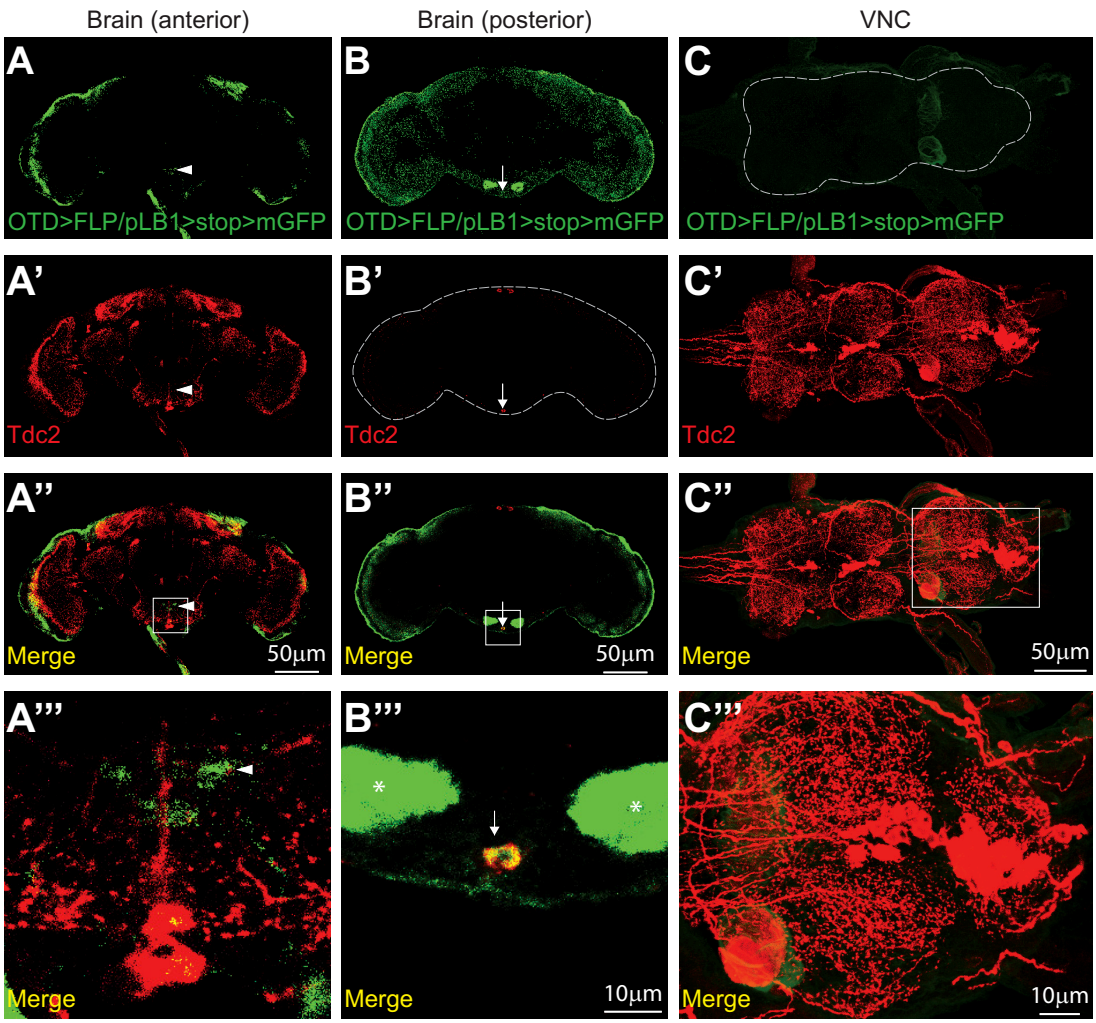

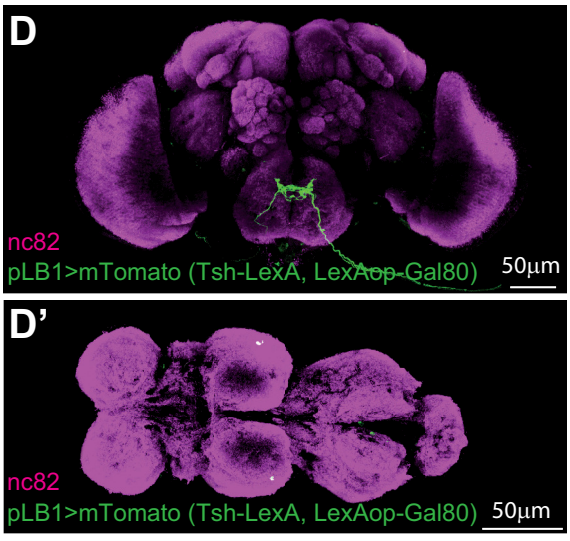

Figure 5—figure supplement 1. OTD-FLP is expressed in pLB1+ neurons of the head, but not of the thorax whileTsh-LexA, LexAop-Gal80 efficiently silences pLB1-Gal4 in the thorax. (**A–C'''**); Immunodetection of cells co-expressing pLB1-Gal4 and OTD-FLP (OTD>FLP/pLB1>stop >mGFP) and

Figure 5—figure supplement 1 continued on next page

Figure 5—figure supplement 1 continued

producing the enzyme Tdc2 in the anterior (**A–A'''**) and posterior (**B–B'''**) parts of the brain as well as in the VNC (**C–C'''**). (**D–D'**); Immunodetection of cells expressing pLB1-Gal4/UAS-Tomato-mCD8 (pLB1>mTomato) in the brain, but not the VNC of flies co-expressing Tsh-LexA/LexAop-Gal80. For the homogeneity of the different images, the red signal corresponding to Tomato-mCD8 was converted in green. For (**A–C'''**), pLB1+/OTD+/Tdc2+ neurons were detected in the brain. Arrows indicate cell bodies and arrowheads projection of pLB1+ neurons; no signal was detected in the VNC. In (**B'''**), asterisks correspond to background. (**A'''**, **B''' and C'''**) correspond to magnification of the area delimited by the box in (**A''**, **B'' and C''**). For (**D**), pLB1 is expressed in the brain. For (**D'**), pLB1 was not detected in the VNC. Details including n values and genotypes can be found in the detailed lines, conditions and, statistics for the figure section.

DOI: https://doi.org/10.7554/eLife.50559.023

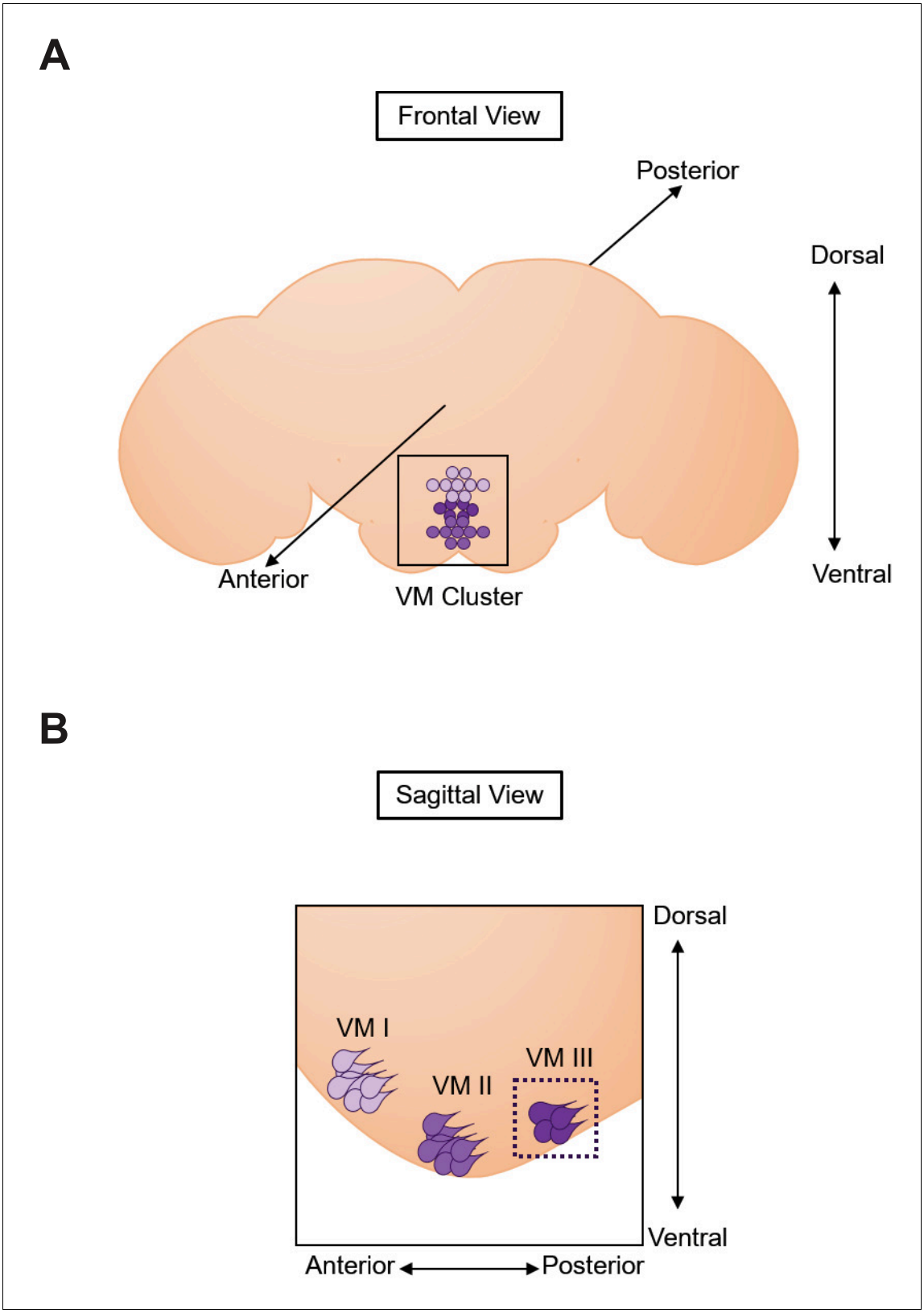

Figure 8—figure supplement 1. The *in vivo* and *ex vivo* real-time Calcium imaging approaches focused on neurons present in the VM II/III octopaminergic sub-cluster. Scheme representing a frontal view (**A**) of a brain and a sagittal view (**B**) of the octopaminergic VM cluster. The VM cluster is located ventrally along the midline in the frontal view (**A**). Three main sub-clusters (neurons represented with colored circles) can be delineated along

Figure 8—figure supplement 1 continued on next page

Figure 8—figure supplement 1 continued

the antero-posterior axis as represented in the sagittal view (**B**). We focused on the VM II/III sub-clusters for the *in vivo* approach and only on the most posterior group (VM III sub-cluster), delineated by a dashed line in (**B**) for the *ex-vivo* assays.

DOI: https://doi.org/10.7554/eLife.50559.031

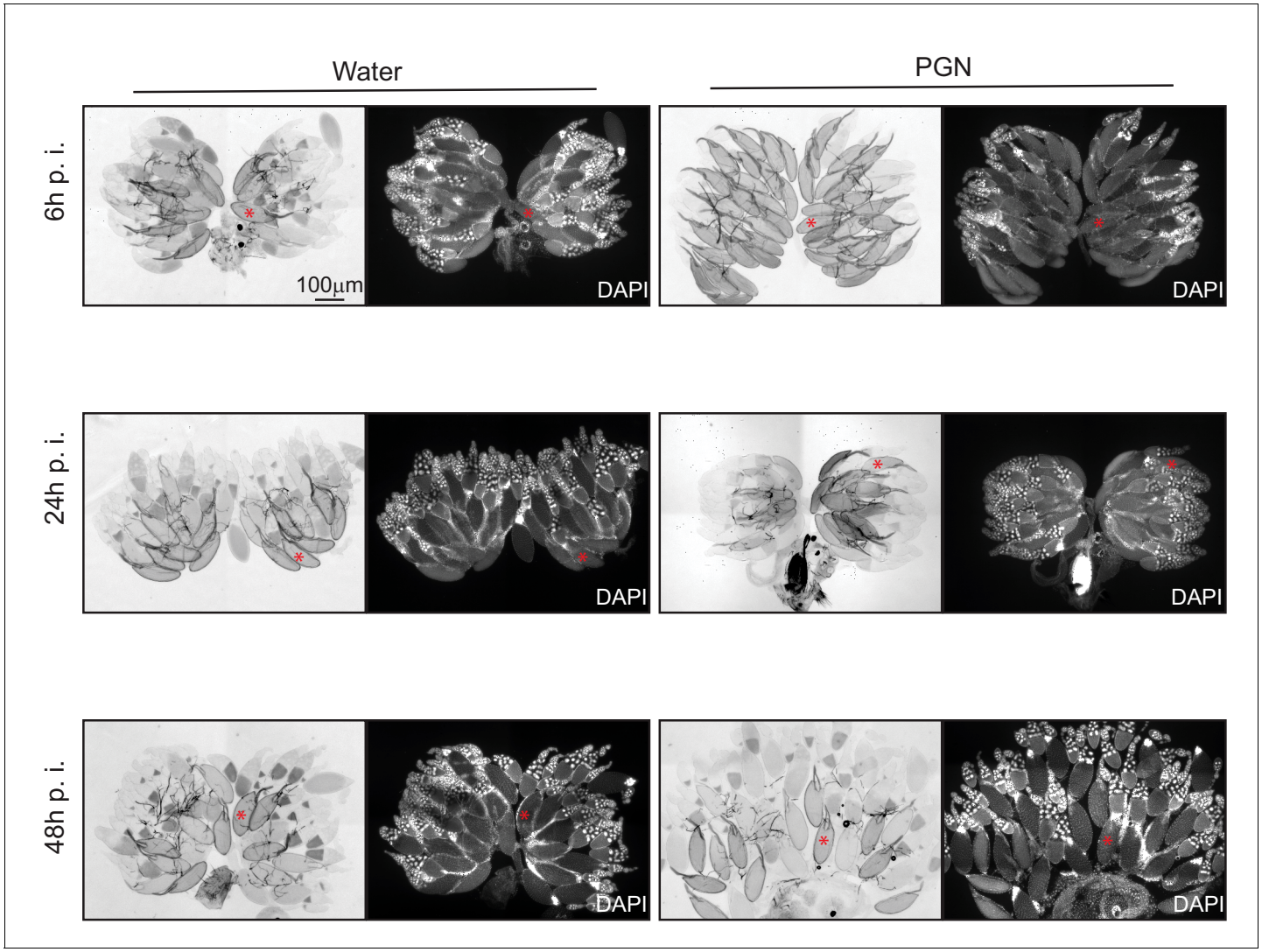

Figure 9—figure supplement 1. Peptidoglycan exposure leads to a reversible accumulation of stage 14 oocytes. Peptidoglycan injection triggers stage 14 oocyte accumulation that is reversed by 24 hours (24h). Ovaries seen with transmission light microscopy and DAPI staining from control flies (water injected) or peptidoglycan-injected animals 6h, 24h and 48h post-treatment (p.i.). Prototypical stage 14 oocyte is indicated with a red asterisk. Details including n values and genotypes can be found in the detailed lines, conditions and, statistics for the figure section.

DOI: https://doi.org/10.7554/eLife.50559.037

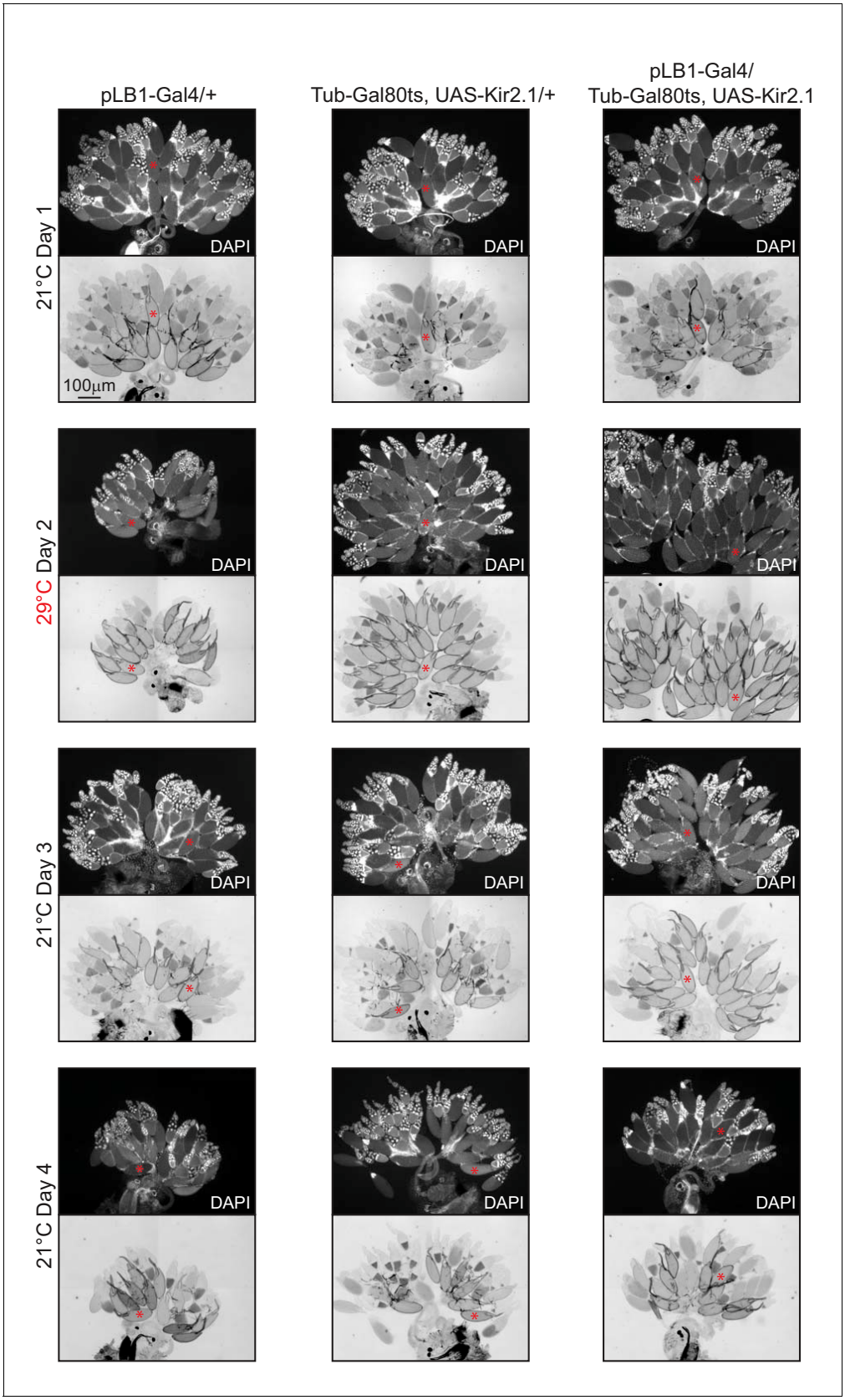

Figure 9—figure supplement 2. Conditional inactivation of pLB1+ neurons leads to a reversible accumulation of stage 14 oocytes. Conditional inactivation of the pLB1+ neurons in pLB1-Gal4/Tub-Gal80^{ts}, UAS-Kir2.1 flies triggers a reversible stage 14 oocytes accumulation. Ovaries from control

Figure 9—figure supplement 2 continued on next page

Figure 9—figure supplement 2 continued

flies (pLB1-Gal4/+ and Tub-G80^{ts}, UAS-Kir2.1/+) and test animals (pLB1-Gal4/Tub-Gal80^{ts}, UAS-Kir2.1) are seen with transmission light microscopy and DAPI staining over the course of 4 days and two different temperatures. Prototypical stage 14 oocyte is indicated with a red asterisk. Details including n values and genotypes can be found in the detailed lines, conditions and, statistics for the figure section.

DOI: https://doi.org/10.7554/eLife.50559.038

Manuscript 3

Dual mode of detection of bacteria-derived peptidoglycan by *Drosophila* gustatory neurons

Ambra Masuzzo[1 $], Claudia Steiner[2,3 $], Gérard Manière[4 $], Yaël Grosjean[4], Frédéric Marion-Poll[2,3], Léopold Kurz[1 *], Julien Royet[1 *¤]

1 : Aix-Marseille Université, CNRS, IBDM, Marseille, France

2 : Evolution, Génomes, Comportement, Ecologie, CNRS, IRD, Univ Paris-Sud, Université Paris-Saclay, Gif-sur-Yvette, France.

3 : AgroParisTech, Université Paris-Saclay, Paris, France.

4 : Centre des Sciences du Goût et de l'Alimentation, AgroSup Dijon, CNRS, INRA, Université Bourgogne Franche-Comté, F-21000 Dijon, France

[$] co-first author, [*] co-corresponding authors

[¤] Lead contact

SUMMARY

Probing the external microbial world is a major function of the eukaryotes nervous system. The identification of beneficial or pathogenic bacteria is of paramount importance for the host. In *Drosophila*, the NF-κB/IMD pathway is activated in immune cells upon recognition of bacteria-derived peptidoglycan by PGRP proteins. We show that one of these peptidoglycan-interacting proteins, called PGRP-LB, is expressed in some proboscis's bitter taste neurons. Calcium imaging reveals that peptidoglycan activates not solely bitter but also sweet neurons. Our results show an implication of the PGRP/IMD pathway in peptidoglycan transduction in bitter neurons expressing PGRP-LB, whereas this module seems dispensable for peptidoglycan detection in sweet neurons. Furthermore, we show how flies integrate both neuronal signals in their behavioral response to peptidoglycan. This demonstrates that flies use the same bacterial elicitor and signaling module to sense bacterial presence via the peripheral nervous system and trigger an anti-bacterial response in immune-competent cells.

KEYWORDS

Drosophila, Peptidoglycan, Taste neurons, Peptidoglycan Recognition Proteins, NF-κB pathway, Bitter neuron, Sweet neurons, Oviposition

INTRODUCTION

Since parasites can dramatically reduce the fitness of their hosts, natural selection should favor defense mechanisms that can efficiently protect them against disease-causing microbes. Historically, much work has focused on dissecting the mechanisms that regulate the humoral and cellular immunities, the main armed branches of the host against invading pathogens. However, hosts can also engage in behaviors to avoid microorganisms or to reduce the consequences of the infection on them or their progeny. Social insects, such as termites can ascertain the virulence of the *Metarhizium* and *Beauveria* fungi and keep away from the most virulent strains [1], while *Apis mellifera* workers are able to detect larvae infected with the fungus *Ascosphaera apis* and remove them from the nest [2]. The molecular mechanisms behind these behavioral responses to microbes, which require a molecular dialog between the microorganism and the host nervous system, are less well-characterized. Genetically tractable models such as *Caenorhabditis elegans* or *Drosophila melanogaster* are very well suited to elucidate them [3, 4, 5]. Devoid of adaptative immunity like all invertebrates, *Drosophila* has emerged as a well-adapted model to unravel the proteins and signaling modules that control the innate immune responses against bacteria [6, 7, 8, 9]. Essential to them are two NF-κB signaling pathways called Toll and IMmune Deficiency (IMD) whose activation triggers the production of immune effectors, such as antimicrobial peptides (AMPs), in immune-competent cells [6, 10, 11, 12]. This activation depends on the detection of bacteria-derived peptidoglycan (PGN) by host pattern recognition receptor (PRR) belonging to the PeptidoGlycan Recognition Protein (PGRP) family [13, 14]. Recent work has shown that signaling components of the NF-κB pathway, including the transcription factor Relish, and the upstream PGRP sensors are expressed and functionally required outside the immune system and more specifically in some neurons of the central nervous system (CNS) [15]. Direct recognition of bacteria-derived PGN by few brain octopaminergic VM III neurons leads to their inhibition and, in turn, to an egg-laying reduction in PGN-exposed females [16]. Hence, by detecting a ubiquitous bacteria cell wall component via dedicated PRRs, few brain neurons can adapt the female physiology to its infectious status. The peripheral nervous system (PNS) of *Drosophila* and more specifically its gustatory and olfactory systems are also implicated in microbe-induced behaviors. By activating a subclass of olfactory neurons that express Or56a, the bacterial odorant geosmin induces pathogen avoid-

ance by inhibiting oviposition, chemotaxis, and feeding [17]. In contrast, bacterial volatiles commonly produced during decomposition of plant material such as ammonia and certain amines, are highly attractive to flies [18]. Furthermore, Or30a-dependent detection of bacteria-derived short-chain fatty acid induces attraction in larvae[19]. Previous works demonstrated that bacterial cell wall components like lipopolysaccharide (LPS) and PGN are sensed by *Drosophila's* gustatory sensory system [20]. LPS detection is mediated by esophageal gustatory bitter neurons expressing the chemosensory cation channel TrpA1 (Transient receptor potential cation channel subfamily A member 1) that triggers feeding and oviposition avoidance [21]. PGN instead triggers grooming behavior in *Drosophila* upon stimulation of wing margins and legs but the nature of gustatory sensory neurons and receptors involved in this behavior remain elusive[22]. In addition, bacteria have been shown to manipulate host behavior by modifying host chemosensory response or pheromone production [23, 24, 25].

We now present data demonstrating that PGN is detected by sensilla present on the *Drosophila* labellum, a major organ of the peripheral taste system. Furthermore, we show that some gustatory receptor neurons (GRNs) housed in these sensilla express the peptidoglycan sensing molecule PGRP-LB[26, 27, 28, 29]. Although the expression of PGRP-LB is restricted to a subpopulation of labellar bitter neurons, calcium imaging revealed that bitter and sweet sensory neurons can be stimulated by PGN. We found that the activation of bitter neurons by PGN requires a functional PGRP/IMD signaling, whereas the activation of sweet neurons through PGN is likely independent of it. Moreover, we present the consequences of PGN detection by taste sensory system on different host behaviors. We demonstrate that PGN promotes feeding in flies and that this behavior is negatively modulated by the IMD pathway in PGRP-LB expressing bitter neurons. Furthermore, a site-specific manipulation of the IMD pathway activity in bitter sensory neurons leads to an egg-lay drop related to the activation of those neurons. Our findings suggest that bacterial peptidoglycan elicits context-dependent opposing host behaviors that are mediated through the activation of distinct molecular pathways in different subclasses of taste neurons. Combined with previous studies, these data demonstrate that the PGRP/IMD module is not only active in immune tissues to trigger the production of antibacterial effectors but also in neurons of the CNS and the PNS to modulate the behavior of flies that are either in contact with or infected by bacteria.

RESULTS

A peptidoglycan binding protein is expressed in some gustatory bitter neurons

Peptidoglycan, one of the major constituents of the bacteria cell wall, is the main elicitor of the antibacterial response in *Drosophila,* and more generally in insects. Its interaction with host receptors belonging to the PGRP family triggers the production by immune-competent cells of NF-κB-dependent immune effectors such as AMPs [13, 14, 30]. Our previous work has shown that some of these PGN sensing molecules are expressed and required outside immune cells and specifically in neurons of the CNS. The direct detection of bacteria-derived PGN by the cytosolic protein PGRP-LE in a small subset of brain neurons modulates oviposition of infected females in an NF-κB-dependent manner [15, 16]. To identify the brain cells whose activity can be modulated upon PGN exposure, we previously made use of a reporter line, pLB1^{Gal4}, that partially recapitulates the endogenous expression of one PGRP protein (called PGRP-LB)[16]. We now noticed that in addition to being expressed in some neurons of the brain, this line also labeled neuronal projections that originated from cells of the PNS. In pLB1^{Gal4}/UAS-GFP-mCD8 flies, the GFP signal was observed in the Sub-Esophageal Zone (SEZ) where gustatory neurons send their axonal projections (Figures 1A and 1B) [31, 32]. Accordingly, some spare cell bodies present at the extremity of the proboscis at the position of sensory neurons were detected (Figure 1C). Since the only known function of the PGRP proteins is to interact with bacteria-derived PGN, we hypothesized that at least some of the gustatory neurons are able to detect and eventually to respond to this microbe-associated molecular pattern.

Some proboscis sensilla can be stimulated by peptidoglycan

The *Drosophila* labellum is possessing around 60 external taste sensilla that are classified according to their morphology (Figure 2B)[28, 29]. Each sensillum has a single pore at the tip and houses two to four gustatory receptor neurons. The moment the fly is probing the environment with its proboscis, attractive and repulsive tastants enter the sensillum through the pore and eventually activate the corresponding GRNs. In order to test if labellar GRNs detect PGN, we performed electrophysiological tip recordings of individual sensilla stimulated with purified PGN or electrolyte solution (tricholine citrate; TCC) alone (Figure 2; Table S1)**.** While PGN elicited weak responses in some long (L) sensilla, stronger responses were observed in intermediate (I) and short (S) sensilla (Figure 2A). Response patterns among I and S type sensilla were diverse ranging from non-responsive (I_7, I_8, I_9, S_1, S_4, S_6) to highly responsive sensilla (I_2,

I_3, I_4, S_5, S_7, S_{10}) (Figure 2A), whereby the PGN response of the latter was dose-dependent (Figures 2C and 2D).

Both sweet and bitter neurons can respond to peptidoglycan

Among the sensilla that respond strongly to PGN, some belong to the I type (I_3, I_4, I_5) that commonly house two GRNs, one sweet and one bitter [33]. Thus, we focused on these neuronal subclasses and tested which one was activated by PGN. For that purpose, we expressed the calcium sensor GCaMP in sweet ($Gr5a^{Gal4}$) or bitter ($Gr66a^{Gal4}$) sensing neurons. Calcium response was measured *in vivo* by GFP quantification in neuronal taste projections of the SEZ after stimulating the fly's labellum with PGN, water, sucrose, or caffeine. Intriguingly, a response to PGN was observed in both Gr5a (Figures 3A and 3B; Video S1) and Gr66a neurons (Figures 3C and 3D; Video S2). Moreover, we confirmed that sweet neurons respond to PGN by using another driver ($Gr64f^{Gal4}$) that widely targets these neurons (Figure S1). Compared to the corresponding positive controls, PGN responses of sweet and bitter sensory neurons were generally weaker and represented on average around 30 % of the sucrose and caffeine response. These results demonstrate that PGN can activate both bitter and sweet sensing taste neurons.

pLB1 neurons are a subset of bitter neurons able to respond to peptidoglycan

From the above results, we hypothesized that both sweet- and bitter-neuron responses to PGN can be linked to PGRP proteins expression. However, double staining between pLB1 and Gr66a revealed that all pLB1 neurons are Gr66a positive (Gr66a+) although they only represent a sub-population of them (Figures 4A and 4B). Indeed, while there are around 25 Gr66a+ neurons in the proboscis, we identified only 10-14 pLB1+ neurons [34, 35, 36]. We confirmed this result by using genetic intersectional strategy between $pLB1^{Gal4}$ and $Gr66a^{LexA}$ (Figure S2A) and by using another driver that broadly targets bitter neurons (i.e. $Gr32a^{LexA}$) (Figure S2B). In addition, we assessed whether the expression of the Gal4 inhibitor Gal80 in Gr66a neurons ($Gr66a^{LexA}$/$LexAop^{Gal80}$) would suppress the expression of GFP in pLB1 neurons ($pLB1^{Gal4}$/UAS-GFP-mCD8). No signal was detected in $pLB1^{Gal4}$/UAS-GFP-mCD8 flies expressing the Gal80 repressor, demonstrating that all the pLB1 neurons in the proboscis are bitter (Figures S2C and S2D). Lastly, imaging using a reporter line in which the endogenous PGRP-LB protein has been GFP-tagged at the locus demonstrated that the endogenous PGRP-LB protein is also expressed

in these neurons (Figure 4C). Consistently, we did not detect any cells, neither neuron nor axon, that are simultaneously pLB1+ and Gr5a+ (Figures 4D and 4E). We next assessed using GCaMP whether pLB1 neurons were able to respond *in vivo* to PGN as well as to bitter and sweet neuron elicitors, i.e. caffeine and sucrose, respectively [37, 38 39]. We found that pLB1 neurons were able to respond to PGN in a dose-dependent manner and that these neurons responded to caffeine, but not to sucrose, confirming their bitter nature (Figures 5A and 5B; Figure S3; Videos S3 and S4). Altogether, these results showed that although both sweet and bitter neurons are capable of responding to PGN, those that express the PGRP-LB protein, and potentially downstream NF-κB pathway effectors, belong to a subclass of bitter neurons.

Bitter neurons respond to PGN in a PGRP-LC/IMD-dependent but Relish-independent manner

Since some of the gustatory cells respond to PGN, we tested whether the canonical upstream PGN sensors and downstream IMD/NF-κB pathway components were necessary to transduce the PGN signal. For that purpose, *in vivo* calcium imaging in pLB1 neurons was performed in various IMD mutant background flies stimulated by PGN or by caffeine. Since PGN can be sensed either at the plasma membrane via the PGRP-LC protein or inside the cell via the cytosolic PGRP-LE protein, we performed the assay in both mutants [40, 41, 42]. While caffeine response was unaffected by PGRP-LC or PGRP-LE inactivation (Figure S4A), PGN ability to activate pLB1 neurons was specifically blocked in PGRP-LC mutants (Figure 5C). This result indicates that Gr66a+/pLB1+ neurons use mainly the membrane-associated receptor PGRP-LC to detect the PGN. Since previous reports demonstrated that elements of the IMD pathway are expressed and functionally required in some neurons[15, 16], their implication in mediating the effect of PGN was further tested and confirmed by the strong reduction of calcium signal in neurons of *Dredd* mutant flies (Figure 5C). The conserved ability of *Dredd* mutant bitter neurons to respond to caffeine (Figure S4A) demonstrated that their unresponsiveness to PGN was neither secondary to neuron death nor to a loss of cell functionality. To ensure that the IMD pathway was required cell-autonomously in pLB1 neurons, we used RNAi-mediated cell-specific inactivation. Functional downregulation of the IMD transducer Fadd in pLB1 or GR66a cells only was sufficient to block calcium response after PGN stimulation (Figures 5D and 5E). These neurons remained responsive to caffeine demonstrating that Fadd inactivation specifically impaired the response of these neurons to PGN (Figures S4B and S4C). Since most of the

reported IMD-dependent responses have been shown to be mediated by the NF-κB transcription factor Relish, we tested its implication in bitter neurons response to PGN [6, 10]. Intriguingly, the calcium response of pLB1+ neurons upon proboscis stimulation by PGN or caffeine was not statistically different between *Relish* null mutants and wild-type controls (Figure 5C; Figure S4A). Altogether, these data demonstrate that a subset of Gr66a bitter neurons that are pLB1+ can respond to PGN in an IMD-pathway dependent manner, but independently of the canonical Relish trans-activator.

The response of bitter neurons to peptidoglycan does not require TrpA1

A previous work has shown that another ubiquitous component of the Gram-negative bacterial cell wall, LPS, is able to stimulate esophageal bitter neurons via the TrpA1 cation channel expressed in Gr66a neurons [21]. To assess whether TrpA1 is implicated in the response of pLB1 neurons to PGN, we performed *in vivo* calcium imaging in a mutant background (*dTrpA1*). The fact that PGN-dependent activation of pLB1 cells is conserved in TrpA1 mutants demonstrated that PGN and LPS are detected by different receptors and triggers different pathways in bitter neurons (Figure 5C; Figure S4A).

Sweet neurons respond to peptidoglycan independently of the IMD pathway

The above results showed that although sweet neurons are responsive to PGN, they are pLB1 negative and are therefore less likely to express components of the IMD pathway compared to bitter neurons. Nonetheless, we tested whether, as for bitter neurons, sweet neurons response to PGN was mediated by the IMD pathway. While Fadd-RNAi expression in Gr66a and pLB1 cells completely abolished the response to PGN, it did not affect calcium release in Gr5a sweet neurons (Figure 5F). These results showed that if both sweet and bitter neurons respond to PGN, they use two different sensing and transducing machineries for PGN. Whereas in bitter neurons PGN is sensed by the classical PGRP-LC receptor and required the activity of some of the IMD pathway components, activation of sweet neurons by the same compound is likely to be independent of both the classical PGRP proteins and the downstream IMD signaling module.

Flies attraction to peptidoglycan is modulated by the IMD pathway

Our data demonstrate that PGN is detected by sweet and bitter neurons whose activation is well documented and triggers among other phenotypes attraction or aversion behaviors respectively [32]. Thus, we tested how PGN is perceived at the organism level using the MultiCAFE assay, a classical feeding two-choice test (Figure S5A)[43]. Our results showed that PGN is appetitive since flies prefer sucrose solution with PGN to pure sucrose solution. Besides, flies exhibited no bias for neither of the capillaries (Figure 6A; Figures S6B and S7B). Also, we tested the evaporation rates of a pure sucrose solution and a solution containing PGN over time. No differences were observed, demonstrating that the preference for the PGN solutions is not due to different evaporation rates of the tested liquids (Figure S5B). The PGN preference was dose-dependent (Figure 6A), lasted for a few hours (Figure 6B), and was observed in both sexes (Figure S5C). Importantly, when PGN was tested in a solution alone, without sucrose, no preference was observed (Figure S5D). Since PGN can activate sweet and bitter neurons, we asked whether the observed feeding behavior corresponded to the integration of multiple sensory inputs and more specifically to a combination of attraction and repulsion. Since our results indicate that PGN is sensed by sweet and bitter neurons in an IMD-independent and IMD-dependent manner, respectively, we tested the feeding behavior of IMD pathway mutant flies exposed to PGN containing solutions. As expected from the IMD-independent sweet neurons response to PGN, PGN attraction in a MultiCAFE assay was not decreased in IMD mutant backgrounds (Figures 5F and 6C; Figure S6A). Interestingly, the fly's attraction toward PGN was enhanced in *Dredd* and *PGRP-LC* mutants suggesting that IMD-dependent bitter neuron activation is antagonistic to sweet neuron activation by PGN. In order to test whether the bitter neuron response to PGN requires pLB1+ neurons, we inactivated these cells using Kir2.1. The inactivation of pLB1 neurons in flies led to an increased attraction to PGN indicating that the aversive response to PGN depends on GR66a+/pLB1+ neurons (Figure 6D; Figure S7A). This involvement of pLB1+ cells prompted us to assess whether the IMD pathway was required cell-autonomously for the modulation of the attraction toward PGN. However, our results using RNAi-mediated cell-specific inactivation of Fadd did not show an altered feeding preference compared to the control (Figure 6D; Figure S7A). Importantly, the attraction toward sucrose and repulsion toward caffeine were neither impaired in IMD pathway mutants nor pLB1^{Gal4}/UAS-Kir2.1 or pLB1^{Gal4}/UAS-Fadd^{IR} flies (Figures S6C and S7C). These data demonstrate that whereas the IMD pathway is dispensable for the fly attraction to PGN, this signaling

module can modulate the inputs from the Gr5a neurons following PGN exposure and this regulation requires the activity of the pLB1+/Gr66a+ cells.

Activation of the IMD pathway in bitter but not in sweet neurons impairs female egg-laying

The above results demonstrated that although both types of gustatory neurons are responsive to PGN, only in bitter neurons, this response is IMD-dependent. To evaluate the phenotypical consequences associated with IMD pathway activation specifically in the Gr66a cells, we overexpressed the upstream signaling receptor PGRP-LCa in these cells. In other contexts, this ectopic expression has been shown to be sufficient to trigger the signaling cascade in the absence of bacterial elicitors [44]. One phenotype associated with PGRP-LCa overexpression in Gr66a cells was a decrease in female egg-laying (Figure 7A). This phenotype which was confirmed using $Gr32a^{Gal4}$ (Figure S8A), was not observed when PGRP-LCa was overexpressed in Gr5a or Gr64f sweet neurons (Figure 7B; Figure S8B). These results that suggest that IMD pathway activation in bitter neurons reduces female egg-laying were further confirmed by showing that this effect could be suppressed by the simultaneous RNAi-mediated Fadd inactivation in Gr66a cells (Figure 7C). We previously demonstrated that PGN-dependent IMD pathway activation in a subset of brain octopaminergic neurons was sufficient to reduce female egg-laying[16], a phenomenon reproduced with Kir2.1 overexpression in these cells, suggesting the PGN-dependent inactivation of those neurons. Importantly, inactivating the Gr66a cells via Kir2.1 expression did not phenocopy the egg-laying drop suggesting that PGRP-LCa overexpression triggered Gr66a+ neuron activation (Figure 7D). Consistently, Gr66a cells activation via TrpA1 overexpression decreased female egg-laying (Figure S8C). Taken together, these data support a model in which activation of Gr66a cells by PGN leads to an IMD-dependent activation of these neurons which *in fine*, provokes an egg-laying drop.

DISCUSSION

This study demonstrates that some neurons of the gustatory system exposed to a microbe-loaded environment are able to detect the presence of bacteria by sensing one of its main conserved and ubiquitous cell wall components, peptidoglycan. In bitter neurons, this detection is mediated by the IMD pathway PGRP-LC receptor and therefore probably not by classical Gr proteins such as Gr66a. The PGN signal is transduced by the known cytosolic members of the IMD pathway such as Fadd and Dredd. Together with previous reports, these results confirm the key role played by the PGN/PGRP module in regulating many of the interactions between bacteria and flies. This specific recognition step, which takes place at the cell membrane via PGRP-LC or inside the cells via PGRP-LE, has been shown to control the production of antibacterial effectors by immune-competent cells, to modify the egg-laying rate of infected females and to allow the physiological adaptation of the flies to their infectious status [15, 16, 42, 45, 46, 47]. Interestingly however, if the initial MAMP/PRR recognition event is conserved among these processes, the downstream molecular mechanisms that transduce the signal are context-dependent. Whereas the PGN-dependent activation of an immune response in adipocytes, hemocytes or enterocytes and the inhibition of VUM III octopaminergic brain neurons rely on the nuclear NF-κB/Relish protein, the transcriptionally regulated effectors are likely to be different [7, 16]. The AMPs that are the main NF-κB-dependent mediators of the antibacterial response, seem to be dispensable for the reduction of oviposition in infected flies (AM, LK, JR, personal communications). The response of bitter neurons to PGN uses a non-canonical IMD pathway in which NF-κB/Relish is not required. Interestingly, PGRP-LC and some downstream IMD components are also required at the pre-synaptic terminal of *Drosophila* motoneurons for robust presynaptic homeostatic plasticity [48, 49]. The local modulation of the presynaptic vesicle release, which occurs in seconds following inhibition of postsynaptic glutamate receptors, required PGRP-LC, Tak1 but is also Relish-independent. These and our present data raise important questions regarding how the activation of the upstream elements of the IMD cascade is modifying neuronal activity, a topic for future studies. Earlier biochemical studies have shown that IMD signaling is rapid, occurring in seconds, a time frame consistent with its role at the synapse and now in bitter neurons signal transduction[50]. If, as expected for cells expressing immune signaling components, bitter neurons respond to PGN, the response of

sweet neurons to PGN raises the question of the nature of the elicitor and of the cellular sensor. One possible ligand is to be found in the composition of the PGN itself. PGN is a polymer consisting of sugars and amino acids that form a mesh-like layer outside the plasma membrane [51]. The sugar component which consists of alternating residues of N-acetylglucosamine and N-acetylmuramic acid could potentially be detected by gustatory receptors on sweet neurons. Such sugars will not activate the bitter neurons since optimum recognition of PGN by PGRP-LC requires that the sugar backbone remains attached to the peptide bridge [52]. Finally, as both cell types respond to PGN using different pathways, another hypothesis is that a yet to identify PGN sensor will be expressed on both sweet and bitter neurons. In bitter neurons, a PGRP/IMD dependent module would be a permissive signal that upon stimulation by environmental bacteria will modulate the expression of this PGN sensor in these cells. However, since the PGN response is Relish-independent, we do not favor this hypothesis.

Our data show that flies can perceive the bacteria cell wall component PGN via two neuronal subclasses triggering behaviors that integrate antagonistic signals (Figure 8). Whereas the stimulation of sweet neurons seems to promote feeding in *Drosophila*, this behavior is counterbalanced by inputs coming from bitter neurons. These findings stand in contrast to observations made for another cell wall component in Gram-negative bacteria, called LPS, which triggers feeding avoidance in *Drosophila* through the activation of bitter neurons[21]. While LPS induced avoidance behavior is mediated through the chemosensory cation channel TrpA1, we show that PGN induced activation of bitter neurons seems to be independent of it. We demonstrate that the bitter response upon PGN stimulation is dependent on the IMD pathway that not only negatively regulates a feeding preference for PGN but also controls ovipositional avoidance. Thus, PGN is a very striking molecule activating distinct taste pathways, which in turn trigger opposing behaviors. Acetic acid is another tastant with similar qualities that has been described in *Drosophila* before[53]. Produced by certain bacteria during fermentation, acetic acid can be nutritious as well as toxic for flies. Flies exhibit conflicting behaviors in response to acetic acid ranging from attraction to repulsion that are mediated through the activation of sugar and bitter sensory neurons.

Despite the ability of PGN to activate sweet sensory neurons, we observed that PGN is only appetitive if combined with a nutritious sugar solution. This indicates that PGN is probably rather an informative environmental cue for flies without any relevant nutritious value. It is

known that flies can distinguish nutritive sugars and non-nutritive sugars. Despite their common detection through labial taste sensilla, non-nutritive sugars are ingested to a lesser extent than nutritive ones [54]. However, the binary response of the fly toward PGN is logically consistent as this molecule may signal a threat as well as an environment sufficiently modified by microbes to favor nutrition, egg-lay and larval growth. In addition, it is most probable that the behavior of flies in a natural environment corresponds to a highly complex integration of multiple intricate signals perceived by different sensory systems of the animal.

In nature, PGN is likely detected in combination with other tastants and odors, which detected alone may lead to an array of conflicting behaviors but in combination will yield in one context-dependent behavioral output [21, 55]. Consequently, it may be hazardous to expect clear phenotypes, or to make sense of the observed ones when testing a single molecule of the permanent environment of the fly while this molecule is not especially deleterious per se, but rather informative for the animal. The PGN is an interesting case as on one hand, an internal sensing of this molecule indicates an infection, the uncontrolled growth of a bacteria or a breach in a physical barrier. On the other hand, the perception of this same molecule in the environment might be a clue, among other, to suggest a favorable environment or a place heavily contaminated. As far as PGN perception is concerned, other levels of regulation are expected [17, 19, 56]. Indeed, the pLB1 line used in this study to probe the neurons that can respond to PGN is only labelling a subclass of GR66a positive neurons. This suggests that the response to PGN is likely to be not homogenous among all bitter neurons. Besides, the pLB1 line partially recapitulates the endogenous expression of PGRP-LB, an enzyme that by cleaving the PGN into non-immunogenic muropeptides, buffers the PGN-dependent IMD response [42, 57, 58]. It is therefore possible that non-pLB1 bitter neurons will also respond to PGN and that this response might be attenuated in pLB1 neurons. Further experiments will be needed to determine how PGN is sensed in sweet neurons and how the inputs coming from taste neurons are integrated in the CNS.

FIGURE LEGENDS

Figure 1. pLB1 is expressed in neurons located in the proboscis.

Immunodetection of cells expressing pLB1^{Gal4}/UAS-GFP-mCD8 (pLB1+).

(A) Schematic representing the fly head and the projections of pLB1+ peripheral neurons (green). The proboscis is an appendix dedicated to the feeding process and hosting neurons for the detection of tastants. The cell bodies of pLB1+ neurons are located in sensilla exposed to the environment and project axons to the brain, specifically in the sub-esophageal zone (SEZ).

(B) In the brain, pLB1+ cells send projections in the SEZ with a reproducible pattern. The panel on the right is a magnification of the SEZ delineated by the box.

(C) The projections seen in the SEZ arise from neurons whose cell bodies are located in the tip of the proboscis, the labellum (sagittal view). The panel on the right is a magnification of the labellum delineated by the box. Neuronal dendrites directed to the environment and prototypical of taste neurons are visible (arrowheads).

In (B and C), scale bar, 50 µm.

Figure 2. Labellar sensilla respond when exposed to peptidoglycan.

(A) Electrophysiological responses of labellar sensilla to peptidoglycan (PGN; 100 µg/mL). The corresponding response from the control diluent tricholine citrate (TCC; 30 mM) was subtracted from each value (see Table S1 for values). Mean ± SEM, N ≥ 5 for each sensillum. *p < 0.05; **p < 0 .01; ***p < 0.001; non-parametric t-test, Mann-Whitney test.

(B) Schematic representing the localization of chemosensory taste bristles on the labellum. One half of the labellum with 29 taste sensilla is represented. Taste sensilla comprise different classes based on their morphology; L sensilla (blue), I sensilla (green), and S sensilla (red). Classification of sensilla is based on Weiss et al.[29]. Arrows point to sensilla robustly responding to PGN.

(C) Dose-dependent response to PGN in I_3 (top) and S_5 (bottom) sensilla. Mean ± SEM, N ≥ 8 for I_3, and N ≥ 7 for S_5. Responses to PGN solutions are compared to the response to TCC. *p < 0.05; **p < 0 .01; non-parametric t-test, Mann-Whitney test.

(D) Sample traces of physiological recordings from I_3 and S_5 in response to increasing concentrations of PGN and the control traces for TCC.

Figure 3. Sweet and bitter neurons respond to peptidoglycan.

(A-D) Real-time calcium imaging using the calcium indicator GCaMP6s to assess the *in vivo* neuronal activity in the sub-esophageal zone (SEZ) of sweet taste neurons ($Gr5a^{Gal4}$/UAS-GCaMP6s) (A and B) or bitter taste neurons ($Gr66a^{Gal4}$/UAS-GCaMP6s) (C and D).

(A and C) Representative images (top) and averaged ± SEM time course of the GCaMP6s intensity variations (ΔF/F%) (bottom). The addition of the chemical at a specific time is indicated by the arrow. The images illustrate the GCaMP6s intensity before and after the addition of either water as negative control (left panels), peptidoglycan (PGN; middle panels), or a positive control (sucrose or caffeine, right panels). The images represent the average intensity of 4 frames before or after the treatments. Scale bar, 20 µm.

(B and D) Averaged fluorescence intensity of peaks ± SEM for control, PGN, sucrose, or caffeine-stimulated flies (N ≥7 for each treatment). *** indicates $p < 0.0001$; non-parametric t-test, Mann-Whitney test.

(See also Figure S1; Videos S1 and S2).

Figure 4. pLB1 cells are a subset of Gr66a neurons.

(A and B) Immunodetection in the brain (A) and detection in the proboscis (B) of cells expressing $pLB1^{Gal4}$/UAS-GFP-mCD8 (pLB1+) as well as Gr66a-RFP (Gr66a+).

(A) Top left is a view of a large portion of the brain, the other panels are magnifications of the sub-esophageal zone delineated by the box.

(B) All the pLB1+ cells (arrowheads) are Gr66a+ while not all the Gr66a+ cells (arrows) are pLB1+.

(C) Detection in the proboscis of cells producing the endogenous PGRP-LB (PGRP-LB::GFP) as well as Gr66a-RFP (Gr66a+). All the PGRP-LB::GFP+ cells (arrowheads) are Gr66a+ while not all the Gr66a+ cells (arrows) are PGRP-LB::GFP+.

(D and E) Immunodetection in the brain (D) and detection in the proboscis (E) of cells pLB1+ as well as Gr5a+ via genetic intersectional strategy ($pLB1^{Gal4}$, $Gr5a^{LexA}$/UAS*frt*STOP*frt*-GFPmCD8, LexAopFLP). Only the cells co-expressing both drivers will produce GFP.

All the images of the proboscis are sagittal views. Scale bar,50 µm.

(See also Figure S2).

Figure 5. pLB1 and Gr66a, but not Gr5a neurons respond to peptidoglycan in an IMD-dependent way.

Real-time calcium imaging using the calcium indicator GCaMP6s to assess the *in vivo* neuronal activity in the sub-esophageal zone (SEZ) of pLB1+ neurons (pLB1^{Gal4}/UAS-GCaMP6s) (A-D), bitter taste neurons (Gr66a^{Gal4}/UAS-GCaMP6s) (E) or sweet taste neurons (Gr5a^{Gal4}/UAS-GCaMP6s) (F).

(A) Representative images of the SEZ (top) and averaged ± SEM time course of the GCaMP6s intensity variations (ΔF/F%) (bottom). The addition of the chemical at a specific time is indicated by the arrow. The images illustrate the GCaMP6s intensity before and after the addition of water (negative control), peptidoglycan (PGN), caffeine, or sucrose. The images represent the average intensity of 4 frames before or after the treatments. Scale bar is 20 µm.

(B) Averaged fluorescence intensity of peaks ± SEM for pLB1^{Gal4}/UAS-GCaMP6s flies exposed to water, different PGN concentrations, caffeine or sucrose.

(C) Averaged fluorescence intensity of peaks ± SEM for pLB1^{Gal4}/UAS-GCaMP6s flies in different mutant backgrounds exposed to PGN (100 µg/mL).

(D-F) Averaged fluorescence intensity of peaks ± SEM for pLB1^{Gal4}/UAS-GCaMP6s (D) Gr66a^{Gal4}/UAS-GCaMP6s (E) or Gr5a^{Gal4}/UAS-GCaMP6s (F) animals expressing Fadd-RNAi (UAS-Fadd^{IR}) and exposed to PGN (100 µg/mL).

(B-F) N ≥ 6 for each treatment. *** indicates $p < 0.0001$; non-parametric t-test, Mann-Whitney test.

(See also Figures S3 and S4; Videos S3 and S4).

Figure 6. Gustatory preference for peptidoglycan is modulated by the IMD pathway.

(A) Feeding preference (consumption) in MultiCAFE assay for increasing concentrations of peptidoglycan (PGN), after 2 hours (h).

(B) Feeding preference (consumption) in MultiCAFE assay for PGN over time (1 – 3 h).

(C) Feeding preference index in MultiCAFE assay for PGN after 2 h in different mutant strains of the IMD pathway including corresponding controls (similar genetic background).

(D) Feeding preference index in MultiCAFE assay for PGN after 2 h in flies with inactivated pLB1 cells (pLB1^{Gal4}/UAS-Kir2.1) and in flies in which the IMD pathway has been specifically inactivated in pLB1 cells (pLB1^{Gal4}/UAS-Fadd^{IR}).

(A-D) The median with interquartile range is shown from at least two independent trials with a minimum of 25 females per genotype and condition.

Wilcoxon matched-pairs (A and B), non-parametric t-test, Mann-Whitney test (C and D). *p < 0.05; **p < 0 .01; ***p < 0.001; ns p > 0.05.

(See also Figures S5, S6 and S7).

Figure 7. Activation of the IMD pathway in Gr66a, but not Gr5a cells impairs egg-laying.

(A and B) Eggs laid per female per 24 hours (24 h) for flies overexpressing PGRP-LCa (UAS-LCa) in bitter neurons ($Gr66a^{Gal4}$/UAS-LCa) (A) or sweet neurons ($Gr5a^{Gal4}$/UAS-LCa) (B).

(C) Eggs laid per female per 24 hours for flies overexpressing PGRP-LCa and Fadd-RNAi (UAS-$Fadd^{IR}$) in bitter neurons ($Gr66^{Gal4}$/UAS-LCa, UAS-$Fadd^{IR}$).

(D) Eggs laid per female per 24 hours for flies with inactivated bitter neurons ($Gr66a^{Gal4}$/UAS-Kir2.1).

In (A-D), shown are the average numbers of eggs laid per fly per 24 h ± SEM from at least two independent trials with at least 20 females per trial, genotype and condition used. *** indicates p < 0.0001; ns indicates p > 0.05; non-parametric ANOVA, Dunn's multiple comparison test.

(See also Figure S8).

Figure 8. Model: effect of peptidoglycan on fly gustatory neurons.

Peptidoglycan (PGN) is an essential cell wall component of all bacteria. Free PGN is released during bacterial proliferation. In *Drosophila*, it is detected by peptidoglycan recognition proteins (PGRPs). The detection of PGN in immune-competent tissues (e.g. the intestine and the fat body) leads to the activation of the IMD pathway and finally to the NFκB-dependent expression of antimicrobial-coding genes. Here we show that some PGN sensors are expressed in a subset of bitter neurons in the proboscis. In these cells (red in this figure), PGN detection by the membrane-associated receptor PGRP-LC induces calcium level increase. This neuronal response requires other members of the IMD pathway components such as Fadd or Dredd, whereas the transcription factor NFκB is not required. The IMD pathway activation in these bitter neurons is sufficient to reduce female egg-laying. Furthermore, we show that sweet neurons (in blue) also respond to PGN with an increase of cellular calcium. In this case, however, the response to PGN is independent of the IMD pathway. We hypothesize that PGN

recognition in sweet neurons is mediated by sugar receptor/s typical of this type of neurons. The integration of signals coming from both sweet and bitter neurons leads to the modulation of the fly feeding behavior towards PGN.

SUPPLEMENTAL FIGURES

Figure S1. GR64f sweet neurons respond to peptidoglycan, related to Figure 3.

Real-time calcium imaging using the calcium indicator GCaMP6s to reflect the *in vivo* neuronal activity in the sub-esophageal zone (SEZ) of sweet neurons ($Gr64f^{Gal4}$/UAS-GCaMP6s).

(A) Representative images of the SEZ (top) and averaged ± SEM time course of the GCaMP6s intensity variations (ΔF/F%) (bottom). The addition of the chemical at a specific time is indicated by the arrow. The images illustrate the GCaMP6s intensity before and after addition of either water (negative control; left panels), peptidoglycan (PGN; middle panels), or sucrose (positive control; right panels). The images represent the average intensity of 4 frames before or after the treatments. Scale bar, 20 µm.

(B) Averaged fluorescence intensity of peaks ± SEM for flies exposed to chemicals (N ≥ 6 for each treatment). ** indicates $p < 0.001$; non-parametric t-test, Mann-Whitney test.

Figure S2. pLB1 neurons in the labellum are exclusively bitter, related to Figure 4.

(A) Immunodetection in brain (top) and detection in the proboscis (bottom) of cells pLB1+ as well as Gr66a+ via genetic intersectional strategy ($pLB1^{Gal4}$, $Gr66a^{LexA}$/UAS*frt*STOP*frt*-GFPmCD8, LexAopFLP). Arrows point to pLB1+/Gr66a+ cellular bodies. The top right panel is a magnification of the sub-esophageal zone delineated by the box.

(B) Immunodetection in the brain of cells pLB1+ as well as Gr32a+ via genetic intersectional strategy ($pLB1^{Gal4}$; UAS*frt*STOP*frt*GFPmCD8, LexAopFLP/$Gr32a^{LexA}$). The lower panel is a magnification of the sub-esophageal zone delineated by the box.

(C and D) Immunodetection in brain (C) and detection in the proboscis (D) of cells pLB1+ and Gr66a- (pLB1+/Gr66a-) via the expression of the Gal4 inhibitor Gal80 specifically in Gr66a+ cells ($pLB1^{Gal4}$; UAS-GFP-mCD8/$Gr66a^{LexA}$, LexAopGal80). In (C), the right panels is a magnification of the sub-esophageal zone delineated by the box.

All the images of the proboscis are sagittal views. Scale bar, 50 µm.

Figure S3. pLB1 cells respond to peptidoglycan in a dose-dependent manner, related to Figure 5.

Real-time calcium imaging using the calcium indicator GCaMP6s to assess the *in vivo* neuronal activity in the sub-esophageal zone (SEZ) of pLB1+ neurons. Representative images of the SEZ (top) and averaged ± SEM time course of the GCaMP6s intensity variations (ΔF/F%) (bottom). The addition of the chemical at a specific time is indicated by the arrow. The images illustrate the GCaMP6s intensity before and after the addition of different peptidoglycan (PGN) concentrations. The images represent the average intensity of 4 frames before or after the treatments. Scale bar, 20 µm.

Figure S4. Mutations in the IMD pathway do not impair the response of pLB1+ cells to caffeine, related to Figure 5.

(A-C) Real-time calcium imaging using the calcium indicator GCaMP6s to assess the *in vivo* neuronal activity in the SEZ of pLB1+ (A and B) or Gr66a+ (C) neurons.

(A) Averaged fluorescence intensity of peaks ± SEM for $pLB1^{Gal4}$/UAS-GCaMP6s flies in different mutant backgrounds exposed to caffeine (10mM).

(B and C) Averaged fluorescence intensity of peaks ± SEM for $pLB1^{Gal4}$/UAS-GCaMP6s (B) or $Gr66a^{Gal4}$/UAS-GCaMP6s (C) animals expressing Fadd-RNAi (UAS-$Fadd^{IR}$) and exposed to caffeine (10mM).

In (A-C), N ≥ 4 for each condition. ns indicates $p > 0.05$; non-parametric t-test, Mann-Whitney test.

Figure S5. Like females, males prefer a sucrose solution containing peptidoglycan in MultiCAFE assay, related to Figure 6.

(A) Schematic representing the two-choice capillary feeding assay (MultiCAFE assay) to quantify the feeding preference between a pure sucrose solution and a sucrose solution containing peptidoglycan (PGN; 500 µg/mL) or caffeine (10mM). Single flies are in a chamber with a choice between two solutions in capillaries. Images are taken regularly over time to quantify the consumption as well as to control the evaporation.

(B) Evaporation rates in MultiCAFE assay of a pure sucrose solution and a sucrose solution containing peptidoglycan over time (1-3 h).

(C) Feeding preference (consumption) in *Drosophila* males for PGN in MultiCAFE assay over time (1-3 h), N ≥ 15. Median with interquartile range, Wilcoxon matched-pairs, $*p < 0.05$.

(D) Feeding preference (consumption) in MultiCAFE assay for pure PGN solution (without sucrose). Wilcoxon matched-pairs, none statistical significance, N ≥ 15.

Figure S6. IMD pathway mutants are comparable to controls for sucrose consumption and aversion toward caffeine, related to Figure 6.

(A-C) Control tests for feeding behavior in mutants of the IMD pathway and their corresponding controls (similar genetic background).

(A) Feeding response (consumption) in MultiCAFE assay to peptidoglycan (PGN), N ≥ 28.

(B) Feeding response (consumption) in MultiCAFE assay to sugar only, side preference test, N ≥ 28.

(C) Feeding response (consumption) in MultiCAFE assay to caffeine, N ≥ 17.

(A-C) Median with interquartile range is shown, Wilcoxon matched-pairs, *$p < 0.05$; **$p < 0.01$; ***$p < 0.001$; ns $p > 0.05$.

Figure S7. Kir2.1 and Fadd^{IR} treated flies are comparable to controls for sucrose consumption and aversion toward caffeine, related to Figure 6.

Control tests for feeding behavior of Kir2.1 and Fadd-RNAi (Fadd^{IR}) treated flies including GAL4 driver and UAS reporter lines.

(A) Feeding response (consumption) in MultiCAFE assay to peptidoglycan (PGN; 500 µg/mL), N ≥ 31.

(B) Feeding response (consumption) in MultiCAFE assay to sugar only (5mM), side preference test, N ≥ 13.

(C) Feeding response (consumption) in MultiCAFE assay to caffeine (10mM), N ≥ 14.

(A-C) Median with interquartile range is shown, Wilcoxon matched-pairs, *$p < 0.05$; **$p < 0.01$; ***$p < 0.001$; ns $p > 0.05$.

Figure S8. Activation of the IMD pathway in Gr32a, but not Gr64f cells impairs egg-laying capacity, related to Figure 8.

(A-C) Eggs laid per female per 24 hours (h) for flies overexpressing PGRP-LCa (UAS-LCa) in bitter neurons (Gr32a^{Gal4}/UAS-LCa) (A), sweet neurons (Gr64f^{Gal4}/UAS-LCa) (B) and for flies with activated bitter neurons (Gr66a^{Gal4}/UAS-TrpA1) (C).

(C) TrpA1 chanel is inactive at 23 °C and active at 29 °C which leads to an increased activity of the neuron. While the increase in temperature from 23°C to 29°C increases the egg-lay of controls, activation of Gr66a+ cells via TrpA1 at 29°C blocks this modification.
(A-C) Shown are the average numbers of eggs laid per fly per 24 h ± SEM from at least two independent trials, except only one trial for (C) with at least 20 females per genotype and condition used. ** indicates $p < 0.001$; *** indicates $p < 0.0001$; ns indicates $p > 0.05$, non-parametric ANOVA, Dunn's multiple comparison test.

Table S1. Taste sensilla respond to peptidoglycan, related to Figure 2.
Electrophysiological responses of different taste sensilla to peptidoglycan (PGN; 100µg/mL) and the control tricholine citrate (TCC; 30mM). The values represent the mean response in spikes per second including SEM.

Video S1. Gr5a+ neurons respond *in vivo* to PGN, related to Figure 3.
Real-time calcium imaging using the calcium indicator GCaMP6s to assess the *in vivo* neuronal activity in the sub-esophageal zone of sweet neurons ($Gr5a^{Gal4}$/UAS-GCaMP6s). Effect of peptidoglycan solution stimulation (100 µg/mL). GFP signal was recorded every 500 ms.

Video S2. Gr66a+ neurons respond *in vivo* to PGN, related to Figure 3.
Real-time calcium imaging using the calcium indicator GCaMP6s to assess the *in vivo* neuronal activity in the sub-esophageal zone of bitter neurons ($Gr66a^{Gal4}$/UAS-GCaMP6s). Effect of peptidoglycan solution stimulation (100 µg/mL). GFP signal was recorded every 500 ms.

Video S3. pLB1+ neurons respond *in vivo* to PGN, related to Figure 5.
Real-time calcium imaging using the calcium indicator GCaMP6s to assess the *in vivo* neuronal activity in the sub-esophageal zone of pLB1 neurons ($pLB1^{Gal4}$/UAS-GCaMP6s). Effect of peptidoglycan solution stimulation (100 µg/mL). GFP signal was recorded every 500 ms.

Video S4. pLB1+ neurons respond *in* vivo to caffeine, related to Figure 5.
Real-time calcium imaging using the calcium indicator GCaMP6s to assess the *in vivo* neuronal activity in the sub-esophageal zone of pLB1 neurons ($pLB1^{Gal4}$/UAS-GCaMP6s). Effect of caffeine solution stimulation (10mM). GFP signal was recorded every 500 ms.

METHODS

Fly stocks

All flies were maintained at 25°C on a standard cornmeal/agar medium on a 12 h:12 h light-dark cycle with a relative humidity of 70%.The strains used are the following: pLB1^{Gal4} [15]; PGRP-LB::GFP [16]; w (BDSC:3605); yw ; Canton-S; Gr64f^{Gal4}; Gr5a^{Gal4}; Gr5a^{Gal4} (BDSC:57592, [59]); Gr5a^{LexA} [60, 61] (Gently provided by Dong Min Shin); Gr66a^{LexA} ([62]; gently provided by K. Scott's Lab); Gr32a^{LexA} [63] (gently provided by A. Dahanukar's lab); Gr32a^{Gal4} (BDSC:57622); Gr66a^{Gal4} ; Gr66a-RFP(X4) (BDSC:60691); UAS-TrpA1 (BDSC:26264,[64]); UAS-Kir2.1 (BDSC:6595); 40XUAS-mCD8GFP (BDSC:32195); UAS-Fadd-RNAi[65]; UAS*frt*STOP*frt*GFPmCD8 (BDSC:30125); 8XLexAop2-FLP (BDSC:55819); UAS-GCaMP6s (BDSC:42746). UAS-PGRP-LCa [66]; PGRP-LC^{E12} [44]; PGRP-LE^{112} [40], Dredd^{D55} [67]; Relish^{E20} [47]; TrpA1^{1} [21].

Tastants

For electrophysiological recordings, *in vivo* calcium imaging and MultiCAFE assays tastants were dissolved in autoclaved purified distilled water. For electrophysiological recordings, the electrolyte tricholine citrate (TCC, 30mM, Sigma-Aldrich) was added to the tastant solution. For *in vivo* calcium imaging tastants were diluted in Millipore Q water. All tastant solutions were freshly prepared and stored in aliquots at -20°C for a maximum duration of six months. Peptidoglycan was obtained from InvivoGen (PGN-EK Catalog # tlrl-pgnek, InvivoGen, USA), while sucrose and caffeine were obtained from Sigma-Aldrich (USA).

Electrophysiology

Electrophysiological recordings were performed by using the tip-recording method. 3-7-day-old non-starved flies were anesthetized on ice and immobilized with extra fine strips of tape on a pad of modelling clay (patafix, UHU, Germany). The fly's body was electrically grounded with a silver wire whereby the fly and electrode were connected through an electrolyte gel (Redux®, Parker Laboratories, Inc, USA). Recordings were performed on labellar taste sensilla. Individual sensilla were stimulated by covering their tip for 2 s with a glass recording electrode containing the tastant solution. Electrical signals were recorded by a preamplifier (TasteProbe DTP-02, Syntech, Netherlands), further amplified 50-100 times and band-pass filtered at 30-3000 Hz (USBPBP^{TM}-S1, Alligator technologies, USA). Sensilla responses were analyzed using

the software dbWave (available at http://perso.numericable.fr/frederic.marion-poll/deterrents/tk/dbwave/index.htm) and quantified by counting the number of spikes during a period of 1 s starting from 200 ms after the stimulation. Tastant solutions were tested in 1 min intervals to avoid adaptation. Spike frequency was calculated by counting the total number of spikes for each recording since extracellular recordings of taste sensilla in *Drosophila* are difficult to sort [68]. Most of the electrophysiological recordings were performed in males. But there was no significant difference between sexes.

***In vivo* calcium imaging**

In vivo calcium imaging experiments were performed on 5-7-day-old mated females. Flies were starved for 24 h before any experiments. Flies of the appropriate genotype were anesthetized on ice for 1 h. Female flies were suspended by the neck on a plexiglass block (2 x 2 x 2.5 cm), with the proboscis facing the center of the block. Flies were immobilized using an insect pin (0.1 mm diameter) placed on the neck. The ends of the pin were fixed on the block with beeswax (Deiberit 502, Siladent, 209212). The head was then glued on the block with a drop of rosin (Gum rosin, Sigma-Aldrich -60895-, dissolved in ethanol at 70 %) to avoid any movements. The anterior part of the head was thus oriented towards the objective of the microscope. Flies were placed in a humidified box for 1 h to allow the rosin to harden without damaging the living tissues. A plastic coverslip with a hole corresponding to the width of the space between the two eyes was placed on top of the head and fixed on the block with beeswax. The plastic coverslip was sealed on the cuticle with two-component silicon (Kwik-Sil, World Precision Instruments) leaving the proboscis exposed to the air. Ringer's saline (130 mM NaCl, 5 mM KCl, 2 mM $MgCl_2$, 2 mM $CaCl_2$, 36 mM saccharose, 5 mM HEPES, pH 7.3, was placed on the head[69]. The antenna area, the tracheas, and the fat body were removed. The gut was cut without damaging the brain and taste nerves to allow visual access to the anterior ventral part of the sub-esophageal zone. The exposed brain was rinsed twice with Ringer's saline. GCaMP6s fluorescence was viewed with a Leica DM600B microscope under a 25x water objective. GCaMP6s was excited using a Lumencor diode light source at 482 nm ± 25. Emitted light was collected through a 505-530 nm band-pass filter. Images were collected every 500 ms using a Hamamatsu/HPF-ORCA Flash 4.0 camera and processed using Leica MM AF 2.2.9. Stimulation was performed by applying 140 µL of tastant solution diluted in water on the pro-

boscis. Each experiment consisted of a recording of 10 images before stimulation and 30 images after stimulation. Data were analyzed as previously described by using FIJI (https://fiji.sc/)[69]. In all experiments implicating pLB1^{Gal4}, this driver and the UAS-GCaMP6s transgenes are homozygous. In experiments using Gr5a^{Gal4} or Gr66a^{Gal4}, these drivers and the UAS-GCaMP6s transgenes are heterozygous.

Immunostaining and imaging

Immunostaining and imaging were performed as previously described [16]. Brains from adult females were dissected in Phosphate-buffered saline (PBS ref) and fixed for 15 min in 4% paraformaldehyde (Electron Microscopy Sciences, Cat # 15714-S) at room temperature (RT). Afterward, brains were washed three times for 10 min in PBS-T (PBS + 0.3% Triton X-100 REF) and blocked in 2,5% bovine serum albumin (BSA; Sigma-Aldrich) in PBS-T for 30 min. After saturation, samples were incubated with the first antibody diluted in 0,5% BSA in PBS-T overnight at 4°C. The following day, brains were washed three times and incubated with the secondary antibody diluted in 0,5% BSA in PBS-T for 2h at RT. Next, samples were washed for 10 min in PBS-T and mounted on slides using Vectashield (Vector Laboratories, Ca, USA) fluorescent mounting medium. In the case of proboscises, no immunostaining was performed. Proboscises of adult females were dissected in PBS, rinsed with PBS and directly mounted on slides using Vectashield fluorescent mounting medium. The tissues were visualized directly after.

For the immunostaining the first antibodies used are the following: Chicken anti-GFP (Aves Labs Cat#GFP-1020, RRID:AB_10000240. Dilution 1:1000), rabbit anti-RFP (Rockland Cat#600-401-379, RRID:AB_2209751. Dilution 1:1000), mouse anti-NC82 (DSHB Cat#nc82,RRID:AB_2314866. Dilution 1:40). The secondary antibodies used are the following: Alexa Fluor 488 Donkey anti-Chicken IgY (IgG) (H+L) (Jackson ImmunoResearch Labs Cat#703-545-155, RRID:AB_2340375. Dilution 1:500), Alexa Fluor568 donkey anti-mouse IgG (H+L) (Thermo Fisher Scientific Cat#A10037, RRID:AB_2534013. Dilution 1:500), Alexa Fluor647 donkey anti-mouse IgG (H+L) (Jackson ImmunoResearch Labs Cat#715-605-151, RRID:AB_2340863. Dilution 1:500), Alexa Fluor 568 donkey anti-rabbit IgG (H+L) (Thermo Fisher Scientific Cat#A10042, RRID:AB_2534017. Dilution 1:500).

Images were captured with either a Leica SP8 confocal microscope (in this case, tissues were scanned with 20X oil immersion objective) or an LSM 780 Zeiss confocal microscope (20x air

objective was used). For the detection of endogenous PGRP-LB::GFP, images were captured with a Spinning Disk Ropper 2 Cam (20x or 40x air objective were used). Images were processed using Adobe Photoshop.

Feeding assay

Multiple choice capillary feeder (MultiCAFE) assay was adapted from Sellier et al, [70]. 2-4-day-old flies were anesthetized on ice, sorted according to their sex, and eventually transferred to vials (9.5 cm, Ø 2.5 cm, Dutscher, France) containing humidified cotton balls. After a starvation period of 20-24 h, each fly was transferred in a chamber (0.6 cm x 2.4 cm x 0.3 cm) that was integrated in a plastic support (7.6 cm x 10.8 cm x 0.8 cm, Sculpteo, France) composed of ten chambers in total. Each fly was given the choice between two capillaries (5 µL, Hirschmann, Germany), containing control or test solution. The control solution was a pure 5 mM sucrose solution, while the test solution was a 5mM sucrose solution mixed with peptidoglycan at different concentrations (50, 100, 500 µg/mL). As controls, we performed a no-choice assay where both capillaries contained the pure 5mM sucrose solution and another two-choice assay replacing peptidoglycan by the bitter compound caffeine (10mM), which has been shown to induce avoidance behavior in *Drosophila* at high concentrations [37, 71]. All tested solution contained 0.125 mg/mL of blue dye (erioglaucine, Sigma-Aldrich, USA). The support with the chambers containing the flies was clamped to the lid of a plastic Tupperware (12.2 cm x 9 cm x 0.7 cm, LocknLock, Korea). Afterward, the lid was tightly attached to the corresponding tupperware box (24.2 cm x 21.8 cm x 18 cm) containing a moist paper towel. The tupperware was then placed in a climate chamber (T: 25°C, H: 80%, illuminated). A digital camera (Logitech, Switzerland) attached to the bottom of the tupperware recorded the liquid levels in the capillaries as images (one image per min) for 1-3 h. To determine the evaporation rate of each solution during the individual tests, flies were placed only in eight of the ten available chambers while the remaining two contained only the capillaries but no flies. The liquid level changes in the capillaries were analyzed with the image processing software platform (icy) using the customized plugin MultiCAFE. Liquid level changes in the capillaries were used to determine the consumption rate of individual flies and evaporation rates. The actual consumption of flies was calculated as followed: liquid level changes of capillaries in chambers with flies – liquid level changes of capillaries in chambers without flies.

Oviposition assay

Oviposition assays were performed as previously described [16]. Eclosed flies were raised at 25°C or RT, in case of experiments involving the thermosensitive transgene UAS-TrpA1. 5-day-old mated females were anesthetized on a CO_2 pad and singularly transferred in tubes with fresh media and dry yeast (Fermipan) added on top of each tube right before the egg-lay period. Flies were let to lay eggs for 24 h at 29°C or 23°C in control conditions for experiments involving UAS-TrpA1. After the 24 h, eggs were counted.

Statistical analysis

GraphPad Prism software was used for statistical analyses. For electrophysiology*, in vivo* Calcium imaging and MultiCAFE assay analysis non-parametric unpaired Mann-Whitney two-tailed tests were performed. For comparing absolute consumption in MultiCAFE assay the non-parametric Wilcoxon matched-pairs signed-rank test was used. In the case of oviposition assay, we used the non-parametric unpaired ANOVA, Kruskal-Wallis test, and Dunn's post-test.

ACKNOWLEDGMENTS

We thank Emilie Avazeri and Annelise Viallat-Lieutaud for technical help. We thank members of the Royet's laboratory for their comments on the manuscript. This work was supported by (ANR-11-LABX-0054) (Investissements d'Avenir–Labex INFORM), ANR BACNEURODRO (ANR-17-CE16-0023-01) and ANR PEPTIMET (ANR-18-CE15-0018-02), Equipe Fondation pour la Recherche Médicale (EQU201903007783) and l'Institut Universitaire de France to J.R. Y.G. laboratory is supported by the "Centre National de la Recherche Scientifique", the "Université de Bourgogne Franche-Comté", the Conseil Régional Bourgogne Franche-Comte (PARI grant), the FEDER (European Funding for Regional Economical Development), and the European Council (ERC starting grant, GliSFCo-311403).

AUTHOR CONTRIBUTIONS

Genetic epistasis and imaging and oviposition assay were performed by A.M. and L.K.. Multi-CAFE assay and electrophysiology experiments were performed by C.S.. Calcium imaging was performed by G.M.. Results were analyzed and interpreted by A.M., C. S., G.M., Y. G., F. M.P., L. K., and J. R.. The original draft was written by J.R.. Reviewing and editing were performed by all authors. Supervision: L.K., Y.G., F.M.P. and J.R. Funding acquisition: Y.G., F.M.P. and J.R.

REFERENCES

1. Mburu, D.M. *et al.* Relationship between virulence and repellency of entomopathogenic isolates of Metarhizium anisopliae and Beauveria bassiana to the termite Macrotermes michaelseni. *J Insect Physiol* **55**, 774-780 (2009).

2. Swanson, J.A. *et al.* Odorants that induce hygienic behavior in honeybees: identification of volatile compounds in chalkbrood-infected honeybee larvae. *J Chem Ecol* **35**, 1108-1116 (2009).

3. Hoffman, C. & Aballay, A. Role of neurons in the control of immune defense. *Curr Opin Immunol* **60**, 30-36 (2019).

4. Aranha, M.M. & Vasconcelos, M.L. Deciphering Drosophila female innate behaviors. *Curr Opin Neurobiol* **52**, 139-148 (2018).

5. Sayin, S., Boehm, A.C., Kobler, J.M., De Backer, J.F. & Grunwald Kadow, I.C. Internal State Dependent Odor Processing and Perception-The Role of Neuromodulation in the Fly Olfactory System. *Front Cell Neurosci* **12**, 11 (2018).

6. Zhai, Z., Huang, X. & Yin, Y. Beyond immunity: The Imd pathway as a coordinator of host defense, organismal physiology and behavior. *Dev Comp Immunol* **83**, 51-59 (2018).

7. Buchon, N., Silverman, N. & Cherry, S. Immunity in Drosophila melanogaster--from microbial recognition to whole-organism physiology. *Nat Rev Immunol* **14**, 796-810 (2014).

8. Martino, M.E., Ma, D. & Leulier, F. Microbial influence on Drosophila biology. *Curr Opin Microbiol* **38**, 165-170 (2017).

9. You, H., Lee, W.J. & Lee, W.J. Homeostasis between gut-associated microorganisms and the immune system in Drosophila. *Curr Opin Immunol* **30**, 48-53 (2014).

10. Myllymaki, H., Valanne, S. & Ramet, M. The Drosophila imd signaling pathway. *J Immunol* **192**, 3455-3462 (2014).

11. Lindsay, S.A. & Wasserman, S.A. Conventional and non-conventional Drosophila Toll signaling. *Dev Comp Immunol* **42**, 16-24 (2014).

12. De Gregorio, E., Spellman, P.T., Tzou, P., Rubin, G.M. & Lemaitre, B. The Toll and Imd pathways are the major regulators of the immune response in Drosophila. *EMBO J* **21**, 2568-2579 (2002).

13. Royet, J., Gupta, D. & Dziarski, R. Peptidoglycan recognition proteins: modulators of the microbiome and inflammation. *Nat Rev Immunol* **11**, 837-851 (2011).

14. Kurata, S. Peptidoglycan recognition proteins in Drosophila immunity. *Dev Comp Immunol* **42**, 36-41 (2014).

15. Kurz, C.L., Charroux, B., Chaduli, D., Viallat-Lieutaud, A. & Royet, J. Peptidoglycan sensing by octopaminergic neurons modulates Drosophila oviposition. *Elife* **6** (2017).

16. Masuzzo, A. *et al.* Peptidoglycan-dependent NF-kappaB activation in a small subset of brain octopaminergic neurons controls female oviposition. *Elife* **8** (2019).

17. Stensmyr, M.C. *et al.* A conserved dedicated olfactory circuit for detecting harmful microbes in Drosophila. *Cell* **151**, 1345-1357 (2012).

18. Min, S., Ai, M., Shin, S.A. & Suh, G.S. Dedicated olfactory neurons mediating attraction behavior to ammonia and amines in Drosophila. *Proc Natl Acad Sci U S A* **110**, E1321-1329 (2013).

19. Depetris-Chauvin, A., Galagovsky, D., Chevalier, C., Maniere, G. & Grosjean, Y. Olfactory detection of a bacterial short-chain fatty acid acts as an orexigenic signal in Drosophila melanogaster larvae. *Sci Rep* **7**, 14230 (2017).

20. Yanagawa, A., Neyen, C., Lemaitre, B. & Marion-Poll, F. The gram-negative sensing receptor PGRP-LC contributes to grooming induction in Drosophila. *PLoS One* **12**, e0185370 (2017).

21. Soldano, A. *et al.* Gustatory-mediated avoidance of bacterial lipopolysaccharides via TRPA1 activation in Drosophila. *Elife* **5** (2016).

22. Yanagawa, A. *et al.* LPS perception through taste-induced reflex in Drosophila melanogaster. *J Insect Physiol* **112**, 39-47 (2019).

23. Sharon, G. *et al.* Commensal bacteria play a role in mating preference of Drosophila melanogaster. *Proc Natl Acad Sci U S A* **107**, 20051-20056 (2010).

24. wong, A.C., Wang, Q.P., Morimoto, J.,Senior, A.M, Lihoreau, M., Neely, G.G, Simpson, S.J., Ponton, F. Gut Microbiota Modifies Olfactory-Guided Microbial Preferences and Foraging Decisions in Drosophila. *Current biology* **27**, 2397-2404 (2017).

25. Keesey, I.W. *et al.* Pathogenic bacteria enhance dispersal through alteration of Drosophila social communication. *Nat Commun* **8**, 265 (2017).

26. Chen, Y.D. & Dahanukar, A. Recent advances in the genetic basis of taste detection in Drosophila. *Cell Mol Life Sci* **77**, 1087-1101 (2020).

27. French, A. *et al.* Drosophila Bitter Taste(s). *Front Integr Neurosci* **9**, 58 (2015).

28. Montell, C. A taste of the Drosophila gustatory receptors. *Curr Opin Neurobiol* **19**, 345-353 (2009).

29. Weiss, L.A., Dahanukar, A., Kwon, J.Y., Banerjee, D. & Carlson, J.R. The molecular and cellular basis of bitter taste in Drosophila. *Neuron* **69**, 258-272 (2011).

30. Kleino, A. & Silverman, N. The Drosophila IMD pathway in the activation of the humoral immune response. *Dev Comp Immunol* **42**, 25-35 (2014).

31. Kwon, J.Y., Dahanukar, A., Weiss, L.A. & Carlson, J.R. A map of taste neuron projections in the Drosophila CNS. *J Biosci* **39**, 565-574 (2014).

32. Marella, S. *et al.* Imaging taste responses in the fly brain reveals a functional map of taste category and behavior. *Neuron* **49**, 285-295 (2006).

33. Shanbhag, S.R., Park, S.K., Pikielny, C.W. & Steinbrecht, R.A. Gustatory organs of Drosophila melanogaster: fine structure and expression of the putative odorant-binding protein PBPRP2. *Cell Tissue Res* **304**, 423-437 (2001).

34. Thorne, N., Chromey, C., Bray, S. & Amrein, H. Taste perception and coding in Drosophila. *Curr Biol* **14**, 1065-1079 (2004).

35. Wang, Z., Singhvi, A., Kong, P. & Scott, K. Taste representations in the Drosophila brain. *Cell* **117**, 981-991 (2004).

36. Dunipace, L., Meister, S., McNealy, C. & Amrein, H. Spatially restricted expression of candidate taste receptors in the Drosophila gustatory system. *Curr Biol* **11**, 822-835 (2001).

37. Moon, S.J., Kottgen, M., Jiao, Y., Xu, H. & Montell, C. A taste receptor required for the caffeine response in vivo. *Curr Biol* **16**, 1812-1817 (2006).

38. Dahanukar, A., Lei, Y.T., Kwon, J.Y. & Carlson, J.R. Two Gr genes underlie sugar reception in Drosophila. *Neuron* **56**, 503-516 (2007).

39. Jiao, Y., Moon, S.J. & Montell, C. A Drosophila gustatory receptor required for the responses to sucrose, glucose, and maltose identified by mRNA tagging. *Proc Natl Acad Sci U S A* **104**, 14110-14115 (2007).

40. Takehana, A. *et al.* Peptidoglycan recognition protein (PGRP)-LE and PGRP-LC act synergistically in Drosophila immunity. *EMBO J* **23**, 4690-4700 (2004).

41. Kaneko, T. *et al.* PGRP-LC and PGRP-LE have essential yet distinct functions in the drosophila immune response to monomeric DAP-type peptidoglycan. *Nat Immunol* **7**, 715-723 (2006).

42. Charroux, B. *et al.* Cytosolic and Secreted Peptidoglycan-Degrading Enzymes in Drosophila Respectively Control Local and Systemic Immune Responses to Microbiota. *Cell Host Microbe* **23**, 215-228 e214 (2018).

43. Ja, W.W. *et al.* Prandiology of Drosophila and the CAFE assay. *Proc Natl Acad Sci U S A* **104**, 8253-8256 (2007).

44. Gottar, M. *et al.* The Drosophila immune response against Gram-negative bacteria is mediated by a peptidoglycan recognition protein. *Nature* **416**, 640-644 (2002).

45. Zhai, Z., Boquete, J.P. & Lemaitre, B. Cell-Specific Imd-NF-kappaB Responses Enable Simultaneous Antibacterial Immunity and Intestinal Epithelial Cell Shedding upon Bacterial Infection. *Immunity* **48**, 897-910 e897 (2018).

46. Guo, L., Karpac, J., Tran, S.L. & Jasper, H. PGRP-SC2 promotes gut immune homeostasis to limit commensal dysbiosis and extend lifespan. *Cell* **156**, 109-122 (2014).

47. Hedengren, M. *et al.* Relish, a central factor in the control of humoral but not cellular immunity in Drosophila. *Mol Cell* **4**, 827-837 (1999).

48. Harris, N. *et al.* The Innate Immune Receptor PGRP-LC Controls Presynaptic Homeostatic Plasticity. *Neuron* **88**, 1157-1164 (2015).

49. Harris, N., Fetter, R.D., Brasier, D.J., Tong, A. & Davis, G.W. Molecular Interface of Neuronal Innate Immunity, Synaptic Vesicle Stabilization, and Presynaptic Homeostatic Plasticity. *Neuron* **100**, 1163-1179 e1164 (2018).

50. Stoven, S., Ando, I., Kadalayil, L., Engstrom, Y. & Hultmark, D. Activation of the Drosophila NF-kappaB factor Relish by rapid endoproteolytic cleavage. *EMBO Rep* **1**, 347-352 (2000).

51. Wheeler, R., Chevalier, G., Eberl, G. & Gomperts Boneca, I. The biology of bacterial peptidoglycans and their impact on host immunity and physiology. *Cell Microbiol* **16**, 1014-1023 (2014).

52. Stenbak, C.R. *et al.* Peptidoglycan molecular requirements allowing detection by the Drosophila immune deficiency pathway. *J Immunol* **173**, 7339-7348 (2004).

53. Devineni, A.V., Sun, B., Zhukovskaya, A. & Axel, R. Acetic acid activates distinct taste pathways in Drosophila to elicit opposing, state-dependent feeding responses. *Elife* **8** (2019).

54. Fujita, M. & Tanimura, T. Drosophila evaluates and learns the nutritional value of sugars. *Curr Biol* **21**, 751-755 (2011).

55. Lopez-Requena, A. *et al.* Roles of Neuronal TRP Channels in Neuroimmune Interactions. In: nd & Emir, T.L.R. (eds). *Neurobiology of TRP Channels*: Boca Raton (FL), 2017, pp 277-294.

56. Chin, S.G., Maguire, S.E., Huoviala, P., Jefferis, G. & Potter, C.J. Olfactory Neurons and Brain Centers Directing Oviposition Decisions in Drosophila. *Cell Rep* **24**, 1667-1678 (2018).

57. Paredes, J.C., Welchman, D.P., Poidevin, M. & Lemaitre, B. Negative regulation by amidase PGRPs shapes the Drosophila antibacterial response and protects the fly from innocuous infection. *Immunity* **35**, 770-779 (2011).

58. Zaidman-Remy, A. *et al.* The Drosophila amidase PGRP-LB modulates the immune response to bacterial infection. *Immunity* **24**, 463-473 (2006).

59. Kwon, J.Y., Dahanukar, A., Weiss, L.A. & Carlson, J.R. Molecular and cellular organization of the taste system in the Drosophila larva. *J Neurosci* **31**, 15300-15309 (2011).

60. Kim, H. *et al.* Drosophila Gr64e mediates fatty acid sensing via the phospholipase C pathway. *PLoS Genet* **14**, e1007229 (2018).

61. Mishra, D. *et al.* The molecular basis of sugar sensing in Drosophila larvae. *Curr Biol* **23**, 1466-1471 (2013).

62. Thistle, R., Cameron, P., Ghorayshi, A., Dennison, L. & Scott, K. Contact chemoreceptors mediate male-male repulsion and male-female attraction during Drosophila courtship. *Cell* **149**, 1140-1151 (2012).

63. Fan, P. *et al.* Genetic and neural mechanisms that inhibit Drosophila from mating with other species. *Cell* **154**, 89-102 (2013).

64. Hardie, R.C. *et al.* Calcium influx via TRP channels is required to maintain PIP2 levels in Drosophila photoreceptors. *Neuron* **30**, 149-159 (2001).

65. Khush, R.S., Cornwell, W.D., Uram, J.N. & Lemaitre, B. A ubiquitin-proteasome pathway represses the Drosophila immune deficiency signaling cascade. *Curr Biol* **12**, 1728-1737 (2002).

66. Maillet, F., Bischoff, V., Vignal, C., Hoffmann, J. & Royet, J. The Drosophila peptidoglycan recognition protein PGRP-LF blocks PGRP-LC and IMD/JNK pathway activation. *Cell Host Microbe* **3**, 293-303 (2008).

67. Leulier, F., Rodriguez, A., Khush, R.S., Abrams, J.M. & Lemaitre, B. The Drosophila caspase Dredd is required to resist gram-negative bacterial infection. *EMBO Rep* **1**, 353-358 (2000).

68. Meunier, N., Marion-Poll, F., Lansky, P. & Rospars, J.P. Estimation of the individual firing frequencies of two neurons recorded with a single electrode. *Chem Senses* **28**, 671-679 (2003).

69. Silbering, A.F., Bell, R., Galizia, C.G. & Benton, R. Calcium imaging of odor-evoked responses in the Drosophila antennal lobe. *J Vis Exp* (2012).

70. Sellier, M.J., Reeb, P. & Marion-Poll, F. Consumption of bitter alkaloids in Drosophila melanogaster in multiple-choice test conditions. *Chem Senses* **36**, 323-334 (2011).

71. Meunier, N., Marion-Poll, F., Rospars, J.P. & Tanimura, T. Peripheral coding of bitter taste in Drosophila. *J Neurobiol* **56**, 139-152 (2003).

Figure 1

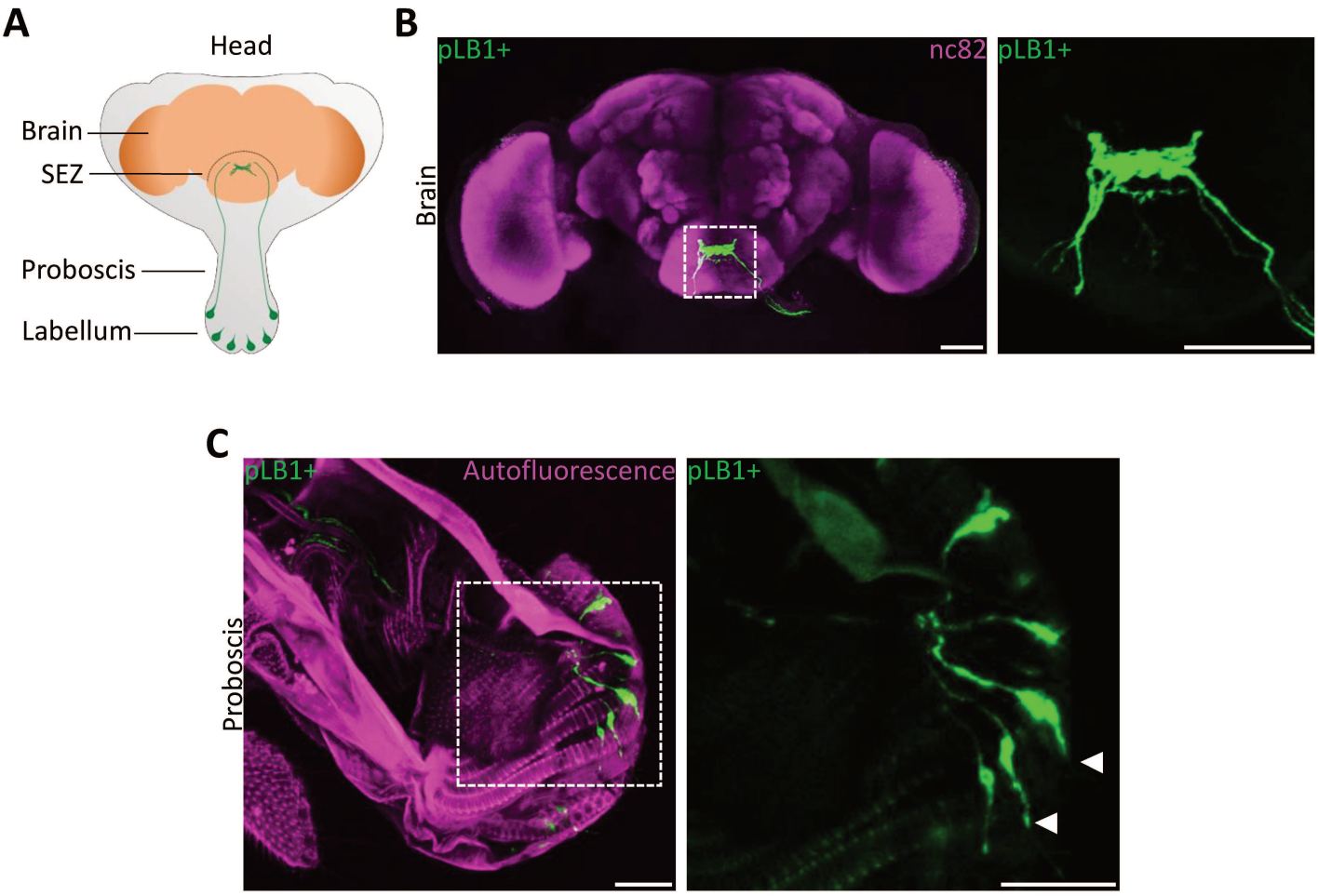
A
Head
Brain
SEZ
Proboscis
Labellum
B
pLB1+
nc82
Brain
pLB1+
C
pLB1+
Autofluorescence
Proboscis
pLB1+

Figure 2

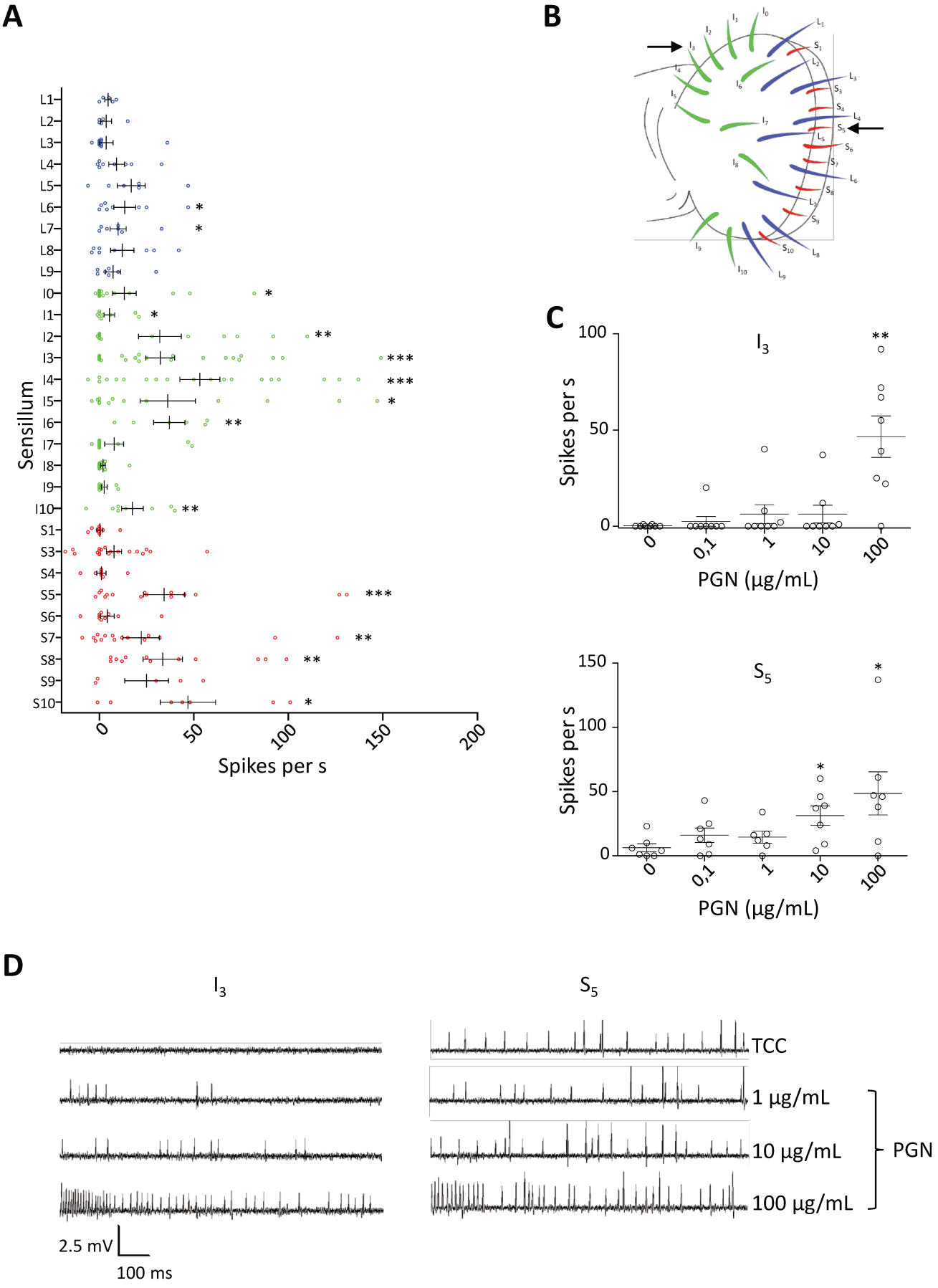
A
Sensillum
L1
L2
L3
L4
L5
L6
L7
L8
L9
I0
I1
I2
I3
I4
I5
I6
I7
I8
I9
I10
S1
S3
S4
S5
S6
S7
S8
S9
S10
0
50
100
150
200
Spikes per s
B
C
I3
Spikes per s
PGN (µg/mL)
0
0,1
1
10
100
S5
D
I3
S5
TCC
1 µg/mL
10 µg/mL
100 µg/mL
PGN
2.5 mV
100 ms

Figure 3

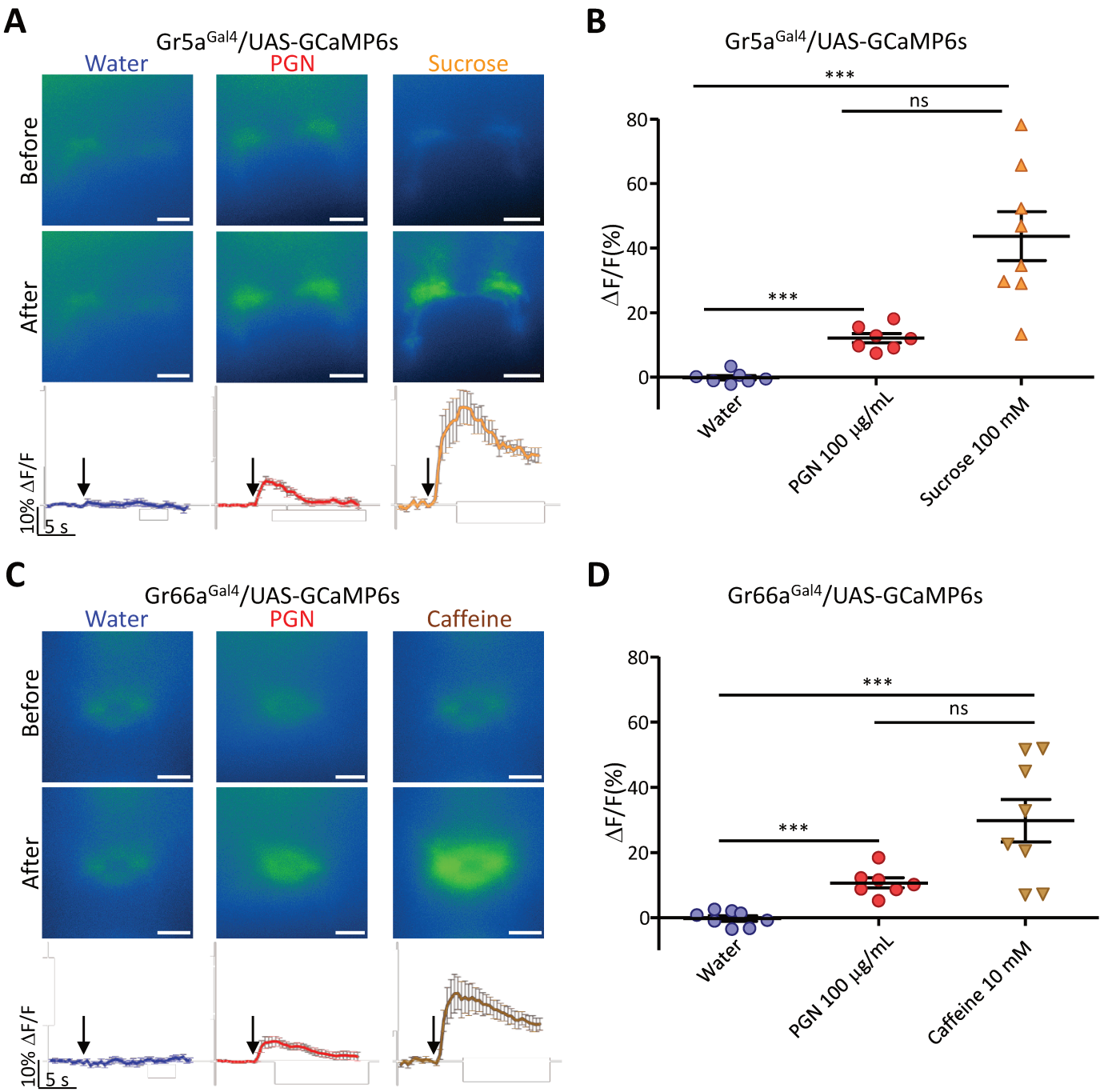
A
Gr5a^{Gal4}/UAS-GCaMP6s
Water
PGN
Sucrose
Before
After
10% ΔF/F
5 s
B
Gr5a^{Gal4}/UAS-GCaMP6s
***
ns
***
ΔF/F(%)
80
60
40
20
0
Water
PGN 100 µg/mL
Sucrose 100 mM
C
Gr66a^{Gal4}/UAS-GCaMP6s
Water
PGN
Caffeine
Before
After
10% ΔF/F
5 s
D
Gr66a^{Gal4}/UAS-GCaMP6s
***
ns
***
ΔF/F(%)
80
60
40
20
0
Water
PGN 100 µg/mL
Caffeine 10 mM

Figure 4

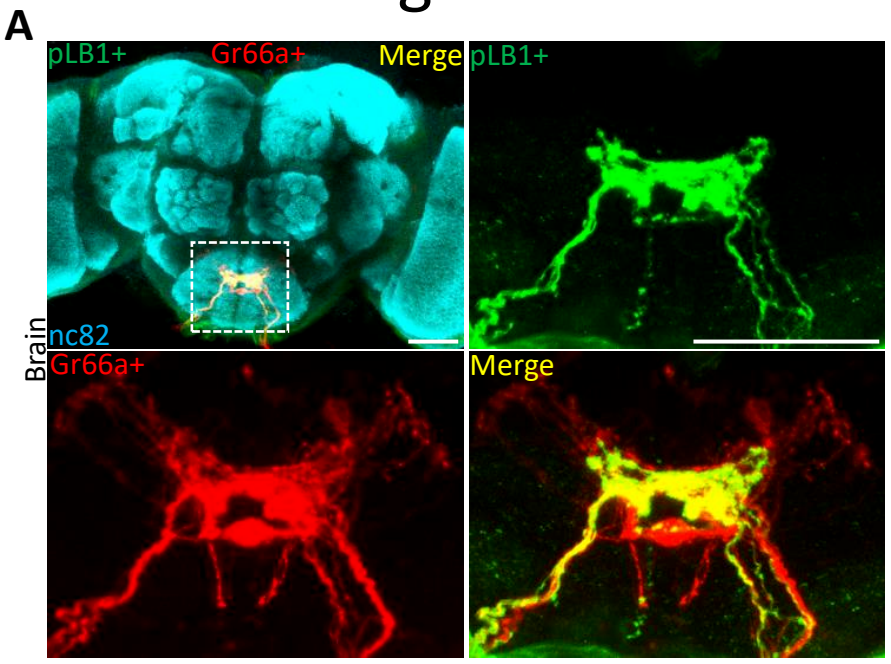
A
pLB1+
Gr66a+
Merge
nc82
Brain
pLB1+
Gr66a+
Merge

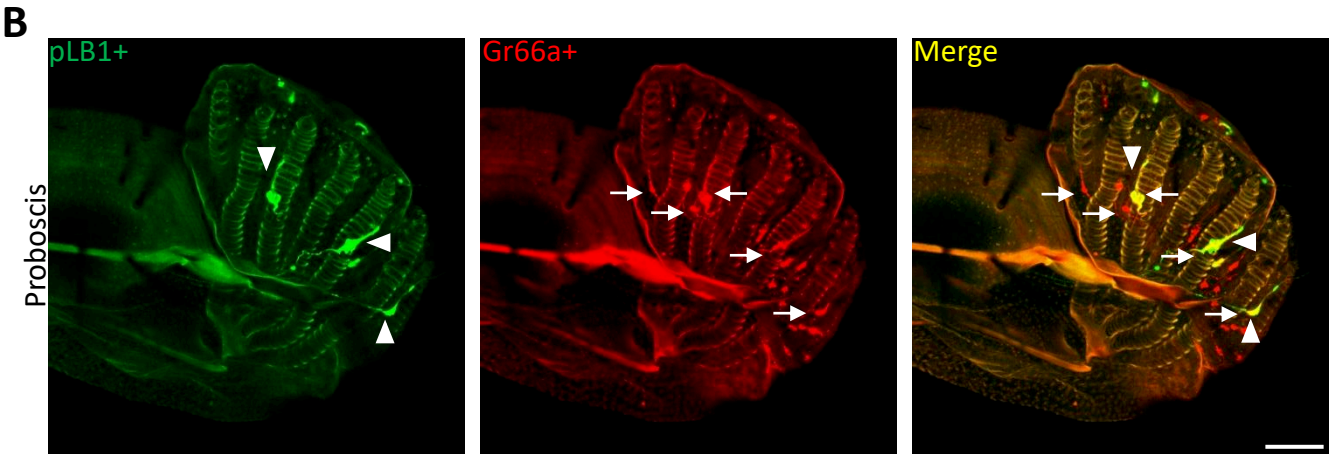
B
pLB1+
Gr66a+
Merge
Proboscis

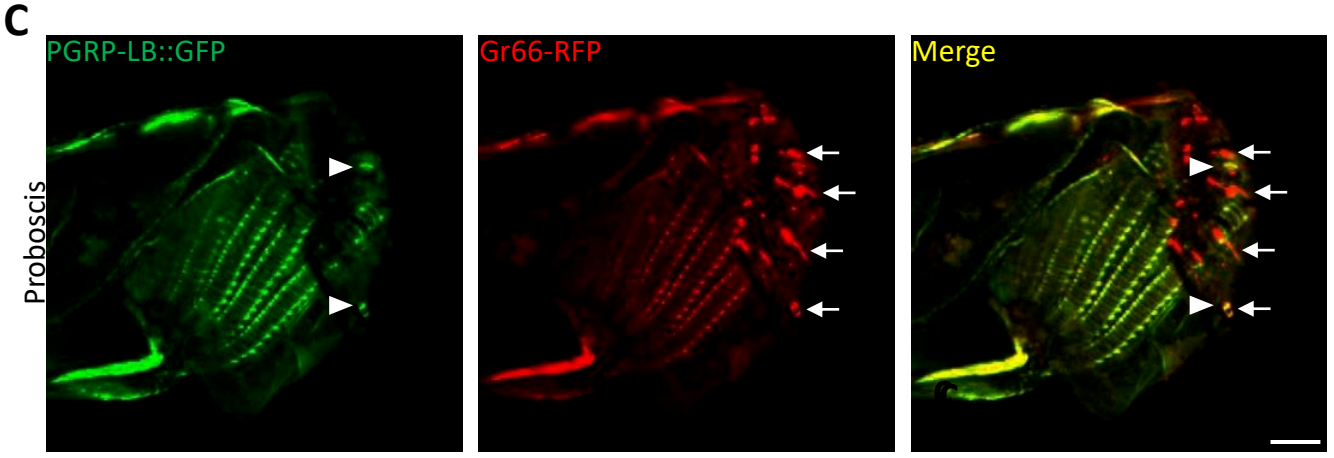
C
PGRP-LB::GFP
Gr66-RFP
Merge
Proboscis

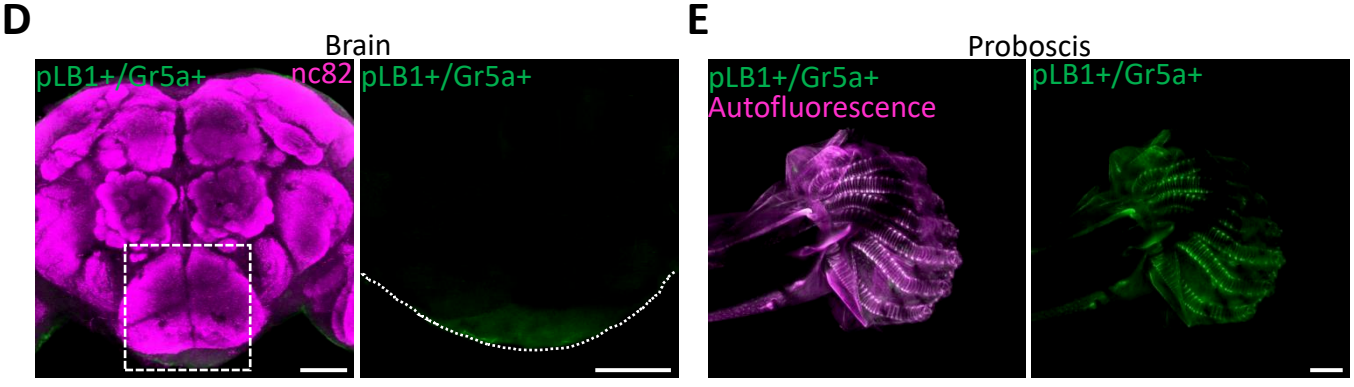
D
Brain
pLB1+/Gr5a+
nc82
pLB1+/Gr5a+
E
Proboscis
pLB1+/Gr5a+
Autofluorescence
pLB1+/Gr5a+

Figure 5

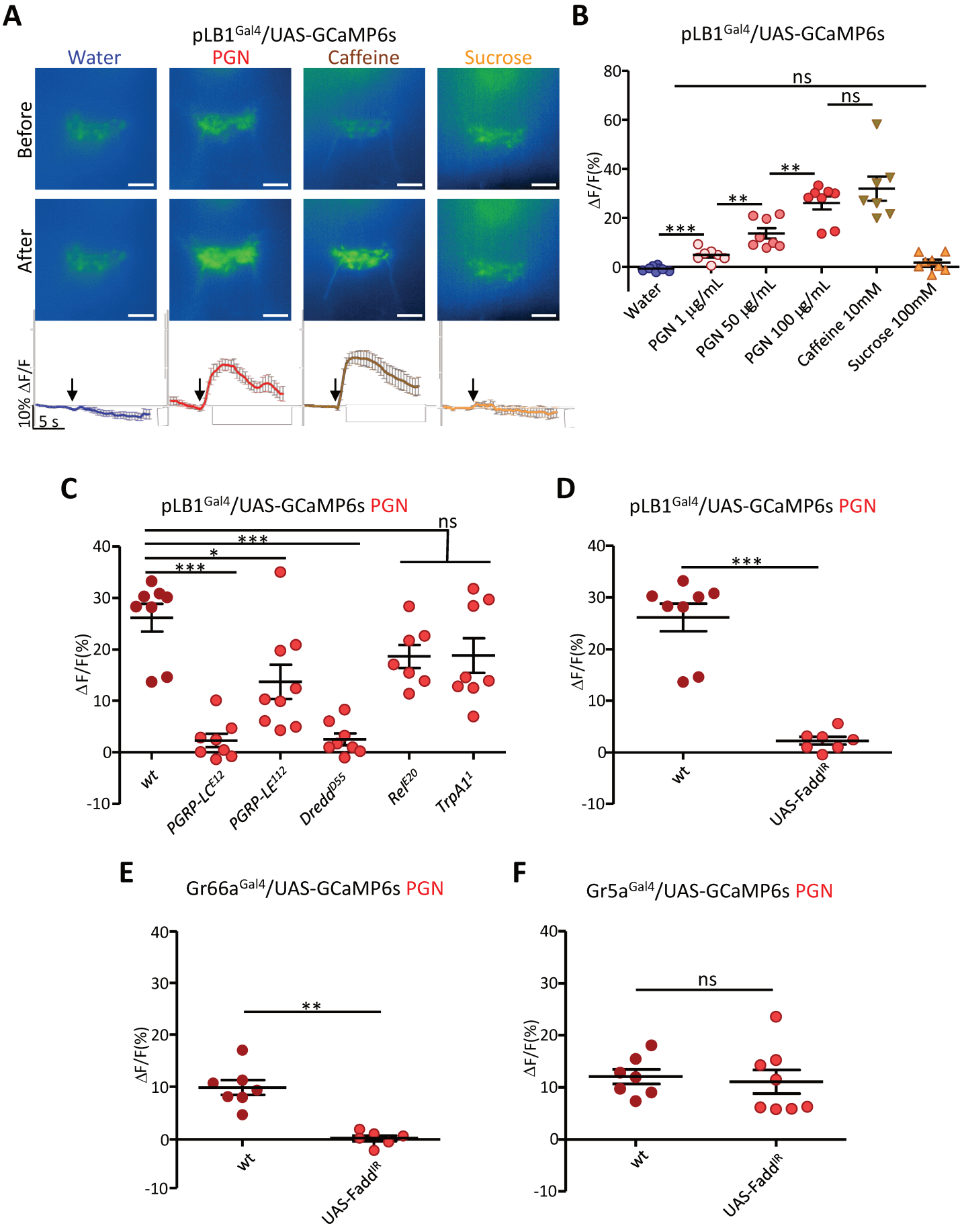
A
pLB1Gal4/UAS-GCaMP6s
Water
PGN
Caffeine
Sucrose
Before
After
10% ΔF/F
5 s
B
pLB1Gal4/UAS-GCaMP6s
ΔF/F(%)
ns
ns
**
**
***
Water
PGN 1 µg/mL
PGN 50 µg/mL
PGN 100 µg/mL
Caffeine 10mM
Sucrose 100mM
C
pLB1Gal4/UAS-GCaMP6s PGN
ΔF/F(%)
ns
***
*
***
wt
PGRP-LCE12
PGRP-LE112
DreddD55
RelE20
TrpA11
D
pLB1Gal4/UAS-GCaMP6s PGN
ΔF/F(%)
***
wt
UAS-FaddIR
E
Gr66aGal4/UAS-GCaMP6s PGN
ΔF/F(%)
**
wt
UAS-FaddIR
F
Gr5aGal4/UAS-GCaMP6s PGN
ΔF/F(%)
ns
wt
UAS-FaddIR

Figure 6

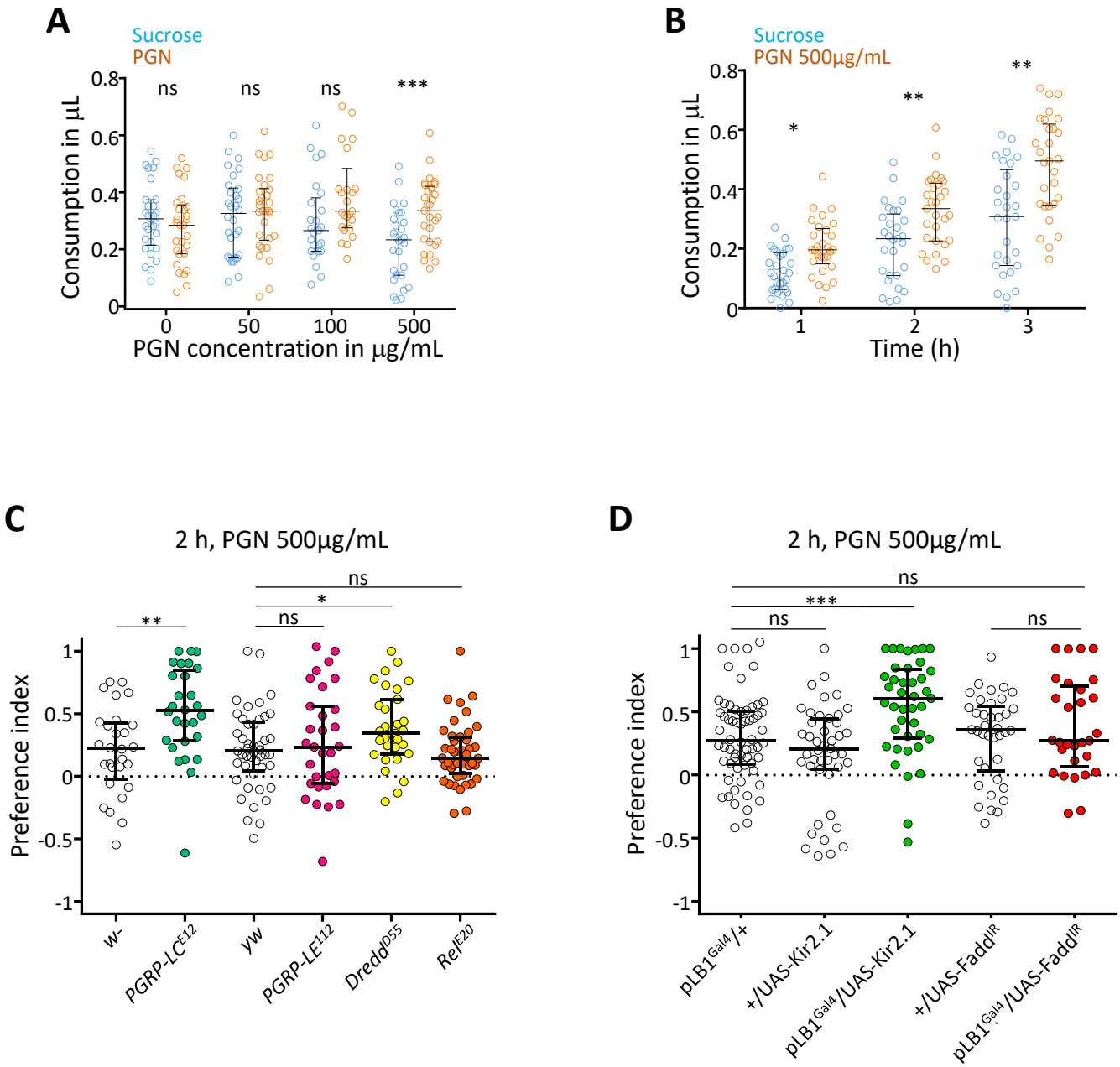
A
Sucrose
PGN
ns
ns
ns
***
Consumption in µL
0
0.2
0.4
0.6
0.8
0
50
100
500
PGN concentration in µg/mL
B
Sucrose
PGN 500µg/mL
*
**
**
Consumption in µL
0
0.2
0.4
0.6
0.8
1
2
3
Time (h)
C
2 h, PGN 500µg/mL
**
ns
*
ns
Preference index
1
0.5
0
-0.5
-1
w-
PGRP-LC^E12
yw
PGRP-LE^112
Dredd^D55
Rel^E20
D
2 h, PGN 500µg/mL
ns
***
ns
ns
Preference index
1
0.5
0
-0.5
-1
pLB1^Gal4/+
+/UAS-Kir2.1
pLB1^Gal4/UAS-Kir2.1
+/UAS-Fadd^IR
pLB1^Gal4/UAS-Fadd^IR

Figure 7

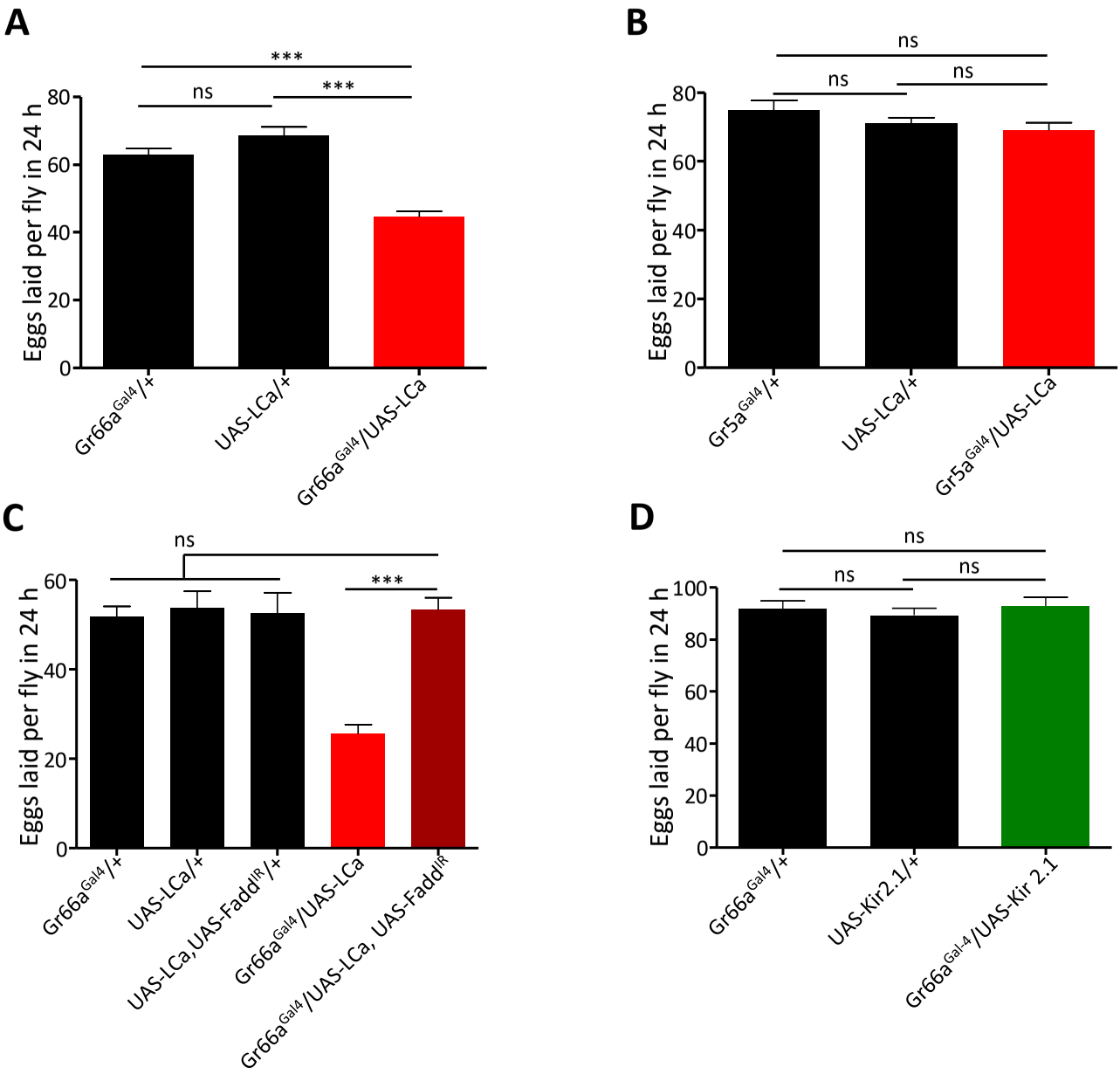
A
***
ns
***
Eggs laid per fly in 24 h
0
20
40
60
80
Gr66a Gal4/+
UAS-LCa/+
Gr66a Gal4/UAS-LCa
B
ns
ns
ns
Eggs laid per fly in 24 h
0
20
40
60
80
Gr5a Gal4/+
UAS-LCa/+
Gr5a Gal4/UAS-LCa
C
ns
***
Eggs laid per fly in 24 h
0
20
40
60
Gr66a Gal4/+
UAS-LCa/+
UAS-LCa, UAS-Fadd IR/+
Gr66a Gal4/UAS-LCa
Gr66a Gal4/UAS-LCa, UAS-Fadd IR
D
ns
ns
ns
Eggs laid per fly in 24 h
0
20
40
60
80
100
Gr66a Gal4/+
UAS-Kir2.1/+
Gr66a Gal-4/UAS-Kir 2.1

Figure 8

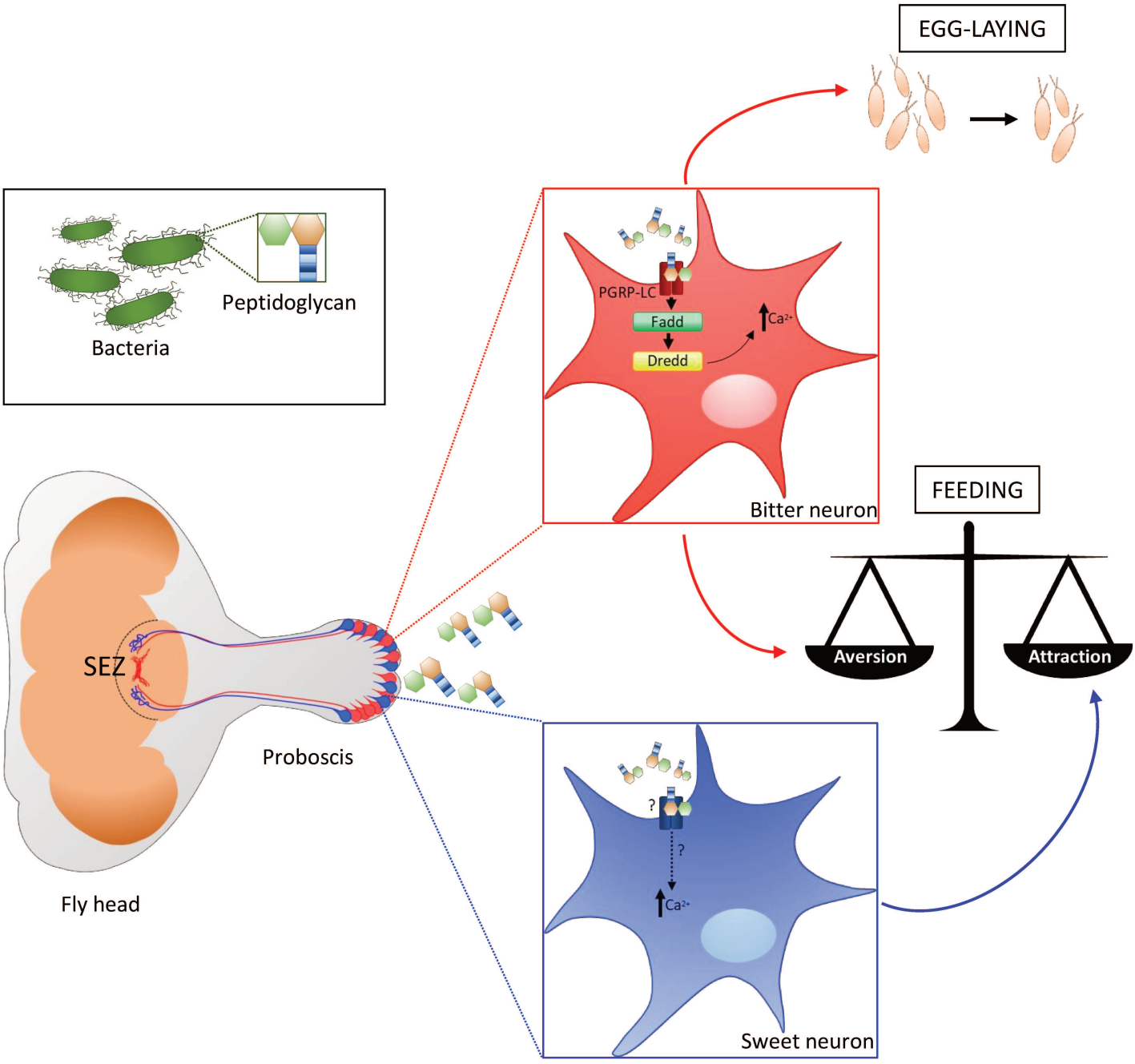
EGG-LAYING
Peptidoglycan
Bacteria
PGRP-LC
Fadd
Dredd
Ca2+
Bitter neuron
FEEDING
Aversion
Attraction
SEZ
Proboscis
Fly head
?
?
Ca2+
Sweet neuron

Figure S1

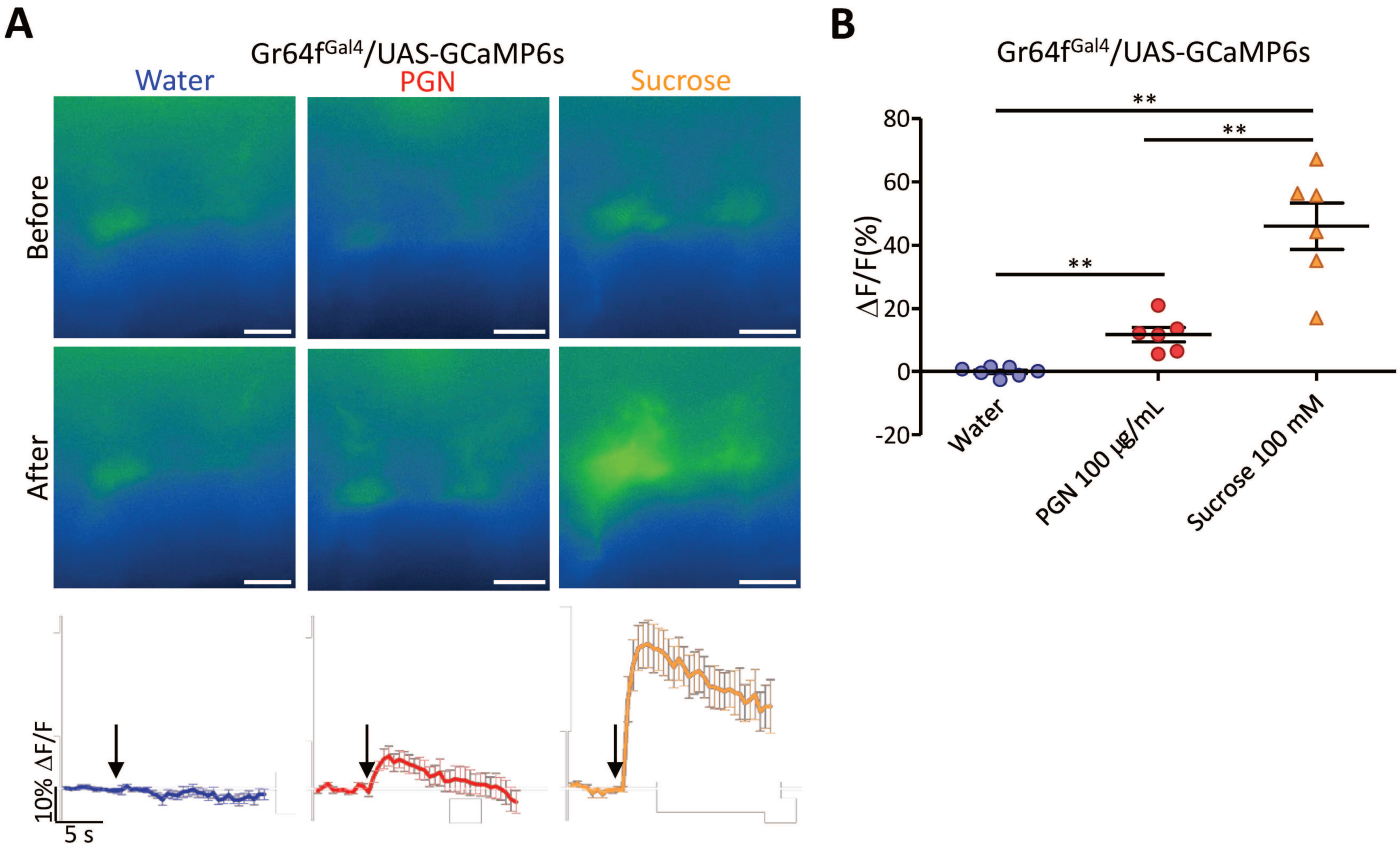
A
Gr64f^Gal4/UAS-GCaMP6s
Water
PGN
Sucrose
Before
After
10% ΔF/F
5 s
B
Gr64f^Gal4/UAS-GCaMP6s
ΔF/F(%)
80
60
40
20
0
-20
**
**
**
Water
PGN 100 μg/mL
Sucrose 100 mM

Figure S2

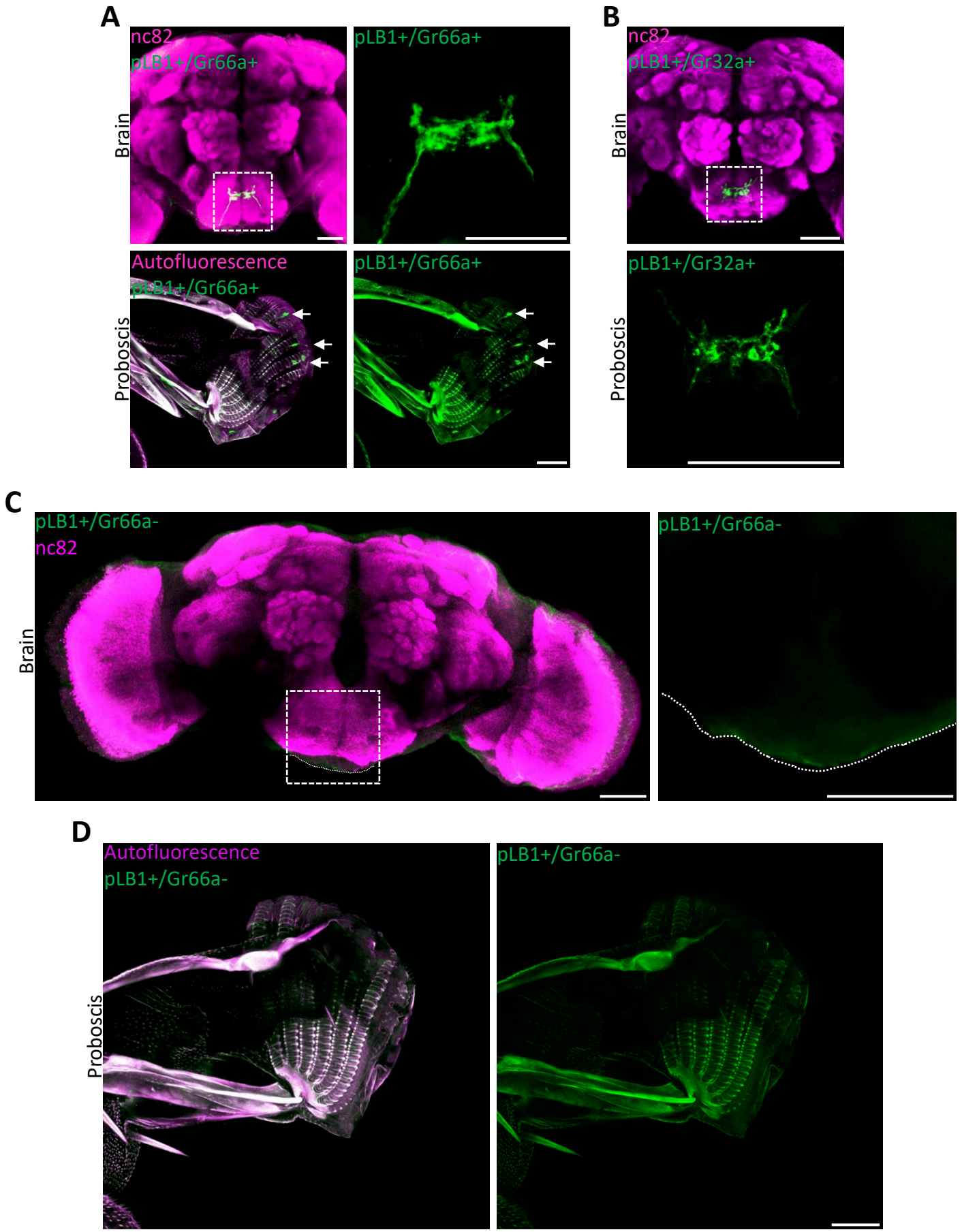
A
nc82
pLB1+/Gr66a+
pLB1+/Gr66a+
Brain
Autofluorescence
pLB1+/Gr66a+
pLB1+/Gr66a+
Proboscis
B
nc82
pLB1+/Gr32a+
Brain
pLB1+/Gr32a+
Proboscis
C
pLB1+/Gr66a-
nc82
pLB1+/Gr66a-
Brain
D
Autofluorescence
pLB1+/Gr66a-
pLB1+/Gr66a-
Proboscis

Figure S3

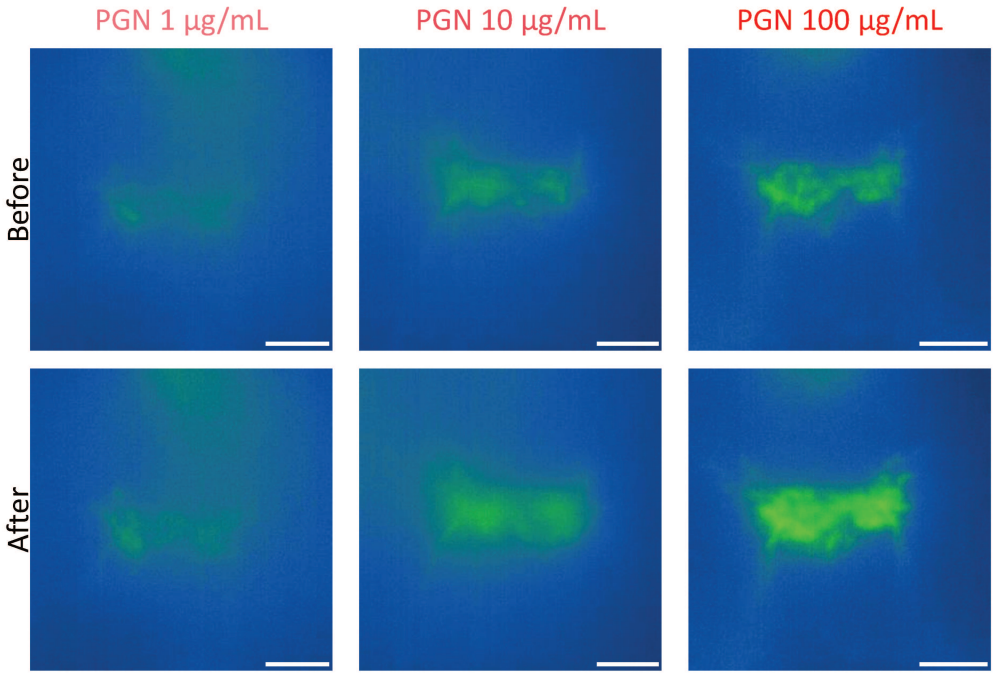

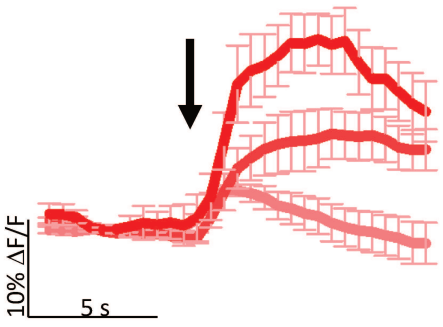

Figure S4

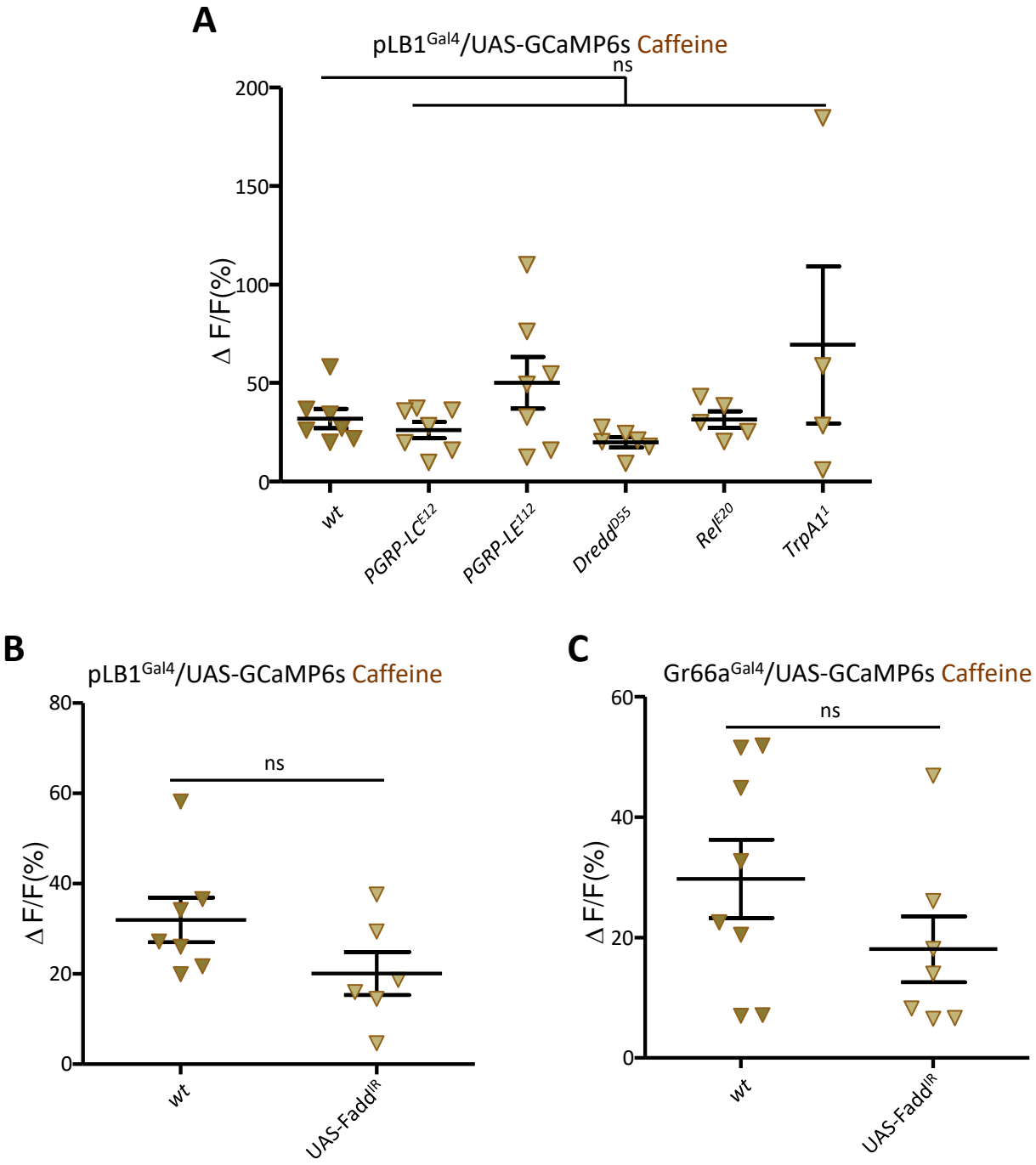
A
pLB1Gal4/UAS-GCaMP6s Caffeine
ns
200
150
100
50
0
Δ F/F(%)
wt
PGRP-LCE12
PGRP-LE112
Dredd D55
RelE20
TrpA11
B
pLB1Gal4/UAS-GCaMP6s Caffeine
ns
80
60
40
20
0
Δ F/F(%)
wt
UAS-FaddIR
C
Gr66aGal4/UAS-GCaMP6s Caffeine
ns
60
40
20
0
Δ F/F(%)
wt
UAS-FaddIR

Figure S5

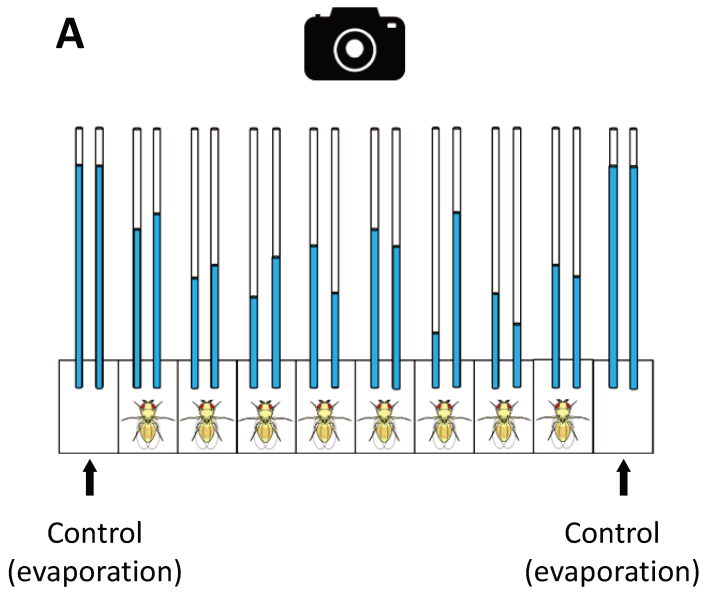
A
Control
(evaporation)
Control
(evaporation)

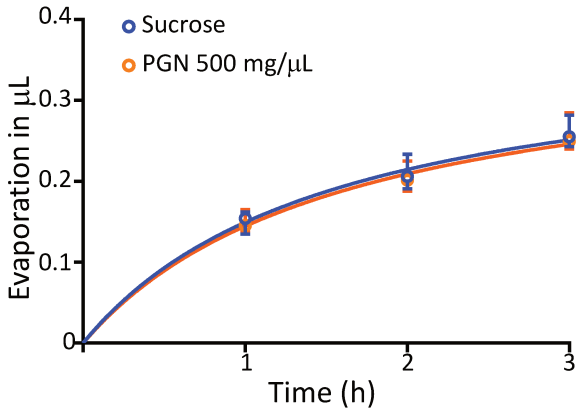
B
Sucrose
PGN 500 mg/µL
Evaporation in µL
0.4
0.3
0.2
0.1
0
1
2
3
Time (h)

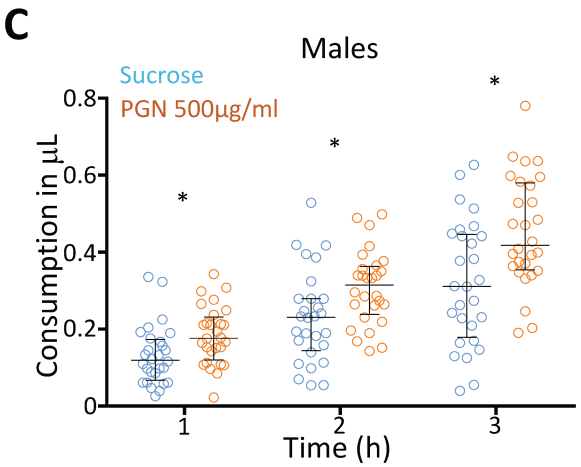
C
Males
Sucrose
PGN 500µg/ml
Consumption in µL
0.8
0.6
0.4
0.2
0
*
*
*
1
2
3
Time (h)

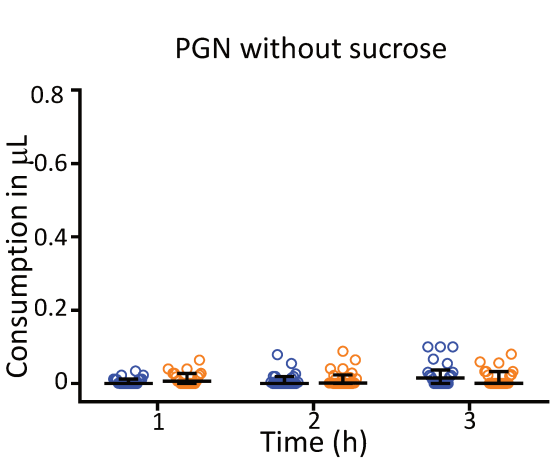
D
PGN without sucrose
Consumption in µL
0.8
0.6
0.4
0.2
0
1
2
3
Time (h)

Figure S6

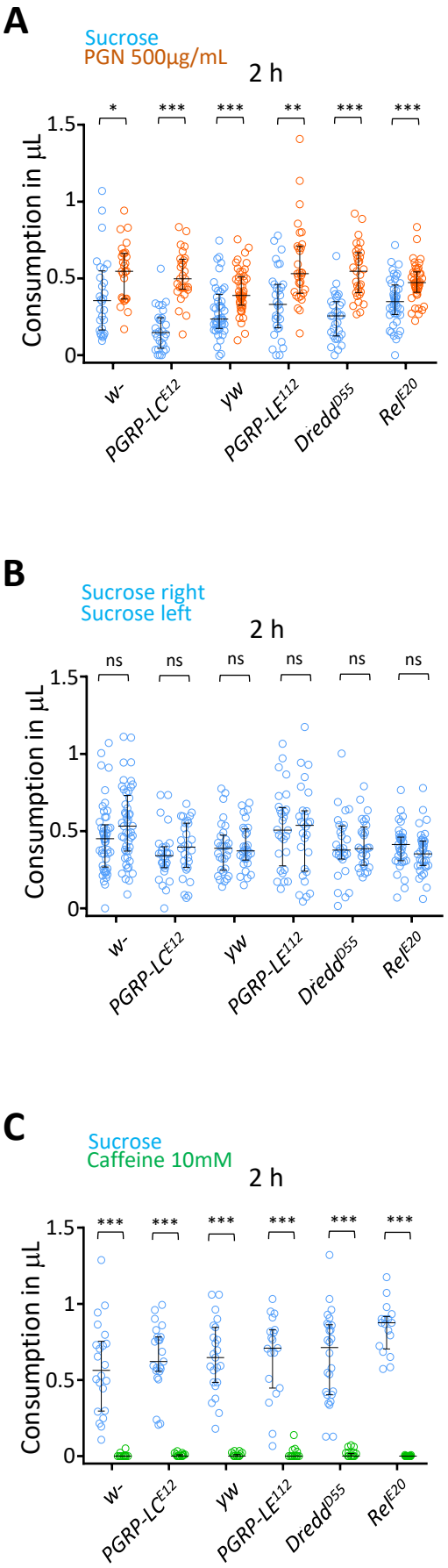
A
Sucrose
PGN 500µg/mL
2 h
Consumption in µL
w-
PGRP-LC^E12
yw
PGRP-LE^112
Dredd^D55
Rel^E20
B
Sucrose right
Sucrose left
2 h
ns
C
Sucrose
Caffeine 10mM
2 h

Figure S7

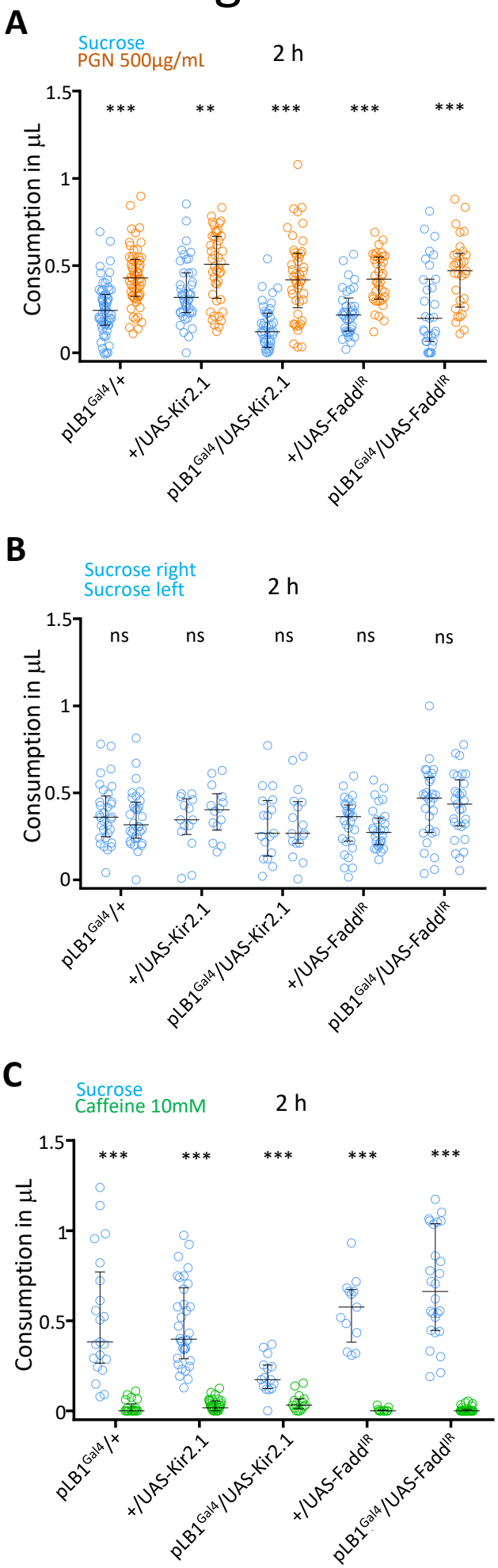
A
Sucrose
PGN 500µg/mL
2 h
Consumption in µL
1.5
1
0.5
0
***
**
***
***
***
pLB1Gal4/+
+/UAS-Kir2.1
pLB1Gal4/UAS-Kir2.1
+/UAS-FaddIR
pLB1Gal4/UAS-FaddIR
B
Sucrose right
Sucrose left
2 h
Consumption in µL
1.5
1
0.5
0
ns
ns
ns
ns
ns
pLB1Gal4/+
+/UAS-Kir2.1
pLB1Gal4/UAS-Kir2.1
+/UAS-FaddIR
pLB1Gal4/UAS-FaddIR
C
Sucrose
Caffeine 10mM
2 h
Consumption in µL
1.5
1
0.5
0
***
***
***
***
***
pLB1Gal4/+
+/UAS-Kir2.1
pLB1Gal4/UAS-Kir2.1
+/UAS-FaddIR
pLB1Gal4/UAS-FaddIR

Figure S8

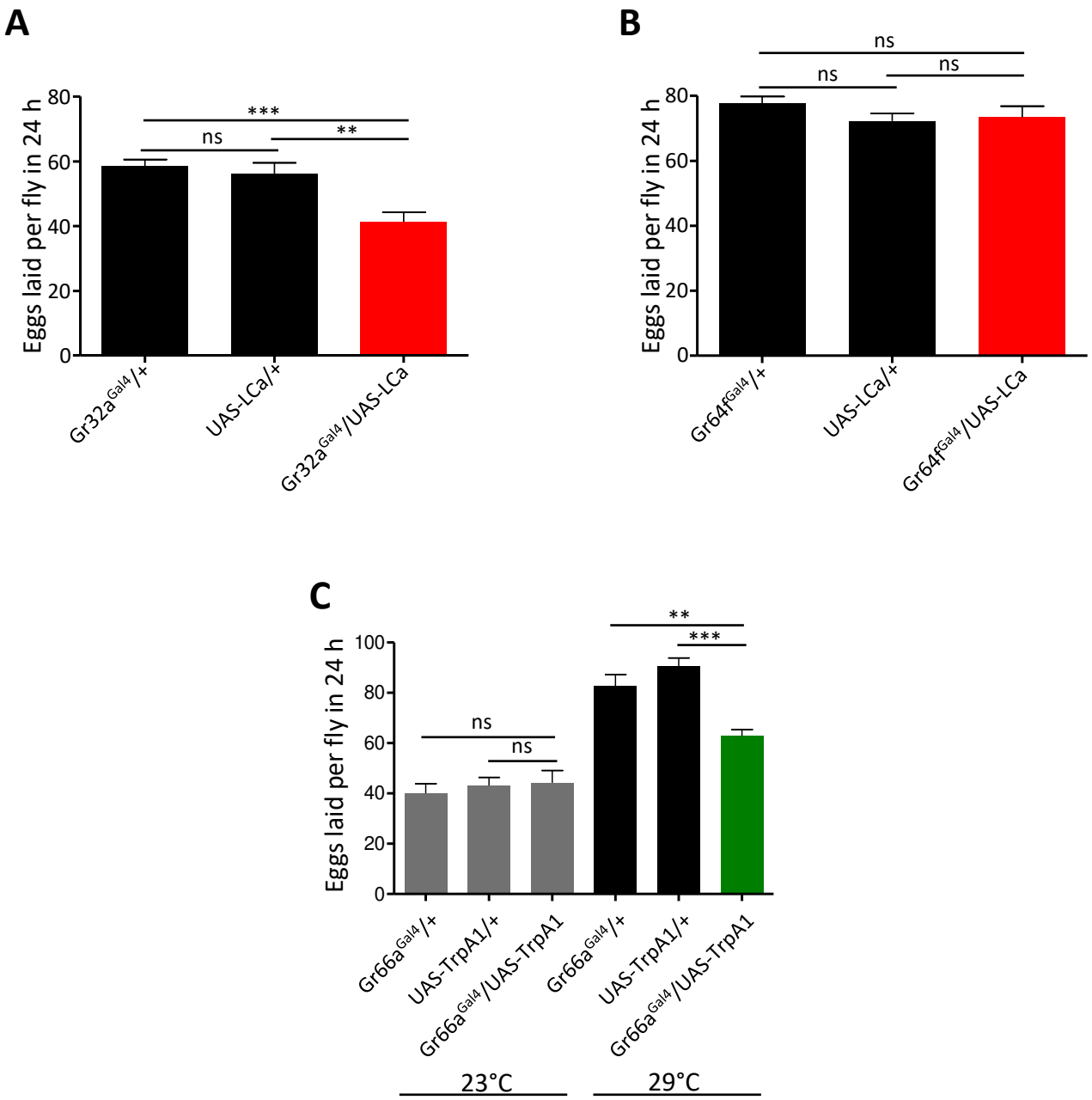
A
Eggs laid per fly in 24 h
0
20
40
60
80
***
ns
**
Gr32a Gal4 /+
UAS-LCa/+
Gr32a Gal4 /UAS-LCa
B
Eggs laid per fly in 24 h
0
20
40
60
80
ns
ns
ns
Gr64f Gal4 /+
UAS-LCa/+
Gr64f Gal4 /UAS-LCa
C
Eggs laid per fly in 24 h
0
20
40
60
80
100
ns
ns
**
***
Gr66a Gal4 /+
UAS-TrpA1/+
Gr66a Gal4 /UAS-TrpA1
Gr66a Gal4 /+
UAS-TrpA1/+
Gr66a Gal4 /UAS-TrpA1
23°C
29°C

Conclusive remarks and future perspectives

During my thesis, I had the opportunity to work in this amazing and still poorly understood field that is behavioral immunity. Animals tightly co-evolved with microbes and developed different strategies to avoid or fight pathogens or take advantage of beneficial microorganisms. Importantly, behavioral responses to microbes are crucial not only in the context of the infection but also in daily animal life. Indeed, animals have to promptly decide where to feed, to lay their eggs or with whom to mate, all decisions that need to be balanced with the animal internal state. The global picture becomes even more complex if we consider the fact that bacteria evolved strategies to bias their host behavior (Elya et al., 2018). It is becoming clear that numerous mechanisms and cellular and molecular players are involved in these interactions. During my thesis, I tried to elucidate some of these mechanisms, being aware of the great complexity of host-pathogen interactions.

In the first work, which I co-authored with Seydou Keita, a previous student in our team, we showed that *D. melanogaster* larvae decrease food uptake when exposed to the opportunistic pathogen *E.c.c.15*. (**Article 1**). This decrease was not observed or to a much lower extent with other bacteria species suggesting that specific *E.c.c.15* produced molecules might be sensed by larvae. Consistently, we showed that the *E.c.c.15* virulence factor *evf*, that mediates bacterial gut persistence, was partially implicated in this phenotype. However, since our assays were performed during a short time window (1 hour), we concluded that the mechanism by which *evf* favorites food uptake might not only be associated with gut persistence. We have shown that the main pathways that control the gut local immune response are not required for this response. In contrast, larvae mutants for the cation channel TRPA1 or the olfactory co-receptor Orco do not show a decrease in food uptake following *E.c.c.15* exposure. Further studies will be of interest to understand in which cells these proteins are required to modulate this behavioral response. TRPA1 is expressed in enteroendocrine cells and sensory neurons and is involved in sensing noxious stimuli (Kang et al., 2010; Kim et al., 2010). In esophageal bitter neurons, TRPA1 senses bacterial LPS, leading to aversive behaviors (Soldano et al., 2016). Since TRPA1 is a pleiotropic channel, it might also detect *E.c.c.15* derived molecules. Orco is broadly expressed in olfactory sensory neurons, suggesting that larvae could detect some specific *E.c.c.15* odorants. One possibility is that TRPA1 and Orco might act in different cells to regulate feeding behavior. However, we can not exclude the hypothesis that Orco and TRPA1 act in the same cells. It has been shown that two pathways involving TRPA1 and OR83a, another olfactory co-receptor, are required in ORNs to avoid citronellal (Kwon et al., 2010). Similarly, Orco and TRPA1 could act in the same ORNs to modulate food uptake.

The olfactory system seems to play a central role in bacterial detection in *D. melanogaster* (Depetris-Chauvin et al., 2017; Mansourian et al., 2016; Stensmyr et al., 2012). Intriguingly, in adult flies, the olfactory system mediates initial attraction toward *E.c.c.15* in double choice assays. However, in this case, the attraction is mediated by the receptor Gr63a (Charroux et al., 2020). Furthermore, the detection of bacteria via the olfactory system seems to be a conserved function. The worm *C.elegans* uses its olfactory system to avoid pathogenic bacteria such as *S.marcescens* or *P.aeruginosa* (Pradel et al., 2007; Zhang et al., 2005). Recently, it has been shown that mice olfactory neurons of the vomeronasal organ respond to bacterial-produced N-formylated peptides (Rivière et al., 2009). However, it still is not known how the detection of bacteria by mammal olfactory neurons could influence animal behavior.

In the second work (**Article 2**), we identified a population of few octopaminergic (Tdc2+) neurons in the brain VM cluster, which modulate egg-laying upon PGN exposure. These neurons also express PGRP-LB (pLB1+), a negative regulator of the IMD pathway, which buffers this response. Also, we showed that the pLB1+/Tdc2+ neurons modulated egg-laying via the IMD pathway. Calcium imaging experiments revealed that these neurons directly sense PGN. This recognition leads to a decrease in the cytoplasmic calcium, and thus we concluded that PGN inhibits these neurons. Previously it has been shown that the egg-laying drop is due to an accumulation of mature eggs in the ovaries (Kurz et al., 2017). We proposed that egg retention is likely caused by a defect in follicle cell trimming, a process mediated by octopamine and necessary for ovulation.
Some important questions remain still open and are of interest for future studies. The first unsolved point is how the PGN reaches the pLB1+/Tdc2+ neurons in the brain. We do not know yet if the PGN overcome the BBB or is sensed in peripheral nervous termini. However, the *ex vivo* PGN application in the fly brain triggers a calcium decrease, suggesting that the PGN is able to overcome the BBB. Interestingly, in mice, PGN traces are detectable in the developing brain of healthy animals. Moreover, PRRs, such as PGLYRP-2 and NOD-1 are expressed in the brain of mice during different postnatal development windows, suggesting a potential role for PGN in brain development. Furthermore, *PGLYRP-2* knockout mice show alteration in their social behavior similar to germ-free animals, suggesting a possible role of PGLYRP-2 -mediated PGN detection in behavior modulation (Arentsen et al., 2017). Further studies and, as well, the development of tools for PGN or/and PGN-PRRs detection are needed to understand how PGN overcomes the BBB. Another question pertains to the mechanism by which PGN is recognized by some octopaminergic neurons. We have previously shown that the intracellular receptor PGRP-LE is required for the egg-laying drop (Kurz et al., 2017). While we might expect that PGRP-LE-mediated PGN recognition

activates the IMD pathway in pLB1+/Tdc2+ neurons, we have not yet demonstrated that the same receptor is mediating the calcium response. Epistatic studies would clarify the role of PGRP-LE in the calcium response. Related to this point, we do not know yet how the IMD cascade and the calcium response in the identified neurons are linked. Another important question is how the activation of the IMD pathway modulates egg-laying behavior. NF-κB/ Relish transcription factor regulates the expression of hundreds of genes (De Gregorio et al., 2002). We hypothesized that this transcription factor might regulate the expression of the enzymes required for octopamine biosynthesis i.e. Tdc2 and Tβh. Importantly, when we knock down Tβh in pLB1 cells we observed a decrease in egg-laying, suggesting that octopamine decrease might lead to this phenotype. However, we were unable to detect canonical NF-kB binding sites on the upstream regulatory sequences of Tdc2 and Tβh. NF-κB/ Relish regulates the expression of AMPs, which function in the humoral immune response against pathogens. Recently, AMP expression in the fly brain has been implicated in behavior modulation (Barajas-Azpeleta et al., 2018; Dissel et al., 2015; Toda et al., 2019). We, however, excluded that AMPs are the NF-kB targets that induce an egg-laying drop post-infection. Indeed, infected females in which all AMPs have been deleted still presented an egg-laying drop post (data not shown in the article). Another important point to address is the identification of the neuronal circuit underlying PGN-dependent egg-laying decrease. Since we observed descending pLB1+/Tdc2+ fibers, one possibility would be that these fibers project in the VNC to synapse with downstream neurons, which will, in turn, modulate egg-laying. It would be important to know if the neuronal circuit which regulates egg-laying upon infection differs from the one which regulates egg-laying after mating (Wang et al., 2020). In the same context, it would be interesting to know whether there are upstream neurons to the pLB1+/Tdc2+ neurons. Moreover, the identified pLB1+/Tdc2+ neurons are not dimorphic, opening the possibility that they have a specific role in males.

The egg-laying retention of infected flies might represent an example of sickness behavior. The significance of this behavioral response remains unclear. By retaining their eggs, flies might save energy that they can devote to the immune response. In this context, it would be interesting to know whether the quality of the immune response is different when we abrogate the behavioral response to PGN. Another possibility is that flies might associate their infectious state with the presence of harmful bacteria in the surrounding environments. In this case, flies would retain their eggs to protect their offspring. The female infectious state could also impact the quality and survival of embryos. Studies on the "quality" of the offspring of infected flies would clarify this point.

Noteworthy is the role of octopamine in mediating microbe-host interactions. A recent study showed that xylose isomerase produced by the gut commensal *Lactobacillus brevis* modulates fly

locomotor activity by acting, through an unknown mechanism, in octopaminergic neurons (Schretter et al., 2018). Furthermore, octopamine seems to play a crucial role in the modulation of the immune response against pathogens. In some insects, *in vitro* studies have shown that octopamine enhances phagocytosis of pathogens, favoring their elimination (Baines and Downer, 1994; Diehl-Jones et al., 1996). In *C.elegans,* octopamine is a negative regulator of the immune response. However, in the presence of pathogenic bacteria such as *P.aeruginosa*, octopamine production is inhibited, leading to an increase in the expression of immune genes (Sellegounder et al., 2018). In mammals, norepinephrine, which is closely related to invertebrate octopamine, acts directly in immune cells such as macrophages and ILC2 cells and enhances pathogen clearance (Gabanyi et al., 2016; Matheis et al., 2020). Thus, octopamine might mediate host-pathogen interactions by modulating both the canonical immune response and the behavioral immune response. It would be interesting to test whether octopamine also controls the immune response in *D. melanogaster*.

An essential point of our results was that among the identified pLB1 neurons, only a subset is octopaminergic and regulates egg-laying. Indeed, other pLB1 and non-octopaminergic neurons were identified. This result prompted us to identify and characterize these cells (**Manuscript 3**). Some of them were housed in the fly labella, where taste sensory neurons (GRNs) are present. Electrophysiological studies demonstrated that some sensilla in the labellum respond to PGN. We showed that pLB1 neurons in the proboscis are a subpopulation of bitter Gr66a+ GRNs. *In vivo* calcium imaging showed that these neurons respond to PGN and that this response requires the PGN receptor PGRP-LC. Moreover, epistatic studies showed that the response of these pLB1+/Gr66a+ neurons to PGN depends on other elements of the IMD pathway, but, unexpectedly not on the transcription factor NF-κB/ Relish. Furthermore, we tested the response to PGN of sweet GRNs (Gr5a+) and we found that these neurons also respond to PGN. However, this response is independent of the IMD pathway. These results lead us to assess the effects of PGN detection by these neurons on the fly behavior. We showed that flies are attracted to high PGN concentrations, and this attraction is exacerbated in fly mutants for elements of the IMD pathway. This result suggests that the IMD pathway negatively modulates the attraction to PGN. Moreover, the inactivation of bitter neurons leads to an increased attraction towards PGN, suggesting that PGN detection by bitter neurons inhibits the preference for this bacterial compound. Since PGN detection in bitter neurons relies on some elements of the IMD pathway, we speculate that this pathway also modulates the behavioral response to PGN. However, while the knockdown of an element of the pathway (i.e. Fadd) in LB1+ cells caused a drastic decrease in the calcium response, it was not

sufficient to increase the attraction towards PGN. To solve this discrepancy between calcium and behavioral response, we are currently assessing the implication of the IMD pathway in the behavioral response with different tools. In our work, we also showed that the induction of the IMD pathway in Gr66a+ (but not in Gr5a+) neurons by overexpressing PGRP-LC triggers a decrease in egg-laying. Notably, it is known that bitter neurons in the labellum contact octopaminergic neurons in the VM to mediate aggression in males (Andrews et al., 2014). Since octopamine also regulates egg-laying, it would be interesting to identify the downstream neurons that modulate egg-laying. In this context, a future objective would be to identify the downstream neurons that modulate the feeding behavior towards PGN. Furthermore, it remains unclear how signals coming from two different types of GRNs that mediate opposite behaviors are integrated. Does this integration occur at the receptor level or in the CNS? Further work is needed to answer this important question. Also, we did not investigate whether only the pLB1+/Gr66a+ neurons are required for PGN sensing. A future point to investigate is whether pLB1-/Gr66a+ neurons respond to PGN. One surprising result of this project was that only part of the IMD pathway elements is implicated in both the calcium and the behavioral response to PGN, while the NF-κB/ Relish transcription factor is not. Notably, it has been shown that PGRP-LC together with other downstream elements of the IMD pathway is required for the modulation of the presynaptic homeostatic potentiation in neuromuscular junctions. This role is, in the short-term, independent from the transcription factor NF-κB/ Relish (Harris et al., 2018; N. Harris et al., 2015). These results suggest that part of this pathway may have acquired a specialized role in neurons, independently from its role in immune cells. Why gustatory neurons for different taste modalities have evolved two different mechanisms to sense PGN is also unclear. The identification of the receptor in sweet GRNs could help to clarify this point. The obvious suspects are the sugar gustatory receptors. Since the PGN backbone includes sugar moieties, PGN may be recognized by these receptors. In contrast, PGRPs are receptors specifically dedicated to the recognition of PGN and they recognize muropetides made of both disaccharidic and peptidic components. The competition for PGN recognition by these two types of neurons might be mediated by different receptors. At last, how PGN-dependent signaling might be integrated with other inputs is still unexplored. We predict that different bacterial cues are differently sensed by sensory neurons. For instance, bitter GRNs sensing of both *E.c.c.15* and bacterial LPS leads to aversive behavior (Charroux et al., 2020; Soldano et al., 2016). Thus, many other bacterial cues are sensed together with the PGN and the integration of these signals determines the fly behavior.

Here I showed different mechanisms by which bacterial detection modulate animals behavior. It has emerged that different neurons and pathways are implicated in the detection of bacterial cues and

trigger specific behaviors. Bacterial PGN is a unique signature of bacteria that is sensed by immune tissues and neurons. Detection by immune cells triggers the production of AMPs. Neuronal sensing of PGN leads to behavioral responses and might be fundamental for the animal to evaluate its internal state and the environment. PGN is detected by both octopaminergic neurons in the brain and by sensory taste neurons in the labella. Moreover, two classes of sensory taste neurons, associated with opposite behaviors, respond to PGN by potentially different molecular mechanisms. The detection of circulating PGN by neurons in the brain might inform the fly about its infectious state. Furthermore, the PGN detection in the environment, together with other bacterial cues, might be essential for the fly to evaluate feeding and/or oviposition site. Importantly, PGN detection in octopaminergic neurons and bitter GRNs is mediated by the IMD pathway, whereas PGN sensing in sweet GRNs does not require this pathway. Many points remain to be solved: how is the IMD pathway implicated with the calcium response in PGN sensing neurons? How are integrated PGN-related inputs coming from sweet and bitter GRNs? Which are the molecular actors involved in PGN detection in sweet GRNs? What is the reason for the different PGN detection mechanisms in bitter and sweet GRNs? These are some exciting questions for the future.

Bibliography

Adamo, S.A., 2006. Comparative psychoneuroimmunology: evidence from the insects. Behav. Cogn. Neurosci. Rev. 5, 128–140. https://doi.org/10.1177/1534582306289580

Adamo, S.A., Bartlett, A., Le, J., Spencer, N., Sullivan, K., 2010. Illness-induced anorexia may reduce trade-offs between digestion and immune function. Anim. Behav. 79, 3–10. https://doi.org/10.1016/j.anbehav.2009.10.012

Agaisse, H., Perrimon, N., 2004. The roles of JAK/STAT signaling in Drosophila immune responses. Immunol. Rev. 198, 72–82. https://doi.org/10.1111/j.0105-2896.2004.0133.x

Ai, M., Min, S., Grosjean, Y., Leblanc, C., Bell, R., Benton, R., Suh, G.S.B., 2010. Acid sensing by the Drosophila olfactory system. Nature 468, 691–695. https://doi.org/10.1038/nature09537

Ainsley, J.A., Pettus, J.M., Bosenko, D., Gerstein, C.E., Zinkevich, N., Anderson, M.G., Adams, C.M., Welsh, M.J., Johnson, W.A., 2003. Enhanced locomotion caused by loss of the Drosophila DEG/ENaC protein Pickpocket1. Curr. Biol. CB 13, 1557–1563. https://doi.org/10.1016/s0960-9822(03)00596-7

Al-Anzi, B., Tracey, W.D., Benzer, S., 2006. Response of Drosophila to Wasabi Is Mediated by painless, the Fly Homolog of Mammalian TRPA1/ANKTM1. Curr. Biol. 16, 1034–1040. https://doi.org/10.1016/j.cub.2006.04.002

Allen, A.M., Neville, M.C., Birtles, S., Croset, V., Treiber, C.D., Waddell, S., Goodwin, S.F., 2020. A single-cell transcriptomic atlas of the adult Drosophila ventral nerve cord. eLife 9, e54074. https://doi.org/10.7554/eLife.54074

Amrein, H., 2016. Chapter 14 - Mechanism of Taste Perception in Drosophila, in: Zufall, F., Munger, S.D. (Eds.), Chemosensory Transduction. Academic Press, pp. 245–269. https://doi.org/10.1016/B978-0-12-801694-7.00014-7

Amrein, H., Thorne, N., 2005. Gustatory Perception and Behavior in Drosophila melanogaster. Curr. Biol. 15, R673–R684. https://doi.org/10.1016/j.cub.2005.08.021

Anderson, K.V., Bokla, L., Nüsslein-Volhard, C., 1985a. Establishment of dorsal-ventral polarity in the drosophila embryo: The induction of polarity by the Toll gene product. Cell 42, 791–798. https://doi.org/10.1016/0092-8674(85)90275-2

Anderson, K.V., Jürgens, G., Nüsslein-Volhard, C., 1985b. Establishment of dorsal-ventral polarity in the Drosophila embryo: Genetic studies on the role of the Toll gene product. Cell 42, 779–789. https://doi.org/10.1016/0092-8674(85)90274-0

Andrews, J.C., Fernández, M.P., Yu, Q., Leary, G.P., Leung, A.K.W., Kavanaugh, M.P., Kravitz, E.A., Certel, S.J., 2014. Octopamine Neuromodulation Regulates Gr32a-Linked Aggression and Courtship Pathways in Drosophila Males. PLoS Genet. 10. https://doi.org/10.1371/journal.pgen.1004356

Arakawa, H., Cruz, S., Deak, T., 2011. From models to mechanisms: odorant communication as a key determinant of social behavior in rodents during illness-associated states. Neurosci. Biobehav. Rev. 35, 1916–1928. https://doi.org/10.1016/j.neubiorev.2011.03.007

Aranha, M.M., Vasconcelos, M.L., 2018. Deciphering Drosophila female innate behaviors. Curr. Opin. Neurobiol., Systems Neuroscience 52, 139–148. https://doi.org/10.1016/j.conb.2018.06.005

Arentsen, T., Qian, Y., Gkotzis, S., Femenia, T., Wang, T., Udekwu, K., Forssberg, H., Diaz Heijtz, R., 2017. The bacterial peptidoglycan-sensing molecule Pglyrp2 modulates brain development and behavior. Mol. Psychiatry 22, 257–266. https://doi.org/10.1038/mp.2016.182

Avila, F.W., Qazi, M.C.B., Rubinstein, C.D., Wolfner, M.F., 2012. A requirement for the neuromodulators octopamine and tyramine in Drosophila melanogaster female sperm storage. Proc. Natl. Acad. Sci. 109, 4562–4567. https://doi.org/10.1073/pnas.1117689109

Bacon, J.P., Thompson, K.S., Stern, M., 1995. Identified octopaminergic neurons provide an arousal mechanism in the locust brain. J. Neurophysiol. 74, 2739–2743. https://doi.org/10.1152/jn.1995.74.6.2739

Baines, D., Downer, R.G., 1994. Octopamine enhances phagocytosis in cockroach hemocytes: involvement of inositol trisphosphate. Arch. Insect Biochem. Physiol. 26, 249–261. https://doi.org/10.1002/arch.940260402

Balfanz, S., Strünker, T., Frings, S., Baumann, A., 2005. A family of octopamine [corrected] receptors that specifically induce cyclic AMP production or Ca2+ release in Drosophila melanogaster. J. Neurochem. 93, 440–451. https://doi.org/10.1111/j.1471-4159.2005.03034.x

Banerjee, U., Girard, J.R., Goins, L.M., Spratford, C.M., 2019. Drosophila as a Genetic Model for Hematopoiesis. Genetics 211, 367–417. https://doi.org/10.1534/genetics.118.300223

Bangham, J., Jiggins, F., Lemaitre, B., 2006. Insect Immunity: The Post-Genomic Era. Immunity 25, 1–5. https://doi.org/10.1016/j.immuni.2006.07.002

Barajas-Azpeleta, R., Wu, J., Gill, J., Welte, R., Seidel, C., McKinney, S., Dissel, S., Si, K., 2018. Antimicrobial peptides modulate long-term memory. PLoS Genet 14, e1007440. https://doi.org/10.1371/journal.pgen.1007440

Basbous, N., Coste, F., Leone, P., Vincentelli, R., Royet, J., Kellenberger, C., Roussel, A., 2011. The Drosophila peptidoglycan-recognition protein LF interacts with peptidoglycan-recognition protein LC to downregulate the Imd pathway. EMBO Rep. 12, 327–333. https://doi.org/10.1038/embor.2011.19

Basset, A., Khush, R.S., Braun, A., Gardan, L., Boccard, F., Hoffmann, J.A., Lemaitre, B., 2000. The phytopathogenic bacteria Erwinia carotovora infects Drosophila and activates an immune response. Proc. Natl. Acad. Sci. 97, 3376–3381. https://doi.org/10.1073/pnas.97.7.3376

Belvin, M.P., Jin, Y., Anderson, K.V., 1995. Cactus protein degradation mediates Drosophila dorsal-ventral signaling. Genes Dev. 9, 783–793. https://doi.org/10.1101/gad.9.7.783

Benton, R., Vannice, K.S., Gomez-Diaz, C., Vosshall, L.B., 2009. Variant ionotropic glutamate receptors as chemosensory receptors in Drosophila. Cell 136, 149–162. https://doi.org/10.1016/j.cell.2008.12.001

Beshel, J., Zhong, Y., 2013. Graded Encoding of Food Odor Value in the Drosophila Brain. J. Neurosci. 33, 15693–15704. https://doi.org/10.1523/JNEUROSCI.2605-13.2013

Bischoff, V., Vignal, C., Duvic, B., Boneca, I.G., Hoffmann, J.A., Royet, J., 2006. Downregulation of the Drosophila Immune Response by Peptidoglycan-Recognition Proteins SC1 and SC2. PLOS Pathog. 2, e14. https://doi.org/10.1371/journal.ppat.0020014

Boillat, M., Challet, L., Rossier, D., Kan, C., Carleton, A., Rodriguez, I., 2015. The vomeronasal system mediates sick conspecific avoidance. Curr. Biol. CB 25, 251–255. https://doi.org/10.1016/j.cub.2014.11.061

Boman, H.G., Nilsson, I., Rasmuson, B., 1972. Inducible Antibacterial Defence System in Drosophila. Nature 237, 232–235. https://doi.org/10.1038/237232a0

Bos, N., Lefèvre, T., Jensen, A.B., d'Ettorre, P., 2012. Sick ants become unsociable. J. Evol. Biol. 25, 342–351. https://doi.org/10.1111/j.1420-9101.2011.02425.x

Bosco-Drayon, V., Poidevin, M., Boneca, I.G., Narbonne-Reveau, K., Royet, J., Charroux, B., 2012. Peptidoglycan Sensing by the Receptor PGRP-LE in the Drosophila Gut Induces Immune Responses to Infectious Bacteria and Tolerance to Microbiota. Cell Host Microbe 12, 153–165. https://doi.org/10.1016/j.chom.2012.06.002

Braunig, null, 1997. The peripheral branching pattern of identified dorsal unpaired median (DUM) neurones of the locust. Cell Tissue Res. 290, 641–654. https://doi.org/10.1007/s004410050970

Bräunig, P., Burrows, M., 2004. Projection patterns of posterior dorsal unpaired median neurons of the locust subesophageal ganglion. J. Comp. Neurol. 478, 164–175. https://doi.org/10.1002/cne.20287

Bray, S., Amrein, H., 2003. A Putative Drosophila Pheromone Receptor Expressed in Male-Specific Taste Neurons Is Required for Efficient Courtship. Neuron 39, 1019–1029. https://doi.org/10.1016/S0896-6273(03)00542-7

Brown, L., Wolf, J.M., Prados-Rosales, R., Casadevall, A., 2015. Through the wall: extracellular vesicles in Gram-positive bacteria, mycobacteria and fungi. Nat. Rev. Microbiol. 13, 620–630. https://doi.org/10.1038/nrmicro3480

Brunet Avalos, C., Maier, G.L., Bruggmann, R., Sprecher, S.G., 2019. Single cell transcriptome atlas of the Drosophila larval brain. eLife 8, e50354. https://doi.org/10.7554/eLife.50354

Buchon, N., Broderick, N.A., Chakrabarti, S., Lemaitre, B., 2009. Invasive and indigenous microbiota impact intestinal stem cell activity through multiple pathways in Drosophila. Genes Dev. 23, 2333–2344. https://doi.org/10.1101/gad.1827009

Burke, C.J., Huetteroth, W., Owald, D., Perisse, E., Krashes, M.J., Das, G., Gohl, D., Silies, M., Certel, S., Waddell, S., 2012. Layered reward signalling through octopamine and dopamine in Drosophila. Nature 492, 433–437. https://doi.org/10.1038/nature11614

Busch, S., Selcho, M., Ito, K., Tanimoto, H., 2009. A map of octopaminergic neurons in the Drosophila brain. J. Comp. Neurol. 513, 643–667. https://doi.org/10.1002/cne.21966

Busch, S., Tanimoto, H., 2010. Cellular configuration of single octopamine neurons in Drosophila. J. Comp. Neurol. 518, 2355–2364. https://doi.org/10.1002/cne.22337

Cameron, P., Hiroi, M., Ngai, J., Scott, K., 2010. The molecular basis for water taste in Drosophila. Nature 465, 91–95. https://doi.org/10.1038/nature09011

Cao, Y., Chtarbanova, S., Petersen, A.J., Ganetzky, B., 2013. Dnr1 mutations cause neurodegeneration in Drosophila by activating the innate immune response in the brain. Proc Natl Acad Sci U A 110, E1752-60. https://doi.org/10.1073/pnas.1306220110

Capo, F., Chaduli, D., Viallat-Lieutaud, A., Charroux, B., Royet, J., 2017. Oligopeptide Transporters of the SLC15 Family Are Dispensable for Peptidoglycan Sensing and Transport in ***Drosophila***. J. Innate Immun. 9, 483–492. https://doi.org/10.1159/000475771

Cardoso, V., Chesné, J., Ribeiro, H., García-Cassani, B., Carvalho, T., Bouchery, T., Shah, K., Barbosa-Morais, N.L., Harris, N., Veiga-Fernandes, H., 2017. Neuronal regulation of type 2 innate lymphoid cells via neuromedin U. Nature 549, 277–281. https://doi.org/10.1038/nature23469

Caruso, R., Warner, N., Inohara, N., Núñez, G., 2014. NOD1 and NOD2: signaling, host defense, and inflammatory disease. Immunity 41, 898–908. https://doi.org/10.1016/j.immuni.2014.12.010

Chamaillard, M., Hashimoto, M., Horie, Y., Masumoto, J., Qiu, S., Saab, L., Ogura, Y., Kawasaki, A., Fukase, K., Kusumoto, S., Valvano, M.A., Foster, S.J., Mak, T.W., Nuñez, G., Inohara, N., 2003. An essential role for NOD1 in host recognition of bacterial peptidoglycan containing diaminopimelic acid. Nat. Immunol. 4, 702–707. https://doi.org/10.1038/ni945

Chandrashekar, J., Hoon, M.A., Ryba, N.J.P., Zuker, C.S., 2006. The receptors and cells for mammalian taste. Nature 444, 288–294. https://doi.org/10.1038/nature05401

Chang, C.-I., Chelliah, Y., Borek, D., Mengin-Lecreulx, D., Deisenhofer, J., 2006. Structure of Tracheal Cytotoxin in Complex with a Heterodimeric Pattern-Recognition Receptor. Science 311, 1761–1764. https://doi.org/10.1126/science.1123056

Charlu, S., Wisotsky, Z., Medina, A., Dahanukar, A., 2013. Acid sensing by sweet and bitter taste neurons in Drosophila melanogaster. Nat. Commun. 4, 2042. https://doi.org/10.1038/ncomms3042

Charrière, G.M., Ip, W.E., Dejardin, S., Boyer, L., Sokolovska, A., Cappillino, M.P., Cherayil, B.J., Podolsky, D.K., Kobayashi, K.S., Silverman, N., Lacy-Hulbert, A., Stuart, L.M., 2010. Identification of Drosophila Yin and PEPT2 as Evolutionarily Conserved Phagosome-associated Muramyl Dipeptide Transporters. J. Biol. Chem. 285, 20147–20154. https://doi.org/10.1074/jbc.M110.115584

Charroux, B., Capo, F., Kurz, C.L., Peslier, S., Chaduli, D., Viallat-lieutaud, A., Royet, J., 2018. Cytosolic and Secreted Peptidoglycan-Degrading Enzymes in Drosophila Respectively Control Local and Systemic Immune Responses to Microbiota. Cell Host Microbe 23, 215-228.e4. https://doi.org/10.1016/j.chom.2017.12.007

Charroux, B., Daian, F., Royet, J., 2020. Drosophila Aversive Behavior toward Erwinia carotovora carotovora Is Mediated by Bitter Neurons and Leukokinin. iScience 23, 101152. https://doi.org/10.1016/j.isci.2020.101152

Charroux, B., Rival, T., Narbonne-Reveau, K., Royet, J., 2009. Bacterial detection by Drosophila peptidoglycan recognition proteins. Microbes Infect. 11, 631–636. https://doi.org/10.1016/j.micinf.2009.03.004

Chen, Y., Amrein, H., 2014. Enhancing perception of contaminated food through acid-mediated modulation of taste neuron responses. Curr. Biol. CB 24, 1969–1977. https://doi.org/10.1016/j.cub.2014.07.069

Chen, Y.-C.D., Dahanukar, A., 2020. Recent advances in the genetic basis of taste detection in Drosophila. Cell. Mol. Life Sci. 77, 1087–1101. https://doi.org/10.1007/s00018-019-03320-0

Chen, Y.-C.D., Dahanukar, A., 2017. Molecular and Cellular Organization of Taste Neurons in Adult Drosophila Pharynx. Cell Rep. 21, 2978–2991. https://doi.org/10.1016/j.celrep.2017.11.041

Chen, Z., Wang, Q., Wang, Z., 2010. The Amiloride-Sensitive Epithelial Na+ Channel PPK28 Is Essential for Drosophila Gustatory Water Reception. J. Neurosci. 30, 6247–6252. https://doi.org/10.1523/JNEUROSCI.0627-10.2010

Chiu, I.M., Heesters, B.A., Ghasemlou, N., Von Hehn, C.A., Zhao, F., Tran, J., Wainger, B., Strominger, A., Muralidharan, S., Horswill, A.R., Bubeck Wardenburg, J., Hwang, S.W., Carroll, M.C., Woolf, C.J., 2013. Bacteria activate sensory neurons that modulate pain and inflammation. Nature 501, 52–57. https://doi.org/10.1038/nature12479

Chiu, I.M., von Hehn, C.A., Woolf, C.J., 2012. Neurogenic inflammation and the peripheral nervous system in host defense and immunopathology. Nat. Neurosci. 15, 1063–1067. https://doi.org/10.1038/nn.3144

Cho, B., Spratford, C.M., Yoon, S., Cha, N., Banerjee, U., Shim, J., 2018. Systemic control of immune cell development by integrated carbon dioxide and hypoxia chemosensation in Drosophila. Nat Commun 9, 2679. https://doi.org/10.1038/s41467-018-04990-3

Choe, K.-M., 2002. Requirement for a Peptidoglycan Recognition Protein (PGRP) in Relish Activation and Antibacterial Immune Responses in Drosophila. Science 296, 359–362. https://doi.org/10.1126/science.1070216

Christiaens, J.F., Franco, L.M., Cools, T.L., De Meester, L., Michiels, J., Wenseleers, T., Hassan, B.A., Yaksi, E., Verstrepen, K.J., 2014. The fungal aroma gene ATF1 promotes dispersal of yeast cells through insect vectors. Cell Rep 9, 425–32. https://doi.org/10.1016/j.celrep.2014.09.009

Chu, B., Chui, V., Mann, K., Gordon, M.D., 2014. Presynaptic Gain Control Drives Sweet and Bitter Taste Integration in Drosophila. Curr. Biol. 24, 1978–1984. https://doi.org/10.1016/j.cub.2014.07.020

Chu, C., Artis, D., Chiu, I.M., 2020. Neuro-immune Interactions in the Tissues. Immunity 52, 464–474. https://doi.org/10.1016/j.immuni.2020.02.017

Clemmons, A.W., Lindsay, S.A., Wasserman, S.A., 2015. An Effector Peptide Family Required for Drosophila Toll-Mediated Immunity. PLOS Pathog. 11, e1004876. https://doi.org/10.1371/journal.ppat.1004876

Cloud-Hansen, K.A., Peterson, S.B., Stabb, E.V., Goldman, W.E., McFall-Ngai, M.J., Handelsman, J., 2006. Breaching the great wall: peptidoglycan and microbial interactions. Nat. Rev. Microbiol. 4, 710–716. https://doi.org/10.1038/nrmicro1486

Clyne, P.J., Warr, C.G., Carlson, J.R., 2000. Candidate Taste Receptors in Drosophila. Science 287, 1830–1834. https://doi.org/10.1126/science.287.5459.1830

Cole, S.H., Carney, G.E., McClung, C.A., Willard, S.S., Taylor, B.J., Hirsh, J., 2005. Two Functional but Noncomplementing Drosophila Tyrosine Decarboxylase Genes DISTINCT ROLES FOR NEURAL TYRAMINE AND OCTOPAMINE IN FEMALE FERTILITY. J. Biol. Chem. 280, 14948–14955. https://doi.org/10.1074/jbc.M414197200

Corfas, G., Dudai, Y., 1989. Habituation and dishabituation of a cleaning reflex in normal and mutant Drosophila. J. Neurosci. 9, 56–62. https://doi.org/10.1523/JNEUROSCI.09-01-00056.1989

Court, R., Namiki, S., Armstrong, J.D., Börner, J., Card, G., Costa, M., Dickinson, M., Duch, C., Korff, W., Mann, R., Merritt, D., Murphey, R.K., Seeds, A., Shirangi, T., Simpson, J.H., Truman, J.W., Tuthill, J., Williams, D., Shepherd, D., 2020. A Systematic Nomenclature for the Drosophila Ventral Nervous System. bioRxiv 122952. https://doi.org/10.1101/122952

Crocker, A., Sehgal, A., 2008. Octopamine regulates sleep in drosophila through protein kinase A-dependent mechanisms. J. Neurosci. Off. J. Soc. Neurosci. 28, 9377–9385. https://doi.org/10.1523/JNEUROSCI.3072-08a.2008

Croset, V., Schleyer, M., Arguello, J.R., Gerber, B., Benton, R., 2016. A molecular and neuronal basis for amino acid sensing in the Drosophila larva. Sci. Rep. 6, 34871. https://doi.org/10.1038/srep34871

Cui, M., Jiang, P., Maillet, E., Max, M., Margolskee, R.F., Osman, R., 2006. The heterodimeric sweet taste receptor has multiple potential ligand binding sites. Curr. Pharm. Des. 12, 4591–4600. https://doi.org/10.2174/138161206779010350

Dahanukar, A., Foster, K., van der Goes van Naters, W.M., Carlson, J.R., 2001. A Gr receptor is required for response to the sugar trehalose in taste neurons of Drosophila. Nat. Neurosci. 4, 1182–1186. https://doi.org/10.1038/nn765

Dahanukar, A., Lei, Y.-T., Kwon, J.Y., Carlson, J.R., 2007. Two Gr genes underlie sugar reception in Drosophila. Neuron 56, 503–516. https://doi.org/10.1016/j.neuron.2007.10.024

Dantzer, R., 2001. Cytokine-Induced Sickness Behavior: Where Do We Stand? Brain. Behav. Immun. 15, 7–24. https://doi.org/10.1006/brbi.2000.0613

Dantzer, R., O'Connor, J.C., Freund, G.G., Johnson, R.W., Kelley, K.W., 2008. From inflammation to sickness and depression: when the immune system subjugates the brain. Nat. Rev. Neurosci. 9, 46–56. https://doi.org/10.1038/nrn2297

Davie, K., Janssens, J., Koldere, D., De Waegeneer, M., Pech, U., Kreft, Ł., Aibar, S., Makhzami, S., Christiaens, V., Bravo González-Blas, C., Poovathingal, S., Hulselmans, G., Spanier, K.I., Moerman, T., Vanspauwen, B., Geurs, S., Voet, T., Lammertyn, J., Thienpont, B., Liu, S., Konstantinides, N., Fiers, M., Verstreken, P., Aerts, S., 2018. A Single-Cell Transcriptome Atlas of the Aging Drosophila Brain. Cell 174, 982-998.e20. https://doi.org/10.1016/j.cell.2018.05.057

De Gregorio, E., Spellman, P.T., Tzou, P., Rubin, G.M., Lemaitre, B., 2002. The Toll and Imd pathways are the major regulators of the immune response in Drosophila. EMBO J. 21, 2568–2579. https://doi.org/10.1093/emboj/21.11.2568

de Roode, J.C., Lefevre, T., 2012. Behavioral Immunity in Insects. Insects 3, 789–820. https://doi.org/10.3390/insects3030789

Deady, L.D., Shen, W., Mosure, S.A., Spradling, A.C., Sun, J., 2015. Matrix Metalloproteinase 2 Is Required for Ovulation and Corpus Luteum Formation in Drosophila. PLOS Genet. 11, e1004989. https://doi.org/10.1371/journal.pgen.1004989

Deady, L.D., Sun, J., 2015. A Follicle Rupture Assay Reveals an Essential Role for Follicular Adrenergic Signaling in Drosophila Ovulation. PLOS Genet. 11, e1005604. https://doi.org/10.1371/journal.pgen.1005604

Delventhal, R., Carlson, J.R., 2016. Bitter taste receptors confer diverse functions to neurons. eLife 5, e11181. https://doi.org/10.7554/eLife.11181

Depetris-Chauvin, A., Galagovsky, D., Chevalier, C., Maniere, G., Grosjean, Y., 2017. Olfactory detection of a bacterial short-chain fatty acid acts as an orexigenic signal in Drosophila melanogaster larvae. Sci Rep 7, 14230. https://doi.org/10.1038/s41598-017-14589-1

Diehl-Jones, W.L., Mandato, C.A., Whent, G., Downer, R.G.H., 1996. Monoaminergic regulation of hemocyte activity. J. Insect Physiol., Mediators of Insect Immunity 42, 13–19. https://doi.org/10.1016/0022-1910(95)00078-X

Diogenes, A., Ferraz, C.C.R., Akopian, A.N., Henry, M.A., Hargreaves, K.M., 2011. LPS sensitizes TRPV1 via activation of TLR4 in trigeminal sensory neurons. J. Dent. Res. 90, 759–764. https://doi.org/10.1177/0022034511400225

Dissel, S., Seugnet, L., Thimgan, M.S., Silverman, N., Angadi, V., Thacher, P.V., Burnham, M.M., Shaw, P.J., 2015. Differential activation of immune factors in neurons and glia contribute to individual differences in resilience/vulnerability to sleep disruption. Brain Behav Immun 47, 75–85. https://doi.org/10.1016/j.bbi.2014.09.019

Donnelly, C.R., Chen, O., Ji, R.-R., 2020. How Do Sensory Neurons Sense Danger Signals? Trends Neurosci. https://doi.org/10.1016/j.tins.2020.07.008

Doyle, R.J., Chaloupka, J., Vinter, V., 1988. Turnover of cell walls in microorganisms. Microbiol. Rev. 52, 554–567.

Du, E.J., Ahn, T.J., Kwon, I., Lee, J.H., Park, J.-H., Park, S.H., Kang, T.M., Cho, H., Kim, T.J., Kim, H.-W., Jun, Y., Lee, H.J., Lee, Y.S., Kwon, J.Y., Kang, K., 2016. TrpA1 Regulates Defecation of Food-Borne Pathogens under the Control of the Duox Pathway. PLOS Genet. 12, e1005773. https://doi.org/10.1371/journal.pgen.1005773

Dubnau, J., Tully, T., 1998. GENE DISCOVERY IN DROSOPHILA: New Insights for Learning and Memory. Annu. Rev. Neurosci. 21, 407–444. https://doi.org/10.1146/annurev.neuro.21.1.407

Dunipace, L., Meister, S., McNealy, C., Amrein, H., 2001. Spatially restricted expression of candidate taste receptors in the Drosophila gustatory system. Curr. Biol. CB 11, 822–835. https://doi.org/10.1016/s0960-9822(01)00258-5

Dweck, H.K.M., Ebrahim, S.A.M., Retzke, T., Grabe, V., Weißflog, J., Svatoš, A., Hansson, B.S., Knaden, M., 2018. The Olfactory Logic behind Fruit Odor Preferences in Larval and Adult Drosophila. Cell Rep. 23, 2524–2531. https://doi.org/10.1016/j.celrep.2018.04.085

Dziarski, R., Gupta, D., 2005. Staphylococcus aureus Peptidoglycan Is a Toll-Like Receptor 2 Activator: a Reevaluation. Infect. Immun. 73, 5212–5216. https://doi.org/10.1128/IAI.73.8.5212-5216.2005

Dziarski, R., Platt, K.A., Gelius, E., Steiner, H., Gupta, D., 2003. Defect in neutrophil killing and increased susceptibility to infection with nonpathogenic gram-positive bacteria in peptidoglycan recognition protein-S (PGRP-S)-deficient mice. Blood 102, 689–697. https://doi.org/10.1182/blood-2002-12-3853

Dziarski, R., Tapping, R.I., Tobias, P.S., 1998. Binding of bacterial peptidoglycan to CD14. J. Biol. Chem. 273, 8680–8690. https://doi.org/10.1074/jbc.273.15.8680

Dziedziech, A., Shivankar, S., Theopold, U., 2020. Drosophila melanogaster Responses against Entomopathogenic Nematodes: Focus on Hemolymph Clots. Insects 11, 62. https://doi.org/10.3390/insects11010062

E, L., Zhou, T., Koh, S., Chuang, M., Sharma, R., Pujol, N., Chisholm, A.D., Eroglu, C., Matsunami, H., Yan, D., 2018. An Antimicrobial Peptide and Its Neuronal Receptor Regulate Dendrite Degeneration in Aging and Infection. Neuron 97, 125-138 e5. https://doi.org/10.1016/j.neuron.2017.12.001

El-Kholy, S., Stephano, F., Li, Y., Bhandari, A., Fink, C., Roeder, T., 2015. Expression analysis of octopamine and tyramine receptors in Drosophila. Cell Tissue Res. 361, 669–684. https://doi.org/10.1007/s00441-015-2137-4

Elya, C., Lok, T.C., Spencer, Q.E., McCausland, H., Martinez, C.C., Eisen, M., 2018. Robust manipulation of the behavior of Drosophila melanogaster by a fungal pathogen in the laboratory. Elife 7. https://doi.org/10.7554/eLife.34414

Enjin, A., Zaharieva, E.E., Frank, D.D., Mansourian, S., Suh, G.S.B., Gallio, M., Stensmyr, M.C., 2016. Humidity sensing in Drosophila. Curr. Biol. CB 26, 1352–1358. https://doi.org/10.1016/j.cub.2016.03.049

Erspamer, V., Boretti, G., 1951. Identification and characterization, by paper chromatography, of enteramine, octopamine, tyramine, histamine and allied substances in extracts of posterior salivary glands of octopoda and in other tissue extracts of vertebrates and invertebrates. Arch. Int. Pharmacodyn. Ther. 88, 296–332.

Ertürk-Hasdemir, D., Broemer, M., Leulier, F., Lane, W.S., Paquette, N., Hwang, D., Kim, C.-H., Stöven, S., Meier, P., Silverman, N., 2009. Two roles for the Drosophila IKK complex in the activation of Relish and the

induction of antimicrobial peptide genes. Proc. Natl. Acad. Sci. U. S. A. 106, 9779–9784. https://doi.org/10.1073/pnas.0812022106

Falk, R., Bleiser-Avivi, N., Atidia, J., 1976. Labellar taste organs of Drosophila melanogaster. J. Morphol. 150, 327–341. https://doi.org/10.1002/jmor.1051500206

Feng, K., Palfreyman, M.T., Häsemeyer, M., Talsma, A., Dickson, B.J., 2014. Ascending SAG Neurons Control Sexual Receptivity of Drosophila Females. Neuron 83, 135–148. https://doi.org/10.1016/j.neuron.2014.05.017

Ferrandon, D., Imler, J.-L., Hetru, C., Hoffmann, J.A., 2007. The Drosophila systemic immune response: sensing and signalling during bacterial and fungal infections. Nat. Rev. Immunol. 7, 862–874. https://doi.org/10.1038/nri2194

Ferrandon, D., Jung, A.C., Criqui, M., Lemaitre, B., Uttenweiler-Joseph, S., Michaut, L., Reichhart, J., Hoffmann, J.A., 1998. A drosomycin-GFP reporter transgene reveals a local immune response in Drosophila that is not dependent on the Toll pathway. EMBO J. 17, 1217–1227. https://doi.org/10.1093/emboj/17.5.1217

Ferraz, C.C.R., Diógenes, A., Henry, M.A., Hargreaves, K.M., 2011. LPS from Porphyromonas gingivalis Sensitizes Capsaicin-Sensitive Nociceptors. J. Endod. 37, 45–48. https://doi.org/10.1016/j.joen.2007.07.001

Fields, P.E., Woodring, J.P., 1991. Octopamine mobilization of lipids and carbohydrates in the house cricket, Acheta domesticus. J. Insect Physiol. 37, 193–199. https://doi.org/10.1016/0022-1910(91)90069-C

Fischer, C.N., Trautman, E.P., Crawford, J.M., Stabb, E.V., Handelsman, J., Broderick, N.A., 2017. Metabolite exchange between microbiome members produces compounds that influence Drosophila behavior. Elife 6. https://doi.org/10.7554/eLife.18855

Flood, T.F., Iguchi, S., Gorczyca, M., White, B., Ito, K., Yoshihara, M., 2013. A single pair of interneurons commands the Drosophila feeding motor program. Nature 499, 83–87. https://doi.org/10.1038/nature12208

Foster, J.A., McVey Neufeld, K.-A., 2013. Gut–brain axis: how the microbiome influences anxiety and depression. Trends Neurosci. 36, 305–312. https://doi.org/10.1016/j.tins.2013.01.005

Fowler, M.A., Montell, C., 2013. Drosophila TRP channels and animal behavior. Life Sci. 92, 394–403. https://doi.org/10.1016/j.lfs.2012.07.029

Freeman, E.G., Wisotsky, Z., Dahanukar, A., 2014. Detection of sweet tastants by a conserved group of insect gustatory receptors. Proc. Natl. Acad. Sci. U. S. A. 111, 1598–1603. https://doi.org/10.1073/pnas.1311724111

Freeman, M.R., 2015. *Drosophila* Central Nervous System Glia. Cold Spring Harb. Perspect. Biol. 7, a020552. https://doi.org/10.1101/cshperspect.a020552

French, A.S., Sellier, M.-J., Agha, M.A., Guigue, A., Chabaud, M.-A., Reeb, P.D., Mitra, A., Grau, Y., Soustelle, L., Marion-Poll, F., 2015. Dual Mechanism for Bitter Avoidance in Drosophila. J. Neurosci. 35, 3990–4004. https://doi.org/10.1523/JNEUROSCI.1312-14.2015

Fujii, S., Yavuz, A., Slone, J., Jagge, C., Song, X., Amrein, H., 2015. Drosophila Sugar Receptors in Sweet Taste Perception, Olfaction, and Internal Nutrient Sensing. Curr. Biol. 25, 621–627. https://doi.org/10.1016/j.cub.2014.12.058

Gabanyi, I., Muller, P.A., Feighery, L., Oliveira, T.Y., Costa-Pinto, F.A., Mucida, D., 2016. Neuro-immune Interactions Drive Tissue Programming in Intestinal Macrophages. Cell 164, 378–391. https://doi.org/10.1016/j.cell.2015.12.023

Ganguly, A., Pang, L., Duong, V.-K., Lee, A., Schoniger, H., Varady, E., Dahanukar, A., 2017. A Molecular and Cellular Context-Dependent Role for Ir76b in Detection of Amino Acid Taste. Cell Rep. 18, 737–750. https://doi.org/10.1016/j.celrep.2016.12.071

Garver, L.S., Wu, J., Wu, L.P., 2006. The peptidoglycan recognition protein PGRP-SC1a is essential for Toll signaling and phagocytosis of Staphylococcus aureus in Drosophila. Proc. Natl. Acad. Sci. U. S. A. 103, 660–665. https://doi.org/10.1073/pnas.0506182103

Gendrin, M., Welchman, D.P., Poidevin, M., Hervé, M., Lemaitre, B., 2009. Long-Range Activation of Systemic Immunity through Peptidoglycan Diffusion in Drosophila. PLOS Pathog. 5, e1000694. https://doi.org/10.1371/journal.ppat.1000694

Georgel, P., Kappler, C., Langley, E., Gross, I., Nicolas, E., Reichhart, J.M., Hoffmann, J.A., 1995. Drosophila immunity. A sequence homologous to mammalian interferon consensus response element enhances the activity of the diptericin promoter. Nucleic Acids Res. 23, 1140–1145.

Georgel, P., Naitza, S., Kappler, C., Ferrandon, D., Zachary, D., Swimmer, C., Kopczynski, C., Duyk, G., Reichhart, J.-M., Hoffmann, J.A., 2001. Drosophila Immune Deficiency (IMD) Is a Death Domain Protein that Activates Antibacterial Defense and Can Promote Apoptosis. Dev. Cell 1, 503–514. https://doi.org/10.1016/S1534-5807(01)00059-4

Girardin, S.E., Boneca, I.G., Carneiro, L.A.M., Antignac, A., Jéhanno, M., Viala, J., Tedin, K., Taha, M.-K., Labigne, A., Zähringer, U., Coyle, A.J., DiStefano, P.S., Bertin, J., Sansonetti, P.J., Philpott, D.J., 2003. Nod1 detects a unique muropeptide from gram-negative bacterial peptidoglycan. Science 300, 1584–1587. https://doi.org/10.1126/science.1084677

Gobert, V., Gottar, M., Matskevich, A.A., Rutschmann, S., Royet, J., Belvin, M., Hoffmann, J.A., Ferrandon, D., 2003. Dual Activation of the Drosophila Toll Pathway by Two Pattern Recognition Receptors. Science 302, 2126–2130. https://doi.org/10.1126/science.1085432

Godinho-Silva, C., Cardoso, F., Veiga-Fernandes, H., 2019. Neuro–Immune Cell Units: A New Paradigm in Physiology. Annu. Rev. Immunol. 37, 19–46. https://doi.org/10.1146/annurev-immunol-042718-041812

Goldstein, D.S., 2010. Adrenal Responses to Stress. Cell. Mol. Neurobiol. 30, 1433–1440. https://doi.org/10.1007/s10571-010-9606-9

Gottar, M., Gobert, V., Matskevich, A.A., Reichhart, J.-M., Wang, C., Butt, T.M., Belvin, M., Hoffmann, J.A., Ferrandon, D., 2006. Dual Detection of Fungal Infections in Drosophila via Recognition of Glucans and Sensing of Virulence Factors. Cell 127, 1425–1437. https://doi.org/10.1016/j.cell.2006.10.046

Guntur, A.R., Gou, B., Gu, P., He, R., Stern, U., Xiang, Y., Yang, C.-H., 2017. H2O2-Sensitive Isoforms of Drosophila melanogaster TRPA1 Act in Bitter-Sensing Gustatory Neurons to Promote Avoidance of UV During Egg-Laying. Genetics 205, 749–759. https://doi.org/10.1534/genetics.116.195172

Gupta, D., Kirkland, T.N., Viriyakosol, S., Dziarski, R., 1996. CD14 Is a Cell-activating Receptor for Bacterial Peptidoglycan. J. Biol. Chem. 271, 23310–23316. https://doi.org/10.1074/jbc.271.38.23310

Ha, E.-M., Lee, K.-A., Park, S.H., Kim, S.-H., Nam, H.-J., Lee, H.-Y., Kang, D., Lee, W.-J., 2009a. Regulation of DUOX by the Gαq-Phospholipase Cβ-Ca2+ Pathway in Drosophila Gut Immunity. Dev. Cell 16, 386–397. https://doi.org/10.1016/j.devcel.2008.12.015

Ha, E.-M., Lee, K.-A., Seo, Y.Y., Kim, S.-H., Lim, J.-H., Oh, B.-H., Kim, J., Lee, W.-J., 2009b. Coordination of multiple dual oxidase–regulatory pathways in responses to commensal and infectious microbes in drosophila gut. Nat. Immunol. 10, 949–957. https://doi.org/10.1038/ni.1765

Ha, E.-M., Oh, C.-T., Bae, Y.S., Lee, W.-J., 2005a. A Direct Role for Dual Oxidase in Drosophila Gut Immunity. Science 310, 847–850. https://doi.org/10.1126/science.1117311

Ha, E.-M., Oh, C.-T., Ryu, J.-H., Bae, Y.-S., Kang, S.-W., Jang, I., Brey, P.T., Lee, W.-J., 2005b. An Antioxidant System Required for Host Protection against Gut Infection in Drosophila. Dev. Cell 8, 125–132. https://doi.org/10.1016/j.devcel.2004.11.007

Hall, J.C., 2003. Genetics and molecular biology of rhythms in Drosophila and other insects. Adv. Genet. 48, 1–280. https://doi.org/10.1016/s0065-2660(03)48000-0

Hanson, M.A., Dostálová, A., Ceroni, C., Poidevin, M., Kondo, S., Lemaitre, B., 2019. Synergy and remarkable specificity of antimicrobial peptides in vivo using a systematic knockout approach. eLife 8, e44341. https://doi.org/10.7554/eLife.44341

Hanson, M.A., Lemaitre, B., 2020. New insights on Drosophila antimicrobial peptide function in host defense and beyond. Curr. Opin. Immunol., Innate immunity 62, 22–30. https://doi.org/10.1016/j.coi.2019.11.008

Harris, D.T., Kallman, B.R., Mullaney, B.C., Scott, K., 2015. Representations of Taste Modality in the Drosophila Brain. Neuron 86, 1449–1460. https://doi.org/10.1016/j.neuron.2015.05.026

Harris, N., Braiser, D.J., Dickman, D.K., Fetter, R.D., Tong, A., Davis, G.W., 2015. The Innate Immune Receptor PGRP-LC Controls Presynaptic Homeostatic Plasticity. Neuron 88, 1157–1164. https://doi.org/10.1016/j.neuron.2015.10.049

Harris, N., Fetter, R.D., Brasier, D.J., Tong, A., Davis, G.W., 2018. Molecular Interface of Neuronal Innate Immunity, Synaptic Vesicle Stabilization, and Presynaptic Homeostatic Plasticity. Neuron 100, 1163-1179 e4. https://doi.org/10.1016/j.neuron.2018.09.048

Hart, B.L., 1988. Biological basis of the behavior of sick animals. Neurosci. Biobehav. Rev. 12, 123–137. https://doi.org/10.1016/s0149-7634(88)80004-6

Hasegawa, M., Yang, K., Hashimoto, M., Park, J.-H., Kim, Y.-G., Fujimoto, Y., Nuñez, G., Fukase, K., Inohara, N., 2006. Differential Release and Distribution of Nod1 and Nod2 Immunostimulatory Molecules among Bacterial Species and Environments. J. Biol. Chem. 281, 29054–29063. https://doi.org/10.1074/jbc.M602638200

Häsemeyer, M., Yapici, N., Heberlein, U., Dickson, B.J., 2009. Sensory Neurons in the Drosophila Genital Tract Regulate Female Reproductive Behavior. Neuron 61, 511–518. https://doi.org/10.1016/j.neuron.2009.01.009

Heinze, J., Walter, B., 2010. Moribund ants leave their nests to die in social isolation. Curr. Biol. CB 20, 249–252. https://doi.org/10.1016/j.cub.2009.12.031

Hoyer, S.C., Eckart, A., Herrel, A., Zars, T., Fischer, S.A., Hardie, S.L., Heisenberg, M., 2008. Octopamine in male aggression of Drosophila. Curr. Biol. CB 18, 159–167. https://doi.org/10.1016/j.cub.2007.12.052

Hu, Y., Han, Y., Shao, Y., Wang, X., Ma, Y., Ling, E., Xue, L., 2015. Gr33a Modulates Drosophila Male Courtship Preference. Sci. Rep. 5, 7777. https://doi.org/10.1038/srep07777

Hughes, S.E., Miller, D.E., Miller, A.L., Hawley, R.S., 2018. Female Meiosis: Synapsis, Recombination, and Segregation in Drosophila melanogaster. Genetics 208, 875–908. https://doi.org/10.1534/genetics.117.300081

Hugot, J.-P., Chamaillard, M., Zouali, H., Lesage, S., Cézard, J.-P., Belaiche, J., Almer, S., Tysk, C., O'Morain, C.A., Gassull, M., Binder, V., Finkel, Y., Cortot, A., Modigliani, R., Laurent-Puig, P., Gower-Rousseau, C., Macry, J., Colombel, J.-F., Sahbatou, M., Thomas, G., 2001. Association of NOD2 leucine-rich repeat variants with susceptibility to Crohn's disease. Nature 411, 599–603. https://doi.org/10.1038/35079107

Hussain, A., Zhang, M., Üçpunar, H.K., Svensson, T., Quillery, E., Gompel, N., Ignell, R., Kadow, I.C.G., 2016. Ionotropic Chemosensory Receptors Mediate the Taste and Smell of Polyamines. PLOS Biol. 14, e1002454. https://doi.org/10.1371/journal.pbio.1002454

Iatsenko, I., Kondo, S., Mengin-Lecreulx, D., Lemaitre, B., 2016. PGRP-SD, an Extracellular Pattern-Recognition Receptor, Enhances Peptidoglycan-Mediated Activation of the Drosophila Imd Pathway. Immunity 45, 1013–1023. https://doi.org/10.1016/j.immuni.2016.10.029

Iliadi, K.G., Iliadi, N., Boulianne, G.L., 2017. Drosophila mutants lacking octopamine exhibit impairment in aversive olfactory associative learning. Eur. J. Neurosci. 46, 2080–2087. https://doi.org/10.1111/ejn.13654

Inohara, N., Ogura, Y., Fontalba, A., Gutierrez, O., Pons, F., Crespo, J., Fukase, K., Inamura, S., Kusumoto, S., Hashimoto, M., Foster, S.J., Moran, A.P., Fernandez-Luna, J.L., Nuñez, G., 2003. Host recognition of bacterial muramyl dipeptide mediated through NOD2. Implications for Crohn's disease. J. Biol. Chem. 278, 5509–5512. https://doi.org/10.1074/jbc.C200673200

Irazoki, O., Hernandez, S.B., Cava, F., 2019. Peptidoglycan Muropeptides: Release, Perception, and Functions as Signaling Molecules. Front. Microbiol. 10. https://doi.org/10.3389/fmicb.2019.00500

Ito, K., Shinomiya, K., Ito, M., Armstrong, J.D., Boyan, G., Hartenstein, V., Harzsch, S., Heisenberg, M., Homberg, U., Jenett, A., Keshishian, H., Restifo, L.L., Rössler, W., Simpson, J.H., Strausfeld, N.J., Strauss, R., Vosshall, L.B., 2014. A Systematic Nomenclature for the Insect Brain. Neuron 81, 755–765. https://doi.org/10.1016/j.neuron.2013.12.017

Jackson, F.R., You, S., Crowe, L.B., 2020. Regulation of rhythmic behaviors by astrocytes. WIREs Dev. Biol. 9, e372. https://doi.org/10.1002/wdev.372

Jaeger, A.H., Stanley, M., Weiss, Z.F., Musso, P.-Y., Chan, R.C., Zhang, H., Feldman-Kiss, D., Gordon, M.D., 2018. A complex peripheral code for salt taste in Drosophila. eLife 7, e37167. https://doi.org/10.7554/eLife.37167

Jan, Y.N., Jan, L.Y., 1994. Genetic Control of Cell Fate Specification in Drosophila Peripheral Nervous System. Annu. Rev. Genet. 28, 373–393. https://doi.org/10.1146/annurev.ge.28.120194.002105

Janeway, C.A., 1989. Approaching the asymptote? Evolution and revolution in immunology. Cold Spring Harb. Symp. Quant. Biol. 54 Pt 1, 1–13. https://doi.org/10.1101/sqb.1989.054.01.003

Jang, I.-H., Chosa, N., Kim, S.-H., Nam, H.-J., Lemaitre, B., Ochiai, M., Kambris, Z., Brun, S., Hashimoto, C., Ashida, M., Brey, P.T., Lee, W.-J., 2006. A Spätzle-Processing Enzyme Required for Toll Signaling Activation in Drosophila Innate Immunity. Dev. Cell 10, 45–55. https://doi.org/10.1016/j.devcel.2005.11.013

Järbrink-Sehgal, E., Andreasson, A., 2020. The gut microbiota and mental health in adults. Curr. Opin. Neurobiol., Brain, gut, and immune system interactions 62, 102–114. https://doi.org/10.1016/j.conb.2020.01.016

Jarret, A., Jackson, R., Duizer, C., Healy, M.E., Zhao, J., Rone, J.M., Bielecki, P., Sefik, E., Roulis, M., Rice, T., Sivanathan, K.N., Zhou, T., Solis, A.G., Honcharova-Biletska, H., Vélez, K., Hartner, S., Low, J.S., Qu, R., de Zoete, M.R., Palm, N.W., Ring, A.M., Weber, A., Moor, A.E., Kluger, Y., Nowarski, R., Flavell, R.A., 2020. Enteric Nervous System-Derived IL-18 Orchestrates Mucosal Barrier Immunity. Cell 180, 50-63.e12. https://doi.org/10.1016/j.cell.2019.12.016

Jeong, Y.T., Shim, J., Oh, S.R., Yoon, H.I., Kim, C.H., Moon, S.J., Montell, C., 2013. An Odorant-Binding Protein Required for Suppression of Sweet Taste by Bitter Chemicals. Neuron 79, 725–737. https://doi.org/10.1016/j.neuron.2013.06.025

Jiang, P., Cui, M., Zhao, B., Snyder, L.A., Benard, L.M.J., Osman, R., Max, M., Margolskee, R.F., 2005. Identification of the cyclamate interaction site within the transmembrane domain of the human sweet taste receptor subunit T1R3. J. Biol. Chem. 280, 34296–34305. https://doi.org/10.1074/jbc.M505255200

Jiang, P., Ji, Q., Liu, Z., Snyder, L.A., Benard, L.M.J., Margolskee, R.F., Max, M., 2004. The Cysteine-rich Region of T1R3 Determines Responses to Intensely Sweet Proteins. J. Biol. Chem. 279, 45068–45075. https://doi.org/10.1074/jbc.M406779200

Jiao, Y., Moon, S.J., Montell, C., 2007. A Drosophila gustatory receptor required for the responses to sucrose, glucose, and maltose identified by mRNA tagging. Proc. Natl. Acad. Sci. U. S. A. 104, 14110–14115. https://doi.org/10.1073/pnas.0702421104

Jiao, Y., Moon, S.J., Wang, X., Ren, Q., Montell, C., 2008. Gr64f is Required in Combination with other Gustatory Receptors for Sugar Detection in Drosophila. Curr. Biol. CB 18, 1797–1801. https://doi.org/10.1016/j.cub.2008.10.009

Jones, W.D., Cayirlioglu, P., Kadow, I.G., Vosshall, L.B., 2007. Two chemosensory receptors together mediate carbon dioxide detection in Drosophila. Nature 445, 86–90. https://doi.org/10.1038/nature05466

Joo, H.-S., Fu, C.-I., Otto, M., 2016. Bacterial strategies of resistance to antimicrobial peptides. Philos. Trans. R. Soc. B Biol. Sci. 371. https://doi.org/10.1098/rstb.2015.0292

Joseph, R.M., Carlson, J.R., 2015. Drosophila Chemoreceptors: A Molecular Interface Between the Chemical World and the Brain. Trends Genet. TIG 31, 683–695. https://doi.org/10.1016/j.tig.2015.09.005

Joseph, R.M., Sun, J.S., Tam, E., Carlson, J.R., 2017. A receptor and neuron that activate a circuit limiting sucrose consumption. eLife 6. https://doi.org/10.7554/eLife.24992

Kain, P., Dahanukar, A., 2015. Secondary taste neurons that convey sweet taste and starvation in the Drosophila brain. Neuron 85, 819–832. https://doi.org/10.1016/j.neuron.2015.01.005

Kaneko, T., Goldman, W.E., Mellroth, P., Steiner, H., Fukase, K., Kusumoto, S., Harley, W., Fox, A., Golenbock, D., Silverman, N., 2004. Monomeric and Polymeric Gram-Negative Peptidoglycan but Not Purified LPS Stimulate the Drosophila IMD Pathway. Immunity 20, 637–649. https://doi.org/10.1016/S1074-7613(04)00104-9

Kaneko, T., Yano, T., Aggarwal, K., Lim, J.-H., Ueda, K., Oshima, Y., Peach, C., Erturk-Hasdemir, D., Goldman, W.E., Oh, B.-H., Kurata, S., Silverman, N., 2006. PGRP-LC and PGRP-LE have essential yet distinct functions in the drosophila immune response to monomeric DAP-type peptidoglycan. Nat. Immunol. 7, 715–723. https://doi.org/10.1038/ni1356

Kang, K., Pulver, S.R., Panzano, V.C., Chang, E.C., Griffith, L.C., Theobald, D.L., Garrity, P.A., 2010. Analysis of Drosophila TRPA1 reveals an ancient origin for human chemical nociception. Nature 464, 597–600. https://doi.org/10.1038/nature08848

Kazlauskas, N., Klappenbach, M., Depino, A.M., Locatelli, F.F., 2016. Sickness Behavior in Honey Bees. Front. Physiol. 7. https://doi.org/10.3389/fphys.2016.00261

Keesey, I.W., Koerte, S., Khallaf, M.A., Retzke, T., Guillou, A., Grosse-Wilde, E., Buchon, N., Knaden, M., Hansson, B.S., 2017. Pathogenic bacteria enhance dispersal through alteration of Drosophila social communication. Nat Commun 8, 265. https://doi.org/10.1038/s41467-017-00334-9

Kim, H., Kirkhart, C., Scott, K., 2017. Long-range projection neurons in the taste circuit of Drosophila. eLife 6, e23386. https://doi.org/10.7554/eLife.23386

Kim, L.K., Choi, U.Y., Cho, H.S., Lee, J.S., Lee, W., Kim, J., Jeong, K., Shim, J., Kim-Ha, J., Kim, Y.-J., 2007. Down-Regulation of NF-κB Target Genes by the AP-1 and STAT Complex during the Innate Immune Response in Drosophila. PLOS Biol. 5, e238. https://doi.org/10.1371/journal.pbio.0050238

Kim, M., Lee, J.H., Lee, S.Y., Kim, E., Chung, J., 2006. Caspar, a suppressor of antibacterial immunity in Drosophila. Proc. Natl. Acad. Sci. 103, 16358–16363. https://doi.org/10.1073/pnas.0603238103

Kim, S.H., Lee, Y., Akitake, B., Woodward, O.M., Guggino, W.B., Montell, C., 2010. Drosophila TRPA1 channel mediates chemical avoidance in gustatory receptor neurons. Proc. Natl. Acad. Sci. U. S. A. 107, 8440–8445. https://doi.org/10.1073/pnas.1001425107

Kim, T., Yoon, J., Cho, H., Lee, W., Kim, J., Song, Y.-H., Kim, S.N., Yoon, J.H., Kim-Ha, J., Kim, Y.-J., 2005. Downregulation of lipopolysaccharide response in drosophila by negative crosstalk between the AP1 and NF-κB signaling modules. Nat. Immunol. 6, 211–218. https://doi.org/10.1038/ni1159

Kim, Y.-S., Ryu, J.-H., Han, S.-J., Choi, K.-H., Nam, K.-B., Jang, I.-H., Lemaitre, B., Brey, P.T., Lee, W.-J., 2000. Gram-negative Bacteria-binding Protein, a Pattern Recognition Receptor for Lipopolysaccharide and β-1,3-Glucan That Mediates the Signaling for the Induction of Innate Immune Genes in Drosophila melanogaster Cells. J. Biol. Chem. 275, 32721–32727. https://doi.org/10.1074/jbc.M003934200

Kitamoto, T., 2002. Targeted expression of temperature-sensitive dynamin to study neural mechanisms of complex behavior in Drosophila. J. Neurogenet. 16, 205–228. https://doi.org/10.1080/01677060216295

Kleino, A., Myllymäki, H., Kallio, J., Vanha-aho, L.-M., Oksanen, K., Ulvila, J., Hultmark, D., Valanne, S., Rämet, M., 2008. Pirk Is a Negative Regulator of the Drosophila Imd Pathway. J. Immunol. 180, 5413–5422. https://doi.org/10.4049/jimmunol.180.8.5413

Klose, C.S.N., Mahlakõiv, T., Moeller, J.B., Rankin, L.C., Flamar, A.-L., Kabata, H., Monticelli, L.A., Moriyama, S., Putzel, G.G., Rakhilin, N., Shen, X., Kostenis, E., König, G.M., Senda, T., Carpenter, D., Farber, D.L., Artis, D., 2017. The neuropeptide neuromedin U stimulates innate lymphoid cells and type 2 inflammation. Nature 549, 282–286. https://doi.org/10.1038/nature23676

Knecht, Z.A., Silbering, A.F., Ni, L., Klein, M., Budelli, G., Bell, R., Abuin, L., Ferrer, A.J., Samuel, A.D., Benton, R., Garrity, P.A., 2016. Distinct combinations of variant ionotropic glutamate receptors mediate thermosensation and hygrosensation in Drosophila. eLife 5. https://doi.org/10.7554/eLife.17879

Knell, R.J., Webberley, K.M., 2004. Sexually transmitted diseases of insects: distribution, evolution, ecology and host behaviour. Biol. Rev. Camb. Philos. Soc. 79, 557–581. https://doi.org/10.1017/s1464793103006365

Kocks, C., Cho, J.H., Nehme, N., Ulvila, J., Pearson, A.M., Meister, M., Strom, C., Conto, S.L., Hetru, C., Stuart, L.M., Stehle, T., Hoffmann, J.A., Reichhart, J.-M., Ferrandon, D., Rämet, M., Ezekowitz, R.A.B., 2005. Eater, a Transmembrane Protein Mediating Phagocytosis of Bacterial Pathogens in Drosophila. Cell 123, 335–346. https://doi.org/10.1016/j.cell.2005.08.034

Koh, T.-W., He, Z., Gorur-Shandilya, S., Menuz, K., Larter, N.K., Stewart, S., Carlson, J.R., 2014. The Drosophila IR20a clade of ionotropic receptors are candidate taste and pheromone receptors. Neuron 83, 850–865. https://doi.org/10.1016/j.neuron.2014.07.012

Koon, A.C., Ashley, J., Barria, R., DasGupta, S., Brain, R., Waddell, S., Alkema, M.J., Budnik, V., 2011. Autoregulatory and paracrine control of synaptic and behavioral plasticity by octopaminergic signaling. Nat. Neurosci. 14, 190–199. https://doi.org/10.1038/nn.2716

Koon, A.C., Budnik, V., 2012. Inhibitory Control of Synaptic and Behavioral Plasticity by Octopaminergic Signaling. J. Neurosci. 32, 6312–6322. https://doi.org/10.1523/JNEUROSCI.6517-11.2012

Kounatidis, I., Chtarbanova, S., Cao, Y., Hayne, M., Jayanth, D., Ganetzky, B., Ligoxygakis, P., 2017. NF-kappaB Immunity in the Brain Determines Fly Lifespan in Healthy Aging and Age-Related Neurodegeneration. Cell Rep 19, 836–848. https://doi.org/10.1016/j.celrep.2017.04.007

Krashes, M.J., DasGupta, S., Vreede, A., White, B., Armstrong, J.D., Waddell, S., 2009. A Neural Circuit Mechanism Integrating Motivational State with Memory Expression in Drosophila. Cell 139, 416–427. https://doi.org/10.1016/j.cell.2009.08.035

Kuo, T.H., Pike, D.H., Beizaeipour, Z., Williams, J.A., 2010. Sleep triggered by an immune response in Drosophila is regulated by the circadian clock and requires the NFkappaB Relish. BMC Neurosci 11, 17. https://doi.org/10.1186/1471-2202-11-17

Kuraishi, T., Hori, A., Kurata, S., 2013. Host-microbe interactions in the gut of Drosophila melanogaster. Front. Physiol. 4. https://doi.org/10.3389/fphys.2013.00375

Kurz, C.L., Charroux, B., Chaduli, D., Viallat-Lieutaud, A., Royet, J., 2017. Peptidoglycan sensing by octopaminergic neurons modulates Drosophila oviposition. eLife 6, e21937. https://doi.org/10.7554/eLife.21937

Kwon, Y., Kim, S.H., Ronderos, D.S., Lee, Y., Akitake, B., Woodward, O.M., Guggino, W.B., Smith, D.P., Montell, C., 2010. Drosophila TRPA1 Channel Is Required to Avoid the Naturally Occurring Insect Repellent Citronellal. Curr. Biol. 20, 1672–1678. https://doi.org/10.1016/j.cub.2010.08.016

Le, Y., Murphy, P.M., Wang, J.M., 2002. Formyl-peptide receptors revisited. Trends Immunol. 23, 541–548. https://doi.org/10.1016/S1471-4906(02)02316-5

LeDue, E.E., Chen, Y.-C., Jung, A.Y., Dahanukar, A., Gordon, M.D., 2015. Pharyngeal sense organs drive robust sugar consumption in Drosophila. Nat. Commun. 6, 6667. https://doi.org/10.1038/ncomms7667

LeDue, E.E., Mann, K., Koch, E., Chu, B., Dakin, R., Gordon, M.D., 2016. Starvation-Induced Depotentiation of Bitter Taste in Drosophila. Curr. Biol. CB 26, 2854–2861. https://doi.org/10.1016/j.cub.2016.08.028

Lee, H.-G., Rohila, S., Han, K.-A., 2009. The Octopamine Receptor OAMB Mediates Ovulation via Ca2+/Calmodulin-Dependent Protein Kinase II in the Drosophila Oviduct Epithelium. PLoS ONE 4. https://doi.org/10.1371/journal.pone.0004716

Lee, H.-G., Seong, C.-S., Kim, Y.-C., Davis, R.L., Han, K.-A., 2003. Octopamine receptor OAMB is required for ovulation in Drosophila melanogaster. Dev. Biol. 264, 179–190. https://doi.org/10.1016/j.ydbio.2003.07.018

Lee, K.-A., Kim, B., Bhin, J., Kim, D.H., You, H., Kim, E.-K., Kim, S.-H., Ryu, J.-H., Hwang, D., Lee, W.-J., 2015. Bacterial Uracil Modulates Drosophila DUOX-Dependent Gut Immunity via Hedgehog-Induced Signaling Endosomes. Cell Host Microbe 17, 191–204. https://doi.org/10.1016/j.chom.2014.12.012

Lee, K.-A., Kim, S.-H., Kim, E.-K., Ha, E.-M., You, H., Kim, B., Kim, M.-J., Kwon, Y., Ryu, J.-H., Lee, W.-J., 2013. Bacterial-Derived Uracil as a Modulator of Mucosal Immunity and Gut-Microbe Homeostasis in Drosophila. Cell 153, 797–811. https://doi.org/10.1016/j.cell.2013.04.009

Lee, K.-Z., Ferrandon, D., 2011. Negative regulation of immune responses on the fly. EMBO J. 30, 988–990. https://doi.org/10.1038/emboj.2011.47

Lee, M.J., Sung, H.Y., Jo, H., Kim, H.-W., Choi, M.S., Kwon, J.Y., Kang, K., 2017. Ionotropic Receptor 76b Is Required for Gustatory Aversion to Excessive Na+ in Drosophila. Mol. Cells 40, 787–795. https://doi.org/10.14348/molcells.2017.0160

Lee, W.-J., Kim, S.-H., 2014. Role of DUOX in gut inflammation: lessons from Drosophila model of gut-microbiota interactions. Front. Cell. Infect. Microbiol. 3. https://doi.org/10.3389/fcimb.2013.00116

Lee, Y., Kang, M.J., Shim, J., Cheong, C.U., Moon, S.J., Montell, C., 2012. Gustatory Receptors Required for Avoiding the Insecticide l-Canavanine. J. Neurosci. 32, 1429–1435. https://doi.org/10.1523/JNEUROSCI.4630-11.2012

Lee, Y., Kim, S.H., Montell, C., 2010. Avoiding DEET through insect gustatory receptors. Neuron 67, 555–561. https://doi.org/10.1016/j.neuron.2010.07.006

Lee, Y., Moon, S.J., Montell, C., 2009. Multiple gustatory receptors required for the caffeine response in Drosophila. Proc. Natl. Acad. Sci. U. S. A. 106, 4495–4500. https://doi.org/10.1073/pnas.0811744106

Lee, Y., Poudel, S., Kim, Y., Thakur, D., Montell, C., 2018. Calcium taste avoidance in Drosophila. Neuron 97, 67-74.e4. https://doi.org/10.1016/j.neuron.2017.11.038

Lemaitre, B., Hoffmann, J., 2007. The Host Defense of Drosophila melanogaster. Annu. Rev. Immunol. 25, 697–743. https://doi.org/10.1146/annurev.immunol.25.022106.141615

Lemaitre, B., Kromer-Metzger, E., Michaut, L., Nicolas, E., Meister, M., Georgel, P., Reichhart, J.M., Hoffmann, J.A., 1995. A recessive mutation, immune deficiency (imd), defines two distinct control pathways in the Drosophila host defense. Proc. Natl. Acad. Sci. 92, 9465–9469. https://doi.org/10.1073/pnas.92.21.9465

Lemaitre, B., Nicolas, E., Michaut, L., Reichhart, J.-M., Hoffmann, J.A., 1996. The Dorsoventral Regulatory Gene Cassette spätzle/Toll/cactus Controls the Potent Antifungal Response in Drosophila Adults. Cell 86, 973–983. https://doi.org/10.1016/S0092-8674(00)80172-5

Lesperance, D.N., Broderick, N.A., 2020. Microbiomes as modulators of Drosophila melanogaster homeostasis and disease. Curr Opin Insect Sci 39, 84–90. https://doi.org/10.1016/j.cois.2020.03.003

Leulier, F., Parquet, C., Pili-Floury, S., Ryu, J.-H., Caroff, M., Lee, W.-J., Mengin-Lecreulx, D., Lemaitre, B., 2003. The Drosophila immune system detects bacteria through specific peptidoglycan recognition. Nat. Immunol. 4, 478–484. https://doi.org/10.1038/ni922

Leulier, F., Vidal, S., Saigo, K., Ueda, R., Lemaitre, B., 2002. Inducible Expression of Double-Stranded RNA Reveals a Role for dFADD in the Regulation of the Antibacterial Response in Drosophila Adults. Curr. Biol. 12, 996–1000. https://doi.org/10.1016/S0960-9822(02)00873-4

Leung, B., Forbes, M.R., Baker, R.L., 2001. Nutritional stress and behavioural immunity of damselflies. Anim. Behav. 61, 1093–1099. https://doi.org/10.1006/anbe.2001.1693

Li, J., Terry, E.E., Fejer, E., Gamba, D., Hartmann, N., Logsdon, J., Michalski, D., Rois, L.E., Scuderi, M.J., Kunst, M., Hughes, M.E., 2017. Achilles is a circadian clock-controlled gene that regulates immune function in Drosophila. Brain Behav Immun 61, 127–136. https://doi.org/10.1016/j.bbi.2016.11.012

Li, X., Staszewski, L., Xu, H., Durick, K., Zoller, M., Adler, E., 2002. Human receptors for sweet and umami taste. Proc. Natl. Acad. Sci. U. S. A. 99, 4692–4696. https://doi.org/10.1073/pnas.072090199

Li, Yong, Hoffmann, J., Li, Yang, Stephano, F., Bruchhaus, I., Fink, C., Roeder, T., 2016. Octopamine controls starvation resistance, life span and metabolic traits in Drosophila. Sci. Rep. 6, 35359. https://doi.org/10.1038/srep35359

Liberles, S.D., Horowitz, L.F., Kuang, D., Contos, J.J., Wilson, K.L., Siltberg-Liberles, J., Liberles, D.A., Buck, L.B., 2009. Formyl peptide receptors are candidate chemosensory receptors in the vomeronasal organ. Proc. Natl. Acad. Sci. 106, 9842–9847. https://doi.org/10.1073/pnas.0904464106

Lim, J., Sabandal, P.R., Fernandez, A., Sabandal, J.M., Lee, H.-G., Evans, P., Han, K.-A., 2014. The Octopamine Receptor Octβ2R Regulates Ovulation in Drosophila melanogaster. PLOS ONE 9, e104441. https://doi.org/10.1371/journal.pone.0104441

Lim, J.-H., Kim, M.-S., Kim, H.-E., Yano, T., Oshima, Y., Aggarwal, K., Goldman, W.E., Silverman, N., Kurata, S., Oh, B.-H., 2006. Structural basis for preferential recognition of diaminopimelic acid-type peptidoglycan by a subset of peptidoglycan recognition proteins. J. Biol. Chem. 281, 8286–8295. https://doi.org/10.1074/jbc.M513030200

Liman, E.R., Zhang, Y.V., Montell, C., 2014. Peripheral coding of taste. Neuron 81, 984–1000. https://doi.org/10.1016/j.neuron.2014.02.022

Lindsay, S.A., Wasserman, S.A., 2014. Conventional and non-conventional Drosophila Toll signaling. Dev. Comp. Immunol. 42, 16–24. https://doi.org/10.1016/j.dci.2013.04.011

Ling, F., Dahanukar, A., Weiss, L.A., Kwon, J.Y., Carlson, J.R., 2014. The Molecular and Cellular Basis of Taste Coding in the Legs of Drosophila. J. Neurosci. 34, 7148–7164. https://doi.org/10.1523/JNEUROSCI.0649-14.2014

Liu, C., Plaçais, P.-Y., Yamagata, N., Pfeiffer, B.D., Aso, Y., Friedrich, A.B., Siwanowicz, I., Rubin, G.M., Preat, T., Tanimoto, H., 2012. A subset of dopamine neurons signals reward for odour memory in Drosophila. Nature 488, 512–516. https://doi.org/10.1038/nature11304

Liu, C., Xu, Z., Gupta, D., Dziarski, R., 2001. Peptidoglycan Recognition Proteins: A NOVEL FAMILY OF FOUR HUMAN INNATE IMMUNITY PATTERN RECOGNITION MOLECULES. J. Biol. Chem. 276, 34686–34694. https://doi.org/10.1074/jbc.M105566200

Liu, T., Starostina, E., Vijayan, V., Pikielny, C.W., 2012. Two Drosophila DEG/ENaC Channel Subunits Have Distinct Functions in Gustatory Neurons That Activate Male Courtship. J. Neurosci. 32, 11879–11889. https://doi.org/10.1523/JNEUROSCI.1376-12.2012

Liu, T., Wang, Y., Tian, Y., Zhang, J., Zhao, J., Guo, A., 2020. The receptor channel formed by ppk25, ppk29 and ppk23 can sense the Drosophila female pheromone 7,11-heptacosadiene. Genes Brain Behav. 19, e12529. https://doi.org/10.1111/gbb.12529

Liu, W., Zhang, K., Li, Y., Su, W., Hu, K., Jin, S., 2017. Enterococci Mediate the Oviposition Preference of Drosophila melanogaster through Sucrose Catabolism. Sci. Rep. 7, 13420. https://doi.org/10.1038/s41598-017-13705-5

Lu, B., LaMora, A., Sun, Y., Welsh, M.J., Ben-Shahar, Y., 2012. ppk23-Dependent Chemosensory Functions Contribute to Courtship Behavior in Drosophila melanogaster. PLoS Genet. 8. https://doi.org/10.1371/journal.pgen.1002587

Lu, X., Wang, M., Qi, J., Wang, H., Li, X., Gupta, D., Dziarski, R., 2006. Peptidoglycan recognition proteins are a new class of human bactericidal proteins. J. Biol. Chem. 281, 5895–5907. https://doi.org/10.1074/jbc.M511631200

Ma, Z., Stork, T., Bergles, D.E., Freeman, M.R., 2016. Neuromodulators signal through astrocytes to alter neural circuit activity and behavior. Nature 539, 428–432. https://doi.org/10.1038/nature20145

Maillet, F., Bischoff, V., Vignal, C., Hoffmann, J., Royet, J., 2008. The Drosophila Peptidoglycan Recognition Protein PGRP-LF Blocks PGRP-LC and IMD/JNK Pathway Activation. Cell Host Microbe 3, 293–303. https://doi.org/10.1016/j.chom.2008.04.002

Makhijani, K., Alexander, B., Rao, D., Petraki, S., Herboso, L., Kukar, K., Batool, I., Wachner, S., Gold, K.S., Wong, C., O'Connor, M.B., Bruckner, K., 2017. Regulation of Drosophila hematopoietic sites by Activin-beta from active sensory neurons. Nat Commun 8, 15990. https://doi.org/10.1038/ncomms15990

Malamud, J.G., Mizisin, A.P., Josephson, R.K., 1988. The effects of octopamine on contraction kinetics and power output of a locust flight muscle. J. Comp. Physiol. A 162, 827–835. https://doi.org/10.1007/BF00610971

Manfruelli, P., Reichhart, J.-M., Steward, R., Hoffmann, J.A., Lemaitre, B., 1999. A mosaic analysis in Drosophila fat body cells of the control of antimicrobial peptide genes by the Rel proteins Dorsal and DIF. EMBO J. 18, 3380–3391. https://doi.org/10.1093/emboj/18.12.3380

Mansourian, S., Corcoran, J., Enjin, A., Lofstedt, C., Dacke, M., Stensmyr, M.C., 2016. Fecal-Derived Phenol Induces Egg-Laying Aversion in Drosophila. Curr Biol 26, 2762–2769. https://doi.org/10.1016/j.cub.2016.07.065

Marella, S., Fischler, W., Kong, P., Asgarian, S., Rueckert, E., Scott, K., 2006. Imaging taste responses in the fly brain reveals a functional map of taste category and behavior. Neuron 49, 285–295. https://doi.org/10.1016/j.neuron.2005.11.037

Marion, E., Song, O.-R., Christophe, T., Babonneau, J., Fenistein, D., Eyer, J., Letournel, F., Henrion, D., Clere, N., Paille, V., Guérineau, N.C., Saint André, J.-P., Gersbach, P., Altmann, K.-H., Stinear, T.P., Comoglio, Y., Sandoz, G., Preisser, L., Delneste, Y., Yeramian, E., Marsollier, L., Brodin, P., 2014. Mycobacterial toxin induces analgesia in buruli ulcer by targeting the angiotensin pathways. Cell 157, 1565–1576. https://doi.org/10.1016/j.cell.2014.04.040

Matheis, F., Muller, P.A., Graves, C.L., Gabanyi, I., Kerner, Z.J., Costa-Borges, D., Ahrends, T., Rosenstiel, P., Mucida, D., 2020. Adrenergic Signaling in Muscularis Macrophages Limits Infection-Induced Neuronal Loss. Cell 180, 64-78.e16. https://doi.org/10.1016/j.cell.2019.12.002

Matsunami, H., Amrein, H., 2003. Taste and pheromone perception in mammals and flies. Genome Biol. 4, 220. https://doi.org/10.1186/gb-2003-4-7-220

Mellroth, P., Steiner, H., 2006. PGRP-SB1: An N-acetylmuramoyl l-alanine amidase with antibacterial activity. Biochem. Biophys. Res. Commun. 350, 994–999. https://doi.org/10.1016/j.bbrc.2006.09.139

Meng, X., Khanuja, B.S., Ip, Y.T., 1999. Toll receptor-mediated Drosophila immune response requires Dif, an NF-κB factor. Genes Dev. 13, 792–797.

Mentel, T., Duch, C., Stypa, H., Wegener, G., Müller, U., Pflüger, H.-J., 2003. Central modulatory neurons control fuel selection in flight muscle of migratory locust. J. Neurosci. Off. J. Soc. Neurosci. 23, 1109–1113.

Mercer, A.R., Menzel, R., 1982. The effects of biogenic amines on conditioned and unconditioned responses to olfactory stimuli in the honeybeeApis mellifera. J. Comp. Physiol. 145, 363–368. https://doi.org/10.1007/BF00619340

Meseguer, V., Alpizar, Y.A., Luis, E., Tajada, S., Denlinger, B., Fajardo, O., Manenschijn, J.-A., Fernández-Peña, C., Talavera, A., Kichko, T., Navia, B., Sánchez, A., Señarís, R., Reeh, P., Pérez-García, M.T., López-López, J.R., Voets, T., Belmonte, C., Talavera, K., Viana, F., 2014. TRPA1 channels mediate acute neurogenic inflammation and pain produced by bacterial endotoxins. Nat. Commun. 5, 3125. https://doi.org/10.1038/ncomms4125

Meunier, N., Marion-Poll, F., Rospars, J.-P., Tanimura, T., 2003. Peripheral coding of bitter taste in Drosophila. J. Neurobiol. 56, 139–152. https://doi.org/10.1002/neu.10235

Meyerhof, W., 2005. Elucidation of mammalian bitter taste. Rev. Physiol. Biochem. Pharmacol. 154, 37–72. https://doi.org/10.1007/s10254-005-0041-0

Miceli-Richard, C., Lesage, S., Rybojad, M., Prieur, A.-M., Manouvrier-Hanu, S., Häfner, R., Chamaillard, M., Zouali, H., Thomas, G., Hugot, J.-P., 2001. CARD15 mutations in Blau syndrome. Nat. Genet. 29, 19–20. https://doi.org/10.1038/ng720

Michel, T., Reichhart, J.-M., Hoffmann, J.A., Royet, J., 2001. Drosophila Toll is activated by Gram-positive bacteria through a circulating peptidoglycan recognition protein. Nature 414, 756–759. https://doi.org/10.1038/414756a

Middleton, C.A., Nongthomba, U., Parry, K., Sweeney, S.T., Sparrow, J.C., Elliott, C.J.H., 2006. Neuromuscular organization and aminergic modulation of contractions in the Drosophila ovary. BMC Biol. 4, 17. https://doi.org/10.1186/1741-7007-4-17

Min, S., Ai, M., Shin, S.A., Suh, G.S.B., 2013. Dedicated olfactory neurons mediating attraction behavior to ammonia and amines in Drosophila. Proc. Natl. Acad. Sci. U. S. A. 110, E1321-1329. https://doi.org/10.1073/pnas.1215680110

Miyamoto, T., Amrein, H., 2014. Diverse roles for the Drosophila fructose sensor Gr43a. Fly (Austin) 8, 19–25. https://doi.org/10.4161/fly.27241

Miyamoto, T., Amrein, H., 2008. Suppression of male courtship by a Drosophila pheromone receptor. Nat. Neurosci. 11, 874–876. https://doi.org/10.1038/nn.2161

Miyamoto, T., Slone, J., Song, X., Amrein, H., 2012. A fructose receptor functions as a nutrient sensor in the Drosophila brain. Cell 151, 1113–1125. https://doi.org/10.1016/j.cell.2012.10.024

Monastirioti, M., 2003. Distinct octopamine cell population residing in the CNS abdominal ganglion controls ovulation in Drosophila melanogaster. Dev. Biol. 264, 38–49. https://doi.org/10.1016/j.ydbio.2003.07.019

Monastirioti, M., Charles E. Linn, J., White, K., 1996. Characterization of Drosophila Tyramine β-HydroxylaseGene and Isolation of Mutant Flies Lacking Octopamine. J. Neurosci. 16, 3900–3911. https://doi.org/10.1523/JNEUROSCI.16-12-03900.1996

Monastirioti, M., Linn, E., 1996. Characterization of Drosophila Tyramine @Hydroxylase Isolation of Mutant Flies Lacking Octopamine. Fruit Flies 12.

Moon, S.J., Köttgen, M., Jiao, Y., Xu, H., Montell, C., 2006. A taste receptor required for the caffeine response in vivo. Curr. Biol. CB 16, 1812–1817. https://doi.org/10.1016/j.cub.2006.07.024

Moon, S.J., Lee, Y., Jiao, Y., Montell, C., 2009. A Drosophila gustatory receptor essential for aversive taste and inhibiting male-to-male courtship. Curr. Biol. CB 19, 1623–1627. https://doi.org/10.1016/j.cub.2009.07.061

Moriyama, S., Brestoff, J.R., Flamar, A.-L., Moeller, J.B., Klose, C.S.N., Rankin, L.C., Yudanin, N.A., Monticelli, L.A., Putzel, G.G., Rodewald, H.-R., Artis, D., 2018. β2-adrenergic receptor-mediated negative regulation of group 2 innate lymphoid cell responses. Science 359, 1056–1061. https://doi.org/10.1126/science.aan4829

Morris, O., Liu, X., Domingues, C., Runchel, C., Chai, A., Basith, S., Tenev, T., Chen, H., Choi, S., Pennetta, G., Buchon, N., Meier, P., 2016. Signal Integration by the IκB Protein Pickle Shapes Drosophila Innate Host Defense. Cell Host Microbe 20, 283–295. https://doi.org/10.1016/j.chom.2016.08.003

Murata, S., Brockmann, A., Tanimura, T., 2017. Pharyngeal stimulation with sugar triggers local searching behavior in Drosophila. J. Exp. Biol. 220, 3231–3237. https://doi.org/10.1242/jeb.161646

Nagashima, H., Mahlakõiv, T., Shih, H.-Y., Davis, F.P., Meylan, F., Huang, Y., Harrison, O.J., Yao, C., Mikami, Y., Urban, J.F., Caron, K.M., Belkaid, Y., Kanno, Y., Artis, D., O'Shea, J.J., 2019. Neuropeptide CGRP Limits Group 2 Innate Lymphoid Cell Responses and Constrains Type 2 Inflammation. Immunity 51, 682-695.e6. https://doi.org/10.1016/j.immuni.2019.06.009

Naitza, S., Rossé, C., Kappler, C., Georgel, P., Belvin, M., Gubb, D., Camonis, J., Hoffmann, J.A., Reichhart, J.-M., 2002. The Drosophila Immune Defense against Gram-Negative Infection Requires the Death Protein dFADD. Immunity 17, 575–581. https://doi.org/10.1016/S1074-7613(02)00454-5

Nakagawa, T., Pellegrino, M., Sato, K., Vosshall, L.B., Touhara, K., 2012. Amino Acid Residues Contributing to Function of the Heteromeric Insect Olfactory Receptor Complex. PLOS ONE 7, e32372. https://doi.org/10.1371/journal.pone.0032372

Nakamura, N., Lill, J.R., Phung, Q., Jiang, Z., Bakalarski, C., de Mazière, A., Klumperman, J., Schlatter, M., Delamarre, L., Mellman, I., 2014. Endosomes are specialized platforms for bacterial sensing and NOD2 signalling. Nature 509, 240–244. https://doi.org/10.1038/nature13133

Namiki, S., Dickinson, M.H., Wong, A.M., Korff, W., Card, G.M., 2018. The functional organization of descending sensory-motor pathways in Drosophila. eLife 7, e34272. https://doi.org/10.7554/eLife.34272

Nathanson, J.A., Greengard, P., 1973. Octopamine-Sensitive Adenylate Cyclase: Evidence for a Biological Role of Octopamine in Nervous Tissue. Science 180, 308–310. https://doi.org/10.1126/science.180.4083.308

Nayak, S.V., Singh, R.N., 1983. Sensilla on the tarsal segments and mouthparts of adult Drosophila melanogaster meigen (Diptera : Drosophilidae). Int. J. Insect Morphol. Embryol. 12, 273–291. https://doi.org/10.1016/0020-7322(83)90023-5

Nehme, N.T., Liégeois, S., Kele, B., Giammarinaro, P., Pradel, E., Hoffmann, J.A., Ewbank, J.J., Ferrandon, D., 2007. A Model of Bacterial Intestinal Infections in Drosophila melanogaster. PLOS Pathog. 3, e173. https://doi.org/10.1371/journal.ppat.0030173

Nelson, G., Chandrashekar, J., Hoon, M.A., Feng, L., Zhao, G., Ryba, N.J.P., Zuker, C.S., 2002. An amino-acid taste receptor. Nature 416, 199–202. https://doi.org/10.1038/nature726

Nelson, G., Hoon, M.A., Chandrashekar, J., Zhang, Y., Ryba, N.J., Zuker, C.S., 2001. Mammalian sweet taste receptors. Cell 106, 381–390. https://doi.org/10.1016/s0092-8674(01)00451-2

Neuhaus, F.C., Baddiley, J., 2003. A Continuum of Anionic Charge: Structures and Functions of d-Alanyl-Teichoic Acids in Gram-Positive Bacteria. Microbiol. Mol. Biol. Rev. 67, 686–723. https://doi.org/10.1128/MMBR.67.4.686-723.2003

Neyen, C., Poidevin, M., Roussel, A., Lemaitre, B., 2012. Tissue- and Ligand-Specific Sensing of Gram-Negative Infection in *Drosophila* by PGRP-LC Isoforms and PGRP-LE. J. Immunol. 189, 1886–1897. https://doi.org/10.4049/jimmunol.1201022

Neyen, C., Runchel, C., Schüpfer, F., Meier, P., Lemaitre, B., 2016. The regulatory isoform rPGRP-LC resolves immune activation through ESCRT-mediated receptor clearance. Nat. Immunol. 17, 1150–1158. https://doi.org/10.1038/ni.3536

Ni, L., Bronk, P., Chang, E.C., Lowell, A.M., Flam, J.O., Panzano, V.C., Theobald, D.L., Griffith, L.C., Garrity, P.A., 2013. A gustatory receptor paralog controls rapid warmth avoidance in Drosophila. Nature 500, 580–584. https://doi.org/10.1038/nature12390

Ni, L., Klein, M., Svec, K.V., Budelli, G., Chang, E.C., Ferrer, A.J., Benton, R., Samuel, A.D., Garrity, P.A., 2016. The Ionotropic Receptors IR21a and IR25a mediate cool sensing in Drosophila. eLife 5. https://doi.org/10.7554/eLife.13254

Ogura, Y., Bonen, D.K., Inohara, N., Nicolae, D.L., Chen, F.F., Ramos, R., Britton, H., Moran, T., Karaliuskas, R., Duerr, R.H., Achkar, J.P., Brant, S.R., Bayless, T.M., Kirschner, B.S., Hanauer, S.B., Nuñez, G., Cho, J.H., 2001. A frameshift mutation in NOD2 associated with susceptibility to Crohn's disease. Nature 411, 603–606. https://doi.org/10.1038/35079114

Paik, D., Monahan, A., Caffrey, D.R., Elling, R., Goldman, W.E., Silverman, N., 2017. SLC46 Family Transporters Facilitate Cytosolic Innate Immune Recognition of Monomeric Peptidoglycans. J. Immunol. 199, 263–270. https://doi.org/10.4049/jimmunol.1600409

Palma, J.M., Corpas, F.J., del Río, L.A., 2011. Proteomics as an approach to the understanding of the molecular physiology of fruit development and ripening. J. Proteomics 74, 1230–1243. https://doi.org/10.1016/j.jprot.2011.04.010

Paquette, N., Broemer, M., Aggarwal, K., Chen, L., Husson, M., Ertürk-Hasdemir, D., Reichhart, J.-M., Meier, P., Silverman, N., 2010. Caspase-mediated cleavage, IAP binding, and ubiquitination: linking three mechanisms crucial for Drosophila NF-kappaB signaling. Mol. Cell 37, 172–182. https://doi.org/10.1016/j.molcel.2009.12.036

Paredes, J.C., Welchman, D.P., Poidevin, M., Lemaitre, B., 2011. Negative Regulation by Amidase PGRPs Shapes the Drosophila Antibacterial Response and Protects the Fly from Innocuous Infection. Immunity 35, 770–779. https://doi.org/10.1016/j.immuni.2011.09.018

Park, J.-H., Kwon, J.Y., 2011a. Heterogeneous Expression of Drosophila Gustatory Receptors in Enteroendocrine Cells. PLOS ONE 6, e29022. https://doi.org/10.1371/journal.pone.0029022

Park, J.-H., Kwon, J.Y., 2011b. A systematic analysis of Drosophila gustatory receptor gene expression in abdominal neurons which project to the central nervous system. Mol. Cells 32, 375–381. https://doi.org/10.1007/s10059-011-0128-1

Park, J.T., Uehara, T., 2008. How Bacteria Consume Their Own Exoskeletons (Turnover and Recycling of Cell Wall Peptidoglycan). Microbiol. Mol. Biol. Rev. MMBR 72, 211–227. https://doi.org/10.1128/MMBR.00027-07

Park, J.-W., Kim, C.-H., Kim, J.-H., Je, B.-R., Roh, K.-B., Kim, S.-J., Lee, H.-H., Ryu, J.-H., Lim, J.-H., Oh, B.-H., Lee, W.-J., Ha, N.-C., Lee, B.-L., 2007. Clustering of peptidoglycan recognition protein-SA is required for sensing lysine-type peptidoglycan in insects. Proc. Natl. Acad. Sci. 104, 6602–6607. https://doi.org/10.1073/pnas.0610924104

Park, S.K., Mann, K.J., Lin, H., Starostina, E., Kolski-Andreaco, A., Pikielny, C.W., 2006. A Drosophila protein specific to pheromone-sensing gustatory hairs delays males' copulation attempts. Curr. Biol. CB 16, 1154–1159. https://doi.org/10.1016/j.cub.2006.04.028

Pauls, D., Blechschmidt, C., Frantzmann, F., el Jundi, B., Selcho, M., 2018. A comprehensive anatomical map of the peripheral octopaminergic/tyraminergic system of Drosophila melanogaster. Sci. Rep. 8, 15314. https://doi.org/10.1038/s41598-018-33686-3

Pinho-Ribeiro, F.A., Baddal, B., Haarsma, R., O'Seaghdha, M., Yang, N.J., Blake, K.J., Portley, M., Verri, W.A., Dale, J.B., Wessels, M.R., Chiu, I.M., 2018. Blocking Neuronal Signaling to Immune Cells Treats Streptococcal Invasive Infection. Cell 173, 1083-1097.e22. https://doi.org/10.1016/j.cell.2018.04.006

Poirotte, C., Massol, F., Herbert, A., Willaume, E., Bomo, P.M., Kappeler, P.M., Charpentier, M.J.E., 2017. Mandrills use olfaction to socially avoid parasitized conspecifics. Sci. Adv. 3, e1601721. https://doi.org/10.1126/sciadv.1601721

Poltorak, A., 1998. Defective LPS Signaling in C3H/HeJ and C57BL/10ScCr Mice: Mutations in Tlr4 Gene. Science 282, 2085–2088. https://doi.org/10.1126/science.282.5396.2085

Pool, A.-H., Scott, K., 2014. Feeding regulation in Drosophila. Curr. Opin. Neurobiol. 0, 57–63. https://doi.org/10.1016/j.conb.2014.05.008

Possidente, D.R., Murphey, R.K., 1989. Genetic control of sexually dimorphic axon morphology in Drosophila sensory neurons. Dev. Biol. 132, 448–457. https://doi.org/10.1016/0012-1606(89)90241-8

Pradel, E., Zhang, Y., Pujol, N., Matsuyama, T., Bargmann, C.I., Ewbank, J.J., 2007. Detection and avoidance of a natural product from the pathogenic bacterium Serratia marcescens by Caenorhabditis elegans. Proc Natl Acad Sci U A 104, 2295–300. https://doi.org/10.1073/pnas.0610281104

Qiao, H., Keesey, I.W., Hansson, B.S., Knaden, M., 2019. Gut microbiota affects development and olfactory behavior in Drosophila melanogaster. J Exp Biol 222. https://doi.org/10.1242/jeb.192500

Ragab, A., Buechling, T., Gesellchen, V., Spirohn, K., Boettcher, A.-L., Boutros, M., 2011. Drosophila Ras/MAPK signalling regulates innate immune responses in immune and intestinal stem cells. EMBO J. 30, 1123–1136. https://doi.org/10.1038/emboj.2011.4

Rämet, M., Manfruelli, P., Pearson, A., Mathey-Prevot, B., Ezekowitz, R.A.B., 2002. Functional genomic analysis of phagocytosis and identification of a Drosophila receptor for E. coli. Nature 416, 644–648. https://doi.org/10.1038/nature735

Reichhart, J. m., Meister, M., Dimarcq, J. l., Zachary, D., Hoffmann, D., Ruiz, C., Richards, G., Hoffmann, J. a., 1992. Insect immunity: developmental and inducible activity of the Drosophila diptericin promoter. EMBO J. 11, 1469–1477. https://doi.org/10.1002/j.1460-2075.1992.tb05191.x

Rezával, C., Nojima, T., Neville, M.C., Lin, A.C., Goodwin, S.F., 2014. Sexually Dimorphic Octopaminergic Neurons Modulate Female Postmating Behaviors in Drosophila. Curr. Biol. 24, 725–730. https://doi.org/10.1016/j.cub.2013.12.051

Rezával, C., Pavlou, H.J., Dornan, A.J., Chan, Y.-B., Kravitz, E.A., Goodwin, S.F., 2012. Neural Circuitry Underlying Drosophila Female Postmating Behavioral Responses. Curr. Biol. 22, 1155–1165. https://doi.org/10.1016/j.cub.2012.04.062

Rivière, S., Challet, L., Fluegge, D., Spehr, M., Rodriguez, I., 2009. Formyl peptide receptor-like proteins are a novel family of vomeronasal chemosensors. Nature 459, 574–577. https://doi.org/10.1038/nature08029

Robertson, H.M., Warr, C.G., Carlson, J.R., 2003. Molecular evolution of the insect chemoreceptor gene superfamily in Drosophila melanogaster. Proc. Natl. Acad. Sci. 100, 14537–14542. https://doi.org/10.1073/pnas.2335847100

Rodríguez-Valentín, R., López-González, I., Jorquera, R., Labarca, P., Zurita, M., Reynaud, E., 2006. Oviduct contraction in Drosophila is modulated by a neural network that is both, octopaminergic and glutamatergic. J. Cell. Physiol. 209, 183–198. https://doi.org/10.1002/jcp.20722

Roeder, T., 2005. Tyramine and octopamine: ruling behavior and metabolism. Annu. Rev. Entomol. 50, 447–477. https://doi.org/10.1146/annurev.ento.50.071803.130404

Roeder, T., 1999. Octopamine in invertebrates. Prog. Neurobiol. 59, 533–561. https://doi.org/10.1016/s0301-0082(99)00016-7

Rohrscheib, C.E., Bondy, E., Josh, P., Riegler, M., Eyles, D., van Swinderen, B., Weible, M.W., 2nd, Brownlie, J.C., 2015. Wolbachia Influences the Production of Octopamine and Affects Drosophila Male Aggression. Appl Env. Microbiol 81, 4573–80. https://doi.org/10.1128/AEM.00573-15

Roper, S.D., Chaudhari, N., 2017. Taste buds: cells, signals and synapses. Nat. Rev. Neurosci. 18, 485–497. https://doi.org/10.1038/nrn.2017.68

Royet, J., Charroux, B., 2013. Mechanisms and consequence of bacteria detection by the Drosophila gut epithelium. Gut Microbes 4, 259–263. https://doi.org/10.4161/gmic.24386

Royet, Julien, Dziarski, R., 2007. Peptidoglycan recognition proteins: pleiotropic sensors and effectors of antimicrobial defences. Nat. Rev. Microbiol. 5, 264–277. https://doi.org/10.1038/nrmicro1620

Royet, J., Dziarski, R., 2007. Peptidoglycan recognition proteins: pleiotropic sensors and effectors of antimicrobial defences. Nat Rev Microbiol 5, 264–77. https://doi.org/10.1038/nrmicro1620

Royet, J., Gupta, D., Dziarski, R., 2011. Peptidoglycan recognition proteins: modulators of the microbiome and inflammation. Nat Rev Immunol 11, 837–51. https://doi.org/10.1038/nri3089

Rubinstein, C.D., Wolfner, M.F., 2013. Drosophila seminal protein ovulin mediates ovulation through female octopamine neuronal signaling. Proc. Natl. Acad. Sci. 110, 17420–17425. https://doi.org/10.1073/pnas.1220018110

Rytz, R., Croset, V., Benton, R., 2013. Ionotropic receptors (IRs): chemosensory ionotropic glutamate receptors in Drosophila and beyond. Insect Biochem. Mol. Biol. 43, 888–897. https://doi.org/10.1016/j.ibmb.2013.02.007

Ryu, J.-H., Kim, S.-H., Lee, H.-Y., Bai, J.Y., Nam, Y.-D., Bae, J.-W., Lee, D.G., Shin, S.C., Ha, E.-M., Lee, W.-J., 2008. Innate Immune Homeostasis by the Homeobox Gene Caudal and Commensal-Gut Mutualism in Drosophila. Science 319, 777–782. https://doi.org/10.1126/science.1149357

Sánchez-Alcañiz, J.A., Zappia, G., Marion-Poll, F., Benton, R., 2017. A mechanosensory receptor required for food texture detection in Drosophila. Nat. Commun. 8, 14192. https://doi.org/10.1038/ncomms14192

Sang, J., Rimal, S., Lee, Y., 2019. Gustatory receptor 28b is necessary for avoiding saponin in Drosophila melanogaster. EMBO Rep. 20. https://doi.org/10.15252/embr.201847328

Sato, K., Pellegrino, M., Nakagawa, Takao, Nakagawa, Tatsuro, Vosshall, L.B., Touhara, K., 2008. Insect olfactory receptors are heteromeric ligand-gated ion channels. Nature 452, 1002–1006. https://doi.org/10.1038/nature06850

Sato, K., Tanaka, K., Touhara, K., 2011. Sugar-regulated cation channel formed by an insect gustatory receptor. Proc. Natl. Acad. Sci. 108, 11680–11685. https://doi.org/10.1073/pnas.1019622108

Sauma, S., Casaccia, P., 2020. Gut-brain communication in demyelinating disorders. Curr. Opin. Neurobiol., Brain, gut, and immune system interactions 62, 92–101. https://doi.org/10.1016/j.conb.2020.01.005

Schaller, M., 2006. Parasites, Behavioral Defenses, and the Social Psychological Mechanisms through Which Cultures Are Evoked. Psychol. Inq. 17, 96–101.

Schleifer, K.H., Kandler, O., 1972. Peptidoglycan types of bacterial cell walls and their taxonomic implications. Bacteriol. Rev. 36, 407–477.

Schretter, C.E., Vielmetter, J., Bartos, I., Marka, Z., Marka, S., Argade, S., Mazmanian, S.K., 2018. A gut microbial factor modulates locomotor behaviour in Drosophila. Nature 563, 402. https://doi.org/10.1038/s41586-018-0634-9

Schwaerzel, M., Monastirioti, M., Scholz, H., Friggi-Grelin, F., Birman, S., Heisenberg, M., 2003. Dopamine and Octopamine Differentiate between Aversive and Appetitive Olfactory Memories in *Drosophila*. J. Neurosci. 23, 10495–10502. https://doi.org/10.1523/JNEUROSCI.23-33-10495.2003

Scott, K., 2018. Gustatory Processing in Drosophila melanogaster. Annu. Rev. Entomol. 63, 15–30. https://doi.org/10.1146/annurev-ento-020117-043331

Scott, K., Brady, R., Cravchik, A., Morozov, P., Rzhetsky, A., Zuker, C., Axel, R., 2001. A Chemosensory Gene Family Encoding Candidate Gustatory and Olfactory Receptors in Drosophila. Cell 104, 661–673. https://doi.org/10.1016/S0092-8674(01)00263-X

Selcho, M., Pauls, D., 2019. Linking physiological processes and feeding behaviors by octopamine. Curr. Opin. Insect Sci., Neuroscience • Special section on Evolutionary Genetics and Genomics 36, 125–130. https://doi.org/10.1016/j.cois.2019.09.002

Selcho, M., Pauls, D., Jundi, B. el, Stocker, R.F., Thum, A.S., 2012. The Role of octopamine and tyramine in Drosophila larval locomotion. J. Comp. Neurol. 520, 3764–3785. https://doi.org/10.1002/cne.23152

Sellegounder, D., Yuan, C.H., Wibisono, P., Liu, Y., Sun, J., 2018. Octopaminergic Signaling Mediates Neural Regulation of Innate Immunity in Caenorhabditis elegans. MBio 9. https://doi.org/10.1128/mBio.01645-18

Shakhar, K., Shakhar, G., 2015. Why Do We Feel Sick When Infected—Can Altruism Play a Role? PLoS Biol. 13. https://doi.org/10.1371/journal.pbio.1002276

Shanbhag, S.R., Park, S.K., Pikielny, C.W., Steinbrecht, R.A., 2001. Gustatory organs of Drosophila melanogaster: fine structure and expression of the putative odorant-binding protein PBPRP2. Cell Tissue Res. 304, 423–437. https://doi.org/10.1007/s004410100388

Sharon, G., Segal, D., Ringo, J.M., Hefetz, A., Zilber-Rosenberg, I., Rosenberg, E., 2010. Commensal bacteria play a role in mating preference of Drosophila melanogaster. Proc Natl Acad Sci U A 107, 20051–6. https://doi.org/10.1073/pnas.1009906107

Shibata, T., Sekihara, S., Fujikawa, T., Miyaji, R., Maki, K., Ishihara, T., Koshiba, T., Kawabata, S., 2013. Transglutaminase-Catalyzed Protein-Protein Cross-Linking Suppresses the Activity of the NF-κB–Like Transcription Factor Relish. Sci. Signal. 6, ra61–ra61. https://doi.org/10.1126/scisignal.2003970

Shim, J., Lee, Y., Jeong, Y.T., Kim, Y., Lee, M.G., Montell, C., Moon, S.J., 2015. The full repertoire of Drosophila gustatory receptors for detecting an aversive compound. Nat. Commun. 6, 8867. https://doi.org/10.1038/ncomms9867

Shim, J., Mukherjee, T., Mondal, B.C., Liu, T., Young, G.C., Wijewarnasuriya, D.P., Banerjee, U., 2013. Olfactory control of blood progenitor maintenance. Cell 155, 1141–53. https://doi.org/10.1016/j.cell.2013.10.032

Shimono, K., Fujimoto, A., Tsuyama, T., Yamamoto-Kochi, M., Sato, M., Hattori, Y., Sugimura, K., Usui, T., Kimura, K., Uemura, T., 2009. Multidendritic sensory neurons in the adult Drosophila abdomen: origins, dendritic morphology, and segment- and age-dependent programmed cell death. Neural Develop. 4, 37. https://doi.org/10.1186/1749-8104-4-37

Silbering, A.F., Rytz, R., Grosjean, Y., Abuin, L., Ramdya, P., Jefferis, G.S.X.E., Benton, R., 2011. Complementary function and integrated wiring of the evolutionarily distinct Drosophila olfactory subsystems. J. Neurosci. Off. J. Soc. Neurosci. 31, 13357–13375. https://doi.org/10.1523/JNEUROSCI.2360-11.2011

Sinakevitch, I., Strausfeld, N.J., 2006. Comparison of octopamine-like immunoreactivity in the brains of the fruit fly and blow fly. J. Comp. Neurol. 494, 460–475. https://doi.org/10.1002/cne.20799

Singh, R.N., 1997. Neurobiology of the gustatory systems of Drosophila and some terrestrial insects. Microsc. Res. Tech. 39, 547–563. https://doi.org/10.1002/(SICI)1097-0029(19971215)39:6<547::AID-JEMT7>3.0.CO;2-A

Slone, J., Daniels, J., Amrein, H., 2007. Sugar receptors in Drosophila. Curr. Biol. CB 17, 1809–1816. https://doi.org/10.1016/j.cub.2007.09.027

Soldano, A., Alpizar, Y.A., Boonen, B., Franco, L., López-Requena, A., Liu, G., Mora, N., Yaksi, E., Voets, T., Vennekens, R., Hassan, B.A., Talavera, K., 2016. Gustatory-mediated avoidance of bacterial lipopolysaccharides via TRPA1 activation in Drosophila. eLife 5, e13133. https://doi.org/10.7554/eLife.13133

Sombati, S., Hoyle, G., 1984. Generation of specific behaviors in a locust by local release into neuropil of the natural neuromodulator octopamine. J. Neurobiol. 15, 481–506. https://doi.org/10.1002/neu.480150607

Starostina, E., Liu, T., Vijayan, V., Zheng, Z., Siwicki, K.K., Pikielny, C.W., 2012. A Drosophila DEG/ENaC Subunit Functions Specifically in Gustatory Neurons Required for Male Courtship Behavior. J. Neurosci. 32, 4665–4674. https://doi.org/10.1523/JNEUROSCI.6178-11.2012

Steck, K., Walker, S.J., Itskov, P.M., Baltazar, C., Moreira, J.-M., Ribeiro, C., 2018. Internal amino acid state modulates yeast taste neurons to support protein homeostasis in Drosophila. eLife 7, e31625. https://doi.org/10.7554/eLife.31625

Steiner, H., Hultmark, D., Engström, Å., Bennich, H., Boman, H.G., 1981. Sequence and specificity of two antibacterial proteins involved in insect immunity. Nature 292, 246–248. https://doi.org/10.1038/292246a0

Stenbak, C.R., Ryu, J.-H., Leulier, F., Pili-Floury, S., Parquet, C., Hervé, M., Chaput, C., Boneca, I.G., Lee, W.-J., Lemaitre, B., Mengin-Lecreulx, D., 2004. Peptidoglycan Molecular Requirements Allowing Detection by the

Drosophila Immune Deficiency Pathway. J. Immunol. 173, 7339–7348. https://doi.org/10.4049/jimmunol.173.12.7339

Stensmyr, M.C., Dweck, H.K., Farhan, A., Ibba, I., Strutz, A., Mukunda, L., Linz, J., Grabe, V., Steck, K., Lavista-Llanos, S., Wicher, D., Sachse, S., Knaden, M., Becher, P.G., Seki, Y., Hansson, B.S., 2012. A conserved dedicated olfactory circuit for detecting harmful microbes in Drosophila. Cell 151, 1345–57. https://doi.org/10.1016/j.cell.2012.09.046

Stevenson, P.A., Spörhase-Eichmann, U., 1995. Localization of octopaminergic neurones in insects. Comp. Biochem. Physiol. A Physiol. 110, 203–215. https://doi.org/10.1016/0300-9629(94)00152-J

Stocker, R.F., 1994. The organization of the chemosensory system in Drosophila melanogaster: a rewiew. Cell Tissue Res. 275, 3–26. https://doi.org/10.1007/BF00305372

Stocker, R.F., Schorderet, M., 1981. Cobalt filling of sensory projections from internal and external mouthparts in Drosophila. Cell Tissue Res. 216, 513–523. https://doi.org/10.1007/BF00238648

Strober, W., Murray, P.J., Kitani, A., Watanabe, T., 2006. Signalling pathways and molecular interactions of NOD1 and NOD2. Nat. Rev. Immunol. 6, 9–20. https://doi.org/10.1038/nri1747

Suh, G.S.B., Wong, A.M., Hergarden, A.C., Wang, J.W., Simon, A.F., Benzer, S., Axel, R., Anderson, D.J., 2004. A single population of olfactory sensory neurons mediates an innate avoidance behaviour in Drosophila. Nature 431, 854–859. https://doi.org/10.1038/nature02980

Sullivan, K., Fairn, E., Adamo, S.A., 2016. Sickness behaviour in the cricket Gryllus texensis: Comparison with animals across phyla. Behav. Processes 128, 134–143. https://doi.org/10.1016/j.beproc.2016.05.004

Sun, H., Bristow, B.N., Qu, G., Wasserman, S.A., 2002. A heterotrimeric death domain complex in Toll signaling. Proc. Natl. Acad. Sci. 99, 12871–12876. https://doi.org/10.1073/pnas.202396399

Sun, H., Towb, P., Chiem, D.N., Foster, B.A., Wasserman, S.A., 2004. Regulated assembly of the Toll signaling complex drives Drosophila dorsoventral patterning. EMBO J. 23, 100–110. https://doi.org/10.1038/sj.emboj.7600033

Sung, H.Y., Jeong, Y.T., Lim, J.Y., Kim, H., Oh, S.M., Hwang, S.W., Kwon, J.Y., Moon, S.J., 2017. Heterogeneity in the Drosophila gustatory receptor complexes that detect aversive compounds. Nat. Commun. 8, 1484. https://doi.org/10.1038/s41467-017-01639-5

Suver, M.P., Mamiya, A., Dickinson, M.H., 2012. Octopamine Neurons Mediate Flight-Induced Modulation of Visual Processing in Drosophila. Curr. Biol. 22, 2294–2302. https://doi.org/10.1016/j.cub.2012.10.034

Swarup, S., Morozova, T.V., Sridhar, S., Nokes, M., Anholt, R.R.H., 2014. Modulation of Feeding Behavior by Odorant-Binding Proteins in Drosophila melanogaster. Chem. Senses 39, 125–132. https://doi.org/10.1093/chemse/bjt061

Swarup, S., Williams, T.I., Anholt, R.R.H., 2011. Functional dissection of Odorant binding protein genes in Drosophila melanogaster. Genes Brain Behav. 10, 648–657. https://doi.org/10.1111/j.1601-183X.2011.00704.x

Takehana, A., Katsuyama, T., Yano, T., Oshima, Y., Takada, H., Aigaki, T., Kurata, S., 2002. Overexpression of a pattern-recognition receptor, peptidoglycan-recognition protein-LE, activates imd/relish-mediated antibacterial defense and the prophenoloxidase cascade in Drosophila larvae. Proc. Natl. Acad. Sci. 99, 13705–13710. https://doi.org/10.1073/pnas.212301199

Takehana, A., Yano, T., Mita, S., Kotani, A., Oshima, Y., Kurata, S., 2004. Peptidoglycan recognition protein (PGRP)-LE and PGRP-LC act synergistically in Drosophila immunity. EMBO J. 23, 4690–4700. https://doi.org/10.1038/sj.emboj.7600466

Tang, H., 2009. Regulation and function of the melanization reaction in Drosophila. Fly (Austin) 3, 105–111. https://doi.org/10.4161/fly.3.1.7747

Tauber, J.M., Brown, E.B., Li, Y., Yurgel, M.E., Masek, P., Keene, A.C., 2017. A subset of sweet-sensing neurons identified by IR56d are necessary and sufficient for fatty acid taste. PLOS Genet. 13, e1007059. https://doi.org/10.1371/journal.pgen.1007059

Tauszig-Delamasure, S., Bilak, H., Capovilla, M., Hoffmann, J.A., Imler, J.-L., 2002. Drosophila MyD88 is required for the response to fungal and Gram-positive bacterial infections. Nat. Immunol. 3, 91–97. https://doi.org/10.1038/ni747

Thistle, R., Cameron, P., Ghorayshi, A., Dennison, L., Scott, K., 2012. Contact chemoreceptors mediate male-male repulsion and male-female attraction during Drosophila courtship. Cell 149, 1140–1151. https://doi.org/10.1016/j.cell.2012.03.045

Thoma, V., Knapek, S., Arai, S., Hartl, M., Kohsaka, H., Sirigrivatanawong, P., Abe, A., Hashimoto, K., Tanimoto, H., 2016. Functional dissociation in sweet taste receptor neurons between and within taste organs of Drosophila. Nat. Commun. 7, 10678. https://doi.org/10.1038/ncomms10678

Thorne, N., Amrein, H., 2008. Atypical expression of Drosophila gustatory receptor genes in sensory and central neurons. J. Comp. Neurol. 506, 548–568. https://doi.org/10.1002/cne.21547

Thorne, N., Chromey, C., Bray, S., Amrein, H., 2004. Taste perception and coding in Drosophila. Curr. Biol. CB 14, 1065–1079. https://doi.org/10.1016/j.cub.2004.05.019

Toda, H., Williams, J.A., Gulledge, M., Sehgal, A., 2019. A sleep-inducing gene, nemuri, links sleep and immune function in Drosophila. Science 363, 509–515. https://doi.org/10.1126/science.aat1650

Toda, H., Zhao, X., Dickson, B.J., 2012. The Drosophila female aphrodisiac pheromone activates ppk23(+) sensory neurons to elicit male courtship behavior. Cell Rep. 1, 599–607. https://doi.org/10.1016/j.celrep.2012.05.007

Towb, P., Galindo, R.L., Wasserman, S.A., 1998. Recruitment of Tube and Pelle to signaling sites at the surface of the Drosophila embryo. Development 125, 2443–2450.

Tsubouchi, A., Yano, T., Yokoyama, T.K., Murtin, C., Otsuna, H., Ito, K., 2017. Topological and modality-specific representation of somatosensory information in the fly brain. Science 358, 615–623. https://doi.org/10.1126/science.aan4428

Tydell, C.C., Yount, N., Tran, D., Yuan, J., Selsted, M.E., 2002. Isolation, characterization, and antimicrobial properties of bovine oligosaccharide-binding protein. A microbicidal granule protein of eosinophils and neutrophils. J. Biol. Chem. 277, 19658–19664. https://doi.org/10.1074/jbc.M200659200

Tydell, C.C., Yuan, J., Tran, P., Selsted, M.E., 2006. Bovine peptidoglycan recognition protein-S: antimicrobial activity, localization, secretion, and binding properties. J. Immunol. Baltim. Md 1950 176, 1154–1162. https://doi.org/10.4049/jimmunol.176.2.1154

Tzou, P., Ohresser, S., Ferrandon, D., Capovilla, M., Reichhart, J.M., Lemaitre, B., Hoffmann, J.A., Imler, J.L., 2000. Tissue-specific inducible expression of antimicrobial peptide genes in Drosophila surface epithelia. Immunity 13, 737–748. https://doi.org/10.1016/s1074-7613(00)00072-8

Ueno, K., Ohta, M., Morita, H., Mikuni, Y., Nakajima, S., Yamamoto, K., Isono, K., 2001. Trehalose sensitivity in Drosophila correlates with mutations in and expression of the gustatory receptor gene Gr5a. Curr. Biol. 11, 1451–1455. https://doi.org/10.1016/S0960-9822(01)00450-X

Unckless, R.L., Howick, V.M., Lazzaro, B.P., 2016. Convergent Balancing Selection on an Antimicrobial Peptide in Drosophila. Curr. Biol. CB 26, 257–262. https://doi.org/10.1016/j.cub.2015.11.063

Vallet-Gely, I., Lemaitre, B., Boccard, F., 2008. Bacterial strategies to overcome insect defences. Nat. Rev. Microbiol. 6, 302–313. https://doi.org/10.1038/nrmicro1870

Venken, K.J.T., Simpson, J.H., Bellen, H.J., 2011. Genetic manipulation of genes and cells in the nervous system of the fruit fly. Neuron 72, 202–230. https://doi.org/10.1016/j.neuron.2011.09.021

Venu, I., Durisko, Z., Xu, J., Dukas, R., 2014. Social attraction mediated by fruit flies' microbiome. J Exp Biol 217, 1346–52. https://doi.org/10.1242/jeb.099648

Verlinden, H., Vleugels, R., Marchal, E., Badisco, L., Pflüger, H.-J., Blenau, W., Broeck, J.V., 2010. The role of octopamine in locusts and other arthropods. J. Insect Physiol., Locust Research in the Age of Model Organisms In honor of M.P. Pener's 80th Birthday 56, 854–867. https://doi.org/10.1016/j.jinsphys.2010.05.018

Vijayan, V., Thistle, R., Liu, T., Starostina, E., Pikielny, C.W., 2014. Drosophila Pheromone-Sensing Neurons Expressing the ppk25 Ion Channel Subunit Stimulate Male Courtship and Female Receptivity. PLoS Genet. 10. https://doi.org/10.1371/journal.pgen.1004238

Vodovar, N., Vinals, M., Liehl, P., Basset, A., Degrouard, J., Spellman, P., Boccard, F., Lemaitre, B., 2005. Drosophila host defense after oral infection by an entomopathogenic Pseudomonas species. Proc. Natl. Acad. Sci. 102, 11414–11419. https://doi.org/10.1073/pnas.0502240102

Wallrapp, A., Riesenfeld, S.J., Burkett, P.R., Abdulnour, R.-E.E., Nyman, J., Dionne, D., Hofree, M., Cuoco, M.S., Rodman, C., Farouq, D., Haas, B.J., Tickle, T.L., Trombetta, J.J., Baral, P., Klose, C.S.N., Mahlakõiv, T., Artis, D., Rozenblatt-Rosen, O., Chiu, I.M., Levy, B.D., Kowalczyk, M.S., Regev, A., Kuchroo, V.K., 2017. The neuropeptide NMU amplifies ILC2-driven allergic lung inflammation. Nature 549, 351–356. https://doi.org/10.1038/nature24029

Wang, F., Wang, K., Forknall, N., Patrick, C., Yang, T., Parekh, R., Bock, D., Dickson, B.J., 2020. Neural circuitry linking mating and egg laying in Drosophila females. Nature 579, 101–105. https://doi.org/10.1038/s41586-020-2055-9

Wang, L., Gilbert, R.J.C., Atilano, M.L., Filipe, S.R., Gay, N.J., Ligoxygakis, P., 2008. Peptidoglycan recognition protein-SD provides versatility of receptor formation in Drosophila immunity. Proc. Natl. Acad. Sci. 105, 11881–11886. https://doi.org/10.1073/pnas.0710092105

Wang, L., Han, X., Mehren, J., Hiroi, M., Billeter, J.-C., Miyamoto, T., Amrein, H., Levine, J.D., Anderson, D.J., 2011. Hierarchical chemosensory regulation of male-male social interactions in Drosophila. Nat. Neurosci. 14, 757–762. https://doi.org/10.1038/nn.2800

Wang, Z., Singhvi, A., Kong, P., Scott, K., 2004. Taste Representations in the Drosophila Brain. Cell 117, 981–991. https://doi.org/10.1016/j.cell.2004.06.011

Wang, Z.-M., Li, X., Cocklin, R.R., Wang, Minhui, Wang, Mu, Fukase, K., Inamura, S., Kusumoto, S., Gupta, D., Dziarski, R., 2003. Human peptidoglycan recognition protein-L is an N-acetylmuramoyl-L-alanine amidase. J. Biol. Chem. 278, 49044–49052. https://doi.org/10.1074/jbc.M307758200

Weber, A.N.R., Tauszig-Delamasure, S., Hoffmann, J.A., Lelièvre, E., Gascan, H., Ray, K.P., Morse, M.A., Imler, J.-L., Gay, N.J., 2003. Binding of the Drosophila cytokine Spätzle to Toll is direct and establishes signaling. Nat. Immunol. 4, 794–800. https://doi.org/10.1038/ni955

Weiss, L.A., Dahanukar, A., Kwon, J.Y., Banerjee, D., Carlson, J.R., 2011. The molecular and cellular basis of bitter taste in Drosophila. Neuron 69, 258–272. https://doi.org/10.1016/j.neuron.2011.01.001

Werner, T., Liu, G., Kang, D., Ekengren, S., Steiner, H., Hultmark, D., 2000. A family of peptidoglycan recognition proteins in the fruit fly Drosophila melanogaster. Proc. Natl. Acad. Sci. 97, 13772–13777. https://doi.org/10.1073/pnas.97.25.13772

Wicher, D., Schäfer, R., Bauernfeind, R., Stensmyr, M.C., Heller, R., Heinemann, S.H., Hansson, B.S., 2008. Drosophila odorant receptors are both ligand-gated and cyclic-nucleotide-activated cation channels. Nature 452, 1007–1011. https://doi.org/10.1038/nature06861

Williams, J.A., Sathyanarayanan, S., Hendricks, J.C., Sehgal, A., 2007. Interaction between sleep and the immune response in Drosophila: a role for the NFkappaB relish. Sleep 30, 389–400. https://doi.org/10.1093/sleep/30.4.389

Winnig, M., Bufe, B., Kratochwil, N.A., Slack, J.P., Meyerhof, W., 2007. The binding site for neohesperidin dihydrochalcone at the human sweet taste receptor. BMC Struct. Biol. 7, 66. https://doi.org/10.1186/1472-6807-7-66

Wolf, A.J., Reyes, C.N., Liang, W., Becker, C., Shimada, K., Wheeler, M.L., Cho, H.C., Popescu, N.I., Coggeshall, K.M., Arditi, M., Underhill, D.M., 2016. Hexokinase Is an Innate Immune Receptor for the Detection of Bacterial Peptidoglycan. Cell 166, 624–636. https://doi.org/10.1016/j.cell.2016.05.076

Wolf, A.J., Underhill, D.M., 2018. Peptidoglycan recognition by the innate immune system. Nat. Rev. Immunol. 18, 243–254. https://doi.org/10.1038/nri.2017.136

Wong, A.C., Wang, Q.P., Morimoto, J., Senior, A.M., Lihoreau, M., Neely, G.G., Simpson, S.J., Ponton, F., 2017. Gut Microbiota Modifies Olfactory-Guided Microbial Preferences and Foraging Decisions in Drosophila. Curr Biol 27, 2397-2404 e4. https://doi.org/10.1016/j.cub.2017.07.022

Xu, C.S., Januszewski, M., Lu, Z., Takemura, Shin-ya, Hayworth, K.J., Huang, G., Shinomiya, K., Maitin-Shepard, J., Ackerman, D., Berg, S., Blakely, T., Bogovic, J., Clements, J., Dolafi, T., Hubbard, P., Kainmueller, D., Katz, W., Kawase, T., Khairy, K.A., Leavitt, L., Li, P.H., Lindsey, L., Neubarth, N., Olbris, D.J., Otsuna, H., Troutman, E.T., Umayam, L., Zhao, T., Ito, M., Goldammer, J., Wolff, T., Svirskas, R., Schlegel, P., Neace, E.R., Knecht, C.J., Alvarado, C.X., Bailey, D.A., Ballinger, S., Borycz, J.A., Canino, B.S., Cheatham, N., Cook, M., Dreher, M., Duclos, O., Eubanks, B., Fairbanks, K., Finley, S., Forknall, N., Francis, A., Hopkins, G.P., Joyce, E.M., Kim, S., Kirk, N.A., Kovalyak, J., Lauchie, S.A., Lohff, A., Maldonado, C., Manley, E.A., McLin, S., Mooney, C., Ndama, M., Ogundeyi, O., Okeoma, N., Ordish, C., Padilla, N., Patrick, C., Paterson, T., Phillips, E.E., Phillips, E.M., Rampally, N., Ribeiro, C., Robertson, M.K., Rymer, J.T., Ryan, S.M., Sammons, M., Scott, A.K., Scott, A.L., Shinomiya, A., Smith, C., Smith, K., Smith, N.L., Sobeski, M.A., Suleiman, A., Swift, J., Takemura, Satoko, Talebi, I., Tarnogorska, D., Tenshaw, E., Tokhi, T., Walsh, J.J., Yang, T., Horne, J.A., Li, F., Parekh, R., Rivlin, P.K., Jayaraman, V., Ito, K., Saalfeld, S., George, R., Meinertzhagen, I., Rubin, G.M., Hess, H.F., Scheffer, L.K., Jain, V., Plaza, S.M., 2020. A Connectome of the Adult Drosophila Central Brain. bioRxiv 2020.01.21.911859. https://doi.org/10.1101/2020.01.21.911859

Yamamoto, D., Jallon, J.-M., Komatsu, A., 1997. Genetic Dissection of Sexual Behavior in Drosophila Melanogaster. Annu. Rev. Entomol. 42, 551–585. https://doi.org/10.1146/annurev.ento.42.1.551

Yanagawa, A., Couto, A., Sandoz, J.-C., Hata, T., Mitra, A., Ali Agha, M., Marion-Poll, F., 2019. LPS perception through taste-induced reflex in Drosophila melanogaster. J. Insect Physiol. 112, 39–47. https://doi.org/10.1016/j.jinsphys.2018.12.001

Yang, C., Rumpf, S., Xiang, Y., Gordon, M.D., Song, W., Jan, L.Y., Jan, Y.-N., 2009. Control of the Postmating Behavioral Switch in Drosophila Females by Internal Sensory Neurons. Neuron 61, 519–526. https://doi.org/10.1016/j.neuron.2008.12.021

Yang, C.-H., Belawat, P., Hafen, E., Jan, L.Y., Jan, Y.-N., 2008. Drosophila egg-laying site selection as a system to study simple decision-making processes. Science 319, 1679–1683. https://doi.org/10.1126/science.1151842

Yang, N.J., Chiu, I.M., 2017. Bacterial Signaling to the Nervous System through Toxins and Metabolites. J. Mol. Biol. 429, 587–605. https://doi.org/10.1016/j.jmb.2016.12.023

Yano, T., Mita, S., Ohmori, H., Oshima, Y., Fujimoto, Y., Ueda, R., Takada, H., Goldman, W.E., Fukase, K., Silverman, N., Yoshimori, T., Kurata, S., 2008. Autophagic control of listeria through intracellular innate immune recognition in drosophila. Nat. Immunol. 9, 908–916. https://doi.org/10.1038/ni.1634

Yao, C.A., Carlson, J.R., 2010. Role of G-Proteins in Odor-Sensing and CO2-Sensing Neurons in Drosophila. J. Neurosci. 30, 4562–4572. https://doi.org/10.1523/JNEUROSCI.6357-09.2010

Yao, C.A., Ignell, R., Carlson, J.R., 2005. Chemosensory coding by neurons in the coeloconic sensilla of the Drosophila antenna. J. Neurosci. Off. J. Soc. Neurosci. 25, 8359–8367. https://doi.org/10.1523/JNEUROSCI.2432-05.2005

Yapici, N., Cohn, R., Schusterreiter, C., Ruta, V., Vosshall, L.B., 2016. A Taste Circuit that Regulates Ingestion by Integrating Food and Hunger Signals. Cell 165, 715–729. https://doi.org/10.1016/j.cell.2016.02.061

Yapici, N., Kim, Y.-J., Ribeiro, C., Dickson, B.J., 2008. A receptor that mediates the post-mating switch in Drosophila reproductive behaviour. Nature 451, 33–37. https://doi.org/10.1038/nature06483

Yarmolinsky, D.A., Zuker, C.S., Ryba, N.J.P., 2009. Common sense about taste: from mammals to insects. Cell 139, 234–244. https://doi.org/10.1016/j.cell.2009.10.001

Youn, H., Kirkhart, C., Chia, J., Scott, K., 2018. A subset of octopaminergic neurons that promotes feeding initiation in Drosophila melanogaster. PloS One 13, e0198362. https://doi.org/10.1371/journal.pone.0198362

Zaidman-Rémy, A., Hervé, M., Poidevin, M., Pili-Floury, S., Kim, M.-S., Blanot, D., Oh, B.-H., Ueda, R., Mengin-Lecreulx, D., Lemaitre, B., 2006. The Drosophila Amidase PGRP-LB Modulates the Immune Response to Bacterial Infection. Immunity 24, 463–473. https://doi.org/10.1016/j.immuni.2006.02.012

Zhang, Y., Lu, H., Bargmann, C.I., 2005. Pathogenic bacteria induce aversive olfactory learning in Caenorhabditis elegans. Nature 438, 179–84. https://doi.org/10.1038/nature04216

Zhang, Y.V., Ni, J., Montell, C., 2013a. The Molecular Basis for Attractive Salt Taste Coding in Drosophila. Science 340, 1334–1338. https://doi.org/10.1126/science.1234133

Zhang, Y.V., Raghuwanshi, R.P., Shen, W.L., Montell, C., 2013b. Food experience–induced taste desensitization modulated by the Drosophila TRPL channel. Nat. Neurosci. 16, 1468–1476. https://doi.org/10.1038/nn.3513

Zhao, G.Q., Zhang, Y., Hoon, M.A., Chandrashekar, J., Erlenbach, I., Ryba, N.J.P., Zuker, C.S., 2003. The receptors for mammalian sweet and umami taste. Cell 115, 255–266. https://doi.org/10.1016/s0092-8674(03)00844-4

Zhong, L., Hwang, R.Y., Tracey, W.D., 2010. Pickpocket is a DEG/ENaC protein required for mechanical nociception in Drosophila larvae. Curr. Biol. CB 20, 429–434. https://doi.org/10.1016/j.cub.2009.12.057

Zhou, C., Huang, H., Kim, S.M., Lin, H., Meng, X., Han, K.-A., Chiang, A.-S., Wang, J.W., Jiao, R., Rao, Y., 2012. Molecular Genetic Analysis of Sexual Rejection: Roles of Octopamine and Its Receptor OAMB in Drosophila Courtship Conditioning. J. Neurosci. 32, 14281–14287. https://doi.org/10.1523/JNEUROSCI.0517-12.2012

Zhou, C., Rao, Yong, Rao, Yi, 2008. A subset of octopaminergic neurons are important for Drosophila aggression. Nat. Neurosci. 11, 1059–1067. https://doi.org/10.1038/nn.2164

Zhou, R., Silverman, N., Hong, M., Liao, D.S., Chung, Y., Chen, Z.J., Maniatis, T., 2005. The role of ubiquitination in Drosophila innate immunity. J. Biol. Chem. 280, 34048–34055. https://doi.org/10.1074/jbc.M506655200

Annex 1

Trends in Neurosciences

CellPress REVIEWS

Review

How Bacteria Impact Host Nervous System and Behaviors: Lessons from Flies and Worms

Ambra Masuzzo,[1] Martina Montanari,[1] Léopold Kurz,[1] and Julien Royet[1,*]

Behavior is the neuronally controlled, voluntary or involuntary response of an organism to its environment. An increasing body of evidence indicates that microbes, which live closely associated with animals or in their immediate surroundings, significantly influence animals' behavior. The extreme complexity of the nervous system of animals, combined with the extraordinary microbial diversity, are two major obstacles to understand, at the molecular level, how microbes modulate animal behavior. In this review, we discuss recent advances in dissecting the impact that bacteria have on the nervous system of two genetically tractable invertebrate models, *Drosophila melanogaster* and *Caenorhabditis elegans*.

Microbes Influence Animal Behavior

Microorganisms, which appeared on our planet more than 3.5 billion years ago, later coevolved with animals. From this cohabitation, a significant interdependency arose between hosts and their surrounding or associated microbes, which had profound effects on metazoan biology, fitness, reproduction, and physiology. It is therefore no surprise that **allochthonous** (see Glossary) and **autochthonous** microorganisms also have important influences on animal behavior [1,2]. While a large number of microbes are pathogenic and pose a threat to an animal's survival, others, such as those forming the symbiotic **microbiota**, play beneficial roles for the host [3,4]. Hence, when navigating in their environment, animals benefit from being able to differentiate between beneficial and harmful microorganisms. They can, for example, taste and smell chemical compounds produced by microbes and use this sensory information to avoid pathogenic microbes. Timely detection of harmful bacteria is expected to be beneficial in many ways for the host. By decreasing exposure to a pathogen, it increases its survival chance and limits the spreading of the threat to its sibling and progeny. It also reduces energetic expenses by preventing the activation of the costly immune response (Box 1). In other circumstances, microorganisms are precious sources of information indicative of favorable sites for foraging, laying offspring, as well as nursing and raising them [5,6]. Microorganisms can also alter the behavior of the host once they have infected them [7]. While some of these behavioral changes are seen as side effects inherent to the modulation of host homeostasis, genetic studies have demonstrated that others result from a direct molecular dialog between the microorganism and the host nervous system. They could represent a noncanonical immune response aimed at reducing the consequences of the infection for the host or its offspring. Dissecting these peculiar interorganism interactions is certainly an important field of research for the coming years. However, the enormous diversity of microbes that cohabit with animals and the highly complex organization of the eukaryotic nervous system complicate the task. Elucidating the causal relationship between host–microbe interactions and behavioral changes can undoubtedly benefit from the use of relatively simple and genetically tractable models. In past years, studies in two invertebrate model systems, *Drosophila melanogaster* and *Caenorhabditis elegans*, have not only unraveled the extreme pleiotropic modes of interactions that take place between microorganisms and the nervous system of animals but have also begun to reveal the nature of the microbial elicitors, the type of neurons that detect them, and the behavioral consequences associated with their reciprocal interactions.

Highlights

Animals can probe, via their sensory neuronal systems, the surrounding environment and the microorganisms that inhabit it. This information is used by animals to adapt their behaviors accordingly.

Drosophila melanogaster and *Caenorhabditis elegans* are useful models to identify the bacteria metabolites and components of the cell wall that are detected by sensory neurons. Some of these bacteria-derived compounds are species-specific, whereas others are more universal.

Some of the bacteria-derived metabolites can affect flies' behavior by directly impacting the function of some of the central nervous system neurons.

In some cases, the same bacterial elicitors and signaling modules are used by the infected host to sense bacterial presence via the nervous system and to trigger an antibacterial response in immune-competent cells.

Production or release of neurotransmitters upon bacterial infection controls immune response intensity in *C. elegans*.

By either producing neurotransmitters or releasing molecules that modulate host neurotransmitter level or activity, gut-associated bacteria influence the behaviors of flies and worms.

[1]Aix-Marseille Université, CNRS, IBDM, Marseille, France

*Correspondence:
julien.royet@univ-amu.fr (J. Royet).

© 2020 Elsevier Ltd. All rights reserved.

Box 1. *D. melanogaster* and *C. elegans* Antibacterial Responses

D. melanogaster: to study antibacterial responses in *D.* melanogaster, flies are typically either infected by wounding the thoraxic cuticle with a contaminated needle or by feeding on bacteria-contaminated medium. Genetic and genomic studies revealed the pivotal role for the TOLL and IMD signaling cascades in *D. melanogaster* antimicrobial response [79,80]. These signaling pathways can be activated locally in exposed epithelia as well as systemically in the fat body. Activation of these pathways depends on the detection of bacteria-derived peptidoglycan by PGRP sensor proteins [22]. These pathways culminate in the translocation of NF-κB to the nucleus, leading to infection-specific upregulation of AMPs dedicated to clear the infection. The cell-mediated immune system relies on blood cells and is induced by epithelial damage and detection of foreign particles in the hemocoel [81]. Hemocytes seal epithelial wounds, encapsulate and terminate parasites, and engulf apoptotic corpses or bacteria. *D. melanogaster* has three major lineages of hemocytes: plasmatocytes with phagocytic capacity, crystal cells that are implicated in the melanization process, and lamellocytes that encapsulate large foreign bodies.

C. elegans: bacteria can infect and kill nematodes [82]. *C. elegans* feeds on bacteria and their standard food in laboratory settings is a slow replicating strain of *E. coli*. To expose nematodes to other bacteria such as *P. aeruginosa* or *S. marcescens*, the animals are deposited on a plate seeded with the desired microbe; accordingly, in some respects, these infections can be considered as natural. This protocol allows worms to seek the bacteria, to flee the bacterial lawn, or to make choices between two strains or species. During the feeding process, bacteria are pumped in the pharynx, then grinded, and a bacterial lysate fills the intestinal lumen. Infections are principally characterized by bacteria able to survive and proliferate within the intestinal lumen, leading to the precocious death of the animal. Septic injury is not a model extensively used. The main pathways involved in the antibacterial responses in *C. elegans* are the TGF-β, the p38/MAPK, and Wnt pathways and the responding cells are those exposed to the threat. TOL-1, homolog of the *D. melanogaster* Toll has not been found in *C. elegans* immune response. When analyzing the upstream events leading to defense activation, it appeared that detection of modified self rather than interactions with microbe-associated molecular patterns like LPS or PGN is used by this invertebrate. Indeed, chemicals perturbing central processes like translation are inducers of the immune response. The same is true with the ToxA bacterial toxin that impairs the ribosomal activity [83].

In this review, we will provide an overview of recent achievements in both animal models, with a specific emphasis on the interactions between bacteria and the host nervous system. The first part will be devoted to the mechanisms involved in bacteria detection by neurons. We will then discuss current knowledge related to the modulation of the immune response by neuronal inputs. Lastly, we will illustrate how some 'immune' proteins are also implicated in neuronally controlled host behaviors under infected or physiological conditions.

C. elegans Detects and Avoids Pathogenic Bacteria through its Sensory Neurons

The nematode *C. elegans* is present in soils, where it encounters a variety of bacteria species [8]. As expected for a bacterivorous animal, it thrives in media containing innocuous food sources such as *Escherichia coli*, but escapes from those contaminated with pathogenic species, which can be life-threatening [9]. For an animal constantly foraging in bacteria and using a bacterial lysate as food source, the classical self/non-self paradigm does not strictly apply (Box 1). How then is the worm distinguishing between innocuous and pathogenic bacteria? In laboratory conditions, *C. elegans* avoids *Serratia marcescens*, which can digest the worm's eggshell and produce deadly compounds. This lawn-avoidance behavior is mediated by two head olfactory neurons exposed to the environment (AWB), that are part of the amphid, the largest chemosensory organ of the nematode (Box 2). Triggered by the *Serratia*-produced serrawetin W2, this lawn-behavior requires the Toll-like receptor TOL-1 [10]. In this prey–predator race, *C. elegans* also escapes from nematicide molecules produced by *Streptomyces*. Avoidance of *Streptomyces*-produced dodecanoic acid requires the expression of the G-protein coupled receptor (GPCR), SRB-6, in a subset of head (ASH, ADL, ADF) and tail (PHA, PHB) chemosensory neurons [11]. Unexpectedly, in two-choice assays between innocuous bacteria and *S. marcescens or Pseudomonas aeruginosa*, *C. elegans* is initially attracted to pathogenic bacteria. Only after some hours of exposure, trained animals learn to avoid pathogens and exit the bacterial lawn. This delay may correspond to a period during which nematodes learn to avoid odors of pathogenic bacteria and generate memory of the encounter. Other data, discussed later, suggest that it results from the development of the infection and it is associated with host damages. Exposure to

Glossary

Aerotaxis: oxygen-dependent migration.
Allochthonous: allochthonous bacteria are non-resident bacteria species that live in the animal environment and can eventually infect it.
Antimicrobial peptides (AMPs): small molecular weight proteins with broad spectrum antimicrobial activity against bacteria, viruses, and fungi. These evolutionarily conserved peptides are usually positively charged and have both a hydrophobic and hydrophilic side that enables them to be both soluble in aqueous environments yet able to penetrate lipid-rich membranes.
Autochthonous: autochthonous bacteria are resident bacteria species that live in association with the host. Typically, some are species that form the microbiota.
Axenic: germ-free.
Dysbiosis: imbalance in host-associated microbial communities that can be associated with diseases.
Frass: excrement or other refuse left by insects and their larvae.
Gnotobiotic: germ-free animals that have been associated with controlled bacteria species.
Interneurons: nerve cells that relay impulses between projection neurons, for instance, between sensory neurons and motor neurons.
Lipopolysaccharide (LPS): present in almost all Gram-negative bacteria, LPS is the major outer surface membrane component. It consists of a polysaccharide region that is anchored in the outer bacterial membrane by lipid A. Its detection by *ad hoc* PRR triggers an immune response.
Lymph gland: larval organ in which most of the *D. melanogaster* hemopoietic cells are generated.
Microbiota: communities of microorganisms that live in or on an animal. The species that live in the intestine form the gut microbiota.
Octopamine: monoamine closely related to mammalian norepinephrine. This neurotransmitter, which acts through G protein-coupled receptors, regulates many behaviors in invertebrates.
Odorant receptor: insect odorant receptors are transmembrane ionotropic receptors that may also use metabotropic signaling. Most insect odorant receptors function in the presence of another shared receptor known as Orco.

Box 2. *C. elegans* Nervous System

The nematode does not possess a so-called brain, even though nearly a third of its somatic cells are neurons, with adult hermaphrodite *C. elegans* possessing 302 neurons (https://www.wormatlas.org/). Thanks to its invariable developmental pattern and intensive studies, including reconstruction based on serial electron micrographs, the exact position of each neuron as well as the neuronal connectivity are known. Each neuron has its own name, using a system of three to four letters (e.g., AFD). Most of the neurons are located in the head around the pharynx in an area called the nerve ring, others are longitudinal, around the vulva or close to the tail. There are currently 32 designated chemosensory neurons and their functions can range from proprioceptors to oxygen sensors or chemosensors. Four chemosensory organs have been described with amphids (in the heads) and phasmids (in the tail) being the largest chemosensory organs of worms. These specialized groups of cells are made of support and socket cells, which define a sensillum that is an opening through which dendrites of sensory neurons are exposed to the external milieu. Interestingly, the chemosensory neurons directly contact neuronal circuits (interneurons and motoneurons) dedicated to forward or backward movement. However, chemosensory neurons are exclusive and one cell controls either attraction or repulsion, but not both. Chemosensory neurons can be dedicated to volatile compounds (1-octanol, diacetyl) as well as water-diluted molecules (NaCl), with more than one specific receptor expressed in the dendrite of each neuron. The candidate proteins to mediate chemosensation are GPCRs and the nematode genome encodes around 1300 of them. Contrary to chemosensation, the neurons necessary for the response to oxygen are exposed to the nematode internal fluids and the receptors are guanylyl cyclases combined with hemes. Pheromone sensing is also present with a complex chemical lexical. Thus, nematodes navigate in the environment, integrate cues from oxygen and carbon dioxide levels, are attracted towards putative food source, can sense the population density, are repulsed when exposed to noxious chemicals, and are capable of learning with a memory lasting several days.

pathogens also upregulates the expression of serotonin in the ADF chemosensory neurons. Serotonin functions through MOD-1, a serotonin-gated chloride channel expressed in sensory **interneurons**, to promote olfactive aversive learning [12]. Recent studies dissected the molecular and cellular bases and characterized the neuronal network underlying this behavior [13–15]. In sum, in parallel to food-seeking behaviors that allow them to search and identify beneficial bacteria, nematodes perceive and react to biotic stress via dedicated neuronal circuits.

C. elegans Senses Local Gas Concentration to Detect Bacteria

Modifications that microorganisms cause to their environment are also a source of information for the worm. Local concentrations of oxygen are important cues used by *C. elegans* to move in its environment, a phenomenon called **aerotaxis** behavior [16]. Usually attracted by low O_2 and high CO_2 concentrations that are indicative of bacteria-enriched substrates, worms use gas-level sensing to mount protective avoidance behavior. Under high bacterial density conditions, *P. aeruginosa* produces secondary metabolites such as phenazine-1-carboxamide and pyochelin. Detection of these metabolites by ASJ neurons (amphids) activates the production of the transforming growth factor (TGF)-β family member DAF-7 that, in turn, inhibits DAF-3 signaling in the adjacent RIM/RIC interneurons [17]. This neuronal activation leads the worm to seek higher oxygen environments, away from potential pathogens. Bacterially produced CO_2 is another cue used by nematodes to escape pathogens. Defective CO_2 detection by gas-sensing BAG neurons positively correlates with a defect in avoidance of *Serratia* [18]. In this context, the TOL-1 receptor and downstream signaling events are required to specify the fate of BAG chemosensory neurons. In addition, *C. elegans*, which, unlike most metazoans lacks nitric oxide synthase and consequently cannot synthesize NO, uses this gas as an environmental cue to avoid *P. aeruginosa* [19]. This response is mediated by the ASJ chemosensory neurons and requires NO-mediated activation of receptor guanylate cyclase and cyclic nucleotide-gated ion channels (DAF-11 and GCY-27). *P. aeruginosa* mutants deficient for NO production fail to elicit avoidance. These results demonstrate that gases produced by microbial respiration are important molecular cues used by nematodes to avoid metabolically active pathogens. However, since both pathogenic and harmless microbes respire aerobically and produce CO_2, the sole presence of this gas does not indicate whether the microbes that produced it are harmful. *C. elegans* might reserve this option to feed on attenuated or dead microbes that would otherwise be pathogenic and probably integrate other cues to distinguish pathogenic from non-pathogenic bacteria (Figure 1).

NF-κB: nuclear factor kappa-light-chain-enhancer of activated B cells, is a protein complex that controls the transcription of DNA. NF-κB is found in almost all animal cell types and is involved in cellular responses to stimuli such as stress, cytokines, free radicals, and bacterial or viral antigens. Three NF-κB members exist in flies (Relish, Dorsal, and DIF). It has not been found in *C. elegans*.

Pattern recognition receptors (PRRs): germline-encoded host sensors, which detect molecules typical for the microbes. They are proteins expressed mainly in cells of the innate immune system but also some neuronal cells.

Peptidoglycan (PGN): polymers of sugars and amino acids that form a mesh-like layer outside the plasma membrane of most bacteria, thus constituting the cell wall.

Peptidoglycan recognition proteins (PGRPs): receptors that play essential roles in triggering the antibacterial innate immune response in invertebrates. Although their main ligand is the bacteria-derived peptidoglycan, some family members can be activated by other bacterial ligands. They are also present in mammalian proteomes [25].

Sensory neurons: nerve cells responsible for converting external stimuli from the environment into internal electrical impulses.

TrpA1: transient receptor potential cation channel, subfamily A, member 1, is an ion channel located on the plasma membrane of many human and animal cells. It is one of the most promiscuous TRP ion channels with many identified ligands such as LPS.

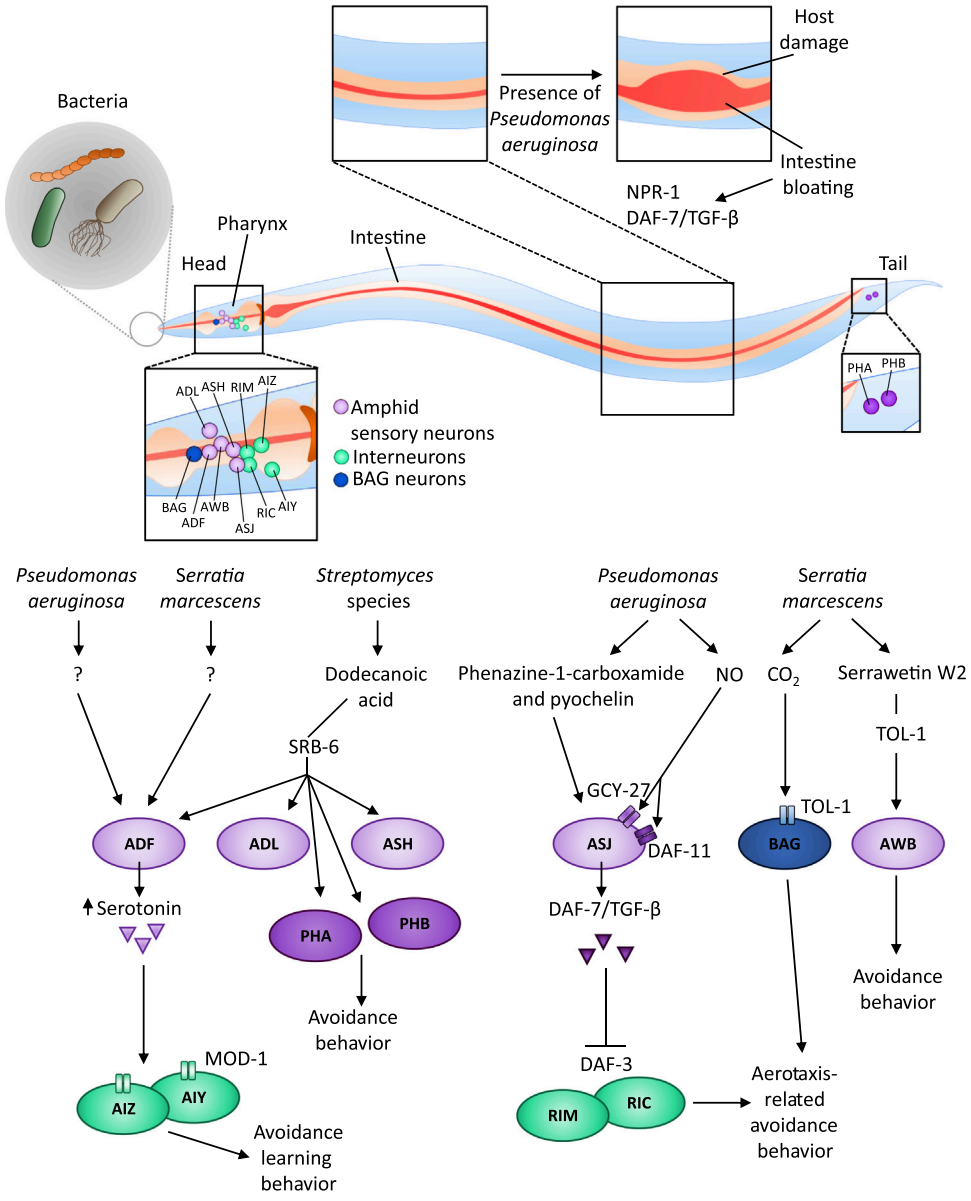

Figure 1. Interactions of Bacteria with the *Caenorhabditis elegans* Nervous System. Some bacteria species produce metabolites that, upon sensing by the amphid sensory neurons, trigger pathogen avoidance. Depending on the species, the bacterial trigger and the host sensing neurons have not always been identified. Different mechanisms underlie pathogen avoidance; these include avoidance learning behavior and aerotaxis-related avoidance behavior. Avoidance can also be triggered after the ingestion of the pathogen. How these gut-associated bacteria induce worm escape is not yet clear. While some authors propose that intestine bloating is the trigger, others state that tissue damages occurring from intestinal infection are a key component of aversive learning response. Integration of several inputs, including the aforementioned ones, might allow the animal to fine-tune its reaction towards bacteria. Abbreviations: NO, nitric oxide; TGF-β, transforming growth factor beta; TOL-1, Toll-like receptor.

Bacterial Detection Mainly Requires the Olfactory and Gustatory Systems of *D. melanogaster*

D. melanogaster lives primarily on rotten fruits populated by microbes that synergistically ferment organic substrates to produce active compounds and metabolites [20,21]. Detecting these

chemosensory molecules helps the flies to find nutrient-rich food, to select hospitable zones for egg-laying, and to avoid ecological niches contaminated with pathogens. In *D. melanogaster*, tastants and volatiles are detected by hundreds of gustatory and olfactory neurons distributed on multiple body parts, including the antennae, maxillary palps, proboscis, wing margins, legs, and ovipositor [22] (Box 3). Some constitutive elements of the bacterial cell wall and membrane can be directly sensed by these neurons. Detection of bacterial **lipopolysaccharide (LPS)** by the esophageal bitter neurons via the **TrpA1** receptor triggers feeding and oviposition avoidance [23]. When applied onto wing margins or legs, bacteria cell wall **peptidoglycan (PGN)** induces grooming behavior [24]. Unpublished data from our group indicate that PGN can also be detected by fly gustatory bitter neurons via the classical immune **pattern recognition receptor (PRR)** of the **peptidoglycan recognition proteins (PGRPs)** family [25] (A. Masuzzo, L. Kurz, and J. Royet unpublished data). As for *C. elegans*, the fly olfactory system plays a key role in adapting behavior to the presence of bacteria. *D. melanogaster* larvae fed with the opportunistic pathogen *Erwinia carotovora* drastically reduce food intake [26]. This feeding blockage requires the universal olfactory coreceptor *Orco* and TrpA1. Geosmin, a volatile odorant produced by some fungi and bacteria acts as a strong fly repellent that can override innate attraction to vinegar and other food-related odorants [27]. Its activity is mediated by a single class of neurons expressing the **odorant receptor** 56a (Or56a) and which target the DA2 glomerulus in the antennal lobe. Carnivore feces are enriched in bacteria that produce phenols. Phenol detection by Or46a olfactory neurons present in the fly palp triggers oviposition aversion [28]. Activation of the geosmin and phenol circuitry is sufficient to induce a reduction in oviposition, suggesting that they are powerful signals for the presence of potential infectious sites containing harmful microbes. Consistently, these signals have been shown to also be aversive in other insect

Box 3. *D. melanogaster* Olfactory and Gustatory Systems

Gustatory System

D. melanogaster can detect basic taste, including sugar, bitter, salt, and acid. The fly taste system is distributed over the whole body. Dose-dependent activation of different taste cells provides a simple mechanism to encode taste modality and tastant concentration. Taste bristles, present on labellum, legs, wings, and ovipositor, house dendrites of underlying gustatory receptors neurons (GRNs), which are thus exposed to the environment. On each dendrite different gustatory receptors (GRs), that bind different chemicals, can be coexpressed. GRNs are named according to receptors they express and their induced behaviors. In addition to peripheral taste bristles, GRNs are also located in three clusters that line the pharynx, to monitor food as it enters the esophagus. Taste information is integrated through different mechanisms in primary taste neurons. Adverse tastants can inhibit the activity of appetizing taste neural circuits, as well as the internal state, and can modulate the sensitivity of sweet and bitter neurons. GRNs from the labellum, pharynx, and some of those in the legs project their axons to the subesophageal zone (SEZ) of the brain, whereas wing and few leg GRNs project to the thoracic ganglion. The SEZ is a primary gustatory center, with characteristic activation patterns defined based on the origin of the taste information and the type of tastants. Higher brain centers, where taste information is conveyed from the SEZ, are largely unknown. Second-order sweet projection neurons, relaying taste information from SEZ to the mechanosensory and motor center (AMMC), have been identified. The AMMC is a center for processing of multisensory information; it also receives inputs from olfactory and auditory neurons. Recent work identified taste projection neurons that project to the superior lateral protocerebrum and convey taste information to the mushroom body (MB); in the MB calyx, taste inputs continue to be segregated according to the taste modality and origin [84–86].

Olfactory System

D. melanogaster detects odors through the antenna and maxillary palp. These olfactory organs are covered by sensory bristles, which house dendrites of underlying olfactory sensory neurons (OSNs). Each OSN generally expresses a single olfactory receptor, belonging to one of the two families of olfactory receptor genes, ORs or IRs, and transmits information to one or two spatially invariant glomeruli in the antennal lobe (AL). In the AL, sensory neurons interact with projection neurons that project towards the upper brain centers and with local neurons whose projections are limited to the AL. Each projection neuron receives information from a single glomerulus and projects its axon to the protocerebrum and from here to the lateral horn (LH) and the MB. The LH is thought to be important for instinctive olfactory behaviors since premotor neurons receive input in the LH that may lead to an olfactory behavioral response. MB is important for learning and memory. It receives olfactory, gustatory, and visual input, allowing multimodal processing and memory [87].

species. Besides protecting flies from detrimental bacteria, the olfactory system can also mediate fly attraction to microbes. Indeed, the detection of bacterial short-chain fatty acid by Or30a neurons acts as an orexigenic signal for the larvae [29]. Optimal identification of a given bacteria species presumably requires the integration of multiple sensory modalities. Consistently, when given the choice between a sugar only and an *E. carotovora carotovora*-contaminated solution, flies are first attracted by the bacteria and after a few hours repulsed by it. While the initial attractive phase depends on the olfactory Gr63a neurons, the second repulsive phase requires the bitter taste Gr66a neurons. Interestingly, by providing a food source for the flies, *E. carotovora* facilitates the potentiation of bitter neurons allowing the avoidance behavior to be established [30]. Altogether, these data demonstrate the roles played by the fly and worm **sensory neurons** in detecting environmental bacteria and mounting behaviors to either avoid them if they are toxic or, on the contrary, to move towards them and feed on them when they are beneficial (Figure 2).

Intestinal Bacteria Impact *C. elegans* Behavior

The gut microbiota is mainly composed of bacteria species that are either neutral or beneficial for the host. However, the ingestion of pathogenic bacteria together with environmental and genetic variations can lead to **dysbiosis** with detrimental consequences for the host. How these quantitative or qualitative changes in gut bacteria populations alter host behavior is a growing area of research. For the nematode that feeds on bacteria and empties its intestine content within minutes, the existence of gut microbiota is still debated (Box 1). However, some reports have shown that some gut bacteria can affect *C. elegans* behavior. To avoid being killed by *P. aeruginosa*, worms move away after a few hours of contact with the pathogen. Although this delayed response has been attributed to olfaction-dependent aversive learning (see earlier), it has been proposed that lawn avoidance is a consequence of the damages caused by the ingested bacteria. This is supported by the lack of lawn avoidance of non-pathogenic bacteria or avirulent mutants of *P. aeruginosa*. Furthermore, the avoidance behavior observed in *C. elegans* fed with *E. coli* producing double-stranded RNA that inactivates genes required for fundamental cellular activities, also reinforces the hypothesis of cellular damage sensing [31]. As in the case of pathogen-avoidance, noxious RNAi-dependent avoidance also engages a serotonergic circuit since it is reduced in the serotonin biosynthetic mutant *tph-1*. Another model has emerged from reports studying bacteria sensing by the gut epithelium [32,33]. Mutant worms defective in either pharyngeal pumping (*phm-2*) or defecation motor program (DMP) present an increased gut bacterial load that is correlated with an avoidance response. Since inhibition of gut colonization abrogates the escape response, bacterial colonization and consequent bloating of the intestine could be perceived as a danger signal by the worm. Increased avoidance caused by the *phm-2* mutation also requires TPH-1-mediated serotonin biosynthesis but is independent of NPR-1-mediated neuropeptide signals [32]. Moreover, the avoidance caused by increased colonization in the *DMP* mutants requires NPR-1 and the two neuropeptides FLP-18 and FLP-21, although serotonin biosynthesis plays a negligible role here [33]. It remains unclear what might cause this discrepancy.

Moreover, in contrast to the aforementioned results [17], the rapid chemosensation of *P. aeruginosa*-derived phenazine-1-carboxamide and pyochelin, which leads to the induction of DAF-7/TGF-β in ASJ neurons, does not correlate with the avoidance behavior [34]. Instead, bloating of the intestinal lumen induces the avoidance behavior via modulation of both DAF-7/TGF-β and the GPCR NPR-1 neuroendocrine pathways, which results in a preference for O_2 and thus in pathogen avoidance behavior [34]. Since there is no general agreement on how gut-associated bacteria trigger avoidance in *C. elegans*, further work will be needed to determine the relative contribution of gut bacteria sensing and/or gut bacteria host damage induction to this

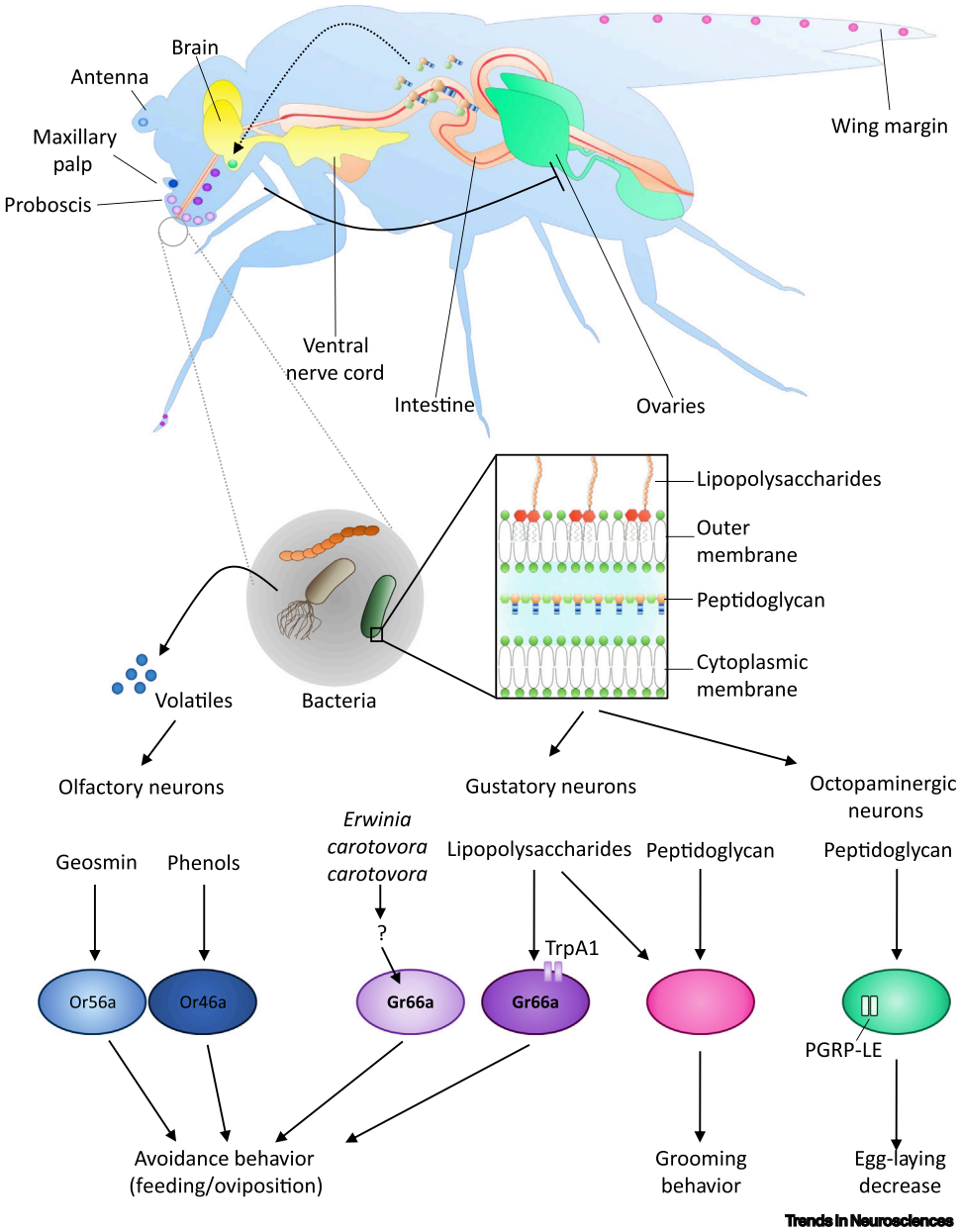

Figure 2. Interactions of Bacteria with the *Drosophila melanogaster* Nervous System. Environmental bacteria produce metabolites and volatiles that can be directly sensed by the fly olfactory and gustatory neurons. The same is true for constituents of the bacteria cell wall such as lipopolysaccharide and peptidoglycan (PGN). Subsequent activation of sensory neurons induces host behavior changes such as bacteria avoidance or modulation in food intake, egg-laying rate, or grooming. Some bacteria cell wall components such as PGN can enter the body cavity and directly act on brain octopaminergic neurons to modulate the egg-laying rate. Abbreviation: PGRP, peptidoglycan recognition protein.

phenomenon. The consideration of the timing seems to be crucial to understand this behavior, which certainly results from the integration of several inputs. Whereas bacteria-induced innate processes are expected to be rapid, slower kinetics would be expected for a behavior secondary to changes in the internal state of the infected animal.

Gut Bacteria-Dependent Neuropeptides Affect *C. elegans* Behavior

In the complex network of influences that *P. aeruginosa* can exert on *C. elegans* behavior, insulin-like neuropeptides also play a role. When exposed to *P. aeruginosa*, worms present an upregulation of the neuroendocrine peptide INS-11 in the intestine. By inhibiting the expression of *ins-6* in ASI neurons and serotonin synthesis in ADF neurons, INS-11 negatively regulates aversive learning behavior [35,36]. The decrease in learning abilities upon pathogen exposure might appear as a disadvantage for the host. However, aversive learning behavior has to be balanced with the need to resume eating and produce progeny. If the balance is too strongly tilted to one side or another, nematodes might be unable to recognize and avoid pathogens, or they might starve and become less fertile. Consistently, *ins-11* loss-of-function mutants that are inefficient in seeking new sources of food consume more energy and have fewer offspring (Figure 1). Host behavior can also be affected by neuropeptides produced by gut bacteria. Released by the commensal *Providencia*, the bioamine tyramine is converted to **octopamine** by the *C. elegans* tyramine β-hydroxylase. Octopamine, in turn, targets the OCTR-1 octopamine receptor on ASH nociceptive neurons to modulate an aversive olfactory response. Food choice assays demonstrate that worms are preferentially colonized by *Providencia* and that this selection bias requires bacterially produced tyramine and host octopamine signaling. Hence, a neurotransmitter produced by a gut bacterium can mimic the functions of the cognate host molecule and override host control of a sensory decision and thereby promotes fitness of both the host and the microorganism [37].

Bacteria-Derived Compounds Can Be Sensed Internally by *D. melanogaster* Neurons

Contrary to *C. elegans*, the existence of the gut microbiota in *D. melanogaster* is well established and studies involving **gnotobiotic** and **axenic** flies are possible [38,39]. While the pleiotropic roles played by gut-associated bacteria in fly development and physiology are amply documented, their influence on behavior is only beginning to be elucidated [40]. By acting via the olfactory system, gut-associated bacteria can influence fly preferences in food-seeking and choice of egg-laying sites [41–43]. However, internal bacteria can also alter neuronally controlled behaviors independently of the sensory system. When compared with their conventionally reared sibling, axenic flies show enhanced locomotion [44]. Gut recolonization by *Lactobacillus brevis* is sufficient to bring locomotion back to normal levels. Genetic and biochemical data demonstrated that bacteria-produced xylose isomerase is critical to sustaining normal fly locomotion. Although the exact mechanisms involved remain unclear, xylose isomerase mediates its effects by inactivating the central nervous system neurons that produce octopamine. The same neuromodulator is central to another bacteria-induced behavior modification in the fruit fly. When mated females are infected by bacteria, they reduce their oviposition to spare the energy required to fight infection or to prevent progeny development in a nonfavorable environment [45]. Previous work has revealed that during an immune response, the detection of bacteria-derived PGN by PGRP receptors triggers an **NF-κB**-dependent production of **antimicrobial peptides (AMP)** in immune cells [46] (Box 1). Surprisingly, the same bacterial elicitor and the same signaling pathway regulate the reduction of female oviposition following bacterial infection [45]. PGN sensing by PGRP-LE and NF-κB activation in a few octopaminergic neurons in the fly brain are sufficient to modulate egg-laying in infected females [47]. Therefore, a unique bacteria cell wall constituent and a common host signaling cascade are used in immune cells to mount an immune response and in brain neurons to control fly behavior following infection. While it is well established that gut-borne PGN can cross the gut epithelium to reach circulating hemolymph, its mode of access to the brain remains unknown [48,49]. Interestingly, the biogenic amine octopamine was also shown to mediate the effects that the endosymbiotic *Wolbachia* bacteria can exert on *D. melanogaster* male aggressivity [50]. Finally, pathogens can also modulate host behavior to their advantage. By changing the pheromone levels in the **frass** of the flies they infect,

Pseudomonas entomophila attracts healthy flies, leading to their contamination and favoring pathogen dispersal [51]. Fly mating behavior can also be influenced by bacteria that are associated with the host. Isogenic *D. melanogaster* populations prefer mating with partners with similar microbiota. Although it has been proposed that gut-associated bacteria influence mating preferences by changing host sex pheromone levels, the exact mechanism is still unclear [52] (Figure 2).

C. elegans Neurotransmitters Modulate the Immune Response

Historically seen as a role for immune cells only, mounting a specific and efficient response against pathogens clearly requires the contribution of non-immune tissues. In this context, the nervous system appears essential to tune immunity according to physiological contexts and to coordinate behavioral and immune responses upon microbial exposure. Work in *C. elegans* has revealed how neurotransmitters modulate the immune response [53,54]. For instance, serotonin synthesized in cephalic ADF chemosensory neurons signals to rectal cells. The signaling in these posteriorly located cells, which depend on the Gα-protein GAO, suppresses the immune response and limits pathogen clearance rate [55]. Dopamine produced in CEP neurons acts through the ASG neurons to inhibit intestine immune signaling upon *P. aeruginosa* exposure [56].

Endogenously produced by RIC neurons, octopamine binds to OCTR-1, an octopamine receptor, to suppress immunity [57]. Indeed, OCTR-1 signaling in ASH and ASI sensory neurons downregulates the translation of immune genes and the unfolded protein response (UPR) pathway in non-neuronal tissues [58–60]. However, this specific aspect linking immune regulation and noncanonical UPR is still debated and has been shown to depend on nematode culture conditions [61,62]. Since octopamine-producing neurons are inhibited when exposed to *P. aeruginosa* but not to the harmless *E. coli*, this neuronal break could allow the worm to adapt its immune response to the nature of encountered bacteria. More generally, these negative regulations could function to mitigate immune response or to restore protein homeostasis after infection. This is well illustrated for the GPCR-encoding *npr-8* gene, which is expressed in amphid neurons (AWB, ASJ, AWC) and negatively regulates the expression of collagen genes in the worm cuticle [63]. Thus, NPR-8 production influences host defense against pathogens by modulating the physical barrier. However, in contrast to these previous examples, the neuro-immune connection can also reinforce host defense. In *C. elegans* infected by *Staphylococcus aureus*, neuronally produced acetylcholine functions in an endocrine fashion to engage muscarinic receptors in the intestinal epithelium and induce Wnt-dependent expression of host defense genes [64]. The establishment of an adapted antibacterial enteric response depends also on neuro-immune interactions that took place early in life, during developmental processes. Expression of *orln-1* in the olfactory AWC neurons is critical for olfactory receptor differentiation during larval development. Loss-of-function mutant analysis indicates that ORLN-1 acts non-cell autonomously to repress p38 MAPK-dependent immune responses in the intestine [65]. These data suggest that low activity of neuronal ORLN-1 de-represses the p38 MAPK PMK1 pathway to prime the immune response in the intestine, thus allowing challenges by bacterial pathogens encountered during larval development to be handled (Figure 1). Thus, the worm nervous system not only detects pathogenic bacteria leading to avoidance behavior, but also modulates the activation of canonical immune pathways in non-neuronal cells in both physiological and infected conditions.

Neuronal Signaling Influences Fly Cellular Immunity

In contrast to *C. elegans, D. melanogaster* possesses circulating immune cells that can engulf and eliminate invasive bacteria (Box 1). These professional phagocytes, called plasmatocytes, are mainly produced by the hematopoietic organ called the **lymph gland** and released into the blood. Their numbers and properties vary in response to developmental and environmental

cues, some of which are of neuronal origin [66]. Activin-β, a TGF-β family ligand that is expressed by sensory neurons of the peripheral nervous system, regulates the proliferation and adhesion of hemocytes. Agonist-mediated activation and transient silencing of these sensory neurons affect resident hemocyte numbers and localization [67]. Environmentally derived neuronal signals also control fly hematopoiesis. Activation of fly olfactory neurons leads to the secretion of GABA from neurosecretory cells into the circulation. Upon binding to its metabotropic receptors expressed on hematopoietic progenitors, GABA regulates the balance between maintenance and differentiation of these progenitors in the lymph gland [68]. One candidate upstream sensor is the odorant receptor Or42, although the ligand(s) involved is still unknown. Neurons have also been implicated in connecting environmental gas level cues to myeloid differentiation. Both the inactivation of CO_2-sensing neurons and the stimulation of hypoxia-sensing neurons lead to an increase of hypoxia-inducible factor-α in downstream neurons. In turn, these neurons release the JAK/STAT ligand Unpaired-3, which triggers Insulin-like peptide-6 production by the fat body cells. Once released into the circulation this hormone promotes crystal cell (one blood cell type) differentiation in the lymph gland [69]. It would be of significant interest to decipher if and how bacterial infection directly modulates the activation of these olfactory and gas-sensitive neurons that function upstream of hematopoietic differentiation.

New Roles for Old Friends: The Multiple Roles of NF-κB and AMPs in Neuronal Tissues

The interplay between the immune and the neuronal systems is also revealed by the growing number of proteins historically considered as immune effectors or regulators for which a function in the nervous system has been observed. An example of how immune protein activity has extended beyond host defense has been described for the proinflammatory cytokine interleukin (IL)-17. When worms are exposed to 21% O_2, they tend to aggregate. Impairment of IL-17 receptors in RMG interneurons induces defects in O_2-dependent social behaviors. IL-17 can act directly on neurons to modulate their responsiveness to presynaptic input and circuit sensitivity to O_2. Knowing that O2 level-dependent aggregation and bordering of *C. elegans* are influenced by the presence of bacteria, IL-17 signaling may have played a role in ancestral nervous systems in the regulation of behavioral responses to bacteria [70,71]. Similarly, a role in the regulation of neuronal function and behavior by immune proteins has been reported in the fruit fly. In *D. melanogaster* neuromuscular junctions, perturbation of neurotransmitter receptors in the muscle cell enhances neurotransmitter release from the motor neuron, a phenomenon called presynaptic homeostatic potentiation (PHP). The immune pattern recognition receptor PGRP-LC and some downstream pathway components of the NF-κB/IMD (immune deficiency) pathway are required presynaptically to regulate PHP. However, the NF-κB/IMD signaling bifurcates downstream of the PGRP-LC receptor to achieve immediate modulation of the presynaptic release apparatus via the TGF-β activated kinase (Tak1) and prolonged maintenance of the homeostatic response via the transcription factor NF-κB/Relish [72,73]. Since PHP has no obvious links with bacterial immunity, it is possible that PGRP-LC is activated at the synapse by an endogenous ligand. Besides the regulation of neuronal function, the NF-κB/Relish protein has also been involved in sleep regulation. Together with other immune effectors, it turns out to be upregulated upon sleep deprivation [74]. Consistently, flies mutant for NF-κB/Relish exhibit a reduced sleep period and, unlike their wild type siblings, are unable to increase sleep upon bacterial infection [75]. Since both phenotypes are rescued by providing NF-κB/Relish in fat body cells, it is likely that NF-κB-regulated genes produced by fat body cells modulate sleep behavior. As mentioned earlier, the canonical NF-κB antibacterial pathway functions in octopaminergic neurons to regulate oviposition. Although AMPs seem dispensable for this response (A. Masuzzo, L. Kurz, and J. Royet personal communication), they have been implicated in other neuronal activities. Nemuri, a peptide with antimicrobial properties expressed in few brain neurons is induced

upon sleep deprivation. Flies in which Nemuri is overexpressed in neurons survive infection by *S. marcescens* or *Streptococcus pneumoniae* better than control flies. Nemuri could therefore act by prolonging sleep to promote fly survival after infection [76]. Moreover, gain-of-function experiments suggest that when expressed in neurons (Drosocin) or glial cells (Metchnikowin) some AMPs could contribute to resilience to sleep deprivation [77]. Finally, genetic inactivation of *Achilles*, a neuronal gene showing a highly rhythmic expression pattern, results in dramatically high levels of immune response effectors, including AMPs [78]. As a result, flies are more resistant to immune challenge with bacteria. Other biological effects of immune genes on nervous function include memory formation. Diptericin B and the bacteria sensor GNBP-like3 are upregulated following behavioral training. Knock-down experiments revealed that while they both regulate long-term memory, Diptericin B functions in the head fat body and GNBP-like3 in neurons to prevent memory deficit [79]. AMPs are produced as a result of immune stimulation, so it can be imagined that the formation of memories related to the event that determined their production may be beneficial for the fly. In contrast to previous examples, recent reports revealed that AMPs may also play a role in neurodegenerative diseases. Indeed, AMP accumulation has been shown to induce neuronal damage in flies. Hyperactivation of innate immunity in the brain as a result of genetic mutations or bacterial injection causes neurodegeneration linked to the neurotoxic effects of AMPs [80]. With age, flies present an NF-κB-dependent constitutive AMP gene expression in glial cells, which is accompanied by progressive neurodegeneration and locomotion decline [81]. Similarly, aging-associated expression of the AMP NLP-29 causes dendrite degeneration in *C. elegans*. By activating the orphan GPRC NPR-12, NLP-29 induces autophagy to mediate aging-associated dendrite degeneration, a mechanism also observed after infection by the fungus *Drechmeria coniospora* [82]. This finding supports the existence of signaling pathways possibly linking microbial defense to degeneration. The growing number of immune proteins and pathways involved in neuronal functions raises the broader question of how precisely should one delineate the range of phenomena to be considered strictly as immune response and whether the definition of an immune cell should be expanded or reconsidered.

Concluding Remarks and Future Perspectives

In the thousands-of-pieces puzzle of the network that underlies microbe interactions with the nervous system of animals, work in recent years, focusing mostly on a few specific bacteria species and animal models, has begun to assemble some of the pieces. While some trends are emerging, such as the role of octopamine in mediating many of these interactions, our knowledge remains fairly rudimentary, with many unanswered questions (see Outstanding Questions). There is a good chance that, as the number of bacteria species studied increases, the number of mechanisms and molecules involved increases in concert. And this without mentioning other non-bacterial parasites, such as viruses or fungi, some of which are also capable of altering the behavior of the hosts they infect [7]. Much work, therefore, still lies ahead. It can be hoped that some of the insights gained using studies in *C. elegans*, *D. melanogaster*, and other invertebrate models will be useful for elucidating how bacteria impact on cognitive functions and fundamental behavior patterns in higher eukaryotes.

Acknowledgments

We thank Marie Meister for comments on the manuscript. This work was supported by Investissements d'Avenir–Labex INFORM (ANR-11-LABX-0054), ANR BACNEURODRO (ANR-17-CE16-0023-01) and ANR PEPTIMET (ANR-18-CE15-0018-02), Equipe Fondation pour la Recherche Médicale (EQU201903007783), and l'Institut Universitaire de France to J.R.

References

1. de Roode, J.C. and Lefevre, T. (2012) Behavioral immunity in insects. *Insects* 3, 789–820
2. Lefevre, T. *et al.* (2012) Defence strategies against a parasitoid wasp in *Drosophila*: fight or flight? *Biol. Lett.* 8, 230–233
3. Storelli, G. *et al.* (2011) *Lactobacillus plantarum* promotes *Drosophila* systemic growth by modulating hormonal signals through TOR-dependent nutrient sensing. *Cell Metab.* 14, 403–414

Outstanding Questions

C. elegans sense gas levels to move away from putative pathogenic bacteria. Since both beneficial and harmful bacteria are metabolically active and produce CO_2, how is the distinction made by the worm? Knowing that *D. melanogaster* is also able to sense CO_2 via dedicated receptors, is this modality also used by flies to avoid pathogenic bacteria?

Work in *C. elegans* demonstrates that neuropeptide production can modulate the intensity of the immune response. In flies, neuropeptides have been reported to impact the differentiation of hematopoietic progenitors and hence the cellular branch of the immune response. Does bacteria detection by the sensory system also impact the humoral arm of the immune response of *D. melanogaster*?

Are the molecular mechanisms that regulate bacteria–neuron interactions universal across bacteria, or alternatively, are they bacteria species-specific?

Peptidoglycan receptor proteins and downstream NF-κB signaling are used in fly immune cells to mount an antibacterial response, in some brain neurons to modify egg-laying of infected animals, and at the neuromuscular junction to control presynaptic homeostatic potentiation. What is the rationale for this shared usage and how did it come to be that such a unique signaling cascade is used in biological contexts that are so different? Are the downstream NF-κB effectors shared between these functions or are they function-specific?

Antimicrobial peptides are one of the main immune effectors in *C. elegans* and *D. melanogaster*. Recent reports indicate that some are also expressed in neurons to control behaviors such as memory or sleep. How are these small cationic peptides able to modify neuronal activity and, consequently, animal behavior?

Bacteria can produce many compounds potentially detected by the host sensory systems. How do animals integrate bacterial inputs detected by multiple types of sensory neurons to display *ad hoc* behavioral responses when in contact with a given bacteria species?

4. Shin, S.C. *et al.* (2011) *Drosophila* microbiome modulates host developmental and metabolic homeostasis via insulin signaling. *Science* 334, 670–674
5. Lafferty, K.D. and Shaw, J.C. (2013) Comparing mechanisms of host manipulation across host and parasite taxa. *J. Exp. Biol.* 216, 56–66
6. Liu, W. *et al.* (2017) Enterococci mediate the oviposition preference of *Drosophila melanogaster* through sucrose catabolism. *Sci. Rep.* 7, 13420
7. Elya, C. *et al.* (2018) Robust manipulation of the behavior of *Drosophila melanogaster* by a fungal pathogen in the laboratory. *eLife* 7, e34414
8. Felix, M.A. and Duveau, F. (2012) Population dynamics and habitat sharing of natural populations of *Caenorhabditis elegans* and *C. briggsae*. *BMC Biol.* 10, 59
9. Zecic, A. *et al.* (2019) The nutritional requirements of *Caenorhabditis elegans*. *Genes Nutr.* 14, 15
10. Pradel, E. *et al.* (2007) Detection and avoidance of a natural product from the pathogenic bacterium *Serratia marcescens* by *Caenorhabditis elegans*. *Proc. Natl. Acad. Sci. U. S. A.* 104, 2295–2300
11. Tran, A. *et al.* (2017) *C. elegans* avoids toxin-producing *Streptomyces* using a seven transmembrane domain chemosensory receptor. *eLife* 6, e23770
12. Zhang, Y. *et al.* (2005) Pathogenic bacteria induce aversive olfactory learning in *Caenorhabditis elegans*. *Nature* 438, 179–184
13. Jin, X. *et al.* (2016) Distinct circuits for the formation and retrieval of an imprinted olfactory memory. *Cell* 164, 632–643
14. Ha, H.I. *et al.* (2010) Functional organization of a neural network for aversive olfactory learning in *Caenorhabditis elegans*. *Neuron* 68, 1173–1186
15. Zhang, X. and Zhang, Y. (2012) DBL-1, a TGF-beta, is essential for *Caenorhabditis elegans* aversive olfactory learning. *Proc. Natl. Acad. Sci. U. S. A.* 109, 17081–17086
16. Gray, J.M. *et al.* (2004) Oxygen sensation and social feeding mediated by a *C. elegans* guanylate cyclase homologue. *Nature* 430, 317–322
17. Meisel, J.D. *et al.* (2014) Chemosensation of bacterial secondary metabolites modulates neuroendocrine signaling and behavior of *C. elegans*. *Cell* 159, 267–280
18. Brandt, J.P. and Ringstad, N. (2015) Toll-like receptor signaling promotes development and function of sensory neurons required for a *C. elegans* pathogen-avoidance behavior. *Curr. Biol.* 25, 2228–2237
19. Hao, Y. *et al.* (2018) Thioredoxin shapes the *C. elegans* sensory response to *Pseudomonas* produced nitric oxide. *eLife* 7, e36833
20. Fischer, C.N. *et al.* (2017) Metabolite exchange between microbiome members produces compounds that influence *Drosophila* behavior. *eLife* 6, e18855
21. Christiaens, J.F. *et al.* (2014) The fungal aroma gene ATF1 promotes dispersal of yeast cells through insect vectors. *Cell Rep.* 9, 425–432
22. Joseph, R.M. and Carlson, J.R. (2015) *Drosophila* chemoreceptors: a molecular interface between the chemical world and the brain. *Trends Genet.* 31, 683–695
23. Soldano, A. *et al.* (2016) Gustatory-mediated avoidance of bacterial lipopolysaccharides via TRPA1 activation in *Drosophila*. *eLife* 5, e13133
24. Yanagawa, A. *et al.* (2019) LPS perception through taste-induced reflex in *Drosophila melanogaster*. *J. Insect Physiol.* 112, 39–47
25. Royet, J. *et al.* (2011) Peptidoglycan recognition proteins: modulators of the microbiome and inflammation. *Nat. Rev. Immunol.* 11, 837–851
26. Keita, S. *et al.* (2017) *Drosophila* larvae food intake cessation following exposure to *Erwinia* contaminated media requires odor perception, Trpa1 channel and evf virulence factor. *J. Insect Physiol.* 99, 25–32
27. Stensmyr, M.C. *et al.* (2012) A conserved dedicated olfactory circuit for detecting harmful microbes in *Drosophila*. *Cell* 151, 1345–1357
28. Mansourian, S. *et al.* (2016) Fecal-derived phenol induces egg-laying aversion in *Drosophila*. *Curr. Biol.* 26, 2762–2769
29. Depetris-Chauvin, A. *et al.* (2017) Olfactory detection of a bacterial short-chain fatty acid acts as an orexigenic signal in *Drosophila melanogaster* larvae. *Sci. Rep.* 7, 14230
30. Charroux, B. *et al.* (2020) *Drosophila* aversive behavior toward *Erwinia carotovora* is mediated by bitter neurons and leukokinin. *iScience* 23, 101152
31. Melo, J.A. and Ruvkun, G. (2012) Inactivation of conserved *C. elegans* genes engages pathogen- and xenobiotic-associated defenses. *Cell* 149, 452–466
32. Kumar, S. *et al.* (2019) Lifespan extension in *C. elegans* caused by bacterial colonization of the intestine and subsequent activation of an innate immune response. *Dev. Cell* 49, 100–117
33. Singh, J. and Aballay, A. (2019) Microbial colonization activates an immune fight-and-flight response via neuroendocrine signaling. *Dev. Cell* 49, 89–99
34. Singh, J. and Aballay, A. (2019) Intestinal infection regulates behavior and learning via neuroendocrine signaling. *eLife* 8, e50033
35. Chen, Z. *et al.* (2013) Two insulin-like peptides antagonistically regulate aversive olfactory learning in *C. elegans*. *Neuron* 77, 572–585
36. Lee, K. and Mylonakis, E. (2017) An intestine-derived neuropeptide controls avoidance behavior in *Caenorhabditis elegans*. *Cell Rep.* 20, 2501–2512
37. O'Donnell, M.P. *et al.* (2020) A neurotransmitter produced by gut bacteria modulates host sensory behaviour. *Nature* 583, 415–420
38. Broderick, N.A. and Lemaitre, B. (2012) Gut-associated microbes of *Drosophila melanogaster*. *Gut Microbes* 3, 307–321
39. Martino, M.E. *et al.* (2018) Bacterial adaptation to the host's diet is a key evolutionary force shaping *Drosophila-Lactobacillus* symbiosis. *Cell Host Microbe* 24, 109–119
40. Lesperance, D.N. and Broderick, N.A. (2020) Microbiomes as modulators of *Drosophila melanogaster* homeostasis and disease. *Curr. Opin. Insect Sci.* 39, 84–90
41. Venu, I. *et al.* (2014) Social attraction mediated by fruit flies' microbiome. *J. Exp. Biol.* 217, 1346–1352
42. Wong, A.C. *et al.* (2017) Gut microbiota modifies olfactory-guided microbial preferences and foraging decisions in *Drosophila*. *Curr. Biol.* 27, 2397–2404
43. Qiao, H. *et al.* (2019) Gut microbiota affects development and olfactory behavior in *Drosophila melanogaster*. *J. Exp. Biol.* 222, jeb192500
44. Schretter, C.E. *et al.* (2018) A gut microbial factor modulates locomotor behaviour in *Drosophila*. *Nature* 563, 402–406
45. Kurz, C.L. *et al.* (2017) Peptidoglycan sensing by octopaminergic neurons modulates *Drosophila* oviposition. *eLife* 6, e21937
46. Royet, J. and Dziarski, R. (2007) Peptidoglycan recognition proteins: pleiotropic sensors and effectors of antimicrobial defences. *Nat. Rev. Microbiol.* 5, 264–277
47. Masuzzo, A. *et al.* (2019) Peptidoglycan-dependent NF-kappaB activation in a small subset of brain octopaminergic neurons controls female oviposition. *eLife* 8, e50559
48. Charroux, B. *et al.* (2018) Cytosolic and secreted peptidoglycan-degrading enzymes in *Drosophila* respectively control local and systemic immune responses to microbiota. *Cell Host Microbe* 23, 215–228
49. Basset, A. *et al.* (2000) The phytopathogenic bacteria *Erwinia carotovora* infects *Drosophila* and activates an immune response. *Proc. Natl. Acad. Sci. U. S. A.* 97, 3376–3381
50. Rohrscheib, C.E. *et al.* (2015) *Wolbachia* influences the production of octopamine and affects *Drosophila* male aggression. *Appl. Environ. Microbiol.* 81, 4573–4580
51. Keesey, I.W. *et al.* (2017) Pathogenic bacteria enhance dispersal through alteration of *Drosophila* social communication. *Nat. Commun.* 8, 265
52. Sharon, G. *et al.* (2010) Commensal bacteria play a role in mating preference of *Drosophila melanogaster*. *Proc. Natl. Acad. Sci. U. S. A.* 107, 20051–20056
53. Styer, K.L. *et al.* (2008) Innate immunity in *Caenorhabditis elegans* is regulated by neurons expressing NPR-1/GPCR. *Science* 322, 460–464
54. Reddy, K.C. *et al.* (2009) A polymorphism in npr-1 is a behavioral determinant of pathogen susceptibility in *C. elegans*. *Science* 323, 382–384
55. Anderson, A. *et al.* (2013) Serotonergic chemosensory neurons modify the *C. elegans* immune response by regulating G-protein signaling in epithelial cells. *PLoS Pathog.* 9, e1003787

56. Cao, X. and Aballay, A. (2016) Neural inhibition of dopaminergic signaling enhances immunity in a cell-non-autonomous manner. *Curr. Biol.* 26, 2329–2334
57. Sellegounder, D. *et al.* (2018) Octopaminergic signaling mediates neural regulation of innate immunity in *Caenorhabditis elegans*. *MBio* 9, e01645-18
58. Sun, J. *et al.* (2011) Neuronal GPCR controls innate immunity by regulating noncanonical unfolded protein response genes. *Science* 332, 729–732
59. Liu, Y. *et al.* (2016) Neuronal GPCR OCTR-1 regulates innate immunity by controlling protein synthesis in *Caenorhabditis elegans*. *Sci. Rep.* 6, 36832
60. Cao, X. *et al.* (2017) Distinct roles of sensory neurons in mediating pathogen avoidance and neuropeptide-dependent immune regulation. *Cell Rep.* 21, 1442–1451
61. George-Raizen, J.B. *et al.* (2014) Dynamically-expressed prion-like proteins form a cuticle in the pharynx of *Caenorhabditis elegans*. *Biol. Open* 3, 1139–1149
62. Kim, D.H. and Ewbank, J.J. (2018) Signaling in the innate immune response. *WormBook* 2018, 1–35
63. Sellegounder, D. *et al.* (2019) Neuronal GPCR NPR-8 regulates *C. elegans* defense against pathogen infection. *Sci. Adv.* 5, eaaw4717
64. Labed, S.A. *et al.* (2018) Intestinal epithelial Wnt signaling mediates acetylcholine-triggered host defense against infection. *Immunity* 48, 963–978
65. Foster, K.J. *et al.* (2020) Innate immunity in the *C. elegans* intestine is programmed by a neuronal regulator of AWC olfactory neuron development. *Cell Rep.* 31, 107478
66. Banerjee, U. *et al.* (2019) Drosophila as a genetic model for hematopoiesis. *Genetics* 211, 367–417
67. Makhijani, K. *et al.* (2017) Regulation of *Drosophila* hematopoietic sites by Activin-beta from active sensory neurons. *Nat. Commun.* 8, 15990
68. Shim, J. *et al.* (2013) Olfactory control of blood progenitor maintenance. *Cell* 155, 1141–1153
69. Cho, B. *et al.* (2018) Systemic control of immune cell development by integrated carbon dioxide and hypoxia chemosensation in *Drosophila*. *Nat. Commun.* 9, 2679
70. Flynn, S.M. *et al.* (2020) MALT-1 mediates IL-17 neural signaling to regulate *C. elegans* behavior, immunity and longevity. *Nat. Commun.* 11, 2099
71. Chen, C. *et al.* (2017) IL-17 is a neuromodulator of *Caenorhabditis elegans* sensory responses. *Nature* 542, 43–48
72. Harris, N. *et al.* (2015) The innate immune receptor PGRP-LC controls presynaptic homeostatic plasticity. *Neuron* 88, 1157–1164
73. Harris, N. *et al.* (2018) Molecular interface of neuronal innate immunity, synaptic vesicle stabilization, and presynaptic homeostatic plasticity. *Neuron* 100, 1163–1179
74. Williams, J.A. *et al.* (2007) Interaction between sleep and the immune response in *Drosophila*: a role for the NFkappaB relish. *Sleep* 30, 389–400
75. Kuo, T.H. *et al.* (2010) Sleep triggered by an immune response in *Drosophila* is regulated by the circadian clock and requires the NFkappaB Relish. *BMC Neurosci.* 11, 17
76. Toda, H. *et al.* (2019) A sleep-inducing gene, nemuri, links sleep and immune function in *Drosophila*. *Science* 363, 509–515
77. Dissel, S. *et al.* (2015) Differential activation of immune factors in neurons and glia contribute to individual differences in resilience/vulnerability to sleep disruption. *Brain Behav. Immun.* 47, 75–85
78. Li, J. *et al.* (2017) Achilles is a circadian clock-controlled gene that regulates immune function in *Drosophila*. *Brain Behav. Immun.* 61, 127–136
79. Barajas-Azpeleta, R. *et al.* (2018) Antimicrobial peptides modulate long-term memory. *PLoS Genet.* 14, e1007440
80. Cao, Y. *et al.* (2013) Dnr1 mutations cause neurodegeneration in *Drosophila* by activating the innate immune response in the brain. *Proc. Natl. Acad. Sci. U. S. A.* 110, E1752–E1760
81. Kounatidis, I. *et al.* (2017) NF-kappaB immunity in the brain determines fly lifespan in healthy aging and age-related neurodegeneration. *Cell Rep.* 19, 836–848
82. Lezi, E. *et al.* (2018) An antimicrobial peptide and its neuronal receptor regulate dendrite degeneration in aging and infection. *Neuron* 97, 125–138
83. McEwan, D.L. *et al.* (2012) Host translational inhibition by *Pseudomonas aeruginosa* exotoxin A triggers an immune response in *Caenorhabditis elegans*. *Cell Host Microbe* 11, 364–374
84. Kirkhart, C. and Scott, K. (2015) Gustatory learning and processing in the *Drosophila* mushroom bodies. *J. Neurosci.* 35, 5950–5958
85. Kain, P. and Dahanukar, A. (2015) Secondary taste neurons that convey sweet taste and starvation in the *Drosophila* brain. *Neuron* 85, 819–832
86. Kim, H. *et al.* (2017) Long-range projection neurons in the taste circuit of *Drosophila*. *eLife* 6, e23386
87. Amin, H. and Lin, A.C. (2019) Neuronal mechanisms underlying innate and learned olfactory processing in *Drosophila*. *Curr. Opin. Insect Sci.* 36, 9–17